MODERN ELECTROCHEMISTRY 1

ELECTROCHEMISTRY 1
ELECTROCHEMISTRY 1

Ionics

SECOND EDITION

JOHN O'M. BOCKRIS and AMULYA K. N. REDDY

VOLUME 1

MODERN ELECTROCHEMISTRY

SECOND EDITION

Ionics

This page intentionally left blank

VOLUME 1

MODERN ELECTROCHEMISTRY

SECOND EDITION

Ionics

John O'M. Bockris
Distinguished Professor of Chemistry
Texas A&M University
College Station, Texas

and

Amulya K. N. Reddy
President
International Energy Initiative
Bangalore, India

KLUWER ACADEMIC PUBLISHERS
NEW YORK, BOSTON, DORDRECHT, LONDON, MOSCOW

eBook ISBN: 0-306-46909-X
Print ISBN: 0-306-45554-4

Created in the United States of America

Visit Kluwer Online at: http://kluweronline.com
and Kluwer's eBookstore at: http://ebooks.kluweronline.com

To P. Debye and E. Hückel

This page intentionally left blank

PREFACE TO THE FIRST EDITION

This book had its nucleus in some lectures given by one of us (J.O'M.B.) in a course on electrochemistry to students of energy conversion at the University of Pennsylvania. It was there that he met a number of people trained in chemistry, physics, biology, metallurgy, and materials science, all of whom wanted to know something about electrochemistry. The concept of writing a book about electrochemistry which could be understood by people with very varied backgrounds was thereby engendered. The lectures were recorded and written up by Dr. Klaus Muller as a 293-page manuscript. At a later stage, A.K.N.R. joined the effort; it was decided to make a fresh start and to write a much more comprehensive text.

Of methods for direct energy conversion, the electrochemical one is the most advanced and seems the most likely to become of considerable practical importance. Thus, conversion to electrochemically powered transportation systems appears to be an important step by means of which the difficulties of air pollution and the effects of an increasing concentration in the atmosphere of carbon dioxide may be met. Corrosion is recognized as having an electrochemical basis. The synthesis of nylon now contains an important electrochemical stage. Some central biological mechanisms have been shown to take place by means of electrochemical reactions. A number of American organizations have recently recommended greatly increased activity in training and research in electrochemistry at universities in the United States. Three new international journals of fundamental electrochemical research were established between 1955 and 1965.

In contrast to this, physical chemists in U.S. universities seem—perhaps partly because of the absence of a modern textbook in English—out of touch with the revolution in fundamental interfacial electrochemistry which has occurred since 1950. The fragments of electrochemistry which are taught in many U.S. universities belong not to the space age of electrochemically powered vehicles, but to the age of thermo-

dynamics and the horseless carriage; they often consist of Nernst's theory of galvanic cells (1891) together with the theory of Debye and Hückel (1923).

Electrochemistry at present needs several kinds of books. For example, it needs a textbook in which the whole field is discussed at a strong theoretical level. The most pressing need, however, is for a book which outlines the field at a level which can be understood by people entering it from different disciplines who have no previous background in the field but who wish to use modern electrochemical concepts and ideas as a basis for their own work. It is this need which the authors have tried to meet.

The book's aims determine its priorities. In order, these are:

1. Lucidity. The authors have found students who understand advanced courses in quantum mechanics but find difficulty in comprehending a field at whose center lies the quantum mechanics of electron transitions across interfaces. The difficulty is associated, perhaps, with the interdisciplinary character of the material: a background knowledge of physical chemistry is not enough. Material has therefore sometimes been presented in several ways and occasionally the same explanations are repeated in different parts of the book. The language has been made informal and highly explanatory. It retains, sometimes, the lecture style. In this respect, the authors have been influenced by *The Feynman Lectures on Physics.*

2. Honesty. The authors have suffered much themselves from books in which proofs and presentations are not complete. An attempt has been made to include most of the necessary material. Appendices have been often used for the presentation of mathematical derivations which would obtrude too much in the text.

3. Modernity. There developed during the 1950s a great change in emphasis in electrochemistry away from a subject which dealt largely with solutions to one in which the treatment at a molecular level of charge transfer across interfaces dominates. This is the "new electrochemistry," the essentials of which, at an elementary level, the authors have tried to present.

4. Sharp variation is standard. The objective of the authors has been to begin each chapter at a very simple level and to increase the level to one which allows a connecting up to the standard of the specialized monograph. The standard at which subjects are presented has been intentionally variable, depending particularly on the degree to which knowledge of the material appears to be widespread.

5. One theory per phenomenon. The authors intend a *teaching book*, which acts as an introduction to graduate studies. They have tried to present, with due admission of the existing imperfections, a simple version of that model which seemed to them at the time of writing to reproduce the facts most consistently. They have for the most part refrained from presenting the detailed pros and cons of competing models in areas in which the theory is still quite mobile.

In respect to references and further reading: no detailed references to the literature have been presented, in view of the elementary character of the book's contents, and the corresponding fact that it is an introductory book, largely for beginners. In the

"further reading" lists, the policy is to cite papers which are classics in the development of the subject, together with papers of particular interest concerning recent developments, and in particular, reviews of the last few years.

It is hoped that this book will not only be useful to those who wish to work with modern electrochemical ideas in chemistry, physics, biology, materials science, etc., but also to those who wish to begin research on electron transfer at interfaces and associated topics.

The book was written mainly at the Electrochemistry Laboratory in the University of Pennsylvania, and partly at the Indian Institute of Science in Bangalore. Students in the Electrochemistry Laboratory at the University of Pennsylvania were kind enough to give guidance frequently on how they reacted to the clarity of sections written in various experimental styles and approaches. For the last four years, the evolving versions of sections of the book have been used as a partial basis for undergraduate, and some graduate, lectures in electrochemistry in the Chemistry Department of the University.

The authors' acknowledgment and thanks must go first to Mr. Ernst Cohn of the National Aeronautics and Space Administration. Without his frequent stimulation, including very frank expressions of criticism, the book might well never have emerged from the Electrochemistry Laboratory.

Thereafter, thanks must go to Professor B. E. Conway, University of Ottawa, who gave several weeks of his time to making a detailed review of the material. Plentiful help in editing chapters and effecting revisions designed by the authors was given by the following: Chapters IV and V, Dr. H. Wroblowa (Pennsylvania); Chapter VI, Dr. C. Solomons (Pennsylvania) and Dr. T. Emi (Hokkaido); Chapter VII, Dr. E. Gileadi (Tel-Aviv); Chapters VIII and IX, Prof. A. Despic (Belgrade), Dr. H. Wroblowa, and Mr. J. Diggle (Pennsylvania); Chapter X, Mr. J. Diggle; Chapter XI, Dr. D. Cipris (Pennsylvania). Dr. H. Wroblowa has to be particularly thanked for essential contributions to the composition of the Appendix on the measurement of Volta potential differences.

Constructive reactions to the text were given by Messers. G. Razumney, B. Rubin, and G. Stoner of the Electrochemistry Laboratory. Advice was often sought and accepted from Dr. B. Chandrasekaran (Pennsylvania), Dr. S. Srinivasan (New York), and Mr. R. Rangarajan (Bangalore).

Comments on late drafts of chapters were made by a number of the authors' colleagues, particularly Dr. W. McCoy (Office of Saline Water), Chapter II; Prof. R. M. Fuoss (Yale), Chapter III; Prof. R. Stokes (Armidale), Chapter IV; Dr. R. Parsons (Bristol), Chapter VII; Prof. A. N. Frumkin (Moscow), Chapter VIII; Dr. H. Wroblowa, Chapter X; Prof. R. Staehle (Ohio State), Chapter XI. One of the authors (A.K.N.R.) wishes to acknowledge his gratitude to the authorities of the Council of Scientific and Industrial Research, India, and the Indian Institute of Science, Bangalore, India, for various facilities, not the least of which were extended leaves of absence. He wishes also to thank his wife and children for sacrificing many precious hours which rightfully belonged to them.

This page intentionally left blank

PREFACE

The textbook *Modern Electrochemistry* by Bockris and Reddy originated in the needs of students at the Energy Conversion Institute of the University of Pennsylvania in the late 1960s. People trained in various disciplines from mathematics to biology wanted to understand the new high-energy-density storage batteries and the doubling of the efficiency of energy conversion offered by fuel cells over heat engines. The task was to take a group that seemed to be above average in initiative and present electrochemistry well enough to meet their needs.

The book turned out to be a great success. Its most marked characteristic was—is—lucidity. The method used was to start off at low level and then move up in a series of very small steps. Repetition is part of the technique and does not offend, for the lesson given each time is the same but is taught differently.

The use of the book spread rapidly beyond the confines of energy conversion groups. It led to the recognition of *physical* electrochemistry—the electrochemical discipline seen from its roots in physics and physical chemistry, and not as a path to superior chemical analysis. The book outlined electrochemical science for the first time in a molecular way, paying due heed to thermodynamics as bedrock but keeping it as background. The success of the effort has been measured not only by the total sales but by the fact that another reprinting had to be made in 1995, 25 years after the first one. The average sales rate of the first edition is even now a dozen copies a month!

Given this background, the challenge of writing a revised edition has been a memorable one. The changes in the state of electrochemical science in the quarter century of the book's life have been broad and deep. Techniques such as scanning tunneling microscopy enable us to *see atoms* on electrodes. Computers have allowed a widespread development of molecular dynamics (MD) calculations and changed the balance between informed guesses and the timely adjustment of parameters in force laws to enable MD calculations to lead to experimental values. The long-postponed introduction of commercial electric cars in the United States has been realized and is

the beginning of a great step toward a healthier environment. The use of the new room-temperature molten salts has made it possible to exploit the advantage of working with pure liquid electrolytes—no solvent—without the rigors of working at 1000 °C.

All the great challenges of electrochemistry at 2000 A.D. do not have to be addressed in this second edition for this is an *undergraduate* text, stressing the teaching of *fundamentals* with an occasional preview of the advancing frontier.

The basic attributes of the book are unchanged: lucidity comes first. Since the text is not a graduate text, there is no confusing balancing of the merits of one model against those of another; the most probable model at the time of writing is described. Throughout it is recognized that theoretical concepts rise and fall; a theory that lasts a generation is doing well.

These philosophies have been the source of some of the choices made when balancing what should be retained and what rewritten. The result is quite heterogeneous. Chapters 1 and 2 are completely new. The contributions from neutron diffraction measurements in solutions and those from other spectroscopic methods have torn away many of the veils covering knowledge of the first 1–2 layers of solvent around an ion. Chapter 3 also contains much new material. Debye and Huckel's famous calculation is two generations old and it is surely time to move toward new ideas. Chapter 4, on the other hand, presents much material on transport that is phenomenological—material so basic that it must be presented but shows little variation with time.

The last chapter, which is on ionic liquids, describes the continuing evolution that is the result of the development of low-temperature molten salts and the contributions of computer modeling. The description of models of molten silicates contains much of the original material in the first edition, for the models described there are those still used today.

A new feature is the liberal supply of problems for student solution—about 50 per chapter. This idea has been purloined from the excellent physical chemistry textbook by Peter Atkins (W. H. Freeman). There are exercises, practice in the use of the chapter's equations; problems (the chapter's material related to actual situations); and finally, a few much more difficult tasks which are called "microresearch problems," each one of which may take some hours to solve.

The authors have not hesitated to call on colleagues for help in understanding new material and in deciding what is vital and what can be left for the literature. The authors would particularly like to thank John Enderby (University of Bristol) for his review of Chapter 2; Tony Haymet (University of Sydney) for advice on the weight to be given to various developments that followed Debye and Hückel's ground-breaking work and for tutoring us on computational advances in respect to electrolytic ion pairs. Michael Lyons (University of Dublin) is to be thanked for allowing the present authors use of an advanced chapter on transport phenomena in electrolytes written by him. Austin Angell (Arizona State University of Tempe) in particular and Douglas Inman

(Imperial College) have both contributed by means of criticisms (not always heeded) in respect to the way to present the material on structure in pure electrolytes.

Many other electrochemists have helped by replying to written inquiries.

Dr. Maria Gamboa is to be thanked for extensive editorial work, Ms. Diane Dowdell for her help with information retrieval, and Mrs. Janie Leighman for her excellence in typing the many drafts.

Finally, the authors wish to thank Ms. Amelia McNamara and Mr. Ken Howell of Plenum Publishing for their advice, encouragement, and patience.

This page intentionally left blank

ACKNOWLEDGMENTS

In writing a book of this type, the authors have accessed the advice of many colleagues, often by telephone discussions and sometimes in written exchanges.

A few individuals, however, deserve mention for having done much more than normal collegial cooperation implies.

Thus, the chapter on solvation was greatly helped by consultation and correspondence with Professor J. E. Enderby (University of Bristol).

In respect to Chapter 3, advice was sought from and given by Professor Harold Friedman (University of New York at Stony Brook) and Professor J. C. Rasaiah (University of Maine).

Professor Antony Haymet (University of Sydney, Australia) was particularly helpful in the giving of his latest work, sometimes unpublished, and the giving of advice, both in writing and in telephone discussions.

Chapter 4 is rewritten to a lesser degree than the other chapters but the new material has been discussed with Professor B. E. Conway (University of Ottawa).

Chapter 5 was greatly improved by discussions and several letter exchanges with Professor Austin Angel (Arizona State University at Tempe) and to some extent with Professor Douglas Inman (Imperial College of Science and Technology, London University).

This page intentionally left blank

CONTENTS

CHAPTER 2

ION–SOLVENT INTERACTIONS

CHAPTER 3

ION–ION INTERACTIONS

CHAPTER 4

ION TRANSPORT IN SOLUTIONS

CHAPTER 5

IONIC LIQUIDS

This page intentionally left blank

NOMENCLATURE

Symbol	*Name*	*SI unit*	*Other units frequently used*
GENERAL			
A	area of an electrode–solution interface	$\mathbf{m^2}$	
a_i	activity of species i		
c_i	concentration of species i	$\mathbf{mol\ m^{-3}}$	M, N
c^0	bulk concentration	$\mathbf{mol\ m^{-3}}$	M, N
E	total energy	J	
F	force	N	
f_c	frictional coefficient	J	
f_i	partition function of species i		
$g_{i,j}$	radial pair distribution function		
k, ν	frequency	$\mathbf{s^{-1}}$	
k	wave vector $(= 2\pi/\lambda)$	$\mathbf{m^{-1}}$	
m	mass	kg	
n	number of moles		
N	number of molecules		
p	momentum		
p_r	radial momentum		
P	pressure	Pa	atm

For each symbol the appropriate SI unit is given. Multiples and submultiples of these units are equally acceptable and are often more convenient. For example, although the SI unit of concentration is $\mathbf{mol\ m^{-3}}$, concentrations are frequently expressed in $\mathbf{mol\ dm^{-3}}$ (or M), $\mathbf{mol\ cm^{-3}}$, or $\mathbf{mmol\ dm^{-3}}$.

Symbol	*Name*	*SI unit*	*Other units frequently used*
P_i^*	vapor pressure of species *i*	Pa	atm
r, d, l	distance	m	Å
T	thermodynamic temperature	K	°C
t	time	s	
U	potential energy	J	
V	volume	m^3	
v	velocity	$m\ s^{-1}$	
W	work	J	
w_i	weight fraction of species *i*		
x_i	molar fraction of species *i*		
μ	reduced mass		
ρ	density	$kg\ m^{-3}$	
τ	relaxation time	s	
λ	wavelength	m	
$\tilde{\nu}$	wavenumber	m^{-1}	
θ	angle	°	

ION– AND MOLECULE-RELATED QUANTITIES

a	distance of closest approach	m	Å
p	quadrupole moment of water	debye cm^2	
q	Bjerrum parameter	m	
z_i	charge number of an ion *i*		
α'	symmetry factor		
α_i	polarizability of species *i*	$m^3\ molecule^{-1}$	
$\alpha_{d,i}$	distortion polarizability of species *i*	$m^3\ molecule^{-1}$	
β	compressibility	Pa^{-1}	
μ	dipole moment	debye	esu cm
κ^{-1}	Debye–Hückel reciprocal length	m	

THERMODYNAMICS OF A SIMPLE PHASE

E_{pzc}, *p.z.c.*	potential of zero charge	V
E_a	energy of activation	$J\ mol^{-1}$
ΔG	molar Gibbs free-energy change	$J\ mol^{-1}$
ΔH	heat or enthalpy change	$J\ mol^{-1}$
K	equilibrium constant of the reaction	

Symbol	*Name*	*SI unit*	*Other units frequently used*
K_A, K_D	association constant and dissociation constant		
ΔS	entropy change	$J\ K^{-1} mol^{-1}$	eu
X	electric field	$V\ m^{-1}$	
μ_i	chemical potential of species i	$J\ mol^{-1}$	
$\bar{\mu}_i$	electrochemical potential of species i	$J\ mol^{-1}$	
ρ	charge density C	m^3	
ε	dielectric constant		
$\hat{\varepsilon}(\omega)$	complex permittivity		
ψ	electrostatic potential between two points	V	

ACTIVITIES IN ELECTROLYTIC SOLUTIONS AND RELATED QUANTITIES

$\alpha_{\pm}$	mean activity	
γ_i, f_i	activity coefficient of species i	
$f_{\pm}$, $\gamma_{\pm}$	stoichiometric mean	
	molar activity coefficient	
f_{IP}	activity coefficient for the ion pairs	
	ionic strength	

MASS TRANSPORT

D_i	diffusion coefficient of species i	$m^2\ s^{-1}$
J_B	flux density of species B	$mol\ m^{-2} s^{-1}$
Re	Reynolds number	
v_d	drift velocity	$m\ s^{-1}$
η	viscosity	poise

CHARGE TRANSPORT PROPERTIES OF ELECTROLYTES

q_i	charge of species i	C
R	resistance of the solution	Ω
$1/R$	conductance	S, Ω^{-1}
σ	specific conductivity	$S\ m^{-1}$ or $\Omega^{-1}\ m^{-1}$
Λ_m	molar conductivity of an electrolyte	$S\ m^2\ mol^{-1}$ or $\Omega^{-1}\ m^2\ mol^{-1}$
Λ	equivalent conductivity	$S\ m^2\ mol^{-1}\ eq^{-1}$ or $\Omega^{-1}\ m^2\ mol^{-1}\ eq^{-1}$
t_i	transport number of ionic species i in an electrolytic solution	number

Symbol	*Name*	*SI unit*
$\vec{\mu}_{abs}$	absolute mobility	$m\ s^{-1}\ N^{-1}$
μ_i, $(\mu_{conv})_i$	conventional (electrochemical) mobility of species *i*	$m^2\ V^{-1}\ s^{-1}$

KINETIC PARAMETERS

I	electric current	A
j	current density	$A\ m^{-2}$
$\vec{k}$, $\overleftarrow{k}$	rate constants	
ν_i	stoichiometric number of species *i*	

STATISTICS AND OTHER MATHEMATICAL SYMBOLS

$C(t)$	autocorrelation function
$G_{A,B}(r)$	pair correlation function
g_o	probability distribution coefficient
I	moment of inertia
P_r	probability
$\langle x \rangle$	average value of variable *x*
$\langle x^2 \rangle$	mean square value of variable *x*
x_{rms}	root-mean-square value of variable *x*
$\bar{y}$	Laplace transform of *y*
θ	fraction number, e.g. fraction of ions associated
erf(*y*)	error function
$x_{\pm}$	mean value of variable *x*

USEFUL CONSTANTS

Symbol	*Name*	*Value*
c_0	velocity of light	$2.998 \times 10^{10}\ cm\ s^{-1}$
e_0	electron charge	$1.602 \times 10^{-19}\ C$
F	Faraday's constant = $e_0 N_A$	$9.649 \times 10^{5}\ C\ mol^{-1}$
h	Planck's constant	$6.626 \times 10^{-34}\ J\ s$
k	Boltzmann's constant	$1.380 \times 10^{-23}\ J\ K^{-1}$
m_e	mass of electron	$9.110 \times 10^{-31}\ kg$
m_p	mass of proton	$1.673 \times 10^{-27}\ kg$
N_A	Avogadro's number	$6.022 \times 10^{23}\ mol^{-1}$
ε_0	permittivity of free space	$8.854 \times 10^{-12}\ C^2\ N^{-1} m^{-2}$
0 K	absolute zero of temperature	–273.15 °C
π	pi	3.14159...

Useful Unit Conversion Factors

Potential	*Length*	*Volume*	*Mass*	*Force*	*Pressure*	*Energy*
1 V	1 m	$1\ m^3$	1 g	1 N	1 Pa	1 J
$1\ J\ C^{-1}$	100 cm	$1000\ dm^3$	10^{-3} kg	10^5 dynes	$1\ N\ m^{-2}$	10^7 ergs
	1000 mm	1000 liters			10^{-5} bar	0.239 cal
	$10^6\ \mu m$				9.872×10^{-6} atm	6.242×10^{18} eV
	10^9 nm				7.502×10^{-3} mmHg	
	10^{10} Å				7.502×10^{-3} torr	
	10^{12} pm					

This page intentionally left blank

CHAPTER 1

ELECTROCHEMISTRY

1.1. A STATE OF EXCITEMENT

Electrochemistry was born from a union between biochemistry and electricity and is the essential discipline among the chemical sciences needed to prepare society for near-future times. The birth of electrochemistry happened over 200 years ago (1791) in Bologna, Italy, where Luigi Galvani was dissecting a frog: "One of those who was assisting me touched lightly and by chance the point of his scalpel to the internal crural nerves of the frog (an electric machine was nearby), then suddenly all the muscles of its limbs were seen to be contracted …"

Galvani's discovery was followed nine years later by that of his compatriot, Volta, who communicated to the Royal Society in London an amazing thing: If one used a pasteboard membrane to separate silver plates from zinc plates, and wetted the ensemble with salt water, an electric current flowed. Volta called his device "the artificial electric organ."

These past events in Italy resonate in a modern decision of the California state legislature. In 2002, California will begin limiting the number of "emitting" vehicles that may be sold in the state, with sales of these being completely eliminated by 2017. Volta's discovery is the basis for the development by U.S. automakers of an emission-free vehicle—one that is electrochemically powered.

In 1923, Debye and Hückel wrote a paper describing for the first time a credible theory of the properties of ionically conducting solutions. In 1994, Mamantov and Popov edited a book in which the first chapter is called "Solution Chemistry: A Cutting Edge in Modern Technology." The book describes some frontiers of the electrochemistry of today: chloraluminate-organic systems that make room-temperature molten salts the basis of high-energy electricity storers; the use of vibrational spectroscopy to study ion-ion interactions; and the application of the molecular dynamic technique to the ionic solutions unfolded by Debye and Hückel just one lifetime before.

Take another gigantic leap along the timeline of electrochemical discovery and application. Consider Michael Faraday,[1] that London superstar who in 1834 discovered the relation between the amount of electricity consumed and the amount of metal produced in solid form from some invisible particles in solution. In 1995, more than a century later, Despic and Popov wrote an article that described electroforming of (almost) anything from its ion in solution: powders or dendrites, whiskers or pyramids, in laminar shapes of any chosen composition (including that of semiconductors) or indeed in nanometer sizes. This is what has become of Faraday's electrodeposition at the cutting edge, as well as in practical applications such as electrodissolution to shape metal parts in the making of Rolls Royce cars.

Of all these jumps in electrochemistry, each separated by around a century, there is one that best of all shows how electrochemistry is both deep-rooted and at the frontier of the twenty-first century. It was the pedant Julius Tafel who found, in 1905, that electric currents passing across metal–solution interfaces could be made to increase exponentially by changing the electric potential of the electrode across the surface of which they passed. In this way, he complemented the finding in ordinary kinetics made by Arrhenius 16 years earlier. Arrhenius's equation tells us that an increase of temperature increases the rate of chemical reaction exponentially:

$$\text{Velocity}_{\text{thermal}} \propto A e^{-E_a/RT} \tag{1.1}$$

where A and E_a are constants, with E_a representing the activation energy.

Corresponding to this, Tafel found a similar equation:

$$\text{Velocity}_{\text{echem}} = B e^{-\alpha VF/RT} \tag{1.2}$$

where B, α, and F are constants. The term αVF (a constant α times a potential V times a quantity of electricity F) represents energy; one can see that the two equations are related.

To what did Tafel's discovery lead in our lifetime? To the first moon landing in 1969! In the 64 years from Tafel's discovery of how electrochemical reaction rates vary with potential, it had become possible to take his equation and use it in the development of an electrochemical fuel cell that produced electricity from chemicals directly without moving parts. This was firstly done by Groves in 1939. Those 64 years following Tafel's discovery had been well used, particularly at Cambridge University in England, by Tom Bacon (a descendant of the seventeenth-century Bacon, Baron Verulam, whom some see as the founder of Science as we know it). Tom Bacon established in practice what theorists had for long reasoned: that the electrochemical fuel cell produced electrical energy from chemical fuels at twice the efficiency of a

[1]Despite his achievements, Faraday was subject to the whip of religious discipline. When he accepted an invitation to visit Buckingham Palace to receive an award from Queen Victoria, and missed a religious service, his church told him that he had preferred Mammon to God and ought to leave the church!

heat engine driving a generator. Thus, when the NASA pioneers turned to the design of the first space vehicles—low weight being at a premium—they chose the electrochemical fuel cell (which provides the same amount of energy as conventional cells at half the weight) as the source of auxiliary power in space. These cells are used in all U.S. space vehicles and will be likely to power the first mass produced electric cars.[2]

These few examples grew out of the chest of treasures opened up by Galvani and by Volta. Diabetics will soon be able to check their glucose levels by glancing at a wrist meter that measures sugar content electrochemically. Tritium, an essential component of nuclear weaponry, may be made electrochemically at a fraction of the cost of its production in a nuclear reactor.

Holding off dielectric breakdown in water by means of electrochemically formed coatings can allow condenser plates to store gargantuan energies for powering the lasers of the Star Wars weaponry. Electrochemistry can be used to consume domestic wastes with no noxious effluents reaching the air. The North Sea oil platforms are protected by corrosion inhibitors that slow down the electrochemical reactions that deteriorate the metal in the rigs.

In this book, an attempt will be made to present the basis of all this new technology, but in a way in which the first consideration is a lucid explanation. Before we look closely at the individual parts of the territory, it is good to have a look at the whole country from above.

1.2. TWO KINDS OF ELECTROCHEMISTRY

According to the philosophers, all science is one, but that is not how it seems in the case of electrochemistry. The two main types do not at first seem to be strongly connected (see Fig. 1.1). These are the physical chemistry of ionically conducting solutions (ionics) and the physical chemistry of electrically charged interfaces (electrodics).

This text discusses four aspects of ionic electrochemistry: ion–solvent interactions, ion–ion interactions, ion transport in solution, and ionic liquids.

The physical chemistry of ionic solutions deals with ions and solvents and how ions interact dynamically with water as they move about in solutions. The study of ion–ion interactions tells us how ions associate, sometimes even forming polymers in solution. These interactions are important for the new spectroscopic techniques, neutron diffraction and infrared spectroscopy; and for molecular dynamics (MD).

The study of transport covers diffusion and conductance of ions in solution, where much of the basis is phenomenological.

---

[2]Batteries carry the active material, the reaction of which produces electricity. Fuel cells store the fuel used to produce electricity in a fuel tank. Batteries limit the range of electric cars to ~150 miles. However, electric cars powered by fuel cells are limited only by the size of the fuel tank.

IONICS	ELECTRODICS
Concerns ions in solution and in the liquids arising from melting solids composed of ions.	Concerns the region between an electronic and an ionic conductor and the transfer of electric charges across it.

Fig. 1.1. A way to divide the two quite different aspects of the field of electrochemistry. In this book, the point of view is presented that the electrodic area should be the realm associated with electrochemistry. Ionics is a necessary adjunct field (just as is the theory of electrons in metals and semiconductors, which is adequately dealt with in books on the solid state).

The last part of ionic electrochemistry, ionics, is about "pure electrolytes." A few decades back this electrochemistry would have been all about high-temperature liquids (liquid common salt at 850 °C was the role model). However, this has changed, and the temperatures for eliminating the solvent have decreased considerably. Some molten salts are now room temperature liquids. At the other end of the temperature scale are the molten silicates, where large polyanions predominate. These are important not only in the steel industry, where molten silicate mixtures form blast furnace slags, but also in the corresponding frozen liquids, the glasses.

The other half of electrochemistry, electrodics, in vol. 2 has surpassed ionics in its rate of growth and is coming into use in enterprises such as the auto industry, to obtain electrochemical power sources for transportation. Such a change in the way we power our cars is seen by many as the only way to avoid the planetary warming caused by the CO_2 emitted by internal combustion engines.

Our discussion of electrodics starts with a description of the *interfacial region* between the metal and solution phases. This is the stage on which the play is to be performed. It involves the kinetics of electrons moving to and fro across areas with immensely strong electric field strengths (gigavolts per meter) that are unavailable in the laboratory. This is the heart of electrochemistry—the mechanism of electrically controlled surface reactions.

Electrons are quantal particles and much basic electrochemistry in the past few decades has been quantal in approach, so a simplified description of the current state of this field is given.

After this, the text moves to the main applications of electrochemistry. There is the conversion of light to electricity and the photosplitting of water to yield pure hydrogen as a storage medium for electricity produced from solar light. Some organic reactions are better carried out under electrochemical conditions, because one can vary the energy of the available electrons so easily (i.e., by changing V in Tafel's law). The stability of materials (corrosion protection) is indeed a vast area, but the basic mechanisms are all electrochemical and deserve a whole chapter. There are two other

important and growing areas of electrochemistry: bioelectrochemistry and the most active and expanding of all, the electrochemistry of cleaner environments.

What is the connection between the two main areas in electrochemistry—the science of solutions (ionics) and that of charge transfer across solid–solution interfaces (electrodics)? There is indeed a close connection. The interfacial region at electrodes (and all wet surfaces, including the surface of plants undergoing photosynthesis) is surrounded by ions in solution (or in the moisture films on surfaces). Thus it is important that we know all about them. The electrode is the stage; the solution is the theater and the audience. It is also the place that supplies the players—ions and solvent—while electrons are clearly supplied from resources in the wings.

1.3. SOME CHARACTERISTICS OF ELECTRODICS

Electron transfer between two phases is the fundamental act of electrochemistry (see Fig. 1.2) and governs much in nature. Until well past the middle of this century, there was no knowledge of the breadth of interfacial charge transfer. It used to be thought of as something to do with metals. All that is changed. Now we know it involves semiconductors and insulators, also, insofar as these bodies are in contact with ion-containing liquids. For example, proteins undergo electron charge transfer when they are in contact with glucose in solution.

The fundamental act in electrochemistry (the simple act of Fig. 1.2) is prevalent in nature, and that is why electrodics is such an important part of science. It is a vast

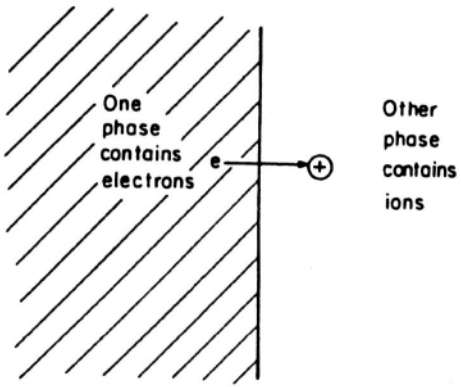

Fig. 1.2. The fundamental act in electrochemistry. Often, the electron-containing phase is a metal and the ion-containing phase is an aqueous solution. However, germanium in contact with a molten salt would also involve electron- and ion-containing systems.

field underlying all those phenomena in chemistry, biology, and engineering that involve real (and therefore moist or wet) surfaces.

1.4. PROPERTIES OF MATERIALS AND SURFACES

It is now well recognized that the properties of most materials are controlled by the properties of their surfaces. Furthermore, most surfaces are "wet." The quotation marks are used because "wet" does not here mean "placed in a solution." It can also mean "covered by a film of moisture." How pervasive are—in this sense—wet surfaces! Indeed, most outdoor and some indoor surfaces are in contact with invisible films of moisture, and the presence of these films is a required element in the corrosion and decay of metals. Thoroughly dry surfaces, removed from contact with air, do not corrode.

Wet surfaces have interfacial regions. One is in the solid, the other is in the solution. Across these regions are super-intense electric fields that accelerate or decelerate the passage of electrons from solid to solution and vice versa.

Corrosion—the gradual decay of materials—occurs in many ways, all involving electrochemical surface reactions. The essence of it is the electrochemical dissolution of atoms in the surface into the ion-containing film that is in contact with the corroding metal. However, such dissolution has to be accompanied by a counter-reaction and this is often the electrochemical decomposition of water to form hydrogen on the metal surface. If that occurs, the H in the form of minute protons, H^+, may enter the metal, diffuse about, and cause a weakening of metal–metal bonds and hence stress-corrosion cracking.

Local mechanical stress also plays an important part in determining the behavior of materials: combined with electrochemical corrosion, it may lead to bridges collapsing and ships splitting in half.[3]

Is friction electrochemical also? At least on moist surfaces, the distance between surface promontories—the protrusions of the metal–metal contacts—is controlled by the repulsion of like charges from ions adsorbed from electrolyte-containing moisture films onto surfaces. Indeed, if a pendulum swings on a fulcrum containing a metal-metal contact, its rate of decay (which is increased by the friction of the contact) maximizes when the interfacial excess electrical charge is a minimum; the friction therefore is a maximum (because the metal contacts, unrepelled by charges, are in closer contact).

1.4.1. Interfaces in Contact with Solutions Are Always Charged

Even when a solid–solution interface is at equilibrium (i.e., nothing net happening), electron transfer occurs at the same speed in each direction, for there are excess

[3]This can happen when the front and back of a ship are momentarily suspended on the peaks of waves in rough weather.

electric charges on both sides of the interface. Consider the interior of a metal. It consists of a lattice of metallic ions populated by electrons in the plasma state that are mobile and moving randomly at about 10^3 km s^{-1}.

Now, in a thought experiment, an extremely thin, sharp knife cuts the metal in half at great speed. Moreover, this imaginary act occurs under a solution of ions. Consider only one of the two surfaces formed by the knife. The electrons near the new surface are suddenly confronted with a boundary, which they overshoot or undershoot. Within 10^{-9} s, ions in the solution nearest to the metal arrange themselves to present a whole load of possible receiver or donor states for electrons. Depending on how the balance of tendencies goes, the electrons will either depart from the metal and head for the receiver states in solution leaving the surface of the metal positively charged, or take on board a load of electrons from the ions that have turned up from the solution, making the metal surface negatively charged. Whichever way it happens, the surface of the metal now has an excess positive or negative electric charge. The interior remains electroneutral (see Fig. 1.3).

Now, this argument can be generalized. It indicates that an uncharged metal or electron conductor in an ionic solution always manifests an excess surface electric charge, and the gigavolt per meter field, which results from having this sheet of excess electric charge on the metal facing a layer of opposite charge on the solution layer in contact with it, has extremely far-reaching consequences for the properties of the interface and eventually of the material beneath it.

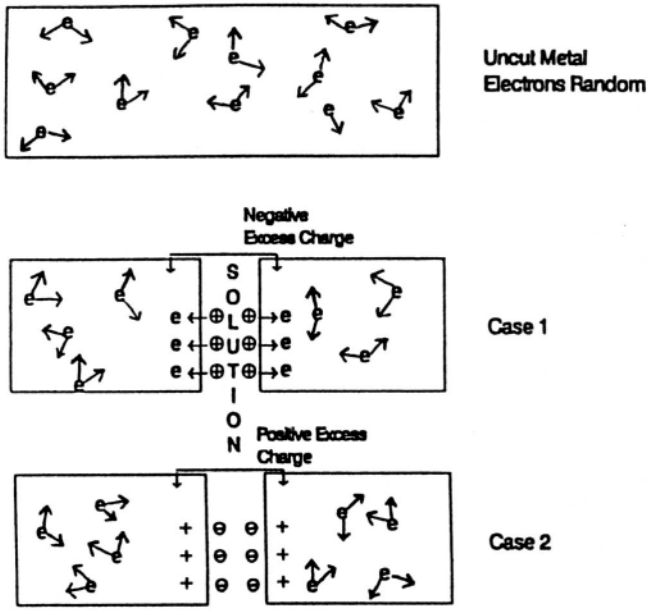

Fig. 1.3. Surfaces in solution carry a net excess charge.

1.4.2. The Continuous Flow of Electrons across an Interface: Electrochemical Reactions

It has been argued in the preceding section that all surfaces carry an excess electric charge, i.e., that surfaces in contact with ionic solutions are electrified. However, the argument was made by considering an isolated piece of material unconnected to a source or sink of electrons.

Suppose now that the metal, an electronic conductor, is connected to a power supply,[4] i.e., to a source of electrons so large in capacity that, say, 10^{19} to 10^{20} electrons[5] drawn from the source leave it unaffected in any significant way. To make the discussion specific, assume that the electronic conductor is a platinum plate and the ionically conducting phase is an aqueous solution of HI.

Then, by connecting the electrical power source to the platinum plate, it becomes possible for electrons to flow from the source to the surface of the plate. Before this was done, the electrified platinum–solution interface was in equilibrium. Under these equilibrium conditions, the platinum plate had a net surface electric charge, and the ionically conducting solution had an equal excess electric charge, though opposite in sign. Furthermore, the passage of electrons across the interface, which is associated with electron-transfer reactions, is occurring at an equal rate in the two directions. What happens when a disequilibrating shower of extra charges from the power source arrives at the surface of the platinum? The *details* of what happens, the mechanism, is a long story, told partly in the following chapters. However, the essence of it is that the new electrons overflow, as it were, the metal plate and *cross the metal–solution interface* to strike and neutralize ions in the layer of solution in contact with the metal, e.g., hydrogen ions produced in solution from the ionization of HI in the solution phase. This process can proceed continuously because the power source supplying the electrons can be thought of as infinite in capacity and the ionic conductor also has an abundance of ions in it; these tend to migrate up to the metal surface to capture there some of the overflowing electrons.

What is being described here is an *electrochemical reaction;* i.e., it is a *chemical transformation involving the transfer of electrons across an interface,* and it can be written in familiar style as

$$2\,H^+ + 2\,e \rightarrow H_2$$

The hydrogen ions are "discharged" (neutralized) on the electrode and there is an evolution of hydrogen outside the solution, as a gas.

---

[4]Actually, a power supply has two terminals and one must also consider how the metal–electrolyte interface is connected to the other terminal; however, this consideration is postponed until the next section.

[5]An Avogadro number ($\sim 10^{24}$) of electrons deposited from ions in solution produces 1 gram-equivalent (g-eq) of metal passed across an interface between metal and solution; hence 10^{19} to 10^{20} electrons produce 10^{-5} to 10^{-4} g-eq of material.

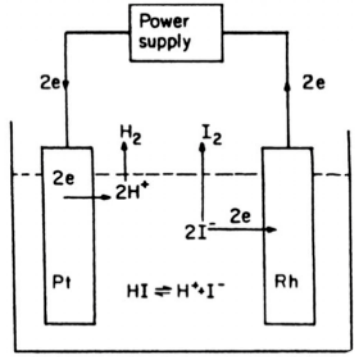

Fig. 1.4. The electrochemical reactor.

The simplicity of such a formulation should not obscure the fact that what has been described is a remarkable and distinctive part of chemistry. An electric current, a controllable electron stream, has been made to react in a controlled way with a chemical substance and produce another *new chemical substance.* That is what a good deal of electrochemistry is about—*it is about the electrical path for producing chemical transformations*. Much of electrochemistry is also connected with the other side of this coin, namely, the production of electric currents *and therefore electric power* directly from changes in chemical substances. This is the method of producing electrical energy without moving parts (see fuel cells, Chapter 13 in vol II).

1.4.3. Electrochemical and Chemical Reactions

There is another aspect of the electrochemical reaction that has just been described. It concerns the effect on the iodide ions of hydrogen iodide, which must also have been present in the HI solution in water. Where do they go while the hydrogen ions are being turned into hydrogen molecules?

The I^- ions have not yet appeared because only half of the picture has been shown. In a real situation, one immerses another electronic conductor in the same solution (Fig. 1.4). Electrical sources have two terminals. The assumption of a power source pumping electrons into a platinum plate in contact with an ionic solution is essentially a thought experiment. In the real situation, one immerses another electronic conductor in the same solution and connects this second electronic conductor to the other terminal of the power source. Then, whereas electrons from the power source pour into the platinum plate, they would flow *away from* the second electronic conductor (made, e.g., of rhodium) and back to the power source. It is clear that, if we want a system that can operate for some time with hydrogen ions receiving electrons from the

[6]There is not much limit on the kind of chemical substance; for example, it does not have to be an ion. $C_2H_4 + 4\,H_2O \rightarrow 2\,CO_2 + 12\,H^+ + 12\,e$ is as much an electrochemical reaction as is $2\,H^+ + 2\,e \rightarrow H_2$.

platinum plate, then iodide ions have to give up electrons to the rhodium plate at the same rate as the platinum gives up electrons. Thus, the whole system can function smoothly without the loss of electroneutrality that would occur were the hydrogen ions to receive electrons from the platinum without a balancing event at the other plate. Such a process would be required to remove the negatively charged ions, which would become excess ones once the positively charged hydrogen ions had been removed from the solution.

An assembly, or system, consisting of one electronic conductor (usually a metal) that acts as an electron source for particles in an ionic conductor (the solution) and another electronic conductor acting as an electron sink receiving electrons from the ionic conductor is known as an *electrochemical cell*, or *electrochemical system*, or sometimes an *electrochemical reactor*.

We have seen that electron-transfer reactions can occur at one charged plate. What happens if one takes into account the second plate? There, the electron transfer is from the solution to the plate or electronic conductor. Thus, if we consider the two electronic conductor–ionic conductor interfaces (namely, the whole cell), there is no *net* electron transfer. The electron outflow from one electronic conductor equals the inflow to the other; that is, *a purely chemical reaction* (one not involving net electron transfer) *can be carried out in an electrochemical cell*. Such net reactions in an electrochemical cell turn out to be formally identical to the familiar thermally induced reactions of ordinary chemistry in which molecules collide with each other and form new species with new bonds. There are, however, fundamental differences between the ordinary chemical way of effecting a reaction and the less familiar electrical or electrochemical way, in which the reactants collide not with each other but with separated "charge-transfer catalysts," as the two plates which serve as electron-exchange areas might well be called. One of the differences, of course, pertains to the facility with which the rate of a reaction in an electrochemical cell can be controlled; all one has to do is electronically to control the power source. This ease of control arises because the electrochemical reaction rate is the rate at which the power source pushes out and receives back electrons after their journey around the circuit that includes (Figs. 1.4 and 1.5) the electrochemical cell.

Thus, one could write the electrochemical events as

$$2\,HI \xrightarrow[\text{solution}]{\text{in}} 2\,H^+ + 2\,I^-$$

$$2\,H^+ + 2\,e \xrightarrow[\text{plate}]{\text{at the Pt}} H_2\uparrow \qquad (1.3)$$

$$2\,I^- \xrightarrow[\text{plate}]{\text{at the Rh}} I_2 + 2\,e$$

$$\text{net reaction: } 2\,HI \rightarrow H_2 + I_2$$

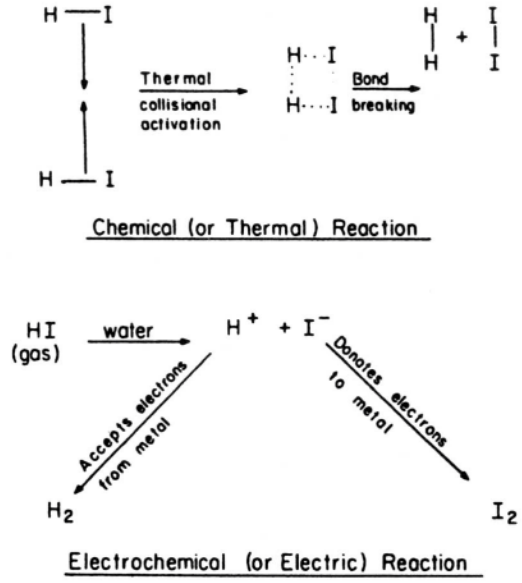

Fig. 1.5. The chemical and electrochemical methods of carrying out reactions. In the electrochemical method, the particles do not collide with each other but with separated sources and sinks of electrons.

Thus, from an overall point of view (not thinking of the molecular-level mechanism), this net cell reaction is identical to that which would occur if one heated hydrogen iodide and produced hydrogen and iodine by a purely chemical, or thermal, reaction.

There is another way in which the electrical method of carrying out chemical reactions is distinct from the other methods for achieving chemical changes (Fig. 1.5). The ordinary reactions of chemistry, such as the homogeneous combination of H_2 and I_2 or the heterogeneous combinations of H_2 and O_2, occur because thermally energized molecules occasionally collide and, during the small time they stay together, change some bonds to form a new arrangement. Correspondingly, photochemical reactions occur when photons strike molecules and give them extra energy so that they break up and form new compounds. In a similar way, the high-energy particles emanating from radioactive substances can energize molecules, which then react. The electrical method of causing chemical transformations is different from the other three methods of provoking chemical reactivity in that the overall electrochemical cell reaction is composed of two separate electron-transfer reactions that occur at *spatially separated*

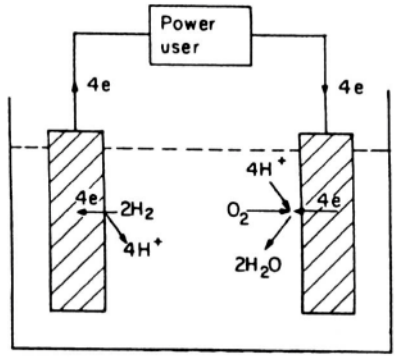

Fig. 1.6. Grove was the first to obtain electric power directly from a chemical reaction.

electrode–electrolyte interfaces and are each susceptible to electrical control as far as rate (electron flow) is possible.

If electrical energy provokes and controls chemical reactions, chemical reactions working in the other direction can presumably give rise to a flow of electricity. Thus, two reactant substances may be allowed to undergo spontaneous electron transfer at the separated (electrode) sites, which is characteristic of the electrochemical way of bringing about chemical reactions, and then the electrons transferred in the two reactions at the two interfaces will surge spontaneously through an electrical load, for example, the circuit of an electric motor (Fig. 1.6). In this reverse process, also, there is a unique aspect when one compares it with the production of available energy from thermally induced chemical reactions. It can be shown (see Chapter 13 in vol 2) that the fraction of the total energy of the chemical reaction that can be converted to mechanical energy is intrinsically much greater in the electrical than in the chemical way of producing energy. This is a useful property when one considers the economics of running a transportation system by means of a fuel cell–electric motor combination rather than by means of the energy produced in the combustion of gasoline.

1.5. THE RELATION OF ELECTROCHEMISTRY TO OTHER SCIENCES

1.5.1. Some Diagrammatic Presentations

Let us look at Fig. 1.7 to see something of the parentage of conventional electrochemistry, in both the ionic and electrodic aspects. We could also look at these relations in a different way and make the central thought a charge transfer at interfaces, while stressing the interdisciplinary character of the fields involved in studying it. Such

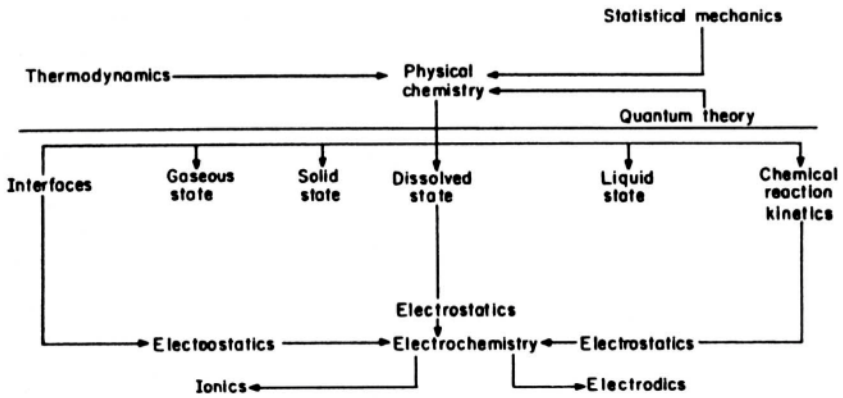

Fig. 1.7. Physical chemistry and electrochemistry.

a view is implied in Fig. 1.8, where space limits the number of disciplines mentioned that are associated with the study of electrified interfaces.

Apart from the large number of areas of knowledge associated with modern electrochemistry, there are many areas to which it contributes or in which it plays an essential role. Thus, much surface chemistry under real conditions involves moisture; hence the electrified interfaces for which electrochemical concepts are relevant are as wide in application as practical surface chemistry itself. This, together with the fact that the subject embraces interactions between electric currents and materials (i.e., between two large areas of physics and chemistry), implies a widespread character for the phenomena subject to electrochemical considerations (Fig. 1.8).

1.5.2. Some Examples of the Involvement of Electrochemistry in Other Sciences

1.5.2.1. *Chemistry.* There are many parts of mainline chemistry that originated in electrochemistry. The third law of thermodynamics grew out of observations on the temperature variations of the potential of electrochemical reactions occurring in cells. The concepts of pH and dissociation constant were formerly studied as part of the electrochemistry of solutions. Ionic reaction kinetics in solution is expressed in terms of the electrochemical theory developed to explain the "activity" of ions in solution. Electrolysis, metal deposition, syntheses at electrodes, plus half of the modern methods of analysis in solution depend on electrochemical phenomena. Many biomolecules in living systems exist in the colloidal state, and the stability of colloids is dependent on the electrochemistry at their contact with the surrounding solution.

1.5.2.2. *Metallurgy.* The extraction of metals from their compounds dissolved in molten salts, the separation of metals from mixtures in solution, and the

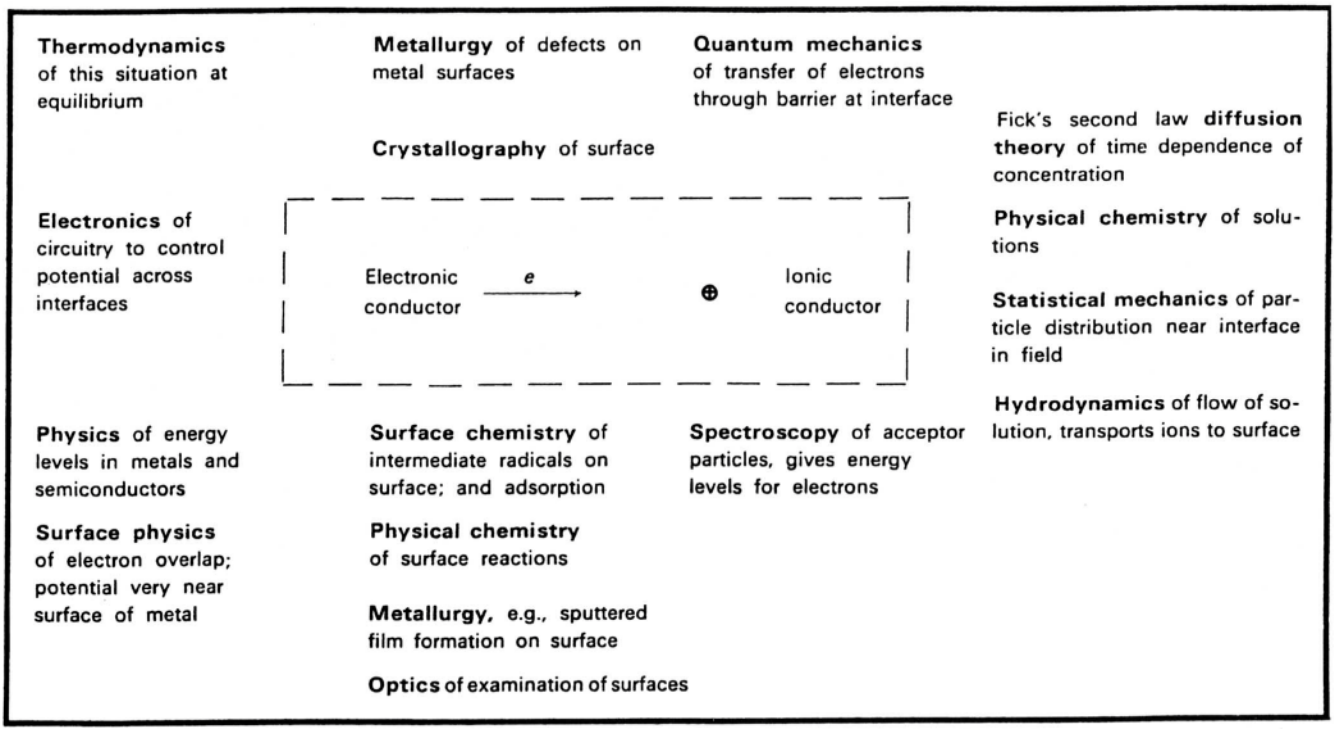

Fig. 1.8. Some disciplines involved in the study of charge transfer at interfaces.

protection of metals from corrosive decay are among the many applications of electrochemistry in metallurgy.

1.5.2.3. *Engineering.* Electrochemical engineering is the basis of a large portion of the nonferrous metals industries, in particular, the production of aluminum by deposition from a molten salt containing aluminum oxide. As noted earlier, electrochemical energy converters, fuel cells, provide the on-board power for space vehicles, and there are prospects of evolving from the thermal to the electrochemical method of utilizing the energy of chemical reactions. One of the most important applications is the prospect of clean, pollution-free electrical on-board power for automobiles. Environmental issues, in general, as well as the real threat of global warming from CO_2 buildup, favor clean electrochemical processes.

1.5.2.4. *Biology.* Food is converted to energy by biochemical mechanisms that have an efficiency much greater than that of some corresponding forms of energy conversion involving the heat-engine principle. Such high efficiency in energy conversion involves electrochemical reactions in the mitochondrion, a part of the biological cell. Correspondingly, the transmission of impulses through nerves, as well as the stability of blood and the functioning of many of the macromolecules involved in biological processes, depends on aspects of electrochemistry that concern electrochemical charge transport and the repulsion between bodies bearing the same electrical charge. The formation of blood clots and the resulting heart attack are influenced by the electrical charge on the arterial wall and that on the colloidal particles in blood.

1.5.2.5. *Geology.* An example of electrochemistry in geology concerns certain types of soil movements. The movement of earth under stress depends on its viscosity as a slurry; that is, a viscous mixture of suspended solids in water with a consistency of very thick cream. Such mixtures of material exhibit thixotropy,[7] which depends on the interactions of the double layers between colloidal particles. These in turn depend on the concentration of ions, which affects the field across the double layer and causes the colloidal structures upon which the soil's consistency depends to repel each other and remain stable. Thus, in certain conditions the addition of ionic solutions to soils may cause a radical increase in their tendency to flow.

1.5.3. Electrochemistry as an Interdisciplinary Field, Distinct from Chemistry

All fields in chemistry (e.g., that of the liquid state or of reaction kinetics) are connected to each other and, indeed, fields treated under chemistry tend, as time goes on, to move toward the more sophisticated level attained in physics. Chemists undertake approximate treatments of relatively complicated problems that are not yet

[7]Thus, certain soils, when appropriately agitated, suddenly become much less viscous and start to flow easily, a dangerous thing if there is a house on top.

simplified enough for physicists to approach them in a more exact way. However, the connections between chemistry and physics (e.g., the study of liquids and gaseous reaction kinetics) largely occur through the parent areas of chemistry (see Fig. 1.7), for example, statistical and quantum mechanics. A direct connection to areas just outside chemistry does not immediately follow, e.g., liquids and reaction kinetics.

In *electro*chemistry, however, there is an immediate connection to the physics of current flow and electric fields. Furthermore, it is difficult to pursue interfacial electrochemistry without knowing some principles of theoretical structural metallurgy and electronics, as well as hydrodynamic theory. Conversely (see Section 1.5.2), the range of fields in which the important steps are controlled by the electrical properties of interfaces and the flow of charge across them is great and exceeds that of other areas in which physical chemistry is relevant.[8] In fact, so great is the range of topics in which electrochemical considerations are relevant that a worker who is concerned with the creation of passive films on metals and their resistance to environmental attack is scarcely in intellectual contact with a person who is interested in finding a model for why blood clots or someone seeking to solve the quantum mechanical equations for the transfer of electrons across interfaces.

This widespread involvement with other areas of science suggests that in the future electrochemistry will be treated increasingly as an interdisciplinary area as, for example, materials science is, rather than as a branch of physical chemistry.

At the same time, there is a general tendency at present to break down the older formal disciplines of physical, inorganic, and organic chemistry and to make new groupings. That of materials science—the solid-state aspects of metallurgy, physics, and chemistry—is one. Energy conversion—the energy-producing aspects of nuclear fission, electrochemical fuel cells, photovoltaics, thermionic emission, magnetohydrodynamics, and so on—is another. Electrochemistry would be concerned with the part played by electrically charged interfaces and interfacial charge transfers in chemistry, metallurgy, biology, engineering, etc.

1.6. THE FRONTIER IN IONICS: NONAQUEOUS SOLUTIONS

Studies of ionic solutions have been overwhelmingly aqueous in the hundred years or so in which they have been pursued. This has been a blessing, for water has a dielectric constant, ε, of ~80, about ten times larger than the range for most nonaqueous solvents. Hence, because the force between ions is proportional to $1/\varepsilon$, the tendency of ions in aqueous solutions to attract each other and form groups is relatively small, and structure in aqueous solutions is therefore on the *simple* side. This enabled a start to be made on the theory of ion–ion attraction in solutions.

[8] As apart from areas of basic science (e.g., quantum mechanics) that primarily originate in physics and underlie all chemistry, including, of course, electrochemistry.

If one goes to a nonaqueous solvent system (an organic one such as acetonitrile, CH_3CN; or a pure electrolyte such as the KNO_3-$NaNO_3$ eutectic), the dielectric constant is more in the range of 2–20, and there is a greater tendency than that in aqueous solutions for ions of opposite sign to get together and stay together. Further, the bonding that develops is not purely Coulombic but may involve solvent and H-bond links, some of them unexpected. Figure 1.9 shows dimethyl sulfoxide (DMSO) with the molecular distances in picometers.

Electrochemical measurements (mainly conductances) have been made in both the organic and the pure electrolyte kind of nonaqueous solution for at least two generations. Why, then, is there talk of nonaqueous electrochemistry as one of the *frontiers* of the field?

One reason is that much better methods of detecting impurities (parts per billion) now exist and hence of purifying solvents (and keeping them pure—they all tend to pick up water). However, there is a greater reason and that is the emergence of several new methods for determining structure. These are

1. X-ray diffraction measurements *in solution* (a development of the earliest method of structural determination)
2. X-ray absorption measurements of fine structure in solution (EXAFS)
3. Neutron diffraction
4. Infrared (IR) and Raman spectroscopy

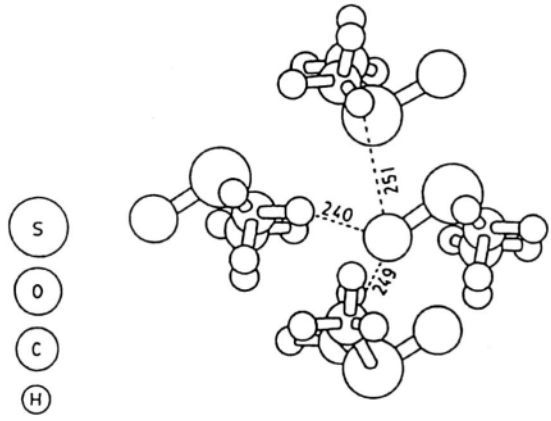

Fig. 1.9. Molecular arrangement in DMSO. Numbers indicate intermolecular distances in picometers. (Reprinted from G. Mamantov and A. I. Popov, *Chemistry of Nonaqueous Solutions: Current Progress,* p. 188. VCH Publishers, New York, 1992.)

Later in this book we will discuss these new tools, how they work, and what they bring to electrochemistry. They have provided the ionics electrochemist with a new kind of microscope.

Although this is still introductory material, three rather general points may be made.

1. Until the 1980s, the major methods of investigation in ionics were nonspectroscopic. For example, conductance results were used to infer the existence of complex ions. Alternatively and typically, the change of the dielectric constant of a solution as a function of the concentration of ions (measurements at various frequencies) was interpreted in terms of structural hypotheses about ion–solvent interactions.

The new optical and spectroscopic methods are more discerning, more definite in what they reveal. For example, in solutions of $AgNO_3$ in water and in dimethylformamide, one used to speak of ion-pair formation, $Ag^+NO_3^-$. By now it is known that there are several kinds of ion pairs. For example, the ions may be in direct contact or they may be separated by a solvent molecule. The concentration of the free ions (if they give vibration spectra) can be followed. In general, an enormous increase in detail (corresponding to an increase in knowledge of the variety of particles present in the nonaqueous systems) has become available.

2. Amazing bonds have been revealed by the new methods. For example, Perelygin found that thiocyanates of the alkali metals form groups in acetonitrile. Valence theory is sometimes hard put to interpret the unusual forms found:

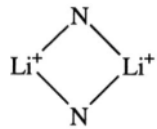

3. Few measurements of the so-called "driving force,"[9] the Gibbs free energy, ΔG°, have become available as yet; however, for a number of reactions in organic nonaqueous solutions it is *entropy* driven, that is, ΔG° is driven to a negative value over the positive (endothermic) ΔH° by a positive ΔS° and its influence as $T\Delta S^\circ$ in the basic thermodynamic equation: $\Delta G^\circ = \Delta H^\circ - T\Delta S^\circ$.

Necessity does seem to be the mother of invention. This nonaqueous electrochemistry has great practical value, for example, in new high-energy-density batteries and fuel cells—just the things needed for electricity storage and production (respectively) on board nonpolluting electric cars.

---

[9]Clearly, a standard free *energy* difference cannot be a driving*force*. However, the larger the negative value of ΔG°, the more will be the tendency of a reaction, with reactants and products in their standard states, to proceed.

1.7. A NEW WORLD OF RICH VARIETY: ROOM-TEMPERATURE MOLTEN SALTS

The image in most chemists' minds of a "molten salt" is probably liquid NaCl at 900 °C. There are many such "pure electrolytes" that have the great advantage of a large electrochemical "window"; that is, one can carry out electrode processes in them over a much greater range of cell potentials than is possible in aqueous solutions, where the range is limited by the evolution of H_2 if the potential becomes too negative and of O_2 if it becomes too positive.

This situation has been radically altered during the past 20 years or so by work that has been led (in separate and individual ways) by three U.S. electrochemists, namely, Osteryoung, Hussey, and Wilkes, respectively. Thus, the first truly room-temperature pure electrolyte (i.e., a system consisting of ions without a solvent) was due to Osteryoung et al. in 1975. This is 1-(1-butylpyridinium chloride) (BupyCl):

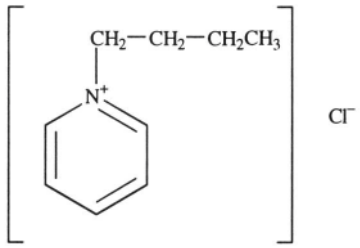

Wilkes, in particular, has developed the use of l-methyl-3-ethylimidazolonium chloride (MeEtInCl):

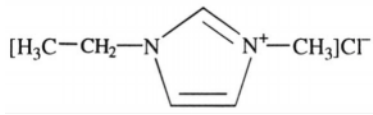

Compounds of these two electrolytes are leading members in the extensive development of this new chemistry. For example, it has been possible to investigate tetrachlorobenzoquinone in $AlCl_3$-BupyCl at an electrode consisting of glassy carbon; changing the potential of this electrode changes the oxidation state of the quinone. The resulting absorption spectrum is shown in Fig. 1.10. Reactions involving Cu, Ag, Au, Co, Rh, Ir, Mo, W, etc. have all been investigated in room-temperature molten salts.

A fertile field exists here for batteries and fuel cells: a rechargeable couple involving the considerable electrical energy that can be stored in Al and O_2 can be developed. In the first aqueous Al cell, developed by Solomon Zaromb in 1960, the product of the anodic dissolution of Al was the insoluble $Al(OH)_3$, and no electrical recharge was possible.

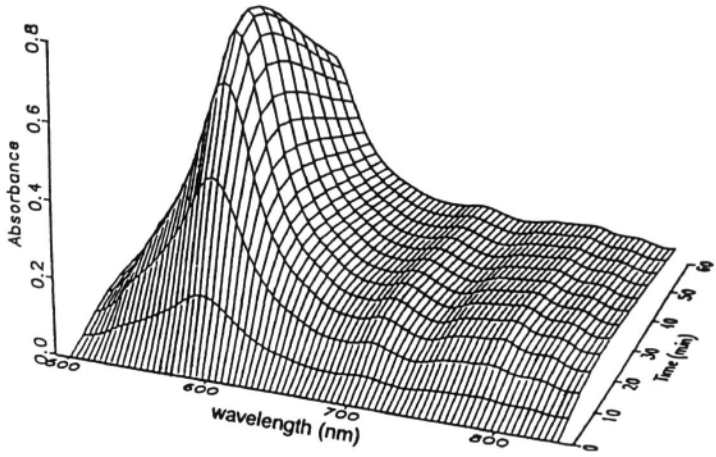

Fig. 1.10. Absorption spectra of a 4.59-m*M* solution of perylene in 44.4–55.6 mol% $AlCl_3$-MeEtimCl melt taken at 5-minute intervals during 60-min electrolysis at a platinum screen optically transparent electrode (OTE). The applied potential was –1.85 V, and the OTE path length was 0.10 cm. (Reprinted from J. E. Coffield, G. Mamantov, S. P. Zingg, G. P. Smith, and A. C. Buchanan, *J. Electrochem. Soc.* **139:** 355, 1992.)

1.8. ELECTROCHEMICAL DETERMINATION OF RADICAL INTERMEDIATES BY MEANS OF INFRARED SPECTROSCOPY

Electrochemical reactions on electrodes involve consecutive reactions with several steps. Knowledge of the reactants and products in each step may provide a valuable piece of evidence by means of which the pathway—and sometimes even the rate-determining step—can be identified.

Two difficulties exist before this can be done. First, the concentrations of surface species are, at most, 10^{-9} mol cm^{-2}, about 10^{15} atoms cm^{-2}, depending on the size of the radical or intermediate molecule to be observed. However, light for any spectroscopic method has to go through a layer of solution before it strikes the electrode. Now a square centimeter of a 0.1 *M* solution 1 mm thick contains about 10^{19} ions. The signal from the radicals on the electrode has to compete with much stronger signals from this layer.

To overcome these hurdles, one has to have a supersensitive measurement and then some way of separating the *surface* signal from competing signals of the same frequency produced by molecules or ions in the adhering solution.

How this could be done was first shown by Neugebauer and co-workers in 1981 (but it was developed particularly by Alan Bewick and Stan Pons in the 1980s). In spectroscopy, in general, it is possible to enhance and elicit a given line by repeating

its spectra many hundreds of times. The signal is enhanced when the spectrum is repeated if it always occurs at the same frequency. Any false blips in the intensity–wavelength relation are determined by random fluctuations—they won't be enhanced by repetition because they don't always occur at the same wavelength. To separate the surface signal from the solution spectrum Greenler's theorem was used. According to this theorem, if the incident angle of the beam from the vertical is very high (e.g., 88–89°), there is a radical difference between the information carried by the parallel and vertical components of the polarized light beam reflected through the solution from the electrode. The parallel component carries both the surface and the solution information; the vertical carries only the solution information. Hence, if the polarities of beams reflected from the surface of an electrode in solution are alternated from parallel to vertical and then vertical to parallel several hundred thousand times per second, and the strength of the signals of the vertical components is subtracted from that of the parallel ones at various wavelengths in the IR region, there should remain (according to Greenler's theorem) the lines characteristic of the surface species only.

Of course, this is a rough outline of a sophisticated and complex technique. The solution layer in contact with the electrode should be very thin to reduce competition

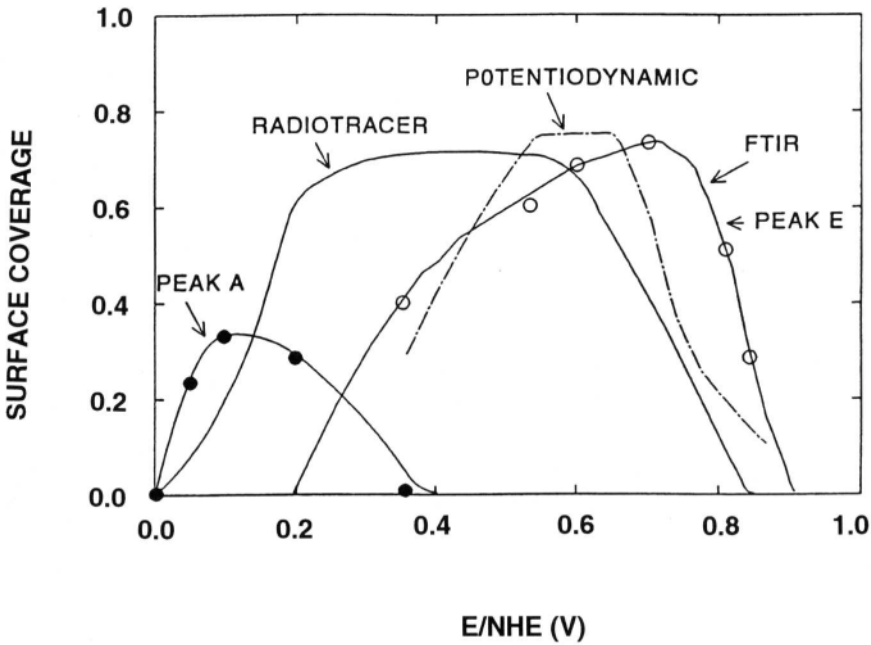

Fig. 1.11. Relative areas of two peaks (A and E) as a function of electrode potential. (Reprinted from K. Chandrasekaran, J. C. Wass, and J. O'M. Bockris, *J. Electrochem. Soc.* **137**: 519, 1990.)

from the ions and molecules in solution (separating parallel and vertical beam information by subtracting the vertical from that of the parallel signal is only an approximation for metal–solution systems). This technique is called Fourier transform IR absorption spectroscopy (FTIRAS). The Fourier transform is used in the mathematics of calculating the results. While the process is complex, the results are relatively simple and helpful. One of these is shown in Fig. 1.11.

This methodology reveals the tell-tale signal of bonds present in intermediate radicals on the electrode surface if the electrochemical reaction is operating in a steady state, i.e., the reaction is in its final pathway with the final rate-determining step. The exciting possibility of advanced versions of the FTTRAS technique is that really rapid (millisecond) changes in the spectra of the surface radicals can be recorded. Then, changes in the nature and concentration of radicals that may occur during the switching-on phase of the electrical current could be measured. This can provide much information on the buildup and structure of the pathway of the reaction occurring on the surface. When this happens, fast-reacting surface spectroscopic measurements will become a principal aid to studies of mechanisms in electrochemistry.

1.9. RELAY STATIONS PLACED INSIDE PROTEINS CAN CARRY AN ELECTRIC CURRENT

The body contains several thousand different enzymes that are catalysts for specific bioreactions. Without them, biochemical pathways in the body would not function.

Diabetics have a need for a glucose meter that would show the glucose concentration in the blood at any moment without having to take a sample. If the glucose builds up too much, the meter would send out a signal telling the wearer of the need for insulin.

Glucose gets oxidized with the cooperation of an enzyme called glucose oxidase, which has a molecular diameter of 86 Å. Suppose we could immobilize glucose oxidase on an organic semiconductor such as polypyrrole, and the electrons produced when glucose in the blood is oxidized could be brought out through the glucose oxidase to work a meter on the wrist: our aim would be achieved, and diabetics could monitor their condition at any time by a glance at the wrist.[10]

One could carry this idea further. Since enzymes are so specific in reacting to only certain molecules, one could imagine a future "general diagnoser," a plaque with a series of enzymes adsorbed on microelectrodes that are exposed to the blood, with each able to pick out the molecules that indicate the presence of specific diseases. Oxidation reactions would provide electrons and an electrical signal would indicate the disease through the circuitry, which would identify the enzyme from which the current originated. For such an idea to work, one must have electronic conductivity of

[10]A wrist glucose meter? Not yet, but several are in development.

the enzyme because eventually the electrons from the reaction on its surface (in contact with the blood) must get through the 10 nm of enzyme to the metallic circuitry of the wrist meter.

Now, most enzymes are centered on a specific redox atom (e.g., Fe) and in order to be oxidized or reduced, the electron, the effector of the act, must travel through the enzyme to the so-called heme group, the vital Fe-containing group, as in hemoglobin, for example.

Enzymes are complex organic substances and are not expected to be good electron conductors at all. If an electron is going to get to and from the heme group to an outside contact, the best hope is quantum mechanical tunneling. However, there is a limit to the jump length in tunneling; it is about 2 nm. Supposing the heme group is in the middle of the enzyme glucose oxidase; then, as it is ~9 nm across, the electron would have to jump ~4 nm, which is not possible.

Adam Heller in 1986 devised and achieved the solution to this, which is illustrated in Fig. 1.12. With his associate, Y. Degani, Heller introduced extra redox centers into

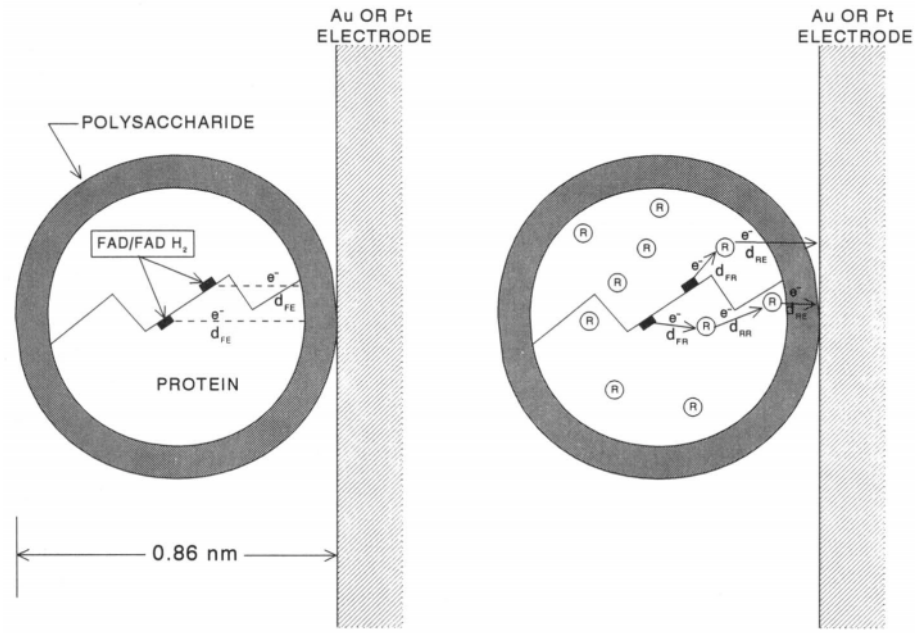

Fig. 1.12. Schematic drawing of the glucose oxidase molecule, showing the electron-transfer distances involved in the various steps of moving an electron from its two flavin adenine dinucleotide/reduced flavin adenine dinucleotide **(FAD/FADH$_2$)** centers to a metal electrode. Left: The enzyme before modification. Right: The modified enzyme, after chemical attachment of an array of electron transfer relays ("R"). (Reprinted from Y. Degani and A. Heller, *J. Phys. Chem.* **91**: 1286, 1987.)

glucose oxidase. The result was duly electrifying—the enzyme became radically more conducting than before.

1.10. SPECULATIVE ELECTROCHEMICAL APPROACH TO UNDERSTANDING METABOLISM

We eat and various biochemical processes produce glucose from some of the food molecules. We breathe and the oxygen changes the glucose to gluconic acid, and finally by way of the ubiquitous enzymes, to CO_2. On the way, we get mechanical energy to operate our muscles, including the heart pump, which drives the fuel-carrying blood around the body circuit. This is metabolism, and one thing about it that is not well understood is why the energy conversion (chemical energy of the oxidation of food to mechanical energy of the body) is so efficient (50%), compared with the efficiency of a normal heat engine (~25%).

The reaction that gives chemical energy to heat engines in cars (hydrocarbon oxidation) has to obey the Carnot cycle efficiency limitation $(1 - T_{low}/T_{high})$. With T_{low} around body temperature (37 °C), the metabolic T_{high} would have to be 337 °C to explain this metabolic efficiency in terms of a heat engine. Thus, the body energy conversion mechanism cannot use this means to get the energy by which it works.

However, there are electrochemical energy converters (fuel cells), such as the one shown in Fig. 1.6. An electrochemical energy converter is not restrained by the Carnot efficiency of 25% and can have efficiencies up to $\Delta H/\Delta G$ for the heat content and free energy changes in the oxidation reactions involved in digesting food. This ratio is often as much as 90% (cf. Chapter 13).

Hence, to explain the high metabolism of > 50%, we are forced into proposing an electrochemical path for metabolism. How might it work? Such a path was proposed by Felix Gutmann in 1985 and the idea is shown in a crude way in Fig. 1.13.

Mitochondria are tiny systems found in every biological cell, and they are known to be the seat of the body's energy conversion. Suppose one could identify certain organic groups on the mitochondria as electron acceptors and other groups as electron donors—microelectrodes, in fact. Glucose diffuses into the cell and becomes oxidized at the electron acceptors. At the electron donor groups, O_2 is reduced using the electrons provided by the glucose. The mitochondrion has made millions of micro fuel cells out of its two kinds of electrodic groups and now has electrical energy from these cells to give—and at an efficiency typical of fuel cells of ~50%.

There is much more to the story—how energy in living systems is stored, for example, and finally how it is transported to all the body parts which use it—this is discussed in Chapter 14. This electrochemical (and vectorial) approach to metabolism, which was proposed in 1986, is not yet widely accepted by tradition-bound biologists, but it has one tremendous thing going for it—it solves the problem of why the efficiency of the conversion of the chemicals in food to mechanical energy is so much higher than it can be in alternative energy conversion pathways.

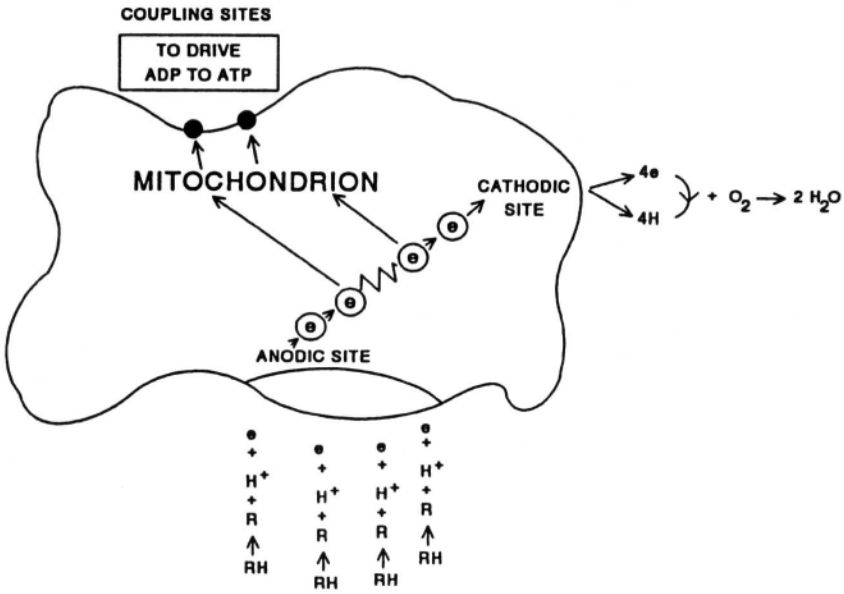

Fig. 1.13. Schematic representation of the principle of the biological fuel cell concept. R and RH represent the oxidized and reduced form of a bio-molecule. ADP is adenosine diphosphate; ATP is adenosine triphospate. (Reprinted from J. O'M. Bockris and S. U. M. Khan, *Surface Electrochemistry,* p. 699. Plenum Press, New York, 1993.)

1.11. THE ELECTROCHEMISTRY OF CLEANER ENVIRONMENTS

Many of the problems of the environment are caused by the fact that the main method by which we obtain the energy to run our civilization is still by means of the combustion of fossil fuels. This has two unacceptable effects. The first—and little realized—is that inhaling gasoline vapors has proved to be carcinogenic to laboratory animals, and there is an indication that it is one of the causes of the increased spread of cancer among humans. The second is that the CO_2 injected into the atmosphere by combustion is causing global warming.

Electrochemical Technology is involved in a major way in the only alternative to oil and gasoline as an energy source which also avoids the hazards of nuclear power. Thus, the collection of solar light and its conversion by means of photovoltaics to electricity and then the electrochemical splitting of water to yield clean hydrogen, would provide an inexhaustible replacement for fossil fuels (see Chapter 15). A pilot plant to do this now exists at Neunburg vorm Wald, in southern Germany.

However, electrochemistry will have to play a broader role than this if sustainable and clean energy is to become a reality. It provides a general approach that is superior to conventional chemical approaches for two reasons.

1. Concentration and temperature determine the rate at which chemical processes take place. Electrochemical processes are equally affected by these variables, but also are controlled in selectivity of reaction by the electrical potential of the electrode (see Section XXX). Hence, there is an extra variable that controls chemical processes that occur electrochemically rather than chemically. Moreover, this variable is applied easily by turning the knob on an electrical power source.

2. When electrochemical processes are used to clean up carbonaceous material, the only gas produced is CO_2—there are no noxious products of partial combustion, such as NO and CO, to be injected into the atmosphere. When hydrogen is used in a fuel cell to produce electric power, it is made by splitting water and it produces water right back again as a by-product of the power generation.

This book contains several examples of electrochemical clean-up processes (see Chapter 15), but one is briefly described here. It is in the cleanup of wastewater, defined as water having impurities in the range of 5–500 ppm. There is a problem in using an electrochemical approach because of the low electrical conductance of the water. However, in one of the several electrochemical companies developed around Texas A&M University, Duncan Hitchens has solved the problem as shown in Fig. 1.14.

A proton exchange membrane on the right draws off protons cathodically; the platinized iridium in the middle presents a large area for anodic oxidation. The arrangement makes the current pathway so small that the low conductivity of the

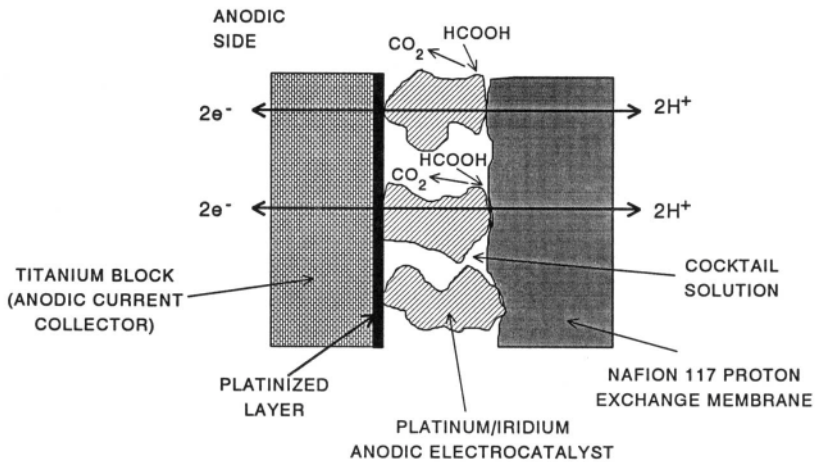

Fig. 1.14. Schematic representation of wastewater treatment process. (Reprinted from O. J. Murphy, G. D. Hitchens, L. Kaba, and C. E. Verostko, *Water Res.* **26:** 443, 1992.)

polluted water does not matter. By flowing wastewater through an electrochemical reactor of this type, impurities are reduced about a thousand times.

1.12. SCIENCE, TECHNOLOGY, ELECTROCHEMISTRY, AND TIME

1.12.1. Significance of Interfacial Charge-Transfer Reactions

It is informative in this chapter to make some attempt to place electrochemistry among the sciences and obtain the relative measure of its significance. It is difficult to do this for a field, the modern phase of which dates back only 50 years. Let us try, but let us realize that what we are doing here is speculating, although we will give some of the reasoning that supports our conclusions.

First, we can ask a relative question: Is interfacial electrochemistry simply a special aspect of reaction kinetics, somewhat analogous to photochemistry? In photochemistry, one might say, one studies the effect of energy packets (photons) striking molecules; in electrochemistry, one studies the effect of striking molecules dissolved in solution with electrons emitted from electrically charged conductors.

Or does interfacial electrochemistry have a greater significance? The evidence for tending to this latter view is as follows:

1. Interfacial electrochemistry has a high degree of prevalence in the practical world compared with other branches of knowledge outside physics. A way to appreciate this is to realize how often one is concerned with electrochemical phenomena outside the laboratory. For example, one starts a car and listens to its radio on battery power; television pictures are transmitted from space vehicles to the earth by fuel-cell power; a sports car may be made of electrochemically extracted aluminum; the water that is in one's coffee may be obtained by electrochemical deionization from impure or brackish water; some persons ride in electrically powered cars; one wears clothes of nylon produced from adiponitrile, which is electrochemically synthesized; one adds an inhibitor to the radiator fluid of a car to reduce electrochemical corrosion. Finally, one thinks by using electrochemical mechanisms in the brain, and one's blood remains liquid as long as the electrochemical potential at the interface between the corpuscles and their solution remains sufficiently high and of the same sign.

2. This ubiquitous role for electrified interfaces throughout many aspects of science suggests that electrochemistry should not be regarded as only a *branch* of chemistry. Rather, while most chemists have concentrated upon *thermally activated* reactions and their mechanisms, with electrochemical reactions as some special academic subcase, there is a parallel type of chemistry based not on the collisions of molecules and the energy transfers that underlie these collisions but on interfacial electron transfers. It is this latter chemistry that seems to underlie much of what goes on in the world around us, for example, in photosynthesis, in metabolism, and in the

decay of metallic structures. The examples of alternative thermal and electrical approaches to common chemical events given in Table 1.1 may illustrate this.

1.12.2. The Relation between Three Major Advances in Science, and the Place of Electrochemistry in the Developing World

If one stands sufficiently removed from one's specialization in the sciences and looks as far back as the nineteenth century, then three great scientific contributions stand out as measured by their impact on science and technology. They are

1. The electromagnetic theory of light due to Maxwell (nineteenth century)
2. The theory of relativistic mechanics due to Einstein (nineteenth century)
3. The theory of quantum mechanics originating with the work of Planck, Einstein, and Bohr and developed by Schrödinger, Heisenberg, Born, and Dirac (twentieth century)

It is important to recall why these contributions to physics and chemistry are regarded as so outstanding. Maxwell's theory provides the basis for the transfer of energy and communication across distances and the delivery of mechanical power on command as a consequence of the controlled application of electric currents causing magnetic fields. The significance of relativistic mechanics is that it helps us understand the universe around us—great bodies, far away, traveling very fast. Quantum mechanics is the basis of solid-state devices and transistor technology. It led to a revolution in thinking; for example, we now know that macroscopic and microscopic systems behave in fundamentally different ways. It allows us to understand how small particles can penetrate barriers otherwise insurmountable (a realization that helps us understand the functioning of fuel cells). A fourth contribution, the discovery of *over unity* processes—machines that seem to produce more energy than was put in—hold promise for great advances. However, this work is still in a very early stage and we cannot yet gauge its technological significance.[11]

How is the eventual magnitude of a contribution in science weighed? Is it not the degree to which the applications that arise from it eventually change everyday life? Is not the essence of our present civilization the attempt to control our surroundings?

It is in this light that one may judge the significance of the theory of electrified interfaces and thus electrochemistry. It is of interest to note how interfacial charge-transfer theories are based on a combination of the electric currents of Maxwell's theory and the quantum-mechanical tunneling of electrons through energy barriers.

---

[11]Over-unity machines are claimed by their inventors to be emerging, as seen in the late 1990s. Their mechanisms are far from clear as yet. They seem to involve nuclear reactions under very low temperature situations, or alternatively, they are machines that are claimed to convert the zero point energy of their surroundings to electricity. If (as seems likely) they become commercialized in the early decades of the new century, the cost of electricity will fall and a great augmentation of the electrical side of chemistry will occur.

Examples of Alternative Thermal and Electrochemical Paths in Chemical Events

Phenomenon or Process	Thermal	Electrochemical
The determination of free-energy changes and equilibrium constants in chemical reactions	Determine equilibrium constant and use $\Delta G^\circ = -RT \ln K$	Determine thermodynamic cell potential and use $\Delta G^\circ = -nFE$
Synthesis, e.g., water from hydrogen and oxygen	Occurs heterogeneously presumably by non-charge-transfer collisional processes $H_2 + {}^1\!/_2O_2 \rightarrow H_2O$	Occurs in electrochemical cell by reactions $H_2 \rightarrow 2\,H^+ + 2\,e$ ${}^1\!/_2O_2 + 2H^+ + 2\,e \rightarrow H_2O$ $H_2 + {}^1\!/_2O_2 \rightarrow H_2O$
Biochemical digestion	Series of enzyme-catalyzed chemical reactions	Some enzymatic reactions may act through electrochemical mechanisms analogous to the local cell theory of corrosion
Many so-called chemical reactions, e.g., chemical synthesis of Ti	$TiCl_4 + 2\,Mg \rightarrow Ti + 2\,MgCl_2$ (apparently a thermal collisional reaction)	$2\,Mg \rightarrow 2\,Mg^{2+} + 4e$ $Ti^{4+} + 4\,e \rightarrow Ti$ $4\,Cl^- \rightarrow 4\,Cl^-$
Production of electrical energy	$H_2 + {}^1\!/_2O_2$ explodes, produces heat, expands gas, causes piston to move, and drives generator	H_2 and O_2 ionize on electrodes, as above in this column, and produce current
Storage of electrical energy	Electricity pumps water up to height and allows it to fall on demand to drive generator	Allow to cause some electrochemical change, e.g., $Cd^{2+} + 2\,e \rightarrow Cd$, $Ni^{2+} \rightarrow Ni^{4+} + 2\,e$, which will be reversed on demand
Synthesis of inorganic and organic material, e.g., Al, adiponitrile	$2\,Al_2O_3 + 3\,C \rightarrow 3\,CO_2 + 4\,Al$; Tetrahydrofuran $\rightarrow$ 1,4-dichlorobutane $\rightarrow$ adiponitrile	$Al^{3+} + 3\,e \rightarrow Al$ $H_2C{=}HC{-}CN \xrightarrow[\text{coupling}]{\text{cathodic}} NC{-}(CH_2)_4{-}CN$
Spreading of cracks through metal	Amount of stress at the apex of a crack per unit area is so high that the crack is propagated into the metal bulk	Bottom of crack dissolves anodically, obtaining current from local cell formed with surface (which is an electron donor, probably to O_2 from air)

A number of illustrations have been given to support the statement that electrochemical mechanisms are relevant to many fields of science. The nineteenth century contributed to physics the theory of electromagnetism. The twentieth century contributed to physics the relativistic theory and the quantum theory. In the twenty-first century, it seems reasonable to assume that the major preoccupations will be in the direction of working out how we can make a sustainable world that continues to have an abundant supply of energy, and that does not suffocate in its own refuse or become too hot to live on because of the continued use of oil and coal as fuels.

Two very general types of probable advances can be expected. One is in the direction noted; for example the development of practical devices for the production of cheap electricity, or the development of prosthetic devices operated by the electric circuits of the body.

The other type will be those developments necessary as a result of the interference with nature over the past 50 years; for example, electrically powered vehicles to avoid increasing the CO_2 content of the atmosphere and processes to reduce pollution in our water supply.

Electrochemistry is the core science upon which many of these electrically oriented advances of the next few decades will depend for their practical execution (see Fig. 1.15). It underlies electrically powered synthesis, extractions (including fresh from brackish water), machining, stabilization of materials, storage of energy in the form of electricity, efficient conversion to electricity of the remaining fossil fuels, and

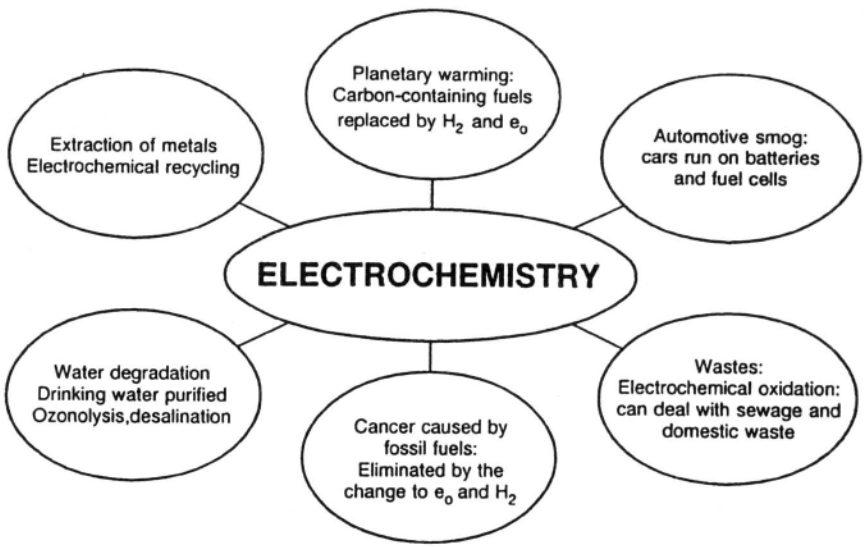

Fig. 1.15. Electrochemistry as a core science for the development of a sustainable society.

the basis for understanding much in molecular biology. The fixing of CO_2 and its photoconversion to methanol (a fuel) is also a prospect.

It is worthwhile thinking also that urban areas are likely to develop as a function of the availability of electricity from solar or nuclear sources. There will also be an increasing need to invest resources in preventing the exhaustion of many vital metals.[12]

The forms in which energy will be transmitted will be electricity with hydrogen as a storage medium. Towns in the 21st century will tend to be self-contained. Little material mass will leave or enter them. The processes on which towns will run will be all electrical, and those involving matter therefore electrochemical. Transportation will use energy stored in hydrogen and in condensers. Manufacturing and machining processes and recovery of materials used or discarded will all be electrochemical. Polluted liquids will be cleaned in packed bed electrolysers (Fig. 1.16). Wastes will be processed electrochemically in molten salts. Medical electronics—the electronic-electrodic combination in medical research—will be highly developed toward various combinations of humans and machines.

Thus, it seems reasonable to expect the achievement of several electrochemically based innovations by 2050: the provision of cheap heat electrically from storage units charged during off-peak times; electrochemically powered vehicles, including ships; an economical and massive solar conversion system; hydrogen storage and transmission to avoid systems that add further CO_2 to the atmosphere; extensive use of electrochemical machining and electrochemically based tools; an internal fuel-cell-powered heart; and electrometallurgical extractions of materials on a large scale from the moon (their transfer to earth will be easy because of the moon's low gravity). An immediately developable area lies in the electrochemical aspects of molecular biology (the replacement of electrically functioning body parts) and in the development of circuitry that will join the brain and its electrochemical mechanisms to artificial limbs with their electrochemical functions and perhaps even to circuits not connected to the body. Cyborgs, the person-machine combination, will become a part of life.

Let us therefore read this book with some sense of where we are on the scale of time, in the development of that great revolution begun in the eighteenth century. For it was then that we discovered how to make heat give mechanical power. However, this great discovery, and all that it has produced, has brought with it an unacceptable penalty—the pollution and planetary warming caused by the use of heat to produce mechanical power. We are just at the point on the time scale where we must wean ourselves away from oil (that mother's milk) and other CO_2-producing fuels that ran the first century of technology and find how to support the population of our overburdened planet by the use of fusion energy (from the sun, itself, or perhaps from the benign energy of low-temperature nuclear reactors). However, as we move away from pollution, CO_2, and planetary warming, it is certain that a greatly enhanced

[12]Only iron and aluminum are present in amounts to last hundreds of years. Unless they are recycled, many metals will be exhausted in the twenty-first century.

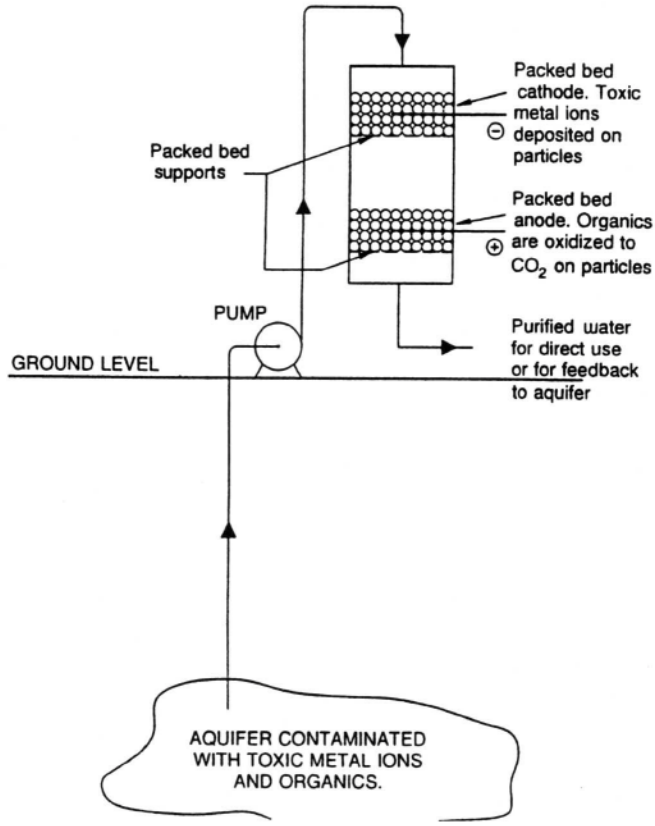

Fig. 1.16. Electrochemical treatment of a contaminated aquifer.

dependence on electricity as a clean source of energy will have to occur. This book stands as a guide on how to achieve this great transition to a sustainable world.

Further Reading

Books

1. D. B. Hibbert, *Dictionary of Electrochemistry*, Wiley, New York (1984).
2. A. J. Fry and W. E. Britton, eds., *Topics in Organic Electrochemistry*, Plenum Press, New York (1986).
3. J. Goodisman, *Electrochemistry: Theoretical Foundations, Quantum and Statistical Mechanics, Thermodynamics, Solid State*, Wiley, New York (1987).
4. O. Murphy, S. Srinivasen, and B. E. Conway, *Electrochemistry in Transition: 20–21st Century*, American Chemical Society, Washington D.C. (1988).

5. K. Scott, *Electrochemical Reaction Engineering*, Academic Press, New York (1993).
6. V. S. Bagotsky, *Fundamentals of Electrochemistry*, Plenum Press, New York (1993).
7. N. Masuko, O. Tetsuya, and Y. Fukunaka, *New Trends and Approaches in Electrochemical Technology*, Kodansha, Tokyo (1993).
8. J. Lipkowski and P. N. Ross, *Structure of Electrified Interfaces*, VCH Publishers, New York (1993).
9. J. O'M. Bockris and S. U. M. Khan, *Surface Electrochemistry*, Plenum Press, New York (1993).
10. J. Wang, *Analytical Electrochemistry*, VCH Publishers, New York (1994).
11. *Electrochemical Engineering in the Environment*, Institution of Chemical Engineers, Rugby, UK (1994).
12. C. A. C. Sequeira, *Environmentally Oriented Electrochemistry*, Elsevier, Amsterdam (1994).
13. R. C. Alkire and D. M. Kolb, Eds., *Advances in Electrochemical Science and Engineering*, V.C.H. Weinheim, New York (1995).
14. F. Goodridge and K. Scott, *Electrochemical Process Engineering: A Guide to the Design of Electrolytic Plant*, Plenum Press, New York (1995).
15. J. A. G. Drake, *Electrochemistry and Clean Energy*, Royal Society of Chemistry, Cambridge (1995).
16. I. Rubenstein, *Physical Electrochemistry: Principles, Methods, and Applications*, M. Dekker, New York (1995).
17. R. J. D. Miller, G. L. McLendon, A. J. Nozik, W. Schmickler, and F. Willig, *Surface Electron Transfer Processes*, VCH Publishers, New York (1995).
18. W. Schmickler, *Interfacial Electrochemistry*, Oxford University Press, Oxford (1996).

Monograph Series

1. J. O'M. Bockris, B. E. Conway, and E. Yeager, eds., *Comprehensive Treatise of Electrochemistry, Vol. 10*, Plenum Press, New York (1986).
2. J. O'M. Bockris, B. E. Conway, and R. White, eds., *Modern Aspects of Electrochemistry, Vol. 29*, Plenum Press, New York (1995).
3. A. J. Bard, ed., *Journal of Analytical Chemistry: The Series of Advances, Vol. 17*, M. Dekker, New York (1991).
4. H. Gerischer and C. W. Tobias, eds., *Advances in Electrochemistry and Electrochemical Engineering, Vol. 13*, Wiley, New York (1984).
5. H. Gerischer and C. W. Tobias, eds., *Advances in Electrochemical Science and Engineering, Vol. 3*, VCH Publishers, New York (1994).
6. D. Pletcher, ed., *Electrochemistry, Vol. 10*, The Royal Society of Chemistry, London (1985).
7. A. J. Bard, ed., *Encyclopedia of Electrochemistry of the Elements, Vol. 15*, M. Dekker, New York (1984).
8. *The Electrochemical Society Series*, Wiley, New York.
9. J. Lipkowski and N. P. Ross, eds., *Frontiers of Electrochemistry*, VCH Publishers, New York (1996).

10. International Union of Pure and Applied Chemistry (IUPAC), *Monographs in Electroanalytical Chemistry and Electrochemistry*, M. Dekker, New York (1995).
11. J. Braunstein, G. Mamantov, and G. P. Smith, eds., *Advances in Molten Salt Chemistry*, Vol. 6, Plenum Press, New York (1987).

Journals

1. Electrochemical themes are often treated in other journals of physical chemistry (e.g., *Journal of Physical Chemistry*) and occasionally in journals of chemical physics.
2. Journal of the Electrochemical Society, P. A. Kohl, ed., The Electrochemical Society, Inc., Pennington, NJ.
3. *Interface*, L. P. Hunt, ed., The Electrochemical Society, Inc., Pennington, NJ.
4. *Electrochimica Acta,* R. D. Armstrong, ed., Elsevier Science Ltd. for the International Society of Electrochemistry (ISE), Oxford.
5. *Journal of Applied Electrochemistry*, A. A. Wragg, ed., Chapman and Hall, London.
6. *Langmuir*, W. A. Steel, ed., The American Chemical Society, Washington, DC.
7. *Journal of Colloid and Interface Science*, Darsh T. Wasan, ed., Academic Press, Orlando, FL.
8. *Russian Journal of Electrochemistry (Elektrokhimiya)*, Yakov M. Kolotyrkin, ed., Interperiodica Publishing, Moscow.
9. *Journal of Electroanalytical Chemistry*, R. Parsons, ed., Elsevier Science, S. A., Lausanne, Switzerland.
10. *Corrosion Science*, J. C. Scully, ed., Elsevier Science Ltd., Oxford.
11. *Corrosion*, J. B. Lumsden, ed., National Association of Corrosion Engineers International, Houston, TX.
12. *Bioelectrochemistry and Bioenergetics*, H. Berg, ed., Elsevier Science, S.A., Lausanne, Switzerland.

CHAPTER 2

ION–SOLVENT INTERACTIONS

2.1. INTRODUCTION

Aristotle noted that one could separate water from a solution by means of evaporation. Some two millennia later, Fourcroy in 1800 focused attention on the *interaction* of a solute with its solvent.

These early observations serve to introduce a subject—the formation of mobile ions in solution—that is as basic to electrochemistry as is the process often considered its fundamental act: the transfer of an electron across the double layer to or from an ion in solution. Thus, in an electrochemical system (Fig. 2.1), the electrons that leave an electronically conducting phase and cross the region of a solvent in contact with it (the interphase) must have an ion as the bearer of empty electronic states in which the exiting electron can be received (electrochemical reduction). Conversely, the filled electronic states of these ions are the origin of the electrons that enter the metal in the

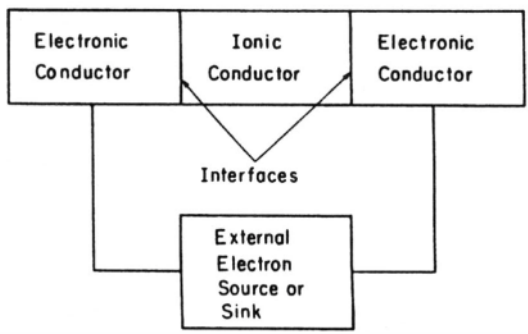

Fig. 2.1. The essential parts of an electrochemical system.

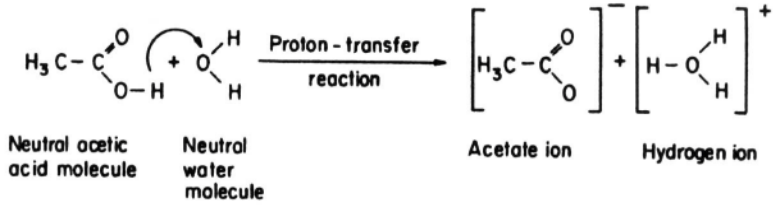

Fig. 2.2. The chemical method of producing ionic solutions.

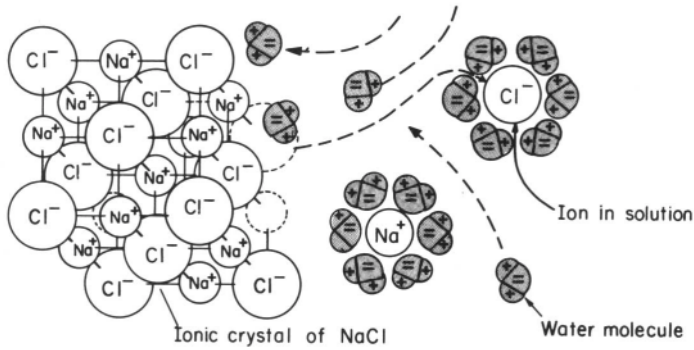

Fig. 2.3. Dissolution of an ionic crystal by the action of a solvent.

reverse electron-transfer reactions involved in electrochemical oxidation reactions. These basic electrochemical processes are shown in Fig. 2.1.

There are two distinct ways that mobile ions form in solution to create the ionically conducting phases that make up the solution side of an electrode–solution system (one half of the electrochemical system shown in Fig. 2.1).

The first one is illustrated in Fig. 2.2. It applies to ion formation in a solvent where the solute is a neutral molecule; in Fig. 2.2 it is acetic acid, CH_3COOH. The figure shows the reaction between solute and solvent that forms the ions in the solvent, and therefore the solution. A characteristic of solutions formed in this way is that usually[1] the ionic concentration is a rather small fraction (e.g., about 0.1%) of the solute molecules are ionized to give ions (Table 2.1).

The second (perhaps more frequently applicable) method of forming mobile ions in solution is quite different: it involves the dissolution of a solid lattice of ions such as the lattice of the often-cited sodium chloride. Some attempt to show what happens in this type of ion formation is reproduced in Fig. 2.3. It is as though the solvent, colliding with the walls of the crystal, gives the ions in the crystal lattice a better deal

[1]However, HCl is a molecule and when this molecule ionizes by reacting with a water molecule, (it does so rather fully), nearly 100% of the molecule can become ionized.

TABLE 2.1
Ionic Concentrations in Pure Water, Pure Acetic Acid, and Acetic Acid Solution

	Ionic Concentration (g-ions dm^{-3} at 298 K)
Pure water	10^{-7}
Pure acetic acid	$10^{-6.5}$
0.1 *N* acetic acid solution	10^{-3}

energetically than they have within the lattice. It entices them out of the lattice and into the solution.[2]

Of course, this implies that there is a considerable energy of interaction between the lattice ions and the solvent molecules. It is this ion–solvent interaction, the immediate cause of the formation of conducting ionic solutions from salts, that is the subject of this chapter.

2.2. BREADTH OF SOLVATION AS A FIELD

The wide range of areas affected by solvation can be seen when one considers the basic role hydration plays in; for example, geochemistry, and indeed in the whole hydrosphere. The pH of natural waters, with all the associated biological effects, is affected by the dissolution of $CaCO_3$ from river beds; and the degree of this dissolution, like any other, is determined by the solvation of the ions concerned. Alternatively, consider the modern environmental problem of acid rain. The basic cause is the formation of atmospheric SO_2 as a result of burning fossil fuels. The pH reached in naturally occurring water is a result of the dissolution of SO_2 in rain and the subsequent creation of the sulfuric acid; H_2SO_4, because the stability of the H^+ and SO_4^{2-} ions that arise is determined by their hydration. The acidity of natural waters then depends upon the original concentration of SO_2 in the air as well as the action of various associated ionic reactions which tend to counter the pH change the SO_2 causes, but which, because they involve ions, themselves depend for their energetics on the ions' solvation energies.

It has already been implied that ion–solvent interactions have widespread significance in electrochemistry, and some of the ramifications of this were discussed in

[2]In this process (and up to a certain concentration) all the ions in the lattice salt become mobile solution ions, although when the ionic concentration gets high enough, the negative and positive ions (*anions* and *cations*, respectively) start to *associate* into nonconducting ion pairs. The specific conductance of salt solutions therefore passes through a maximum, if plotted against concentration.

[3]In this chapter, *solvation* and *hydration* will both be used to describe the interaction of an ion with its surroundings. Clearly, solvation is the general term but most cases of it are in fact hydration.

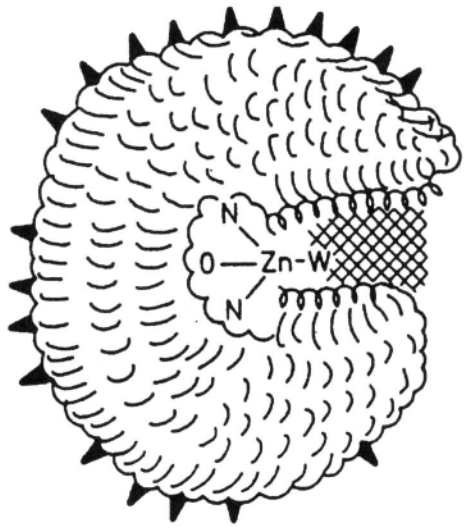

Fig. 2.4. Schematic view of carboxypeptidase A. The coordination sphere around Zn at the bottom of the groove is shown (W = water). The curly lining of the pocket symbolizes hydrophobic residues and the hatched area indicates "organized" water molecules. The small pointed figures at the outer surface refer to polar side groups solvated by the external solvent. (Reprinted from R. R. Dogonadze, A. A. Komyshev, and J. Ulstrup "Theoretical Approach in Solvation," in *The Chemical Physics of Solvation,* Part A, R. R. Dogonadze, E. Kalman, A. A. Kornyshev, and J. Ulstrup, eds., Elsevier, New York, 1985.)

Chapter 1. However, ionic hydration[3] also plays a leading role in biology. Figure 2.4 shows how the structure of an enzyme depends upon hydration. The diagram indicates how there are effects from "organized water" (i.e., water molecules associated with the Zn nucleus of the carboxypeptidase A) as well as some hydrophobic effects.

This mention of hydrophobicity serves to introduce a lesser mentioned field, that in which solute–solute interactions combine to force *out* solvent molecules, in direct contrast to the more normal ionic hydration effects in which the ions draw solvent molecules into themselves. Such hydrophobic effects occur, for example, when there are large solute groups present (e.g., neutral hydrocarbons in water) and sometimes with large charged groups such as NR_4^+ ions, the size of which can cause attractive–dispersive interactions between the ions and organic molecules to compete with ion–solvent attraction.

TABLE 2.2
Some Approaches to the Investigation of Solvation

From the Properties of Solutions	From Spectroscopic and Other Approaches[a]
Mobility of ions	NMR
Individual partial molar volumes	Raman
Activities of the solvent	EXAFS
Compressibilities of solutions	Neutron diffraction
Vibration potentials	Model calculations using statistical mechanics
Dielectric constants	Monte Carlo
Individual ionic entropies	Molecular dynamics

[a]NMR, nuclear magnetic resonance; EXAFS, extended X-ray absorption fine structure. Neutron diffraction deals with momentum transfer: spectroscopic methods with energy transfer.

2.3. A LOOK AT SOME APPROACHES TO SOLVATION DEVELOPED MAINLY AFTER 1980

There are three main approaches to the study of solvation that have been developed largely since the first edition of this book was published in 1970 (Table 2.2).

2.3.1. Statistical Mechanical Approaches

Statistical mechanical approaches apply mainly to deductions about structure and are the basis of interpretations of the entropy of ions in solution and the solution's heat capacity. The entropy of a system can be calculated if the partition functions of the ions and the water molecules surrounding them are known.[4] The partition functions (translatory, rotational, and vibrational) can be obtained from textbook material by assuming a structure of the ion–solvent complex. By comparing calculations based on various assumptions about structure with the values obtained from experiments, certain structures can be shown to be more likely (those giving rise to the calculations that match the experiment), others less probable, and some so far from the experimental values that they may be regarded as impossible.

2.3.2. What Are Monte Carlo and Molecular Dynamics Calculations?

The easy availability of computers of increasing power has greatly encouraged the two approaches described in this section. In the Monte Carlo (MC) approach,

[4]Although these statistical mechanical approaches have been used increasingly in recent times, a paper by Eley and Evans written as early as 1938 is the origin of partition functional treatments of solutions.

random movements of ions in the solution (and the waters near them) are tested by calculating the energy changes they would bring about were they to occur. The ones that happen with the lowest energy (with a negative free-energy change) are those taken to be occurring in reality.

The molecular dynamics (MD) calculations are different from the Monte Carlo ones. Instead of using assumptions about random movements of the ions and solvent molecules and calculating which of the movements is good (lowers energy) or bad (raises it), the molecular dynamics approach works out the potential energy of the molecular entities as they interact with each other. Then, by differentiating these energies with respect to distance, one can derive the force exerted on a given particle at each of the small time intervals (mostly on a femtosecond scale). As a result of such computations, the dynamics of each particle, and hence the distribution function and eventually the properties of the system, can be calculated. The critical quantities to know in this approach are the parameters in the equation for the intermolecular energy of interaction. To compensate for the fact that only interactions between nearest neighbors are taken into account (no exact calculations can be made of multibody problems), these parameters are not calculated from independent data, but an assumption is made that the two-body-problem type of interaction is acceptable and the parameters are computed by using a case for which the answer is known. The parameters thus obtained are used to calculate cases in which the answer is unknown.

The ability of these computational approaches to predict reality is good. A limitation is the cost of the software, which may amount to many thousands of dollars. However, some properties of solutions can be calculated more cheaply than they can be determined experimentally (Section 2.5). Increasing computer power and a lowering of the cost of the hardware indicates a clear trend toward the ability to calculate chemical events.

2.3.3. Spectroscopic Approaches

In the latter half of this century physicochemical approaches have increasingly become spectroscopic ones. Infrared (IR), Raman, and nuclear magnetic resonance (NMR) spectroscopic approaches can be used to register spectra characteristic of the ion–solvent complex. The interpretation of what molecular structures give these spectra then suggests structural features in the complex. On the other hand, the spectroscopic technique does not work well in dilute solutions where the strength of the signal emitted by the ion–solvent interaction is too small for significant determination. This limits the spectroscopic approach to the study of solvation because it is only in dilute solutions that the cations and anions are sufficiently far apart to exert their properties independently. Thus, spectroscopic methods are still only a partial help when applied to solvation. Spectroscopic and solution property approaches are summarized in Table 2.2.

Two other points must be made here:

1. Water is a very special solvent in respect to its structure (Section 2.4) and the fact that nearly all of our knowledge of ions in solutions involves water arises from its universal availability and the fact that most solutions met in practice are aqueous. However, studying the hydration of ions rather than their solvation limits knowledge, and a welcome modern trend is to study nonaqueous solutions as well.

2. Modern theoretical work on solution properties often involves the use of *mean spherical approximation*, or MSA. This refers to models of events in solution in which relatively simple properties are assumed for the real entities present so that the mathematics can be solved analytically and the answer obtained in terms of an analytical solution rather than from a computer program. Thus, it is assumed that the ions concerned are spherical and incompressible. Reality is more complex than that implied by the SE approximations, but they nevertheless provide a rapid way to obtain experimentally consistent answers.

2.4. STRUCTURE OF THE MOST COMMON SOLVENT, WATER

One can start by examining the structure of water in its gaseous form. Water vapor consists of separate water molecules. Each of these is a bent molecule, the H–O–H angle being about 105° (Fig. 2.5). In the gaseous oxygen atom, there are six electrons in the second shell (two 2s electrons and four 2p electrons). When the oxygen atoms enter into bond formation with the hydrogen atoms of adjacent molecules (the liquid phase), there is a blurring of the distinction between the s and p electrons. The six electrons from oxygen and the two from hydrogen interact. It has been found that four pairs of electrons tend to distribute themselves so that they are most likely to be found in four approximately equivalent directions in space. Since the motion of electrons is described by quantum mechanics, according to which one cannot specify precise orbits for the electrons, one talks of the regions where the electrons are likely to be found as orbitals, or blurred orbits. The electron orbitals in which the electron pairs are likely to be found are arranged approximately along the directions joining the oxygen atom to the corners of a tetrahedron (Fig. 2.6). The eight electrons around the oxygen are neither s nor p electrons; they are sp^3 hybrids. Of the four electron orbitals, two are used for the O–H bond, and the remaining two are as free as a lone pair of electrons.

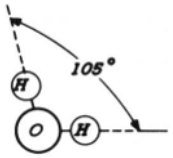

Fig. 2.5. A water molecule is nonlinear.

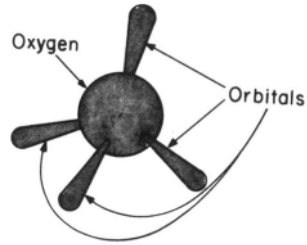

Fig. 2.6. The hybrid orbitals of an oxygen atom.

Because of the repulsion of the electron pairs, the H–O–H angle is not exactly equal to the tetrahedral angle **(109° 28′),** but is a few degrees less than that.

Water molecules vibrate and rotate in the gas phase. In the liquid phase, the rotation is hindered (*libration*) because of the structure (intermolecular H bonds) and the vibrations are modified (Section 2.11.2).

The free orbitals in which are found the electron lone pairs confer an interesting property on the water molecule. The center of gravity (Fig. 2.7) of the negative charge in the water molecule does not coincide with the center of gravity of the positive charge. In other words, there is a separation within the electrically neutral water molecule: it is thus called an electric *dipole.* The *moment* of a dipole is the product of the electrical charge at either end times the distance between the centers of the electrical charge, $q \cdot d$. The dipole moment of water is 1.87 D in the gas phase (but becomes larger when the water molecule is associated with other water molecules) (Section 2.4.2).

In fact, although water can be treated effectively as a dipole (two equal and opposite charges at either end of a straight line), a more accurate representation of the electrical aspects of water is to regard the oxygen atom as having two charges and each hydrogen atom as having one. This model will be studied in the theory of hydration heats (Section 2.15).

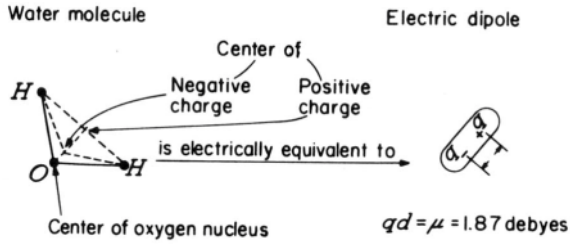

Fig. 2.7. A water molecule can be considered electrically equivalent to a dipole.

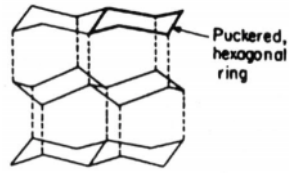

Fig. 2.8. The oxygen atoms in ice, which are located at the intersections of the lines in the diagram, lie in a network of open puckered hexagonal rings.

The availability of the free orbitals (with lone electron pairs) on the oxygen atom contributes not only to the dipolar character of the water molecule but also to another interesting consequence. The two lone pairs can be used for electrostatic bonding to two other hydrogen atoms from a neighboring water molecule. This is what happens in a crystal of ice. The oxygen atoms lie in layers, with each layer consisting of a network of open, puckered hexagonal rings (Fig. 2.8). Each oxygen atom is tetrahedrally surrounded by four other oxygen atoms. In between any two oxygen atoms is a hydrogen atom (Fig. 2.9), which provides a hydrogen bond. At any instant the hydrogen atoms are not situated exactly halfway between two oxygens. Each oxygen has two hydrogen atoms near it (the two hydrogen atoms of the water molecule) at an estimated distance of about 175 pm. Such a network of water molecules contains interstitial regions (between the tetrahedra) that are larger than the dimensions of a water molecule (Fig. 2.10). Hence, a free, nonassociated water molecule can enter the interstitial regions with little disruption of the network structure.

This important property of water, its tendency to form the so-called *H bonds* with certain other atoms, is the origin of its special characteristic, the netting up of many water molecules to form large groups (Fig. 2.10). *H bonds* may involve other types of

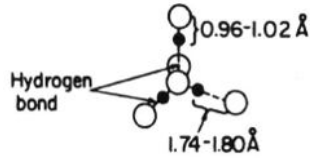

Fig. 2.9. The hydrogen bond between two oxygen atoms (the oxygen and hydrogen atoms are indicated by ○ and •, respectively).

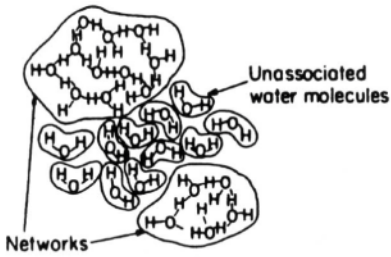

Fig. 2.10. Schematic diagram to show that in liquid water there are networks of associated water molecules and also a certain fraction of free, unassociated water molecules.

atoms, such as Cl, F, O, and S when they are in solution. There is nothing mysterious about the energy behind H bonding; it derives from the positive charge on the proton and the negative one on F^-, for example.

However, H bonding (the value of the bond strength is small, only 10–40 kJ mol^{-1}) does affect the properties of water and is responsible for water's anomalously high boiling point. If one extrapolates the boiling points of the hydrides of the elements in group VI of the Periodic Table to the expected value for the hydride of O, it turns out to be ~ 215 K. The fact that it is actually 158 K higher than that is undoubtedly because individual water molecules are not free to evaporate as the temperature is increased. Many of them bond to each other through the H bonds. The thermal stability of water has had an important effect on the structure of the earth, for if there were no H bonds, the seas would never have formed (they would have remained in the vapor phase) and it is doubtful if life would have begun.

Structural research on water, which originated in a classic paper by Bernal and Fowler, has shown that under most conditions liquid water is best described as a rather broken-down, slightly expanded (Table 2.3) form of the ice lattice (Fig. 2.8). Thus, X-ray and other techniques indicate that in water there is a considerable degree of short-range order that is characteristic of the tetrahedral bonding in ice. Thus, liquid water partly retains the tetrahedral bonding and resulting network structure characteristic of crystalline ice. In addition to the water molecules that are part of the network, some structurally free, nonassociated water molecules can be present in interstitial regions of the network (Fig. 2.10). When a network water molecule breaks its hydrogen bonds with the network, it can move as an interstitial water molecule that can rotate freely. The classification of the water molecules into network water and free (or interstitial) water is not a static one. It is dynamic. As argued in a classic paper by Frank and Wen, clusters of water molecules cooperate to form networks and at the same time the networks can break down. A water molecule may be free in an interstitial

TABLE 2.3
The Structure of Ice and Liquid Water

	Ice	Liquid Water
Mean O–O distance	276 pm	292 pm
Number of oxygen nearest neighbors	4	4.4–4.6

position at one instant and in the next instant it may become held as a unit of the network.[5]

In the 1970s and 1980s, calculational approaches (in addition to the X-ray studies) were added to the tools for the attack on the structure of water. In the molecular dynamics approach, classical mechanics is used to calculate the successive movements of molecules in the structure. Such an approach is dependent on the correctness of the equation that represents the energies of interaction between the particles. The basic equation for these interactions is the "Lennard-Jones 6–12" potential.

$$U_r = -\frac{A}{r^6} + \frac{B}{r^{12}} \tag{2.2}$$

The first term represents the attraction between two molecules and the second the repulsion that also occurs between them.

One of the results of these calculations is that the number of water molecules in an ordered structure near a given water molecule drops away rapidly from the original molecule considered. The similarity of the liquid to solid ice does not remain too far from a given water molecule, i.e., the long-range order present in the solid is soon lost in the liquid.

---

[5] *Radial distribution functions* are met along the path between the results of X-ray and neutron diffraction examinations of water and the deriving of structural information, which is more difficult to do with a liquid than with a solid. Radial distribution functions are, e.g.,

$$\int_0^a 4\pi r^2 g(r) \frac{\sin Sr}{Sr} dr \tag{2.1}$$

and can be seen as proportional to the intensity of the reflected X-ray beam as a function of the incident angle, θ. Thus, in Eq. (2.1) $S = (4\pi/\lambda)\sin \theta/2$. The significance of $4\pi r^2 g(r)dr$ allows one to calculate the number of oxygen atoms between r and $r + dr$. In this way one can derive the number of nearest neighbors in the liquid from any central O. The value is 4 for ice and, rather curiously, increases as the temperature is increased (it is 4.4 at 286 K). This may be due to the disturbing effect of pure H_2O molecules, which increase in number with temperature. Their presence would *add* to the intensity due to the regular pattern and account for values greater than 4.2.

Knowing the distribution functions, $g(r)$, as a function of r from experiment or calculation from a central particle, it is possible to calculate how the water molecules spread out from a central particle. With knowledge of this function, it is possible to calculate various properties of liquid water (e.g., its compressibility), and these can then be compared with experimental values as a test of the calculation.

2.4.1. How Does the Presence of an Ion Affect the Structure of Neighboring Water?

The aim here is to take a microscopic view of an ion inside a solvent. The central consideration is that ions orient dipoles. The spherically symmetrical electric field of the ion may tear water dipoles out of the water lattice and make them point (like compass needles oriented toward a magnetic pole) with the appropriate charged end toward the central ion. Hence, viewing the ion as a point charge and the solvent molecules as electric dipoles, one obtains a picture of ion–dipole forces as the principal source of ion–solvent interactions.

Owing to the operation of these ion–dipole forces, a number of water molecules in the immediate vicinity of the ion (the number will be discussed later) may be trapped and oriented in the ionic field. Such water molecules cease to associate with the water molecules that remain part of the network characteristic of water (Section 2.4.3). They are immobilized except insofar as the ion moves, in which case the sheath of immobilized water molecules moves with the ion. The ion and its water sheath then become a single kinetic entity (there is more discussion of this in Section 2.4.3). Thus, the picture (Fig. 2.11) of a hydrated ion is one of an ion enveloped by a solvent sheath of oriented, immobilized water molecules.

How about the situation far away from the ion? At a sufficient distance from the ion, its influence must become negligible because the ionic fields have become

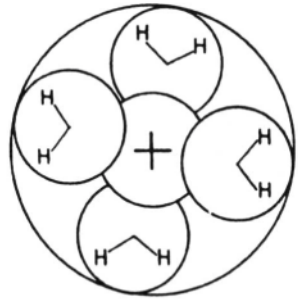

Fig. 2.11. An ion enveloped by a sheath of oriented solvent molecules.

attenuated to virtually zero. The normal structure of water has been re-attained: it is that of bulk water.

In the region between the solvent sheath (where the ionic influence determines the water orientation) and the bulk water (where the ionic influence has ceased to dominate the orientation of water molecules), the ion still has some orienting influence on the water network: it tries to align the water dipoles parallel to the spherically symmetrical ionic field, and the water network tries to convert the water in the in-between region into a tetrahedral arrangement (Fig. 2.12). Caught between the two types of influences, the in-between water adopts some kind of compromise structure that is neither completely oriented nor yet fixed back into the undisturbed water structure shown in Fig. 2.10. The compromising water molecules are not close enough to the ion to become oriented perfectly around it, but neither are they sufficiently far away from it to form part of the structure of bulk water; hence, depending on their distance from the ion, they orient out of the water network to varying degrees. In this intermediate region, the water structure is said to be partly broken down.

One can summarize this description of the structure of water near an ion by referring to three regions (Fig. 2.12). In the *primary*, or structure-enhanced, region next to the ion, the water molecules are oriented out of the water structure and immobilized by the ionic field; they move as and where the ion moves. Then, there is a *secondary*, or structure-broken (SB), region, in which the normal bulk structure of

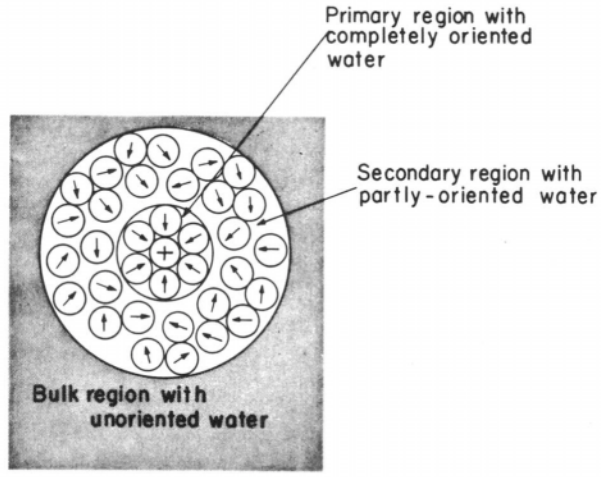

Fig. 2.12. The neighborhood of an ion may be considered to consist of three regions with differing solvent structures: (1) the primary or structure-forming region, (2) the secondary or structure-breaking region, and (3) the bulk region.

water is disturbed to varying degrees. The in-between water molecules, however, do not partake of the translational motion of the ion. Finally, at a sufficient distance from the ion, the water structure is unaffected by the ion and again displays the tetrahedrally bonded networks characteristic of bulk water.

The three regions just described differ in their degree of sharpness. The primary region (discussed in greater detail later), in which there are (at least for the smaller cations) water molecules that share the translational motion of the ion, is a sharply defined region.

In contrast, the secondary region, which stretches from the termination of the primary region to the resumption of the normal bulk structure, cannot be sharply defined; the bulk properties and structure are asymptotically approached.

These structural changes in the primary and secondary regions are generally referred to as solvation (or as hydration when, as is usual, water is the solvent). Since they result from interactions between the ion and the surrounding solvent, one often uses the term "solvation" and "ion–solvent interactions" synonymously; the former is the structural result of the latter.

2.4.2. Size and Dipole Moment of Water Molecules in Solution

In discussions of the *radius of a molecule*, the only well-defined, exact part of the answer lies in the internuclear distances (e.g., between H and O for water), but this distance comprises only part of the radius, albeit the main part. All other measures of the radius of a molecule are affected by some aspect of the occupancy of space that is connected with the packing of the molecule, which varies with circumstances.

In ice (where X-ray measurements of internuclear distances, d, are more exact than those in the liquid), the O–O internuclear distance is accurately known: 280 pm. The distance between the nucleus of oxygen and that of hydrogen (see a space-fitting picture of water, Fig. 2.9) is 138 pm.

The so-called *van der Waals radius*[6] of H can be taken to be 52.8 pm (this is the Bohr radius for the ground state of H). The van der Waals radius of O is ~115 pm and from these values 168 pm is obtained for the radius of water.

Now, several other radii between ca. 140 and 193 pm can be obtained by equating $4/3\ \pi r^3$ to certain volumes (e.g., the close-packed volume of water, or a volume based on the molecular dimensions). Each of these radii is "applicable" as the circumstances dictate.

Thus, the "radius of water" varies, according to the method used to estimate it, between 168 (the model shown in Fig. 2.9) and 193 pm, which arises from measurements on the density of water (and the resulting molar volume of 18 cm^3). The larger

---

[6]The phrase "van der Waals radius" arises as a distinction from "internuclear distance radii." Thus, from the van der Waals equation for the P-V relation in gases (an improvement on the simple gas law $PV=nRT$), a quantity b can be found which refers to the space taken up out of the whole gas volume V by the molecules themselves.

value is too high because it includes the free space in liquid water. The lower value is too low, because it neglects the volume needed to cover some water movements in the liquid. The mean, 181 ± 13 pm, is a regrettably imprecise figure for such an important quantity, but, as can be understood, it all depends upon what one takes into account.

The dipole moment of water in the gas phase is well known as 1.87 D but is 2.42 D in water at 298 K. The reason for the difference is that in liquid water there is electrostatic pull on a given water molecule from the surrounding ones, and this lengthens the distance in the dipoles (Fig. 2.7).

2.4.3. The Ion–Dipole Model for Ion–Solvent Interactions

The preceding description of the solvent surrounding an ion was used as the basis of a structural treatment of ion–solvent interactions initiated by Bernal and Fowler (1933). Their paper is a seminal one for much else in the structural picture of hydration (Section 2.4).

Bernal and Fowler thought of the changes of free energy during solvation as being largely electrostatic in nature. In their picture, the passage of an ion began in the gas phase, and here they took (for most of their calculations) the ions to have a zero potential energy of interaction. Transferring an ion mentally to the interior of the solvent, they thought this to be associated with three energy changes:

1. The ion–dipole interaction caused by the ion's attracting water dipoles in the first layer around the ion (ion–dipole interaction). (*cf.* Appendix 2.2)
2. Then there would be the energy needed to break up the water structure, which occurs when ions enter it.
3. There would be a further allowance for the ion–water interactions "further out" from the first layer to the rest of the solvent surrounding the ion. Such an interaction might be thought to be relatively small, not only because of the increasing distance but because of the increasing dielectric constant; small (near to 6) near the ion but rapidly attaining the value of about 80 (at 25 °C), as near as 1000 pm from the ion. Both these factors would diminish the individual ion–dipole interaction energy.

Bernal and Fowler's calculation remains famous because it grappled for the first time with the structure of water and with ion–solvent interactions on a molecular basis. Better theories have been developed, but most have their roots in the Bernal and Fowler work of 1933.

The modern developments of solvation theory will not be discussed at this point because nearly all the tools for investigating the ion–solvent interaction have become available since 1933. One has to see some of the information they have provided before ion–solvent interactions can be worked out in a more quantitative way.

Further Reading

Seminal

1. M. Born, "Free Energy of Solvation," *Z. Phys.* **1**: 45 (1920).
2. J. D. Bernal and R. H. Fowler, "The Structure of Water," *J. Chem. Phys.* **1**:515 (1933).
3. R. W. Gurney, *Ionic Processes in Solution,* McGraw-Hill, New York (1953).
4. H. S. Frank and W. Y. Wen, "Water Structure Near to Ions," *Faraday Discuss., Chem. Soc.* **24**: 133 (1957).

Monograph

1. B. E. Conway, *Ionic Hydration in Chemistry and Biology*, Elsevier, New York (1981).

Papers

1. C. Sanchez-Castro and L. Blum, *J. Phys. Chem.* **93**: 7478 (1989).
2. E. Guardia and J. A. Padro, *J. Phys. Chem.* **94**: 6049 (1990).
3. B. Guillot, P. Martean, and J. Ubriot, *J. Chem. Phys.* **93**: 6148 (1990).
4. S. Golden and T. R. Tuttle, *J. Phys. Chem.* **93**: 4109 (1990).
5. D. W. Mundell, *J. Chem. Ed.* **67**: 426 (1990).
6. F. A. Bergstrom and J. Lindren, *Inorg. Chem.* **31**: 1525 (1992).
7. Y. Liu and T. Ichiye, *J. Phys. Chem.* **100**: 2723 (1996).
8. A. K. Soper and A. Luzar, *J. Phys. Chem.* **100**: 1357 (1996).
9. B. Madan and K. Sharp, *J. Phys. Chem.* **100**: 7713 (1996).
10. G. Hummer, L. R. Pratt, and A. E. Garcia, *J. Phys. Chem.* **100**: 1206 (1996).

2.5. TOOLS FOR INVESTIGATING SOLVATION

2.5.1. Introduction

The more recently used methods for investigating the structure of the region around the ion are listed (though not explained) in Table 2.2. It is convenient to group the methods shown there as follows.

Several methods involve a study of the properties of solutions in equilibrium and are hence reasonably described as *thermodynamic*. These methods usually involve thermal measurements, as with the heat and entropy of solvation. Partial molar volume, compressibility, ionic activity, and dielectric measurements can make contributions to solvation studies and are in this group.

Transport methods constitute the next division. These are methods that involve measurements of diffusion and the velocity of ionic movement under electric field gradients. These approaches provide information on solvation because the dynamics of an ion in solution depend on the number of ions clinging to it in its movements, so that knowledge of the facts of transport of ions in solution can be used in tests of what entity is actually moving.

A third group involves the *spectroscopic approaches.* These are discussed in Section 2.11.

Finally, computational approaches (including the Monte Carlo and molecular dynamic approaches) are of increasing importance because of the ease with which computers perform calculations that earlier would have taken impractically long times.

2.5.2. Thermodynamic Approaches: Heats of Solvation

The definition of the heat of solvation of a salt is the change in heat content per mole for the imaginary[7] transition of the ions of the salt (sufficiently far apart so that they have negligible energies of interaction between them) from the gas phase into the dissolved state in solution. Again, a simplification is made: the values are usually stated for dilute solutions, those in which the interaction energies between the ions are negligible. Thus, the ion–solvent interaction is isolated.

The actual calorimetric measurement that is made in determining the heat of hydration of the ions of a salt is not the heat of hydration itself, but the heat of its dissolution of the salt in water or another solvent (Fajans and Johnson, 1942). Let this be ΔH_{soln}. Then one can use the first law of thermodynamics to obtain the property which it is desired to find, the heat of hydration. What kind of thought process could lead to this quantity? It is imagined that the solid lattice of the ions concerned is broken up and the ions vaporized to the gaseous state (heat of sublimation). Then one thinks of the ions as being transferred from their positions far apart in the gas phase to the dissolved state in dilute solution (heat of hydration). Finally, the cycle is mentally completed by imagining the dissolved ion reconstituting the salt-lattice ($-\Delta H_{soln}$). It is clear that by this roundabout or cyclical route[8] the sum of all the changes in the cycle should be equal to zero, for the initial state (the crystalline salt) has been re-formed.

This process is sketched in Fig. 2.13.

Thus,

$$L_{sub} + \Delta H_{s,salt} - \Delta H_{soln} = 0 \tag{2.3}$$

---

[7]It *is* an imaginary transition because we don't know any actual way of taking two individual ions from the gas phase and introducing them into a solution without passing through the potential difference, $\Delta\chi$, which occurs across the *surface* of the solution. There is always a potential difference across an interphase, and were ions *actually* to be transferred from the gas phase to the interior of a solution, the energy, $z_i e_o \Delta\chi$, would add to the work one calculates by the indirect method outlined here. It's possible to add this energy of crossing the interphase to the heats of solution of Table 2.4 and the resultant values are consequently called "real heats of solvation," because they represent the actual value that would be obtained if one found an experimental way to go from the vacuum through the interface into the solution.

[8]When, as here, an imaginary cycle is used to embrace as one of its steps a quantity not directly determinable, the process used is called a "Born–Haber cycle." The sum of all the heats in a cycle must be zero.

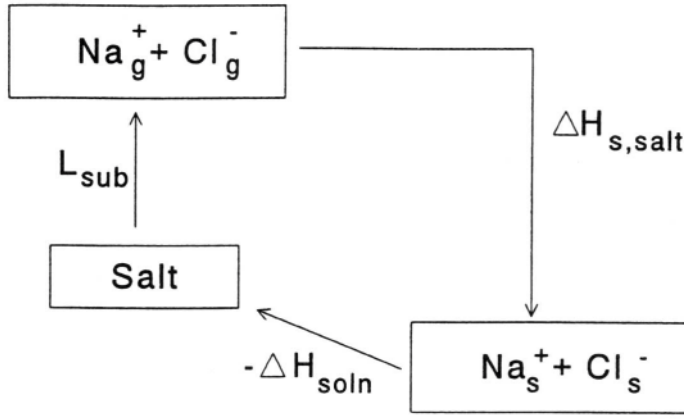

Fig. 2.13. An imaginary cycle–route process.

TABLE 2.4

Heats of Hydration of the Alkali Halides and Quantities Used in Their Derivation[a]

Salt	U_o (calc.)[b]	U^b (T – 291 K)[b]	Initial Heat of Solution, $\Delta H_{soln,o}$	$\Delta H_{s,+} + \Delta H_{s,-}$
Li-F	–245.5	–247.7	1.1	–245.9
–Cl	–201.8	–202.7	–8.6	–211.3
–Br	–191.0	–191.4	–11.1	–202.5
–I	–177.7	–177.6	–14.8	–192.4
Na-F	–217.2	–218.2	0.6	–217.6
–Cl	–185.0	–185.5	1.3	–184.2
–Br	–177.4	–177.8	0.2	–177.6
–T	–165.5	–165.6	–1.4	–167.0
K-F	–194.0	–194.7	–4.1	–198.8
–Cl	–169.2	–169.6	4.4	–165.2
–Br	–162.6	–162.8	5.1	–157.7
–I	–153.8	–153.9	5.1	–148.8
Rb-F	–184.5	–184.9	–5.8	–190.7
–Cl	–163.3	–163.4	4.5	–158.9
–Br	–157.4	–157.4	6.4	–151.0
–I	–149.3	–149.2	6.5	–142.7

[a] Units are kcal mol^{-1}. 1 calorie = 4.184 J.
[b] Lattice energy.

Now, only ΔH_{soln} (the heat of solution) is experimentally measured, and hence the evaluation of the heat of solvation of the salt, $\Delta H_{s,salt}$, by means of Eq. (2.3) involves trusting the reliability of information on the heat of sublimation of the salt, L_{sub}. In some cases, L_{sub} is known reliably (±1%) from calculations. Alternatively, it can be determined experimentally. From L_{sub}, then, and the measured heat of dissolution, ΔH_{soln}, the heat of hydration of the salt concerned in the solvent can be deduced.

Fajans (1962) was the first scientist to put these thoughts into practice. One finds that the determined heats of solvation are relatively small and endothermic (+) for some salts but exothermic (–) for others. However, lattice energies are known to be in the region of several hundreds of kilojoules mol^{-1}, so that, in rough terms [Eq. (2.3)], heats of solvation should not be more than a dozen kilojoules mol^{-1} (numerically) different from lattice energies. In Table 2.4 a compilation is given of the quantities mentioned earlier in the case of the alkali halides.[9] Now, the method described here gives the sum of the heat of hydration of the ions of a salt. The question of how to divide this sum up into individual contributions from each of the ions of a salt requires more than the thermodynamic approach that has been used so far. The way this is done is described in later sections (e.g., in Section 2.6.2 or 2.15.9).

2.5.3. Obtaining Experimental Values of Free Energies and Entropies of the Solvation of Salts

In the preceding section it was shown how to obtain, a little indirectly, the heat of solvation of a salt. However, it is the *free energies* of the participants in a chemical reaction that determine the state of equilibrium so that one cannot leave the situation with only the ΔH determined. Free energy and entropy changes have to be dealt with also.

How can the free energy of a solution be obtained? Consider a saturated solution of a 1:1 salt of the type MA. Because the solid salt lattice is in equilibrium with its ions in solution, the chemical potential of the salt, μ_{MA}, can be expressed in terms of its individual chemical potentials and activities (a_{M^+} and a_{A^-}) in solution,

$$\mu_{MA,crystal} = \mu^{\circ}_{MA,crystal} = \mu_{M^+A^-,soln}$$
$$= \mu^{\circ}_{M^+,soln} + RT \ln(a_{M^+})_{soln,sat} + \mu^{\circ}_{A^-,soln} + RT \ln(a_{A^-})_{soln,sat} \qquad (2.4)$$

In thermodynamic reasoning, there has to be a *standard state.* The standard state for the solid crystal is the substance in its pure state at 298 K. It follows that the standard chemical potential of solution is:

$$\Delta\mu^{\circ}_{soln} = \mu^{\circ}_{M^+,soln} + \mu^{\circ}_{A^-,soln} - \mu^{\circ}_{MA,crystal}$$
$$= -RT \ln [a_{M^+,soln,sat}\, a_{A^-soln,sat}] = -2\, RT \ln a_{\pm(soln,sat)} \qquad (2.5)$$

[9]The alkali halides are chosen as good examples because the lattice energy is particularly well known and reliable.

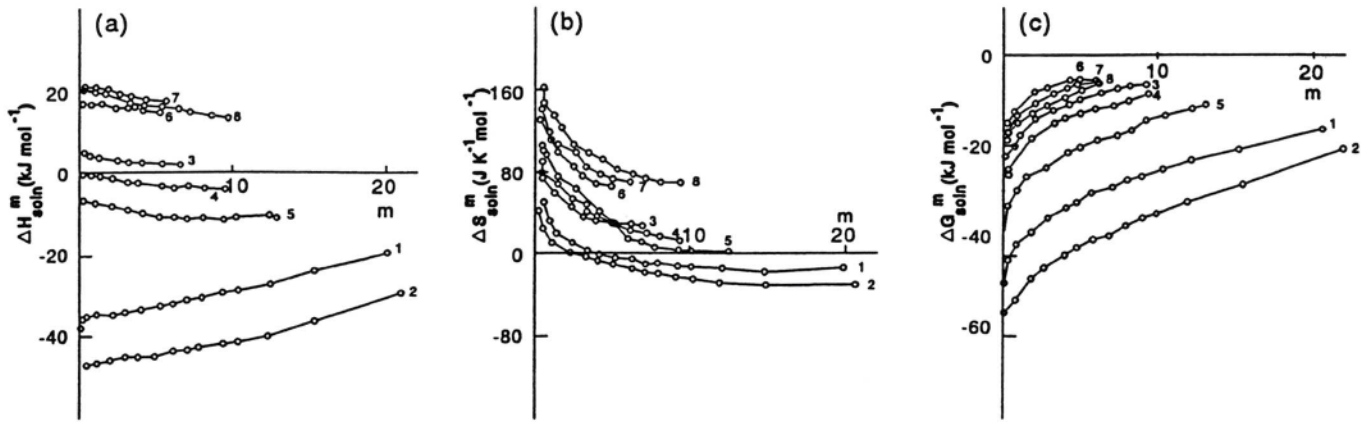

Fig. 2.14. Dependence of $\Delta H_{m,\text{soln}}$, $\Delta S_{m,\text{soln}}$, and $\Delta G_{m,\text{soln}}$ on electrolyte concentration in aqueous solutions for some alkali metal halides at 298.15 K: 1, LiCl; 2, LiBr; 3, NaCl; 4, NaBr; 5, NaI; 6, KCl; 7, KBr; 8, KI. (Reprinted from G. A. Krestov, *Thermodynamics of Solvation*, Ellis Harwood, London, 1991.)

where a is activity of the ion in solution and $a_{\pm(\text{soln,sat})}$ is the mean ionic activity of the solution defined as $a_\pm = (a_+ a_-)^{1/2}$.

Thus, if one knows the mean activity (see Section 2.9.1) of the electrolyte for the condition at which the solution is saturated and in equilibrium with the salt, one has the standard free energy change of solution. To obtain the standard free energy of solvation (hydration) from this, one has also to know the free energy of the salt lattice at 298 K. This is easily obtainable (see any physicochemical text) if there are data on the specific heat of the given salt as a function of temperature, so that the entropy of the salt in its standard state can be determined in the usual way of integrating the $\Delta C_p - T$ relation (where C_p is specific heat) to obtain entropies. Knowing then the standard free energy of solution and that of the salt lattice, one applies reasoning similar to that used earlier for the heats [Eq. (2.3)]. One can thus obtain free energies of hydration of salts. Knowing the $\Delta G°$ and $\Delta H°$ for the hydration process, one may calculate the standard entropy of solvation of the salt from the well-known thermodynamic equation $\Delta G_s^\circ = \Delta H_s^\circ - T\Delta S_s^\circ$. Values of ΔS_s° will be discussed further in Section 2.15.12, which covers the process of splitting up ΔS_s° into its component parts for the individual ions concerned.

Why should one bother with these thermodynamic quantities when the overall aim of this chapter is to determine the structure of liquids near ions? The answer is the same as it would be to the generalized question: What is the utility of thermodynamic quantities? They are the quantities at the base of most physicochemical investigations. They are fully *real*, no speculations or "estimates" are made on the way (at least as far as the quantities for salts are concerned). Their numerical modeling is the challenge that the theoretical approaches must face. However, such theoretical approaches must assume some kind of structure in the solution and only a correct assumption is going to lead to a theoretical result that agrees with experimental results. Thus, such agreement indirectly indicates the structure of the molecules.

Finally, this section ends with a reminder that heats, entropies, and free energies of hydration depend on concentration (Fig. 2.14) and that there are significant changes in values at very low concentrations. It is the latter values that are the desired quantities because at high concentrations the heats and free energies are influenced not only by ion–solvent interactions (which is the objective of the venture) but also by interionic forces, which are much in evidence (Chapter 3) at finite concentrations.

2.6. PARTIAL MOLAR VOLUMES OF IONS IN SOLUTION

2.6.1. Definition

The molar volume of a pure substance can be obtained from density measurements, i.e., ρ = (molecular weight)/(molar volume). The volume contributed to a solution by the addition of 1 mole of an ion is, however, more difficult to determine. In fact, it has to be measured indirectly. This is because, upon entry into a solvent, the

ion changes the volume of the solution not only by its own volume, but by the change due, respectively, to a breakup of the solvent structure near the ion and the compression of the solvent under the influence of the ion's electric field (called *electrostriction*; see Section 2.22).

The effective ionic volume of an ion in solution, the partial molar volume, can be determined via a quantity that *is* directly obtainable. This is the apparent molar volume of a salt, $V_{m,2}$, defined by

$$V_{m,2} = \frac{V - n_1 V_{m,1}}{n_2} \tag{2.6}$$

where V is the volume of a solution containing n_1 moles of the solvent and n_2 moles of the solute and $V_{m,1}$ is the molar volume of the solvent. It is easily obtained by measuring the density of the solution.

Now, if the volume of the solvent were not affected by the presence of the ion, $V - n_1 V_{m,1}$ would indeed be the volume occupied by n_2 moles of ions. However, the complicating fact is that the solvent volume is no longer $V_{m,1}$ per mole of solvent; the molar volume of the solvent is affected by the presence of the ion, and so $V_{m,2}$ is called the *apparent* molar volume of the ion of the salt. Obviously, as when $n_2 \to 0$, the apparent molar volume of the solvent in the solution must become the real one, because the disturbing effect of the ion on the solvent's volume will diminish to zero. Hence, at *finite* concentration, it seems reasonable to write the following equation:

$$\tilde{V} = \tilde{V}^0 + n_2 \left(\frac{\partial V_{m,2}}{\partial n_2} \right)_{T,P,n_1} \tag{2.7}$$

This equation tells one that the density of the solution that gives $V_{m,2}$ for a series of concentrations gives the partial molar volume $\tilde{V}$ at any value of n_2. Knowing $V_{m,2}$ from ρ_{soln} and ρ°, Eq. (2.7) can be used to obtain $\tilde{V}$ as a function of n_2. Extrapolation of $\tilde{V}$ to $n_2 = 0$ gives the partial molar volume of the electrolyte *at infinite dilution*, $\tilde{V}^0$ (i.e., free of interionic effects).

Once partial molar volumes are broken down into the individual partial ionic volumes (see Section 2.6.2), the information given by partial molar volume measurements includes the net change in volume of the solvent that the ion causes upon entry and hence it provides information relevant to the general question of the structure near the ion, that is, its solvation.

2.6.2. How Does One Obtain Individual Ionic Volume from the Partial Molar Volume of Electrolytes?

From an interpretive and structural point of view, it is not much use to know the partial molar volumes of electrolytes unless one can separate them into values for each ion. One way of doing this might be to find electrolytes having ions with the same

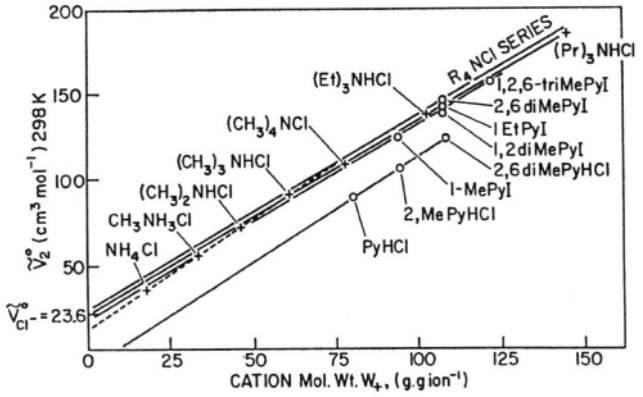

Fig. 2.15. Plot of infinite-dilution partial molar volumes of homologous R_4N^+ chlorides in water against the cation molecular weight, allowing extrapolation to obtain $\tilde{V}^0_{Cl^-}$. (Reprinted from B. E. Conway, *Ionic Hydration in Chemistry and Biophysics*, Elsevier, New York, 1981.)

crystallographic radii (the standard example is KF) and allot to each ion one half of the partial molar volume of the electrolyte. However, this method does not give results in agreement with those of other methods, which agree among themselves. Why is this? It is because electrostriction and the breakdown of the solvent structure in the neighborhood of the ion are not purely Coulombic (depending on simple distance laws), but are also specific (depending to some degree on chemical bonding, like hydrogen bond formation between ion and solvent).

Correspondingly, objections can be made to making a plot of the values of $\tilde{V}$ for the electrolyte against $1/\tilde{V}_{cation}$, and extrapolating to $1/\tilde{V}_{cation} = 0$. At first sight, one thinks this should give the value of the partial molar volume for an anion which is the partner of each of the various cations of increasing size in the data that would make up the plot.[10] However, questions of the specificity of some interactions, the absence of allowance for dead space, etc., make this approach too flawed to be acceptable.

2.6.3. Conway's Successful Extrapolation

Conway has suggested a method that seems to give results in agreement with those of a second entirely different method, the *ionic vibration* method (see later discussion). Conway found that plotting the partial molar volume of a series of electrolytes involving large cations (e.g., a tetraalkylammonium series) and a constant smaller

[10]Of course, if one obtains reliably the value of $\tilde{V}_i^0$ for one ion, then knowing the partial molar volumes for a series of electrolytes containing that one known ion enables the $\tilde{V}_i^0$ for the counterions of a series of electrolytes to be known.

anion, Cl^-, against the *molecular weight* of the cation (instead of the reciprocals of the cations' volumes) is useful. Extrapolation of this plot to zero cation molecular weight should give the partial gram-ionic volume for the partner anion. Conway's plot is given in Fig. 2.15. The method works because the tetraalkylammonium ions are large and hence cause little electrostriction (i.e., compression of the surrounding solvent), which is the reason for the apparent lack of agreement of the other extrapolations. The reason for the apparent absence of other specific effects, such as the structure breaking which the big tetraalkylammonium cations would be expected to produce, is less obvious. The basis for the success claimed by Conway's method is the agreement (particularly for $\tilde{V}^0_{H^+}$) of the values it gives with those of an entirely different method, the ionic vibration approach (Section 2.7). The values for $\tilde{V}^0_{Cl^-}$ and $\tilde{V}^0_{H^+}$ from the present method are found to be 23.6 and –5.7 $cm^3\ mol^{-1}$, respectively. Why is one of these values negative? It can only mean that addition of H^+ to the solution causes more contraction among the surrounding solvent molecules than the volume added by the cation (which in this case is small).

2.7. COMPRESSIBILITY AND VIBRATION POTENTIAL APPROACH TO SOLVATION NUMBERS OF ELECTROLYTES

2.7.1. Relation of Compressibility to Solvation

In 1938, Passynski made the following argument, which relates the compressibility of a solution to the sum of the *primary* solvation numbers of each ion of an electrolyte. Primary here means ions that are so compressed by the ions' field that they themselves have zero compressibility.

Passynski measured the compressibility of solvent (β_0) and solution (β), respectively, by means of sound velocity measurements. The compressible volume of the solution is V and the incompressible part, v ($v/V = \alpha$). The compressibility is defined in terms of the derivative of the volume with respect to the pressure, P, at constant temperature, T. Then,

$$\beta_0 = -\frac{1}{V-v}\left(\frac{\partial(V-v)}{\partial P}\right)_T = -\frac{1}{V-v}\left(\frac{\partial V}{\partial P}\right)_T \tag{2.8}$$

$$\beta = -\frac{1}{V}\left(\frac{\partial V}{\partial P}\right)_T \tag{2.9}$$

Therefore

$$\frac{\beta}{\beta_0} = \frac{V-v}{V} = \frac{V-\alpha V}{V} \tag{2.10}$$

and

$$\alpha = 1 - \frac{\beta}{\beta_0} = \frac{v}{V} \tag{2.11}$$

Let the g-moles of salt be n_2; these are dissolved in n_1 g-moles of solvent. Then, there are $\alpha n_1/n_2$ g-moles of incompressible solvent per g-mole of solute. This was called by Passynski (not unreasonably) the *primary solvation number* of the salt, although it involves the assumption that water held so tightly as to be incompressible will qualify for primary status by traveling with the ion.

To obtain *individual* ionic values, one has to make an assumption. One takes a large ion (e.g., larger than I^-) and assumes its primary solvation number to be zero,[11] so that if the total solvation number for a series of salts involving this big anion is known, the individual hydration numbers of the cations can be obtained. Of course, once the hydration number for the various cations is determined by this artifice, each cation can be paired with an anion (this time including smaller anions, which may have significant hydration numbers). The *total* solvation numbers are determined and then, since the cation's solvation number is known, that for the anion can be obtained.

In Passynski's theory, the basic assumption is that the compressibility of water sufficiently bound to an ion to travel with it is zero. Onori thought this assumption questionable and decided to test it. He used more concentrated solutions (1–4 mol dm^{-3}) than had been used by earlier workers because he wanted to find the concentration at which there was the beginning of an overlap of the primary solvation spheres (alternatively called Gurney co-spheres) of the ion and its attached primary sheath of solvent molecules.

Figure 2.16 shows the plot of the mean molar volume of the solution $\bar{V}_m$ multiplied by the compressibility of the solution β as a function of the molar fraction of the NaCl solute x_2. At $x_2 \approx 0.07$ (~4 mol dm^{-3}), the values for the three temperatures become identical. Onori arbitrarily decided to take this to mean that $\beta\bar{V}_m$ has no further temperature dependence, thus indicating that *all the water in the solution* is now in the hydrated sphere of the ions and these, Onori thought, would have a β with no temperature dependence (for they would be held tight by the ion and be little dependent on the solvent temperature).

These assumptions allow the compressibility of the hydration sheath itself to be calculated (Passynski had assumed it to be negligible). To the great consternation of some workers, Onori found it to be significant—more than one-tenth that of the solvent value.

---

[11]Thus, whether molecules move off with an ion is determined by the struggle between the thermal energy of the solution, which tends to take the water molecule away from the ion into the solvent bulk, and the attractive ion–dipole force. The larger the ion, the less likely it is that the water molecule will remain with the ion during its darting hither and thither in solution. A sufficiently large ion doesn't have an adherent (i.e., primary) solvation shell, i.e., $n_x = 0$.

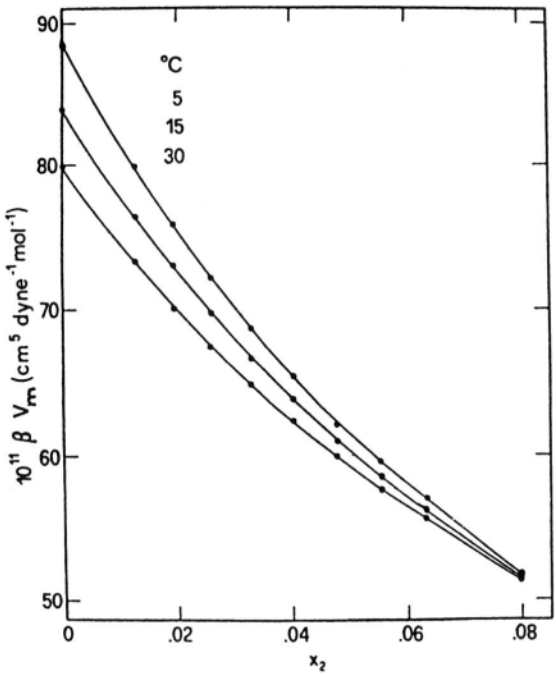

Fig. 2.16. Adiabatic compressibility of aqueous sodium chloride solutions as a function of salt mole fraction, x_2, at various temperatures. The solid line is the calculated compressibility. The expected error is on the order of the dot size. (Reprinted from G. Onori, *J. Chem. Phys.* **89:** 510, 1988.)

Taking into account a finite compressibility of the hydration waters led Onori to suggest solvation numbers that differed from those of Passynski with his assumption of zero compressibility of the inner region of the solvation shell. For example, for a 1.5 *M* solution, Onori has the value 19 for the sum of the solvation numbers of Na^+ and Cl^-, whereas the Passynski at 0.05 *M* solution is 6! However, later on (Section 2.22), when electrostriction is discussed in detail, Onori's estimate will be shown to be unlikely.

2.7.2. Measuring Compressibility: How It Is Done

The most convenient way to measure the compressibility of a liquid or solution is from the velocity of sound in it. A well-known equation derived in physics texts states that

$$\beta = \frac{1}{c_0^2 \rho} \tag{2.12}$$

where c_0 is the velocity of an ultrasonic wave in the medium and ρ is the density.

Note that β determined by this equation is an *adiabatic* β, not an isothermal one, because the local compression that occurs when the ultrasound passes through the solution is too rapid to allow an escape of the heat produced.[12]

A word about a particularly clever sound velocity measurement technique is justified. It is due in its initial form to Richards et al. One creates an ultrasonic vibration by bringing a piezoelectric crystal with oscillations in the megahertz range into contact with a fixed transducer. The latter has one face in contact with the liquid and sends out a beam of sound through it. Another transducer (the receiver) is not fixed and its position is varied with respect to that of the first transducer over distances that are small multiples of the wavelengths of the sound waves ($\sim 5 \times 10^{-3}$ cm). A stepping motor is used to bring about exact movements, and hence positions, of the receiver transducer. As the movable transducer passes through nodes of the sound waves, the piezoelectric crystal on the receiver transducer reacts and its signal is expressed through an electronic circuit to project Lissajous figures (somewhat like figures of eight) on the screen of a cathode ray oscilloscope. When these figures attain a certain configuration, they indicate the presence of a node (the point in a vibration where the amplitude is negligible) and by counting the number of nodes observed for a given distance of travel of the receiver transducer, the distance between two successive nodes—the wavelength of sound in the liquid (λ)—is obtained. The frequency of piezoelectric crystal used (e.g., barium titanate), ν (e.g., 5 MHz), is known. Because

$$\nu\lambda = c_0 \tag{2.13}$$

where c_0 is the velocity of sound needed in Eq. (2.12) for the compressibility, the latter can be found from Eq. (2.13).

2.8. TOTAL SOLVATION NUMBERS OF IONS IN ELECTROLYTES

Total solvation numbers arise directly from the discussion following Passynski's Eq. (2.11), which requires measurements only of the compressibility (β) of the solution (that of the solvent usually being known). Bockris and Saluja used this method in 1972 to obtain the total solvation numbers of both ions in a number of salts (Table 2.5).

In the next section it will be shown how these total solvation numbers for salts can be turned into individual solvation numbers for the ions in the salt by the use of information on what are called "ionic vibration potentials," an electrical potential

[12] A study of the temperature dependence of β shows that it is positive for tetraalkylammonium salts.

TABLE 2.5

Adiabatic Compressibility and Total Solvation Number of Electrolytes as a Function of Concentration at 298 K

c (mol/liter)	Adiabatic Compressibility $\times 10^6$ (bar^{-1})	Total Solvation Number of Salt	c (mol/liter)	Adiabatic Compressibility $\times 10^6$ (bar^{-1})	Total Solvation Number of Salt
	NaF			$BaBr_2$	
1.0	38.72	7.5 ± 0.0	3.29	20.39	7.5 ± 0.0
0.5	41.57	7.9 ± 0.0	1.21	33.60	10.7 ± 0.0
0.1	44.04	8.5 ± 0.3	0.50	39.59	12.4 ± 0.0
0.05	44.35	9.1 ± 0.1	0.14	43.09	14.6 ± 0.2
			0.05	44.1	15.2 ± 0.5
	NaCl				
5.1	26.75	3.9 ± 0.0		BaI_2	
2.0	36.64	4.7 ± 0.0	2.50	26.00	9.1 ± 0.0
0.1	40.04	5.7 ± 0.0	0.50	39.86	11.7 ± 0.0
0.1	44.20	6.5 ± 0.3	0.25	41.99	13.2 ± 0.1
0.05	44.45	6.9 ± 0.5	0.05	44.05	15.4 ± 0.4
			0.025	44.40	16.2 ± 1.0
	NaBr				
5.2	26.93	3.7 ± 0.0		$MgCl_2$	
2.0	35.99	5.1 ± 0.0	4.22	21.61	6.1 ± 0.0
1.1	39.75	5.7 ± 0.0	2.11	29.74	8.4 ± 0.0
0.1	44.23	6.1 ± 0.3	1.05	35.94	10.1 ± 0.0
0.05	44.47	6.3 ± 0.5	0.09	43.88	12.3 ± 0.3
			0.05	44.21	12.8 ± 0.6
	NaI				
5.0	28.78	3.2 ± 0.0		$CaCl_2$	
2.1	36.83	4.4 ± 0.0	4.05	22.90	5.9 ± 0.0
1.0	40.84	4.6 ± 0.0	2.02	30.94	8.0 ± 0.0
0.1	44.28	5.5 ± 0.3	1.00	36.91	9.4 ± 0.0
0.05	44.48	6.1 ± 0.5	0.10	43.82	11.1 ± 0.3
			0.05	44.22	12.1 ± 0.5
	LiCl				
5.0	29.93	3.3 ± 0.0		$SrCl_2$	
2.0	37.15	4.5 ± 0.0	3.11	27.38	6.2 ± 0.0
1.0	40.60	4.9 ± 0.0	1.50	33.91	8.5 ± 0.0
0.1	44.30	5.3 ± 0.3	0.80	38.42	9.5 ± 0.0
0.05	44.49	6.0 ± 0.4	0.10	44.04	8.8 ± 0.3
			0.03	44.45	13.2 ± 0.8

TABLE 2.5
Continued

c (mol/liter)	Adiabatic Compressibility $\times 10^6$ (bar^{-1})	Total Solvation Number of Salt	c (mol/liter)	Adiabatic Compressibility $\times 10^6$ (bar^{-1})	Total Solvation Number of Salt
	KCl				
4.0	29.88	4.0 ± 0.0		$LaCl_3$	
1.0	39.84	5.7 ± 0.0	1.68	28.11	11.6 ± 0.0
0.17	43.90	6.2 ± 0.1	0.34	40.51	15.4 ± 0.0
0.05	44.46	6.6 ± 0.5	0.03	44.23	18.3 ± 0.7
			0.02	44.47	18.9 ± 1.4
	RbCl				
3.5	31.84	4.0 ± 0.0		$CeCl_3$	
1.7	38.13	4.9 ± 0.0	1.68	29.74	9.7 ± 0.0
0.9	41.17	4.9 ± 0.0	0.34	40.73	14.6 ± 0.0
0.1	44.30	5.0 ± 0.2	0.03	44.14	21.5 ± 0.7
0.05	44.50	5.5 ± 0.5	0.02	44.42	22.4 ± 1.3
	CsCl			$ThCl_4$	
5.0	28.15	3.2 ± 0.0	1.25	29.39	14.5 ± 0.0
1.0	42.03	3.2 ± 0.0	0.25	40.90	18.8 ± 0.0
0.1	44.43	3.6 ± 0.3	0.11	42.84	21.0 ± 0.3
0.05	44.52	5.1 ± 0.5	0.05	43.72	22.9 ± 0.5
			0.03	44.19	26.6 ± 1.1
	$BaCl_2$				
1.65	30.90	9.9 ± 0.0			
0.74	37.65	11.6 ± 0.0			
0.50	39.44	12.8 ± 0.0			
0.1	43.65	13.5 ± 0.0			
0.05	44.14	14.6 ± 0.5			

Source: Reprinted from J. O'M. Bockris and P. P. S. Saluja, *J. Phys. Chem.* **76**: 2140, 1972.

difference that can be detected between two electrodes sending sound waves to each other.

2.8.1. Ionic Vibration Potentials: Their Use in Obtaining the Difference of the Solvation Numbers of Two Ions in a Salt

Sound waves pass through matter by exerting a force on the particles in the path of the beam. Transmission of the sound occurs by each particle giving a push to the next particle, and so on.

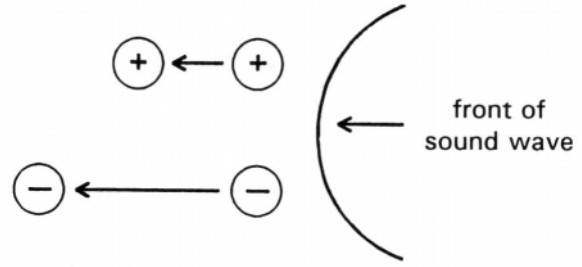

Fig. 2.17. Debye vibronic potential. Schematic on origin. In one phase of the sound waves, both ions are accelerated toward the left. However, small cations tend to be heavier than small anions because the cations carry a larger load of primary hydration water.

When a beam of sound is emitted from a transducer onto a solution that contains cations and anions, each having a different mass, these masses undergo a different degree of displacement per cycle, for while each receives the same pulse from the sound, each has a different inertia. Figure 2.17 shows that the displacement of each ion in one phase of the cycle is canceled in the next. However, there is a net difference in position of the cation and anion which remains and this gives rise to a degree of nonelectroneutrality that can be measured in the form of an ionic vibration potential, usually found to be in the range of $1\text{–}5\ \mu\text{V cm}^{-1}\ \text{s}$.

In 1933 Peter Debye formulated a sophisticated theory about all this.[13] He assumed, as is also intuitively obvious, that the "supersonic emf," that is, the ionic vibration potential produced by the ultrasonic beam, would be proportional to the *difference* of the masses of the moving ions. Debye's expression can be reduced to

$$\Delta E = 1.55 \times 10^{-7}\, a_0 \left(\frac{t_+}{z_+} m_{m,+} - \frac{t_-}{z_-} m_{m,-} \right) \tag{2.14}$$

where a_0 is the velocity amplitude[14] of the ultrasonic wave; t_+ and t_- are the respective transport numbers of cation and anion; and z_+ and z_- are the corresponding charges on cation and anion. The *apparent molar mass*, $m_{m,i}$, of the moving ion is defined as the mass of the solvated ion minus the mass of the solvent displaced, $V_1\rho_1$, where ρ_1 is the density of the solvent and V_1 its volume.

---

[13]It is of interest to note that the lengthy and complex calculation Debye made was published in the same (first) edition of the *Journal of Chemical Physics* as an article by Bernal and Fowler, who first suggested several seminal concepts about the structure of water that are now commonly accepted in solution theory.

[14]The velocity amplitude is measured in cm s^{-1}. It is the ratio of the pressure of the ultrasonic wave to the characteristic acoustic impedance of the media.

Now the mass of the solvated ion $(M_i)_s$ is the sum of the mass of the bare ion, M_i, and that of the primary solvation water, $n_i M_1$, where n_i is the solvation number of the ion and M_1 is the molar weight of the solvent.

Thus:

$$m_{m,i} = M_i + n_i M_1 - V_1 \rho_1 \tag{2.15}$$

If one takes this definition of $m_{m,i}$ and uses it in the above expression for ΔE, one obtains the rather lengthy expression:

$$\left(\frac{t_+}{z_+}\right) n_+ - \left(\frac{t_-}{z_-}\right) n_- = \frac{\Delta E / a_0}{M_1\, 1.55 \times 10^{-7}} - \frac{1}{M_1}\left(\frac{t_+}{z_+} M_+ - \frac{t_-}{z_-} M_-\right)$$

$$+ \frac{\rho_1}{M_1}\left(\frac{t_+}{z_+}(V_1) - \frac{t_-}{z_-}(V_s)\right) \tag{2.16}$$

Now, for the aqueous case, Eq. (2.16) reduces to

TABLE 2.6

Relevant Parameters to Obtain Individual Solvation Numbers

Electrolyte	t_+ (Infinite Dilution)	t_- (Infinite Dilution)	$(V_s)_+$, $cm^3\ mol^{-1}$	$(V_s)_-$, $cm^3\ mol^{-1}$	A	ψ_0/a_0, $\mu V\ cm^{-1}\ s$ 0.05 N	0.1 N	1.0 N	5.0 N
NaF	0.476	0.524	115.8	110.1	−0.20	1.0	1.0	0.9	Insol
NaCl	0.396	0.604	115.8	92.4	0.14	1.1	1.0	0.7	(0.7)
NaBr	0.392	0.608	115.8	90.7	1.66	−2.8	−2.8	−2.6	(−2.6)
NaI	0.395	0.605	115.8	91.5	3.23	−6.4	−6.4	−5.7	(−5.7)
LiCl	0.336	0.664	140.7	92.4	0.40	0.1	0.1	0.05	(0.0)
KCl	0.490	0.510	91.5	92.4	−0.20	1.7	1.7	1.7	(1.7)
RbCl	0.511	0.489	89.9	92.4	−1.42	5.2	5.2	(5.2)	(5.2)
CsCl	0.500	0.500	89.9	92.4	−2.78	8.1	8.1	(8.1)	(8.1)
$BaCl_2$	0.454	0.546	166.4	92.4	−1.35	4.2	4.2	3.6	(3.6)
$BaBr_2$	0.448	0.552	166.4	90.7	−0.03	−1.8	1.6	−0.8	(0.8)
BaI_2	0.452	0.548	166.4	91.5	1.45	−1.7	1.8	−2.0	(2.03)
$MgCl_2$	0.410	0.590	197.9	92.4	0.12	1.1	1.0	1.0	(1.0)
$CaCl_2$	0.438	0.562	176.5	92.4	−0.12	1.1	1.1	1.0	0.8
$SrCl_2$	0.438	0.562	176.5	92.4	−0.70	2.6	2.5	2.1	1.8
$LaCl_3$	0.476	0.524	233.1	92.4	−0.82	3.9	3.7	3.2	(3.2)
$CeCl_3$	0.460	0.540	233.1	92.4	−0.91	3.8	3.8	3.0	2.5
$ThCl_4$	0.485	0.515	330.9	92.4	−0.95	3.4	3.2	2.9	(2.9)

Source: Reprinted from J. O'M. Bockris and P. P. S. Saluja, *J. Phys. Chem.* **76**: 2140, 1972.

TABLE 2.7

Absolute Values of Ionic Solvation Number (SN) vs. Concentration at 298 K

Electrolyte	Concentration	SN of Cation	SN of Anion	Electrolyte	Concentration	SN of Cation	SN of Anion
NaF	1.0	4.0	3.5	$BaBr_2$	3.29	5.7	0.9
	0.5	4.3	3.6		1.21	7.9	1.4
	0.1	4.6	3.9		0.50	9.2	1.6
NaCl	5.1	2.8	1.1		0.14	11.1	1.8
	2.0	3.2	1.5		0.05	11.6	1.8
	1.0	3.8	1.9	BaI_2	2.50	7.4	0.9
	0.1	4.4	2.1		0.50	9.2	1.3
	0.05	4.7	2.2		0.25	10.3	1.5
NaBr	5.2	3.0	0.7		0.05	11.9	1.8
	2.0	3.8	1.3		0.025	12.6	1.8
	1.1	4.2	1.5	$MgCl_2$	6.22	5.1	0.5
	0.1	4.4	1.7		2.11	6.8	0.8
	0.05	4.5	1.8		1.05	8.1	1.0
NaI	5.0	3.1	0.1		0.09	9.7	1.3
	2.1	3.8	0.6		0.05	10.1	1.4
	1.0	4.0	0.6	$CaCl_2$	4.05	4.5	0.7
	0.1	4.3	1.2		2.02	5.0	1.0
	0.05	4.6	1.5		1.00	7.1	1.2

LiCl	5.0	2.6	0.7		0.10	8.3	1.4
	2.0	3.4	1.1		0.05	9.1	1.5
	1.0	3.7	1.2	$SrCl_2$	3.11	4.4	0.9
	0.1	3.9	1.4		1.50	6.0	1.3
	0.05	4.4	1.6		0.80	6.9	1.3
KCl	4.0	2.4	1.6		0.10	6.6	1.1
	1.0	3.3	2.4		0.03	9.8	1.7
	0.17	3.6	2.6	$LaCl_3$	1.68	9.4	0.7
	0.05	3.8	2.8		0.34	12.3	1.0
RbCl	3.5	2.4	1.6		0.03	14.8	1.2
	1.7	2.8	2.1		0.02	15.3	1.2
	0.9	2.8	2.1	$CeCl_3$	1.68	7.5	0.7
	0.1	2.9	2.1		0.34	11.6	1.0
	0.05	3.1	2.4		0.03	17.4	1.4
CsCl	5.0	1.7	1.5		0.02	18.1	1.4
	1.0	1.7	1.5	$ThCl_4$	1.25	11.9	0.6
	0.1	1.9	1.7		0.25	15.4	0.8
	0.05	2.7	2.4		0.11	17.4	0.9
$BaCl_2$	1.65	6.9	1.5		0.05	18.4	1.1
	0.74	8.2	1.7		0.03	22.0	1.1
	0.50	9.0	1.9				
	0.10	9.7	1.9				
	0.05	10.5	2.0				

Source: Reprinted from J. O'M. Bockris and P. P. S. Saluja, *J. Phys. Chem.* **76**: 2140, 1972.

$$\left(\frac{t_+}{z_+}\right)n_+ - \left(\frac{t_-}{z_-}\right)n_- = \frac{\Delta E/a_0}{2.79} + A \tag{2.17}$$

where A depends on the electrolyte.

Bockris and Saluja applied these equations derived by Debye to a number of electrolytes and, using data that included information provided by Conway and by Zana and Yeager, calculated the difference of the solvation numbers of the ions of salts. The relevant parameters are given in Table 2.6.

Now, since the ultrasound method gives the difference of the hydration numbers, while the compressibility method gave the sum, individual values can be calculated (Table 2.7).

2.9. SOLVATION NUMBERS AT HIGH CONCENTRATIONS

2.9.1. Hydration Numbers from Activity Coefficients

A nonspectroscopic method that has been used to obtain hydration numbers at high concentrations will be described here only in qualitative outline. Understanding it quantitatively requires a knowledge of ion–ion interactions, which will be developed in Chapter 3. Here, therefore, are just a few words of introduction.

The basic point is that the mass action laws of chemistry ([A][B]/[AB] = constant) do not work for ions in solution. The reason they do not work puzzled chemists for 40 years before an acceptable theory was found. The answer is based on the effects of electrostatic interaction forces between the ions. The mass action laws (in terms of concentrations) work when there are no charges on the particles and hence no long-range attraction between them. When the particles are charged, Coulomb's law applies and attractive and repulsive forces (dependent on $1/r^2$ where r is the distance between the ions) come in. Now the particles are no longer independent but "pull" on each other and this impairs the mass action law, the silent assumption of which is that ions are free to act alone.

There are several ways of taking the interionic attraction into account. One can work definitionally and deal in a quantity called "*activity*," substituting it for concentration, whereupon (by definition) the mass action law works. Clearly, this approach does not help us understand why charges on the particles make the concentration form of the mass action law break down.

From a very dilute solution (10^{-4} mol dm^{-3}) to about 10^{-2} mol dm^{-3}, the ratio of the activity to the concentration (a_i/c_i or the *activity coefficient*, γ_i) keeps on getting smaller (the deviations from the "independent" state increase with increasing concentration). Then, somewhere between 10^{-2} and 10^{-1} M solutions of electrolytes such as NaCl, the activity coefficient (the arbiter of the deviations) starts to hesitate as to which direction to change with increasing concentration; above 1 mol dm^{-3}, it turns around and *increases* with increasing concentration. This can be seen schematically in Fig. 2.18.

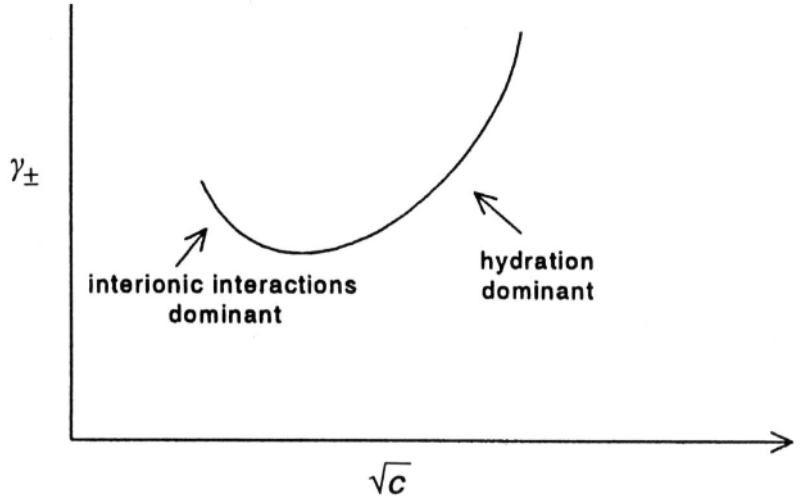

Fig. 2.18. Schematic of the observed trend of $\gamma_\pm$ versus $\sqrt{c}$ curve for salts showing a minimum.

Why does it do this? There may be more than one reason. A reason that was suggested long ago by Bjerrum and developed intensively by Stokes and Robinson in the 1950s is concerned with solvation and has more than historical interest. This is how they argued.

In 1 liter ($1\ dm^3$) of pure water, there are 55.5 mol of water [(1000 g)/(18 g/mol)], all of it available to solvate ions. As ions are added, the water can be divided into two types, the so-called *free water* (unattached to any ions) and the *water associated* with (i.e., hydrating) ions.

The idea is that the water adhering to ions is out of commission as far as functions of the free water go. Only a fraction of the free water is available to solvate the added ions. That is, the effective concentration is increased compared with that which one would calculate if one assumed all the water was active. Thus, in the "concentration" calculation (so and so many moles of ions per liter of water), it is implicitly assumed that all the water molecules are "active." Suppose half the water molecules are temporarily associated with ions; then the *effective* concentration (i.e., the activity) is doubled.

Of course, in this simplified presentation, one assumes that by the time the concentration is so high that the activity coefficient–concentration relation turns upward (Fig. 2.18), the interionic interaction effects, although still there, have been overwhelmed by the effect of ions in reducing free waters. In reality, both this effect and the interionic effects that dominated at lower concentrations (below the minimum) should be taken into account.

By now, the reader will begin to see the point, and how all this is related to determining hydration number. In Chapter 3, a quantitative expression between this

activity coefficient and the concentration will be developed. In it, the unknown is n_h, the *hydration number* of the electrolyte. The sum of the hydration number of the cation and anion will be found and so a measurement of the activity coefficient at a particular concentration (from, e.g., 0.1 mol dm^{-3} up to 10 mol dm^{-3}) will yield the hydration number at that concentration.

A second difficulty is more subtle. The activity coefficient is determined not only by water that is adhering to ions, but also by increasing interionic effects, and our ability to allow for these at very high concentrations such as 5 mol dm^{-3} is not good. Spectroscopy tells us also that ionic association is occurring in these high ranges, but there is not much information on this association for ions that do not have IR spectra (e.g., Na^+ and Cl^-). These matters will be discussed again quantitatively in Chapter 3.

2.10. TRANSPORT

2.10.1. The Mobility Method

The mobility method is a rough-and-ready method for obtaining information on the number of solvent molecules that accompany an ion in motion. Its basic theory is really quite simple. One equates the electrostatic force pulling the ion forward, $z_i e_0 X$ ($z_i e_0$ = charge of the ion; X = electric field gradient), to the viscous resistance to the ion's flow. This view neglects all interionic interactions (Chapter 4) but would apply at sufficiently high dilution. This viscous resistance is given by Stokes' law, $6\pi r \eta v$, where r is the radius of the entity moving through a liquid of viscosity η and at a velocity v. The bulk viscosity is used. However, in reality an ion breaks up the solvent near it as it darts from here to there in the solution, so that a viscosity less than that of the undisturbed bulk water should be used with Stokes' law. Again, to determine the radius of the ion plus the adherent solvent and to determine how many water molecules fit in, one has to know the volume of water attached to the ion. This is not the ordinary bulk volume but a compressed value arising from the effect of the ion's field on normal water.

Finally, the validity of using Stokes' law to find the force of viscous resistance against movement in a liquid has to be questioned. In the original derivation of this formula, the model used was that of a *solid sphere* passing in a stately way in a straight line through a viscous fluid like molasses. The extrapolation to atomic-sized particles that move randomly in a solvent which itself has innumerable complex, dynamic movements might be thought to stretch the equation so far from its original model that it would become inapplicable. Nevertheless, tests (Chapter 5) show that Stokes' law *does* apply, although, depending on the shape of the particle, the 6 (which is valid for spheres) might have to be modified for other shapes (e.g., 4 for cylinders).

Now, from the equivalent conductivity of an electrolyte Λ (Chapter 4, Section 4.3.7) at concentrations low enough so that the ions are virtually free from the influence

of interionic forces, or ion-pair formation, individual ions (none associated into pairs) can be related to the mobility of the ions, u_+ and u_- by the equation (Section 4.4.5).

$$\Lambda = F(u_+ + u_-) \tag{2.18}$$

The transport number (Section 4.5.2) of the cation, t_+, is given by

$$t_+ = \frac{u_+}{u_+ + u_-} = \frac{u_+ F}{\Lambda} \tag{2.19}$$

and

$$u_i = \frac{t_i \Lambda}{F} \tag{2.20}$$

In electrostatics, a charge q under the influence of a field X experiences a force Xq. Here,

$$z_i e_0 X = 6\pi r_S \eta \; u_i \tag{2.21}$$

where r_S is r_{Stokes} (the radius of the ion and its primary solvation shell) and this allows one to use independent knowledge of the mobility, u_i, to obtain the radius of the moving solvated ion (Chapter 3). One also knows the crystallographic radius of the bare ion inside the solvation sheath, r_c. Hence:

$$V_{\text{hydrated water}} = \frac{4}{3}\pi(r_S^3 - r_c^3) \tag{2.22}$$

$$n_s = \frac{r_S^3 - r_c^3}{r_{H_2O}^3} \tag{2.23}$$

TABLE 2.8

Nearest Integer Hydration Number of Electrolytes from the Mobility Method and the Most Probable Value from Independent Experiments

Salt	Hydration Number (nearest integer)	Hydration Number from Other Experimental Methods
LiCl	7	7 ± 1
LiBr	8	7 ± 1
NaCl	4	6 ± 2
KCl	2	5 ± 2
KI	3	4 ± 2

TABLE 2.9
Primary Hydration Numbers from Ionic Mobility Measurements

Ion	Li^+	Na^+	Mg^{2+}	Ca^{2+}	Ba^{2+}	Zn^{2+}	Cd^{2+}	Fe^{2+}	Cu^{2+}	Pb^{2+}
V_s	31.8	15.0	95.2	67.8	48.5	92.3	91.2	92.3	95.0	34.3
n_{min}	3.5	2	10.5	7.5	5	10	10	10	10.5	4
n_{max}	7	4	13	10.5	9	12.5	12.5	12.5	12.5	7.5

Source: Reprinted from B. E. Conway, *Ionic Hydration in Chemistry and Biophysics*, Elsevier, New York, 1981.

is a rough expression for the volume occupied by water molecules that move with one ion. The expression is very approximate (Tables 2.8 and 2.9), because of the uncertainties explained earlier.

On the other hand, the transport or mobility approach to determining the primary hydration number does give a value for what is wanted, the number of water molecules that have lost their own degrees of translational freedom and stay with the ion in its motion through the solution. This approach has the advantage of immediately providing the individual values of the solvation number of a given ion, and not the sum of the values of those of the electrolyte.

Why bother about these hydration numbers? What is the overall purpose of chemical investigation? It is to obtain knowledge of invisible structures, to see how things work. Hydration numbers help to build up knowledge of the environment near ions and aid our interpretation of how ions move.

2.11. SPECTROSCOPIC APPROACHES TO OBTAINING INFORMATION ON STRUCTURES NEAR AN ION

2.11.1. General

There is nothing new about spectroscopic approaches to solvation, the first of which was made more than half a century ago. However, improvements in instrumentation during the 1980s and 1990s, and above all the ready availability of software programs for deconvolving spectra from overlapping, mixed peaks into those of individual entities, have helped spectra give information on structures near an ion. This is not to imply that they supersede alternative techniques, for they do carry with them an Achilles heel in that they are limited in sensitivity. Thus, by and large, only the more concentrated solutions (>0.1 mol dm^{-3}) are open to fruitful examination. This is not good, for in such concentrations, interionic attraction, including substantial ion pairing and more, complicates the spectral response and makes it difficult to compare

information obtained spectroscopically with that obtained using the partial molar volumes and vibration potential methods (Section 2.7).

One point should be noted here: the importance of using a 10% D_2O mixture with H_2O in IR spectroscopic measurements because of the properties of HOD, which contributes a much more clearly resolved spectrum with respect to O-D. Thus, greater clarity (hence information) results from a spectrum in the presence of HOD. However the *chemical* properties (e.g., dipole moment) of HOD are very similar to those of H_2O.

Raman spectra have a special advantage in analyzing species in solution. This is because the integrated intensity of the spectral peaks for this type of spectroscopy is proportional to the concentration of the species that gives rise to them.[15] From observations of the intensity of the Raman peaks, equilibrium constants K can be calculated and hence $\Delta G°$s from the thermodynamic equation $K = e^{-\Delta G°/RT}$ can be derived. Furthermore, if one carries out the Raman experiment at various temperatures, one can determine both the heat and the entropy of solution. Since $\Delta G° = \Delta H° - T\Delta S°$, a plot of ln K against $1/T$ gives the enthalpy of solvation from the slope and the entropy from the intercept. This provides much information on the various relations of ions to water molecules in the first one or two layers near the ion. In particular, the use of a polarized light beam in the Raman experiments provides information on the *shape* of complexes present in a solution.

2.11.2. IR Spectra

In obtaining information on solvation that can be deduced from IR spectra, the first thing that must be understood is that the raw data, the peaks and their frequencies, seldom speak directly but need to be decoded. Spectra in the IR region are mainly messages fed back from the solvent, and it is from the interpretation of evidence for *changes* in the solvent's libration and rotation when ions are introduced (rather than any new peaks) that information on solvation may sometimes be drawn. One has to take the spectrum of the solvent, then that of the solution, and subtract them to obtain the effect of the solute (Fig. 2.19). Vibration spectra have frequencies in the region of 10^{14} s^{-1} but it is usual to refer to the inverse of the wavelength, that is, the *wavenumber*, $\bar{\nu} = 1/\lambda$. Since $c_0 = \nu\lambda$, then $1/\lambda = \nu/c_0$. It turns out then that the wavenumbers of most covalent bonds are numerically in the thousands.[16]

Intramolecular effects can be detected in the near infrared or high-frequency region ($\bar{\nu} \sim 1000$ cm^{-1}). *Intermolecular* effects are seen in the far infrared or low-frequency region ($\bar{\nu}$ down to 100 cm^{-1}). Early measurements showed that ions can cause new peaks to arise that are at distinctly higher wavenumbers than those in pure water. The explanation proposed is that some of the hydrogen bonds present in pure

---

[15]This tends to be the case for all spectra. For other spectra it involves sensitivity factors or nonlinearity at higher concentrations; that is, it is approximate.

[16]A typical value for ν is 9×10^{13} s^{-1} and $c_0 = 3 \times 10^{10}$ cm s^{-1}. Hence, the wave number, $\bar{\nu}$, is $\bar{\nu} = 9 \times 10^{13}/3 \times 10^{10} = 3 \times 10^3$ cm^{-1}.

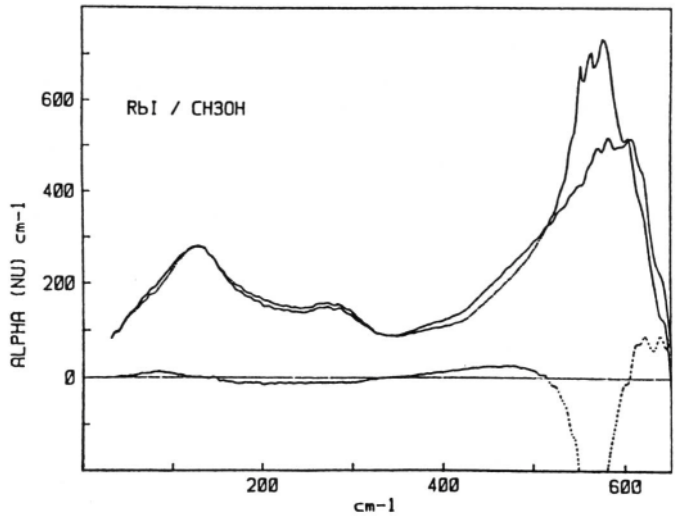

Fig 2.19. The absorption coefficients of pure methanol (Top line) and a solution of 0.4 *M* RbI in CH_3OH (Lower line). The bottom curve represents the difference between the solution absorption band and the solvent absorption band. (Reprinted from B. Guillot, P. Marteau, and J. Obriot, *J. Chem. Phys.* **93**: 6148, 1990.)

water have been broken due to the presence of ions, thus producing some quasi-free water molecules, which are the source of the new peaks.

There is plenty of spectroscopic evidence for a *structure-breaking* effect of ions in aqueous solution (although there is also evidence for formation of new structures). Because an increase in temperature also causes structure breaking, there has arisen the concept of "structural temperature" to describe ionic effects that produce the same degree of damage that would be produced by increasing the temperature. This structure breaking occurs in the "secondary" water (i.e., that outside the primary hydration sphere) because the first sheath of water around the ion is structure forming. Anions, which are usually bigger than cations, have consequently a less tightly held primary co-sphere and their large size makes them more responsible for structure breaking in solution than the corresponding cations.

The far IR (lower energy) spectra ($100\,\mathrm{cm}^{-1}$) show intermolecular effects in which the spectra reflect the effect of ions on the movements of the whole water molecule and (in contradistinction to vibrational movements within individual molecules)[17] are dynamically dominated by the mass of oxygen and not that of hydrogen.

---

[17]For a water molecule, the reduced mass is $1/\tilde{\mu} = 1/M_O + 1/2M_H$ and from Eq. (2.24) the vibrational spectrum is dominated by M_H.

From an interpretation of peaks in the far IR spectral region, one can obtain knowledge of hindered translations among water molecules in ionic solutions. Somewhat surprisingly, the force constants associated with such movements are *lowered* by the presence of ions because ions free some water molecules from the surrounding solvent structures. Thus, force constants are given by $\partial^2 U/\partial r^2$, where U is the potential energy of particle–particle interaction. The librative frequencies (Section 2.4) of water also show up in this region and decrease in the order KF > KC1 > KBr > KI. Thus, ions of smaller radii (higher field and force) give higher librative frequencies, as expected because of the equation

$$\nu = (2\pi)^{-1}\sqrt{k/\tilde{\mu}} \tag{2.24}$$

where k is the force constant (a function of the energy of ion–water interaction) and $\tilde{\mu}$ is the reduced mass of the vibrating entities.

James and Armitage have analyzed the far IR spectra of some ionic solutions and attempted to distinguish waters in the primary hydration shell (those waters that *stay* with the ion as it moves) from waters ("secondary hydration") which, although affected by the ion, are not attracted by it enough to move with it.

Studies that provide more illumination arise from IR measurements in the work of Bergstrom and Lindgren (Table 2.10). They have made IR studies of solutions containing Mn^{2+}, Fe^{2+}, and Co^{2+}, which are transition-metal ions, and also certain lanthanides, La^{3+}, Nd^{3+}, Dy^{3+}, and Yb^{3+}, at a concentration of 0.2–0.3 mol dm^{-3}. They find that the O–D stretching vibrations in HOD (2427 cm^{-1} in the absence of ions) are affected by the presence of these substances (Fig. 2.20). Both the transition-metal ions and the lanthanide elements perturb the HOD molecule in a similar way. However, even the trivalent lanthanide ions (for which stronger effects are expected because of the higher ionic charge) only perturb the nearest-neighbor water molecules (the first

TABLE 2.10

Bergstrom and Lindgren's Determination of Primary Hydration Number from IR Measurements (Transition Metal-Ions and Lanthanides)

Ion	Hydration No.
Mn^{2+}	6.5
Fe^{2+}	7.3
Co^{2+}	6.5
La^{3+}	7.8
Nd^{3+}	8.0
Dy^{3+}	8.7
Yb^{3+}	8.8

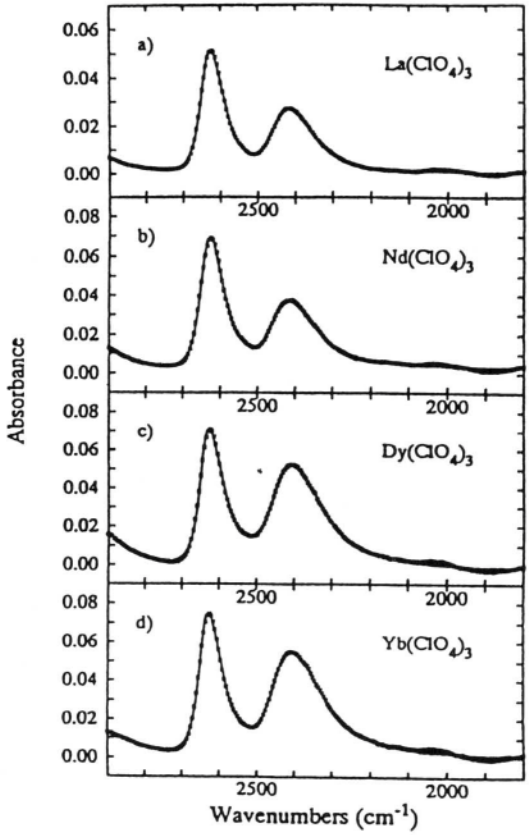

Fig. 2.20. O–D stretching spectra of aqueous solutions of (a) 0.236 *M* $La(ClO_4)_{3+}$ and (b) 0.342 *M* $Nd(ClO_4)_{3+}$ (c) 0.366 *M* $Dy(ClO_4)_{3+}$ and (d) 0.375 *M* $Yb(ClO_4)_{3+}$. The crosses are the observed points, and the solid line is the function fitted to the spectra. See Table 1 for band parameters. T = 20.0 °C, path length = 0.0444 mm, and c(HDO) = 6.00 mol%. (Reprinted from P. A. Bergstrom, *J. Phys. Chem.* **95**: 7650, 1991).

shell around the ion) and there is no effect detectable in the IR spectra on the second and other layers. The hydration numbers thus obtained are given in Table 2.10.

The hydration numbers in the table, deduced from IR spectroscopy, are much lower than values given by nonspectroscopic methods. The latter give hydration numbers for two- and three-valent ions 1.3 times greater than the spectroscopic values. It seems particularly surprising that in the spectroscopic results (Table 2.10) the three-valent ions give hydration numbers little different from those of charge two.

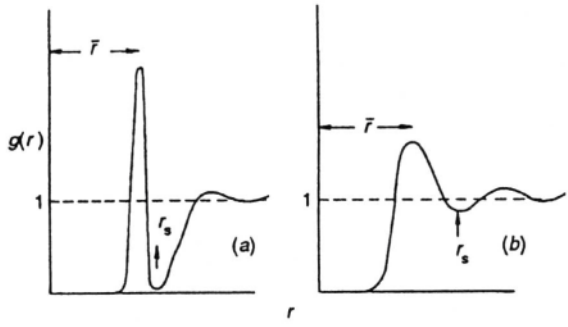

Fig. 2.21. Generic radial distribution functions for (a) a well-coordinated liquid with a long-lived coordination shell and (b) a weakly coordinated liquid. (Reprinted from J. E. Enderby, *Chem. Soc. Rev.* **24**: 159, 1995.)

Evidently the first layer is about the same when filled for both the two- and the three-valent ions, and perhaps the IR spectrum does not register effects given by a second layer of water. One might indeed well expect the first layer of water around an ion to be full, and therefore expect the same for the two- and three-valent cations of similar radii.

The presence of electrolytes in solution is often ill characterized spectroscopically by vague shoulders or bumps that make the interpretation hazardous and lacking in quantitative information on the ion–solvent structure. However, far IR does allow one to understand the spectra and obtain knowledge of the ion–solvent structure. For example, it is important to distinguish contact ion pairs (CIP) in the spectrum. These must be clearly identified and their effects allowed for before the spectrum can be used to obtain knowledge of ion–solvent interactions (Fig. 2.21).

2.11.3. The Neutron Diffraction Approach to Solvation

The seminal event in the foundation of solid-state science was the realization by von Laue that the ordered structure of atoms in a crystalline solid might act as a diffraction grating for X-rays. The corresponding formula by Bragg,

$$n\lambda = 2d \sin \theta \tag{2.25}$$

This represents the path-length difference with θ as the glancing angle (see Section 5.2.3) allowed *d*, the distance between atoms, to be determined for the first time. The path to structure determination was open.

X-ray analysis works when there are indeed ordered rows of atoms in a crystal. It also works in an examination of the structure of molten salts (Chapter 5), when there

is short-range order; the molten salts are somewhat like a disordered solution containing much open space, which some call holes. However, X-ray analysis does not work well for ionic solutions because the ordered elements (solvated ions) turn up only occasionally and are interrupted by relatively large distances of disordered solvent molecules.

Although, as will be seen in this section, the developments of neutron diffraction during the 1980s (Enderby and Neilson) have led to substantial advances in determining the coordination numbers of water molecules around ions, there are still some hurdles to clear before one can use this powerful method:

1. It is necessary to have a *neutron source* and that, in turn, means that only laboratories that have access to a nuclear reactor can do such work.[18]
2. It is desirable to work with D_2O rather than H_2O because of the sharper diffraction patterns obtained are the former. This can become a cost burden.
3. (1) and (2) can be overcome but the last hurdle is too high and must be accepted: the method is limited (as with most of the spectroscopic methods) to solutions of 1 mol dm^{-3} or more,[19] whereas most of the data in the literature concern dilute solutions (e.g., 10^{-3} mol dm^{-3}) where the univalent salts are about 12 nanometers apart (one can, then, picture an isolated ion in its solvation shell).

Having given the obstacles to attainment, let it be said that there are two ways in which neutron diffraction can be used to obtain information on the structure around an ion. In the first (Soper et al., 1977), the objective is the distribution function in the equation:

$$dn_\alpha = 4\pi \rho_\beta g_{\alpha\beta}(r) r^2 dr \tag{2.26}$$

where $\rho_\beta = N_\beta / V$.

This equation refers to a reference ion α and gives the average number of β particles that exist in a spherical shell of radius r and thickness dr (of course, on a time average). The symbol $g_{\alpha\beta}(r)$ is the so-called *distribution function.* For multicomponent systems, one can generalize $g_{\alpha\beta}(r)$ to include all the possible combinations of atoms [e.g., NaCl would have a total of 10 $g_{\alpha\beta}(r)$ values].

---

[18]In U.S. universities, this means that the professor concerned must write a proposal to ask for time on a reactor at, for example, Brookhaven or Oak Ridge or Argonne. Such proposals wait in line until they are evaluated and then, if accepted, the professor's team must move to the reactor for some days of intense activity—probably shift work to make 24-hr per day use of the time allotted.

[19]It is easy to show that the average distance between ions in a solution of 1:1 salt is $(1000/2N_A c)^{1/3}$, where c is the concentration in mol dm^{-3}. For a 1 M solution, this comes to 1.2 nm. However, for an ion of 0.1-nm radius and layer of two waters, the radius is about 0.1 + 4 × 0.16 nm and therefore the internuclear distance between two ions in contact is about 1.4 nm. For the 10^{-3} mol dm^{-3} case, the distance apart is 12.2 nm; i.e., the ions are isolated. Thus, it is very desirable to try to get spectroscopic measurements at these dilute solutions. Only then can the results of spectroscopic work be compared directly with deductions made about solvation (a concentration-dependent property) from measurements of solution properties.

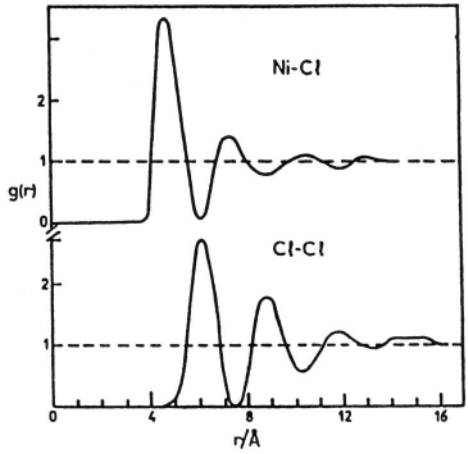

Fig. 2.22. The radial distribution functions g_{NiNi} and $g_{ClCl}(r)$ for a 4.35 *M* solution of $NiCl_2$ in D_2O (neutron results). (Reprinted from J. E. Enderby, "Techniques for the Characterization of Electrodes and Electrochemical Processes," in R. Varma and J. R. Selman, eds., *The Electrochemical Society Series,* Wiley, New York, 1991, p. 110).

It follows that

$$4\pi\rho_\beta \int_0^{r_s} g_{\alpha\beta}(r)\, r^2\, dr$$

is the coordination number, where r_s is the radius of the first shell of water molecules around the ion.

Two extreme types of results are obtained from this approach (which is limited to solutions of C > 0.1 m), and they are shown in Fig. 2.21. The left-hand diagram shows the kind of result in which the molecules are strongly coordinated in a first shell with a lifetime that could vary from, say, 10^{-5} s to hundreds of hours (in exceptional cases). The second diagram is typical of a more weakly coordinated ion in which the

[20]The actual experimental determination (analogous to the Bragg determination of *d*, the distance apart of atoms in crystals) is of $g_{\alpha\beta}$. This is what is done with neutron diffraction. It can also be calculated using molecular dynamics in which the basic assumption is that there is a certain force field between the particles. As explained elsewhere (Section 2.17.4), this is given in terms of the corresponding energy of interaction of pairs of particles. Although the attraction energy is always given by $z_i z_j / \varepsilon r$, there are various versions of the repulsion potential.

lifetime of water molecules is short, perhaps only 10^{-11} s. For multicomponent systems it is possible to have several internuclear distances and, correspondingly, a number of distribution functions. By applying Eq. (2.26) to the data for $g_{\alpha\beta}(r)$, such as that shown in the diagram, one can find out how many water molecules are in the first shell, as in the case of concentrated $NiCl_2$ solutions (Fig. 2.22).

There are always water molecules located around a stationary ion and the structure of these waters will be dominated by the field of the ion (rather than the pull back into the structure of the water). This dominance is stronger the smaller the ion because the ion–solvent interaction is inversely proportional to $1/r^2$. As the schematics of a typical distribution function suggest, there may be a second layer in addition to the first shell of solvent associated with the ion. In this layer the structure is not yet that of bulk water, though such second solvation layers are usually more prominent with divalent ions (they are even more so with 3+ and 4+ ions) and are not seen for univalent ions, in the company of which hydration waters stay for very short times.

Now, the question is how to get information on the more subtle quantity, the hydration *numbers*. Some confusion arises here, for in some research papers the coordination number (the average number of ions in the first layer around the ion) is also called the hydration number! However, in the physicochemical literature, this latter term is restricted to those water molecules that spend at least one jump time with the ion, so that when its dynamic properties are treated, the effective ionic radius seems to be that of the ion plus one or more waters. A startling difference between co-ordination number and solvation number occurs when the ionic radius exceeds about 0.2 nm (Fig. 2.23a).

It is important, then, to find out the time that waters stay with the ion. Thus, one can make an order-of-magnitude calculation for the jump time, by a method shown in Section 4.2.17. It comes to approximately 10^{-10} s.

One could conclude that if a water molecule stays with its ion for more than about 10^{-10} s, it has accompanied the ion in a jump. That is, during the time the water is associated with the ion, it is likely to have made one move with the ion in its sporadic random movements (and therefore counts as a hydration number rather than a static or equilibrium coordination number).[21] Figure shows the ratio of the solvation number to the coordination number. The ratio $\tau_{\text{ion-wait}}/\tau_{\text{water orient}}$ is an important quantity

[21] In the case of ions for which the ion–water binding is very strong (the transition-metal ions particularly), the hydration number may be greater than the coordination number, because more than one shell of waters moves with the ion and the hydration number will encompass *all* the water molecules that move with it, while the coordination number refers to the ions in just the first shell.

However, with larger ions, which have weaker peripheral fields, there is less likelihood that a water molecule will stay for the time necessary to accomplish an ion movement (e.g., > 10^{-10} s). Thus, for larger ions like Cl^- and large cations such as $N(C_2H_5)_4^+$, the coordination number will be 6 or more, but the hydration number may tend to be 0. The hydration number is a dynamic concept; the coordination number is one of equilibrium: it does not depend on the lifetime of the water molecules in the shell but measures their time-averaged value.

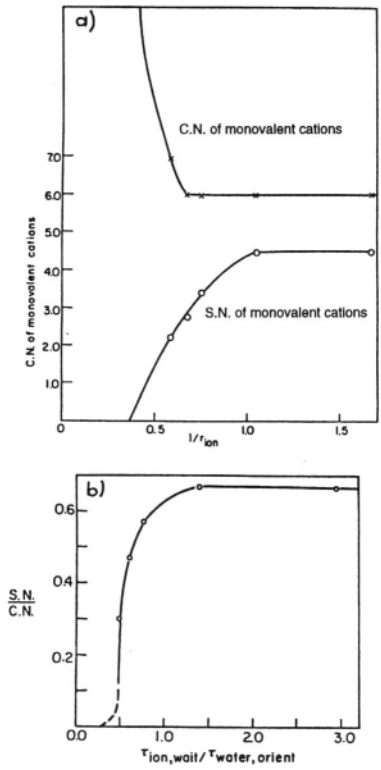

Fig. 2.23. (a) SN and CN of alkali metal cations plotted as reciprocal function of cation radius. (b) SN/CN plotted against $\tau_{ion,wait}/\tau_{ion,orient}$ for monovalent ions. (Reprinted from J. O'M. Bockris and P. P. S. Saluja, *J. Electrochem. Soc.* **119**:1060, 1972.)

because it emphasizes the dynamic character of the solvation number. Thus, $\tau_{ion\text{-}wait}$ represents the time taken for an ion to remain at a given site in its movement into the solution. Correspondingly, $\tau_{water\ orient}$ represents the time for a water molecule (at first fixed within the water structure) to break out of this and orient towards the ion to a position of maximum interactions upon the ions arrival at a given site. In the case (Fig. 2.23b) where this ratio is big enough, the ratio of the solution number to the co-ordination number will be above 0.5.

There is a second way to use neutrons to investigate the structure of ions, particularly with respect to the time of movement of the water molecules. A remarkable advance was accomplished by Hewich, Neilson, and Enderby in 1982. They used *inelastic neutron scattering.* Upon analysis of their results, they found that they could obtain D_H, the diffusion coefficient for displacement of water. The special point they

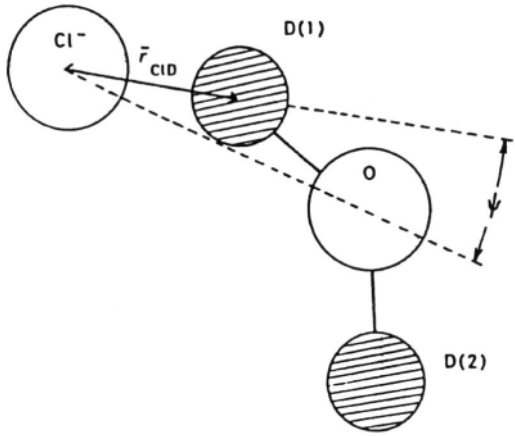

Fig. 2.24. Geometric arrangement of a D_2O molecule close to a chloride ion. (Reprinted from D. H. Powell, A. C. Barnes, J. E. Enderby, G. W. Neilson, and P. H. Salmon, *Faraday Disc. Chem. Soc.* **85**:137, 1988.)

discovered was that certain functions that should have varied in a Lorentzian way with the frequency of the neutrons used were a poor fit to the expected variation and were better deconvoluted into two *D*s, one for water in the inner sphere and one for water in the outer sphere. Thus, this was direct evidence that during the movement of some ions (Ni is the one cited) there is an inner layer of about 6 but an outer layer of about 15 that also moves with the ion. Here, then, the coordination number would be 6 (number of molecules in the inner sphere) and the hydration number would be 6 + 15 = 21.

Finally, in this very general account of neutron interference and scattering applied to ions in solution, it is interesting to note that the tilt angle of the water molecule to the ion can be obtained (Fig. 2.24). Again, Enderby and Neilson are the progenitors of this kind of information and an example (together with one for the wag angle ψ and its variation with concentration) is given here.[†]

Ferrous and ferric ions have been examined in respect to their solvation shells, particularly by NMR methods. For Fe^{2+}, the value obtained for the number of water

[†]John Enderby is Professor of Physics in the H. H. Wills Physics Laboratory of the University of Bristol. Together with his colleague, G. W. Neilson, he has made, arguably more contributions to specific, quantitative, knowledge of the region close to an ion in solution than that of any other worker since 1950. Thus, the developments of the neutron diffraction methods at Bristol have gone far to making it possible (for concentrated solutions at least) to distinguish between waters remaining with an ion during its movements and those which are simply affected by an ion as it passes by.

molecules in a first shell was 5.85 and the lifetime of these waters was relatively long, about 2×10^{-7} s. Thus, because this time is much greater than that needed for a diffusive movement (10^{-10} s), the waters in the first shell are certainly a part of the hydration number. By analogy with Ni^{2+}, it seems likely that the total hydration number is greater than this coordination number because of a second shell containing water with a lifetime greater than 10^{-11} s, which would then also qualify (because its lifetime greatly exceeds a jump time) as contributing to a hydration number. Similar remarks apply to Fe^{3+} but the lifetime of the inner shell is greater (about 6×10^{-3} s) than that for ferrous ions because of the stronger binding to water with ferric rather than ferrous ions.

The Cr^{3+} ion has a special place in the history of solvation because it was the first ion for which the lifetime of the water in its hydration shell was measured. This work was done by Hunt and Taube in 1957. The exchange of water between the hydration shell and the surroundings was slow, so the change in the concentration of the isotope could be measured. The lifetime found is 1.6×10^{7} s (about 6 months). There is evidence of outer-sphere water, so the value for the total hydration water that travels with the ion is much higher than the value of about 6 found for the first shell in transition-metal ions.

The hydration number of the Li^{+} ion has been measured by a number of nonspectroscopic methods and a value of 5 ±1 represents the range of results. The difference method of neutron diffraction gives 6 with reasonable consistency. The lifetime is 3×10^{-9} s, so the value is clearly a hydration number (i.e., it is much greater than 10^{-11} s, so water travels with the ion).

An interesting result is obtained for Cl^{-}. Neutron diffraction work shows the value to be 6, which is in strong disagreement with nonspectroscopic methods, which give the much lower value of 1 or 2. However, light is at once thrown on what seems a breach difficult to mend when the lifetime of the 6 waters around the Cl^{-} is found to be only 10×10^{-11} s; this is on the borderline as viable for a dynamic hydration number. It seems likely, then, that the Cl^{-} moves on average without its hydration water, because its lifetime is barely enough for the time needed ($> 10^{-11}$ s) for wares to travel one jump distance. Thus, the 1 or 2 hydration numbers of other measurements is understandable. It is possible to regard the 6 value as coordination water, but few of the waters manage to stay with the ion when it moves from site to site.

2.11.4. To What Extent Do Raman Spectra Contribute to Knowledge of the Solvation Shell?

Raman spectra have a more involved origin than do IR absorption spectra. They concern the *scattering* of light. This is a subject that was studied in the nineteenth century when Rayleigh showed that the elastic scattering of light (no absorption) was proportional in intensity to λ^{-4}, where λ is the wavelength of the scattered light. In conditions that pertain to the application of this formula, the photon is assumed to "bounce" off the molecules it strikes with the same energy latterly as it had initially.

Smekal predicted a radically different type of scattering in 1923. He suggested that if a beam of light were incident on a solution, the scattered light would contain (apart from the elastically scattered light of unchanged frequency) two more frequencies, one greater and one lesser than the frequency of the incident beam. These would result from a collision of a photon with a molecule in which the photon would indeed (in contrast to Rayleigh's idea) exchange energy with the molecule it struck and bring about a transition in the molecule's vibrational band. Smekal thought that two kinds of energy exchange would occur. The photon might excite the molecule to higher states and the resulting frequency of the scattered light would be lower than the incident frequency (because some energy had been removed from the light). Alternatively, the molecule might give energy to the photon and the emerging photon would have a higher frequency than that of the initial beam. These nonelastic scattering effects predicted by Smekal in 1923–1924 were first experimentally observed by the Indian scientists Raman and Krishnan in 1928.

Thus, in the Raman spectra, it is a frequency shift, a $\Delta\nu$, that is observed. The value of such shifts in the frequency of nonelastically scattered light is not dependent on the exciting frequency,[22] but on the structure of the molecule with which the photon interacts. Thus, the Raman shifts reflect *vibrational* transitions, as do the IR spectra.

One other aspect of Raman spectra must be explained before one can understand how information on structures around ions in solution can be extracted from positive and negative Raman shifts. In Rayleigh scattering, the oscillating dipoles may radiate in all directions with the frequency of the exciting beam. However, in Raman spectra, the radiation depends on the polarizability of the bond. In some molecules, polarizability does not have the same value in all directions and is called nonisotropic. Let it emit light in the *x-y* plane only. Then the intensity ratio (light in the *xy* plane)/(light in the incident beam) is called the *depolarization factor.* For Raman scattering, this depolarization factor gives information on structure, for example, on the degree of symmetry of the entity in the solution, the Raman spectra of which are being observed (Tanaka et al., 1965).

2.11.5. Raman Spectra and Solution Structure

One type of Raman study of solutions concentrates on water–water bonding as it is affected by the presence of ions. Hydrogen bonds give Raman intensities, and the variation of these with ionic concentration can be interpreted in terms of the degree and type of structure of water molecules around ions. The ClO_4^- ion has often been used in Raman studies to illustrate structure-breaking effects because it is a relatively large ion.

In studies of the spectra of intramolecular water and how they are affected by ions, new Raman peaks can be interpreted in terms of the model of solvation suggested by

[22]This must, however, have a frequency greater than that of any of the transitions envisaged, but less than that which would cause an electronic transition.

Bockris in 1949 and by Frank and Evans in 1957. According to these workers, there are two regions. One is in the first (and for polyvalent cations, the second) layer near the ions, where water molecules are tightly bound and give rise to new frequencies. Such waters accompany the ion in its movements in the solution.

There is also a broken-structure region outside the first one to two layers of water molecules around the ion. Here the solvating waters are no longer coordinated, as in the bulk, by other waters, because of the ion's effect, but they are outside the *primary* hydration shell, which moves with the ion. Such intermediate waters, though partly broken out of the bulk water structure, do not accompany an ion in its diffusional motion.

Studies consistent with these ideas were first performed by Walfren in 1971 in H_2O–D_2O mixtures. Concentrations of 1 to 4 mol dm^{-3} were employed to get measurable effects. Thus, at 4 mol dm^{-3}, some 40–50% of the water present is at any moment in the primary hydration sheath!

Intermolecular effects in ionic solutions can also be studied in the Raman region between 200 and 1000 cm^{-1}. Librational modes of water show up here. The intensity of such peaks changes linearly with the ionic concentration. The ν_2 bending mode in the Raman spectra of alkali halides in water was studied by Weston. They may also be interpreted in terms of models of primary hydration (water staying with the ion in motion) and a secondary disturbed region.

Raman spectra can also be used to determine the degree of dissociation of some molecules, namely, those that react with the solvent to give ions (e.g., HC1). If the Raman frequency shifts for the dissociated molecules are known, then they can be used to calculate equilibrium constants at different temperatures. Then, once the temperature coefficient of the equilibrium constant K is known, one can determine $\Delta H°$ and $\Delta S°$ of the dissociation reaction (Section 2.13).

The study of the NO_3^- ion falls into the category of Raman studies that concentrate on interpreting spectra caused by the solute. It illustrates the use of Raman spectra to give structural conclusions via the study of symmetry. The free NO_3^- ion should have what is termed "D_{3h} symmetry" and give rise to three Raman bands corresponding to two degenerate asymmetric stretching modes (ν_3 and ν_4) and one symmetric stretching mode.

Irish and Davis studied the effect of solvation on the spectra of this NO_3^- ion and the splitting of the ν_3 band. They found that H bonding removes the degeneracy of this mode. The symmetry change would be from D_{3h} to C_{2h} and this is interpreted to mean that hydration effects have brought about a nonequivalence of the O atoms in NO_3^-, a most unexpected effect.

2.11.6. Information on Solvation from Spectra Arising from Resonance in the Nucleus

It has been often suggested that nuclear resonance might be used to gain information in solvation studies. Thus, in hydroxylic solvents, electron shielding around the proton should be affected by ions and thus, in terms of changes in nuclear resonance frequencies, solvation-bound water and free water should be distinguishable. It turns

out that this is a nonevent for water because the rapid exchange between the two types, bound and unbound, gives rise to only a broad peak.

In order to obtain information from nuclear resonance, the proceedings must be a bit complicated. One adds a paramagnetic ion to a solution in which the solvation of a diamagnetic entity is to be measured. Then, two types of water around, for example, an Al^{3+} ion, bound and unbound waters, can be distinguished by observing the resulting nuclear magnetic resonance spectra of ^{17}O. The nuclear spin in the ^{17}O interacts with the electron spin vector of the paramagnetic ion added as a helpful auxiliary ion, and this changes the field on the ^{17}O nucleus. This shift in the NMR spectra of ^{17}O between water attached to the ion and bulk water has to be sufficiently large, and this in turn may allow a separation to be made between water bound to the diamagnetic ion and free water. In this rather complex and devious way, it is possible to obtain estimates of the number of waters in the first layer next to an ion.

However, disappointingly, again the values obtained from this NMR spectroscopic approach (e.g., 6 for Al^{3+}, Ga^{3+}, and Be^{2+}) are less than the values obtained for these ions (e.g., 14 for Be^{2+}) from the relatively self-consistent values of mobility, entropy, and compressibility. Is this simply because the nonspectroscopic measurements are usually done at high dilutions (e.g., 10^{-3} mol dm^{-3}) to diminish interionic effects, and the spectroscopic ones have to be done at 0.5 mol dm^{-3} or greater concentrations, because the spectroscopic shifts are relatively insensitive, and hence need the high concentration to score a detectable effect?

Swift and Sayne used concepts similar to those of Bockris and Saluja: if a molecule stays associated with an ion for more than the time needed for a diffusional jump, it "counts" as a primary hydration number. This approach yields approximately 4 solvation molecules for Mg^{2+} and Ca^{2+}, and 5 for Ba^{2+} and Sr^{2+}, whereas nonspectroscopic methods for these systems yield values that are two to three times larger. Does NMR measure only water arranged in a first, octahedral layer in the first shell near the ion and is it insensitive to the rest of the water structure near an ion?

Further Reading

Seminal

1. P. Debye, "The Vibrational Potential in Solution," *J. Chem. Phys.* **1**: 13 (1933).
2. D. D. Eley and M. G. Evans, "Statistical Mechanics of Ions in Solution," *Trans. Faraday Soc.* **34**: 1093 (1938).
3. M. Passynski, "Compressibility and Solvation," *Acta Phys. Chim. USSR* **8**: 385 (1938).
4. K. Fajans and O. Johnson, "Heats of Hydration," *J. Am. Chem. Soc.* **64**: 668 (1942).
5. R. H. Stokes and R. A. Robinson, "Hydration Numbers from Activity Measurements," *J. Am. Chem. Soc.* **70**: 1870 (1948).
6. J. B. Hasted, D. M. Ritson, and C. H. Collie, "Dielectric Constants of Solutions," *J. Chem. Phys.* **16**: 1 (1948).
7. J. O'M. Bockris, "Primary and Secondary Solvation," *Quart. Rev. Chem. Soc. Lond.* **3**: 173 (1949).

8. A. M. Azzam, "Theoretical Calculation of Hydration Numbers," *Z. Phys. Chem. (N.F.)* **33**: 320 (1962).
9. R. Zana and E. Yeager, "Solvation Numbers from Partial Molar Volumes," *J. Phys. Chem.* **71**: 521 (1967).
10. G. E. Walfren, "Spectroscopic Evidence on Hydration," *J. Chem. Phys.* **55**: 768 (1971).
11. J. O'M. Bockris and P. P. S. Saluja, "Hydration Numbers for Partial Molar Volumes and Vibrational Potentials from Solutions," *J. Phys. Chem.* **76**: 2140 (1972).
12. A. K. Soper, G. W. Neilson, J. E. Enderby, and R. A. Howe, "Neutron Diffraction and Coordination Numbers in Solution," *J. Phys. Soc.* **10**: 1793 (1977).
13. N. A. Hewich, G. W. Neilson, and J. E. Enderby, "Deconvolution within Neutron Diffraction Data and the Structure of the Hydration Sheath," *Nature* **297**: 138 (1982).
14. H. Friedman, "Time of residence of water molecules near ions," *Chem. Scripta* ***25***: 42 (1985).

Review

1. G. A. Krestov, *Thermodynamics and Structure in Solvation*, Ellis Harwood, New York (1990).

Papers

1. S. Koda, J. Goto, T. Chikusa, and H. Nomura, *J. Phys. Chem.* **93**: 4959 (1989).
2. G. Omori and A. Santucci, *J. Chem. Phys.* **93**: 2939 (1990).
3. M. Jukiewicz and M. Figlerowicz, *Ultrasonics* **28**: 391 (1990).
4. B. Wilson, R. Georgiadis, and J. A. Bartmess, *J. Am. Chem. Soc.* **113**: 1762 (1991).
5. I. Howell, G. W. Neilson, and P. Chieuk, *J. Mol. Struct.* **250**: 281 (1991).
6. P. A. Bergstrom and J. Lindgren, *Inorg. Chem.* **31**: 1529 (1992).
7. P. A. Bergstrom, J. Lindgren, M. Sandrum, and Y. Zhou, *Inorg. Chem.* **31**: 150 (1992).
8. B. Guillot, P. Martineau, and J. O. Grist, *J. Chem. Phys.* **93**: 6148 (1993).
9. M. Maroncelli, V. P. Kumer, and A. Papazyan, *J. Phys. Chem.* **97**: 13 (1993).
10. J. M. Alia, H. G. M. Edwards, and J. Moore, *Spectrochim. Acta* **16**: 2039 (1995).
11. J. Barthell, *J. Mol. Liquids* **65**: 177 (1995).
12. Y. Tominaga, Y. Wang, A. Fujiwara, and K. Mizoguchi, *J. Molec. Liquids* **65**: 187 (1995).
13. M. J. Shaw and W. E. Geiger, *Organometallics* **15**: 13 (1996).
14. A. E. Johnson and A. B. Myers, *J. Phys. Chem.* **100**: 7778 (1996).
15. A. S. L. Lee and Y. S. Li, *Spectrochim. Acta* **52**: 173 (1996).
16. G. W. Neilson and J. E. Enderby, *J. Phys. Chem.* **100**: 1317 (1996).

2.12. DIELECTRIC EFFECTS

2.12.1. Dielectric Constant of Solutions

The electric field created between two plates of a parallel-plate condenser in a vacuum is greater than the field that exists between the same plates with the same

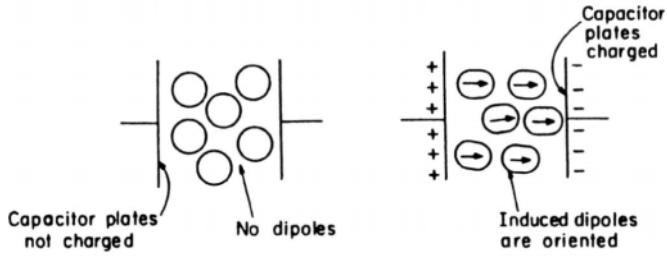

Fig. 2.25. The charge on the capacitor plates induces dipoles in the molecules of a dielectric.

charge on them but separated by a material medium, a so-called dielectric. The model by which dielectrics affect fields is easy to understand at a qualitative level. The molecules of the medium either contain a permanent dipole moment in their structure or have one induced by the field between the plates. Of course, when the field on the condenser plates is switched on, the dipoles orient against it (Fig. 2.25) and cause a counter electric field. The result is that the net electric field between the plates is less than it is when there is no medium between them (Fig. 2.26).

The counter field and the resulting net field can be calculated in mathematical form, but historically a more empirical way has been used; the field in the presence of a dielectric is simply expressed by dividing the field in its absence by an empirical "dielectric constant." The greater the counter field set up by the medium between the plates (Fig. 2.26), the greater the dielectric constant and the less the net electric field.

With this simple background model, then, it is easy to see that there will be a *decrease* of the dielectric constant of solutions (compared with that of the original

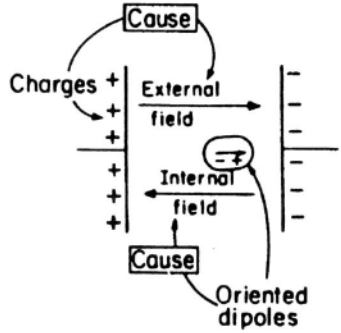

Fig. 2.26. The orientation of dipoles in the dielectric sets up an internal field that is directed counter to the external field produced by the charges on the plates.

TABLE 2.11

Hydration Numbers from Dielectric Increment Measurements

Ion	n	Ion	n
H^+	10	Rb^+	4
Li^+	6	Mg^{2+}	14
Na^+	4	Ba^{2+}	14
K^+	4	La^{3+}	22

Source: From J. B. Hasted, *Aqueous Dielectrics*, Chapman and Hall, London, 1973.

liquid) if ions are added to them. Thus, the ions undergo solvation and, to some critical distance from the ions' center, hold the solvent molecules tightly against the tendency of the field to orient them to oppose the applied field.

Those water molecules that are prevented from orienting ("irrotationally bound") to oppose the field will be withdrawn from those contributing to the counter field and hence the dielectric constant of the ionic solution will be reduced from what the solvent would have without the ions.

There are a number of publications in the field of the structure of ionic solutions that are particularly seminal and although published half a century ago have great influence on present concepts. One of them is the paper by Bernal and Fowler in which the associated structure of water was first established (in 1933) from the interpretation of the original X-ray data on liquids. However, another paper of great importance is that by Hasted, Ritson, and Collie in 1948, for it was here that the dielectric properties of solutions were first recorded on a large scale. In subsequent publications the relation of the dielectric constant of the solution and solvation was first investigated.

Some of the facts that Hasted et al. established are shown in Table 2.11. They found that the lowering of the dielectric constant of 1 *M* solutions is in the range of 10–20%. This can be nicely explained by taking the water in contact with the ion as dielectrically saturated (unable to orient on the demand of the external field), but still having a dielectric constant of only 6,[23] compared with the value of 80 for bulk water unaffected by ions. The table shows the number of water molecules per ion pair that one has to assume are saturated (i.e., irrotationally bound in the vicinity of each ion) to make the above model come out right (i.e., reproduce the measured dielectric constants of solutions). This model leads to a very simple equation for the dielectric constant of a solution:

[23]This value (6) is the dielectric constant of water under conditions of dielectric saturation. The ion's field not only stops the water orienting under the influence of the ac field exerted on the solution, it also breaks up the associated water structure (which made the dielectric constant of water so huge compared with that of other liquids). The 6 represents the counter field offered by the distortion of the positions of the nuclei in H and O and of the electron shells of these atoms.

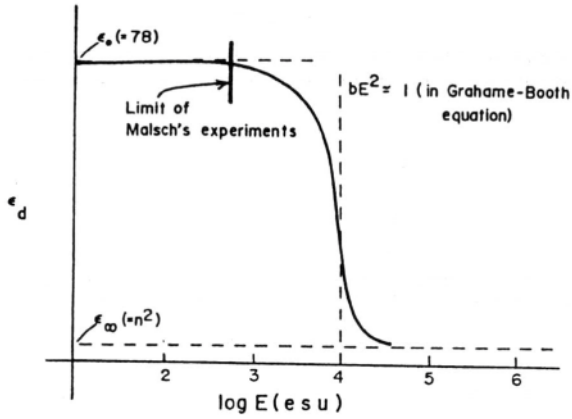

Fig 2.27. Differential dielectric constant ε_d as a function of field that is near an ion. (Reprinted from B. E. Conway, *Ionic Hydration in Chemistry and Biophysics*, Elsevier, New York, 1981.)

$$\varepsilon_{\text{soln}} = 80\left(\frac{55 - c_i n_s}{55}\right) + 6\,\frac{c_i n_s}{55} \tag{2.27}$$

where n_s is the total number of water molecules held by the ion, and c_i is the ionic concentration in mol dm^{-3}. Here, the first term represents the contribution from the bulk water molecules and the second term that from the bounded waters. Thus, measurements of the dielectric constants of ionic solutions provide a way to determine primary hydration numbers, the number of water molecules that stay with an ion while it diffuses in a solution.

Of course the assumption that in ionic solutions there are just two dielectric constants, one at 6 and the other at 80, is a simplification. There must be an intermediate region in the first two or three layers out near the ion in which the dielectric constant varies quite rapidly as one passes from the 6 of the first layer to the 80 a few layers further out.

This broken-down region near the ion was the subject of mathematical discussion by Webb as early as 1926, by Conway et al., and by Booth, whose paper also can be considered seminal. Grahame made an attempt to simplify Booth's equation for the dielectric constant as a function of field strength, and a diagram due to him is shown in Fig. 2.27.

Although the dielectric constant shown here is in terms of the *field* near the ion, not the distance from it, it is fairly[24] simple to find the distance that corresponds to those fields in the diagram and thus know what the dielectric constant is as a function of distance.

---

[24]Only fairly simple because the field itself depends on ε_r, the quantity one is trying to find. There is thus a catch to obtaining the distance corresponding to a certain field. An early solution to the problem was given by Conway, Bockris, and Ammar in 1951.

The main purpose of this section is to give the basis of how measurements of the dielectric constants of ionic solutions can give information on solvation, particularly primary hydration numbers. However, dielectric measurements *as a function of frequency* also give information on the dynamic behavior of water by allowing us to determine the relaxation time of water in ionic solutions and expressing the changes in terms of the number of water molecules bound to the ion.

Dielectric measurements of ionic solutions are also important for another topic that will be dealt with in Section 2.22, namely, electrostriction, the study of the compressive effect of the very strong electric fields produced by ions on the surrounding medium. When one looks into the effect of ions on the frequency at which water undergoes relaxation (i.e., when water no longer reacts to an applied field), it is found that the cation has a greater effect than the anion. The reason is shown in Fig. 2.28. For the cation, the two protons of a solvated water stick out from the ion and are bound to other waters, which restricts their libration and hence their contribution to the dielectric constant. Anions orient the protons of the hydration waters to themselves and away from binding by waters outside the first shell, thus having less binding effect on their movement than do the cations.

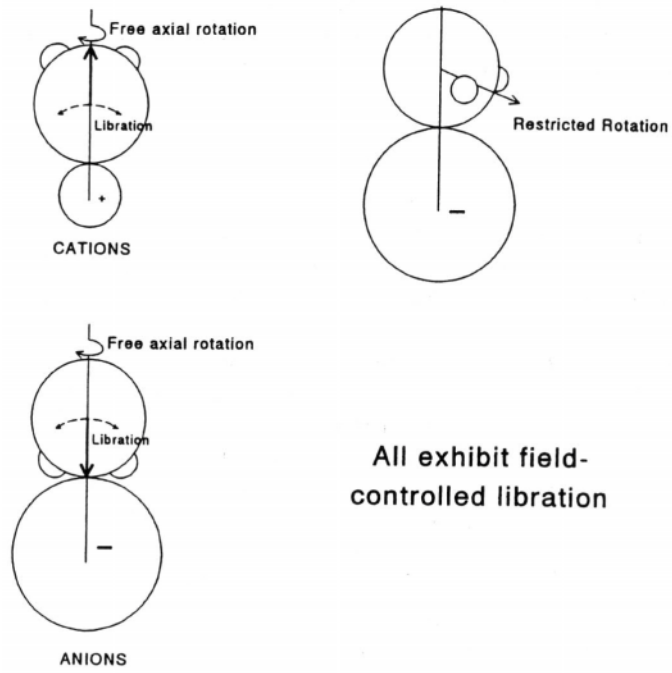

Fig. 2.28. Orientation and rotation possibilities for H_2O dipoles at anions and cations. (Reprinted from B. E. Conway, *Ionic Hydration in Chemistry and Biophysics*, Elsevier, New York, 1981.)

2.12.2. How Does One Measure the Dielectric Constant of Ionic Solutions?

There is much to think about here. If one wishes to measure the dielectric constant of a *liquid*, not a conducting ionic solution, one simply uses an alternating current (ac) bridge containing a capacitor in one of the arms. Then the capacitance is measured in the presence of the liquid, the dielectric constant of which is to be measured, and then without it, i.e., in the presence of air. Since the dielectric constant is near to unity in the latter case, this gives rise to knowledge of the dielectric constant of the liquid because the capacitance of the cell in the bridge arm increases as the dielectric constant increases.

However, when the liquid is a conducting solution, this approach breaks down. The conductance of the solution contributes to the impedance of the cell, which (depending on frequency) may no longer be overwhelmingly capacitative. Hence, the dielectric constant of a conducting liquid cannot be simply measured, because of the conductive components of the impedance.

Two approaches can be used to avoid this difficulty. In the one, which is best used for frequencies well below the relaxation frequency of water, one measures the *force* between two plates that have the conducting liquid between them. This force is independent of the conductance of the liquid or the direction of the field. If d is the distance between the plates, it is easy to show that the force is

$$\text{force} = \frac{E^2 A\varepsilon}{8\pi d^2} \tag{2.28}$$

where E is the potential difference between the plates, A is their area, and ε is the dielectric constant (Fig. 2.26). To obtain measurements that avoid significantly changing the temperature of the solution, d should be minimal. The field between the two plates is small (10^3 V cm^{-1}). Vibrations must also be minimized (e.g., by placing the apparatus on a stone slab supported on an inflated inner tube). An optical lever magnifies the very small movement of the plates.[25] Because everything is known in Eq. (2.28) except , the latter can be measured.

If it is desired to measure the dielectric constant at high frequencies (e.g., 10^7–10^{10} Hz), a different technique is necessary, partly because one may be working in the range of the relaxation time of water. The measurement of this, and the degree to which it is affected by the presence of ions, provides yet another way of finding how many molecules of water are bound to cation and to anion. The technique involves the use of a *wave guide* consisting of a coaxial liquid-filled cell, containing a probe that is moved about until the interference signal between it and an alternator is found to be

[25] A movement of 0.1 mm in the plate can be magnified mote than 100 times by projecting a beam of light reflected from a mirror attached to the plate over a distance of 25 m.

zero. From this (for details of how to do this, see Conway, 1982), it is possible to find the ε of the solution as a function of frequency (and hence the relaxation time of water as a function of the presence of ions). This quantity clearly depends on how many water molecules have been withdrawn from the free solvent, where they can relax, and how many are attached to ions, where they cannot. It therefore leads to primary hydration numbers

Studies of the dielectric constant of solutions and the relaxation times of water in the presence of ions have been refined since the 1980's and indeed difficulties do turn up if one looks at data from measurements over large frequency ranges. The variation of the dielectric constant with frequency has been studied particularly by Winsor and Cole, who used the Fourier transform of time domain reflectometry to obtain dielectric constants of aqueous solutions and the relaxation times in them. Their frequency ranges from over 50 MHz to 9 GHz.

The problem of making significant dielectric constant measurements in these ranges is to separate the relaxation effects of the ionic atmosphere around the ions (Chapter 3) from effects connected with ion-solvent interactions. At low concentrations (< 0.01 mol dm^{-3}), the former effects are less important, but at such concentrations the decrements in the dielectric constant are too small for accurate measurement. Theoretical work makes it clear that a series of measurements over a large range of frequencies (e.g., 1 Hz to 1 GHz) are needed to separate dielectric effects from those due to relaxation of the ionic atmosphere.

Nevertheless, in spite of these warnings, values of dielectric decrements have a sufficiently clear basis to allow their use in discussing the elusive solvation numbers.

2.12.3. Conclusion

Measurements of dielectric constants of solutions allow the deduction of not only how many waters are taken up and held irrotationally by ions, but also how the ions affect the frequency of the movements of molecules near them. This will help a person interested in electrostatic effects calculate the local pressure near an ion (Section 2.22.1).

Further Reading

Seminal

1. J. J. Webb, "Electric Field near an Ion in Solution," *J. Am. Chem. Soc.* **48**: 2589 (1926).
2. J. B. Hasted, D. M. Ritson, and C. H. Collie, "The Dielectric Constants of Ionic Solutions," *J. Chem. Phys.* **16**: 1 (1948).
3. F. Booth, "Dielectric Constant As a Function of the Applied Field," *J. Chem. Phys.* **19**: 1451 (1951).
4. D. C. Grahame, "Electric Field and Dielectric Constant near an Ion," *J. Phys. Chem.* **11**: 1054(1951).

5. J. O'M. Bockris and J. Bowler-Reed, "A Technique for Measuring Dielectric Constants in Conducting Solution," *J. Appl. Phys.* **2**: 74 (1951).

Papers

1. D. Bertolini, M. Cassetari, E. Tombari, and S. Verenesi, *Rev. Sci. Instrum.* **61**: 450 (1990).
2. R. S. Drago, D. C. Feris, and N. Wong, *J. Am. Chem. Soc.* **112**: 8953 (1990).
3. S. Safe, R. K. Mohr, C. J. Montrose, and T. A. Litovitz, *Biopolymers* **31**: 1171 (1991).
4. M. Bruehl and J. T. Hynes, *J. Phys. Chem.* **96**: 4068 (1992).
5. J. Z. Bao, M. L. Swicord, and C. C. Davis, *J. Chem. Phys.* **104**: 4441 (1996).
6. J. L. Buck, *IEEE Transactions* **45**: 84 (1996).

2.13. IONIC HYDRATION IN THE GAS PHASE

Now that some methods for investigating the structure of the ion–solvent complex in solution have been described, it is time to learn systematically what is known about it. One can start by considering systems that avoid the complexity of liquid water. By varying the partial pressure of water vapor while keeping it low (0.1–10kPa), it is possible to find the equilibrium constant between water vapor and the entities represented by a number of ion–solvent aggregates, $M(H_2O)_n^+$, in the gas phase (Kebarle and Godbole, 1968).

Thus, if the equilibrium constant K for one of these equilibria is known, $\Delta G°$ can be derived from the well-known thermodynamic relation $K = \exp(-\Delta G°/RT)$. If K (and hence $\Delta G°$) is known as a function of T, $\Delta H°$ can be obtained from the slope of an In $K - 1/T$ plot and $\Delta S°$ from the intercept.

The seminal work in this field was carried out by Kebarle and it is surprising to note the gap of 30 years between the foundation paper by Bernal and Fowler on solvation in solution and the first examination of the simpler process of hydration in the gas phase. A series of plots showing the concentrations of various hydrate complexes for $Na(H_2O)_n^+$ as a function of the total pressure of water vapor is given in Fig. 2.29.[26]

Now, an interesting thing can be done with the ΔH values obtained as indicated earlier. One takes the best estimate available for the primary hydration number in solution (see, e.g., Tables 2.7 and 2.11). One then calculates the corresponding heat of hydration in the gas phase for this number and compares it with the corresponding individual heat of hydration of the ion in solution. The difference should give the residual amount of interaction heat outside the first layer (because in the gas phase there is no "outside the first layer").

The hydration energy for the outer shell turns out to be 15% of the whole for cations and about 30% for anions. Thus, in hydration of the alkali and halide ions,

[26]In Fig. 2.29 a non-SI unit, the torr, is used. The unit is named for Torricelli, who first discussed the partial vacuum above mercury contained in a tube and found it to be ~1/760 of an atmosphere.

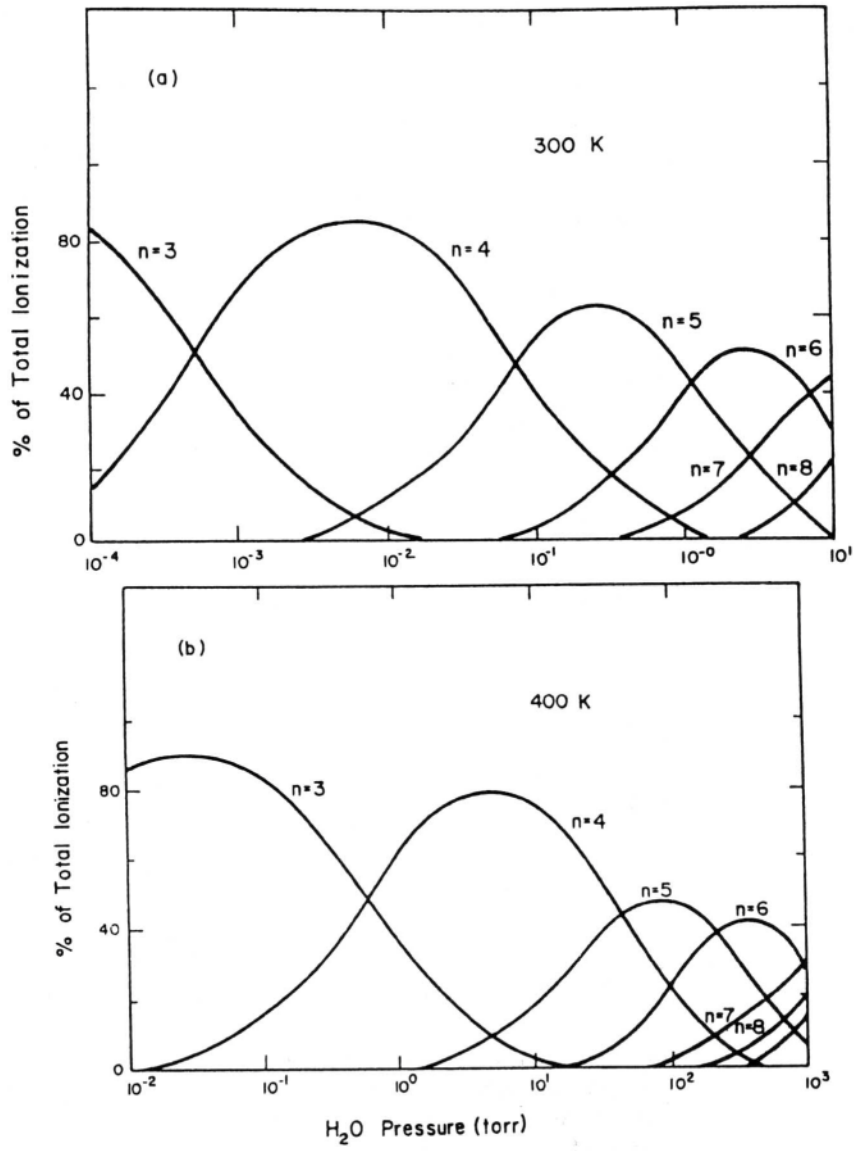

Fig. 2.29. Relative concentrations of Na^+ ion hydrates, $Na(H_2O)_n^+$, in the gas phase at (a) 300 K and (b) 400 K. (Reprinted from B. E. Conway, *Ionic Hydration in Chemistry and Biophysics*, Elsevier, New York, 1981.)

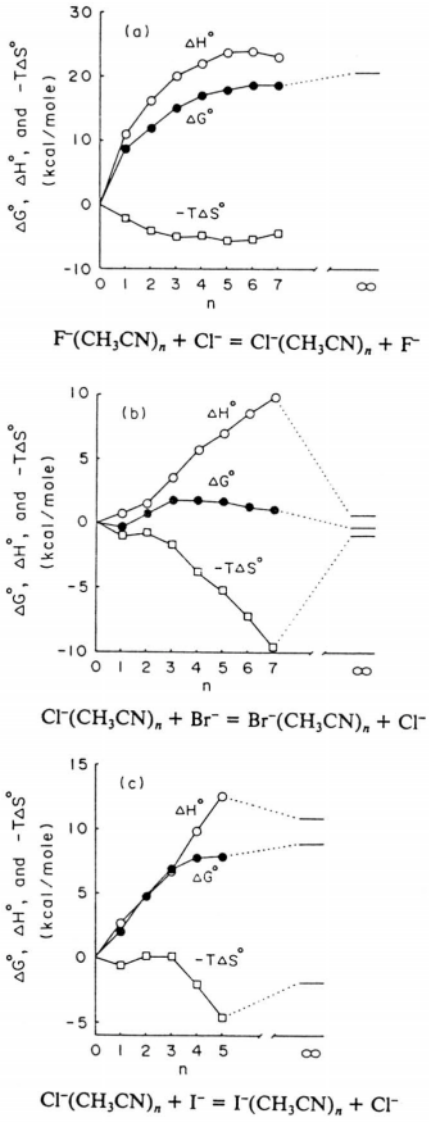

Fig. 2.30. The *n* dependence of differential integrated thermochemical values, $\Delta G°$, $\Delta H°$, and $-T\Delta S°$, for three different solvation reactions. The values with $n = \infty$ correspond to the relative thermochemical values for the bulk hydration of the ions (1 cal = 4.184 J). (Reprinted from K. Hiraoka, S. Mizuse, and S. Yamabe, *J. Phys. Chem.* **92**: 3943,1988.)

between 70 and 85% of the heat of hydration of ions comes from the first shell. One reason for the interest in this result lies in the electrode process field where the traditional theory of the energetics of electron transfer has in the past stressed the outer and not the inner shell solvation as having a major influence on electron transfer, although the present material makes the waters in the first layer those which exert the major control on the ion–solvent interaction energy.

Kebarle used a pulsed electron beam to produce ions for injection into a mass spectrograph that contained the water molecules at a determined, but variable partial pressure. Hiraoka et al. found that $-\Delta G^\circ$ decreases more rapidly with a change in the numbers of water molecules attached to Cl^- than for Br^- and crosses over at $n_h = 4$. Evidence for some degree of covalent bonding occurs for $F^-(CH_3CN)$. The completion of the first solvation shell does not occur until $n_h = 8$ in this case, a surprisingly high number. The trends found are diagrammed in Fig. 2.30.

Hiraoka et al. have also discussed how the results of their measurements on solvation in the gas phase are related to the more usually discussed liquid phase solvation. The first water molecules go onto the ion and are structure-forming.

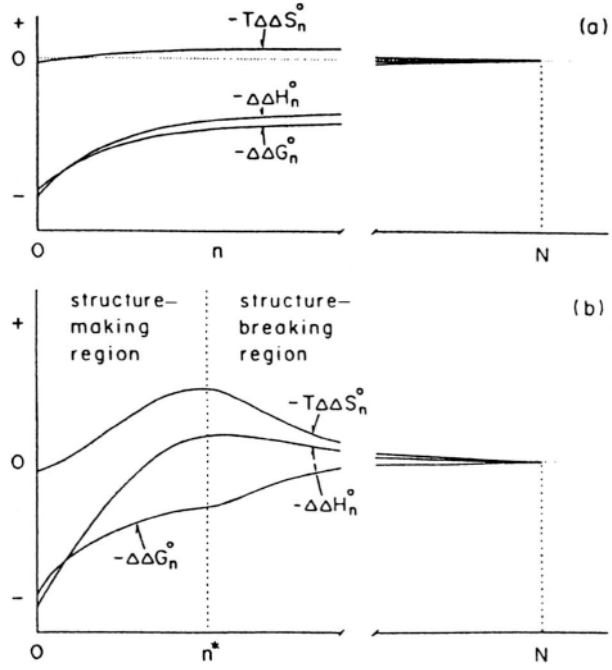

Fig. 2.31. Schematic representation of n dependence of $-\Delta\Delta G_n^\circ$, $-\Delta\Delta H_n^\circ$, and $-T\Delta\Delta S_n^\circ$ for reactions (a) $Cl^-(H_2O)_{n-1} + H_2O = Cl^-(H_2O)_n$ and (b) $Cl^-(CH_3CN)_{n-1} + CH_3CN = Cl^-(CH_3CN)_n$. (Reprinted from K. Hiraoka, S. Mizuse, and S. Yamabe, *J. Phys. Chem.* **92**: 3943, 1988.)

However, as the shell builds up and breaks more and more H bonds in the surrounding solvent, the effect of ions on liquid water begins to become more structure-breaking (Fig. 2.31).

So far, only singly charged ions have been mentioned and there is a good reason for this. A flow of univalent ions can be generated by electron pulses in an atmosphere of water vapor. If the electron energy is sufficiently high to bring about the second ionization of the metal atoms to form M^{2+}, ionization of water also occurs and hence experiments are rendered useless. The results of measurements of equilibria become too complex to interpret. However, in 1984, Yamashita and Fenn introduced a technique that *sprays* ions already in solution into a mass spectroscope. It is possible to spray into the instrument any ions that exist in solution. Such electrospray techniques have opened up an exciting new area of possibilities in gas phase solvation studies, but the database in the 1990s is as yet too sparse to support broader conclusions.

2.14. INDIVIDUAL IONIC PROPERTIES

2.14.1. Introduction

It is usually relatively easy to find the solvation-related property of an *electrolyte* (as, e.g., the heat of hydration, Section 2.5.2) or the partial molar volume (Section 2.6.2) of a salt in solution. However, experiments that reflect the properties of *individual ions* are difficult to devise, the only simple, direct one being the transport number of an ion (Section 2.10) and the associated individual ionic mobility (Section 2.10.1).

It is important to separate the two contributions to ionic solvation in a salt such as NaCl. Thus, the degree of hydration depends first upon the ion–solvent distance. The crystallographic radii of cations are less than those of the parent atom, but those of anions are larger than those of the parent. Cations, therefore, tend to be more hydrated than anions because the attraction rendered by the ion is inversely proportional to its radius. However, when, as with K^+ and F^-, the crystallographic radii are essentially identical, there is even then a nonequal heat of hydration for each ion. This is because the dipole moment of the water molecule is not symmetrically distributed with respect to its geography; its center, which determines the degree of interaction with the ion, is nearer the positive than the negative ion, so that the former is again favored in respect to solvation compared with the latter.

Obtaining the individual properties of ions with solvation numbers from measurements of ionic vibration potentials and partial molar volumes is not necessary in the study of gas phase solvation (Section 2.13), where the individual heats of certain hydrated entities can be obtained from mass spectroscopy measurements. One injects a spray of the solution under study into a mass spectrometer and investigates the time of flight, thus leading to a determination of the total mass of individual ions and adherent water molecules.

2.14.2. A General Approach to Individual Ionic Properties: Extrapolation to Make the Effects of One Ion Negligible

Let it be assumed that the value of the interaction energy of an ion with a solvent is an inverse function of the ion–first water shell distance, r. Then, if one has a series of salts (R_1A, R_2A, . . .) where R is, say, a tetraalkylammonium ion, and the anion is constant, the electrolyte property (e.g., the heat of hydration) can be plotted for the series of RAs, against $1/r_i^n$ (where r represents the cation radius), and the extrapolated value for $1/r_i^n = 0$ is then the individual heat of hydration for the common anion, A^-.

If an accepted value of the property for this one anion can be derived, then, of course, it can be coupled with data for various electrolytes containing this anion. If the data pertain to dilute solutions, avoiding the interfering effects of ion-ion interactions, it is possible to derive the individual value for the heat of hydration of the cations.

This method sounds simple at first. However, there are certain difficulties. One has to decide on a value of n in the plot of $1/r_i^n$ and this may not always be unity or simple. Various terms that affect the calculation of the heat of hydration of ions depend on r^{-2}, r^{-3}, and r^{-4}. Against which one should one plot?

Because the appropriate n is uncertain, it may be a better tactic to make a different extrapolation and plot the property of the electrolyte against the molecular weight of the cation and then extrapolate to zero, as with partial molar volumes, which was illustrated in Fig. 2.15.

Conway and his associates have been foremost in studying individual ionic properties and have published a weighted analysis of many suggested methods for obtaining individual ionic properties (see the reading lists). Among the methods chosen by Conway et al. as excellent, two have been discussed in this chapter so far, namely, extrapolation against cation molecular weight and combining partial molar volume with data on ionic vibration potential to determine individual solvation numbers. Another method with good reliability involves measurements of the heat produced in reversible electrolytic cells, which can be used to deduce individual, ionic entropies, as will be explained in Section 2.15.8. First, though, it is desirable to describe one particular method used for the individual heat of hydration of the proton, clearly a most fundamental quantity.

2.15. INDIVIDUAL HEAT OF HYDRATION OF THE PROTON

2.15.1. Introduction

A particular method of obtaining this fundamental quantity was given by Halliwell and Nyburg in 1963 and although there have been several reexaminations of the process,[27] changes of only about 1 % in a value first calculated in 1963 have been made.

---

[27]These include information on the dynamics of proton hydration.

It seems reasonable therefore to examine the process that gave such a hardy number so reliably.

2.15.2. Relative Heats of Solvation of Ions on the Hydrogen Scale

Consider the unambiguous experimental value ΔH_{HX-H_2O}, the heat of hydration of HX. It is made up of the heats of hydration of H^+ ions and X^- ions.[28]

$$\Delta H_{HX} = \Delta H_{H^+} + \Delta H_{X^-} \tag{2.29}$$

The heat of solvation of X^- ions relative to that of H^+ ions [i.e., $\Delta H_{X^-}(rel)$] can be defined by considering ΔH_{H^+} as an arbitrary zero in Eq. (2.29), that is,

$$\Delta H_{X^-}(rel) = \Delta H_{X^-}(abs) + \Delta H_{H^+}(abs) = \Delta H_{HX} \tag{2.30}$$

Thus, the notation (rel) and (abs) has been inserted to distinguish between the *relative* ΔH_{X^-} value of X^- ions on an arbitrary scale of $\Delta H_{H^+}(abs) = 0$ and the *absolute* or true ΔH_{X^-} values. From Eq. (2.30),

$$\Delta H_{X^-}(rel) = \Delta H_{HX} \tag{2.31}$$

and since ΔH_{HX} (the heat of hydration of an electrolyte) can be experimentally obtained to a precision determined only by measuring techniques (i.e., it includes no structural assumptions), one can see that the relative heat of solvation, $\Delta H_{X^-}(rel)$, is a clear-cut experimental quantity.

Relative heats of solvation can also be defined for positive ions. One writes

$$\Delta H_{MX} = \Delta H_{M^+}(abs) + \Delta H_{X^-}(abs) \tag{2.32}$$

and substitutes for $\Delta H_{X^-}(abs)$ from Eq. (2.30). Thus, one has

$$\Delta H_{X^-}(abs) = \Delta H_{X^-}(rel) - \Delta H_{H^+}(abs) = \Delta H_{HX} - \Delta H_{H^+}(abs) \tag{2.33}$$

which, when inserted into Eq. (2.32), gives

$$\Delta H_{MX} = \Delta H_{M^+}(abs) + \Delta H_{HX} - \Delta H_{H^+}(abs) \tag{2.34}$$

or

---

[28]One should, strictly speaking, write

$$\Delta H_{HX-H_2O} = \Delta H_{H^+-H_2O} + \Delta H_{X^--H_2O}$$

but the $-H_2O$ will be dropped in the subsequent text to make the notation less cumbersome.

TABLE 2.12

Relative Heats of Hydration of Individual Ions, $\Delta H_{H^+}(\text{abs}) = 0$

Ion	Relative Heat of Hydration
Li^+	+136.34
Na^+	+163.68
K^+	+183.74
Rb^+	+188.80
Cs^+	+194.60
F^-	−381.50
Cl^-	−347.50
Br^-	−341.00
I^-	−331.20

$$\Delta H_{M^+}(\text{abs}) - \Delta H_{H^+}(\text{abs}) = \Delta H_{MX} - \Delta H_{HX} \tag{2.35}$$

Taking $\Delta H_{H^+}(\text{abs})$ as an arbitrary zero in this equation permits the definition of the relative heat $\Delta H_{M^+}(\text{rel})$ for the heat of solvation of positive ions

$$\Delta H_{M^+}(\text{rel}) = \Delta H_{M^+}(\text{abs}) - \Delta H_{H^+}(\text{abs}) = \Delta H_{MX} - \Delta H_{HX} \tag{2.36}$$

Since ΔH_{MX} and ΔH_{HX} are unambiguous experimental quantities, so are the relative heats of solvation, $\Delta H_{M^+}(\text{rel})$, of positive ions.

On this basis, a table of relative heats of solvation of individual ions can be drawn up (Table 2.12). These relative heats can be used, as will be promptly shown, to examine the degree of truth in the assumption that ions of equal radii and opposite charge have equal heats of solvation.

2.15.3. Do Oppositely Charged Ions of Equal Radii Have Equal Heats of Solvation?

Consider two ions M_i^+ and X_i^- of *equal radius* r_i *but opposite charge.* If their *absolute* heats of solvation are equal, one expects that

$$\Delta H_{M_i^+}(\text{abs}) - \Delta H_{X_i^-}(\text{abs}) = 0 \tag{2.37}$$

But, from the definition of the *relative* heats of solvation of positive ions [Eq. (2.36)] and of negative ions [Eq. (2.33)], one has by subtraction

$$\Delta H_{M_i^+}(\text{abs}) - \Delta H_{X_i^-}(\text{abs}) = [\Delta H_{M_i^+}(\text{rel}) - \Delta H_{X_i^-}(\text{rel})] + 2\Delta H_{H^+}(\text{abs}) \tag{2.38}$$

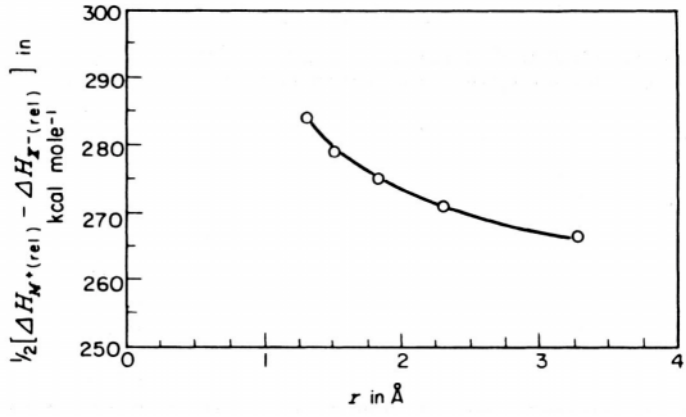

Fig. 2.32. Plot of the difference between the relative heats of hydration of oppositely charged ions with equal radii vs. ionic radius. Values are in kilocalories (1 cal = 4.184 J).

If, therefore, the left-hand side is zero, then one should find, since $\Delta H_{H^+}(\text{abs})$ is a constant, that

$$\Delta H_{M_i^+}(\text{rel}) - \Delta H_{X_i^-}(\text{rel}) = \text{a constant} \tag{2.39}$$

This prediction can easily be checked. One makes a plot of the experimentally known relative heats of solvation of positive and negative ions as a function of ionic radius. By erecting a perpendicular at a radius r_i, one can get the difference $[\Delta H_{M_i^+}(\text{rel}) - \Delta H_{X_i^-}(\text{rel})]$ between the relative heats of solvation of positive and negative ions of radius r_i. By repeating this procedure at various radii, one can make a plot of the differences $[\Delta H_{M^+}(\text{rel}) - \Delta H_{X^-}(\text{rel})]$ as a function of radius. If oppositely charged ions of the same radius have the same absolute heats of hydration, then $[\Delta H_{M^+}(\text{rel}) - \Delta H_{X^-}(\text{rel})]$ should have a constant value independent of radius. It does not (Fig. 2.32).

2.15.4. The Water Molecule as an Electrical Quadrupole

The structural approach to ion–solvent interactions has been developed so far by considering that the electrical equivalent of a water molecule is an idealized dipole, i.e., two charges of equal magnitude but opposite sign separated by a certain distance. Is this an adequate representation of the charge distribution in a water molecule?

Consider an ion in contact with the water molecule; this is the situation in the primary hydration sheath. The ion is close enough to "see" one positively charged region near each hydrogen nucleus and two negatively charged regions corresponding

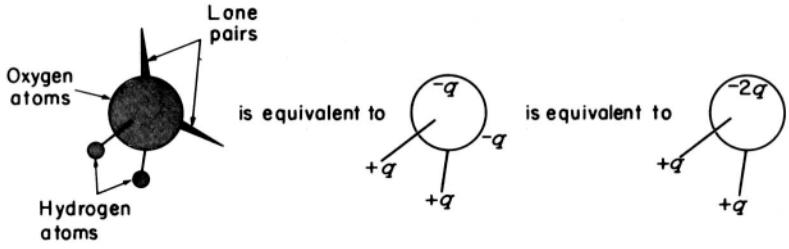

Fig. 2.33. The electrical equivalence between a water molecule and a quadrupole.

to the lone pairs near the oxygen atom. In fact, from this intimate viewpoint, the charge distribution in the water molecule can be represented (Fig. 2.33) by a model with four charges of equal magnitude q: a charge of $+q$ near each hydrogen atom, and two charges each of value $-q$ near the oxygen atom. Thus, rather than consider that the water molecule can be represented by a dipole (an assembly of two charges), a better approximation, suggested by Buckingham (1957), is to view it as a *quadrupole*, i.e., an assembly of four charges. What may this increase in realism of the model do to the remaining discrepancies in the theory of ion-solvent interactions?

2.15.5. The Ion–Quadrupole Model of Ion–Solvent Interactions

The structural calculation of the heat of ion-solvent interactions involves the following cycle of hypothetical steps: (1) A cluster of $n + 1$ water molecules is removed from the solvent to form a cavity; (2) the cluster is dissociated into $n + 1$ independent water molecules; (3) n out of $n + 1$ water molecules are associated with an ion in the gas phase through the agency of ion–dipole forces; (4) the primary solvated ion thus formed in the gas phase is plunged into the cavity; (5) the introduction of the primary solvated ion into the cavity leads to some structure breaking in the solvent outside the cavity; and (6) finally, the water molecule left behind in the gas phase is condensed into the solvent. The heat changes involved in these six steps are W_{CF}, W_D, W_{I-D}, W_{BC}, W_{SB}, and W_C, respectively, where, for $n = 4$.

$$W = W_{CF} + W_D + W_{SB} + W_C = +20 \text{ for positive ions}$$

$$= +30 \text{ for negative ions} \tag{2.40}$$

$$W_{I-D} = -\frac{4N_A z_i e_0 \mu_W}{(r_i + r_W)^2} \tag{2.41}$$

$$W_{BC} = -\frac{N_A (z_i e_0)^2}{2(r_i + 2r_W)}\left(1 - \frac{1}{\varepsilon_W} - \frac{T}{\varepsilon_W{}^2}\frac{\partial \varepsilon_W}{\partial T}\right) \tag{2.42}$$

and the total heat of ion–water interactions is

$$\Delta H_{I\text{-}H_2O} = W + W_{I\text{-}D} + W_{BC} \tag{2.43}$$

If one scrutinizes the various steps of the cycle, it will be realized that for only one step, namely, step 3, does the heat content change [Eq. (2.41)] depending upon whether one views the water molecule as an electrical dipole or quadrupole. Hence, the expressions for the heat changes for all steps *except* step 3 can be carried over as such into the theoretical heat of ion–water interactions, $\Delta H_{I\text{-}H_2O}$, derived earlier. In step 3, one has to replace the heat of ion–dipole interactions, $W_{I\text{-}D}$ [Eq. (2.41)], with the heat of ion–quadrupole interactions (Fig. 2.34).

What is the expression for the energy of interaction between an ion of charge $z_i e_0$ and a quadrupole? The derivation of a general expression requires sophisticated mathematical techniques, but when the water molecule assumes a symmetrical orientation (Fig. 2.35) to the ion, the ion–quadrupole interaction energy can easily be shown to be (Appendix 2.3)

$$E_{I\text{-}Q} = -\frac{z_i e_0 \mu_W}{r^2} \pm \frac{z_i e_0 p_W}{2r^3} \tag{2.44}$$

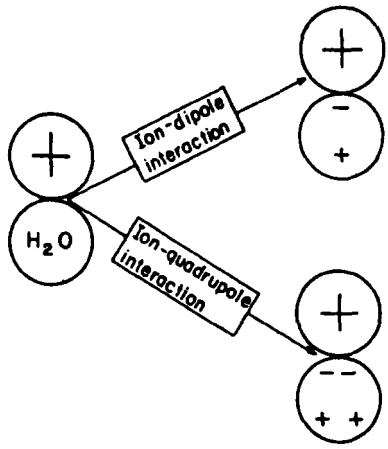

Fig. 2.34. Improvement in the calculation of the ion–water molecule interactions by altering the model of the water molecule from a dipole to a quadrupole.

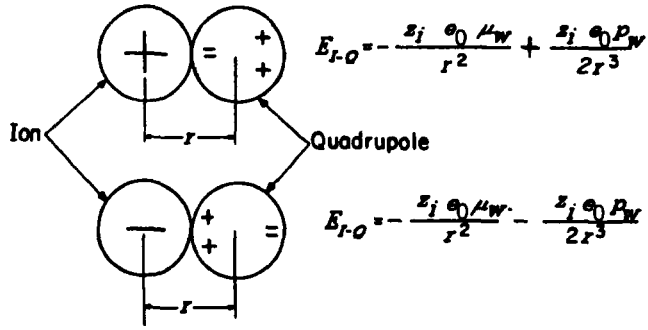

Fig. 2.35. The symmetrical orientation of a quadrupole to an ion.

where the + in the ± is for positive ions, and the – is for negative ions, and p_W is the quadrupole moment (3.9×10^{-26} esu) of the water molecule. It is at once clear that a difference will arise for the energy of interaction of positive and negative ions with a water molecule, a result hardly foreseeable from the rudimentary dipole viewpoint and hence probably accountable for the result shown in Fig. 2.32.

The first term in this expression [Eq. (2.44)] is the dipole term, and the second term is the quadrupole term. It is obvious that with increasing distance r between ion and water molecule, the quadrupole term becomes less significant. Or, in other words, the greater the value of r, the more reasonable it is to represent the water molecule as a dipole. However, as the ion comes closer to the water molecule, the quadrupole term becomes significant, i.e., the error involved in retaining the approximate dipole model becomes more significant.

When the ion is in contact with the water molecule, as is the case in the primary solvation sheath, expression (2.44) for the ion–quadrupole interaction energy becomes

$$E_{I-Q} = -\frac{z_i e_0 \mu_W}{(r_i + r_W)^2} \pm \frac{z_i e_0 p_W}{2(r_i + r_W)^3} \tag{2.45}$$

The quantity E_{I-Q} represents the energy of interaction between one water molecule and one ion. If, however, four water molecules surround one ion and one considers a mole of ions, the heat change W_{I-Q} involved in the formation of a primary solvated ion through the agency of ion–quadrupole forces is given by

$$W_{I-Q} = 4N_A E_{I-Q} = -\frac{4N_A z_i e_0 \mu_W}{(r_i + r_W)^2} \pm \frac{4N_A z_i e_0 p_W}{2(r_i + r_W)^3} \tag{2.46}$$

where, as before, the + in the ± refers to positive ions and the – to negative ions.

Substituting this expression for W_{I-Q} in place of W_{I-D} in expression (2.43) for the heat of ion-water interactions, one has

$$\Delta H_{I\text{-}H_2O} = 20 - \frac{4N_A z_i e_0 \mu_W}{(r_i + r_W)^2} + \frac{4N_A z_i e_0 p_W}{2(r_i + r_W)^3} - \frac{N_A (z_i e_0)^2}{2(r_i + 2r_W)}$$

$$\times \left(1 - \frac{1}{\varepsilon_W} - \frac{T}{\varepsilon_W{}^2} \frac{\partial \varepsilon_W}{\partial T}\right) \tag{2.47}$$

for positive ions and

$$\Delta H_{I\text{-}H_2O} = 30 - \frac{4N_A z_i e_0 \mu_W}{(r_i + r_W)^2} - \frac{4N_A z_i e_0 p_W}{2(r_i + r_W)^3} - \frac{N_A (z_i e_0)^2}{2(r_i + 2r_W)}$$

$$\times \left(1 - \frac{1}{\varepsilon_W} - \frac{T}{\varepsilon_W{}^2} \frac{\partial \varepsilon_W}{\partial T}\right) \tag{2.48}$$

for negative ions (values in kilocals (gram ion)$^{-1}$.

2.15.6. Ion–Induced Dipole Interactions in the Primary Solvation Sheath

At this level of sophistication, one wonders whether there are other subtle interactions that one ought to consider.

For instance, when the water molecule is in contact with the ion, the field of the latter tends to distort the charge distribution in the water molecule. Thus, if the ion is positive, the negative charge in the water molecule tends to come closer to the ion, and the positive charge to move away. This implies that the ion tends to induce an extra dipole moment in the water molecule over and above its permanent dipole moment. For small fields, one can assume that the induced dipole moment μ_{ind} is proportional to the inducing field X

$$\mu_{ind} = \alpha X \tag{2.49}$$

where α, the proportionality constant, is known as the *deformation polarizability* and is a measure of the "distortability" of the water molecule along its permanent dipole axis.

Thus, one must consider the contribution to the heat of formation of the primary solvated ion (i.e., step 3 of the cycle used in the theoretical calculation presented earlier), which arises from interactions between the ion and the dipoles induced in the water molecules of the primary solvent sheath. The interaction energy between a dipole and an infinitesimal charge dq is $-\mu\, dq/r^2$, or, since dq/r^2 is the field dX due to this charge, the interaction energy can be expressed as $-\mu\, dX$. Thus, the interaction energy between the dipole and an ion of charge $z_i e_0$, exerting a field $z_i e_0/r^2$, can be found by,

performing the integration $-\int_0^{z_i e_0/r^2} \mu \, dX$. In the case of permanent dipoles, μ does not depend on the field X and one gets the result (Appendix 2.2):

$$-\int_0^{z_i e_0/r^2} \mu \, dX = -\frac{z_i e_0}{r^2}\mu \tag{2.50}$$

For induced dipoles, however, $\mu_{ind} = \alpha X$, and, hence,

$$-\int_0^{z_i e_0/r^2} \mu \, dX = -\int_0^{z_i e_0/r^2} \alpha X \, dX = -\left[\frac{\alpha X^2}{2}\right]_0^{z_i e_0/r^2} = \alpha\frac{(z_i e_0)^2}{2r^4} \tag{2.51}$$

Considering a mole of ions and four water molecules in contact with an ion, the heat of ion–induced dipole interactions is

$$-\frac{4N_A\alpha(z_i e_0)^2}{2(r_i + r_W)^4}$$

Introducing this induced dipole effect into the expression for the heat of ion-solvent interactions [Eqs. (2.47) and (2.48)], one has

$$\Delta H_{I\text{–}H_2O} = 20 - \frac{4N_A z_i e_0 \mu_W}{(r_i + r_W)^2} + \frac{4N_A z_i e_0 p_W}{2(r_i + r_W)^3} - \frac{N_A(z_i e_0)^2}{2(r_i + 2r_W)}\left(1 - \frac{1}{\varepsilon_W} - \frac{T}{\varepsilon_W^2}\frac{\partial \varepsilon_W}{\partial T}\right) - \frac{4N_A\alpha(z_i e_0)^2}{2(r_i + r_W)^4} \tag{2.52}$$

for positive ions, and

$$\Delta H_{I\text{–}H_2O} = 30 - \frac{4N_A z_i e_0 \mu_W}{(r_i + r_W)^2} - \frac{4N_A z_i e_0 p_W}{2(r_i + r_W)^3} - \frac{N_A(z_i e_0)^2}{2(r_i + 2r_W)}\left(1 - \frac{1}{\varepsilon_W} - \frac{T}{\varepsilon_W^2}\frac{\partial \varepsilon_W}{\partial T}\right) - \frac{4N_A\alpha(z_i e_0)^2}{2(r_i + r_W)^4} \tag{2.53}$$

for negative ions.

2.15.7. How Good Is the Ion–Quadrupole Theory of Solvation?

A simple test for the validity of these theoretical expressions (2.52) and (2.53) can be constructed. Consider two ions M_i^+ and X_i^- of equal radius but opposite charge. The

difference $\Delta H_{M_i^+}(\text{abs}) - \Delta H_{X_i^-}(\text{abs})$ in their absolute heats of hydration is obtained by subtracting Eq. (2.53) from Eq. (2.52). Since the signs of the dipole term,

$$\frac{4N_A z_i e_0 \mu_W}{(r_i + r_W)^2}$$

the Born charging term,

$$\frac{N_A (z_i e_0)^2}{2(r_i + 2r_W)} \left(1 - \frac{1}{\varepsilon_W} - \frac{T}{\varepsilon_W{}^2} \frac{\partial \varepsilon_W}{\partial T}\right)$$

and the induced dipole term,

$$\alpha \frac{4N_A (z_i e_0)^2}{2(r_i + r_W)^4}$$

are invariant with the sign of the charge of the ion, they cancel out in the subtraction (as long as the orientation of a dipole near a cation is simply the mirror image of that near an anion). The quadrupole term, however, does not cancel out because it is positive for positive ions and negative for negative ions. Hence, one obtains[29]

$$\Delta H_{M_i^+}(\text{abs}) - \Delta H_{X_i^-}(\text{abs}) = -41 + \frac{4N_A z_i e_0 p_W}{(r_i + r_W)^3} \tag{2.54}$$

It is seen from this equation that the quadrupolar character of the water molecule would make oppositely charged ions of equal radii have radius-dependent differences in their heats of hydration (Fig. 2.32). Further, Eq. (2.38) has given

$$\Delta H_{M_i^+}(\text{abs}) - \Delta H_{X_i^-}(\text{abs}) = \Delta H_{M_i^+}(\text{rel}) - \Delta H_{X_i^-}(\text{rel}) + 2\Delta H_{H^+}(\text{abs}) \tag{2.38}$$

By combining Eqs. (2.38) and (2.54), the result is

$$\Delta H_{M_i^+}(\text{rel}) - \Delta H_{X_i^-}(\text{rel}) = -2\Delta H_{H^+}(\text{abs}) - 41 + \frac{4N_A z_i e_0 p_W}{(r_i + r_W)^3} \tag{2.55}$$

Thus, the ion–quadrupole model of ion–solvent interactions predicts that if the experimentally available differences $\Delta H_{M_i^+}(\text{rel}) - \Delta H_{X_i^-}(\text{rel})$ in the relative heats of solvation of oppositely charged ions of equal radii r_i are plotted against $(r_i + r_W)^{-3}$, one should get a straight line with a slope $+4N_A z_i e_0 p_W$. From Fig. 2.36, it can be seen that

[29]Expression (2.54) is based on the assumption of the radius independence of $W_+ - W_- = 84 - 125 = 41$ kJ (gram ion)$^{-1}$ and the constancy of n with radius over the interval concerned.

the experimental points do give a straight line unless the ionic radius falls below about 13 nm. Further, the theoretical slope $(4.51\ \text{kJ mol}^{-1}\ \text{nm}^3)$ is in fair agreement with the experimental slope $(3.80\ \text{kJ mol}^{-1}\ \text{nm}^3)$.

It can therefore be concluded that by considering a quadrupole model for the water molecule, one can not only explain why oppositely charged ions of equal radius have differing heats of hydration (Fig. 2.32), but can also quantitatively predict the way these differences in the heats of hydration will vary with the radius of the ions concerned.

What are we seeking in this section? The objective is a method to unscramble the individual heats of hydration from values known for the salt, i.e., for at least two individual ions.

An elegant method of obtaining such experimental values is now at hand. Starting from the experimentally proved linearity of $\Delta H_{M_i^+}(\text{rel}) - \Delta H_{X_i^-}(\text{rel})$ vs. $(r_i + r_W)^{-3}$ (Fig. 2.36), one can take Eq. (2.55) and, following Halliwell and Nyburg, extrapo-

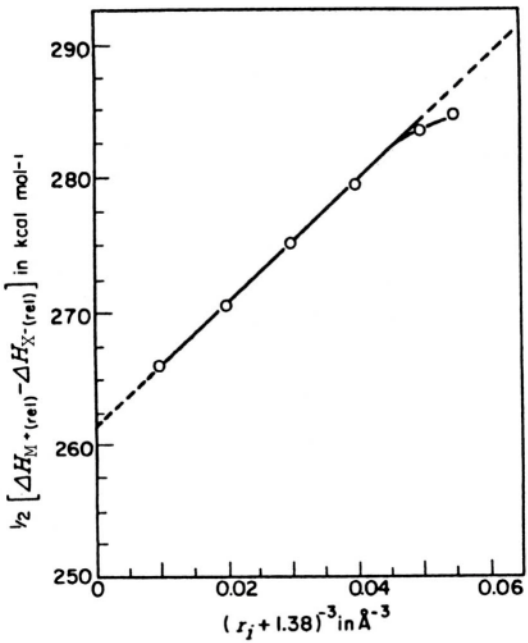

Fig. 2.36. The plot of half the difference in the relative heats of hydration of positive and negative ions of the same radii versus $(r_i + 1.38)^{-3}$. The solid line is through experimental points and the dotted line is the extrapolation of the straight line going through the experimental points (1 cal = 4.184 J; 1 Å = 100 pm).

Å = 100 pm)

TABLE 2.13

Quasi-Experimental Absolute Heats of Hydration of Various Individual Ions

Ion	Absolute Heat of Hydration (kcal. (gram ion)$^{-1}$)
Li^+	−129.7
Na^+	−102.3
K^+	−82.3
Rb^+	−77.2
CS^+	−71.4
F^-	−115.5
Cl^-	−81.5
Br^-	−75.0
I^-	−65.2

late the $\Delta H_{M_i^+}(\text{rel}) - \Delta H_{X_i^-}(\text{rel})$ vs. $(r_i + r_W)^{-3}$ plot to infinite radius, i.e., to $(r_i + r_W)^{-3} \rightarrow 0$. The intercept, which is 2184 kJ mol^{-1}, is then equal to $-2\Delta H_{H^+}(\text{abs}) - 41$, or $\Delta H_{H^+}(\text{abs}) = -1113$ kJ mol^{-1}.

Once one has thus obtained the experimental absolute heat of hydration of the proton, one can use it in combination with experimental values of H^+-containing electrolytes (e.g., HC1) to obtain absolute values of the heat of hydration of other ions, (Table 2.13). Such an approach has a better basis than an older method in which the salt considered had equal radii and the absolute heat of solvation of each was equal to half that of the whole. However, this assumption of the equality of the heats of hydration of ions with the same radius is just not true (Fig. 2.32).

Conway and Soloman corrected Halliwell and Nyburg's (1963) value for the numerical value of the dipole moment of water and got −1117 kJ mol^{-1}. Then, Lister, Nyburg, and Doyntz reattacked the calculation using a different series of ions of the same size. They got −1096 kJ mol^{-1}.

The best value in the late 1990s is −1110 kJ mol^{-1} (*cf.* the original value of −1113). As stated earlier, knowledge of the absolute heat of hydration of H^+ allows individual heats of hydration of anions to be obtained from the corresponding heats for an electrolyte, HX. Knowing the individual heats for some typical X^- ions allows one to couple these values with the heats of hydration of MXs and obtain individual values for M^+ ions. A few values are given in Table 2.13.

2.15.8. How Can Temperature Coefficients of Reversible Cells Be Used to Obtain Ionic Entropies?

In Section 2.13, it was shown how it is possible to obtain the entropy of solvation for an electrolyte, but that left open the separation into the individual entropies of solvation for each ion.

A well-known thermodynamic expression for the change in entropy $\Delta S°$ of a process is

$$\Delta S = -\frac{\partial \Delta G}{\partial T} \tag{2.56}$$

with ΔG as the free-energy change.

Furthermore, when an electrochemical cell works in a thermodynamically reversible way (see Vol. 2, Chapter 7),

$$\Delta G° = -nFE \tag{2.57}$$

where n is the number of electrons for one step of the overall reaction.

It follows from Eq. (2.56) that

$$\Delta S = nF\frac{\partial E}{\partial T} \tag{2.58}$$

Now, this ΔS of a *cell* reaction must be composed of the entropies of at least two different ions in solution (because two electrode reactions are involved, one at each electrode), so that Eq. (2.58) cannot lead directly to an individual ionic entropy.

However, in 1941, Lee and Tai considered the potential and temperature coefficients of the following cells:

1. $Hg(ecm) \mid Hg_2Cl_2(sat), KCl(a_{Cl^-} = 1) \mid Hg$ E_1
2. $H_2 \mid Hg_2Cl_2(sat), HCl(a_{H^+} = 1) \mid Hg$ E_2
3. $Hg(ecm) \mid HCl(a_{H^+} = 1) \mid H_2$ E_3

The suffix (ecm) for cells 1 and 3 represents the term "electrocapillary maximum" and can be regarded (Vol. 2, Chapter 6) as a potential at which the electrode has zero charge.

Lee and Tai assumed that the potential at which the excess charge on the electrode is zero also indicates an interfacial potential difference of zero. This would not be consistent with the viewpoint of workers in the late 1990s (Vol. 2, Chapter 6), but let it be assumed to be so for now and follow Lee and Tai's reasoning.

Contemplating then cell (3),[30] if the Hg electrode does not contribute to the temperature coefficient of the potentials measured, then E_3 of the cell (being equivalent to $\Delta S°$) must yield here the entropy difference $(\frac{1}{2}S_{H_2} - S_{H^+})$ of the ion undergoing a reversible equilibrium reaction at Pt (right-hand electrode, cell 3) with H_2 in the gas phase and H^+ in solution at unit activity.

---

[30] In fact, Lee and Tai made measurements on cells (1) and (2) and obtained data on cell (3) by observing that $E_3 = E_1 - E_2$.

TABLE 2.14

Absolute Standard Partial Gram-Ionic Entropies of H^+ and Cl^- Ions[a]

Author(s)	$\bar{S}^\circ_{Cl^-}$	Discrepancy between Values with Various Electrolytes	Value of $\bar{S}^\circ_{H^+}$
Eastman (NaCl, KCl, HCl)	18.5 (288 K)	0.2	-5.0 ± 1.87
Crockford and Hall (NaCl, KCl, NH_4Cl, HCl)	19.8 (285.5 K)	1.8	-6.3 ± 3.8
Lange and Hesse (HCl)	18.2 (298 K)		−4.7
Lee and Tai	Value obtained using electrode at ecm		−5.4

Source: Reprinted from B. E. Conway, *Ionic Hydration in Chemistry and Biophysics*, Elsevier, New York, 1981.

[a]Units are cal K^{-1} mol^{-1}. 1 cal = 4.184 J.

However, the entropy of H_2 in the gas phase is well known and hence $S^\circ_{H^+}$ can be obtained. Lee and Tai, in fact, obtained $-22.6\ J\ K^{-1}\ mol^{-1}$ for $S^\circ_{H^+}$, the absolute standard entropy of H^+ in solution.

What of Lee and Tai's assumption that a charge-free surface involves no potential contribution to the cell? In fact, work done much later suggests that the missing temperature coefficient is only 0.01, so that the error Lee and Tai introduced by their outmoded assumption is indeed negligible.

Other work on the temperature coefficient of cells gave rise to a more complex analysis, but produced essentially the same result as that of Lee and Tai. Thus, Table 2.14 can be taken to indicate a result of $-20.9\ J\ K^{-1}\ mol^{-1}$ for this important quantity, $S^\circ_{H^+}$.

Having obtained the individual value of the gram-ionic entropy of the hydrogen ion in solution, the individual *entropy of hydration* can be obtained by a straightforward calculation of the value of $(S_{H^+})_{gas}$ from statistical mechanical reasoning.

To use this value of S_{H^+} to obtain the individual ionic entropies of other ions in solution, it is necessary to know values for the entropy of hydration of a number of electrolytes containing H^+. Thereafter, the value of the entropy of the counterion can be obtained. It can then be used in conjunction with entropies of hydration of electrolytes containing the counterion to determine the absolute entropies of partner ions in the electrolyte containing the constant anion. Of course, in all cases, the value of the entropy of the ion in the gaseous state must be subtracted from that of the ion in solution to give the entropy of hydration [i.e., $\Delta S_{hyd} = (S_i)_{soln} - (S_i)_{gas}$].

These considerations of individual entropies take it for granted that values of $(S)_{hyd}$ for a group of electrolytes are known (Table 2.15). This is acceptable pedagogically because in Section 2.5.3 one learned how to obtain ΔH_s and ΔG_s. So, the equation

TABLE 2.15

Entropies of Hydration of Individual Ions at 298 K and Quantities Used in Their Derivation[a,b]

Ion	Conventional $\bar{S}_i^\circ$	$\tilde{S}_i$ (assuming $\bar{S}^\circ_{H^+} = -5.0$)	$S^\circ_{i,g}$	$\Delta S^\circ_{s,i}$ [c]
H^+	0	−5.0	26.0	−31.0
Li^+	4.7	−0.3	31.8	−32.1
Na^+	14.0	9.0	35.3	−26.3
K^+	24.2	19.2	36.9	−17.7
Rb^+	28.7	23.7	39.3	−15.6
NH_4^+	26.4	21.4	—	—
Ag^+	17.5	12.5	39.9	−27.4
Tl^+	30.5	25.5	41.9	−16.4
Mg^{2+}	−31.6	−41.6	35.5	−77.1
Ca^{2+}	−11.4	−21.4	37.0	−58.4
Sr^{2+}	−7.3	−17.3	39.3	−56.6
Ba^{2+}	2.3	−7.7	40.7	−48.4
Zn^{2+}	−25.7	−35.7	38.5	−74.2
Cd^{2+}	−16.4	−26.4	40.1	−66.5
Fe^{2+}	−25.9	−25.9	38.0	−73.9
Cu^{2+}	−26.5	−36.5	38.5	−75.0
Sn^{2+}	−4.9	−14.9	40.3	−55.2
Pb^{2+}	3.9	−6.1	41.9	−48.0
Al^{4+}	−76.0	−91.0	35.9	−126.8
F^-	−2.3	3.0	34.8	−31.8
Cl^-	13.5	18.5	36.7	−18.2
Br^-	19.7	24.7	39.1	−14.4
I^-	25.3	30.3	40.4	−10.1
OH^-	−2.5	2.5	—	
NO_3^-	35.0	40.0	—	—
ClO_4^-	43.6	48.6	—	—
SO_4^{2-}	4.4	5.6	—	—
CO_3^{2-}	−13.0	−3.0	—	—
PO_4^{3-}	−45.0	−30.0	—	—

Source: Reprinted from B. E. Conway, *Ionic Hydration in Chemistry and Biophysics*, Elsevier, New York, 1981.

[a] Based on Latimer's scale of conventional ionic entropies. Units are cal K^{-1} mol^{-1}.

[b] 1 cal = 4.184 J.

[c] Ionic entropy of hydration as $\Delta S^\circ_{s,i} = \bar{S}^\circ_i - S^\circ_{i,g}$ when $S^\circ_{i,g}$ is the gas-phase ionic entropy.

$\Delta S_s = (\Delta H_s - \Delta G_s)/T$ can be used to obtain ΔS_s, the entropy of hydration of an electrolyte.

However, there is a direct method to obtain ΔS_s, via the thermodynamics of reversibly behaving cells *without* any special assumptions. Thus, consider a cell that is assumed to be run in a thermodynamically reversible way:

$$H_2 \mid HCl \mid Hg_2Cl_2 \mid Hg$$

The overall reaction is

$$H_2 + Cl_2 \rightarrow 2\,H^+ + 2\,Cl^-$$

Now:

$$\Delta S = -nF\frac{\partial E}{\partial T} \tag{2.59}$$

However, the entropies of H_2 and Cl_2 in the gas phase can easily be calculated so that the sum of the entropies of H^+ and Cl^- in solution can be obtained. The value H^+ in solution is known (2.15.8). It is fairly easy to devise these kinds of cells, which have been used in obtaining much data.

2.15.9. Individual Ionic Properties: A Summary

In Section 2.15, methods for obtaining the properties of individual ions (their hydration numbers, heats, and entropies) have been considered. Starting with a general method—extrapolation to eliminate the effect of a partner on the value of the (easily obtainable) corresponding electrolyte property—two special cases were dealt with: how one obtains the individual values of the heat of hydration of the proton and then its entropy.

Values of the thermal properties of individual ions do not have the same status as thermodynamic properties (for these are assumption-free). For thermodynamic properties, only the accuracy of the experimental determination can be questioned. For example, in electrochemical cells, are they being operated in equilibrium as required? Thus, determining the values of the properties of individual ions always involves some assumption—that it is appropriate to extrapolate according to a certain $1/r^n$ law, for example—and therefore the values will always be open to improvement. Some of the newer values increasingly refer to nonaqueous solutions.

2.15.10. Model Calculations of Hydration Heats

In the 1970s Bockris and Saluja developed models incorporating and extending ideas proposed by Eley and Evans, Frank and Wen, and Bockris and Reddy. Three basic models of ionic hydration that differ from each other in the structure in the first coordination shell were examined. The features of these models are given in Table 2.16. The notations chosen for the models were 1A, 1B, 1C; 2A, 2B, 2C; and 3A, 3B, 3C, where 1, 2, and 3 refer to three basic hydration models, and A, B, and C refer to the subdivision of the model for the structure-broken (SB) region. These models are all defined in Table 2.16. A model due to Bockris and Reddy (model 3 in Table 2.16 and Fig. 2.37) recognizes the distinction between *coordination number* (CN) and *solvation number* (SN).

TABLE 2.16
Models of Ionic Solvation

Model 1		
First coordination shell		
a. CN = 4 for all monovalent ions b. No distinction between SN and CN		
Second layer (SB region)		
Model A	Model B	Model C
Molecules in the first shell are H bonded to those in the SB region; rest of the solvent as bulk	SB region consists of dimers formed from monomers drawn from liquid water	SB region consists of monomers, some of which librate with respect to molecules in the first shell
Model 2		
First coordination shell		
a. CN ranges from 6 to 8 for monovalent ions b. No distinction between SN and CN		
Second layer (SB region)		
Model A	Model B	Model C
Model 3		
First coordination shell		
a. CN ranges from 6 to 8 for monovalent ions b. Distinction between SN and CN		
Second layer (SB region)		
Model A	Model B	Model C

In the concept of nonsolvated coordinated water, it is assumed that an ion exists in two states in the solution. It is either stationary or engaged in diffusional movement. As an ion arrives at a new site after a movement, its situation in respect to coordination by water is of two types. Clearly, the water molecules must always have some degree of orientation in the direction of their dipoles in the first layer around the ion. It is practical to divide these molecules into two types. There will be those oriented so that these dipoles interact maximally with the ion, and another type that is oriented so that the dipoles are oriented at 90° to the ion and do not interact with it at all. The coordination number refers to the total number of water molecules in the first layer around the ion, independently of how they are oriented.

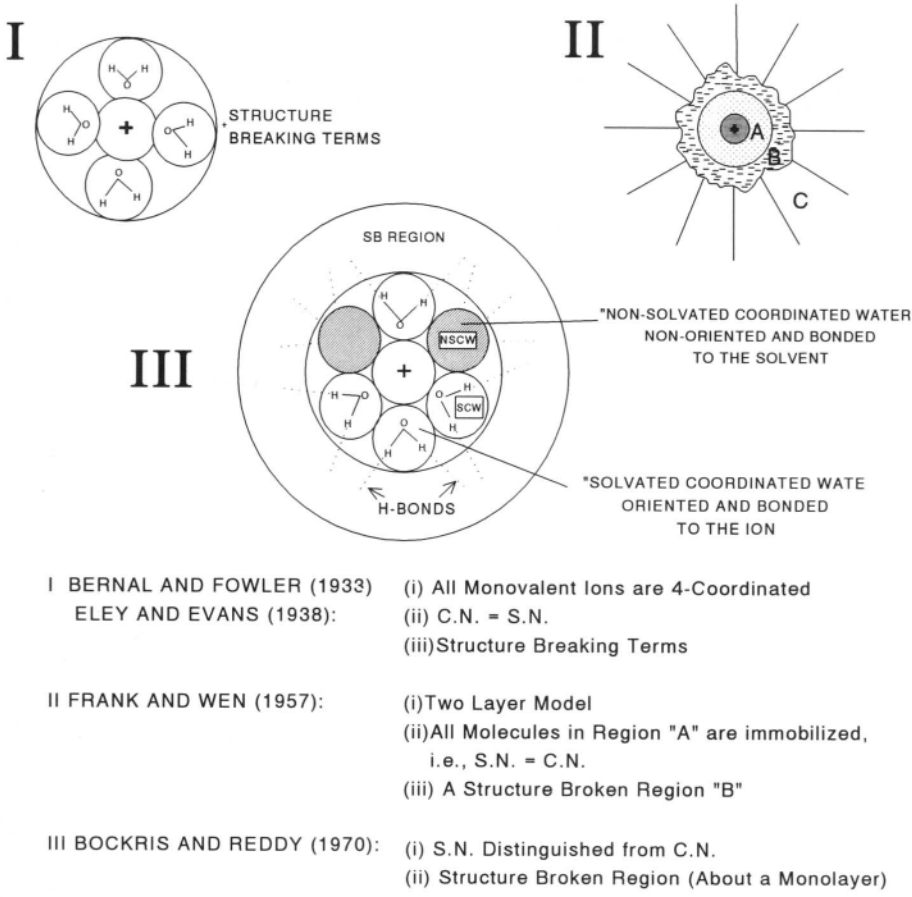

Fig. 2.37. Models for the region near an ion. (Reprinted from J. O.'M. Bockris and P. P. S. Saluja, *J. Phys. Chem.* **76**: 2298,1972.)

The *dynamic* solvation number (as distinguished from the *static* coordination number) is the number of these water molecules *that remain with the ion for at least one diffusive movement.* When an ion arrives at a new site, it may remain there long enough to influence a number of the surrounding water molecules to come out of the water structure and become part of the primary solvation shell that moves with the ion. Conversely, it may remain at a given site for a time so brief that it does not have an effect on the waters that are relatively stable and fixed tightly in the water structure that surrounds it. In the solvent structure these latter may still be thought of as part of the coordinating waters of the ion, but their dipoles have not had sufficient time to rotate into the attractive position ($\cos\theta = 1$), such as that of the solvationally coordinated waters represented by the letters SCW.

2.15.11. Heat Changes Accompanying Hydration

The following steps in a cycle (Fig. 2.38 and Tables 2.17 and 2.18) are carried out in calculating the heat of hydration (ΔH_h): (1) the evaporation of n water molecules from liquid water to the gas phase ($\Delta H_1 = n\Delta H_{evap}$), where n is the number of molecules in the first shell in a given model and ΔH_{evap} is the heat of evaporation ($42.2\ kJ\ mol^{-1}$); (2) the gain on interaction of an ion with n water molecules in the gas phase ($\Delta H_2 = n\Delta H_{ion\text{-}w}$), where $\Delta H_{ion\text{-}w}$ is the ion–water interaction and is negative in sign; (3) a lateral interaction term: $\Delta H_3 = \Sigma\Delta H_{lat}$; (4) the phenomenon known as *Born charging* in which the ion with its coordination shell is returned to the solvent ($\Delta H_4 = \Delta H_{BC}$) (see Appendix 2.1); and (5) the interaction among the molecules in the first shell with molecules in the outer layer and, consequently, structural alterations in the structure-broken region making a net contribution ($\Delta H_5 = \Sigma\Delta H_{SB}$).

The heat of ionic hydration ΔH_h can now be calculated as

$$\Delta H_h = \sum_{z=1}^{5} \Delta H_x \tag{2.60}$$

When all the molecules in the coordination shell are treated as identical, ΔH_h will be given by the cycle in Fig. 2.38.

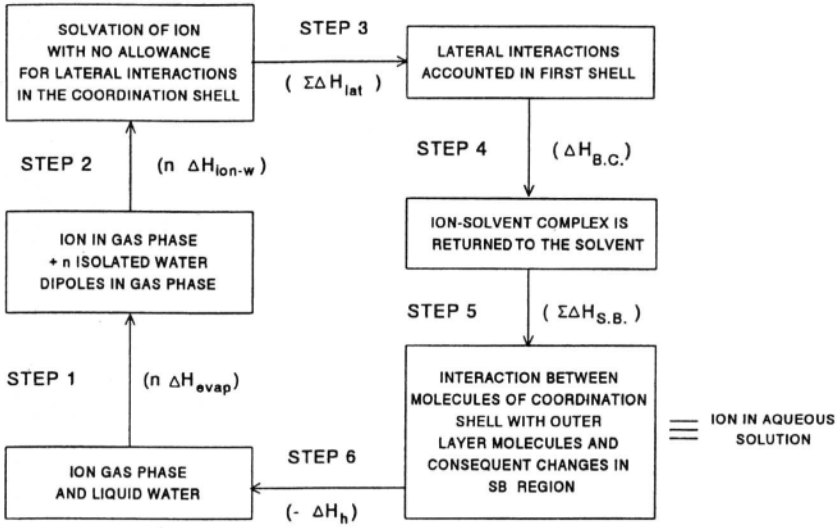

Fig. 2.38. A cycle to separate out various contributions of ion–solvent interactions. (Reprinted from J. O'M. Bockris and P. P. S. Saluja, *J. Phys. Chem.* **76**: 2298,1972.)

TABLE 2.17

Relevant Quantities for Predicting Heat of Hydration, ΔH_h

	Li^+	Na^+	K^+	Rb^+	Cs^+	F^-	Cl^-	Br^-	I^-
τ_{ion}, Å	0.60	0.95	1.33	1.48	1.69	1.36	1.81	1.95	2.16
$\Delta H_{ion\text{-}w} = H_{ion\text{-}SCW}$, kcal mol^{-1}	−29.92	−20.50	−14.75	−13.17	−11.38	−27.23	−18.67	−16.82	−14.51
$\Delta H_{ion\text{-}NSCW}$, kcal mol^{-1}	1.67	2.03	1.41	1.06	1.64	−10.94	−6.84	−5.99	−4.88
n_{CW} (X-ray)	(6)	(6)	(6)	(6)	(7)	(6)	(7)	(7)	(8)
n_{SCW}	(4)	(4)	(3)	(3)	(2)	(4)	(2)	(2)	(1.5)
n_{NSCW}	(2)	(2)	(3)	(3)	(5)	(2)	(5)	(5)	(6.5)
$(\Sigma E_{lat})_{CN\text{-}4}$, kcal	−2.3	−0.8	1.5	1.5	1.5	7.7	4.8	4.2	3.4
$(\Sigma E_{lat})_{CN\text{-}nCW}$, kcal	−20.7	−2.6	2.6	3.2	5.0	21.7	20.0	17.5	22.0
$(\Sigma E_{lat})_{SN \neq CN}$, kcal	−2.3	−0.8	0.0	0.0	0.0	13.75	0.0	0.0	0.0
ΔH_{BC}, kcal	−47.32	−42.91	−38.96	−37.59	−35.84	−38.68	−34.90	−33.87	−32.84
n_{SB}	23.6	28.7	34.8	37.4	41.1	35.3	43.4	46.0	50.2
$\Sigma\Delta H_{SB}$ (model 1A), kcal	−20.2	−20.2	−20.2	−20.2	−20.2	−20.2	−20.2	−20.2	−20.2
$\Sigma\Delta H_{SB}$ (model 2A), kcal	−30.3	−30.3	−30.3	−30.3	−35.4	−30.3	−35.4	−35.4	−40.4
$\Sigma\Delta H_{SB}$ (model 3A), kcal	−35.4	−35.4	−37.9	−37.5	−48.0	−32.8	−48.0	−48.0	−56.8
$\Sigma\Delta H_{SB}$ (model 1–3B), kcal	−64.5	−73.0	−83.0	−87.0	−92.75	−83.75	−96.25	−100.25	−106.7
$\Sigma\Delta H_{SB}$ (model 1C), kcal	−29.7	−31.7	−34.3	−35.3	−36.8	−34.4	−37.8	−38.8	−40.5
$\Sigma\Delta H_{SB}$ (model 2C), kcal	−40.0	−41.7	−44.3	−45.3	−51.8	−44.4	−52.8	−53.8	−60.5
$\Sigma\Delta H_{SB}$ (model 3C), kcal	−44.7	−46.8	−51.8	−52.3	−64.3	−46.9	−65.3	−65.8	−76.7

TABLE 2.18

Ionic Solvation Numbers Obtained in Dilute Solution

Ion	Vibration Potentials + Partial Molar Volumes	Passynski Compressibility	Ulich Entropy	Ulich Mobility	Zana and Yeager	Averages Nearest Integer
Li^+	4.5	5–6	5	3.5	5–6	5 ± 0.4
Na^+	4.5	6–7	4	2.0	7.0	5 ± 0.6
K^+	3.8	6–7	3		6.0	5 ± 1.6
Rb^+	3.0	—	3		—	3 ± 0.0
Cs^+	2.5	—	—		—	—
F^-	4.0	2.0	5		2.0	3 ± 1.2
Cl^-	2.2	0–1	3		1	2 ± 0.8
Br^-	1.8	0	2		0–1	2 ± 0.4
I^-	1.5	0	1		0	1 ± 0.1
Mg^{2+}	10.0	16	13	10.5	15.0	13 ± 2
Ca^{2+}	9.0	—	10	7.5	—	9 ± 0.8
Ba^{2+}	11.0	16	8	5.0	13.0	11 ± 4

$$(\Delta H_h)_{SN=CN} = n\Delta H_{evap} + n\Delta H_{ion\text{-}w} + (\sum \Delta H_{lat})_{SN=CN} + \Delta H_{BC} + (\sum \Delta H_{SB})_{SN=CN} \quad (2.61)$$

When, as suggested by Bockris and Reddy, the number of water molecules that stay with the ion (SN) is distinguished from the number that simply surround the first shell (CN), $\Delta H_{ion\text{-}w}$ will differ for molecules referred to as solvational coordinated water and for those referred to as nonsolvational coordinated water (NSCW). Then ΔH_h will be given by

$$(\Delta H_h)_{SN\neq CN} = n\Delta H_{evap} + n_{SCW}\,\Delta H_{ion\text{-}SCW} + n_{NSCW}\,\Delta H_{ion\text{-}NSCW} + (\sum \Delta H_{lat})_{SN\neq CN} + \Delta H_{BC} + (\sum \Delta H_{SB})_{SN\neq CN} \quad (2.62)$$

Let's now evaluate the different energy terms involved in calculating the heat of hydration of the ions [Eqs. (2.61) and (2.62)] and compare the various models described in Table 2.16.

2.15.11.1. $\Delta H_{ion\text{-}water}$. The energy of an ion interacting with a water molecule oriented along the ionic field is

$$\Delta H_{\text{ion-}w} = \Delta H_{\text{ion-dipole}} + \Delta H_{\text{ion-quadrupole}} + \Delta H_{\text{ion-induced dipole}} \tag{2.63}$$

or

$$\Delta H_{\text{ion-}w} = -\frac{|z|e\mu}{\varepsilon r^2} \pm zep_w \frac{1}{2\varepsilon r^3} - \frac{1}{2}\frac{\alpha_w (zr)^2}{r^4} \tag{2.64}$$

where μ_w, p_w, and α_w are the dipole moment, quadrupole moment, and polarizability of the water molecule. The ion-water distance is symbolized by $r\ (= r_i + r_w)$, where r_i is crystallographic ionic radius and r_w is the radius of the water molecule. The ± sign in the ion–quadrupole term refers to cation and anion, respectively.

Using values of 1.84×10^{-18} esu cm, 3.9×10^{-26} esu cm^2, and 1.444×10^{-24} cm^3 molecule^{-1} for μ_w, p_w, and α_w, respectively, the term $\Delta H_{\text{ion-}SCW}$ can be rewritten as

$$\Delta H_{\text{ion-}SCW}\ (\text{kJ mol}^{-1}) = 60.24\left[\frac{-8.8357}{r^2} \pm \frac{9.3639}{r^3} - \frac{16.6487}{r^4}\right] \tag{2.65}$$

2.15.11.2. $\Delta H_{\text{ion-}NSCW}$. When SN ≠ CN, there will be two interaction energies: (1) the interaction energy of a solvationally coordinated water with the ion, $\Delta H_{\text{ion-}SCW}$; and (2) the interaction energy of nonsolvationally coordinated water (NSCW) with the ion, $\Delta H_{\text{ion-}NSCW}$. The $\Delta H_{\text{ion-}SCW}$ energy is given by Eq. (2.65). An NSCW does not give any average preferred orientation.[31] Before it has time to orient toward the ion, the latter has left the site. Thus, NSCW is still a part of the water structure, but on the average has an H-bonding position blocked by the ion. Thus, its net ion–dipole interaction energy is zero. The interaction energy of an NSCW with the ion arises from the ion–induced dipole, the ion quadrupole, and the dispersion interactions.

Thus,

$$\Delta H_{\text{ion-}NSCW} = \Delta H_{\text{ion-induced dipole}} + \Delta H_{\text{ion-quadrupole}} + \Delta H_{\text{dip}} \tag{2.66}$$

and

$$\Delta H_{\text{ion-}NSCW} = -\frac{1}{2}\frac{\alpha_w (ze)^2}{r^4} \pm \frac{zep_w}{2r^3} - \frac{3}{4}\frac{h\nu\alpha_{\text{ion}}\alpha_w}{r^6} \tag{2.67}$$

[31] Of course, in reality, there will not only be these two positions but also all possible intermediate positions, in which the ion-solvent interaction is given for one solvent molecule by $z_i e_o \mu \cos\theta / \varepsilon_r r^2$. The value of θ is zero for a dipole oriented directly to the ion (cos 0° = 1); and 90° for a distant water molecule (cos 90° = 0). However, there will be all different values of θ in between, and the model presented here does not deal with them. As a simplification; it takes the two extreme situations (all oriented and not at all oriented) and pretends any water molecule belongs to one group or the other.

where α_{ion} is the polarizability of the ion. Values of $\Delta H_{ion\text{-}NSCW}$ calculated from Eq. (2.67) are listed in Table 2.17.

2.15.11.3. ΔH_{lat}. The lateral interactions in the coordination shell for a CN of 4 and 6 can be calculated. A $\Sigma\Delta H_{lat}$ vs. CN plot obtained for CNs of 4 and 6 can be extrapolated. Thus, $\Sigma\Delta H_{lat} \rightarrow 0$ when CN $\rightarrow$ 1, i.e., there is no other molecule to interact with; and for CN = 6, the extrapolation is made to follow the shape of the curve of $\Sigma\Delta H_{lat}$ vs. CN, obtained from the equation

$$\sum \Delta H_{lat} = \frac{D_n \mu_w^2}{r^3} \tag{2.68}$$

where D_n is a geometrical factor depending on the CN. The $(\Sigma\Delta H_{lat})$ arises only from the SCW. Thus, for large ions, which have a low SN, $\Sigma\Delta H_{lat}$ obtained from the $\Sigma\Delta H_{lat}$ vs. CN plot is negligible. Therefore, for large ions ($r_i > 250$ pm), $\Sigma\Delta H_{lat}$ has been neglected.

2.15.11.4. ΔH_{BC} This term can be determined from

$$\Delta H_{BC} = -\frac{N(ze)^2}{2(r_i + 2r_w)}\left[1 - \frac{1}{\varepsilon} - \frac{T}{\varepsilon^2}\left(\frac{\partial \varepsilon}{\partial T}\right)\right] \tag{2.69}$$

Substituting in Eq. (2.69) the appropriate values for ε and $(\partial\varepsilon/\partial T)$, the following equation is obtained:

$$\Delta H_{BC}\,(\text{in kcal mol}^{-1}) = -\frac{6.73z^2}{(r_i + 2r_w)} \tag{2.70}$$

where r_i and r_w are in picometer (pm) units.

2.15.11.5. $\Sigma\Delta H_{SB}$ *(Model A).* This model (Table 2.16) considers H bonding between the molecules in the first layer and those in the region of structure breaking (SB) (Fig. 2.37). The solvated coordinated water (SCW), which is oriented toward the ion, has two H-bonding positions blocked by the ion and offers the remaining two sites for H bonding to the solvent molecules in the SB region (Fig. 2.37). The NSCW is still attached predominantly to the solvent structure but on the average has an H-bonding position blocked by the ion and thus can offer three H-bonding sites to molecules in the SB region. Thus, the net gain in energy from H bonding between molecules in the B region and those in the first layer will be $(2/2)E_{\text{H-bond}}$ for the SCW and $(3/2)E_{\text{H-bond}}$ for NSCW, i.e.,

$$\sum \Delta H_{SB}\,(\text{modelA}) = n_{CW}[(2/2)E_{\text{H-bond}}] \tag{2.71}$$

for the case where the solvation number and the coordination number is the same (SN = CN), and

$$\sum \Delta H_{SB}(\text{modelA}) = n_{SCW}[(2/2)E_{\text{H-bond}}) + n_{SCW}[(3/2)E_{\text{H-bond}}] \qquad (2.72)$$

when the solvation number differs from the coordination number (SN $\neq$ CN). The $E_{\text{H-bond}}$ is the energy of one H bond, equal to –21 kJ mol^{-1}. The numerical values are listed in Table 2.17.

2.15.11.6. $\Sigma\Delta H_{SB}$ *(Model B).* This model (Table 2.16) considers the structure-breaking region as consisting of dimers, which are formed from monomers from liquid water. If the lowering in the potential energy due to formation of a dimer from two monomers is $\Delta E_{m\to d}$, then

$$\sum \Delta H_{SB}(\text{modelB}) = \frac{n_{SB}}{2}(\Delta E_{m\to d}) \qquad (2.73)$$

where n_{SB} is the number of molecules in the SB region per ion, and $\Delta E_{m\to d}$ is taken as the energy of one H bond, i.e., –21 kJ mol^{-1}. Values of $\Sigma\Delta H_{SB}$ (model B) are listed in Table 2.17.

2.15.11.7. $\Sigma\Delta H_{SB}$ *(Model C).* In this model (Table 2.16) the SB region is considered to consist basically of monomers. Some of these monomers are H bonded to the molecules in the first shell. The SCW and NSCW participate in two and three H bonds with molecules in the SB region. The formation of an SB region of monomers can be treated according to the cycle shown in Fig. 2.39. Therefore, one can write

$$\Delta H_{SB} + \Delta H_{\text{evap},SBW} + \Delta H_{\text{cond, }w} = 0 \qquad (2.74)$$

or

$$\Delta H_{SB} = -\Delta H_{\text{evap},SBW} - \Delta H_{\text{cond }w} \qquad (2.75)$$

or

$$\Delta H_{SB} = \Delta H_{\text{evap},w} - \Delta H_{\text{evap},SBW} \qquad (2.76)$$

$\Delta H_{\text{evap},SBW}$ clearly cannot be taken as the heat of evaporation for liquid water. It may be possible to get some rough value for it. In some theories of liquids, a property of interest is that of the free volume, that is, the volume occupied by the liquid minus the volume of the actual molecules considered to occupy "cells." One such theory gives

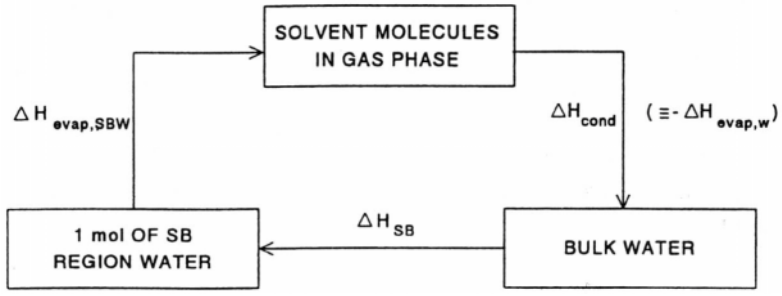

Fig. 2.39. The formation of an SB region of monomers can be treated according to the cycle shown. (Reprinted from J. O'M. Bockris and P. P. S. Saluja, *J. Phys. Chem.* **76**: 2298, 1972.)

$$\ln V_{f,w} = 1 + \ln \frac{RT}{P_w^*} - \frac{\Delta H_{\text{evap},w}}{RT} \tag{2.77}$$

and

$$\ln V_{f,SBW} = 1 + \ln \frac{RT}{P_{SBW}^*} - \frac{\Delta H_{\text{evap},SBW}}{RT} \tag{2.78}$$

Here the P_w^* terms refer to the vapor pressure of bulk water, while P_{SBW}^* is that of the structure-breaking region.

From Eqs. (2.77) and (2.78),

$$\ln \frac{V_{f,SBW}}{V_{f,w}} = -\left(\frac{\Delta H_{\text{evap},SBW} - \Delta H_{\text{evap},w}}{RT}\right) \tag{2.79}$$

on the first-approximation assumption that the vapor pressures of the two forms of water are not significantly different. Using a value of $V_{f,SBW}$ of 0.20 $\text{cm}^3\ \text{mol}^{-1}$ for water in the SB region and 0.40 $\text{cm}^3\ \text{mol}^{-1}$ for $V_{f,w}$

$$\ln \frac{0.20}{0.40} = -\left(\frac{\Delta H_{\text{evap},SBW} - \Delta H_{\text{evap},w}}{RT}\right) \tag{2.80}$$

or

$$\Delta H_{\text{evap},w} - \Delta H_{\text{evap},SBW} = -RT \ln 2 \tag{2.81}$$

Substitution of values from Eq. (2.81) into Eq. (2.76) gives

$$\Delta H_{SB} = -RT \ln 2 = -1.72 \text{ kJ mol}^{-1} \tag{2.82}$$

Thus, for Li^+, where n_{SB} (the number of molecules in the structure-breaking region per ion; see later discussion) is 24, the net contribution of ΔH_{SB} will be –41 kJ. Similar calculations can be carried out for other ions. The net contribution from $\Sigma\Delta H_{SB}$ (model C) comes to

$$\sum \Delta H_{SB}(\text{model C}) = n_{SB}[(2/2)E_{\text{H-bond}}] \tag{2.83}$$

for SN = CN, and

$$\sum \Delta H_{SB}(\text{model C}) = n_{SB}\Delta H_{SB} + n_{SCW}[(2/2)E_{\text{H-bond}}] + n_{SCW}[(3/2)E_{\text{H-bond}}] \tag{2.84}$$

for SN ≠ CN, where ΔH_{SB} in the first term is obtained from Eq. (2.82). The values of $\Sigma\Delta H_{SB}$ (model C) are listed in Table 2.17.

2.15.11.8. n_{SB}. The total number of molecules in the SB region can be calculated by consideration of the close packing of water molecules in the area of a sphere consisting of the ion plus the first layer. Thus, the number of molecules of cross-sectional area πr_w^2 will be given as

$$n_{SB} = \frac{4\pi(r_i + 2r_w)^2}{\pi r_w^2} \tag{2.85}$$

Values of n_{SB} are listed in Table 2.17.

2.15.11.9. *Numerical Evaluation of* ΔH_h. The heats of hydration of monovalent ions have been calculated for the various models by using Eqs. (2.61) and (2.62) and the parameters listed in Table 2.17. The results are shown in Figs. 2.40 and 2.41. From Figs. 2.40 and 2.41 it can be seen that the experimental data for cations fit model 3C of Table 2.16 best, while for the anions, the best fit is with model 3A.

Both models of best fit assume that there is a distinction between the coordination shell and the solvation shell. The difference between cations and anions is that the anion calculations are more consistent with H bonding from the first coordination shell around the ions and the water in the structure-broken region; with the cations, the better model fit is to stress the librating properties of water in the structure-broken region. This difference may arise from the smaller peripheral field strengths of the anions (larger radius) so that there is more time for orientation and H bonding with the (larger amount of) structure-broken waters after an ion arrives in a given region.

All these conclusions must be tempered by continuous reminders that solvation is a dynamic matter and that water molecules are constantly being attracted by the

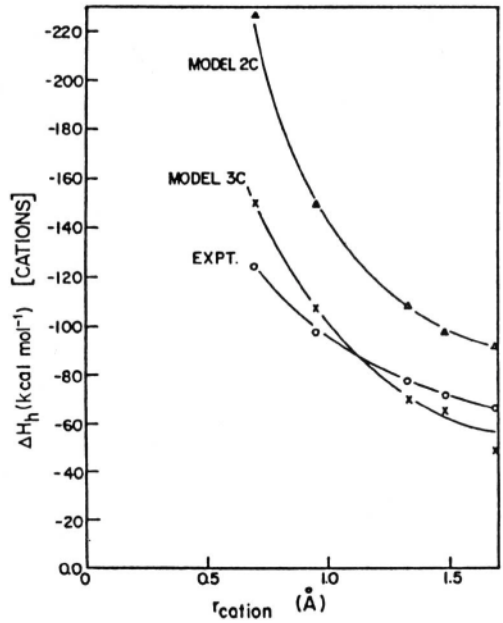

Fig. 2.40. Heat of hydration against radius of cations for various competing models (1 Å = 100 pm; 1 kcal = 4.184 kJ). (Reprinted from J. O'M. Bockris and P. P. S. Saluja, *J. Phys. Chem.* **76**: 2298, 1972.)

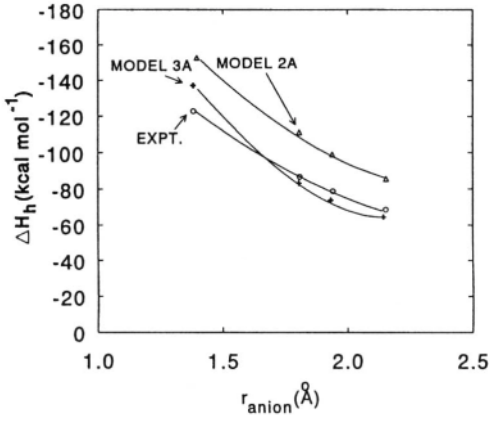

Fig. 2.41. Heat of hydration against radius of anions, for various models (1 Å = 100 pm; 1 kcal=4.184 kJ). (Reprinted from J. O'M. Bockris and P. P. S. Saluja, *J. Phys. Chem.* **76**: 2298,1972.)

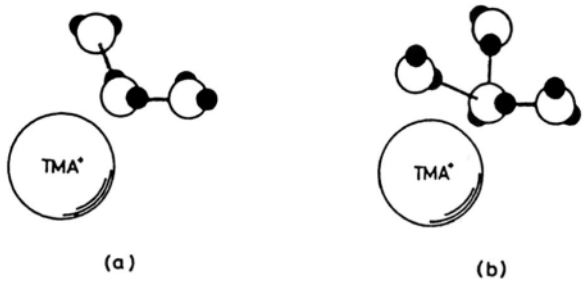

Fig. 2.42. Orientational change of a water molecule in the first hydration shell of a tetramethylammonium ion (TMA^+). (a) A water molecule in the first hydration shell is attached to the TMA^+ ion by charge–electric dipole interaction, (b) Orientational change of a water molecule in the first hydration shell is complemented by formation of another hydrogen bond to an outer water molecule. (Reprinted from Y. Nagano, H. Mizuno, M. Sakiyama, T. Fujiwara, and Y. Kondo, *J. Phys. Chem.* **95**: 2536, 1991.)

ion–dipole forces; but they are also shaken about by the thermal forces, by lateral repulsion between waters, and by the breaking and formation of hydrogen bonds. Orientational changes of waters in the first shell of a tetramethylammonium cation are shown in Fig. 2.42.

2.15.12. Entropy of Hydration: Some Possible Models

The entropy of solvation values reflect solvational structure near an ion. The following discussion of models that are more in agreement with the experimental values of solvational entropies follows the seminal treatment due to Bockris and Saluja in 1982. Models for the region near an ion are shown in Fig. 2.37. The entropy of hydration from the model with no SB region was 170 to 250 $J\ K^{-1}\ mol^{-1}$ lower (more negative) than the experimental values, and was therefore not pursued further.

2.15.13. Entropy Changes Accompanying Hydration

The ΔS_h is the entropy change that accompanies the transition of an ion in the gas phase to an ion in solution (with the arbitrary neglect of any change in crossing the gas–liquid interface).[32] Thus,

---

[32]This does not introduce an error, due to the way in which solvation entropies are calculated. Thus, one calculates the processes of ordering in solution when an ion becomes hydrated and then subtracts the ion's entropy in the gas phase. This is precisely what the experimental value reflects.

$$\Delta S_h = S_{i,\text{soln}} - S_{i,g} \tag{2.86}$$

The second term in the right-hand side of Eq. (2.86) is the entropy of the ion in the gas phase and the first term represents the total entropy change caused upon the entry of the ion into the solution. $S_{i,\text{soln}}$ will be given as

$$[S_{i,\text{soln}}]_{SN=CN} = S_{i,tr} + n_{CW}(S_{i\text{-}CW} - S_{w\text{-}w}) + \Delta S_{BC} + \Delta S_{SB} \tag{2.87}$$

$$[S_{i,\text{soln}}]_{SN\neq CN} = S_{i,tr} + n_{SCW}(S_{i\text{-}SCW} - S_{w\text{-}w}) + n_{NSCW}(S_{i\text{-}NSCW} - S_{w\text{-}w}) + \Delta S_{BC} + \sum \Delta S_{SB} \tag{2.88}$$

where $S_{i,tr}$ is the translational entropy of the ion, $S_{i\text{-}CW}$ is the entropy of coordinated water in the first shell around the ion, $S_{w\text{-}w}$ is the entropy of water in liquid water, ΔS_{BC} is Born-charging entropy, $S_{i\text{-}SCW}$ and $S_{i\text{-}NSCW}$ are the entropy of solvationally coordinated water and nonsolvationally coordinated water, respectively, near the ion, and $\Sigma\Delta S_{SB}$ is the net entropy contribution of the structure-broken region around the ion.

The substitution into Eq. (2.86) of the values of $S_{i,\text{soln}}$ from Eqs. (2.87) and (2.88) gives the entropy of hydration. Relevant terms will be evaluated next.

2.15.13.1. $S_{i,g}$. One uses the Sackur–Tetrode equation for the translational entropy of a monatomic ion in the gas phase and it gives

$$S_{i,g} = \frac{3}{2} R \ln m_{\text{ion}} + 26.0 \tag{2.89}$$

where m_{ion} is the mass of the ion (Table 2.19).

2.15.13.2. ΔS_{BC}. The Born-charging entropy is given by

$$\Delta S_{BC} = \frac{N_A(z_i e_0)^2}{2(r_i + 2r_w)} \frac{1}{2}\left(\frac{\partial \varepsilon}{\partial T}\right) \tag{2.90}$$

which at 298 K becomes

$$\Delta S_{BC} = -\frac{4.09.5 z_i^2}{(r_i + 2r_w)} \quad (\text{J K}^{-1}\ \text{mol}^{-1}) \tag{2.91}$$

where r_i and r_w are in nanometers (Table 2.19).

2.15.13.3. $S_{i,tr}$. The partition function corresponding to "translation" of a particle in a liquid can be written as

TABLE 2.19

Relevant Parameters in Calculations of the Entropy of Ionic Hydration

	Li^+	Na^+	K^+	Rb^+	Cs^+	F^-	Cl^-	Br^-	I^-
$S_{i,g}$	31.8	35.3	36.9	39.2	40.6	34.8	36.7	39.1	40.6
ΔS_{BC}	−2.9	−2.6	−2.4	−2.3	−2.2	−2.4	−2.1	−2.1	−2.0
$\Delta S_{BC} - S_{i,g}$	−34.7	−37.9	−39.3	−41.5	−42.8	−37.2	−38.8	−41.2	−42.6
$S_{rot}(SCW)$	5.62	6.12	6.55	6.70	6.90	5.74	6.24	6.38	6.57
$S_{vib}(SCW)$	0.64	1.65	2.39	2.77	3.08	2.16	2.96	3.33	3.64
$S\ (SCW)$	6.26	7.77	8.94	9.47	9.98	7.90	9.20	9.71	10.21
$S_{rot}(NSCW)$	9.43	9.18	9.66	10.03	10.50	6.94	7.57	7.74	8.02
$S_{vib}(NSCW)$	0.89	2.30	3.36	3.85	4.33	3.14	4.27	4.74	5.16
$S\ (NSCW)$	10.32	11.48	13.02	13.88	14.83	10.08	11.84	12.48	13.18
$\Sigma\Delta S_{SB}$ (model 1A)	10.24	10.24	10.24	10.24	10.24	10.24	10.24	10.24	10.24
$\Sigma\Delta S_{SB}$ (model 2A)	15.36	15.36	15.36	15.36	17.92	15.36	17.92	17.92	20.48
$\Sigma\Delta S_{SB}$ (model 3A)	17.92	17.92	19.20	19.20	24.32	16.64	24.32	24.32	28.80
$\Sigma\Delta S_{SB}$ (model 2C)	32.8	40.4	49.6	53.5	58.6	50.3	62.1	65.9	72.2
$\Sigma\Delta S_{SB}$ (model 3C)	32.3	39.9	48.9	52.8	57.5	50.1	61.0	64.8	71.0

$$f_{tr,\text{ion}} = \frac{(2\pi m_{\text{ion}} kT)^{3/2}}{h^3} V_{f,\text{ion}} \tag{2.92}$$

where $V_{f,\text{ion}}$ is the *free volume available to the ion in solution* described in Section 2.15.11. Therefore, the entropy of translation is

$$S_{i,tr} = R \ln f_{tr,\text{ion}} + RT \frac{\partial \ln f_{tr,\text{ion}}}{\partial T} \tag{2.93}$$

Also,

$$V_{f,\text{soln}} = x_{\text{salt}} V_{f,\text{salt}} + (1 - x_{\text{salt}}) V_{f,\text{water}} \tag{2.94}$$

where $V_{f,\text{soln}}$, $V_{f,\text{salt}}$, and $V_{f,\text{water}}$ are the free volumes of solution, salt, and water, respectively, and x_{salt} is the mole fraction of the salt. Equation (2.94) can be rearranged as

$$V_{f,\text{soln}} = V_{f,\text{water}} + x_{\text{salt}}(V_{f,\text{salt}} - V_{f,\text{water}}) \tag{2.95}$$

and a plot of $V_{f,\text{soln}}$ vs. x_{salt} can then be used to calculate $V_{f,\text{salt}}$.

The $V_{f,\text{soln}}$ can be calculated from the velocity of sound by the expression

$$V_{f,\text{soln}} = \left(\frac{v_{o,g}}{v_{o,\text{soln}}} \right)^3 V_{m,\text{soln}} \tag{2.96}$$

where $v_{o,g} = (\gamma RT/M)^{1/2}$ is the velocity in the gas phase given by kinetic theory, $v_{o,\text{soln}}$ is the velocity of sound in solution, $V_{m,\text{soln}}$ is the molar volume of the solution, $\gamma = C_p/C_v$, and M is the molecular weight. Equation (2.96) at 298.16 K becomes upon substitution of appropriate values:

$$V_{f,\text{soln}} = \left(\frac{18.63 \times 10^4}{v_{o,\text{soln}}} \right)^3 V_{m,\text{soln}} \tag{2.97}$$

The molar volume $V_{m,\text{soln}}$ of a binary solution is given by

$$V_{m,\text{soln}} = \frac{1}{\rho \sum_i (w_i/M_i)} \tag{2.98}$$

where w_i and M_i are the weight fraction and molar weight of the ith component, respectively, and ρ is the density of the solution. For example, for NaCl, Eq. (2.98) reduces to

$$V_{m,\text{soln}} = \frac{18}{(1 - 0.6923w_2)} \tag{2.99}$$

where w_2 is the weight fraction of NaCl in solution. M_{soln} needed to calculate $V_{\phi,\text{soln}}$ is given by

$$M_{\text{soln}} = x_{\text{salt}} M_{\text{salt}} + x_{\text{solv}} M_{\text{solv}} \tag{2.100}$$

where x_{salt} and x_{solv} are the mole fractions of salt and solvent in the solution. Using measurements of the velocity of sound, $V_{m,\text{soln}}$ from Eq. (2.99), and M_{soln} from Eq. (2.100), $V_{f,\text{soln}}$ can be calculated from Eq (2.97) for different mole fractions, x_{salt}, of the salt.

The $V_{f,\text{salt}}$ obtained from the slope of $V_{f,\text{soln}}$ vs. x_{salt} [*cf.* Eq. (2.95)] is near zero and it is inferred that this value indicates a value of zero for the translational entropy of the ion. A similar result was obtained for the solvated complex. Zero translational entropy for a solvated ion is a reasonable conclusion. Thus, for most of its time, the ion is still in a cell in the solution and only occasionally does it jump into a vacancy, or if it shuffles about, its movement is so constrained compared with that of a gas that it may approach zero.

2.15.13.4. $S_{i\text{-SCW}}$. The entropy of solvationally coordinated water is made up of librational ($S_{i,\text{lib}}$) and vibrational ($S_{i,\text{vib}}$) contributions. $S_{i,\text{lib}}$ can be calculated as follows.

$S_{i\text{-lib}}$. The partition function of a particle, f_{rot}, under an electric field is

$$f_{\text{lib}} = \frac{8\pi^2(8\pi^3 I_1 I_2 I_3 k^3 T^3)^{1/3}}{\sigma'_w h^3} \frac{\sinh E_r/kT}{E_r/kT} \tag{2.101}$$

where I_1, I_2, and I_3 are the moments of inertia of the water molecules about three mutually perpendicular axes and E_r is the ion–water interaction energy. The symbol σ'_w is the symmetry factor and is equal to 2 for water. Therefore (see physicochemical texts)

$$S_{i,\text{lib}} = R\left[\frac{\ln 8\pi^2(8\pi^3 I_1 I_2 I_3 k^3 T^3)^{1/3}}{\sigma'_w h^3} + \ln \sinh(E_r/kT) - E_r/kT + \coth(E_r/kT) + 5/2\right] \tag{2.102}$$

In the case of water molecules oriented near the ion, $E_r >> kT$ and Eq. (2.102) becomes

$$S_{i,\text{lib}} = R\left[\ln\frac{8\pi^2(8\pi^3 I_1 I_2 I_3 k^3 T^3)^{1/3}}{\sigma'_w h^3} - \ln E_r/kT - \ln 2 + 5/2\right] \tag{2.103}$$

Inserting numerical values for I_1, I_2, and I_3, S_{lib} at 298.16 K becomes

$$S_{i,\text{lib}} = R[5.57 - \ln E_r/kT] \tag{2.104}$$

Substituting $\Delta H_{\text{ion-}w}$ from Table 2.17 for E_r, $S_{i,\text{lib}}$ for the SCW molecules near ions can be calculated. The quantity E_r represents the sum of the ion–dipole, ion–quadrupole, and ion–induced dipole interactions.

In the computation of the rotational entropies of SCW and NSCW near an ion, the rotation is restricted to libration about the axis perpendicular to the dipole. The third rotation, i.e., about the dipole axis, does not change the orientation of the dipole and may be better calculated as if it were a free rotation. The partition function for this is

$$f_{\text{rot,free}} = \frac{2\pi}{\sigma'}\left(\frac{2\pi I_w kT}{h^2}\right)^{1/2} \tag{2.105}$$

where I_w is the moment of inertia of water molecules about the dipole axis and is 1.9187×10^{-40} g cm^2. Using this partition function in the general equation for entropy in terms of partition function, one calculates $S_{\text{rot,free}} = 14.35$ J K^{-1} mol^{-1}.

Thus,

$$S_{SCW,\text{rot}} = \frac{2}{3} S_{SCW,\text{lib}} + 3.43 \tag{2.106}$$

and

$$S_{NSCW,\text{rot}} = \frac{2}{3} S_{NSCW,\text{lib}} + 3.43 \tag{2.107}$$

$S_{i,\text{vib}}$. The term $S_{i,\text{vib}}$ can be calculated from

$$f_{i,\text{vib}} = \left(2 \sinh \frac{h\nu}{2kT}\right)^{-1} \tag{2.108}$$

and therefore

$$S_{i,\text{vib}} = R \ln\left(2 \sinh \frac{h\nu}{2kT}\right)^{-1} + R\left(\frac{h\nu}{2kT}\right)\coth\left(\frac{h\nu}{2kT}\right) \tag{2.109}$$

where

$$\nu = \frac{1}{2\pi}\sqrt{k/\bar{\mu}} \tag{2.110}$$

and k is the force constant and $\bar{\mu}$ is the reduced mass.

Now

$$k = \left(\frac{\partial^2 U_r}{\partial x^2}\right)_{r=r_{eq}} \tag{2.111}$$

and

$$U_r = -\frac{ze\mu}{r^2} + \frac{A}{r^9} \tag{2.112}$$

Now, at equilibrium, for the ion–water separation

$$\left(\frac{\partial U}{\partial r}\right)_{r=r_{eq}} = 0 \tag{2.113}$$

It follows that

$$A = \frac{2}{9} ze\mu r_{eq}^7 \tag{2.114}$$

From Eqs. (2.112) and (2.114) and expressing the displacements from the equilibrium separation, r_{eq}, as $(r_{eq} + x)$ and $(r_{eq} - x)$, one gets for k:

$$k = \frac{14ze\mu}{r_{eq}^4} \tag{2.115}$$

The numerical form turns out to be

$$k = \frac{123.7 \times 10^4 z}{r_{eq}^4} \qquad \text{(in dyn cm}^{-1}\text{ if } r_{eq} \text{ is in angstroms)} \tag{2.116}$$

Thus, ν can be evaluated by inserting k from Eq. (2.116) into Eq. (2.110). The values of ν, when substituted in Eq. (2.109), give $S_{i,vib}$ (Table 2.19).

2.15.13.5. S_{NSCW}. The term S_{NSCW} is made up of two contributions, $S_{NSCW,lib}$ and $S_{NSCW,vib}$. The librational entropy of the NSCW is obtained from Eqs. (2.104) and (2.107) by inserting the value of $\Delta H_{ion\text{-}NSCW}$ for E_r from row 3 of Table 2.17 (see Table 2.19).

$S_{NSCW,vib}$ can be calculated from Eq. (2.109) if ν_{NSCW} is known. Waters that are not coordinated solvationally with the ion (NSCW) have as attractive force only an ion–induced dipole component (ΔH_h). Thus, the force constant k_{NSCW} can be worked out by using Eqs. (2.111)–(2.114):

$$k_{NSCW} = \frac{10(ze)^2}{r_{eq}^6} \tag{2.117}$$

or in numerical form:

$$k_{NSCW} = \frac{332.9 \times 10^4 z^2}{r_{eq}^6} \tag{2.118}$$

Substitution of k_{NSCW} in Eq. (2.110) gives ν_{NSCW}, which, when used in Eq. (2.109), gives the vibrational contribution to the entropy of an NSCW near ions (Table 2.19).

2.15.13.6. S_{SB} *(Model A).* In this model, the hydrogen-bonded molecule of the SB region is seen as executing one free rotation about the H-bond axis. The two rotations about the axes perpendicular to the H-bond axis will be librational. $S_{\text{rot-H-bond axis}}$ can be obtained from Eq. (2.109) using a frequency represented by a wave-number of 60 cm^{-1} (or 1.80×10^{12} s^{-1}) assigned for the rotational band of a one-hydrogen-bonded species. Thus,

$$S_{\text{rot-H-bond-axis}} = 18.74 \text{ J K}^{-1} \text{ mol}^{-1} \tag{2.119}$$

The entropy corresponding to two librations can be obtained by inserting the librational frequencies, $\nu_{1,\text{lib}}$ and $\nu_{2,\text{lib}}$, in Eq. (2.109). The assignments of these νs, based on the interpretation of the infrared spectrum for two libration frequencies, are 4.35×10^{12} and 5.25×10^{12} s^{-1}. Substituting these values in Eq. (2.109) gives

$$(S_{1,\text{lib}})_{SB} = 11.46 \text{ J K}^{-1} \text{ mol}^{-1} \tag{2.120}$$

$$(S_{2,\text{lib}})_{SB} = 10.08 \text{ J K}^{-1} \text{ mol}^{-1} \tag{2.121}$$

The three vibrations, corresponding to the three translational degrees of freedom, for a molecule involved in a single H bond are assigned frequencies of 1.80×10^{12} s^{-1}. The entropy for these vibrations follows from Eq. (2.109) as

$$S_{SB,\text{vib}} = 3(10.67) = 32.00 \text{ J K}^{-1} \text{ mol}^{-1} \tag{2.122}$$

From Eqs. (2.119) to (2.122)

$$S_{SB,\text{H-bonded}} = 18.74 + 11.46 + 10.08 + 32.00 = 72.29 \text{ J K}^{-1} \text{ mol}^{-1} \tag{2.123}$$

Thus

$$S_{SB}\ (\text{model A}) = n_{SB,\text{H-bonded}}(S_{SB,\text{H-bonded}} - S_{w,w}) \tag{2.124}$$

(Table 2.19).

2.15.13.7. S_{SB} (*Model C*). In this model, the molecules in the SB region, which are not H bonded to the first shell, are taken as *unbonded*, i.e., freely rotating monomers. These molecules are assigned three translational and three rotational degrees of freedom. The intramolecular bond stretching and bending modes are of high frequencies and do not contribute to the entropy of an unbonded molecule.

One has to know the free volume available to the unbonded molecule, $V_{f,SB}$, and its temperature dependence, so that the translational entropy may be calculated. The term $V_{f,SB}$ may be found from sound velocity measurements [Eq. (2.96)]. If one takes a number of unassociated liquids and plots their free volumes V_f obtained from the velocity of sound against their molar weights, an extrapolation through a molar weight of 18 will give $V_{f,SB}$ for a freely rotating monomer of water.[33] A value of 0.2 $\text{cm}^3\ \text{mol}^{-1}$ for $V_{f,SB}$ is obtained. The temperature dependence of $V_{f,SB}$ is obtained from the integration of the heat capacity

$$(C_v)_{SB} = RT^2\left(\frac{\partial^2 \ln V_{f,SB}}{\partial T^2}\right) \tag{2.125}$$

which gives

$$T\frac{\partial \ln V_{f,SB}}{\partial T} = \frac{(C_v)_{SB}}{R} - \frac{F'}{2} - 1.2 \tag{2.126}$$

where $(C_v)_{SB}$ is the heat capacity of the freely rotating monomers in the SB region, F' is the number of degrees of freedom, and the term –1.2 is the integration constant. $(C_v)_{SB}$ has a value of $(6/2)R$ arising from three translational and three rotational degrees of freedom. Thus, from Eq. (2.126)

$$T\frac{\partial \ln V_{f,SB}}{\partial T} = -1.2 \tag{2.127}$$

Using $V_{f,SB}$ of 0.20 $\text{cm}^3\ \text{mol}^{-1}$ and $T(\partial \ln V_{f,SB}/\partial T)$ of –1.2 in the general equation relating entropy to partition function,

$$S = Nk\left(\ln f - T\frac{\partial \ln f}{\partial T}\right)$$

[33]This is to be distinguished from the entropy of *water in water* for which, of course, free-volume values are available directly from measurements of sound velocity.

one finds

$$S_{SB,tr} = 29.29 \text{ J K}^{-1} \text{ mol}^{-1} \tag{2.128}$$

Furthermore, $S_{SB,\text{rot}}$ for three degrees of free rotations is calculated with the same general approach to be 43.85 $\text{J K}^{-1} \text{ mol}^{-1}$. Adding these components together, one obtains a calculated entropy for the structure-broken part of model C, that is,

$$S_{SB,\text{freely rot}} = 29.29 + 43.85 = 73.14 \text{ J K}^{-1} \text{ mol}^{-1} \tag{2.129}$$

Thus, the total entropy for model C is

$$\begin{aligned} \sum \Delta S_{SB} \text{ (model C)} = {} & n_{\text{H-bonded}} (S_{SB,\text{H-bonded}} - S_{w,w}) \\ & + (n_{SB} - n_{\text{H-bonded}})(S_{SB,\text{freely rot}} - S_{w,w}) \end{aligned} \tag{2.130}$$

The values of ΔS_h of models A and C as well as their comparisons with experimental values are shown in Table 2.20 and in Figs. 2.43 and 2.44. It is necessary to reject model 1C because X-ray determinations of the CN indicate not 4, but numbers that vary from 6 to 8 as a function of the ion. The experimental results on solvation numbers have similar inference; a sharp distinction between the solvation numbers of

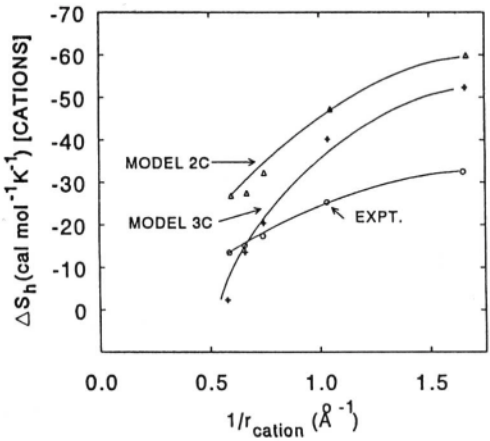

Fig. 2.43. Entropy of hydration against reciprocal of ionic radius for monovalent cations (1 Å = 100 pm; 1 cal = 4.184 J). (Reprinted from J. O'M. Bockris and P. P. S. Saluja, *J. Phys. Chem.* **76**: 2298, 1972.)

TABLE 2.20

Comparison of Calculated and Experimental Values for Entropy of Hydration (calories K^{-1})

Ion	Li^+	Na^+	K^+	Rb^+	Cs^+	F^-	Cl^-	Br^-	I^-
ΔS_h									
Model 1A	−63.42	−60.58	−57.30	−57.38	−56.64	−59.36	−55.76	−56.12	−55.52
Model 2A	−77.78	−71.92	−66.30	−65.32	−67.02	−70.44	−68.48	−67.31	−68.44
Model 3A	−67.10	−62.00	−50.20	−48.30	−36.30	−64.80	−48.90	−47.10	−40.80
Model 1C	−40.0	−29.6	−17.1	−13.3	−7.0	−13.4	−2.6	0.8	7.7
Model 2C	−60.4	−46.9	−32.1	−27.2	−26.4	−35.5	−24.3	−19.4	−17.9
Model 3C	−52.7	−40.0	−20.5	−14.6	−3.2	−31.4	−12.2	−6.6	0.7
ΔS_h (exptl.)[a]	−33.7	−26.2	−17.7	−14.0	−14.0	−31.8	−18.2	−14.5	−9.0

[a]The experimental values refer to $S^\circ_{H^+} = 5.3 \pm 0.3$ e.u.

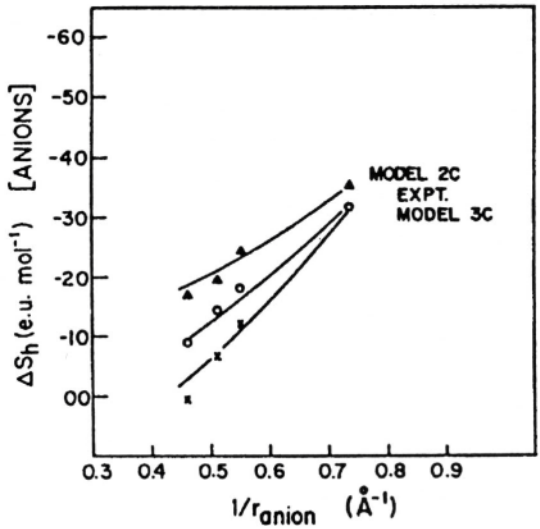

Fig. 2.44. Entropy of hydration against reciprocal of ionic radius for halide ions (1 Å = 100 pm; 1 e.u. = 4.184 J K^{-1} mol^{-1}). (Reprinted from J. O'M. Bockris and P. P. S. Saluja, *J. Phys. Chem.* **76**: 2298, 1972.)

larger and smaller ions is indicated (the SN of Na^+ is 4, and that of I^- is 1.5). Models 2A and 2C turn out, after the calculations have been made, to be the least consistent with the experiments (Figs. 2.43 and 2.44).

Thus, model 3C is the most experimentally consistent model. It is consistent with a model in which there is a difference between coordinated water and solvational water. Some of the waters in the structure-broken region are librating monomers. The entropy choice of 3C is the same as the choice in the heat calculation for cations. However, there is much deviation for the cations (Fig. 2.43) and only the anion model is more consistent with experiments (Figs. 2.43 and 2.44). The model in which two different kinds of coordinating waters in the first shell have been assumed (i.e., a solvational and a nonsolvational coordination number) gives numerically better consistency with experiments than models lacking this feature.

Conclusions for the monovalent ions can be drawn from this fairly detailed analysis. (1) A division of a region around the ion into two parts (Bockris, 1949; Frank and Wen, 1957) is supported. (2) In the first layer around the ion, one can distinguish two kinds of water molecules, referred to as "solvated" and "nonsolvated." (3) The second layer is also one water molecule thick and consists basically of monomers, some of which librate.

2.15.14. Is There a Connection between the Entropy of Solvation and the Heats of Hydration?

It is common in many properties of chemical systems to find that as the ΔH of the property varies in a series of elements, there is a corresponding $T\Delta S$ change that counteracts the ΔH change. The appropriate relations are shown for ionic hydration in Fig. 2.45. Because of the general relation $\Delta G = \Delta H - T\Delta S$, this compensation effect quiets down the variation of ΔG_{solv} among the ions.

An interpretation of this well-known compensation effect has been given by Conway. In this interpretation, ion–dipole attraction is the larger contributor to the ΔH_s values. As it increases (becomes more negative), the vibrational and rotational frequencies will increase and hence the entropy contribution will become more negative. Because $\Delta G = \Delta H - T\Delta S$, the increased negativity of $T\Delta S$ (i.e., a *positive* contribution to ΔG) will compensate for the increasingly negative ΔH_{solv}.

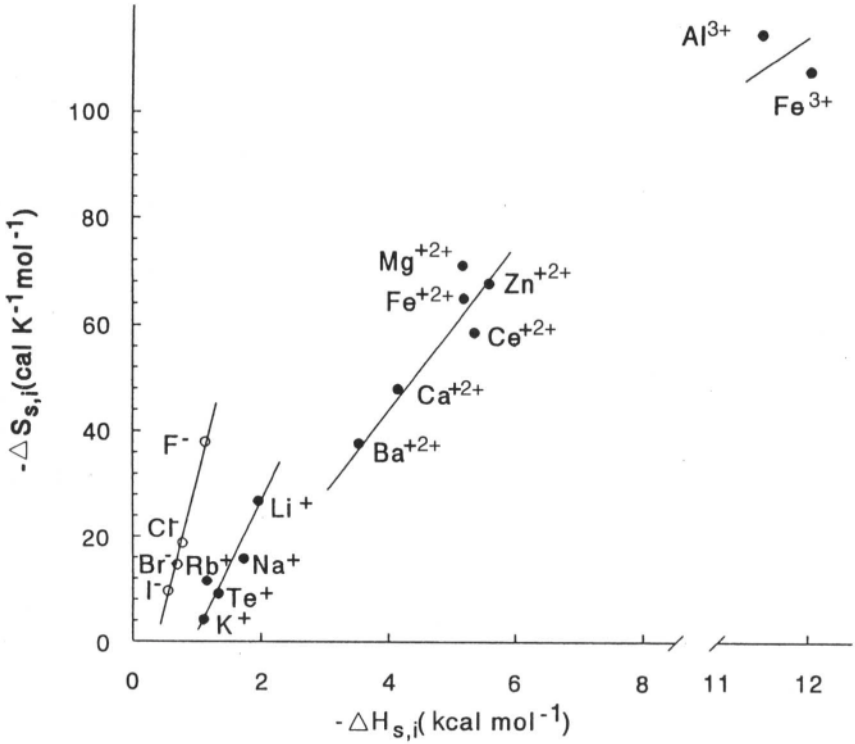

Fig. 2.45. Compensation plot of enthalpies vs. standard entropies of hydration for a number of ions. (Reprinted from D. D. Eley and H. G. Evans, *Trans. Faraday Soc.***34**: 1093, 1938.)

2.15.15. Krestov's Separation of Ion and Solvent Effects in Ion Hydration

Krestov in 1993 broke down the solvent contribution into an "ordering" one—that is, a negative entropy due to the enhanced order brought about by the ordering of the solvent around the ion—and a disordering entropy (i.e., ΔS positive) caused by the solvent breakdown. Temperature affects the ordering part little, but the disordering contribution diminishes with an increase in temperature because the water is already broken up before entry of the ion.

2.16. MORE ON SOLVATION NUMBERS

2.16.1. Introduction

One of the challenges of solvation studies consists in separating effects among the ions of a salt (e.g., those due to the anion and those due to the cation) and this difficulty, that of determining the *individual* solvation heats (see Section 2.15), invades most methods devoted to the determination of individual ionic properties (Fig. 2.46). When it comes to the solvation number of an ion, an unambiguous determination is even more difficult because not all workers in the field understand the importance of distinguishing the coordination number (the nearest-neighbor first-layer number) from

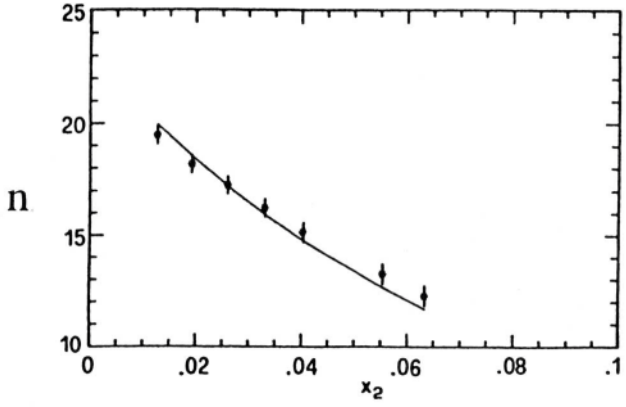

Fig. 2.46. "Hydration number" vs. sodium chloride molar fractions. (•) Experimental data; (–) fitting. (Reprinted from G. Onori and A. Santucci, *J. Chem. Phys.* **93**: 2939, 1990.) The large values arise as a consequence of dropping the assumption of an incompressible hydration sheath.

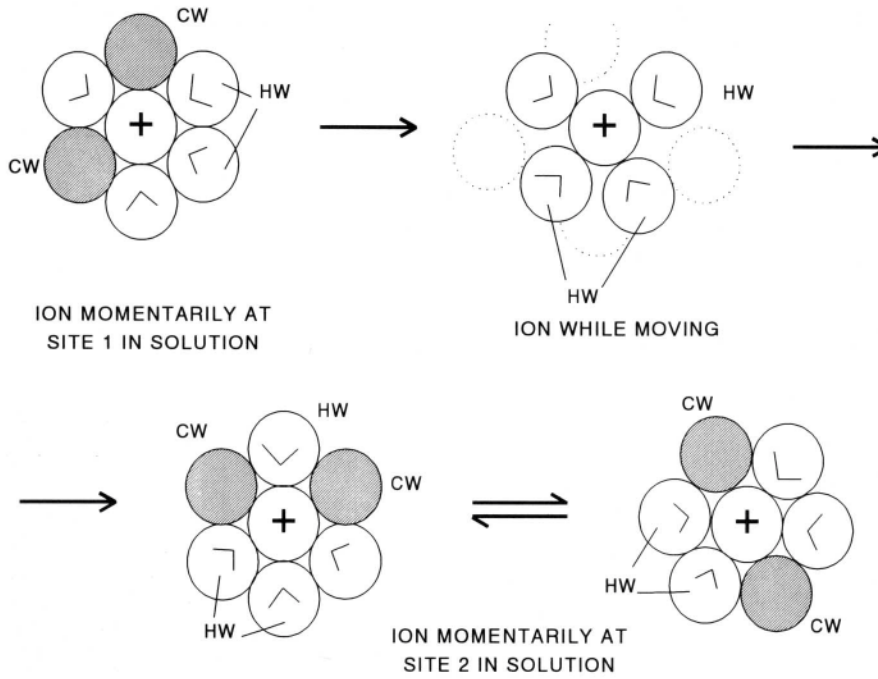

Fig. 2.47. Hydration number *n* in relation to coordination number CN in the motion of an ion in water and in relation to exchange of water molecules. CW, coordinated H_2O; HW, primary hydrating H_2O molecules. (Reprinted from J. O'M. Bockris and P. P. S. Saluja, *J. Phys. Chem.* **76**: 2298, 1972.)

the dynamic solvation number (the number of water molecules that remain with an ion for at least one movement (Fig. 2.47).

Thus, a major misunderstanding is committed by those who confuse solvation numbers with the number of solvent molecules in contact with an ion, the coordination number. It has already been implied and indeed spelled out that the term *solvation number* implies a dynamic concept. Solvation numbers reflect the dynamic situation of the ion as it moves around in the solution. Thus, two hydration numbers may be described, but only one of these is open to numerical determination. This is the so-called *primary hydration number*, that is, the number of water molecules that have lost their own freedom of translational motion and move along with the ion in its random movements in the solution. A *secondary hydration number* refers to the water molecules in the area around the ion that *are affected by* the ion's presence. Clearly, this second quantity depends entirely on the degree of the effect on the solvent molecules outside the first and second layers and hence on the sensitivity of the method being used. It includes waters in the structurally broken-down region out from the first layer of waters attached to the anion.

However, the term *primary salvation number*, although it has apparently a clear definition (see above), is open to further discussion. Thus it may be that a water molecule loses its degree of translational freedom and travels with a given ion as it moves from site to site. The question is, how long does it have to remain the ion's consort to count in the definition? There is no difficulty in accepting "travels with the ion in its movements" when the lifetime of the complex is clearly greater than that needed for registration in some experimental method. Thus, a relatively long lifetime, more than 10^{-6} s, say, would find a strong positive vote on the question of whether such an ion counts primarily as a hydrated molecule. However, it seems better to accept the limit of one jump as the necessary qualification. Thus, if the lifetime of water molecules in contact with an ion is only enough for one jump, it still means that the ion always has water molecules with it on jumping, and the number of these is reasonably taken as the primary hydration (solvation) number.

Another matter concerns the time of "reaction" between a set of water molecules after an ion has just pushed its way into the middle of them. Thus, if the lifetime of molecules in the primary solvation shell is sufficiently short, there must be some jumps in which the ion is bare or at least only minimally clothed. How is the hydration number affected by the time needed for the solvent molecules buried in the solvent layer to break out of that attachment and rotate so that their dipoles are oriented toward the ion to maximize the energy of interaction $(\cos \theta = 1)$?

2.16.2. Dynamic Properties of Water and Their Effect on Hydration Numbers

A critical question one might ask in obtaining a closer concept of the primary hydration number pertains to the average time during which a water molecule stays with an ion during its movements (*cf.* Fig. 2.23). One can begin by repeating yet again the distinction between coordination number and primary hydration water. The coordination number is the number of particles in contact with the ion (independently of whether any of the molecules concerned move with the ion and independently of how they orient in respect to it). It is a matter of geometry, space filling, etc. Now, when an ion moves from one site to the next, not all of the water molecules coordinating it at the beginning of the movement cling to it.

One can see at once that the free volume for coordinating waters is

$$\frac{4}{3}\pi[(r_i + 2r_w)^3 - r_i^3]$$

If water molecules fill this space without regard to directed valences and without accounting for repulsion between head-to-head dipoles, the coordination number could be obtained by dividing the above number by the volume of one water molecule.

For r_i = 70, 100, 150, and 200 pm, the calculated coordination numbers obtained on such a basis are shown in Tables 2.21 and 2.22. Real values should be less, because of lateral repulsion of molecules.

TABLE 2.21
Geometrically Calculated Coordination Numbers (Space Filling) for Univalent Ions[a]

Radius of Ion (Å)	Coordination Number (nearest integer)
0.7	9
1.0	11
1.5	15
2.0	20

[a]The values of the coordination number will be less because the molecules repel each other and the space is not filled.

The solvation numbers would be expected to be zero for sufficiently large ions. For these ions, the ion's field is too weak to hold the dipoles and rises toward (but never equals) the coordination number as the ion's size falls; therefore its Coulombic attraction upon the water molecule increases (Fig. 2.23).

2.16.3. A Reconsideration of the Methods for Determining the Primary Hydration Numbers Presented in Section 2.15

Most[34] of the methods employed to yield primary hydration numbers have already been presented (Section 2.15). Thus, one of the simplest methods, which has been applied to organic molecules as well as ions in solution, is that originated by Passynski. As with most methods, it purports to give the total solvation number for the salt, but this should not be counted as a difficulty. More to the point is Onori's criticism that the primary hydration shell is not incompressible. Onori has measured this while dropping Passynski's assumption, but the solvation numbers he gets seem unreasonably large and may be invalidated by his counter assumption, i.e., that solvation is temperature independent.

The mobility method (Section 2.10.1) has the advantage of yielding individual solvation numbers directly (as long as the transport numbers are known). However, this positive point is offset by the fact that the viscosity term used should be the *local* viscosity near the ion, which will be less than the viscosity of the solvent, which is

[34]Thus the entropy of solvation (Section 2.15.12) can be used to obtain hydration numbers. Knowing the value of ΔS (Section 2.5.3), it is necessary only to know the entropy change of one water molecule as it transfers from a position in a somewhat broken-up water lattice, where it has librative (and some limited translatory) entropy but ends up, after having been trapped by the ion, with only vibrational entropy. The value assigned to this change is generally 25 $\mathrm{J\,K^{-1}\,mol^{-1}}$ of water, so that $n_s = \Delta S_s/25$.

As a rough-and-ready estimate, this will do. However, the method is open to further development, particularly as to the broken-down character of water in the neighborhood of the ion and how this affects the value of 25 $\mathrm{J\,K^{-1}\,mol^{-1}}$ per water molecule.

TABLE 2.22

Comparison of Theoretically and Experimentally Obtained Solvation Numbers

Method	Be^{2+}	Mg^{2+}	Ca^{2+}	Sr^{2+}	Ba^{2+}	Zn^{2+}	Cd^{2+}	Fe^{2+}	Co^{2+}	Ni^{2+}	Sn^{2+}	Pb^{2+}	Cu^{2+}
Theoretical	15.6	13.5	12.3	11.4	11	13.3	12.4	13.1	13.3	13.5	12.9	11.3	13.4
average of: Mobility, Entropy, Compressibility		14	12.2	10.8	9	12.3	12	12.2					12.2

Source: Reprinted from B. E. Conway, *Ionic Hydration in Chemistry and Biophysics*, Elsevier, New York, 1981.

usually used in the calculation. It is interesting to note that the use of raw solvent viscosities does, however, give values that agree (±30%) with the mean of the other five or so nonspectroscopic approaches.

The use of hydration numbers calculated from the effect of ions on the dielectric constant of ionic solutions was seen (Section 2.12.1) at first to be relatively free of difficulties. However, the theory has become more sophisticated since the original conception, and it has been realized that in all but quite dilute solutions, interionic forces affect a straightforward interpretation of the relaxation time, making it important to have sets of data over a wide range of frequencies—1 mHz to 1 GHz. The methods of Yeager and Zana and Bockris and Saluja (Section 2.8.1), which use compressibility measurements to obtain the sum, and the ionic vibration potentials to get the difference, represent an approach to determining hydration number that has the least number of reservations (although there are questions about the degree of residual compressibility of the inner sheath).

Finally, there is the troubling matter that the spectroscopic methods of measurement generally gave results as much as 50% lower (Table 2.10) than the values obtained by the relatively concordant nonspectroscopic methods (compressibility,

TABLE 2.23

Hydration Numbers for Some Alkali Metal and Halide Ions Obtained from MD Calculations and X-Ray and Neutron-Diffraction Experiments[a]

Ion	Solute Salt	Hydration Number	
		MD (conc.)	Diffraction
Li^+	LiCl	5.7	4 ± 1
	LiBr		4 and 6
	LiI	7.1	
Na^+	NaCl	6.6	4
K^+	KF	5.3	2–4
	KCl	6	2 and 4
	KI	1.7–3.2	0.5–5
F^-	CsF	6.3	
	NH_4F		4.5
Cl^-	HCl		4
	LiCl	7.4	Various values in the range 6–9
	NaCl	6.7	6
		7.7 (0.55 M)	6.3
I^-	LiI	7.3	8.8

Source: Reprinted from B. E. Conway, *Ionic Hydration in Chemistry and Biophysics*, Elsevier, New York, 1981.

[a]It seems likely that although these values are called hydration numbers, they are, in fact, coordination numbers.

TABLE 2.24
Summary of Primary Hydration Numbers for Alkali Metal and Halide Ions

	Li^+	Na^+	K^+	Rb^+	F^-	Cl^-	Br^-	I
n^a	5 ± 1	5 ± 1	4 ± 2	3 ± 1	4 ± 1	1 ± 1	1 ± 1	1 ± 1
No. of methods	5	5	4	4	3	3	3	2
n(calc.)	6	5	3	2	5	3	2	0

Source: Reprinted from B. E. Conway, *Ionic Hydration in Chemistry and Biophysics*, Elsevier, New York, 1981.
[a]Based on interpretation of various experimental ionic properties discussed in text.

activity, entropy, mobility, partial ionic volume, vibration potentials, and dielectric constant). There seem to be two interpretations for this marked discrepancy. The first is that the spectroscopic methods are relatively insensitive and for this reason are only applicable to concentrated solutions. However, here the number of water molecules available per ion markedly decreases (5×10^4 water molecules in a 10^{-3} *M* solution and 10 water molecules in a 5 *M* solution) so that there would be a mass tendency toward lower hydration numbers (see Fig. 2.46). Apart from this, in solutions as concentrated as those used, e.g., in neutron diffraction (> 1.5 mol dm^{-3} for 2:1 salts such as $NiCl_2$), the situation becomes complicated for two reasons: (1) the formation of various kinds of ion pairs and triplets and (2) the fact that so much of the water available is part of the hydration sheaths that are the object of investigation. Thus, ionic concentration, which refers conceptually to the number of *free* waters in which the hydrated ion can move, has a different meaning from that when the number of water molecules that are tied up is negligible.

Conversely, spectroscopic methods (particularly NMR and neutron diffraction) can be used to sense the residence time of the water molecules within the solvent sheaths around the ion. Thus, they could offer the most important data still required—a clean quantitative determination of the number of molecules that move with the ion. Unfortunately they only work in concentration regions far higher than those of the other methods. A summary of results from these methods is given in Tables 2.23 and 2.24.

2.16.4. Why Do Hydration Heats of Transition-Metal Ions Vary Irregularly with Atomic Number?

The theoretical discussion of the heats of ion–solvent interactions has been restricted so far to stressing the alkali metal and alkaline earth cations and halide anions. For these ions, a purely electrostatic theory (Section 2.15.10) provides fair coincidence with experiments. However, with the two- and three-valent transition-metal ions, where directed orbital interactions with water may have more influence,

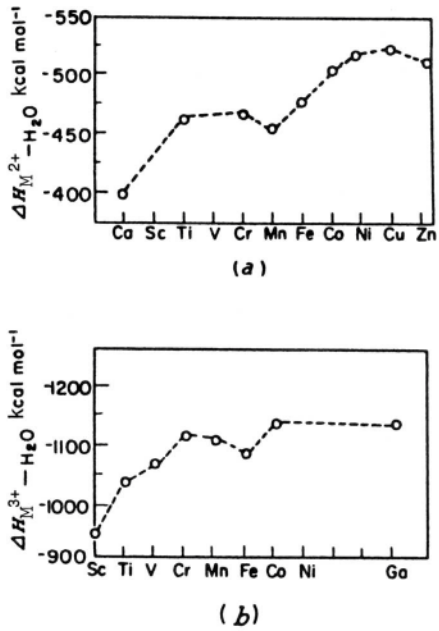

Fig. 2.48. Plot of the heats of hydration of transition-metal ions (and their immediate neighbors) vs. atomic number. (a) Divalent ions; (b) trivalent ions (1 cal = 4.184 J).

interesting and unexpected changes of the hydration heats occur with change of atomic number.

One way of seeing these changes is to plot the experimental heats of hydration of the transition-metal ions against their atomic number. It is seen that in the case of both divalent and trivalent ions, the heats of hydration lie on double-humped curves (Fig. 2.48).

Now, if the transition-metal ions had spherical charge distributions, then one would expect that with increasing atomic number there would be a decreasing ionic radius[35] and thus a smooth and monotonic increase of the heat of hydration as the atomic number increases. The double-humped curve implies therefore the operation

[35]The radius of an ion is determined mainly by the principal quantum number and the effective nuclear charge. As the atomic number increases in the transition-metal series, the principal quantum number remains the same, but the effective charge of the valence electrons increases; hence, the ionic radius should decrease smoothly with an increase in atomic number.

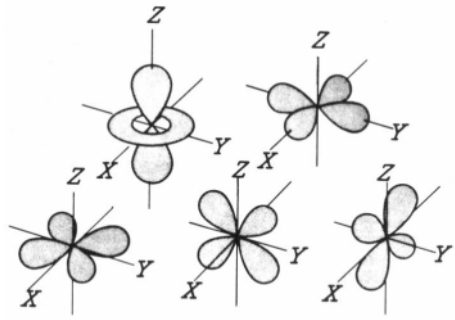

Fig. 2.49. The five 3d orbitals.

of factors that make transition-metal ions deviate from the behavior of charged spheres. What are these factors?

In the case of transition-metal ions, the 3d orbitals are not spherically symmetrical; in fact, they are as shown in Fig. 2.49. In a gaseous ion (i.e., a free unhydrated ion), all the 3d orbitals are equally likely to be occupied because they all correspond to the same energy. Now, consider what happens when the ion becomes hydrated by six[36] water molecules situating themselves at the corners of an octahedron enveloping the ion. The lone electron pairs of the oxygen atoms (of the water molecules) exert a repulsive force on the valence electrons of the ion (Fig. 2.50).

This repulsive force acts to the same extent on all the p orbitals, as may be seen from Fig. 2.51. The d orbitals, however, can be classified into two types: (1) those that are directed along the x, y, and z axes, which are known as the $\mathbf{d}_\varepsilon$ orbitals, and (2) those that are directed between the axes, which are known as the $\mathbf{d}_\gamma$ orbitals. It is clear (Fig. 2.52) that the repulsive field of the lone electron pairs of the oxygen atoms acts more strongly on the $\mathbf{d}_\varepsilon$ orbitals than on the $\mathbf{d}_\gamma$ orbitals. Thus, under the electrical influence of the water molecules of the primary solvation sheath, all the 3d orbitals do not correspond to the same energy. They are differentiated into two groups, the $\mathbf{d}_\varepsilon$ orbitals corresponding to a higher energy and the $\mathbf{d}_\gamma$ orbitals corresponding to a lower energy. This splitting of the 3d orbitals into two groups (with differing energy levels) affects the heat of hydration and makes it deviate from the values expected on the basis of the theory developed earlier in this chapter, which neglected interactions of the water molecules with the electron orbitals in the ion.

Thus, consider a free vanadium ion $\mathbf{V^{2+}}$ and a hydrated vanadium ion. In the case of the free ion, all the five 3d orbitals (the two $\mathbf{d}_\varepsilon$ and the three $\mathbf{d}_\gamma$ orbitals) are equally likely to be occupied by the three 3d electrons of vanadium. This is because in the free ion, all five 3d orbitals correspond to the same energy. In the hydrated $\mathbf{V^{2+}}$ ion,

[36]The figure of six, rather than four, is used because of the experimental evidence that transition-metal ions undergo six coordination in the first shell. Correspondingly, the hydration numbers are 10–15.

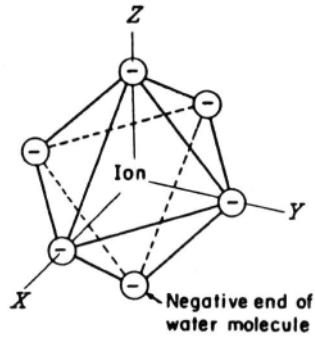

Fig. 2.50. Schematic diagram to show that the valence electrons of the positive ion are subject to the repulsion of the negative ends of the octahedrally coordinating water molecules. The negative charge arises from the presence of lone electron pairs on the oxygen atoms of the water molecules.

however, the $\mathbf{d}_\gamma$ orbitals, corresponding to a lower energy, are more likely to be occupied than the $\mathbf{d}_\varepsilon$ orbitals. This implies that the mean energy of the ion is less when the ion is subject to the electrical field of the solvent sheath than when it is free. Thus, the change in the mean occupancy of the various 3d orbitals, arising from the electrical

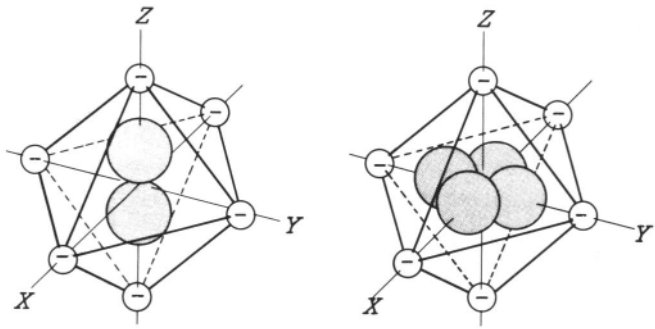

Fig. 2.51. Schematic diagram that shows that the three p orbitals (directed along the axes) are equally affected by the repulsive field of octahedrally coordinating water molecules.

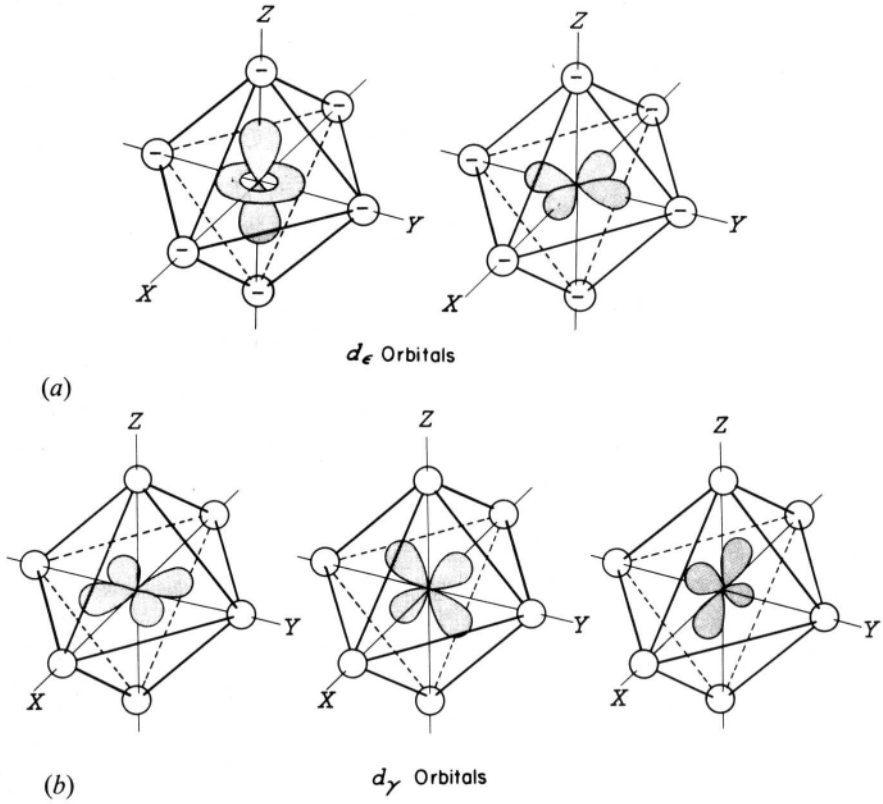

Fig. 2.52. Because the d_ϵ orbitals (a) are directed along the axes and toward the negative ends of the water molecules, they correspond to a higher energy than the d_γ orbitals (b), which are directed between the axes.

field of the water molecules coordinating the ion, has conferred an extra field stabilization (lowering of energy) on the ion–water system and because of this, the heat of hydration is made more negative.

In the case of the hydrated divalent manganese ion, however, its five 3d electrons are distributed[37] among the five 3d orbitals, and the decrease in energy of three electrons in the d_γ orbitals is compensated for by the increase in energy of the two electrons in the d_ϵ orbitals. Thus, the mean energy of the ion in the hydrated state is

[37]The five electrons tend to occupy five different orbitals for the following reason: In the absence of the energy required for electrons with opposite spins to pair up, electrons with parallel spins tend to occupy different oribtals because, according to the Pauli principle, two electrons with parallel spins cannot occupy the same orbital.

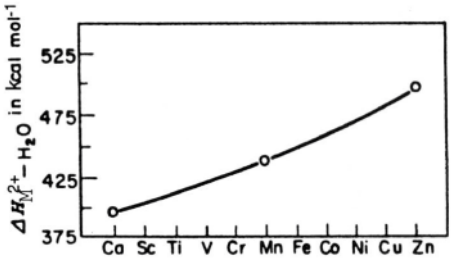

Fig. 2.53. A plot of the heat of hydration of Ca^{2+}, Mn^{2+}, and Zn^{2+} vs. atomic number.

the same as that calculated from a model that neglects interactions affecting the filling of orbitals. Similarly, for Ca^{2+} with no 3d electrons and Zn^{2+} with a completely filled 3d shell, the heat of hydration does not become more negative than would be expected from the electrostatic theory of ion–solvent interactions developed in Section 2.4.3. It can be concluded, therefore, that the experimental heats of hydration of these three ions should vary in a monotonic manner with atomic number as indeed they do (Fig. 2.53).

All the other transition-metal ions, however, should have contributions to their heats of hydration from the field stabilization energy produced by the effect of the field of the water molecules on the electrons in the 3d orbitals. It is these contributions that produce the double-humped curve of Fig. 2.54. If, however, for each ion, the energy[38] corresponding to the water-field stabilization is subtracted from the experimental heat of hydration, then the resulting value should lie on the same smooth curve yielded by plotting the heats of hydration of Ca^{2+}, Mn^{2+}, and Zn^{2+} versus atomic number. This reasoning is found to be true (Fig. 2.54).

The argument presented here has been for divalent ions, but it is equally valid (Fig. 2.55) for trivalent ions. Here, it is Sc^{3+}, Fe^{3+}, and Ga^{3+} which are similar to manganese in that they do not acquire any extra stabilization energy from the field of the water molecules acting on the distribution of electrons in their d levels.

Thus, it is the contribution of the *water-field stabilization energy* to the heat of hydration that is the special feature distinguishing transition-metal ions from the alkali-metal, alkaline-earth-metal, and halide ions in their interactions with the solvent.

This seems quite satisfying, but interesting (and apparently anomalous) results have been observed by Marinelli and Squire and others concerning the energy of interaction of successive molecules as the hydration shell is built up in the gas phase. Thus, it would be expected that the first hydrating water would have the greatest heat of binding, because there are no other molecules present in the hydration shell with

[38]This energy can be obtained spectroscopically.

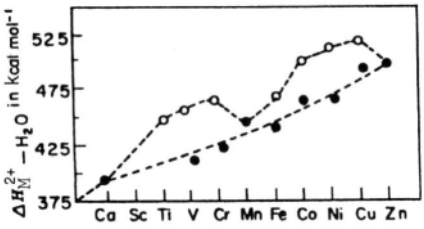

Fig. 2.54. A plot of the heat of hydration of divalent transition-metal ions vs. atomic number (○, experimental values; ●, values after subtracting water-field stabilization energy) (1 cal = 4.184 J).

which to experience lateral repulsion. On the other hand, it is found that with some transition-metal ions (e.g., V, Cr, Fe, and Co), the second water bonds with greater strength than the first!

Rosi and Bauschlicher have made detailed molecular-orbital calculations of the interaction of successive water molecules with transition-metal ions to interpret this anomaly. Their quantum-chemical calculations are able to reproduce the anomalous heats. Depending upon the ion, it is found (in agreement with experiments) that the binding strength of the second hydration water is greater than that of the first.

The anomalous results (the binding energy of the second water being greater than that of the first) can be explained even though the binding energy of hydration water in transition-metal ions is still largely electrostatic. The essential cause is changes in the occupancy of the metal-ion orbitals as a result of differences in repulsion between neighboring waters.

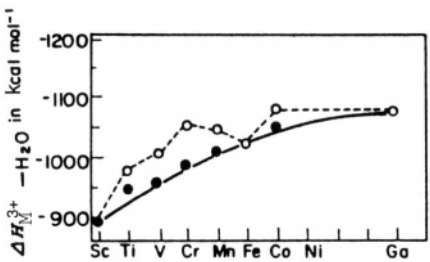

Fig 2.55. A plot of the heat of hydration for trivalent ions.

The key to understanding this surprising result is the interplay between the 4p and the 4s orbitals. The latter can mix in 4p character with its shoelace shape. Such an orbital (effectively an electron cloud) reduces the repulsion between water molecules 1 and 2. Such a reduction allows the bonding energy of the second water to be greater than that of the first. The degree of this mixing of 4p character into 4s (and the resulting effect on bonding) depends on the ion. If the effect is small, repulsion between water molecules 1 and 2 remains great enough for the second water to have a *lesser* bonding energy than the first, as would ordinarily be expected.

Further Reading

Seminal

1. D. D. Eley and M. G. Evans, "Statistical Mechanics in Ionic Solutions," *Trans. Faraday Soc.* **34**: 1093 (1938).
2. S. Lee and M. Tai, "Individual Ionic Entropy of the Proton," *J. Chinese Chem. Soc.* **9**: 60 (1941).
3. F. H. Halliwell and N. C. Nyburg, "Hydration Heat of the Proton," *Trans. Faraday Soc.* **59**: 1126 (1963).
4. J. O'M. Bockris and P. P. S. Saluja, "Model-Based Calculations of Hydration Energies," *J. Phys. Chem.* **76**: 2295 (1972).
5. B. E. Conway, "Individual Ionic Properties," *J. Solution Chem.* **7**: 721 (1978).
6. P. Kebarle and E. W. Godbole, "Hydration in the Gas Phase," *J. Chem. Phys.* **39**: 1131 (1983).

Reviews

1. R. R. Dogonadze, A. A. Kornyshev, and J. Ulstrup, "Theoretical Approaches to Solvation," in *The Chemical Physics of Solvation*, R. R. Dogonadze, E. Kalman, A. A. Kornyshev, and J. Ulstrup, eds., Part A, Elsevier, New York (1985).
2. G. A. Krestov, "Individual Ionic Properties," in *Thermodynamic Structure of Solvation*, Ellis Harwood, New York (1990).

Papers

1. R. C. Keese and A. W. Casheman, *J. Am. Chem. Soc.* **14**: 9015 (1989).
2. J. Marinelli and R. R. Squires, *J. Am. Chem. Soc.* **111**: 4101 (1989).
3. M. Rosi and C. W. Bauschlicher, *J. Chem. Phys.* **90**: 7264 (1989).
4. R. S. Drago, D. C. Feris, and N. Wang, *J. Am. Chem. Soc.* **112**: 8953 (1990).
5. A. D. Paynton and S. E. Feller, *J. Electrochem. Soc.* **137**: 183 (1990).
6. A. G. Sharpe, *J. Chem. Ed.* **67**: 309 (1990).
7. S. Golden and T. R. Tuttle, *J. Phys. Chem.* **95**: 4109 (1991).
8. H. Mizuno and M. Sakiyami, *J. Phys. Chem.* **95**: 2536 (1991).
9. T. F. Magnera, D. E. David, and J. Mich, *Chem. Phys. Lett.* **182**: 363 (1991).
10. P. M. Quereschi, S. Kamoonpuri, and M. Igbal, *J. Chem. Ed.* **68**: 109 (1991).

11. H. Ohtaki and T. Rednai, *Chem. Rev.* **93**: 1157 (1993).
12. Y. Marcus, *Faraday Trans.* **89**: 713 (1993).
13. B. E. Conway and D. P. Wilkinson, "Evolution of Single Ion Entropies," *Electrochim. Acta* **38:** 997 (1993).
14. T. Barthel, *J. Mol. Liquids* **65:** 177 (1995).
15. J. M. Alia, H. G. M. Edwards, and J. Moore, *Spectrochim. Acta* **16:** 2039 (1995).
16. P. Dangelo, A. Dinola, M. Mangani, and N. V. Pavel, *J. Chem. Phys.* **104:**1779 (1996).

2.17. COMPUTER-SIMULATION APPROACHES TO IONIC SOLVATION

2.17.1. General

For about 95% of the history of modern science, since Bacon's work in the seventeenth century, the general idea of how to explain natural phenomena consisted of a clear course: collection of the facts, systemization of them into empirical laws, the invention of a number of alternative and competing intuitive models by which the facts could be qualitatively understood, and, finally, mathematical expression of the more qualitatively successful models to obtain sometimes more and sometimes less numerical agreement with the experimental values. The models that matched best were judged to describe a particular phenomenon better than the other models.

Until the 1960s, one of the difficulties in this approach was the lengthy nature of the calculations involved. Using only mechanical calculators, adequate numerical expression of a model's prediction would often have taken an impractical time.

Electronic calculating machines (the hardware) that can read instructions on how to carry out the calculations (the software) have made it much easier to select models that give the best prediction. However, not only has this technology transformed the possibilities of calculating the consequences of intuitive assumptions (reducing the time needed for calculation from weeks and months to minutes and hours),[39] but it has made possible another approach toward putting experimental results into a theoretical framework. Instead of making up intuitive suppositions as to what might be happening in the system concerned, and seeing how near to reality calculations with competing models can come, the alternative mode is to calculate the forces between the particles concerned and then to use classical mechanics to calculate the properties of the particles without prior assumptions as to what is happening. In physical chemistry, phenomena often result from a series of collisions among particles, and *that* is what can be calculated.

Computational chemistry can be applied to all parts of chemistry, for example, to the design of corrosion inhibitors that are not toxic to marine life. In this section, a

[39]This assumes that a program for the calculation concerned has already been written. If not, it may take an experienced specialist 6 months to write, and cost $50,000 to buy.

brief account will be given of how far this approach has gone in improving our understanding of ionic solvation.

2.17.2. An Early Molecular Dynamics Attempt at Calculating Solvation Number

Palinkas et al. were the first (1972) to calculate the expression:

$$n_s = 4\pi\rho_w \int_{r_i}^{\infty} g_{i-o}(r)\, r^2\, dr \tag{2.131}$$

where ρ_w is the mean density of water molecules, and g_{i-o} is the radial pair distribution function for the pair ion–oxygen. A plot of n_s against r leads to a series of maxima, the first much greater than the second, and the number of waters "under" this peak is the number in the first shell nearest to the ion.

These sophisticated calculations are impressive but they err in representing their results as solvation numbers. They are, rather, coordination numbers and grow larger with an increase in the size of the ion (in contrast to the behavior of the hydration numbers, which decrease as the ion size increases).

2.17.3. Computational Approaches to Ionic Solvation

In considering various computational approaches to solvation, it must first be understood that the ion–water association alone offers a great range of behavior as far as the residence time of water in a hydration shell is concerned. Certain ions form *hydrates* with lifetimes of months. However, for the ions that are nearly always the goal of computation (ions of groups IA and IIA in the Periodic Table and halide ions), the lifetime may be fractions of a nanosecond.

As indicated earlier in this chapter (see Section 2.3), there are three approaches to calculating solvation-related phenomena in solution: Quantum mechanical, Monte Carlo, and molecular dynamics.

The quantum mechanical approach, which at first seems the most fundamental, has major difficulties. It is basically a 0° K approach, neglecting aspects of ordering and entropy. It is suited to dealing with the formation of molecular bonds and reactivity by the formation in terms of electron density maps.[40] However, ionic solutions are *systems* in which order and entropy, its converse, are paramount considerations.

The most fruitful of the three approaches, and the one likely to grow most in the future, is the molecular dynamics approach (Section 2.3.2). Here, a limited system of ions and molecules is considered and the Newtonian mechanics of the movement of

[40]There is a more fundamental difficulty: the great time such calculations take. If they have to deal with more than ten electrons, *ab initio* calculations in quantum mechanics may not be practical.

all the particles in the system is worked out, an impractical task without computers. The foundation of such an approach is knowledge of the intermolecular energy of interaction between a pair of particles. The validity, and particularly the integrity, of the calculations is dependent upon the extent to which the parameters in the equations representing attraction and repulsion can be obtained *independently* of the facts that the computation is to calculate. Thus, if the energy U_r for the interaction of a particle with its surroundings is known, then $\partial U_r/\partial r$ is the force on the particle and hence the acceleration and final velocity can be calculated [e.g., every femtosecond (10^{-15}s)]. With the appropriate use of the equations of statistical mechanics, the properties of a system (particularly the dynamic ones such as diffusion coefficients and the residence times of water molecules) can then be calculated.

In spite of these confident statements, the computation of the properties of ionic solutions is truly difficult. This is partly because of the general limitations of molecular dynamics. Because it is based on classical mechanics, MD cannot deal with situations in which $h\nu/kT > 1$, i.e., quantal situations (e.g., molecular vibrations). Again, MD depends on potential and kinetic energy (as does quantum mechanics), but it does not account for entropy, which is an important characteristic of equilibrium conditions in systems.

Another problem is that long-range Coulombic forces, which are the principal actors in solvation, have to be subjected in practice to a cutoff procedure (thus, they tend to continue to be significant outside the volume of the few hundred particles in the system considered), and the effect of the cutoff on the accuracy of the final calculation is sometimes unclear. For these reasons, much of the computational work on solvation has been carried out with gas-phase clusters, where the essence of the solvational situation is retained but the complexities of liquids are avoided.

2.17.4. Basic Equations Used in Molecular Dynamics Calculations

The basis of MD calculations in solvation is pairwise interaction equations between the ion and the water molecule. The form of these equations depends greatly upon the water molecule model chosen; there are several possibilities.

For example, suppose one can choose a rigid three-point-charge model of water with an internal geometry of 109.47° and 100 pm for the HOH angle and OH distance, respectively. The interaction energy involves a "Lennard-Jones" 6–12 potential for electrostatic interactions between water–water and ion–water pairs, U_{pair}; a nonadditive *polarization energy*, U_{pol}; and a term that includes exchange repulsion for ion–water and water–water pairs, $U_{\text{3-body}}$:

$$U_{\text{total}} = U_{\text{pair}} + U_{\text{pol}} + U_{\text{3-body}} \tag{2.132}$$

The pair additive potential is

$$U_{\text{pair}} = \sum_i \sum_j \frac{A_{ij}}{\mathbf{r}_{ij}^{12}} - \frac{C_{ij}}{\mathbf{r}_{ij}^{6}} + \frac{q_i q_j}{\mathbf{r}_{i,j}} \tag{2.133}$$

the polarization energy is

$$U_{\text{pol}} = \frac{1}{2} \sum \mu_{\text{ind}} X_i^0 \tag{2.134}$$

and a three-body repulsion term is

$$U_{\text{3-body}} = A \exp(-\beta r_{12}) \exp(-\beta r_{13}) \exp(-\gamma r_{23}) \tag{2.135}$$

where μ_{ind} is the induced dipole moment and X_i^0 is the electrostatic field from the charges. The term $\mathbf{r}_{ij}$ is the vector from atom j to atom i, and q_j is the charge on atom j. The distances r_{12} and r_{13} are ion–oxygen distances for the trimer, and r_{23} is the oxygen–oxygen distance for the two water molecules in the trimer. Finally, A, C, and γ are empirical constants.

An iterative approach is often taken to solve the equations. Iteration may be continued until the difference in the induced dipole for successive calculations is 0 to 0.1 D. Typically one uses a system of, say, 215 waters for one ion in a cubic cell with an 1860-pm side. The time step is 1 fs. Coulombic interactions may be cut off at as little as 800 pm. Each set of calculations involves computer software (the cost of which may be very high) and various mathematical procedures to solve the equations of motion.

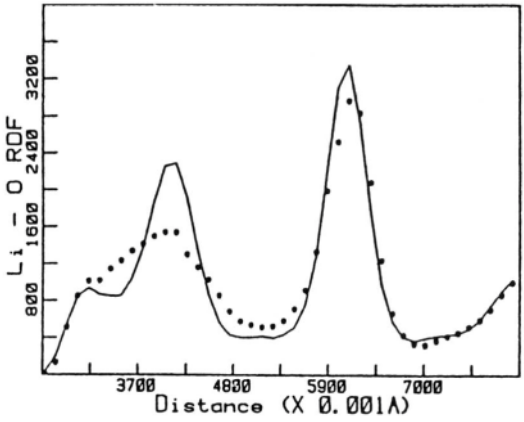

Fig. 2.56. Li-O radial distribution functions (RDFs). The curve represents results from the full-scale MD method. (Reprinted from S. B. Zhu, J. Lee, and G. W. Robinson, *J. Phys. Chem.* **94**: 2114, 1990.)

An example of an Li-O radial distribution function (calculated by MD) is shown in Fig. 2.56. From such calculations one can obtain relaxation features of the rotational and translational motion of the neighboring waters and find the effect of Li^+ or F^-, for example.

What is practical in the later 1990s depends upon whether software able to carry out the computation needed has already been written and is available for about $ 10,000. It is usually economically impractical for university groups to have a program written for each calculation, so that one finds oneself sometimes carrying out a calculation for which there is the software rather than obtaining the software to carry out the needed calculation.

2.18. COMPUTATION OF ION–WATER CLUSTERS IN THE GAS PHASE

Ion–water clusters have been examined by Dang et al., who calculated the interaction between $Na^+(OH_2)_4$, $Na^+(OH_2)_6$, and $Cl^-(H_2O)_4$. Their orientations and structures at various times in the stimulation are shown in Fig. 2.57.

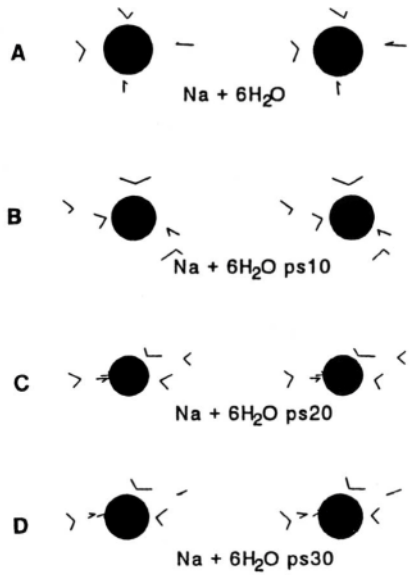

Fig. 2.57. Snapshots of water around the ions of the $Na^+(H_2O)_6$ complex during a simulation of dynamics. (a) 1 ps; (b) 10 ps; (c) 20 ps; (d) 30 ps. (Reprinted from L. X. Dang, J. F. Rice, J. Caldwell, and P. A. Kollman, *J. Am. Chem. Soc.* **113**: 2481,1991.)

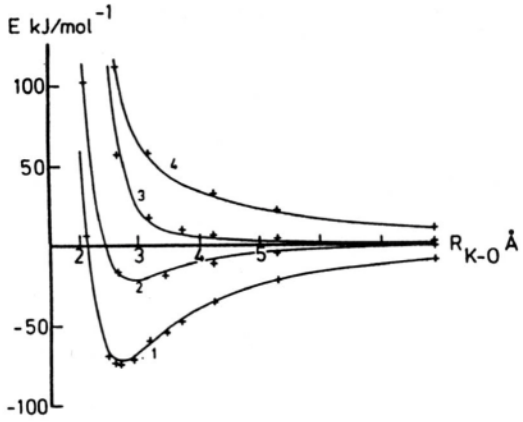

Fig. 2.58. Dependence of $K^+(OH_2)$ interaction energies on the K-O distance for different orientations of the H_2O molecule (1 Å = 100 pm). 1–4 refer to the orientations. (Reprinted from G. G. Malenkov, "Models for the Structure of Hydrated Shells of Simple Ions Based on Crystal Structure Data and Computer Simulation," in *The Chemical Physics of Solvation*, Part A, R. R. Dogonadze, E. Kalman, A. A. Kornyshev, and J. Ulstrup, eds., Elsevier, New York, 1985.)

H–O bonding is important for the Cl^- complex because the Hs are drawn toward the Cl^- and leave the O for H bonding with other waters. The converse is true for $Na^+(OH_2)$ interactions. During simulations, it is found that water molecules transfer from the sheath in contact with the ion to a second sheath in the cluster.

The $Na^+(OH_2)$ turns out to be best fitted with a 4 + 2 structure rather than an octahedral one. It seems likely that the coordination geometries for cluster water in the gas phase and water around the ions in solution differ significantly, but the gas-phase calculations provide an introductory step to the solution ones.

The dependence of the $K^+(OH_2)$ interaction on distance is shown in Fig. 2.58. The ion-O radial distribution functions for $Na^+(H_2O)$ and $K^+(H_2O)$ clusters are shown in Fig. 2.59. A histogram that illustrates the distribution of O–Na–O angles in an $Na(H_2O)_6$ cluster (simulated at 298 K) is shown in Fig. 2.60. Finally, Fig. 2.61 shows the number of water molecules in a sphere of radius r within the cluster.

These diagrams indicate the limit of the hydration shell in the gas-phase ion as the first minimum in the radial distribution function. It is well pronounced for K^+, which has 8 molecules as the calculated coordination number on the cluster; curiously, the sharpness of the definition for Na^+ is less at $N = 6$ (and sometimes 7). The influence

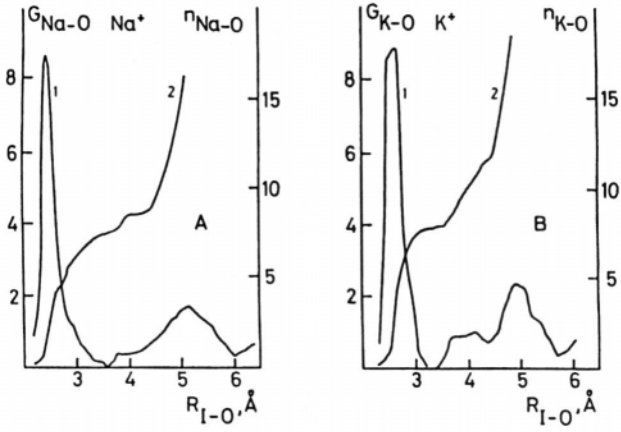

Fig. 2.59. Ion-O radial distribution functions in the ion–$(H_2O)_{199}$ cluster. (a): Na^+, (b) K^+. 1: G_{I-O} (ordinate to the left). 2: Number of H_2O molecules in the sphere of radius R (ordinate to the right). (Reprinted from G. G. Malenkov, "Models for the structure of Hydrated Shells of Simple Ions Based on Crystal Structure Data and Computer Simulation," in *The Chemical Physics of Solvation*, Part A, R. R. Dogonadze, E. Kalman, A. A. Kornyshev, and J. Ulstrup, eds., Elsevier, New York, 1985.)

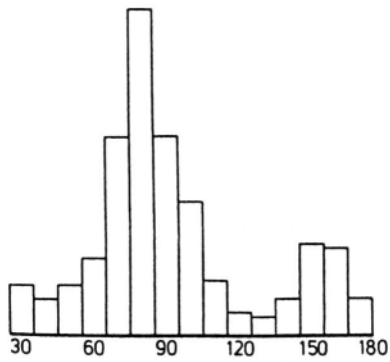

Fig. 2.60. Histogram showing the distribution of O–Na–O angles in a $Na(H_2O)_6$ cluster simulated at 298 K. (Reprinted from G. G. Malenkov, "Models for the Structure of Hydrated Shells of Simple Ions Based on Crystal Structure Data and Computer Simulation," in *The Chemical Physics of Solvation*, Part A, R. R. Dogonadze, E. Kalman, A. A. Kornyshev, and J. Ulstrup, eds., Elsevier, New York, 1985.)

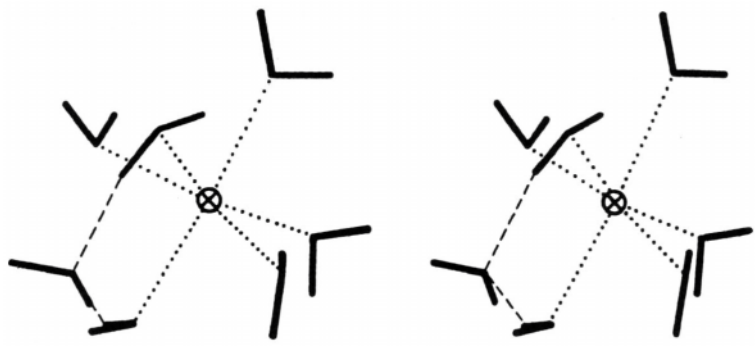

Fig. 2.61. Stereoscopic picture of a "frozen" $Na(H_2O)_7$ cluster. CN = 6. Na–O close contacts (242–245 pm) are shown by dotted lines, hydrogen bonds by dashed lines. (Reprinted from G. G. Malenkov, "Models for the Structure of Hydrated Shells of Simple Ions Based on Crystal Structure Data and Computer Simulation," in *The Chemical Physics of Solvation*, Part A, R. R. Dogonadze, E. Kalman, A. A. Kornyshev, and J. Ulstrup, eds., Elsevier, New York, 1985.)

of the ion on the cluster's structure in these computations becomes negligible at around 700 pm (Fig. 2.62).

If the minimum of the potential corresponds to an Na^+-O separation of 238 pm and a K^+-O separation of 278 pm, then the most probable distances in simulated clusters containing 6 water molecules are about 244 and 284 pm, respectively, at 300 K and about 2 pm less at 5 to 10 K. In Table 2.25, potential parameters that provide such results are given, and the dependence of the ion–water interaction energy on the ion–O distance is shown in Fig. 2.63.

Experimental mass spectrometric data on the hydration of ions in the gas phase that can be compared with calculations of small clusters are available. Full accordance of the computed results with these data is not expected, partly because the aim was to simulate the condensed phase, and the interaction potentials used may not adequately reproduce the properties of small systems in the gas phase at low pressures. However, mass spectrometric data provide reliable experimental information on the hydration of separate ions in the gas phase, and comparison of the results of simulation with these data is an important test of the reliability of the method.

In cluster calculations, an element essential in solution calculations is missing. Thus, intrinsically, gas-phase cluster calculations cannot allow for ionic movement. Such calculations can give rise to average coordination numbers and radial distribution functions, but cannot account for the effect of ions jumping from place to place. Since one important aspect of solvation phenomena is the solvation number (which is intrinsically dependent on ions moving), this is a serious weakness.

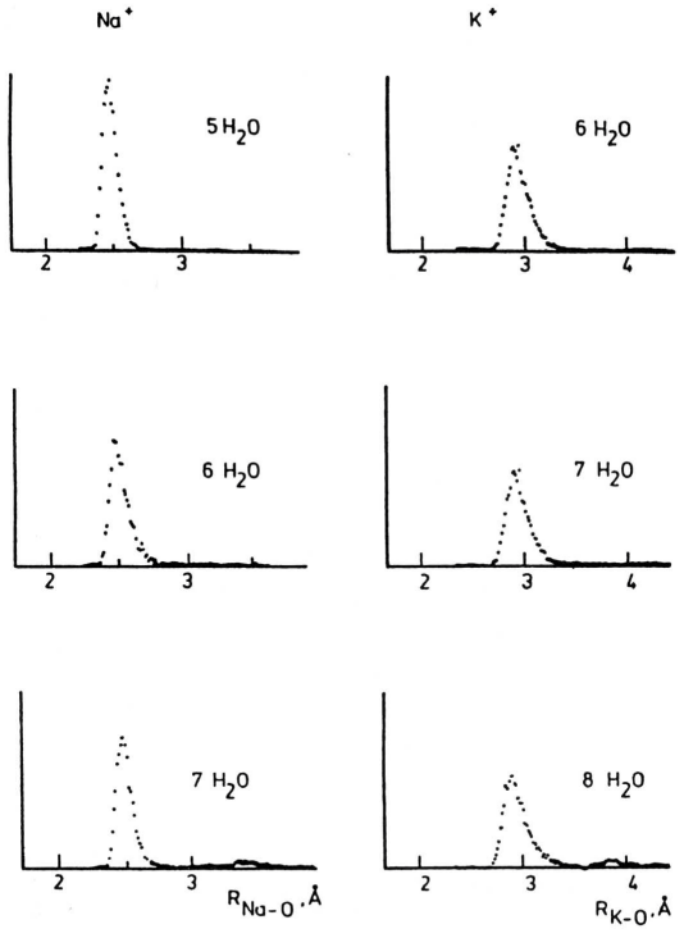

Fig. 2.62. Ion-O radial distribution functions for simulated ion $(H_2O)_n$ clusters (300 K). Ordinate, G_{T-O} in arbitrary units. (Reprinted from G. G. Malenkov, "Models for the Structure of Hydrated Shells of Simple Ions Based on Crystal Structure Data and Computer Simulation," in *The Chemical Physics of Solvation*, Part A, R. R. Dogonadze, E. Kalman, A. A. Kornyshev, and J. Ulstrup, eds., Elsevier, New York, 1985.)

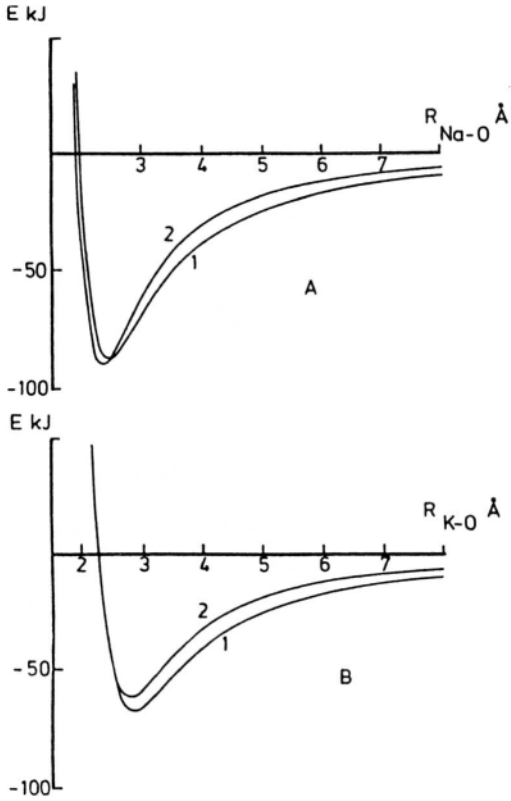

Fig. 2.63. Dependence of ion–H_2O interaction on ion-O distance. 1: Symmetric H_2O molecule orientation (ion-O vector coincides with the water dipole moment direction): 2: lone pair-to-ion orientation. (a) Na^+, (b) K^+ (1 Å = 100 pm). (Reprinted from G. G. Malenkov, "Models for the Structure of Hydrated Shells of Simple Ions Based on Crystal Structure Data and Computer Simulation," in *The Chemical Physics of Solvation*, Part A, R. R. Dogonadze, E. Kalman, A. A. Kornyshev, and J. Ulstrup, eds., Elsevier, New York, 1985.)

TABLE 2.25

Parameters of the Potential Function Used in Equations[a]

$$U_{I\text{-}W} = \sum_{i=1}^{4} \frac{q_i}{r_{O\text{–}I}} - \frac{A_{I\text{–}O}}{r_{I\text{–}O}^{6}} + B_{I\text{–}O} \exp(-C_{I\text{–}O} r_{I\text{–}O}) + \sum_{i=1}^{2} -\frac{A_{I\text{–}H}}{r_{I\text{–}H}^{6}} + B_{I\text{–}H} \exp(-C_{I\text{–}H} \times r_{I\text{–}H})$$

Interaction				
I	j	A_{i-j}	B_{i-j}	C_{i-j}
O	O	4169	34,330,500	4.33
O	H	159	4940	3.90
Na^+	O[b]	6285	4,400,000	4.18
Na^+	O[c]	6285	9,218,000	4.18
K^+	O[b]	8925	377,100	3.50
K^+	O[c]	12,980	569,000	3.50

[a] Distances in angstroms, energy in kJ/mol.
[b] Adjusted to quantum mechanical calculations.
[c] Improved by taking into account crystallographic data.

2.19. SOLVENT DYNAMIC SIMULATIONS FOR AQUEOUS SOLUTIONS

Of the models of water chosen as practical for MD simulation work, the central force model is the best because the effect of ions on intramolecular frequencies can be studied. Heinzinger and Palinkas first used such a model in 1982 to calculate the ion–water pair potentials as a function of the ion–water distance and orientations as shown in Fig. 2.64. Such computations were carried out using 200 water molecules, 8 cations, and 8 anions in a 2.2 M solution. The side of the cube in the computation was 2000 pm.

The time-average positions for Mg^{2+}, F^-, Cs^+, and I^- can be seen in Fig. 2.64. For Mg^{2+}, the arrangement is octahedral but for F^- there is only a small preference for octahedral coordination. On the other hand, Cs^+ and I^- are firmly octahedral. As one goes outward past 400 pm, the preferential orientation is gone except for Li^+ and this seems to form a second shell. It must be again stressed that the numbers are all time-averaged (coordination) numbers and have only a tenuous relation to the time-dependent hydration numbers.

It is possible to calculate diffusion coefficients by computing the mean square displacement distance and dividing by 6t. [The basic relation here is the Einstein–Smoluchowski equation (Section 4.2.6)]. The values are surprisingly good and are shown in Table 2.26.

Both transition times, reorientation of water near the ion and translation, can be calculated. The value for the reorientation time of I^- is 5 ± 2 ps; this is a low value because of the weak field in the water arising from the large size of I^-. The hindered

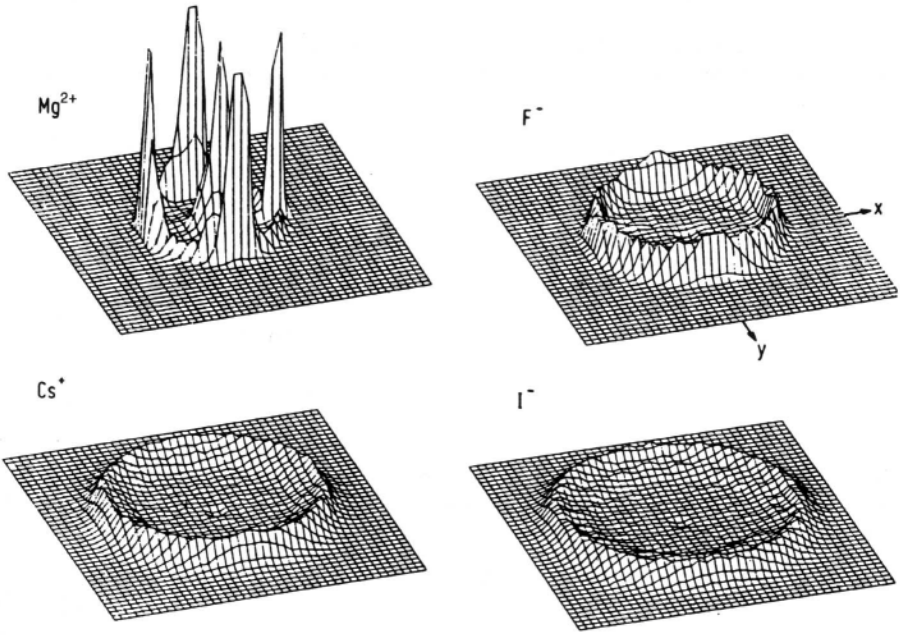

Fig. 2.64. Three-dimensional drawings of the projections of the oxygen atom positions of the six and eight nearest-neighbor water molecules around Mg^{2+} and F^-, and Cs^+ and I^-, respectively, onto the *xy* plane of a coordinate system. The drawings are calculated from MD simulations of 1.1 molal $Mg^{38}Cl_2$ as well as 2.2 molal cs^{18} and $Li^{35}I$ solutions. (Reprinted from K. Heinzinger and G. Palinkas, "Computer Simulation of Ion Solvent Systems," in *The Chemical Physics of Solvation*, Part A, R. R. Dogonadze, E. Kalmar, A. A. Kornyshev, and J. Ulstrup, eds., Elsevier, New York, 1985.)

translation can also be calculated and the frequencies of movement are found to be in the range of the librational modes for water. I^- moves faster than Li^+ because it moves almost bare of water. Li^+ drags with it its hydration number waters.

The work of Guardia and Padro in applying MD to solvation is of particular interest because of the attention given to simulations oriented to the actual calculations

TABLE 2.26

Self-Diffusion Coefficients of Ions and Solvent Water (D_w) in a 2.2 molal LiI Solution Obtained from MD Simulation and Experiments at 305 K[a]

	D_w	D_{Li^+}	D_{I^-}
MD	2.48 ± 0.06	0.7 ± 0.3	1.40 ± 0.15
Experimental	2.35	1.0	1.47

Source: From J. A. Padro and E. Guardia, *J. Phys. Chem.* **94**: 2113, 1990.
[a]Units are 10^5 cm^2 s^{-1}.

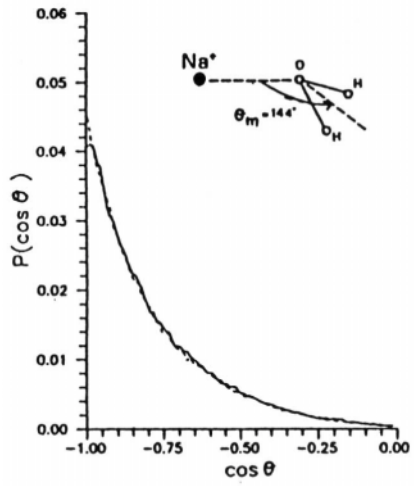

Fig. 2.65. Probability distribution of cos θ for water molecules in the first hydration shell of Na^+ ion. ___, Flexible water,..., rigid water. (Reprinted from E. Guardia and J. A. Padro, *J. Phys. Chem.* **94:** 6049,1990.)

of hydration numbers (and not coordination numbers!) Figure 2.65 shows the flexible water model used.

Among the variations for the water molecule are a rigid and a flexible model, and Guardia and Padro found that significant changes arose with the introduction of flexibility in respect to orientation times. The most important aspect of this work is the computation of the residence times (*cf.* Section 2.11.3).

TABLE 2.27

Residence Times and Hydration Numbers

	Residence Times (picoseconds)		Computed Hydration Numbers	
	Na^+	F^-	Na^+	F^-
Flexible model	38.5	21.4	5.4	5.7
Rigid model	23.8	15.8	5.2	5.4
Computer simulation[a]	9.9	20.3	3.8	4.6
Experimental		5 ± 1	4 ± 1	

Source: From E. Guardia and J. A. Padro, *J. Phys. Chem.* **94**: 2113, 1990.
[a]Data correspond to computer simulations at different temperatures, i.e., 282 K for Na^+ and 278 K for F^-.

The basic idea of calculating a hydration number is to study the number of water molecules in the shell as a function of time. At $t = 0$, the number is the coordination number, and at $t = \tau_{i-w}$, all the waters have been replaced. Then the mean number during this time is taken as the solvation number:

$$n_h = (CN)_{t=0} e^{-\tau_{w-w}/\tau_{i-w}} \tag{2.136}$$

where τ_{w-w} is the residence time for water around water. Although this approach does not take into account the distribution of residence times for the various waters "caught" in different positions when the ions arrive, it does give reasonable values (Table 2.27).

Further Reading

Seminal

1. J. O'M. Bockris and P. P. S. Saluja, "The Time Dependence of Solvation Numbers," *J. Electrochem. Soc.* **119**: 1060(1972).
2. G. Palinkas, W. O. Riede, and K. Heinzinger, "Calculation of Distribution Functions," *Z. Naturforsch.* **32**: 1137 (1972).
3. F. H. Stillinger and A. Rahman, "A Statistical Mechanical Approach to Ionic Solution," *J. Chem. Phys.* **60**: 1545 (1974).

Papers

1. A. Chandra and B. Bagchi, *J. Phys. Chem.* **93:** 6996 (1989).
2. E. Guardia and J. A. Padro, *J. Phys. Chem.* **94:** 2113 (1990).
3. P. Cieplak and P. Kollman, *J. Chem. Phys.* **92:** 6761 (1990).
4. P. A. Kollman, *J. Am. Chem. Soc.* **113:** 2681 (1991).
5. T. Yabe, S. Sankareman, and J. K. Kochi, *J. Phys. Chem.* **95:** 4147 (1991).
6. H. Yu, B. M. Pettitt, and M. Karplus, *J. Am. Chem. Soc.* **113:** 2425 (1991).
7. R. W. Rick and B. J. Berne, *J. Am. Chem. Soc.* **116:** 3949 (1994).
8. P. J. Rossky, K. P. Johnson, and P. B. Babuena, *J. Phys. Chem.* **100:** 2706 (1996).
9. C. C. Pye, W. Rudolph, and R. A. Pourier, *J. Phys. Chem.* **100:** 601 (1996).
10. T. Z. M. Denti, T. C. Beutler, W. F. Vangunsteeren, and F. Diedrich, *J. Phys. Chem.* **100:** 4256 (1996).

2.20. INTERACTIONS OF IONS WITH NONELECTROLYTES IN SOLUTION

2.20.1. The Problem

The picture that has emerged in this book so far is of ions interacting with a solvent and producing the interesting effects that go under the name "solvation." The solvent

structure is not the same after an ion has entered it near the ion. Some of the water molecules are wrenched out of the quasi-lattice and appropriated by the ion as part of its primary solvation sheath. Further off, in the secondary solvation sheaths, the ions produce the telltale effects of structure breaking.

What happens if, in addition to ions and water molecules, molecules of nonelectrolytes are also present in the system? Or what will occur if ions are added to a solution already saturated with nonelectrolyte molecules?

One thing is certain: the fact that the ion takes the water out of circulation for a time means that there will be on average less free water to dissolve the nonelectrolyte. The nonelectrolyte molecules will find themselves suddenly having less water to associate with, and some of them will shun the loneliness imposed by the water's preference for the newly added ions and find it energetically favorable to go back to their parent lattice, i.e., precipitate out. This is the origin of a term from organic chemistry—*salting out.* It means causing a nonelectrolyte to precipitate out of a solution by adding an electrolyte to it to draw off available solvent molecules.

Occasionally, however, the ions are deviants and associate preferentially with the nonelectrolyte solute, shunning the water (hydrophobic effects). In the rare instances where these deviants appear, there is a rapid departure of the nonelectrolyte from the parent lattice and the solubility of the former is *enhanced* rather than decreased. The phenomenon is called *salting in.*

Two aspects of the theory of salting out are considered below. First, the effects of the primary solvation sheath have to be taken into account: how the requisition of water by the ions causes the nonelectrolyte's solubility to decrease. Second, the effects of secondary solvation (interactions outside the solvation sheath) are calculated. The two effects are additive.

2.20.2. Change in Solubility of a Nonelectrolyte Due to Primary Solvation

It is easy to calculate this change of solubility so long as there are data available for the solvation numbers of the electrolyte concerned. Let it be assumed that the normal case holds true and that ions are solvated entirely by water molecules (i.e., the organic present is pushed out). Then recalling that 1 liter of water contains 55.55 moles, the number of water molecules left free to dissolve nonelectrolytes after the addition of ions is $55.55 - c_i n_s$, where n_s is the solvation number of the electrolyte concerned.

Assuming that the solubility of the nonelectrolyte is simply proportional to the number of water molecules outside the hydration sheath, then

$$\frac{S}{S_0} = \frac{55.55 - c_i n_s}{55.55} \tag{2.137}$$

where S_0 is the solubility of the nonelectrolyte before the addition of electrolyte and S that after it.

Assume $n_s = 6$, $c_i = 1\ M$; then from Eq. (2.137), $(S/S_0) = 0.89$. For comparison, with $KClO_4$ as electrolyte, and 2,4-dinitrophenol as nonelectrolyte, the corresponding experimental value is about 0.7. Some further effects must be taken into account.

2.20.3. Change in Solubility Due to Secondary Solvation

It has been stressed that solvation is a far-reaching phenomenon, although only the coordination number and the primary solvation number can be determined. However, there are effects of ions on the properties of solutions that lie outside the radius of the primary hydration sheath. These effects must now be accounted for, insofar as they relate to the solubility of a nonelectrolyte. Let the problem be tackled as though no primary solvation had withdrawn water from the solution. One can write

$$n_{NE,r} = n_{NE,b}\, e^{-\Delta G/RT} \tag{2.138}$$

where $n_{NE,r}$ is the number per unit volume of nonelectrolyte molecules at a distance r from the ion, $n_{NE,b}$ is the same number in the bulk, and the free-energy change ΔG is the work W_r done to remove a mole of water molecules and insert a mole of nonelectrolyte molecules at a distance r from the ion outside the primary solvation sheath.

A first-approximation calculation would be like this. The field X_r of the ion at a distance r falls off with distance according to Coulomb's law[41]

$$X_r = \frac{z_i e_0}{\varepsilon r^2} \tag{2.139}$$

If, now, a dipole (aligned parallel to the ionic field) is moved from infinity, where the field $X_r = 0$, through a distance dr to a point where the corresponding field is dX, the elementary work done is $-\mu\, dX$. Thus, the work to bring a mole of nonelectrolyte molecules from infinity to a distance r is

$$-N_A \int_0^{X_r} \mu_{NE}\, dX$$

and the work done to remove a water molecule to infinity is $N_A \int_0^{X_r} \mu_w\, dX$. The net work of replacing a water molecule by a nonelectrolyte molecule would therefore be given by

[41] Notwithstanding the considerations of Section 2.12.1, the use of the *bulk* dielectric constant of water for dilute solutions of nonelectrolyte is not very inaccurate in the region *outside* the primary solvation sheath. The point is that in this region (i.e., at distances > 500 to 1000 pm from the ion's center), there is negligible structure breaking and therefore a negligible decrease in dielectric constant from the bulk value.

$$W_r = N_A \left(\int_0^{X_r} \mu_w \, dX - \int_0^{X_r} \mu_{NE} \, dX \right) \tag{2.140}$$

Now, the reader will probably be able to see there is a flaw here. Where? The error is easily recognized if one recalls the Debye argument for the average moment of a gas dipole. What is the guarantee that a water dipole far from the ion is aligned parallel to the ionic field? What about the thermal motions that tend to knock dipoles out of alignment? So what matters is the *average* dipole moment of the molecules in the direction of the ionic field. Thus, one has to follow the same line of reasoning as in the treatment of the dielectric constant of a polar liquid and think in terms of the average moment $<\mu>$ of the individual molecule, which will depend in Debye's treatment on the interplay of electrical and thermal forces, and in Kirkwood's treatment also on possible short-range interactions and associations of dipoles. One has therefore

$$W_r = N_A \left(\int_0^{X_r} <\mu_w> dX - \int_0^{X_r} <\mu_{NE}> dX \right) \tag{2.141}$$

Further, with α now the orientation polarizability,

$$<\mu> = \alpha X \tag{2.142}$$

so that

$$W_r = \frac{N_A(\alpha_w - \alpha_{NE})X_r^2}{2} \tag{2.143}$$

This expression for the work of replacing a water molecule by a nonelectrolyte molecule at a distance r from an ion can now be introduced into Eq. (2.138) to give (in number of nonelectrolyte molecules per unit volume)

$$n_{NE,r} = n_{NE,b} \exp\left[\frac{(\alpha_{NE} - \alpha_w)X_r^2}{2kT} \right] \tag{2.144}$$

The exponent of Eq. (2.144) is easily shown to be less than unity at 298 K for most ions. Thus, for distances outside the primary hydration shell of nearly all ions, the field X will be sufficiently small (because of the large dielectric constant of bulk water), so one can expand the exponential and retain only the first two terms, i.e.,

$$n_{NE,r} = n_{NE,b} \left[1 + \frac{(\alpha_{NE} - \alpha_w)X_r^2}{2kT} \right] \tag{2.145}$$

Thus, the *excess number* per unit volume of nonelectrolyte molecules at a distance r from the ion is (in number of molecules per unit volume)

$$n_{NE,r} - n_{NE,b} = \frac{n_{NE,b}(\alpha_{NE} - \alpha_w)X_r^2}{2kT} \tag{2.146}$$

However, this is only the excess number of nonelectrolyte molecules per unit volume at a distance r from the ion. What is required is the total excess number per unit volume throughout the region outside the primary solvation sheath, i.e., in region 2. One proceeds as follows: the excess number, *not* per unit volume, but in a spherical shell of volume $4\pi r^2\,dr$ around the ion, is

$$(n_{NE,r} - n_{NE,b})4\pi r^2\,dr$$

and therefore the total excess number of nonelectrolyte molecules per ion in region 2 is (with r_h equal to the radius of the primary hydration sheath)

$$n_{NE,2} - n_{NE,b} = \int_{r_h}^{\infty} (n_{NE,r} - n_{NE,b})4\pi r^2 dr = \int_{r_h}^{\infty} \frac{n_{NE,b}(\alpha_{NE} - \alpha_w)X_r^2}{2kT} 4\pi r^2 dr \tag{2.147}$$

If one sets $X_r = z_i e_0/(\varepsilon r^2)$, then the excess number of nonelectrolyte molecules caused to be in solution per ion is

$$\frac{4\pi(z_i e_0)^2 n_{NE,b}(\alpha_{NE} - \alpha_w)}{2\varepsilon^2 kT} \int_{r_h}^{\infty} \frac{1}{r^2}\,dr = \frac{4\pi(z_i e_0)^2 n_{NE,b}}{2\varepsilon^2 kTr_h}(\alpha_{NE} - \alpha_w) \tag{2.148}$$

The excess number of nonelectrolyte molecules in a real solution containing c_i moles dm^{-3} of binary electrolyte is given by Eq. (2.148), multiplied by the number of moles per cubic centimeter in the solution, namely, $N_A c_i/1000$. The expression is[42]

$$n_{NE} - n_{NE,b} = \frac{N_A c_i}{1000}\left[\frac{4\pi(z_i e_0)^2 n_{NE,b}(\alpha_{NE} - \alpha_w)}{\varepsilon^2 kTr_h}\right] \tag{2.149}$$

where n_{NE} is the number of nonelectrolyte molecules per cubic centimeter in the solution after addition of the electrolyte.

Hence,

$$\frac{n_{NE} - n_{NE,b}}{n_{NE,b}} = \frac{N_A c_i}{1000}\left[\frac{4\pi(z_i e_0)^2(\alpha_{NE} - \alpha_w)}{\varepsilon^2 kTr_h}\right] \tag{2.150}$$

[42] A factor of 2 has been removed from the denominator of this equation, compared with Eq. (2.148), because there are two ions in the binary electrolyte, each of which is assumed to give the same effect on the solubility.

The terms n_{NE} and $n_{NE,b}$ are numbers of nonelectrolyte molecules per cubic centimeter; $N_A n_{NE} = S$ and $N_A n_{NE,b} = S_0$; these terms were defined in Section 2.20.2. It follows that

$$S = S_0 - \frac{S_0 N_A c_i}{1000}\left[\frac{4\pi(z_i e_0)^2(\alpha_w - \alpha_{NE})}{\varepsilon^2 kTr_h}\right] \tag{2.151}$$

This equation clearly shows the effect of the secondary solvation. It turns out that the orientation polarizabilities α_{NE} and α_w depend on the square of the permanent dipole moments of the molecules. Water has a higher dipole moment than most nonelectrolytes. When $\alpha_w > \alpha_{NE}$, S is less than S_0 and there is salting out. HCN is an example of a substance the dipole moment of which is greater than that of water. (It masquerades as a nonelectrolyte because it is little dissociated in aqueous solution.) Appropriately, HCN is often salted in.

2.20.4. Net Effect on Solubility of Influences from Primary and Secondary Solvation

Equation (2.137) can be written as

$$S_{\text{prim}} = S_0 - K_1 c_i \tag{2.152}$$

Equation (2.151) can be written as

$$S_{\text{sec}} = S_0 - K_2 c_i \tag{2.153}$$

The treatment of the effect of secondary solvation has assumed that the primary solvational effects do not exist. In fact, the secondary solvational effects work on the diminished concentration of nonelectrolyte which arises because of the primary solvation. Hence,

$$S = S_{\text{prim}} - K_2 c_i \tag{2.154}$$

$$= S_0 - K_1 c_i - K_2 c_i \tag{2.155}$$

$$= S_0 - \frac{S_0 c_i n_s}{55.55} - \frac{N_A c_i S_0}{1000}\left[4\pi(z_i e_0)^2 \frac{(\alpha_w - \alpha_{NE})}{\varepsilon^2 kTr_h}\right] \tag{2.156}$$

S as written in Eq. (2.154) has taken into account the primary and secondary solvation and can be identified with the solubility of the nonelectrolyte after addition of ions to the solution. Hence,

$$\frac{S_0 - S}{S_0} = \frac{n_s c_i}{55.55} + \frac{N_A c_i}{1000}\left[\frac{4\pi(z_i e_0)^2(\alpha_w - \alpha_{NE})}{\varepsilon^2 k T r_h}\right] \tag{2.157}$$

or:

$$\Delta S/S_0 = k_1 c_i \tag{2.158}$$

the k_1 is called Setchenow's constant (Fig. 2.66).

There is fair agreement between Eq. (2.158) and experiment. If the nonelectrolyte has a dipole moment less than that of water, it salts out. In the rare cases in which there is a dipole moment in the nonelectrolyte greater than that of water, the nonelectrolyte salts in.

Salting *out* has practical implications. It is part of the electrochemistry of everyday industrial life. One reclaims solvents such as ether from aqueous solutions by salting them out with NaCl. Salting out enters into the production of soaps and the manufacture of dyes. Detergents, emulsion polymerization (rubber), and the concentration of antibiotics and vitamins from aqueous solutions all depend in some part of their

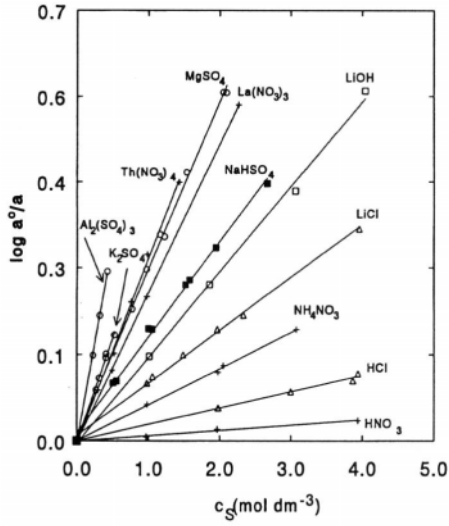

Fig. 2.66. Setchenow plots for oxygen at 310.2 K and 1 atm (101.325 kPa) oxygen partial pressure in aqueous solutions of some representative electrolytes. (Reprinted from W. Lang and R. Zander, *Ind. Eng. Chem. Fundam.* **25**: 775, 1986.)

manufacture upon salting in. However, the salting in with which they are associated is not the rare deviant phenomenon arising when the dipole moment of the nonelectrolyte is greater than that of water. It possesses the characteristic of always being associated with organic electrolytes in which the ions are *large*. Here, even when water has a dipole moment *greater* than that of the nonelectrolyte, which would be expected to give salting out, salting in occurs.

2.20.5. Cause of Anomalous Salting In

The picture given above seems satisfactory as a first approximation and for dilute solutions, but it has this one disturbing feature; namely, there are situations where theory predicts salting out but experiment shows salting in. In such cases, the theory seems to favor ions being surrounded by water whereas in fact they move away from water (hydrophobic effects). Now, it will be recalled that only ion–dipole forces have been reckoned with in treating the interactions among the particles populating the primary solvation shell. Thus, the ion–water and ion–nonelectrolyte forces have been considered to be of the ion–dipole type of directional forces which orient polar particles along the ionic field. Perhaps this restriction is too severe, for there are also nondirectional forces, namely, dispersion forces.

These dispersion forces can be seen classically as follows: The *time-average* picture of an atom may show spherical symmetry because the charge due to the electrons orbiting around the nucleus is smoothed out in time. However, an instantaneous picture of, say, a hydrogen atom would show a proton "here" and an electron "there"—two charges separated by a distance. Thus, every atom has an *instantaneous* dipole moment; of course, the time average of all these oscillating dipole moments is zero.

Now, an instantaneous dipole in one atom will induce an instantaneous dipole in a contiguous atom, and an instantaneous dipole–dipole force will arise. When these forces are averaged over all instantaneous electron configurations of the atoms and thus over time, it is found that the time-averaged result of the interaction is finite, attractive, and nondirectional. Forces between particles that arise in this way are called *dispersion forces*.

Dispersion forces give rise to an interaction energy in which the potential energy of interaction varies as r^{-6}, where r is the distance between the centers of the two substances interacting. Thus, the equation for the dispersive energy of interaction may be written as λ/r^6, where λ is a constant independent of r. The rapid decrease of such forces with increase of distance from the origin makes it unnecessary to consider dispersion interactions outside the primary solvation shell; by then, they have already decreased to an extent that they no longer warrant consideration. Inside the primary hydration sheath, the dispersion interaction can be treated in the same way as the ion–dipole interaction. That is, in the replacement of a water molecule by a nonelectrolyte molecule, one must take into account not only the difference in ion–dipole

interactions but also the difference between the dispersion interactions. Thus, one must reconsider the situation in which the ion interacts with water molecules.

The picture given in the last three sections was that the water would usually be the entity to be predominantly attracted to the ion, so that the amount of water available for the dissolution of the nonelectrolyte would be reduced and its solubility consequently would fall. The only exceptions that were recognized for this were those unusual cases in which the nonelectrolyte had a dipole moment greater than that of water. As for the ion, only its radius and charge played a part in the matter; it did not influence the situation in any more structural way, e.g., in terms of its polarizability.

On what molecular features do dispersion forces depend? What relative attractiveness has a given ion on the one hand for a water molecule, and on the other for a nonelectrolyte? Equations for the dispersive force interactions have been worked out for interactions in the gas phase. A simple version of such equations would be

$$U = \frac{h\nu\alpha_{d\text{-ion}}\alpha_{d\text{-molec}}}{2R^6} \tag{2.159}$$

where the ν is the frequency of vibration of the electron in its lowest energy state, the αs are the *distortion polarizabilities* of the entities indicated, and R is their distance apart. It must be noted at once that the polarizability indicated here, the distortion polarizability, differs from that which enters into the equations for the dipole effects, which has simply been termed α. This latter α, which influences the theory of effects of secondary solvation upon salting out and salting in, is due to the orientation of dipoles against the applied field. The distortion polarizability α_d is due to the stretching of the molecule under the influence of a field. The former polarizability α is connected to the dipole moment of the molecule according to a formula such as Eq. (2.142). The α_d is more complexly connected to the size of the molecule. There is a parallelism with the radius and in spherical symmetry cases it is found that α_d approximately follows r^3, where r is the radius of the molecule.

Now, if the size of the nonelectrolyte (hence $\alpha_{d,\text{molec}}$) is greater than that of the water molecule (and for organic nonelectrolytes this is often so), it is clear from the above equation that the dispersive interaction of a given ion is going to be greater with the nonelectrolyte than with the water. This is a reversal of the behavior regarded as usual when only the permanent dipoles of the water and the nonelectrolyte are taken into account (for the dipole moment of water is higher than that of most nonelectrolytes). In view of the above situation it may be asked, why is not salting in (which happens when the nonelectrolyte outcompetes the water molecule in its attraction to the ion) the normal case? In this section, it is the dispersive interactions which have been the center of attention: they have been suddenly considered in isolation. One has to ask, however, whether the dispersive ion–water (and dispersive ion–nonelectrolyte) interactions will dominate over the ion–dipole interactions. If the ion–dipole interactions dominate the dispersive interactions, the considerations of those earlier sections

are applicable and salting out is the norm, with salting in a rare exception. When the dispersive interactions predominate, it is the other way around; salting in (and hydrophobic effects) becomes the norm.

What factors of structure tend to make the dispersive forces dominate the situation? Clearly, they will be more likely to have a main influence upon the situation if the nonelectrolyte is large (because then the distortion polarizability is large), but there are many situations where quite large nonelectrolytes are still salted *out.* The dispersive interaction contains the *product* of the polarizability of both the ion and the nonelectrolyte (or the ion and water, depending upon which interaction one is considering), so that it is when *both* the ion *and* the nonelectrolyte are large (hence, both the αs are large) that the dispersive situation is likely to dominate the issue, rather than the ion–dipole interaction.

In accordance with this it is found that if one maintains the nonelectrolyte constant[43] and varies the ion in size, though keeping it of the same type, salting in begins to dominate when the ion size exceeds a certain value. A good example is the case of the ammonium ion and a series of tetraalkylammonium ions with increasing size, i.e., NR_4^+, where R is CH_3, C_2H_5, etc. Here, the salting in begins with the methylammonium ion (its α_d is evidently large enough), the ammonium ion alone giving salting out. The degree of salting in increases with an increase in the size of the tetraalkylammonium cation. Thus, the observations made concerning the salting in of detergents, emulsions, and antibiotics by organic ions are, in principle, verified. An attempt has been made to make these considerations quantitative.

This discussion of the effect of ions upon the solubility of nonelectrolytes is sufficiently complicated to merit a little summary. The field is divided into two parts. The first part concerns systems in which the dispersive interactions are negligible compared with the dipole interactions. Such systems tend to contain relatively small ions acting upon dissolved molecules. Here salting out is the expected phenomenon—the solubility of the nonelectrolytes is decreased—and the reverse phenomenon of salting in occurs only in the rare case in which the nonelectrolyte dipole moment is greater than the dipole moment of the solvent. In the other group of solubility effects caused by ions, the ions concerned tend to be large and because distortion polarizability increases with size, this makes the dispersive activity between these large ions and the nonelectrolyte become attractive and dominate this situation so that the organic molecule is pulled to the ions and the water is pushed out. Then salting in (solubility of the nonelectrolyte increases) becomes the more expected situation.

2.20.6. Hydrophobic Effect in Sotvation

Solvation entropies (Section 2.15.13) are negative quantities. Since $\Delta S_{solv} = S_{i,soln} - S_{i,gas}$, this means that the disorder in solution (the entropy) is less than that of the ion

[43]For example, it may be benzoic acid, which is considered a nonelectrolyte because it dissociates to a very small degree.

in the gas phase. The interpretation of this is in terms of the structured presence of water molecules around the ion (low entropy). However, there must be another component in the events that make up the measured entropy, for the ion breaks the water structure; i.e., it increases entropy. This is called the "hydrophobic aspect of solvation." There is a large literature on this phenomenon and it can be seen by its effects on several properties of solutions, not only on ΔH_s and ΔS_s, but also on the partial molar volume, specific heat effect, etc.

Among the early discussions of hydrophobic effects were those of Frank et al. They studied the highly negative entropies of hydration of the rare-gas atoms. These might have been expected to give much less negative values because of the absence of tightly ordered hydration shells. To interpret the order indicated by the highly negative entropies, they suggested that when the normal structure of water was broken down by the dissolution of the rare-gas atoms, a new type of water structure—iceberglike groups—was formed. Such groups arise from the breakup of normal water and thus result from hydrophobicity.

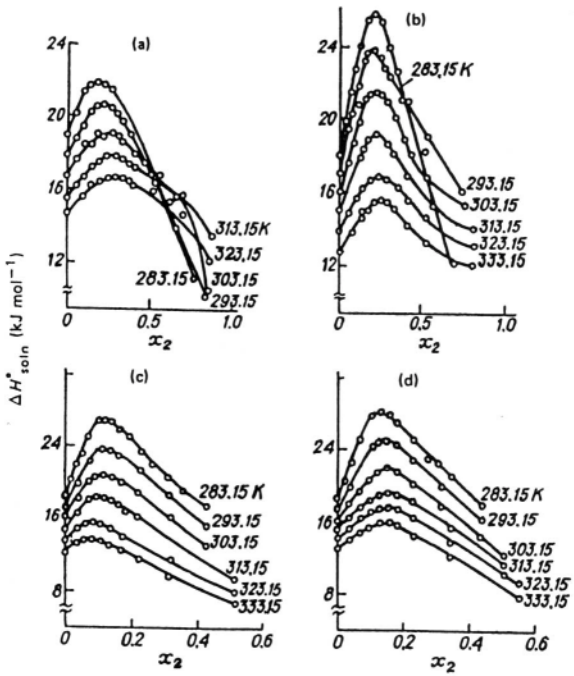

Fig. 2.67. Dependence of ΔH°_{soln} for KCl in aqueous solutions of (a) methanol, (b) ethanol, (c) 1-propanol, and (d) 2-propanol on composition at different temperatures. (Reprinted from G. A. Krestov, *Thermodynamics of Solvation,* Ellis Harwood, London, 1991.)

Frank and Evans, in studying the numbers for the hydrational entropies of ordinary monatomic ions, found them *insufficiently* negative, indicating that, due to structure breaking, the entropy of the ion itself should be larger than that expected if only the ordering effect of the ion is considered.

An interesting variation of the heat of solution (e.g., for KC1) can be observed in water–alcohol mixtures. The position of the maxima of the curves shifts with increasing temperature along the ordinate in conjunction with the decrease of the endothermicity of the KC1 dissolution. This is related to an increasing disruption of the water structure—a hydrophobic effect (Fig. 2.67).

The solubility of noble gases in various solutions (often aqueous–nonaqueous mixtures) gives indications of both *hydrophobic* and *hydrophilic* effects (Fig. 2.68). When substances exhibiting both effects are present, there is a maximum in the solubility of argon. Thus (Fig. 2.68, curve 1) in the system water–acetone, no hydrophilic effects are caused by the added solvent component, and the solubility increases. On the other hand, for systems in which urea is added, there are no hydrophobic effects and the solubility or the gas therefore decreases. In curve 2 of Fig. 2.68, hydrophilic and hydrophobic effects compete (due to the properties of acetamide in water) and there is a maximum on the curve.

Another source of hydrophobic effects arises from solute–solute attraction. The usual effects of interactions between ions of like sign are, of course, repulsive. However, if the ions are sufficiently large, attractive interactions will arise due to

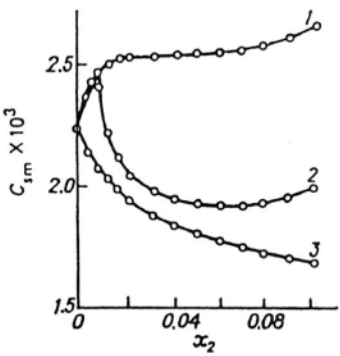

Fig. 2.68. Dependence of solubility of argon in aqueous solutions of (1) acetone, (2) acetamide, and (3) urea (NH_2CON_2H) on composition at 273.15 K. (Reprinted from G. A. Krestov, *Thermodynamics of Solvation*, Ellis Harwood, London, 1991.)

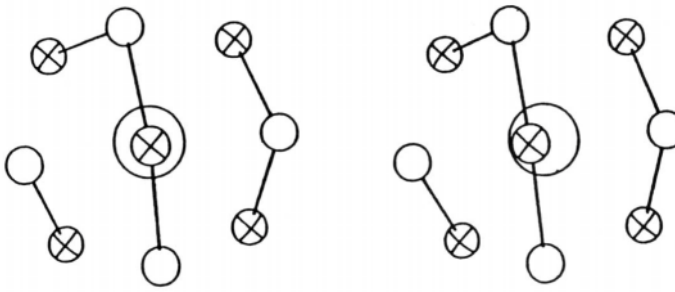

Fig. 2.69. Stereographic view of part of a possible solvation shell. Only a portion of the hydrogen bonds in the solvation shell is shown. Large sphere: nonpolar solute, $\sigma = 320$ pm. Cross-hatched spheres: nearest-neighbor water molecules. Plain spheres: a group of next-nearest-neighbor water molecules located in the solvation shell and surrounding one of the nearest-neighbor molecules, O–O distances range from 290 pm for hydrogen bonds to 320–350 pm otherwise. (Reprinted from E. Grunwald, *J. Am. Chem. Soc.* **108**: 5926, 1986.)

significant dispersion force interaction between the solute particles, and this tends to push water away from the ions; i.e., make it act *hydrophobically.*

These thermodynamic approaches to hydrophobic effects are complemented by spectroscopic studies. Tanabe (1993) has studied the Raman spectra manifested during the rotational diffusion of cyclohexane in water. The values of the diffusion coefficients are approximately half those expected from data for other solvents of the same viscosity, and the interpretations made are in terms of hindered rotation arising from the icebergs presumably formed (*cf.* Frank and Evans) around the cyclohexane.

Correspondingly, NMR studies of the rate at which CH_4 "tumbles" in mixtures of nonaqueous solvents with water show that it is moving approximately ten times faster than the solvent rotation; i.e., it moves independently of the solvent and thus acts hydrophobically.

Simulations of solutions have been used to study hydrophobic effects. Thus, Rossky and Zicki (1994) found that hydration shells of methane and neon remain intact in mixed solvents; this is understandable in terms of clathrate formation—an example of an unusual degree of disordering from the normal structure of water.

Hydrocarbons in water give rise to hydrophobic solvation shells in which the water structure is thoroughly disturbed though still forming a solvation shell around a spherical solute. An example of a calculated situation of this type is shown in Fig. 2.69.

Further Reading

Seminal

1. P. Setchenow, "Salting Out Coefficients," *Z. Phys. Chem.* **4**: 117 (1889).

2. P. Debye and W. McAuley, "Theory of Salting Out," Z. *Phys. Chem.* **26**: 22 (1925).
3. J. O'M. Bockris, J. Bowler-Reed, and J. A. Kitchener, "The Salting In Effect," *Trans. Faraday Soc.* **47**: 184 (1951).
4. R. McDevilt and F. Long, "Salting Out," *Chem. Rev.* **51**: 119 (1952).

Reviews

1. B. E. Conway, *Ionic Hydration in Chemistry and Biology*, pp. 444–465, Elsevier, New York (1981).
2. G. A. Krestov, *Thermodynamics of Solvation*, Ellis Harwood, New York (1991).

Papers

1. W. Lang and R. Zander, *Ind. Eng. Chem. Fundam.* **25**: 775 (1986).
2. J. Butz, P. H. Karpinski, J. Mydiarz, and J. Nyvil, *Ind. Eng. Chem. Prod. Res. Dev.* **25**: 657 (1986).
3. D. C. Leggett, T. F. Jenkins, and P. H. Miyeres, *J. Anal. Chem.* **62**: 1355 (1990).
4. G. Mina-Makarius and K. L. Pinder, *Can. J. Chem. Eng.* **69**: 308 (1991).

2.21. DIELECTRIC BREAKDOWN OF WATER

2.21.1. Phenomenology

Experiment shows that the magnitude of the electric field between two plates depends on the medium contained between them. The quantity *dielectric constant* is used as a measure of the effect of the medium in reducing the field that exists if nothing is there. Water has a particularly large dielectric constant (ca. 78 at 25 °C). This means that if the field between two plates separated by a vacuum amounts to X_0, the field would be reduced to $X_0/78$ if water were used to fill the space between the plates.

Dielectric constants depend little upon the strength of the applied field until extremely high fields are reached—fields greater than 10^6 V cm^{-1}. However, at some critical field strength, a complex phenomenon occurs (Figs. 2.70 and 2.71). It is called *dielectric breakdown.* It can be described in a general way by saying that a dielectric liquid subjected to a sufficiently high electric field suddenly ceases to behave in the customary field-reducing manner. At the same time, a number of characteristic phenomena (e.g., light emission) occur.

What are the phenomena characteristic of dielectric breakdown?[44] The first six in importance are:

[44]The phenomenon occurs for solids, liquids, and gases. Because this chapter is concerned with ionic solutions, the material here is limited to liquids and dilute solutions.

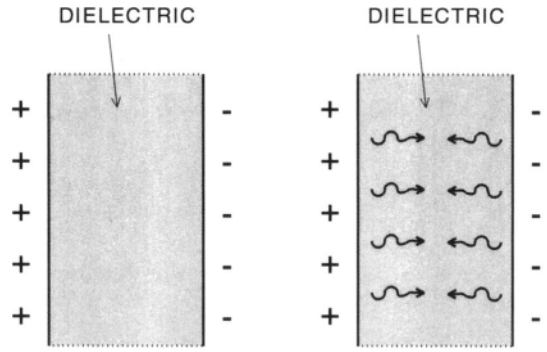

Fig. 2.70. (a) The field between the plates is normal and the water dielectric is chemically stable. Its property as an insulator depends on the concentration of ions but it is highly resistive. (b) When the field applied is sufficiently high, dielectric breakdown occurs; the liquid no longer supports the field and the charges flow away, forming "streamers."

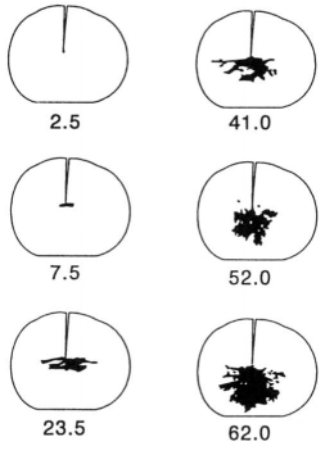

Fig. 2.71. Negative streamer growth in a white naphthenic mineral oil (Marcol 70). Gap: 1.27 cm; voltage step: 185 kV; time in microseconds. (Reprinted from R. E. Tobeozon, *The Liquid State and Its Electrical Properties,* Plenum Press, New York, 1988.)

1. The time between application of an electric field sufficiently high to cause the breakdown phenomena and their occurrence is about 1 μs.
2. Bright, white light is emitted.
3. The most singular and characteristic phenomenon is that called *streamers.* The electrodes concerned emit a piercing series of filaments (Fig. 2.71) that spread out across the solution from the electrode. The filaments turn out to be low-density tubules through the liquid and fade away rapidly after breakdown. These low-density regions in the dielectric remind one of the branchlike growth of trees (Fig. 2.71). The heads of the streamers travel at high velocity, reaching in some systems 1 % of the velocity of light.
4. Although older books give tables of the *breakdown voltage* for a series of different liquids, it is not helpful to describe dielectric breakdown phenomena in terms of the voltage applied between two metal plates. The phenomenon depends on the strength of the *electric field* (volts per unit distance), not upon volts. It is also not enough to state a field strength as the volts between two electrodes immersed in the dielectric divided by the distance between the plates. This is because the phenomenon is known to be critically associated with the *interfacial regions* of the cathode and anode concerned. In such regions, however, there are huge discontinuities in field strength. A total of 30,000 V applied over 10 cm may cause dielectric breakdown, but this may not be directly related to the apparent $3000\ \mathrm{V\ cm^{-1}}$ field across the whole liquid between the plates. It may depend upon the $10^6\ \mathrm{V\ cm^{-1}}$ field very near the surface or even the $10^8\ \mathrm{V\ cm^{-1}}$ over a few nanometers, which can be calculated to occur at the tips of the spikelike micropromontories that exist on many real surfaces.
5. An increase in pressure applied to the liquid suppresses the formation of streamers, which are the most telling sign of breakdown.
6. The critical applied volts (and the associated electric field at the interfaces concerned) that cause breakdown depend upon the conductance of the solution (Fig. 2.72).

2.21.2. Mechanistic Thoughts

Dielectric breakdown is a phenomenon of practical importance; it is by no means only an academic puzzle. One can appreciate this through the analogy between mechanical strength and dielectric strength. Any mechanical structure collapses if too great a stress is placed upon it. Correspondingly, any substance can withstand an electric field only to a certain degree of field strength, after which it ceases to remain an insulator and opens the flood gates for electrons to come across; as a result, the resistance to the applied potential undergoes a catastrophic decline. For example, a condenser may be used with a water dielectric to store great amounts of electrical energy to activate electromagnetic weapons. It then becomes important to know, and

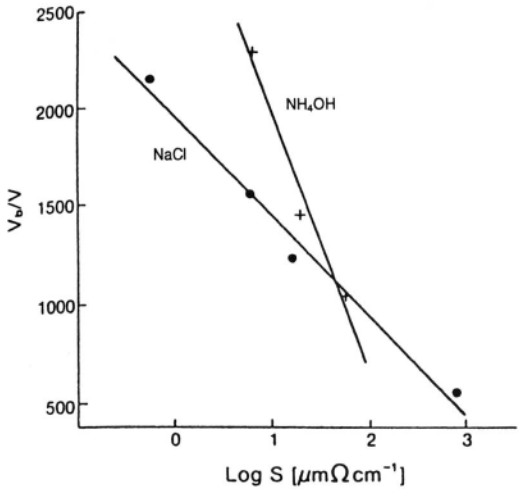

Fig 2.72. The dependence of the breakdown potential (V_b) on the log of conductivity (log S) of NaCl (•) and of NH_4OH (+) solutions. (Reprinted from M. Szklarczyk, R. Kainthla, and J. O'M. Bockris, *J. Electrochem. Soc.* **136**: 2512,

be able to control, the critical field strength, the exceeding of which would break down the dielectric and waste away the electrical energy stored within it.[45]

There is not yet a consensus as to the mechanism of dielectric breakdown in liquids. Research during the last decades of the twentieth century on the breakdown of liquid dielectrics was funded mainly to investigate dielectric breakdown in oils because transformers use oils as dielectrics and sometimes suffer catastrophic dielectric breakdown accompanied by sparking. Insulating oil then catches on fire and equipment costing millions of dollars is damaged beyond repair. Thus, not much laboratory work aimed at determining the mechanism of dielectric breakdown in water *at a molecular level* exists. For example, work in which all is maintained constant except for a systematic change in the nature of the electrode surfaces seems to be conspicuous by its absence.

The most obvious theory—one still held even today by engineers—is that a sufficiently high electric field existing in *the liquid* will eventually place an electrical force on the solvent dipoles, which will cause the force applied to break the chemical

[45]In the Star Wars program of the early 1990s, giant space-borne lasers were to zap enemy missiles as they left their silos. Their ground-based power was to he held in condensers with water or very dilute solutions as the dielectric. Transfer of electrical energy to the orbiting satellite was to be made by beaming it in the megacycle frequency range.

bond and hence destroy its dielectric properties. Thus, μX is the force on a dipole, where X is the electric field and μ is the dipole moment. If $\mu X > \Delta G^{\circ}_{\text{dissocn}}$ for the liquid ($\Delta G^{\circ}_{\text{dissocn}}$ is the standard free energy of a dissociation reaction), it should break down. The results of calculations along these lines for water show that more than 10^7 V cm^{-1} would be needed and this kind of electric field strength could only be attained at an interface. However, even then, breakdown by electrical *tearing apart* does not merit too much attention any more because it has been known since the 1950s that fields at interfaces between electrodes and solutions are on the order of 10^7 V cm^{-1} (Chapter 6), yet water there retains its chemical stability.

On the other hand, most chemists and physicists who have discussed this phenomenon in the 1980s and 1990s observed that the streamers *come from the electrode* and that light is emitted from the electrode. The interfacial region undoubtedly plays the determinative role in the dielectric breakdown of liquids.

One view has concentrated upon seeing water and dilute solutions thereof as if they were intrinsic semiconductors, i.e., semiconductors in which no impurities have been added to provide foreign atoms that could ionize and provide electrons to increase conductance. Such bodies are known to have three vital regions. In one, the electron

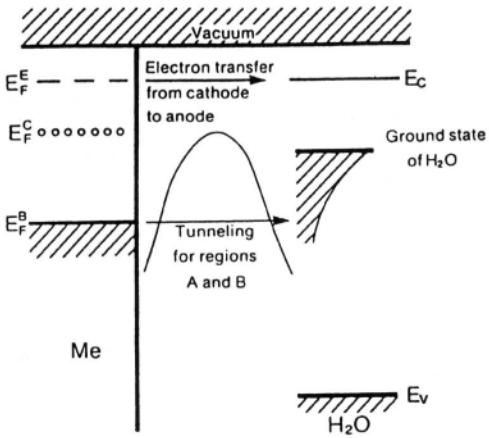

Fig. 2.73. A schematic representation of the Fermi level of the electrons in the electrode and different levels in H_2O. E_F^B, E_F^C, and E_F^E correspond to the position of the Fermi level, E_v and E_c represent the valence and conduction bands of water. The barrier for the electrons at the metal–solution interface is also shown. (Reprinted from M. Szklarczyk, R. Kainthla, and J. O'M. Bockris, *J. Electrochem. Soc.* **136**:2512, 1989.)

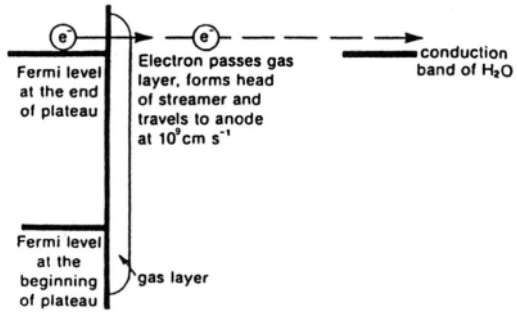

Fig. 2.74. Schematic representation of the transfer of electrons from metal to the conduction band of water before and after the breakdown. The current-potential relation leading to breakdown involves a plateau in which current hardly increases as potential approaches breakdown. (Reprinted from M. Szklarczyk, R. Kainthla, and J. O'M. Bockris, *J. Electrochem. Soc.*, **136**: 2512, 1989.)

energy levels are full and transport by electrons is therefore nonexistent. This *valence band* region is separated from the *conductance band* by what is called an *energy gap*; i.e., between the energy of the band of electron levels that conducts and the band that does not, there is a region in which no electrons exist. However, energetically above the top of the gap in the conduction band, electrons can conduct freely and with a mobility millions of times above that of ions in solution.

A theory put forward by Szklarczyk et al. suggests that the high applied potential (and high resulting field strength in solution) are secondary reflections of the effect they cause on the fundamental Fermi energy level of electrons in this metal. Here are most of the available electrons in a metal. Should it be possible to lift this electron-emitting level in the electrode to sufficiently high levels, the level of the conduction band in water (seen as a semiconductor) would be reached (Fig. 2.73). *This* would be the critical event for breakdown, for if electrons in the metal attained such an energy, they would enter the conduction band of water and behave as electrons in the conduction band of a semiconductor, traveling too rapidly to react chemically with

[46]Distance = (speed)(time). Suppose one allows twice the diameter of water (~ 600 pm) for the distance between the center of a water molecule and that in which an electron could affect a water chemically, and 0.1 of the speed of light for the velocity of passage of a streamer. Then $6 \times 10^{-8} = 3 \times 10^{9}\ \tau$, where τ is the time the water has to recognize an electron; 2×10^{-17}s leaves water unaffected as far as the vibrational and rotational levels are concerned. Even the electrons in water move only about 1/100 of a diameter in such a short time.

water,[46] but forming the head of the streamers and traveling across to the counter electrode. The great outburst of electrons arising from reaching the conduction band in water and flowing through the dielectric (opening of said flood gates, etc.) would precipitate dielectric breakdown (Fig. 2.74).

This section briefly describes an intriguing and practical phenomenon found in water and ionic solutions. A detailed comparison of this new model with experiment would take a disproportionate amount of space. One matter only is mentioned. Does the model stated explain the apparent avalanchelike effect shown in Fig. 2.71? Perhaps. For there are always particles in practical solution, solid particles and some metallic. The phenomena of breakdown are probably determined by many factors. A stream of electrons from the cathodes could cause collisional phenomena in the solution and thus secondary emissions from the particles struck by the electrons, which would then cause many more electron–particle collisions and eventually an avalanche of electrons.

2.22. ELECTROSTRICTION

Ions exert electrical forces on solvent molecules in their vicinity. Because pressure is defined as force per unit area, this means that ions exert a pressure on the solvent and/or other nearby ions. As shown below, this pressure is very high (it may exceed 10^9 Pa) compared with pressures normally encountered in the laboratory.[47]

Phenomena connected with this large pressure are referred to under the title of *electrostriction.* Molecules and ions are squeezed and decrease in size. Electrostriction is the reason that the partial molar volume of ions may become negative, for the volume-decreasing effect of adding them to a system can be greater than the volume increase caused by the addition of the ions themselves.

Effects of this kind are shown in Fig. 2.75. However, electrostriction has its limits. As seen in Fig. 2.75, the value of the compressibility itself is reduced as the electric field (and hence the local pressure) increases. Some details of this are worked out in the next section.

2.22.1. Electrostrictive Pressure near an Ion in Solution

The molar volume of water in the natural state is $18\ \text{cm}^3\ \text{mol}^{-1}$ but if water molecules are close-packed in the liquid state, this volume would become only $12\ \text{cm}^3\ \text{mol}^{-1}$, a reduction of 33%. Thus, the volume available for the effects of electrical constriction by ions on water molecules is as much as $6\ \text{cm}^3\ \text{mol}^{-1}$.

It is easy to calculate a typical pressure exerted by an ion on a water molecule in the first hydration shell. Thus, the energy of interaction of an ion of radius r_i on a water molecule of radius r_w is

[47]When a gas is compressed, the particles come into contact at pressures of a few thousand atmospheres. It is impractical to deal with gases at substantially higher pressures.

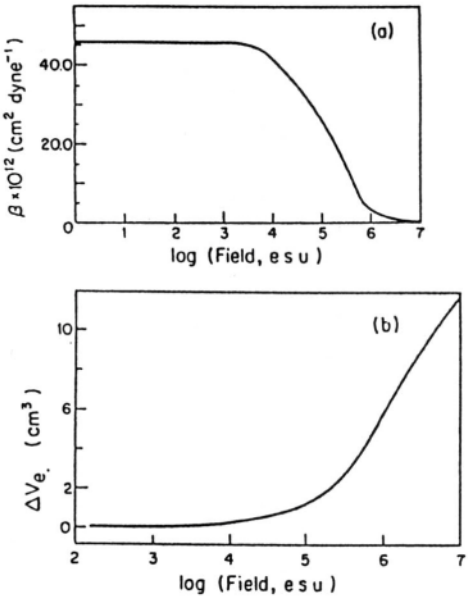

Fig. 2.75. (a) Local compressibility β of water as a function of log(field) near an ion. (b) Electrostriction, ΔV, in water as a function of log(field) near an ion. (Reprinted from B. E. Conway, *Ionic Hydration in Chemistry and Biophysics*, Elsevier, New York, 1981.)

$$U_r = \frac{e_0 \mu \cos \theta_r}{\varepsilon_r r^2} \tag{2.160}$$

Now,

$$F_r \, dr = - dU_r \tag{2.161}$$

where F_r is the force of the ion on the water molecule at a distance r from the ion.

Therefore,

$$F_r = \frac{2e_0 \mu \cos \theta_r}{\varepsilon_r r^3} \tag{2.162}$$

The force calculated here is upon a water molecule in the hydration shell. If one takes the cross section of the water as r_w^2, the pressure (pressure = force/unit

area) at $r = (r_i + r_w)$ with $r_i = 200$ pm, $r_w = 138$ pm, $\mu_w = 1.8$ D, $\varepsilon_r = 6$, and $\theta_r = 0$ is $P \simeq 10^{10}$ Pa.

2.22.2. Maximum Electrostrictive Decrease in the Volume of Water in the First Hydration Shell

The definition of compressibility is

$$\beta = -\frac{1}{V}\left(\frac{\partial V}{\partial P}\right)_T \tag{2.163}$$

Then,[48]

$$\beta\, dP = -\frac{dV}{V} \tag{2.164}$$

and after integration,

$$V_P = V^0 \exp(-\beta P) \tag{2.165}$$

Although β is known to decrease with increase of pressure, it is of interest to make a first approximation by taking β_{water} is constant ($\beta_{P^0} = 4.56 \times 10^{-11}$ Pa^{-1})up to pressures on the order of 10^{10} Pa. Then, for $V^0 = 18$ cm^3 mol^{-1}, Eq. (2.165) becomes

$$V_P = 18 \exp(-4.56 \times 10^{-11} \times 10^{10}) = 11.5 \text{ cm}^3 \text{ mol}^{-1} \tag{2.166}$$

However, water cannot be compressed below the volume of the close-packed structure, 12 cm^3 mol^{-1}. Hence, when the compressibility is taken as pressure independent, the calculated effect of pressure becomes overestimated. What, then, is the relation of β to P?

2.22.3. Dependence of Compressibility on Pressure

It is known empirically that for water

$$\left(\frac{1}{\beta}\right)_p - \left(\frac{1}{\beta}\right)_{p0} = 7.5P \text{ (atm)} \tag{2.167}$$

Hence, at $P = 10^{10}$ Pa, $\beta = 1 \times 10^{-6}$ atm^{-1} $= 1 \times 10^{-11}$ Pa^{-1}. It can be seen that $\beta_P/\beta_{P^0} = 0.22$, a 22% decrease in β compared with that at the standard condition of 10^5 Pa.

---

[48] A pressure of 10^5 Pa = 1 bar $\simeq$ 1 atm is the standard pressure for reporting data, and it is denoted by a superscript null after the variable, e.g., V^0.

TABLE 2.28
Calculated Electrostriction, ΔV_e ($cm^3\ mol^{-1}$), of Water as a Function of Field (Intermediate Fields)

ΔV_e ($cm^3\ mol^{-1}$)	E (esu)[a]	ΔV_e ($cm^3\ mol^{-1}$)	E (esu)[a]
0	0	0.995	6.01×10^4
5×10^{-4}	4×10^2	1.36	1.09×10^5
0.010	2×10^3	1.82	1.82×10^5
0.030	3×10^3	2.36	2.70×10^5
0.085	5.51×10^3	3.17	4.06×10^5
0.201	9.51×10^3	5.08	8.16×10^5
0.536	2.31×10^4	5.71	1.00×10^6

Source: Reprinted from B. E. Conway, *Ionic Hydration in Chemistry and Biophysics*, Elsevier, New York, 1981.
[a] 1 esu = 3.33×10^{-10} coulombs.

This decrease in compressibility with increase in pressure explains the overlarge decrease in volume (44%) due to electrostriction calculated earlier, assuming β to be independent of pressure. It also supports Passynski's approximation $(\beta)_{\text{hydn shell}} = 0$.

In Fig. 2.75 the decrease of β is shown as a function of log X, where X is the electric field in the hydration shell. For an ion of radius 100 pm, this is[49]

$$X = k' \frac{e_0}{\varepsilon r^2} = k' \frac{1.6 \times 10^{-19}}{6(10^{-10})^2} = 2.40 \times 10^{10}\ \text{N C}^{-1} = 2.40 \times 10^{10}\ \text{Vm}^{-1} \qquad (2.168)$$

If one compares this with the Conway relation of local pressure to field, one sees that this field is equivalent in electrostrictional pressure to about 4×10^9 Pa, at which (see above) the compressibility is about 22% of the value at the standard pressure.

Thus in Fig. 2.75(a), the decrease of the molecular volume of water in the hydration sheath of an ion, the radius of which is 100 pm, is about 2 $cm^3\ mol^{-1}$, or about 11% (the first approximation was 44%).

For instance,

at $P = 10^{10}$ Pa, $\beta = 10^{-11}\ \text{Pa}^{-1}$, and from Eq. (2.165),

[49] The Système International of electrical units includes most of the common electrical units, such as volt (V), ampere (A), ohm (Ω), watt (W), and coulomb (C). In this system, Coulomb's law reads

$$F = k' \frac{|q_1 q_2|}{r^2}$$

where $k' = 1/4\pi\varepsilon_0 \sim 9.0 \times 10^9\ \text{N m}^2\ \text{C}^{-2}$. Useful conversions to remember are 1 J = 1 N m and 1 J/C = 1 V, In the cgs system (in which the basic units are the centimeter, gram, and second), the constant k' is defined to be unity, without unit. In this system the unit of electric charge is the *statctmlomb* or esu (electrostatic unit), which is still used in many scientific publications. The conversion factor is, to four significant figures. 1 C = 2.998×10^9 esu.

$$\Delta V = 18[\exp(-10^{-11} \times 10^{10}) - 1] = -1.71 \text{ cm}^3 \quad (2.169)$$

Hence, the compression in the first layer of water molecules around an Na^+ ion would be about (1.71/18) or 10% of the average volume of water in the bulk.

2.22.4. Volume Change and Where It Occurs In Electrostriction

Calculation shows that most of the electrostrictional volume change due to the electrical pressure exerted by an ion in the surrounding solvent arises in the first shell of solvent around it. The calculated volume changes for typical fields are shown in Table 2.28.

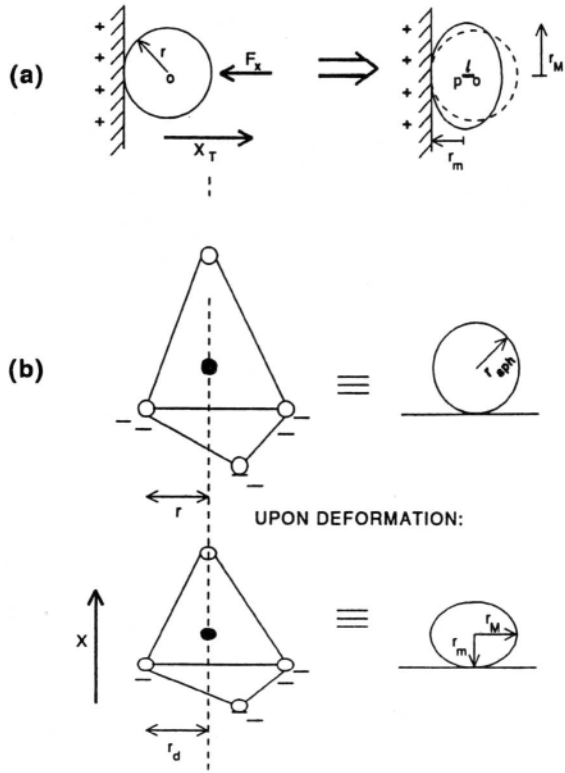

Fig. 2.76. (a) Deformation of the adsorbed ions due to the electric field at the metal–solution interphase. (b) Schematic representation of the bisulfate ion and its equivalent spherical structure before and after its deformation at the interphase. (Reprinted from J. O'M. Bockris, Maria Gamboa-Aldeco, and M. Szklarczyk, *J. Electroanalyt. Chem.* **339:** 335, 1992.)

2.22.5. Electrostriction in Other Systems

This section concentrates on the electrostrictional volume contraction of water molecules in the hydration shell. However, electrostriction is a general phenomenon and whenever there are electric fields on the order of $10^9 - 10^{10}\ V\ m^{-1}$, the compression of ions and molecules is likely to be significant (although less so than occurs by using the compressibility figures usually given in books because these usually neglect the decrease of β with increase of pressure). Bockris and Gamboa have calculated the degree of compression of SO_4^{2-} and Cl^- ions near interfaces. The spherical shape is lost and the ions become lenslike in shape (Fig. 2.76).

Electrostriction in solids is important as the origin of piezoelectric effects. Von Sterkenberg has measured the electrostrictive coefficients in alkaline (earth) fluorides and found electrostriction there to be anisotropic.

Further Reading

Seminal

1. T. J. Webb, "Field and Pressure Near an Ion," *J. Am. Chem. Soc.* **48**: 2589 (1926).
2. H. S. Frank, "Theory of Electrostriction," *J. Chem. Phys.* **23**: 2033 (1955).
3. J. Padova, "Pressure Effects in Ionic Solutions," *J. Chem. Phys.* **39**: 1552 (1963).
4. J. E. Desnoyers, R. E. Verrall, and B. E. Conway, "Electrostriction in Electrolytes," *J. Chem. Phys.* **43**: 243 (1965).

Papers

1. S. W. P. von Sterkenberg, *J. Phys. Appl. Chem.* **17**: 69 (1982).
2. J. L. Ord, *J. Electrochem. Soc.* **138**: 2934 (1991).
3. J. O'M. Bockris, M. Gamboa-Aldeco, and M. Szklarczyk, *J. Electroanal. Chem.* **339**: 355 (1992).
4. S. W. P. von Sterkenberg and Th. Kwaitaal, *J. Appl. Phys.* **25**: 843 (1992).
5. M. Szklarzcyck, in *Modern Aspects of Electrochemistry*, Vol. 25, Ed. J. O'M. Bockris, B. E. Conway, and R. H. White, Plenum, New York (1993).
6. G. Kloos, *J. Appl. Phys.* **28**: 1680 (1995).
7. W. L. Marshall, *J. Solution Chem.* **22**: 539 (1993).
8. T. M. Letcher, J. J. Paul, and R. L. Kay, *J. Solution Chem.* **20**: 1001 (1991).

2.23. HYDRATION OF POLYIONS

2.23.1. Introduction

Most of the ion-exchange resins consist of polyions. A typical one is also the most well known: Nafion, the structure of which is shown in Fig. 2.77; the figure also shows the structure of some proteins (these are often polyelectrolytes).

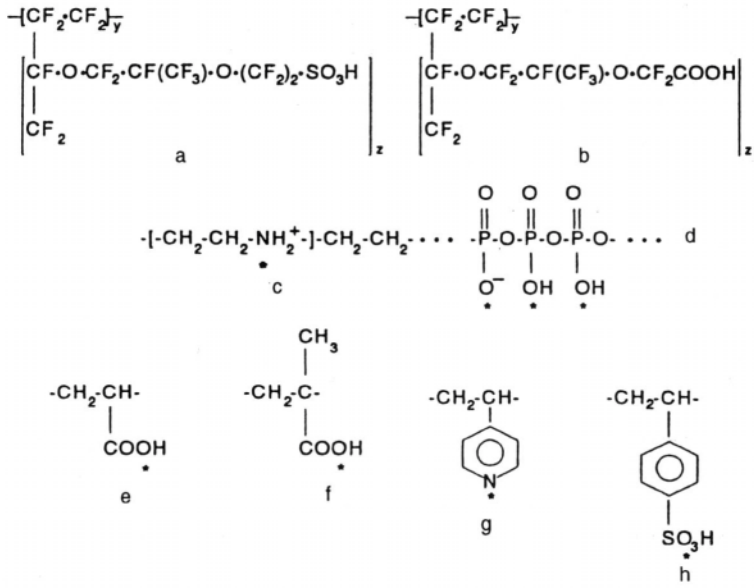

Fig. 2.77. Ion-exchange resins. a = nafion; b = the Asahi structure similar to nation's; c = polyimines; d = polyphosphates; e = polyacrylic acid; f = polymethacrylic acid; g = polyvinylpyridine; h = polysterene sulphonic acid.

In all these structures the interaction of the solvent with the polyelectrolyte is critical for its stability (*cf.* Fig. 2.4). The ion concerned is usually nonspherical and a more typical configuration is cylindrical, as with the linear polyphosphates.

Thus, the ionizing group in many of these materials is in the side chain, as with polyacrylic acid [Fig. 2.77(e)]. Correspondingly, in the linear polyions there are structures of the kind shown in Fig. 2.77(c) and (d).

2.23.2. Volume of Individual Polyions

To obtain the partial molar volume of a series of polyvinyl acid salts containing a cation of tetraalkylammonium, one plots the volume V of the total electrolyte against $1/V_{cation}$ and obtains the partial molar volume by extrapolating the volume of the anion. Such volumes are given in Table 2.29.

2.23.3. Hydration of Cross-Linked Polymers (e.g., Polystyrene Sulfonate)

It is possible to study step-by-step hydration of biomolecules as was first done by Gluckauf. The hydration is localized and connected to ionic binding. Thus, Gregor et al. found that the order of adsorption onto polystyrene was $H^+ > Li^+ > Na^+ > K^+$.

TABLE 2.29

Individual Partial Molar Volumes of Macroions of Weak Polyelectrolytes at 298 K[a]

Weak polyelectrolyte[b] (α)	$\bar{V}_p^0$	V_I	V_{st}	V_e
KPMA (0.95)	43.5*	81.6	−9.1	−29.0
(0.75)	46.6*			−25.9
(0.6)	51.3*			−21.2
(0.4)	60.0*			−12.5
PEI (HCl) (0.8)	29.1	54.7	−21.5	−4.1
TP (HCl) (0.8)	24.9	54.0	−20.3	−8.8
TT (HCl) (0.8)	24.9	53.3	−19.6	−8.8
DT (HCl) (0.8)	24.5	52.0	−18.4	−9.1
ED (HCl) (0.8)	20.3	50.6	−19.2	−11.1

Source: Reprinted from B. E. Conway, *Ionic Hydration in Chemistry and Biophysics*, Elsevier, New York, 1981.

[a]Units are cm^3 monomoles^{-1}. $\bar{V}_p^0$, partial molar volume of the polyion; V_I, ionic volume; V_{st}, volume due to change in the volume of the surrounding water; and V_e, volume due to the electrostriction of the surrounding water.

[b]KPMA, potassium polymethacrylate; PEI, polyethyleneimines; TP, tetraethylene pentamine; TT, triethylene tetramine; DT, diethylene triamine; ED, ethylene diamine.

2.23.4. Effect of Macroions on the Solvent

Macroions, such as proteins, have an effect on the self-diffusion of a solvent. Thus, the presence of the macroion obstructs the solvent's movement. On the other hand, it binds the solvent and substantial fractions of it may be trapped within the molecule.

The fluidity of the solvent is changed because of the structure-breaking effects caused by the presence of macroions. Self-diffusion data on water in the presence of proteins allows one to measure their hydration. This is usually measured in water per gram of anhydrous protein.

2.24. HYDRATION IN BIOPHYSICS

Hydration of biopolymers is a mechanism for stabilizing these materials (Fig. 2.78). When proteins are completely dry, they tend to decompose. One way of evaluating hydration in polyions is to measure the dielectric constant of a solution containing a dissolved protein as a function of concentration at radio frequency. The dielectric constant falls with increase in concentration and the water per polyion can be calculated by assuming that water bound to the protein no longer makes any contribution to the dielectric constant. Thus, Buchanan calculated the irrotationally bound water from such experiments. Some of this water is hidden in cavities within the structure of the protein molecule.

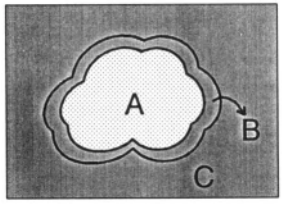

Fig. 2.78. A schematic drawing of protein and water. The regions of the protein and the excluded volume of it are represented as A and A + B, respectively. The regions of solute (low dielectric media) and solvent (high dielectric media) are represented as A and B + C, respectively. (Reprinted from M. Irisa, T. Takahashi, F. Hirata, and T. Yanagida, *J. Mol. Liquids* **65**: 381, 1995.)

As with normal electrolytes (Section 2.12.1), the dielectric constant depends linearly on concentration:

$$\varepsilon = \varepsilon_0(1 - \delta c) \tag{2.170}$$

where:

$$\delta = \frac{\beta}{100}\left[\tilde{V}(\varepsilon_{H_2O} - \varepsilon^{\infty}_{prot}) + N_{w,irr}(\varepsilon_{H_2O} - \varepsilon^{\infty}_{w})\right] \tag{2.171}$$

Here c is the concentration in gram percent, $\tilde{V}$ is the partial specific volume of the protein, $\varepsilon^{\infty}_{prot}$ is the high-frequency value of the dielectric constant of the protein (= 2) or of water (=6) and ε^{∞}_{w} is that. The unknown here is $N_{w,irr}$, the number of irrotationally bound waters and this can then be calculated. It is usual to assume that the water is adjacent to charged groups.

2.24.1. A Model for Hydration and Diffusion of Polyions

For polyelectrolytes containing discrete charged groups, the usual configuration is cylindrical. Thus, the field midway along the chain is described by Conway (1982) as

$$X = \sum_{0}^{n} \frac{ze_0 r}{[r^2 + (2n-1)^2\lambda^2]^{3/2}\varepsilon} \tag{2.172}$$

TABLE 2.30

Free-Energy Changes for the Introduction of a Water Molecule into Pure Water and into Two Cavities in Sulfate-Binding Protein (SBP)[a]

Energy component	Theoretical ΔA for Pure Water	Experimental ΔG for Pure Water	Theoretical ΔA for Hydrated Cavity in SBP	Theoretical ΔA for "Dry" Cavity in SBP
Electrostatic	-8.4 ± 0.3	-8.7	-11.9 ± 0.9	-1.9 ± 0.9
Lennard-Jones	2.0 ± 0.1	2.4	-4.5 ± 0.0	-4.3 ± 0.2
Total	-6.4 ± 0.4	-6.3	-16.4 ± 0.9	-6.2 ± 1.1

[a]Units are kcal/mol.

As expected, ε decreases near the ions concerned. However, the structure of water is disturbed by the field from such charged bodies only 500–600 pm out into the solvent.

2.24.2. Molecular Dynamics Approach to Protein Hydration

Internal water plays a role in the structure of proteins. It is difficult to detect and measure these waters by means of X-rays and therefore statistical thermodynamic calculations may be helpful.

An example of this kind of calculation, due to Wade et al., is the computation of the hydration of two internal cavities in a sulfate-binding protein. The results are given in Table 2.30. The main difference between having a "dry" cavity and having a wet one is the hydration bond energy.

2.24.3. Protein Dynamics as a Function of Hydration

Proteins in the dry state are "frozen." They only open up and start moving if some water is added, as in nature. It turns out that protein movements in, e.g., lysozyme are activated only when there is 0.15 g of water per gram of protein, a good example of the effect of hydration on living processes. However, it is difficult to examine protein dynamics in solution because to make a satisfactory interpretation of the observations, one would have first to do the corresponding spectroscopy in the dry state; this is difficult because of the "frozen" state referred to and a tendency to decompose.

To avoid this difficulty, one technique is to use *reverse micelles.* These materials can host a protein in a small water pool. Reverse micelles are spherical aggregates formed by dissolving amphiphiles in organic solvents. The polar head of the amphiphilic molecule is in the interior of the aggregate and the hydrophobic tail is in the organic phase. The micellar suspension is transparent, and controlled amounts of water can be added.

TABLE 2.31
Results of Protein Hydration

Protein[a]	Concentration Range (mg/ml)	N_{total} (liters/protein)
Cc(A)	15–65	290 ± 30
Mb(A)	14–56	350 ± 40
Ov(dw)	12–49	870 ± 100
Ov(A)	14–60	860 ± 95
Ov(M)	15–58	840 ± 95
BSA(dw)	17–68	1300 ± 140
BSA(A)	11–43	1260 ± 150
BSA(M)	14–61	1410 ± 160
Hb(A)	17–66	1260 ± 140

Source: Reprinted from M. Suzuki, J. Shigematsu, and T. Kodama, *J. Phys. Chem.* **100**: 7282, 1996.
[a]Cc, cytochrome; Mb, myoglobin; Ov, ovalbumin; BSA, bovine serum albumin; Hb, hemoglobin; dw, distilled water; A, buffer A which contained 10 mM KCl and 10 mM sodium borate (pH = 8.0). M, buffer M, which contains 20 mM KCl, 5 mM $MgCl_2$ and 10 mM sodium borate (pH = 7.5).

One can then use the time course of the fluorescence decay. The change in frequency of the emitted light compared with that of the incident light contains information from which the rotational and internal dynamics can be studied.

The rotational frequency in lysozomes decreases with increase of water. This type of study throws some light on protein–micellar interactions and how they are affected by hydration.

X-ray and neutron diffraction measurements on polyion hydration give the number of water molecules involved per repeat group in the structures. About one water molecule per repeat group is the result for polymethyl methacrylate. The results of hydration for a variety of proteins are given in Table 2.31.

2.24.4. Dielectric Behavior of DNA

The rotation of large molecules in solution together with their hydration is the basis of many of the properties of solutions containing polyions. One has to ask questions, however, about the decrement of the dielectric constant in the case of linear polyelectrolytes, which include DNA. Substances such as this exhibit dielectric decrements as expected but it is difficult to account for their magnitude in terms of hydration. Thus, there might be a rotation but this cannot be about the long axis because in such a case δ (Section 2.24) should increase when the molecules are oriented perpendicularly to the electric field and this is not found to be the case.

Could this be behavior in terms of the Maxwell–Wagner dispersion,[50] which would arise through conductivity in the double layer near the polyanion. In support of this, the dielectric constant falls as the frequency increases (Fig. 2.79).

[50]This is the variation of the resistance or capacitance with frequency.

Now, ice has a dielectric dispersion over the range 10^2–10^4 Hz, and water over the range 10 Hz–10^2 Hz. Thus, the high rate of fall of dielectric constant with increased concentration for linear polyelectrolytes may come from the icelike structure of water in their vicinity.

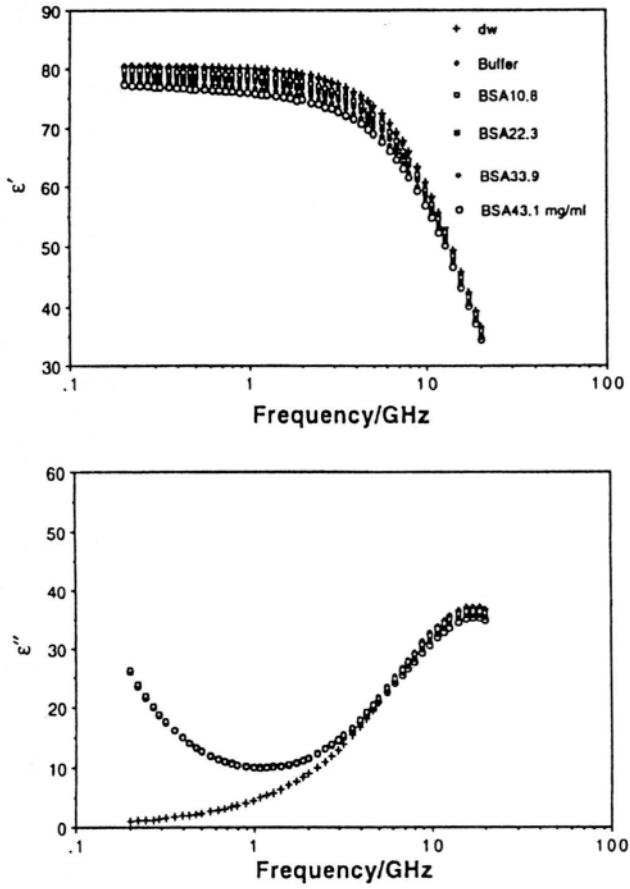

Fig. 2.79. Dielectric spectra of solutions of the protein bovine serum albumin (BSA) at 20.0 ± 0.01 °C. dw, buffer, and the numbers after BSA indicate distilled water, buffer A, and BSA concentrations in mg/ml in buffer A, respectively. (Reprinted from M. Suzuki, J. Shigematsu, and T. Kodama, *J. Phys. Chem.* **100**: 7279, 1996.)

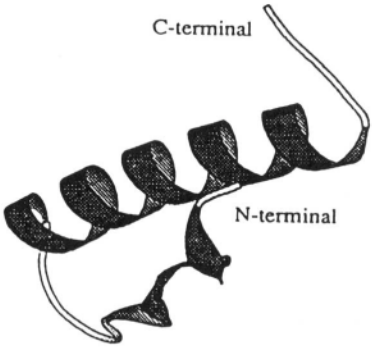

Fig. 2.80. A secondary structure of avian pancreatic polypeptide. (Reprinted from M. Irisa, T. Takahashi, F. Hirata, and T. Yanagida, *J. Mol. Liquids* **65**: 381, 1995.)

2.24.5. Solvation Effects and the α-Helix–Coil Transition

In many biological materials in solution, there is an equilibrium between a coil-like film and a helix[51] (Fig. 2.80). The position of the equilibrium between coil and helix-like forms in biomolecules in solution is determined by hydration. For example, in the solvent $Cl–CH_2–CH_2OH$, light scattering studies show that poly-γ-benzyl glutamate is found to consist of random coils, but in other solvents it forms a helix.

The form and structure of proteins demands hydration. Doty, Imahor, and Klemperer found that a typical structure was 15% α-helix in 0.14 M NaCl, but at pH 4 it changed to 50% α-helix. The change is a function of hydrogen bonding. The main difference between having a "dry" cavity and a wet one is the hydrogen bond energy.

2.25. WATER IN BIOLOGICAL SYSTEMS

2.25.1. Does Water in Biological Systems Have a Different Structure from Water *in Vitro*?

It has been suggested that water in biological systems has a different structure from that of free water. Thus, Szent-Györgyi (the discoverer of vitamin C) was the first to suggest that an icelike structure surrounded proteins and other biomolecules. Cope examined cell hydration and asked whether water is affected by *conformational*

---

[51] A helix is an elongated form of a coil.

[52] *Conformational* refers to spatial arrangements of molecules that can be obtained by rotating groups around bonds.

changes[52] in the protein structure. Much of the water present in a biological cell would be associated with the cell surface and hence have an oriented or rigid structure. Thus, the interior of biological cells contains an interconnecting network of cellular organelles: there is little space inside for free water.

Water in biological systems does indeed have a structure different from that of the bulk, as it does at all interfaces, and the appropriate way to look at the alleged difference in its structure is to realize that there is a large surface-to-volume ratio in cell-like structures so that the fraction of water associated with surfaces is large, and; by definition, under electric fields that are characteristic of the surface of double layers at surface–solution interfaces. Hence, the icelike structure that Szent-Györgyi saw as characteristic of biological systems would be a description of any near-surface water and becomes the norm for biological cell water because most water is near a surface and hence has abnormal structure (Ling and Drost-Hansen, 1975).

2.25.2. Spectroscopic Studies of Hydration of Biological Systems

Zundel reports on the hydration of thin polyelectrolyte ion-exchange membranes subject to progressive increases in water sorption. Spectroscopic observations of these systems reflect the hydration of polyion charge centers in the membranes but in the presence of associated counterions, H_3O^+, which in turn are progressively hydrated. Zundel worked with polysulfonates and found the spectra of unhydrated polymer salts: the cation is attached unsymmetrically to the SO_3^- groups. This mode of attachment leads to a loss of degeneracy[53] in the antisymmetric vibrations.

The fact that this is so allows one to follow the hydration of cation–polyanion association. This also affects the assignment of changes of band frequency in the water molecule as it dissociates with the counterion groups.

In the region of 2000–4000 cm^{-1}, it is possible to obtain Spectroscopic results that reflect the bound water at polyions. These occur at 3000–3700 cm^{-1} in H_2O and 2200–2750 cm^{-1} for D_2O. As the radius of the bound counteranion and polystyrene sulfonate decreases, the OH stretching vibration of the hydration water molecule increases (e.g., from Ba^{2+} to Be^{2+} and from La^{3+} to Sc^{3+}).

These Spectroscopic results are consistent with corresponding thermodynamic results obtained by Gluckauf and Kitt. They found that the greatest values of ΔH and ΔS for sorption occurred during the first water molecule aggregation per ion pair and decreased for subsequent ones.

2.25.3. Molecular Dynamic Simulations of Biowater

So far there have been few in-depth MD simulations of water at the interfaces of cells. As indicated earlier, the results of general studies and Spectroscopic data suggest that much of the water in biological cells is affected by the interface. The fact that the

[53]Degeneracy = more than one state having the same energy.

surface-to-volume ratio is so large in biological cells means that most of the water there is affected by the surface forces. However, this is *not* supported by the MD calculations of Ahlstrom et al., who made an MD simulation of the Ca^{2+}-binding protein, parvalbumin. These workers found, contrary to the expectation arising from knowledge of the high surface-to-volume ratio, that relatively few ions were immobilized (Fig. 2.81) on the surface of the protein. However, they did conclude that the dipole of the waters in contact with the protein was indeed oriented perpendicularly to the protein surface. These findings contradict NMR data that indicate surface waters as having a longer relaxation time than in the bulk. The potential functions of the MD simulation may have been ill chosen. Electron density distributions of water in cells show order out to 1500 pm.

2.26. SOME DIRECTIONS OF FUTURE RESEARCH IN ION–SOLVENT INTERACTIONS

Traditionally, the interaction between particles in chemistry has been based upon empirical laws, principally on Coulomb's law. This law is also the basis of the attractive part of the potential energy used in the Schrödinger equation, but the resultant

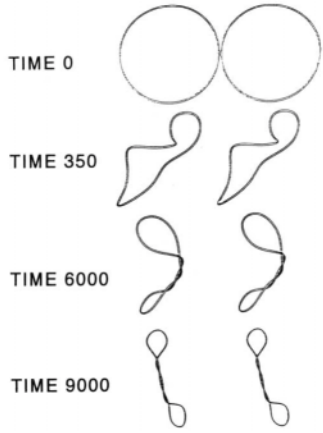

Fig. 2.81. Snapshots from a stochastic dynamics simulation of DNA supercoiling. (Reprinted from P. Ahlstrom, O. Teleman, and B. Jocsom, *J. Am. Chem. Soc.* **110**: 4198, 1988.)

energies of interaction obtained by solving it are then quantized. Such an approach was begun for ion–water interactions by Clementi in the 1970s.

A quantum mechanical approach to ion–water interactions has the up side that it is the kind of development one might think of as inevitable. On the other hand, there is a fundamental difficulty that attends all quantum mechanical approaches to reactions in chemistry. It is that they concern potential energy and do not account for the entropic aspects of the situation. The importance of the latter (*cf.* the basic thermodynamic equation $\Delta G = \Delta H - T\Delta S$) depends on temperature, so that at $T = 0$, the change in entropy in a reaction, ΔS, has no effect. However, in calculations of solvation at ordinary temperatures, the increase in order brought about by the effect of the ion on the water molecules is an essential feature of the situation. Thus, a quantum mechanical approach to solvation can provide information on the energy of individual ion–water interactions (clusters in the gas phase have also been calculated), but one has to ask whether it is relevant to solution chemistry.

Another problem in the quantal approach is that ions in solution are not stationary as pictured in the quantum mechanical calculations. Depending on the time scale considered, they can be seen as darting about or shuffling around. At any rate, they move and therefore the reorientation time of the water when an ion approaches is of vital concern and affects what is a solvation number (waters moving with the ion) and what is a coordination number (Fig. 2.23). However, the Clementi calculations concerned stationary models and cannot have much to do with dynamic solvation numbers.

Finally, Conway points out that the values of the energies obtained by solving the Schrodinger equation and by electrostatics are about the same. But this should be! The quantum mechanical calculations do not infer that the electrostatic ones (Section 2.15.11) are wrong. Indeed, the Schrödinger equations solved by Clementi involved the same energy that was used in the electrostatic method. It is a matter of whether the sophistication of quantization gives increasing insight into the behavior of a real system in solution. The answer in the 1990s is: not yet.

However, science evolves! More will be seen of the quantum mechanical approach to solvation and in particular in nonaqueous solutions when there is more chance of interactions involving overlap of the orbitals of transition-metal ions and those of organic solvent molecules. Covalent bond formation enters little into the aqueous calculations because the bonding orbitals in water are taken up in the bonds to hydrogen. With organic solvents, the quantum mechanical approach to bonding may be essential.

The trend pointing to the future is the molecular dynamics technique, and treatments of this kind were discussed in Section 2.17. The leaders here are Heinzinger and Palinkas (in the 1990's), and the major thing to note is that the technique provides needed information on the *number* of waters in the first shell. The MD method does this by calculating the distribution function (Section 2.17.2) and may also provide information on a second layer, lifetimes of the solvent molecules in the hydration sheath, and so on.

2.27. OVERVIEW OF IONIC SOLVATION AND ITS FUNCTIONS

2.27.1. Hydration of Simple Cations and Anions

The first thing that was dealt with in this chapter was the fundamental question of how things dissolve. Materials have stability in the solid lattice and therefore in the solution there must be energies of interaction that compensate for the lattice energies and thus make it comfortable for the ion to move into the solution. This energy of interaction of solvent and ion is called the *solvation energy*. Solvation and the corresponding water-related hydration are fields having a great breadth of application and indeed one can even see a relevance to environmental problems such as acid rain because the pH of natural waters depends on the stabilization of certain ions in solution, and this depends primarily upon their solvation energies.

It is useful to divide the methods of investigating hydration into four groups. First of all, there are the many methods in which one looks at the ionic solution in the equilibrium state; for example, one can study its compressibility or one can study heats and entropies of hydration and fit the values to various model systems.

Another approach involves measuring the transport of the ion concerned under an applied electric field, its mobility. This approach has a unique aspect: it provides the individual properties of ions directly so long as they are in dilute solution.

Spectra of all kinds (infrared, Raman, nuclear magnetic resonance, neutron diffraction) have been applied to electrolytic solutions for a long time, and the contrast between the indications from such measurements (which involve the grave disadvantage of having to be carried out at high concentrations) and those of other (concordant) methods of investigation (usually carried out in dilute solutions to diminish the effects of ion–ion interactions) in measuring solvation numbers is troubling. It seems likely that the spectroscopic results report the much smaller values obtained in solvation studies at higher ionic concentrations (i.e., lower water concentration). The thermodynamic methods (e.g., partial molar volumes and the Debye vibrational potential) give much higher results than the spectroscopic methods because they measure the situation at high concentrations of water (i.e., low ionic concentrations) or dilute solutions. However, increasingly neutron diffraction and MD methods are being able to provide information on the *time* spent by water molecules in the first and second layer near an ion. By comparing these times with those known for the time an ion spends between its movements in solution, it is becoming increasingly possible to use spectroscopic methods (particularly the recent neutron diffraction methods) to make a distinction between coordination numbers and numbers of waters which travel with the ion, the hydration number.

Finally, there is the theoretical method of approaching ionic solvation including the molecular dynamics simulations. These have become increasingly used because they are cheap and quick. However, MD methods use two-body interaction equations and the parameters used here need experimental data to act as a guide for the determination of parameters that fit.

Most of the data that one gets from the experimental point of view of hydration concerns the net effect of all the ions in the electrolytes, and it is necessary to pull out the quantities corresponding to each ion separately. This is tricky but possible. For example, one can couple a certain anion with a series of cations of increasing size and extrapolate a plot in such a manner that the effect of the cation becomes negligible and that of the anion is isolated. Then, the individual value for that anion can be used to obtain individual values for any cations that can form salts with this anion.

Apart from neutron diffraction, what other method distinguishes between the static or equilibrium coordination number and the dynamic solvation number, the number of solvent molecules that travel with an ion when it moves? One method is to obtain the sum of the solvation numbers for both cation and anion by using a compressibility approach, assuming that the compressibility of the primary solvation shell is small or negligible, then using the vibration potential approach of Debye to obtain the difference in mass of the two solvated ions. From these two measurements it is possible to get the individual ionic solvation numbers with some degree of reliability.

Another approach that can help in getting hydration numbers is the study of dielectric constants—both the static dielectric constants and the dielectric constant as it depends on frequency. Such measurements give a large amount of information about the surrounds of the ion but a good deal more has to be done before the theoretical interpretation can bear the weight of clear structural conclusions. Density, mobility, and entropy measurements may also be informative.

The material so far has all come from discussions of methods of examining hydration and solvation in solutions. It is now good to turn to a simpler field, the study of which began much later—hydration of the gas phase. It was not until high-pressure mass spectroscopy became available that such studies could be easily made. If we had had these studies 50 years ago, it would have been much easier to interpret the values obtained in solution. Thus, the numbers we get from the unambiguous gas-phase results are close to results for the first shell of water around ions in solution, and knowledge of this, and the energies that go with it, helps us greatly in building models in solution.

The models assume that the energies are entirely electrostatic and go about calculation in terms of ion-dipole forces for the first layer, together with correction for the quadrupole properties of water, and for the extra dipole that the ion induces in the water. There are two more steps. One is to take into account the interaction of the ion with distant water molecules, which we do by means of the Born equation, and then finally we take into account the structure-breaking effects of the ions on the surrounding solvent. The agreement between theory and experiment is good and this applies (though somewhat less well) to the corresponding calculation of the entropies of hydration.

A special case, but one of seminal importance, is the heat of hydration of the proton because so much depends upon it. A rather clever method was set out many years ago by Halliwell and Nyburg and although their approach has been reexamined

many times, the numerical values have not changed by more than one percent. The method involves an application of the known *differences* of quadrupole interactions of ions which have the same size but different signs.

2.27.2. Transition-Metal Ions

Our overview of hydration so far is based upon ions which are simple, mostly those from groups IA and IIA. We haven't yet said anything about the ions with more complex electronic structures, for example, the transition-metal ions, two-valent and three-valent entities. There are many who would expect such ions to have valence-force interactions (orbital bond formation) with water molecules, but in fact they don't. It is possible to interpret their hydration heats in terms of electrostatic interactions with water, but one has to be more sophisticated and no longer regard the ions as simple spheres but take into account the shape and direction of their molecular orbitals and how these affect the electrostatics of the interactions with water molecules.

It turns out that the splitting of electron levels in the ions caused by the water molecules changes the electrostatic interaction of the ions with the waters. This in turn makes the course of a plot of individual hydration of transition-metal ions against the radii of the ions no longer a continuous one, which one would expect from first-approximation electrostatic studies, but takes into account some irregularities that can be quite reasonably accounted for. Now, there is also lurking among the literature on ion hydration in the gas phase the surprising (but clearly explainable) fact that the *second* water molecule sometimes has a larger heat of hydration than the first.

2.27.3. Molecular Dynamics Simulations

The last part of our treatment of the central aspects of the chapter concerned molecular dynamics. We showed the power of molecular dynamics simulations in ionic solutions and what excellent agreement can be obtained between, say, the distribution function of water molecules around an ion calculated from molecular dynamics simulation and that measured by neutron diffraction.

However, there has been in the past some semantic confusion in these calculations. Most of them are about distribution functions. Some of the workers concerned assumed that they were calculating hydration numbers when in fact they were calculating time-averaged coordination numbers. Nevertheless, a few groups have indeed been able to calculate the rate at which water molecules react when an ion is brought near them and the lifetime of the water molecules near the ion as it moves. From this, they have calculated hydration numbers that are in fair agreement with those determined experimentally.

2.27.4. Functions of Hydration

The rest of this chapter has been concerned with phenomena and effects that are connected with hydration. The first one (salting out) concerns the solubility of nonelectrolytes as affected by the addition of ions to the solution. Here two effects are

to be dealt with. The first is salting out—the decrease of solubility that the ions cause. This is easily understood because of course the ions remove quite a lot of the waters from availability to the incoming solute by taking them off into temporary inactivity in the hydration shell so that the organic molecule has less water (per liter of solution) to dissolve in and its solubility is thus decreased. Salting in is a little bit more difficult to understand, especially anomalous salting in, which occurs when the equations for salting out indicate that there should be a decrease in the solubility of a nonelectrolyte upon the addition of ions but in fact there is an increase. It turns out that this is caused by dispersion force interactions by which the ions (large ions such as those of the NR_4^+ series are involved here) attract the organic molecules to themselves and push the water out, thus giving more water for the organic molecules to dissolve in and an increased solubility. Such phenomena provide some basis for an interpretation of hydrophobic effects in hydration.

Electrostriction is the study of the effects of squeezing of ions and molecules by the electrical forces that are exerted upon them by the ions we have been dealing with (Section 2.22). It is only recently that modelers have begun to take into account the shapes formed by these compressed bodies. In fact, they do become lenslike in shape (not spheres) and when this is taken into account, agreement between theory and experiment is improved.

Hydrophobic effects are on a list of special phenomena. They are closely tied to salting in because one of the reasons for hydrophobic effects (water pushing-out effects, one could say) is that the ions of the solute tend to attract each other or other nonelectrolytes present and push the water between them out. Structure breaking in a solution, some part of which rejects water in the rearrangements formed, also gives hydrophobic effects.

Polyelectrolytes occur in ion-exchange membranes and thus their study has great material value. They have a central importance in biology and the study of their electrochemistry, as ions, their natural interactions in solution, etc., are important although we are only able to give a short description of them in a chapter of restricted length.

Finally, the question of the structure of biological water is one of far-reaching importance. Some workers in the last few decades have suggested that water in biological systems is special but our answer is that this special structure is so readily explicable that no mystery exists. Biological cells are sized on the micron scale and contain much solid material. The surface-to-volume ratio inside such cells is very large. Most of the waters in cells are in fact surface waters. In this sense, biological water *is* special but only because it has lost the netted-up properties of bulk water and adopted the individual two-dimensional structure of water at all surfaces.

APPENDIX 2.1. THE BORN EQUATION

In the preceding text, particularly in Section 2.15.11, use is made of Born's equation, a famous classical equation first deduced in 1920. This equation is generally

used to express that part of the free energy of the solvation of ions which arises from interactions outside the first, oriented, layers of dipoles near the ion. Thus, sufficiently near the ion, the structure of the water is fairly definite and can be used to write equations that express simple models close enough to reality to be credible (see Appendices 2.2 and 2.3). A molecular picture is more difficult to sustain outside these first one or two layers. It is argued that there it is better to work in terms of continuum electrostatics and to suppress questions concerned with structure in the solution, etc.

The basic model upon which Born's equation rests involves a mental image of a metallic sphere. It is argued that when such a sphere (at first grounded and charge free) is given an electric charge q, this charging process must be equivalent to some amount of energy.

The reasoning is that when a series of small amounts of charge are brought upon the ion, some work has to be done to put them there because after the first charge arrives, the rest of the charge bits (all positive, say) have to push against the repelling interaction between the positive charges themselves and the positive charge already building up on the metallic sphere.

Now, from electrostatics, the work done, W, when there is a change of charge Δq of a body of potential, ψ, is given by

$$dW = \psi \, \Delta q \tag{A2.1.1}$$

In the case of the conducting sphere upon which charge is building, the potential ψ depends upon the charge and so to avoid conceptual trouble [what ψ to use in Eq. (A2.1.1) as q changes], we take an infinitesimally small change of charge dq and argue that for such very very small changes of charge, ψ will be very very nearly constant.

To find the work W done in a real finite buildup of charge, one has to overcome a problem—that ψ itself depends on the degree of charge—and hence express ψ in terms of q.

It is easy to show that for a conducting sphere, the value of ψ is given by

$$\psi = \frac{q}{r} \tag{A2.1.2}$$

With this (and the assumptions) as background, one may write for the work to build up a charge q on the sphere:

$$W = \int_0^q \frac{q}{r} \, dq = \frac{q^2}{2r} \tag{A2.1.3}$$

Now, solvation energy—and Born's equation is usually proposed as giving at least some part of that—is the difference of free energy of an ion *in vacuo* and that of an ion in solution. If this work of charging which has been calculated above is then

taken as the basis for a change of energy upon the transfer from vacuum to solution, one has ($q_{ion} = z_i e_0$):

$$\text{Energy of charging in vacuum: } (z_i e_0)^2/r_i \tag{A2.1.4}$$

$$\text{Energy of charging in solution: } (z_i e_0)^2/\varepsilon r_i \tag{A2.1.5}$$

where ε is the dielectric constant of the solution.

Hence, the work of charging in solution, $(z_i e_0)^2/2r_i\varepsilon$, minus the work of charging the solution, $(z_i e_0)^2/2r_i$, is argued to be a contribution to the solution energy. Therefore, the corresponding energy change or the so-called *Born term* is

$$\Delta G_{\text{Born}} = \frac{(z_i e_0)^2}{2r_i\varepsilon} - \frac{(z_i e_0)^2}{2r_i} = -\frac{(z_i e_0)^2}{2r_i}\left(1 - \frac{1}{\varepsilon}\right) \tag{A2.1.6}$$

This equation is used in most theories of solvation (Section 2.15.10) as though it represented, not the difference in the energy of charging up a conducting sphere *in vacuo* and then in solution, but the energy of interaction of an ion with a solvent.

There are a number of fundamental difficulties with the Born equation, which is still presented in this text because of the prominent part it plays in most theories (it accounts for around one-third of the hydration energy calculated for simple ions).

1. Behind the idea of the work of charging is an assumption that the charging occurs slowly, so that all parts of the system concerned are arranged in their equilibrium configuration. This is arguable. Any real change of charge on an ion in solution occurs in a time of about 10^{-15} s, so fast, indeed, that atomic motions in molecules (e.g., vibrations) are taken to be stationary in comparison (Franck–Condon principle).

2. The thinking behind the deduction of Born's equation is pre-quantal. In reality, atoms do not charge up by the aggregation of a series of infinitesimally small amounts of charge. They become charged by means of the sudden transfer of one electron. The energy of charging an atom to a positive ion is called the ionization energy and is a known quantity. The energy of charging an atom to be a negative ion is called the electron affinity and is also known. Both these energies differ significantly from the Born energy of charging.

3. Although the Born charging energy differs from either the ionization energy or the electron affinity, its values for simple ions are not unreasonable. However, when one comes to apply Born's concepts to protons and electrons, irrational energies result. For example, the Born energy of a proton in the gas phase is ~1000 times the normal range of chemical energies. The corresponding self-energy for an electron alone is greater than $m_e c^2$!

So, Born's equation remains a controversial part of the theory of solvation although there have been many recent attempts striving to justify it. The difficulty resides in the avoidance of molecular-level arguments and in applying continuum electrostatics, which clearly involves fundamental limitations when it comes to atomic

and subatomic charged bodies. However, there is a greater doubt. What is required in calculations of solvation energy is the ion–solvent interaction energy. Does the Born equation measure the difference of two self-energies, which is not a quantity to be used in solvation calculations at all?

APPENDIX 2.2. INTERACTION BETWEEN AN ION AND A DIPOLE

The problem is to calculate the interaction energy between a dipole and an ion placed at a distance r from the dipole center, the dipole being oriented at an angle θ to the line joining the centers of the ion and dipole (Fig. A2.2.1). (By convention, the direction of the dipole is taken to be the direction from the negative end to the positive end of the dipole.)

The ion–dipole interaction energy U_{I-D} is equal to the charge $z_i e_0$ of the ion times the potential ψ_r due to the dipole at the site P of the ion

$$U_{I-D} = z_i e_0 \psi_r \tag{A2.2.1}$$

Thus, the problem reduces to the calculation of the potential ψ_r due to the dipole. According to the law of superposition of potentials, the potential due to an assembly of charges is the sum of the potentials due to each charge. Thus, the potential due to a dipole is the sum of the potentials $+q/r_1$ and $-q/r_2$ due to the charges $+q$ and $-q$, which constitute the dipole and are located at distances r_1 and r_2 from the point P. Thus,

$$\psi_r = \frac{q}{r_1} - \frac{q}{r_2}$$

$$= q\left(\frac{1}{r_1} - \frac{1}{r_2}\right) \tag{A2.2.2}$$

From Fig. A2.2.2, it is obvious that

$$r_1^2 = Y^2 + (z + d)^2 \tag{A2.2.3}$$

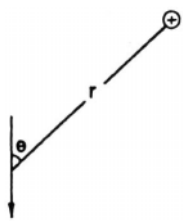

Fig. A2.2.1

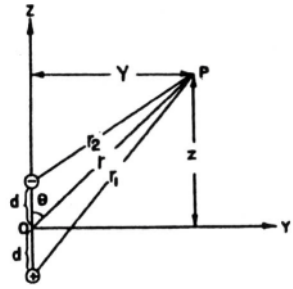

Fig. A2.2.2

and therefore,

$$\frac{1}{r_1} = [Y^2 + (z+d)^2]^{-1/2}$$

$$= [(Y^2 + z^2) + d^2 + 2zd]^{-1/2}$$

$$= (r^2 + d^2 + 2zd)^{-1/2}$$

$$= \frac{1}{r}\left[1 + \left(\frac{d}{r}\right)^2 + \frac{2dz}{r^2}\right]^{-1/2} \qquad \text{(A2.2.4)}$$

At this stage, an important approximation is made, namely, that the distance $2d$ between the charges in the dipole is negligible compared with r. In other words, the approximation is made that

$$1 + \left(\frac{d}{r}\right)^2 + \frac{2dz}{r^2} \approx 1 + \frac{2dz}{r^2} \qquad \text{(A2.2.5)}$$

It is clear that the validity of the approximation decreases, the closer the ion comes toward the dipole, i.e., as r decreases.

Making the above approximation, one has [see Eq. (A2.2.4)]

$$\frac{1}{r_1} \approx \frac{1}{r}\left(1 + \frac{2dz}{r^2}\right)^{-1/2} \qquad \text{(A2.2.6)}$$

which, by the binomial expansion taken to two terms, gives

$$\frac{1}{r_1} = \frac{1}{r}\left(1 - \frac{dz}{r^2}\right) \qquad \text{(A2.2.7)}$$

By similar reasoning,

$$\frac{1}{r_2} = \frac{1}{r}\left(1 + \frac{dz}{r^2}\right) \tag{A2.2.8}$$

By using Eqs. (A2.2.7) and (A2.2.8), Eq. (A2.2.2) becomes

$$\psi_r = -\frac{2dq}{r^2}\frac{z}{r} \tag{A2.2.9}$$

Since $z/r = \cos\theta$ and $2dq$ is the dipole moment μ,

$$\psi_r = -\frac{\mu \cos\theta}{r^2} \tag{A2.2.10}$$

or the ion–dipole interaction energy is given by

$$U_{I-D} = \frac{-z_i e_0 \mu \cos\theta}{r^2} \tag{A2.2.11}$$

APPENDIX 2.3. INTERACTION BETWEEN AN ION AND A WATER QUADRUPOLE

Instead of presenting a sophisticated general treatment for ion–quadrupole interactions, a particular case of these interactions will be worked out. The special case to be worked out is that corresponding to the water molecule being oriented with respect to a positive ion so that the interaction energy is a minimum.

In this orientation (see Fig. A2.3.1), the oxygen atom and a positive ion are on the y axis, which bisects the H–O–H angle. Further, the positive ion, the oxygen atom, and the two hydrogen atoms are all considered in the xy plane. The origin of the xy coordinate system is located at the point Q, which is the center of the water molecule. The ion is at a distance r from the origin.

The ion–quadrupole interaction energy U_{I-Q} is simply given by the charge on the ion times the potential ψ_r at the site of the ion due to the charges of the quadrupole,

$$U_{I-Q} = z_i e_0 \psi_r \tag{A2.3.1}$$

The potential ψ_r is the sum of the potentials due to the four charges q_1, q_2, q_3, and q_4 in the quadrupole (1 and 2 are the positive charges at the hydrogen, and 3 and 4 are the negative charges at the oxygen). That is,

$$\psi_r = \psi_1 + \psi_2 + \psi_3 + \psi_4 \tag{A2.3.2}$$

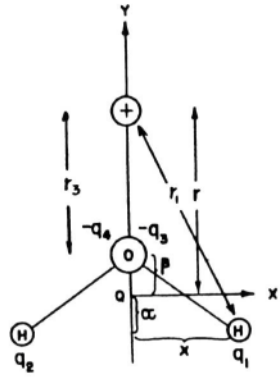

Fig. A2.3.1

Each of these potentials is given by the usual Coulombic expression for the potential

$$\psi_r = \frac{q_1}{r_1} + \frac{q_2}{r_2} - \frac{q_3}{r_3} - \frac{q_4}{r_4} \tag{A2.3.3}$$

where the minus sign appears before the third and fourth terms because q_3 and q_4 are negative charges. Further, the *magnitudes* of all the charges are equal

$$|q_1| = |q_2| = |q_3| = |q_4| = q \tag{A2.3.4}$$

and, because of symmetrical disposition of the water molecule,

$$r_2 = r_1 \quad \text{and} \quad r_4 = r_3 \tag{A2.3.5}$$

Hence, from Eqs. (A2.3.3), (A2.3.4), and (A2.3.5),

$$\psi_r = 2q\left(\frac{1}{r_1} - \frac{1}{r_3}\right) \tag{A2.3.6}$$

It is obvious (see Fig. A2.3.1) that

$$r_1^2 = (r + \alpha)^2 + x^2 \tag{A2.3.7}$$

$$= r^2\left(1 + \frac{\alpha^2 + x^2}{r^2} + \frac{2\alpha}{r}\right) \tag{A2.3.8}$$

and

$$r_3 = r - \beta \tag{A2.3.9}$$

$$= r\left(1 - \frac{\beta}{r}\right) \tag{A2.3.10}$$

Thus,

$$\frac{1}{r_1} = \frac{1}{r}\left(1 + \frac{\alpha^2 + x^2}{r^2} + \frac{2\alpha}{r}\right)^{-1/2} \tag{A2.3.11}$$

and

$$\frac{1}{r_3} = \frac{1}{r}\left(1 - \frac{\beta}{r}\right)^{-1} \tag{A2.3.12}$$

One can now use the binomial expansion, i.e.,

$$(1 \pm m)^{-n} = 1 \mp nm + \frac{n(n+1)}{2} m^2 \mp \cdots \tag{A2.3.13}$$

and drop off all terms higher than the *third*.[53] Thus,

$$\frac{1}{r_1} \approx \left\{ \frac{1}{r} - \frac{1}{2}\frac{\alpha^2 + x^2}{r^3} - \frac{\alpha}{r^2} + \frac{3}{8}\left[\frac{(\alpha^2 + x^2)^2}{r^5} + \frac{4\alpha^2}{r^3} + \frac{4\alpha(\alpha^2 + x^2)}{r^4}\right]\right\} \tag{A2.3.14}$$

and, omitting all terms with powers r greater than 3, one has

$$\frac{1}{r_1} \approx \frac{1}{r} - \frac{\alpha}{r^2} + \frac{1}{2r^3}(2\alpha^2 - x^2) \tag{A2.3.15}$$

Further,

$$\frac{1}{r_3} \approx \frac{1}{r}\left(1 + \frac{\beta}{r} + \frac{\beta^2}{r^2}\right)$$

$$= \frac{1}{r} + \frac{\beta}{r^2} + \frac{\beta^2}{r^3} \tag{A2.3.16}$$

Subtracting Eq. (A2.3.16) from Eq. (A2.3.15), one has

[53] It is at this stage that the treatment of ion–quadrupole interactions diverges from that of ion–dipole interactions (*cf.* Appendix 2.2). In the latter, the binomial expansion was terminated after the second term.

$$\frac{1}{r_1} - \frac{1}{r_3} = -\frac{(\alpha+\beta)}{r^2} + \frac{1}{2r^3}(2\alpha^2 - x^2 - 2\beta^2) \qquad \text{(A2.3.17)}$$

and therefore by substitution of Eq. (A2.3.17) in Eq. (A2.3.6),

$$\psi_r = -\frac{2q(\alpha+\beta)}{r^2} + \frac{1}{2r^3}[2(2q\alpha^2 - 2q\beta^2) - 2qx^2] \qquad \text{(A2.3.18)}$$

The first term on the right-hand side of Eq. (A2.3.18) can be rearranged as follows:

$$2q(\alpha+\beta) = 2q\alpha + 2q\beta$$

$$= \sum (2q)d \text{ where } d = \alpha \text{ or } \beta \qquad \text{(A2.3.19)}$$

Thus, as a first approximation, the water molecule can be represented as a dipolar charge distribution in which there is a positive charge of $-2q$ (due to the H atoms) at a distance α from the origin on the bisector of the H–O–H angle and a charge of $-2q$ (due to the lone electron pair) at a distance $-\beta$ from the origin; it follows that

$$\sum (2q)d = \sum \text{ magnitude of each charge of dipole}$$

$$\times \text{ distance of the charge from origin} \qquad \text{(A2.3.20)}$$

The right-hand side of this expression is the *general* expression for the dipole moment μ, as is seen by considering the situation when $\alpha = \beta$, i.e., $\Sigma(2q)d = (2q)2d$, where $2d$ is the distance between the charges of the dipole, in which case one obtains the familiar expression for the dipole moment μ,

$$\mu = 2q2d \qquad \text{(A2.3.21)}$$

Thus, the first term on the right-hand side of Eq. (A2.3.18) is

$$-\frac{2q(\alpha+\beta)}{r^2} = -\frac{\mu}{r^2} \qquad \text{(A2.3.22)}$$

The second term can be interpreted as follows: Consider $(2q\alpha^2 - 2q\beta^2)$. It can be written thus

$$2q\alpha^2 - 2q\beta^2 = q\alpha^2 + q\alpha^2 + (-q)\beta^2 + (-q)\beta^2$$

$$= \sum q d_y^2 \text{ where } d_y = \alpha \text{ or } \beta \qquad \text{(A2.3.23)}$$

But the general definition of a quadrupole moment is the magnitude of each charge of quadrupole times the *square* of the distance of the charge from the origin. Thus, $\Sigma q d_y^2$ is the y component p_{yy} of the quadrupole moment for the particular coordinate system that has been chosen. Similarly, $\Sigma 2qx^2$ is the x component p_{xx} of the quadrupole moment. Thus,

$$2(2q\alpha^2 - 2q\beta^2) - 2qx^2 = 2p_{yy} - p_{xx} \tag{A2.3.24}$$

One can combine $2p_{yy} - p_{xx}$ into a single symbol and talk of the quadrupole moment p_W of the water molecule in the particular orientation of Fig. A2.3.1.

Hence,

$$2(2q\alpha^2 - 2q\beta^2) - 2qx^2 = p_W \tag{A2.3.25}$$

and therefore by substituting Eqs. (A2.3.22) and (A2.3.25) in Eq. (A2.3.18),

$$\psi_r = -\frac{\mu}{r^2} + \frac{p_W}{2r^3} \tag{A2.3.26}$$

The ion–quadrupole interaction energy [*cf.* Eq. (A2.3.1)] thus becomes

$$U_{I-Q} = -\frac{z_i e_0 \mu}{r^2} + \frac{z_i e_0 p_W}{2r^3} \tag{A2.3.27}$$

When a negative ion is considered, the water molecule turns around through π, and one obtains by an argument similar to that for positive ions

$$U_{I-Q} = -\frac{z_i e_0 \mu}{r^2} - \frac{z_i e_0 p_W}{2r^3} \tag{A2.3.28}$$

EXERCISES

1. The heat of evaporation of water is $2240\ \mathrm{J\ g^{-1}}$. Calculate the total H- bond energy for 1 mole of water, and compare the two values.
2. The Cl^- ion has a radius of 180 pm. Find how much bigger the ion–dipole term is compared with the Born term. The dielectric constant in the Born equation is to be taken as 80.
3. The energy of the I^- ion-water dipole interaction is $-171\ \mathrm{kJ\ mol^{-1}}$ at 298 K. Calculate the radius of a water molecule. Consider $r_{I^-} = 216$ pm and $\mu_W = 1.8$ D. (Contractor)

4. The heat of the chloride ion interaction with water is measured to be $-347.3\ \text{kJ mol}^{-1}$, in which the contribution of the Born charging process is $-152.5\ \text{kJ mol}^{-1}$. If the dielectric constant of water at 298 K is 78.3, estimate its rate of change with temperature at this temperature. Also calculate the percent error introduced in the Born charging term if the dielectric constant is assumed to be independent of temperature. Consider $r_{Cl^-} = 181$ pm and $r_w = 138$ pm. (Contractor)

5. When an F^- comes in contact with water molecules, its ion–quadrupole interaction energy is $-394.6\ \text{kJ mol}^{-1}$. Calculate the quadrupole moment of water ($r_w = 138$ pm, $r_{F^-} = 136$ pm, $\mu_w = 1.8$ D). (Contractor)

6. If the total primary hydration number of NaCl in a 1 M solution is 6, make a rough calculation of the dielectric constant of the solution by assuming that the dielectric constant of pure water is 80 and that of the water molecule in the primary hydration sheath is 6.

7. For an NaCl solution, calculate the concentration at which the so-called "Gurney co-sphere" is reached. (Hint: For 1:1 electrolyte, the average separation l (in Å) $= 9.40c^{-1/3}$, where c is the concentration in mol dm^{-3}. Assume the Gurney co-sphere is two water molecules beyond the ions periphery.) (Xu)

8. Suppose the results from Exercise 7 are true and calculate the solvation number for NaCl. Comment on the reliability of the result. (Xu)

9. (a) A Roman spectrum shows that in a 4.0 *M* NaCl solution, about 40% of the waters are in the primary sheath. Estimate the solvation number n_h. (b) If the SB region consists of only one layer of water molecules, is there any bulk water left in this solution? (Xu)

10. Solvation numbers for Na^+ and CF have been measured at about 5 and 1, respectively. With this information, and recalling that the number of moles per liter of pure water is 55, calculate the dielectric constant of a 5 *M* solution of NaCl. (The dielectric constant of pure water is to be taken as 80 near room temperature; when the water molecules are held immobile in respect to the variations of an applied field, *M* drops to 6.)

11. Calculate the sum of the heats of hydration of K^+ and F^-. The lattice energy is $814.6\ \text{kJ mol}^{-1}$. The heat of the solution is $-17.15\ \text{kJ mol}^{-1}$.

12. Using the Born equation as representing a part of the free energy of hydration of ions, derive an expression for the entropy of Born hydration. According to this, what would be the entropy of Born solvation of the Γ ion with a radius of 200 pm?

13. Calculate the ion–solvent interaction free energy for K^+, Ca^{2+}, F^-, and Cl^- in water. The ionic radii are 133, 99, 136, and 181 pm, respectively, and the dielectric constant for water is 78.3 at 25°C. (Kim)

14. Calculate the entropy change due to ion–solvent interaction for the ions in Exercise 13 using the relation $\partial\varepsilon/\partial T = 0.356/K$ for water. (Kim)

15. Evaluate the heat of solvation for the ions in Exercise 13 in terms of the ion–dipole approach ($r_w = 138$ pm, $\mu_w = 1.8$ D). (Kim)

16. Calculate the difference of the heat of hydration for the tons in Exercise 13 between the ion–quadrupole model and the ion–dipole model ($p_w = 3.9 \times 10^{-8}$ D cm). (Kim)

17. Calculate the absolute heats of hydration of Na^+ and Cl^- using the absolute heat of hydration of H^+ of -1113.0 kJ mol^{-1}. The heat of interaction between HC1 and water is -1454.0 kJ mol^{-1}; the heat of solution of NaOH is $+3.8$ kJ mol^{-1}; and the heat of sublimation of NaCl is $+772.8$ kJ mol^{-1}. (Kim)

18. The adiabatic compressibilities of water and 0.1 *M* NaI solution at 298 K are 4.473×10^{-12} Pa^{-1} and 4.428×10^{-13} Pa^{-1}, respectively. Calculate the hydration number of the NaI solution when the density of the solution is 1.0086 cm^{-3}. (Kim)

19. The adiabatic compressibility of water at 25 °C is 4.473×10^{-12} Pa^{-1}. Calculate the adiabatic compressibility of a 0.101 *M* solution of $CaCl_2$ (density at 25 °C = 1.0059 g cm^{-3}) if the hydration number of the electrolyte is 12. (Contractor)

20. Sound velocity in water is measured to be 1496.95 m s^{-1} at 25 °C. Calculate the adiabatic compressibility of water in Pa^{-1}. (Xu)

21. In the text are data on compressibilities as a function of concentration. Use the Passynski equation to calculate the total solvation number of NaBr at infinite dilution.

22. The definition of compressibility is $\beta = -(1/V)(\partial V/\partial P)_T$. On the (often made but erroneous) assumption that β is constant with pressure, find V as a function of P. Why must your equation be applicable only over a limited range of pressures?

23. Calculate the hydration number of Na^+ when the mobility of the ion in water is 44×10^{-5} cm^2 s^{-1} V^{-1} and the viscosity of the solution is 0.01 poise, $r_{Na^+} = 95$ pm and $r_w = 138$ pm. (Kim)

24. Use the infinite-dilution equality between the accelerative force for ions under an applied electric field and the viscous drag to calculate the hydration number of Cl^- in HC1 aqueous solution, using the result that the transport number of the cation is 0.83, while the equivalent conductivity at infinite dilution is 304 S cm^2 mol^{-1} (25 °C). Take the radius of water as 170 pm and the corresponding viscosity of water as 0.01 poise.

25. Calculate the change of solubility of 2,4-dinitrophenol in water due to primary solvation when 0.1 *M* NaCl is added to the solution and the solvation number of NaCl is assumed to be 5. (Kim)

26. Calculate the change of the solubility of ethyl ether (dielectric constant, 4,3; density, $0.7138\ \text{g cm}^{-3}$) in water due to the secondary solvation shell when 1 *M* of NaCl is added to the solution ($r_{Na^+} = 180$ pm, $r_{Cl^-} = 191$ pm, $r_w = 138$ pm). (Kim)

27. Show that the electrostatic interaction potential energy between two charges Q_1 and Q_2 can be represented by the nonconventional although widely used equation

$$E = \frac{132}{\varepsilon} \frac{Q_1 * Q_2}{R_{12}}$$

where Q_1, Q_2 are expressed in electronic charge units, R_{12} is the distance between the charges expressed in Å, ε is the relative dielectric constant of the medium, and *E is* given in units of kcal/mol. What is the Coulombic interaction between a proton and electron by 1 Å in vacuum? (Contractor)

28. (a) Li^+ has an ionic radius of 60 pm. Calculate the work of charging the lithium ion in vacuum, (b) Repeat the calculation for Cl^{-1}, whose ionic radius is 181 pm. (c) Calculate the work of charging Li^+ surrounded by *bulk* water with a relative dielectric constant of 80 at 293 K. (Contractor)

29. A positive charge of $+e_0$, and a negative charge of $-e_0$ are separated by 53 pm. Calculate their dipole moment. (Contractor)

30. Calculate the effective moment that a gas dipole of water exhibits in the direction of an external field of $10^3\ \text{V cm}^{-1}$ when subject to electrical orienting and thermal randomizing forces at 25 °C. The dipole moment of water $\mu_w = 1.87 \times 10^{-15}$ D. (Contractor)

31. Estimate the average moment of a dipole cluster of water subject to an external electric field of $2.7 \times 10^8\ \text{V cm}^{-1}$. Assume the average of the cosine of the angles between the dipole moment of the central water molecule and those of its bonded neighbors is 1/3 at 298 K. (Contractor)

32. For liquid water, the relative dielectric constant at 25 °C is 78. Calculate its deformation polarizability at this temperature if there are 10^{-3} moles of deformable molecules per unit volume.* Use the average of the cosines of the angles

*The deformable molecules are taken, in this problem to be less than the total number.

between the dipole moment of the central molecule and that of its bonded neighbors as 1/3. (Contractor)

33. Water often comes under extremely strong electric fields as, e.g., in the solvation of ions. By considering the total H-bond energy of water, calculate the electric field strength that will break up H-bonded water. At what field strength would liquid water dissociate, and to what?

34. An IR spectrum has a band at a wavenumber of $1.561 \times 10^3\ cm^{-1}$. What are the wavelength and frequency of the corresponding bond? If the spectrum originates from water, calculate the force constant between O and H.

35. From the data in the text, the self-diffusion coefficients of certain ions (e.g., Li^+ and I^-) are known. The diffusion coefficient is related to the rate constant for diffusion by the equation $\frac{1}{2} l^2 \approx \frac{D}{k}$. What kind of value for l (jump distance) would you think reasonable? With the known values for D (see text), calculate the time the anion resides in one place.

36. The effect of electrolytes on the solubility of nonelectrolytes is generally to decrease the solubility of the nonelectrolyte (salting-out). Taking O_2 as the nonelectrolyte and the relevant solubility data from the text, obtain Setchenow's constant for HCl and $Ac_2(SO_4)_3$. Comment on the great difference.

PROBLEMS

1. Use the data of Table 2.8 to calculate the mean activity coefficient of a 5 *M* NaCl solution, assuming the total hydration number at this high concentration is <3. Values for *A* and *B* of the Debye–Hückel equation can be recovered from the text.

2. Define wavenumber and explain why ions of a small radius tend to give higher librative frequencies in their IR spectra in solution. Why do hydration numbers obtained from spectroscopic data tend to be lower than those from nonspectroscopic methods? Write down the expression for the coordination number of an ion in terms of the distribution function for the O in the first shell with respect to an Na^+ ion. Draw typical plots of g_r as a function of distance from an ion for (a) a strongly hydrated and (b) a weakly hydrated ion, respectively.

3. Explain what is meant by the statement: "The *relative* heat of hydration of I^- is $-1385.7\ kJ\ mol^{-1}$." Halliwell and Nyburg's value for the heat of hydration of protons was $-1087.8\ kJ\ mol^{-1}$. Use this value to establish the absolute heat of hydration of I^-.

4. Calculate the librative and vibrational contributions for the entropy of an Na^+ ion in dilute solutions assuming 6 water molecules in the first shell. Why is it

usual to neglect the translational entropy? (Give a numerical answer involving the free volume of Na^+ in water to this part of the question.)

5. Calculate the heats of interaction between individual ions and water: (a) $\Delta H_{Cl^-\text{-}H_2O}$, (b) $\Delta H_{Na^+\text{-}H_2O}$, and (c) $\Delta H_{Br^-\text{-}H_2O}$ using the experimental values of the heats of interaction between a salt and water, $\Delta H_{S\text{-}H_2O}$ at 25 °C (the Born model is considered valid). (Constantinescu)

Salt	$\Delta H_{S\text{-}H_2O}$ / kJ mol^{-1}	Ionic Radius / / pm	
KF	−827.6	Na^+	95
KCl	−685.3	K^+	133
NaF	−911.2	F^-	136
NaBr	−791.8	Cl^-	181
		Br^-	195

6. Calculate the ion–water interaction for Cl^- using the ion-dipole model at 298 K. Use four coordination. (Contractor)

7. Calculate ΔH_{soln} and ΔH_h for AgCl, AgBr, and AgI and rationalize their low solubility (using the data in Table P.1). (Xu)

8. Calculate $\Delta H_{Cl^-\text{-}H_2O}$ at 298 K. The ionic radius of Cl^- is 1.81 Å. The dielectric constant of water at three temperatures is ε (20°C) = 80.1, ε (25°C) = 78.3, ε (30°C) = 76.54. Use the Born model. (Contractor)

9. Estimate the error introduced by ignoring the size of the solvent molecules in calculating the heat of the Born–charging process of a Cs^+ ion interaction with water–water ($r_{Cs^+} = 169$ pm). (Contractor)

10. Estimate the error introduced in calculating the heat of an NaBr interaction with water by ignoring the distortability of the water molecules $r_{Bi} = 1.95$ Å, $r_{Na^+} = 0.95$ Å, $p_w = 3.9 \times 10^8$ D cm, $\alpha_w = 1.46 \times 10^{-26}$ cm^3, $\varepsilon_w(298\text{ K}) = 78.3$, $\partial\varepsilon_w/\partial T = -0.356$ K^{-1}).

11. (a) Using data for solution enthalpy (ΔH_{soln}) and lattice enthalpy ($\Delta H_{lattice}$) (see Table P.2), calculate the hydration heat for various alkali halides (ΔH_h). Comment on the possible major error source, (b) Using the cation radii data, explain

TABLE P.1

	AgCl	AgBr	AgI
Equilibrium constant, K	1.77×10^{-10}		7.7×10^{-13}
$-S_{soln}$ (kJ K^{-1}mol^{-1})		32.98	51
$-H_{lattice}$ (kJ mol^{-1})			−91

TABLE P.2

	LiCl	LiBr	NaCl	NaBr	KCl	KBr
ΔH_{soln} (kJ/mol)	−37	−48.8	+3.89	−0.6	17.22	19.9
ΔS_{soln} (J/mol)	48	43	110	120	135	140
$\Delta H_{lattice}$ (kJ/mol)	−815	−787	−752	−717	−689	−653
r (cation) (Å)	0.59	0.59	1.02	1.02	1.38	1.38

the trend and the sign of ΔH_{soln}. What is the driving force of the solution process in case $\Delta H_{soln} > 0$? (Xu)

12. Chloride is surrounded by 4 water molecules. Calculate the ion–dipole interaction work ($r_{Cl^-} = 181$ pm). (Contractor)

13. Anomalous salting in is said to occur when the dipole moment of water is greater than that of the organic molecule concerned, but the solubility of the latter *increases* when ions are added to the solution. What kind of model could explain the observation that anomalous salting in occurs when the electrolyte consists of large ions?

    From the model you derive, calculate the minimum radius of ions required to salt-in benzoic acid in a 1 *M* solution of electrolyte. (Take the polarizability as r_i^3, where r_i is the radius of any entity involved.)

14. An ion of charge ze_0 and radius r is transferred from a solvent of dielectric constant ε_i to a solvent of dielectric constant ε_i. Derive an expression for the free-energy change associated with this transfer using the Born model. (Contractor)

15. What is the free-energy change involved in transferring Cl^- from water to a nonpolar medium like carbon tetrachloride with a dielectric constant of 2.23 at 298 K? Is this an energetically favorable process? (Make use of Problem 3.) Water has a dielectric constant of 78.54 at 298 K. (Contractor)

16. Living cells are surrounded by membranes and on either side of the membrane an aqueous environment is present. The interior of the membrane is highly nonpolar. Based on the result of Problem 15, can you explain why it is difficult to transport or move charges across a membrane in a living cell? (Contractor)

17. For a given water molecule, what is the *maximum* number of hydrogen bonds that can be formed with other neighboring water molecules? Are these hydrogen bonds identical in bonding nature for this particular water molecule? Why? If there is a difference in bonding nature for these hydrogen bonds, how would you

Fig. P2.1

differentiate these experimentally? (*Maximum* is emphasized because in a liquid state the actual number of hydrogen bonds per molecule is less than the maximum possible. Even in crystal ice II there are dangling hydrogen atoms, which do not participate in hydrogen bonding.) (Xu)

18. In an ion–solvent interaction model (Fig. P2.1), "solvated coordinated water" has two sites capable of forming hydrogen bonds with water molecules in the SB region. Are these two sites identical in bonding? For "nonsolvated coordinated water," there are three sites for hydrogen bonds. Are these three identical? Why? (Xu)

19. (a) Calculate the volume of bare and solvated ions sheathed by water, using the following ionic and water radii: $r_{Li^+} = 54$ pm, $r_{Na^+} = 102$ pm, $r_{K^+} = 138$ pm, and $r_w = 158$ pm. (b) Suppose the structure-breaking region consists of two layers of water molecules. Calculate the volume of water that has been affected by a single ion. (Xu)

20. Using the above results, calculate the percentage of bulk water in a 0.05 *M* NaCl solution. What if the concentration is 0.5 *M*? Comment on the significance of the result (assume the anion has the same SB structure as for cations ($r_{Cl^-} = 181$ pm). (Xu)

TABLE P.3

c_2, mol dm^{-3}	β (LiCl)	β (NaCl)	β (KCl)	β ($MgCl_2$)
0.05	44.49	44.45	44.46	44.21
0.09				43.88
0.10	44.30	44.20		
1.00	40.60	40.04	39.84	
1.05				35.94
2.00	37.15	36.64		
4.10			29.88	
5.00	29.93	26.75		

TABLE P.4

	LiCl	NaCl	KCl
ε at 25 °C	64.9	66.7	68.1

21. (a) Justify that in a dilute solution solvation number $n_s = [1 - (\beta/\beta_0)] \times (55.56/c_2)$, where c_2 is the electrolyte concentration in mol dm^{-3}. (b) The compressibility of LiCl, NaCl, KCl, and $MgCl_2$ are measured at 25 °C (Table P.3 in 10^{-6} bar^{-1}). Calculate the total solvation number of these electrolytes. (Xu)

22. Table P.4 lists measured dielectric constants at 25 °C for 1.0 *M* LiCl, NaCl, and KC1 solutions, respectively. Calculate the percentage of water in the primary sheath and the total solvation number. Compare the results with those of the compressibility method (see problem 21) and comment on their reliability.

23. The densities of aqueous NaCl solutions at 25°C are given as a function of NaCl molality in Table P.5. (a) Obtain a graph for the partial molar volumes of both water V_1, and NaCl V_2, as a function of NaCl molality. Compare the limiting cases V_1 $(m \to 0)$, V_2 $(m \to \text{sat})$ with those of pure water and pure NaCl molar volumes, V_1° and V_2°, respectively, (b) Calculate V_2 for m = 0.5 and m = 2. (Mussini)

TABLE P.5

m NaCl / mol kg^{-1}	ρ / kg dm^{-3}
0	0.99707
0.11094	1.00158
0.23631	1.00663
0.56874	1.01970
0.85382	1.03071
1.47458	1.05353
2.51393	1.08963
3.09392	1.10849
3.9873	1.13600
5.24324	1.17290
5.4952	1.18030
5.8023	1.18880
5.82267	1.18888

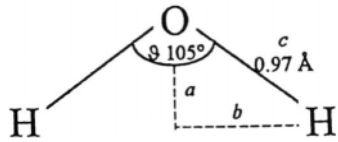

Fig. P2.2

24. (a) Calculate the dipole moment associated with water in the hypothesis of fully ionic OH bondings (i.e., considering a $-2e$ charge on the O atom and a $+ 1e$ charge on each H atom; e = elementary charge taken without sign). Draw the associated vector (refer to Fig. P2.2). (b) Knowing the dipole moment of water, write down an equation expressing it in terms of f the fractional charge on either end of the dipole and x the distance between the center of charge and the atomic nucleus. (c) Determine f and x in the hypothesis of a tetrahedrical angle HOH and draw the corresponding vector T. (Mussini)

25. (a) Write an expression for the potential in a point P of the electric field created by a dipole. (b) Then write an expression for the potential energy of the ion–dipole interaction. (c) Calculate the potential energy, E_p, of an ion-dipole interaction (in $\mathrm{kJ\ mol^{-1}}$) between water ($\mu_w = 1.86$ D) and a z-valent cation, as a function of the distance r, the ion charge z_i, the angle ϑ and the relative permittivity ε_r. (d) Perform a complete calculation for the limiting cases $z_i = 1$, $r = 2$ Å, $\varepsilon_r = 4.5$ and $z_i = 1$, $r = 6$ Å, $\varepsilon_r = 80$. Assume that the relative positions are as in Fig. P.2.3 and the negative end of the water dipole faces the positive ion. (e) Assuming the intermediate values ε_r to increase exponentially, draw a complete E_p versus r characteristic in the interval $2 < r < 6$, and mark the region

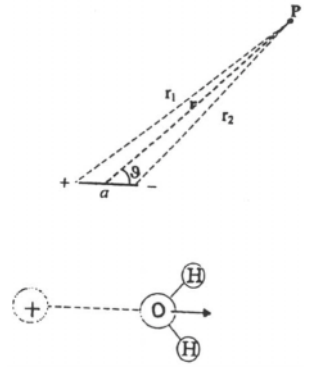

Fig. P2.3

in which the thermal energy, $\sim RT$, is competitive with the electric interaction. (Mussini)

26. The heat of hydration of an electrolyte is obtained by measuring the heat of dissolution at various concentrations and extrapolating its values to $c_{\text{electrolyte}} \approx 0$. This value is then used in conjunction with the lattice energy to yield the desired heat. Explain, then, how the free energy (hence the entropy) of the hydration of an electrolyte is obtained. Apart from the heat of solution, what other essential measurements would be necessary?

27. Table P.6 gives the density of a number of solutions of AgCl. Find the apparent molar volume of the electrolyte at each concentration. Then, by using the method described in the text, find the partial molar volume of the electrolyte at infinite dissolution.

28. The (idealized) radius of a polystyrene styrene sulfonate may be several hundred angstroms. Were you to measure the self-diffusion coefficient, what equation would you use to obtain a measure of the ion's size? Explain the principles (showing appropriate equations) of obtaining an individual ionic entropy and an individual ionic entropy of hydration.

TABLE P.6

c/M	$\rho/\text{g cm}^{-3}$
0.0010294	1.000170
0.0051484	1.000862
0.010904	1.001823
0.018974	1.003175
0.045680	1.00763
0.080311	1.01339
0.11868	1.01970
0.23881	1.03944
0.47773	1.0786
0.84786	1.1396
1.2005	1.1973
1.4717	1.2420
1.7321	1.2846
2.0451	1.3358
2.4640	1.4017

MICRO RESEARCH PROBLEMS

1. Define electrostriction.
   In the functioning of drugs, the physiological effects are dependent on the precise structure of the molecule. Among other reasons, this is because of the need to "fit" onto the structure of a relevant enzyme. In work on theoretical drug designs, some computations are made on models of the organic molecules constituting the drug in a force-free field, i.e., in a hypothetical vacuum.

   Consider an $(-NH_3)^+$ group associated with a designer drug. What happens to the group when it is introduced into a saline solution 0.4 *M* in NaCl? Examine the likely hydration in respect to energy and structure. Calculate the change in volume of the $(-NH_3)^+$ group due to electrostriction. Examine carboxypeptides (Fig. 2.4) and make computations that would lead to an estimate of the stabilization energy due to hydration.

2. (a) The origin of the hydrogen bond is the intermolecular dipole interaction caused by the polarized covalent bond. The existence of this additional intermolecular force accounts for the abnormally high boiling point for water. Using the electronegativity (χ) data provided, try to rationalize semiquantitatively the elevation of boiling point in terms of bond polarization for a series of hydrides (*Fig. 1*). (χ: H 2.2; N 3.0; O 3.4; F 4.0; Zn 1.6. Hint: The total intermolecular force caused by the H bond is proportional to the total number of H bonds and dipole moment of an individual H bond, which in turn vary approximately with X. (b) The elevation of boiling point is by no means unique to hydrogen. Explain the abnormal boiling point of ZnF_2 in the light of the "zinc bond." Compare the "zinc bond" with the hydrogen bond in (a) and account for the especially strong effect of the "zinc bond" on boiling point. (Assume that each ZnF_2 molecule can form 6 Zn bonds.)

CHAPTER 3

ION–ION INTERACTIONS

3.1. INTRODUCTION

A model has been given for the breaking up of an ionic crystal into free ions which stabilize themselves in solution with solvent sheaths. One central theme guided the account, the interaction of an ion with its neighboring water molecules.

However, ion–solvent interactions are only part of the story relating an ion to its environment. When an ion looks out upon its surroundings, it sees not only solvent dipoles but also other ions. The mutual interaction between these ions constitutes an essential part of the picture of an electrolytic solution.

Why are ion–ion interactions important? Because, as will be shown, they affect the equilibrium properties of ionic solutions, and also because they interfere with the drift of ions, for instance, under an externally applied electric field (Chapter 4).

Now, the degree to which these interactions affect the properties of solutions will depend on the mean distance apart of the ions, i.e., on how densely the solution is populated with ions, because the interionic fields are distance dependent. This ionic population density will in turn depend on the nature of the electrolyte, i.e., on the extent to which the electrolyte gives rise to ions in solution.

3.2. TRUE AND POTENTIAL ELECTROLYTES

3.2.1. Ionic Crystals Form True Electrolytes

An important point to recall regarding the dissolution of an ionic crystal (Chapter 2) is that ionic lattices consist of ions *even before they come in contact with a solvent.* In fact, all that a polar solvent does is to use ion–dipole (or ion–quadrupole) forces to disengage the ions from the lattice sites, solvate them, and disperse them in solution.

Such ionic crystals are known as true electrolytes or *ionophores* (the Greek suffix *phore* means "bearer of"; thus, an ionophore is a "substance that bears ions"). When a true electrolyte is melted, its ionic lattice is dismantled and the pure liquid true electrolyte shows considerable ionic conduction (Chapter 2). Thus, the characteristic of a true electrolyte is that in the pure liquid form it is an ionic conductor. All salts belong to this class. Sodium chloride therefore is a typical true electrolyte.

3.2.2. Potential Electrolytes: Nonionic Substances that React with the Solvent to Yield Ions

A large number of substances (e.g., organic acids) show little conductivity in the pure liquid state. Evidently there must be some fundamental difference in structure between organic acids and inorganic salts, and this difference is responsible for the fact that one pure liquid (the true electrolyte) is an ionic conductor and the other is not.

What is this difference between, say, sodium chloride and acetic acid? Electron diffraction studies furnish an answer. They show that gaseous acetic acid consists of separate, neutral molecules and the bonding of the atoms inside these molecules is essentially nonionic. These neutral molecules retain their identity and separate existence when the gas condenses to give liquid acetic acid. Hence, there are hardly any ions in liquid acetic acid and therefore little conductivity.

Now, the first requirement of an electrolyte is that it should give rise to a conducting solution. From this point of view, it appears that acetic acid will never answer the requirements of an electrolyte; it is nonionic. When, however, acetic acid is dissolved in water, an interesting phenomenon occurs: ions are produced, and therefore the solutions conduct electricity. Thus, acetic acid, too, is a type of electrolyte; it is not a true electrolyte, but a potential one ("one which can, but has not yet, become"). Potential electrolytes are also called *ionogens*, i.e., "ion producers."

How does acetic acid, which does not consist of ions in the pure liquid state, generate ions when dissolved in water? In short, how do potential electrolytes work? Obviously, there must be some reaction between neutral acetic acid molecules and water, and this reaction must lead to the splitting of the acetic acid molecules into charged fragments, or ions.

A simple picture is as follows. Suppose that an acetic acid molecule collides with a water molecule and in the process the H of the acetic acid OH group is transferred from the oxygen atom of the OH to the oxygen atom of the H_2O. A proton has been transferred from CH_3COOH to H_2O.

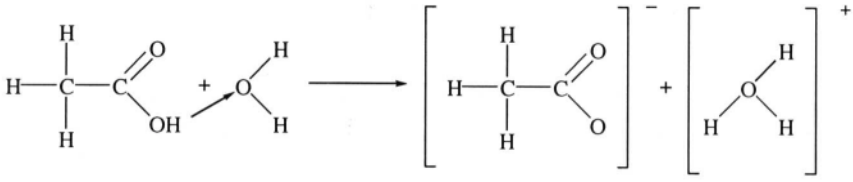

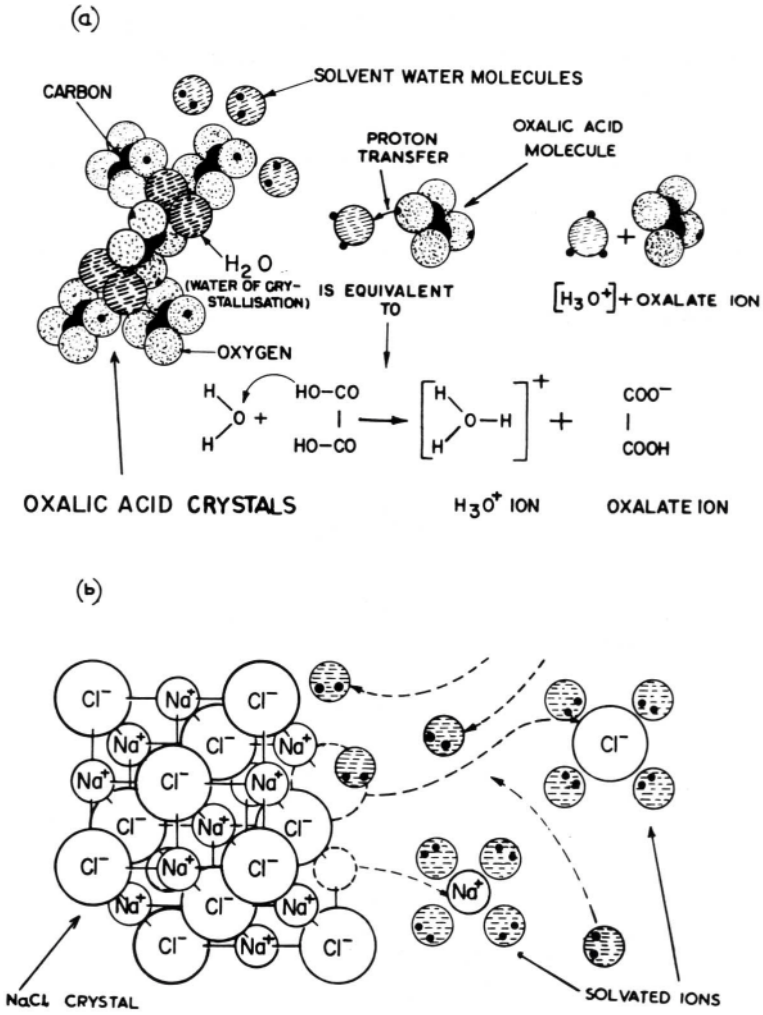

Fig. 3.1. Schematic diagram to illustrate the difference in the way potential electrolytes and true electrolytes dissolve to give ionic solutions: (a) Oxalic acid (a potential electrolyte) undergoes a proton-transfer chemical reaction with water to give rise to hydrogen ions and oxalate ions. (b) Sodium chloride (a true electrolyte) dissolves by the solvation of the Na^+ and Cl^+ ions in the crystal.

The result of the proton transfer is that two ions have been produced: (1) an acetate ion and (2) a hydrated proton. Thus, potential electrolytes (organic acids and most bases) dissociate into ions by ionogenic, or ion-forming, chemical reactions with solvent molecules, in contrast to true electrolytes, which often give rise to ionic solutions by physical interactions between ions present in the ionic crystal and solvent molecules (Fig. 3.1).

3.2.3. An Obsolete Classification: Strong and Weak Electrolytes

The classification into true and potential electrolytes is a modern one. It is based on a knowledge of the structure of the electrolyte: whether in the pure form it consists of an ionic lattice (true electrolytes) or neutral molecules (potential electrolytes) (Fig. 3.2). It is not based on the behavior of the solute in any particular solvent.

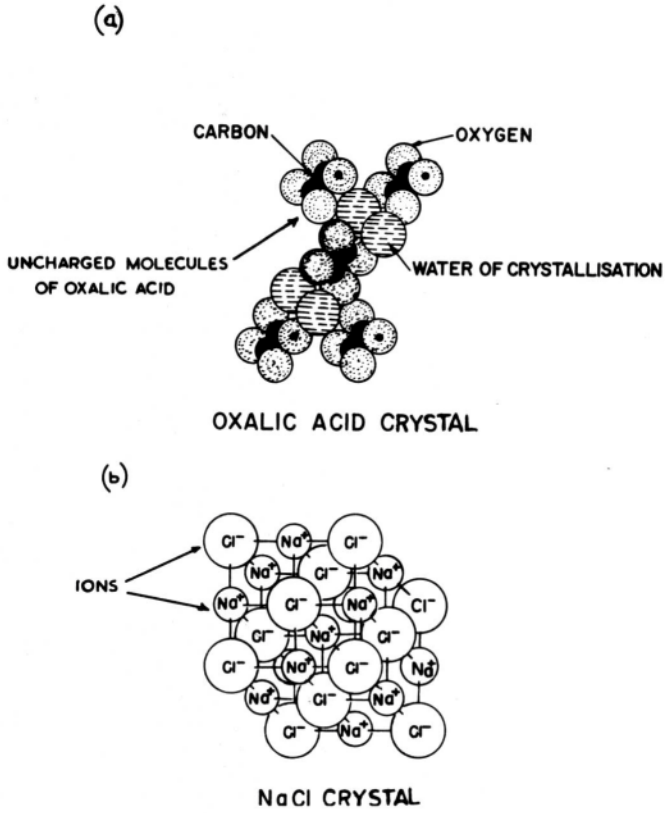

Fig. 3.2. Electrolytes can be classified as (a) potential electrolytes (e.g., oxalic acid), which in the pure state consist of uncharged molecules, and (b) true electrolytes (e.g., sodium chloride), which in the pure state consist of ions.

TABLE 3.1
Conductance Behavior of Substances in Different Media

	Equivalent Conductance	
	Water	Liquid Ammonia
NaCl	106.7	284.0
Acetic acid	4.7	216.6

Historically, however, the classification of electrolytes was made on the basis of their behavior in one particular solvent, i.e., water. *Weak* electrolytes were those that yielded relatively poorly conducting solutions when dissolved in water, and *strong* electrolytes were those that gave highly conducting solutions when dissolved in water.

The disadvantage of this classification into strong and weak electrolytes lies in the following fact: As soon as a different solvent (i.e., a nonaqueous solvent) is chosen, what was a strong electrolyte in water may behave as a weak electrolyte in the nonaqueous solvent. For example, sodium chloride behaves like a strong electrolyte (i.e., yields highly conducting solutions) in water and acetic acid behaves like a weak electrolyte. In liquid ammonia, however, the conductance behavior of acetic acid is similar to that of sodium chloride in water, i.e., the solutions are highly conducting (Table 3.1). This is an embarrassing situation. Can one say: Acetic acid is weak in water and strong in liquid ammonia? What is wanted is a classification of electrolytes that is independent of the solvent concerned. The classification into true and potential electrolytes is such a classification. It does not depend on the solvent, but rather upon the degree of ionicity of the substance constituting the solid lattice.

3.2.4. The Nature of the Electrolyte and the Relevance of Ion–Ion Interactions

Solutions of most potential electrolytes in water generally contain only small concentrations of ions, and therefore ion–ion interactions in these solutions are negligible; the ions are on the average too far apart. The behavior of such solutions is governed predominantly by the position of the equilibrium in the proton-transfer reaction between the potential electrolyte and water.

In contrast, true electrolytes are completely dissociated into ions when the parent salts are dissolved in water. The resulting solutions generally consist only of solvated ions and solvent molecules. The dependence of many of their properties on concentration (and therefore mean distance apart of the ions in the solution) is determined by the interactions between ions. To understand these properties, one must understand ion–ion interactions.

3.3. THE DEBYE–HÜCKEL (OR ION-CLOUD) THEORY OF ION–ION INTERACTIONS

3.3.1. A Strategy for a Quantitative Understanding of Ion–Ion Interactions

The first task in thinking in detail about ion–ion interactions is to evolve a quantitative measure of these interactions.[1] One approach is to follow a procedure similar to that used in the discussion of ion–solvent interactions (Section 2.4). Thus, one can consider an initial state in which ion–ion interactions do not exist (are "switched off") and a final state in which the interactions are in play (are "switched on"). Then, the free-energy change in going from the initial state to the final state can be considered the free energy ΔG_{I-I} of ion–ion interactions (Fig. 3.3).

The final state is obvious; it is ions in solution. The initial state is not so straightforward; one cannot take ions in vacuum, because then there will be ion–solvent interactions when these ions enter the solvent. The following approach is therefore adopted. One conceives of a hypothetical situation in which the ions are there in solution but are nevertheless not interacting. Now, if ion–ion interactions are assumed to be electrostatic in origin, then the imaginary initial state of noninteracting ions implies an assembly of discharged ions.

Thus, the process of going from an initial state of noninteracting ions to a final state of ion–ion interactions is equivalent to taking an assembly of discharged ions, charging them up, and setting the electrostatic charging work equal to the free energy ΔG_{I-I} of ion–ion interactions (Fig. 3.4).

One point about the above procedure should be borne in mind. Since, in the charging process, both the positively charged and negatively charged ionic species are charged up, one obtains a free-energy change that involves *all* the ionic species

[1]The question of how one obtains an experimental measure of ion–ion interactions is discussed in Section 3.4.

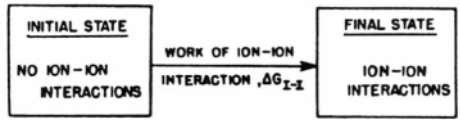

Fig. 3.3. The free energy ΔG_{I-I} of ion–ion interactions is the free-energy change in going from a hypothetical electrolytic solution, in which ion-ion interactions do not operate, to a real solution, in which these interactions do operate.

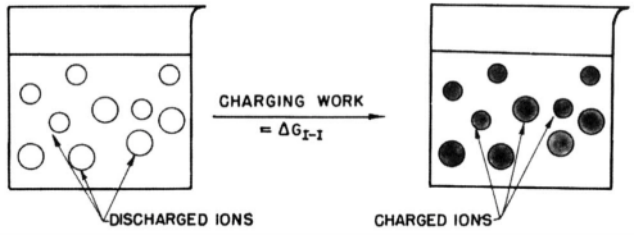

Fig. 3.4. The free energy ΔG_{I-I} of ion–ion interactions is the electrostatic work of taking an imaginary assembly of discharged ions and charging them up to obtain a solution of charged ions.

constituting the electrolyte. Generally, however, the desire is to isolate the contribution to the free energy of ion–ion interactions arising from one ionic species i only. This partial free-energy change is by definition the *chemical-potential change* $\Delta\mu_{i-I}$ arising from the interactions of one ionic species with the ionic assembly.

To compute this chemical-potential change $\Delta\mu_{i-I}$, rather than the free-energy change ΔG_{I-I}, one must adopt an approach similar to that used in the Born theory of solvation. One thinks of an ion of species i and imagines that this reference ion alone of all the ions in solution is in a state of zero charge (Fig. 3.5). If one computes the work of charging up the reference ion (of radius r_i) from a state of zero charge to its final charge of $z_i e_0$, then the charging work W times the Avogadro number N_A is equal to the partial molar free energy of ion–ion interactions, i.e., to the chemical potential of ion–ion interactions:

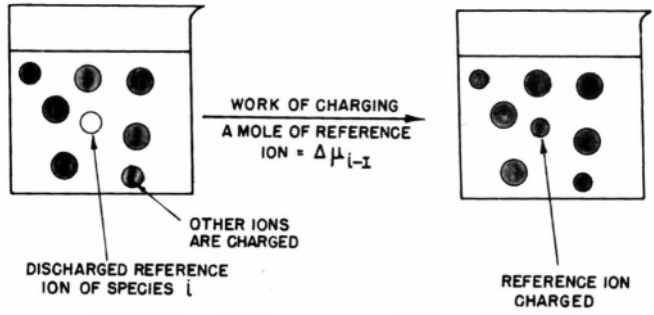

Fig. 3.5. The chemical potential $\Delta\mu_i$ arising from the interactions of an ionic species i with the electrolytic solution is equal to the Avogadro number times the electrostatic work of taking an imaginary solution in which one reference ion alone is discharged and charging this reference ion up to its normal charge.

$$\Delta\mu_{i-I} = N_A W \tag{3.1}$$

Then *as* the work of charging an electrical conductor is proved to be

$$W = 1/2\ [(\text{charge on the conductor}) \times (\text{conductor's electrostatic potential})] \tag{3.2}$$

one obtains

$$\Delta\mu_{i-I} = N_A W = \frac{N_A z_i e_0}{2}\psi \tag{3.3}$$

where ψ is the electrostatic potential of the ion due to the influence on it by the electrostatic interactions of the surrounding field.

The essence of the task therefore in computing the chemical-potential change due to the interactions of the ionic species *i* with the ionic solution is the calculation of the electrostatic potential produced at a reference ion by the rest of the ions in solution. Theory must aim at this quantity.

If one knew the *time-averaged spatial distribution* of the ions, then one could find out how all the other charges are distributed as a function of distance from the reference ion. At that stage, one of the fundamental laws of electrostatics could be used, namely, the law of the superposition of potentials, according to which the potential at a point due to an assembly of charges is the sum of the potentials due to each of the charges in the assembly.

Thus, the problem of calculating the chemical-potential change $\Delta\mu_{i-I}$ due to the interactions between one ionic species and the assembly of all the other ions has been reduced to the following problem: On a time average, how are the ions distributed around any specified ion? If that distribution became known, it would then be easy to calculate the electrostatic potential of the specified ion due to the other ions and then, by Eq. (3.3), the energy of that interaction. Thus, the task is to develop a model that describes the equilibrium spatial distribution of ions inside an electrolytic solution and then to describe that model mathematically.

3.3.2. A Prelude to the Ionic-Cloud Theory

A spectacular advance in the understanding of the distribution of charges around an ion in solution was achieved in 1923 by Debye and Hückel. It is as significant in the understanding of ionic solutions as the Maxwell theory of the distribution of velocities is in the understanding of gases.

Before going into the details of their theory, a moment's reflection on the magnitude of the problem will promote appreciation of their achievement. Consider, for example, a 10^{-3} M (mol dm^{-3}) aqueous solution of sodium chloride. There will be $10^{-6} \times 6.023 \times 10^{23}$ sodium ions per cubic centimeter of solution and the same number of chloride ions, together, of course, with the corresponding number of water molecules. Nature takes these $2 \times 6.023 \times 10^{17}$ ions cm^{-3} and arranges them so that there

is a particular time-averaged[2] spatial distribution of the ions. The number of particles involved is enormous, and the situation appears far too complex for mathematical treatment.

However, there exist conceptual techniques for tackling complex situations. One of them is model building. This involves conceiving a model that contains only the essential features of the real situation. All the thinking and mathematical analysis is done on the (relatively simple) model and then the theoretical predictions are compared with the experimental behavior of the real system. A good model simulates nature. If the model yields wrong answers, then one tries again by changing the imagined model until one arrives at a model, the theoretical predictions of which agree well with experimental observations.

The genius of Debye and Hückel lay in their formulation of a very simple but powerful model for the time-averaged distribution of ions in very dilute solutions of electrolytes. From this distribution they were able to obtain the electrostatic potential contributed by the surrounding ions to the total electrostatic potential at the reference ion and hence the chemical-potential change arising from ion–ion interactions [Eq.(3.3)]. Attention will now be focused on their approach.

The electrolytic solution consists of solvated ions and water molecules. The first step in the Debye–Hückel approach is to select arbitrarily any one ion out of the assembly and call it a *reference ion* or *central ion.* Only the reference ion is given the individuality of a discrete charge. What is done with the water molecules and the remaining ions? The water molecules are looked upon as a continuous dielectric medium. The remaining ions of the solution (i.e., all ions except the central ion) lapse into anonymity, their charges being "smeared out" into a continuous spatial distribution of charge (Fig. 3.6). Whenever the concentration of ions of one sign exceeds that of the opposite sign, there will arise a net or excess charge in the particular region under consideration. Obviously, the total charge in the atmosphere must be of opposite sign and exactly equal to the charge on the reference ion.

Thus, the electrolytic solution is considered to consist of a central ion standing alone in a continuum. Thanks to the water molecules, this continuum acquires a dielectric constant (taken to be the value for bulk water). The charges of the discrete ions that populate the environment of the central ion are thought of as smoothed out and contribute to the continuum dielectric a net charge density (excess charge per unit volume). In this way, water enters the analysis in the guise of a dielectric constant ε; and the ions, except the specific one chosen as the central ion, in the form of an excess charge density ϱ (Fig. 3.7).

---

[2]Using an imaginary camera (with exposure time of $\sim 10^{-12}$ s), suppose that it were possible to take snapshots of the ions in an electrolytic solution. Different snapshots would show the ions distributed differently in the space containing the solution, but the scrutiny of a large enough number of snapshots (say, $\sim 10^{12}$) would permit one to recognize a certain average distribution characterized by average positions of the ions; this is the time-averaged spatial distribution of the ions.

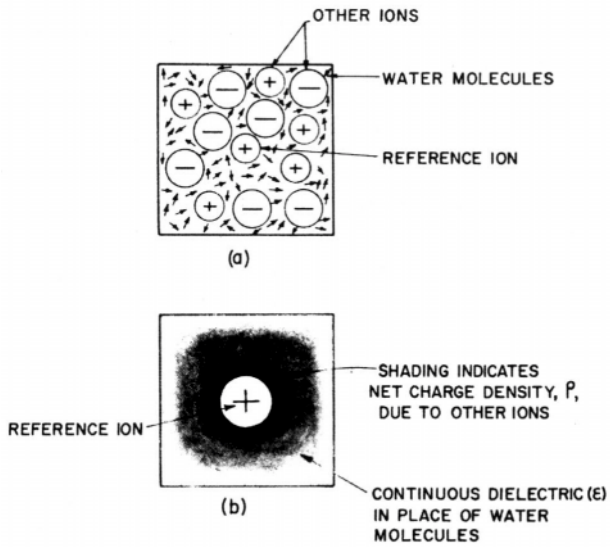

Fig. 3.6. A schematic comparison of (a) the assembly of ions and solvent molecules that constitute a real electrolytic solution and (b) the Debye–Hückel picture in which a reference ion is surrounded by net charge density ϱ due to the surrounding ions and a dielectric continuum of the same dielectric constant ε as the bulk solvent.

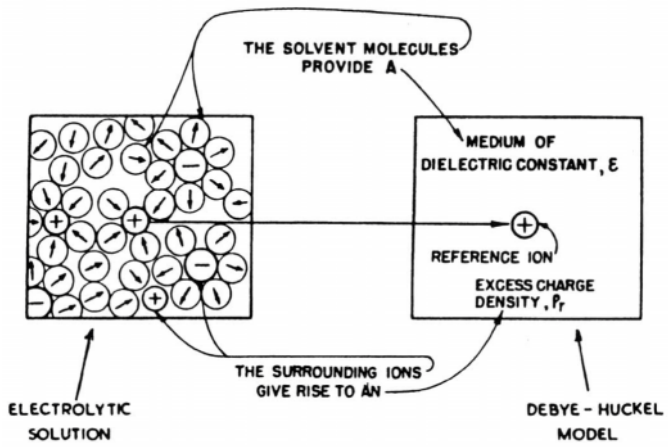

Fig. 3.7. The Debye–Hückel model is based upon selecting one ion as a reference ion, replacing the solvent molecules by a continuous medium of dielectric constant ε and the remaining ions by an excess charge density ϱ_r (the shading usually used in this book to represent the charge density is not indicated in this figure).

Hence, the complicated problem of the time-averaged distribution of ions inside an electrolytic solution reduces, in the Debye–Hückel model, to the mathematically simpler problem of finding out how the excess charge density ρ varies with distance r from the central ion.

An objection may be raised at this point. The electrolytic solution as a whole is electroneutral, i.e., the net charge density ρ is zero. Then why is not $\rho = 0$ everywhere?

So as not to anticipate the detailed discussion, an intuitive answer will first be given. If the central ion is, for example, positive, it will exert an attraction for negative ions; hence, there should be a greater aggregation of negative ions than of positive ions in the neighborhood of the central positive ion, i.e., $\rho \neq 0$. An analogous situation, but with a change in sign, obtains near a central negative ion. At the same time, the thermal forces are knocking the ions about in all directions and trying to establish electroneutrality, i.e., the thermal motions try to smooth everything to $\rho = 0$. Thus, the time average of the electrostatic forces of ordering and the thermal forces of disordering is a local excess of negative charge near a positive ion and an excess of positive charge near a negative ion. Of course, the excess positive charge near a negative ion compensates for the excess negative charge near a positive ion, and the overall effect is electroneutrality, i.e., a ρ of zero for the whole solution.

3.3.3. Charge Density near the Central Ion Is Determined by Electrostatics: Poisson's Equation

Consider an infinitesimally small volume element dV situated at a distance r from the arbitrarily selected central ion, upon which attention is to be fixed during the discussion (Fig. 3.8), and let the net charge density inside the volume element be ρ_r. Further, let the average[3] electrostatic potential in the volume element be ψ_r. The question is: What is the relation between the excess density ρ_r in the volume element and the time-averaged electrostatic potential ψ_r?

One relation between ρ_r and ψ_r is given by Poisson's equation (Appendix 3.1). There is no reason to doubt that there is spherically symmetrical distribution of positive and negative charge and therefore excess charge density around a given central ion. Hence, Poisson's equation can be written as

$$\frac{1}{r^2}\frac{d}{dr}\left(r^2\frac{d\psi_r}{dr}\right) = -\frac{4\pi}{\varepsilon}\rho_r \tag{3.4}$$

where ε is the dielectric constant of the medium and is taken to be that of bulk water, an acceptable approximation for dilute solutions.

---

[3] Actually, there are discrete charges in the neighborhood of the central ion and therefore discontinuous variations in the potential. But because in the Debye–Hückel model the charges are smoothed out, the potential is averaged out.

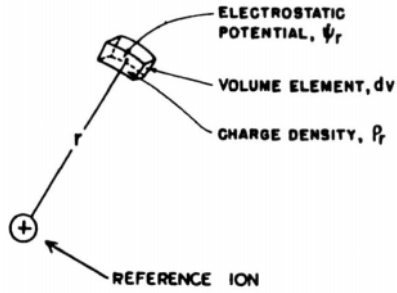

Fig. 3.8. At a distance r from the reference ion, the excess charge density and electrostatic potential in an infinitesimal volume element dV are ϱ_r and ψ_r, respectively.

3.3.4. Excess Charge Density near the Central Ion Is Given by a Classical Law for the Distribution of Point Charges in a Coulombic Field

The excess charge density in the volume element dV is equal to the total ion density (total number of ions per unit volume) times the charge on these ions. Let there be, per unit volume, n_1 ions of type 1, each bearing charge z_1e_0, n_2 of type 2 with charge z_2e_0, and n_i of type i with charge z_ie_0, where z_i is the valence of the ion and e_0 is the electronic charge. Then, the excess charge density ϱ_r in the volume element dV is given by

$$\varrho_r = n_1z_1e_0 + n_2z_2e_0 + \ldots + n_iz_ie_0 \tag{3.5}$$

$$= \sum n_iz_ie_0 \tag{3.6}$$

In order to proceed further, one must link up the unknown quantities $n_1, n_2, \ldots, n_i, \ldots$ to known quantities. The link is made on the basis of the Boltzmann distribution law of classical statistical mechanics. Thus, one writes

$$n_i = n_i^0 e^{-U/(kT)} \tag{3.7}$$

where U can be described either as the change in potential energy of the i particles when their concentration in the volume element dV is changed from the bulk value n_i^0 to n_i or as the work that must be done by a hypothetical external agency against the time average of the electrical and other forces between ions in producing the above

concentration change. Since the potential energy U relates to the time average of the forces between ions rather than to the actual forces for a given distribution, it is also known as the *potential of average force.*

If there are no ion–ion interactional forces, $U = 0$; then, $n_i = n_i^0$, which means that the local concentration would be equal to the bulk concentration. If the forces are attractive, then the potential-energy change U is negative (i.e., negative work is done by the hypothetical external agency) and $n_i > n_i^0$; there is a local accumulation of ions in excess of their bulk concentrations. If the forces are repulsive, the potential-energy change is positive (i.e., the work done by the external agency is positive) and $n_i < n_i^0$; there is local depletion of ions.

In the first instance, and as a first approximation valid for very dilute solutions, one may ignore all types of ion–ion interactions except those deriving from simple Coulombic[4] forces. Thus, short-range interactions (e.g., dispersion interactions) are excluded. This is a fundamental assumption of the Debye–Hückel theory. Then the potential of average force U simply becomes the *Coulombic* potential energy of an ion of charge $z_i e_0$ in the volume element dV, i.e., the charge $z_i e_0$ on the ion times the electrostatic potential ψ_r in the volume element dV. That is,

$$U = z_i e_0 \psi_r \tag{3.8}$$

The Boltzmann distribution law (3.7) thus assumes the form

$$n_i = n_i^0 e^{-z_i e_0 \psi_r/(kT)} \tag{3.9}$$

Now that n_i, the concentration of the ionic species i in the volume element dV, has been related to its bulk concentration n_i^0, the expression (3.6) for the excess charge density in the volume element dV becomes

$$\varrho_r = \sum_i n_i z_i e_0 = \sum_i n_i^0 z_i e_0 e^{-z_i e_0 \psi_r/(kT)} \tag{3.10}$$

3.3.5. A Vital Step in the Debye–Hückel Theory of the Charge Distribution around Ions: Linearization of the Boltzmann Equation

At this point of the theory, Debye and Hückel made a move that was not only mathematically expedient but also turned out to be wise. They decided to carry out the

---

[4]In this book, the term *Coulombic* is restricted to forces (with r^{-2} dependence on distance) which are based directly on Coulomb's law. More complex forces, e.g., those which vary as r^{-4} or r^{-7}, may occur as a net force from the combination of several different Coulombic interactions. Nevertheless, such more complex results of the interplay of several Coulombic forces will be called *non-Coulombic.*

analysis only for systems in which the average electrostatic potential ψ_r would be much smaller than the thermal energy kT. Then:

$$z_i e_0 \psi_r << kT \quad \text{or} \quad \frac{z_i e_0 \psi_r}{kT} << 1 \tag{3.11}$$

Based on this assumption, one can expand the exponential of Eq. (3.10) in a Taylor series, i.e.,

$$e^{-z_i e_0 \psi_r/(kT)} = 1 - \frac{z_i e_0 \psi_r}{kT} + \frac{1}{2}\left(\frac{z_i e_0 \psi_r}{kT}\right)^2 + \ldots \tag{3.12}$$

and neglect all except the first two terms. Thus, in Eq. (3.10),

$$\varrho_r = \sum_i n_i^0 z_i e_0 \left(1 - \frac{z_i e_0 \psi_r}{kT}\right) \tag{3.13}$$

$$= \sum_i n_i{}^0 z_i e_0 - \sum_i \frac{n_i^0 z_i^2 e_0^2 \psi_r}{kT} \tag{3.14}$$

The first term $\Sigma n_i^0 z_i e_0$ gives the charge on the electrolytic solution as a whole. This is zero because the solution as a whole must be electrically neutral. The local excess charge densities near ions cancel out because the excess positive charge density near a negative ion is compensated for by an excess negative charge density near a positive ion. Hence,

$$\sum_i n_i^0 z_i e_0 = 0 \tag{3.15}$$

and one is left with

$$\varrho_r = -\sum_i \frac{n_i^0 z_i^2 e_0^2 \psi_r}{kT} \tag{3.16}$$

3.3.6. The Linearized Poisson–Boltzmann Equation

The stage is now set for the calculation of the potential ψ_r and the charge density ϱ_r in terms of known parameters of the solution.

Notice that one has obtained two expressions for the charge density ϱ_r in the volume element dV at a distance r from the central ion. One has the Poisson equation [Eq. (3.4)]

$$\varrho_r = -\frac{\varepsilon}{4\pi}\left[\frac{1}{r^2}\frac{d}{dr}\left(r^2\frac{d\psi_r}{dr}\right)\right] \tag{3.17}$$

and one also has the "linearized" Boltzmann distribution

$$\varrho_r = -\sum_i \frac{n_i^0 z_i^2 e_0^2 \psi_r}{kT} \tag{3.18}$$

where Σ_i refers to the summation over all species of ions typified by i.

If one equates these two expressions, one can obtain the linearized Poisson–Boltzmann (P–B) expression

$$\frac{1}{r^2}\frac{d}{dr}\left(r^2\frac{d\psi_r}{dr}\right) = \left(\frac{4\pi}{\varepsilon kT}\sum_i n_i^0 z_i^2 e_0^2\right)\psi_r \tag{3.19}$$

The constants in the right-hand parentheses can all be lumped together and called a new constant κ^2, i.e.,

$$\kappa^2 = \frac{4\pi}{\varepsilon kT}\sum_i n_i^0 z_i^2 e_0^2 \tag{3.20}$$

At this point, the symbol κ is used only to reduce the tedium of writing. It turns out later, however, that κ is not only a shorthand symbol; it contains information concerning several fundamental aspects of the distribution of ions around an ion in solution. In Chapter 6 it will be shown that it also contains information concerning the distribution of charges near a metal surface in contact with an ionic solution. In terms of κ, the linearized P–B expression (3.19) is

$$\frac{1}{r^2}\frac{d}{dr}\left(r^2\frac{d\psi_r}{dr}\right) = \kappa^2\psi_r \tag{3.21}$$

3.3.7. Solution of the Linearized P–B Equation

The rather messy-looking linearized P–B equation (3.21) can be tidied up by a mathematical trick. Introducing a new variable μ defined by

$$\psi_r = \frac{\mu}{r} \tag{3.22}$$

one has

$$\frac{d\psi_r}{dr} = \frac{d}{dr}\frac{\mu}{r} = -\frac{\mu}{r^2} + \frac{1}{r}\frac{d\mu}{dr}$$

and therefore

$$\frac{1}{r^2}\frac{d}{dr}\left(r^2\frac{d\psi_r}{dr}\right) = \frac{1}{r^2}\frac{d}{dr}\left(-\mu + r\frac{d\mu}{dr}\right)$$

$$= \frac{1}{r^2}\left(-\frac{d\mu}{dr} + r\frac{d^2\mu}{dr^2} + \frac{d\mu}{dr}\right)$$

$$= \frac{1}{r}\frac{d^2\mu}{dr^2} \tag{3.23}$$

Hence, the differential equation (3.21) becomes

$$\frac{1}{r}\frac{d^2\mu}{dr^2} = \kappa^2\frac{\mu}{r} \tag{3.24}$$

or

$$\frac{d^2\mu}{dr^2} = \kappa^2\mu \tag{3.25}$$

To solve this differential equation, it is recalled that the differentiation of an exponential function results in the multiplication of that function by the constant in the exponent. For example,

$$\frac{d}{dr}e^{\pm\kappa r} = \pm\kappa e^{\pm\kappa r} \tag{3.26}$$

and

$$\frac{d^2}{dr^2}e^{\pm\kappa r} = \kappa^2 e^{\pm\kappa r}$$

Hence, if μ is an exponential function of r, one will obtain a differential equation of the form of Eq. (3.25). In other words, the "primitive" or "origin" of the differential equation must have had an exponential in κr.

Two possible exponential functions, however, would lead to the same final differential equation; one of them would have a positive exponent and the other a negative one [Eq. (3.26)]. The general solution of the linearized P–B equation can therefore be written as

$$\mu = Ae^{-\kappa r} + Be^{+\kappa r} \tag{3.27}$$

where A and B are constants to be evaluated. Or, from Eq. (3.22),

$$\psi_r = A\frac{e^{-\kappa r}}{r} + B\frac{e^{+\kappa r}}{r} \tag{3.28}$$

The constant B is evaluated by using the boundary condition that far enough from a central ion situated at $r = 0$, the thermal forces completely dominate the Coulombic forces, which decrease as r^2, and there is electroneutrality (i.e., the electrostatic potential ψ_r vanishes at distances sufficiently far from such an ion, $\psi_r \to 0$ as $r \to \infty$). This condition would be satisfied only if $B = 0$. Thus, if B had a finite value, Eq. (3.28) shows that the electrostatic potential would shoot up to infinity (i.e., $\psi_r \to \infty$ as $r \to \infty$), a physically unreasonable proposition. Hence,

$$\psi_r = A\frac{e^{-\kappa r}}{r} \tag{3.29}$$

To evaluate the integration constant A, a hypothetical condition will be considered in which the solution is so dilute and on the average the ions are so far apart that there is a negligible interionic field. Further, the central ion is assumed to be a point charge, i.e., to have a radius negligible compared with the distances otherwise to be considered. Hence, the potential near the central ion is, in this special case, simply that due to an isolated point charge of value $z_i e_0$.

This is given directly from Coulomb's law as

$$\psi_r = \frac{z_i e_0}{\varepsilon r} \tag{3.30}$$

At the same time, for this hypothetical solution in which the concentration tends to zero, i.e., $n_i^0 \to 0$, it is seen from Eq. (3.20) that $\kappa \to 0$. Thus, in Eq. (3.29), $e^{-\kappa r} \to 1$, and one has

$$\psi_r = \frac{A}{r} \tag{3.31}$$

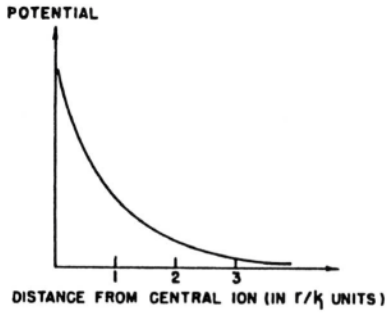

Fig. 3.9. The variation of the electrostatic potential ψ as a function of distance from the central ion expressed in units of r/κ.

Hence, by combining Eqs. (3.30) and (3.31),

$$A = \frac{z_i e_0}{\varepsilon} \tag{3.32}$$

By introducing this expression for A into Eq. (3.29), the result is

$$\psi_r = \frac{z_i e_0}{\varepsilon} \frac{e^{-\kappa r}}{r} \tag{3.33}$$

Here then is the appropriate solution of the *linearized* P–B equation (3.21). It shows how the electrostatic potential varies with distance r from an arbitrarily chosen reference ion (Fig. 3.9).

3.3.8. The Ionic Cloud around a Central Ion

In the imaginative Debye–Hückel model of a dilute electrolytic solution, a reference ion sitting at the origin of the spherical coordinate system is surrounded by the smoothed-out charge of the other ions. Further, because of the local inequalities in the concentrations of the positive and negative ions, the smoothed-out charge of one sign does not (locally) cancel out the smoothed-out charge of the opposite sign; there is a local excess charge density of one sign opposite to that of the central ion.

Now, as explained in Section 3.3.2, the principal objective of the Debye–Hückel theory is to calculate the time-averaged spatial distribution of the excess charge density around a reference ion. How is this objective attained?

The Poisson equation (3.4) relates the potential at r from the sample ion to the charge density at r, i.e.,

$$\frac{1}{r^2}\frac{d}{dr}\left(r^2\frac{d\psi_r}{dr}\right)=-\frac{4\pi}{\varepsilon}\varrho_r \tag{3.4}$$

Further, one has the linearized P–B equation

$$\frac{1}{r^2}\frac{d}{dr}\left(r^2\frac{d\psi_r}{dr}\right)=\kappa^2\psi_r \tag{3.21}$$

From these two equations, one has the linear relation between excess charge density and potential, i.e.,

$$\varrho_r=-\frac{\varepsilon}{4\pi}\kappa^2\psi_r \tag{3.34}$$

and by inserting the solution (3.33) for the linearized P–B equation, the result is

$$\varrho_r=-\frac{z_i e_0}{4\pi}\kappa^2\frac{e^{-\kappa r}}{r} \tag{3.35}$$

Here then is the desired expression for the spatial distribution of the charge density with distance r from the central ion (Fig. 3.10). Since the excess charge density results from an unequal distribution of positive and negative ions, Eq. (3.35) also describes the distribution of ions around a reference or sample ion.

To understand this distribution of ions, however, one must be sufficiently attuned to mathematical language to read the physical significance of Eq. (3.35). The physical ideas implicit in the distribution will therefore be stated in pictorial terms. One can say that the central reference ion is surrounded by a cloud, or atmosphere, of excess charge (Fig. 3.11). This ionic cloud extends into the solution (i.e., r increases), and the excess

Fig. 3.10. The variation of the excess charge density ϱ as a function of distance from the central ion.

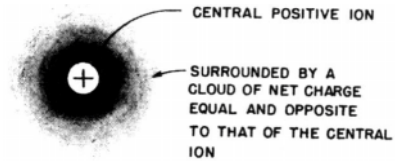

Fig. 3.11. The distribution of excess charge density around a central ion can be pictured as a cloud, or atmosphere, of net charge around the central ion.

charge density ϱ decays with distance r in an exponential way. The excess charge residing on the ion cloud is opposite in sign to that of the central ion. Thus, a positively charged reference ion has a negatively charged ion atmosphere, and vice versa (Fig. 3.12).

Up to now, the charge density at a given distance has been discussed. The total excess charge contained in the ionic atmosphere that surrounds the central ion can, however, easily be computed. Consider a spherical shell of thickness dr at a distance r from the origin, i.e., from the center of the reference ion (Fig. 3.13). The charge dq in this thin shell is equal to the charge density ϱ_r times the volume $4\pi r^2 dr$ of the shell, i.e.,

$$dq = \varrho_r 4\pi r^2 dr \tag{3.36}$$

The total charge q_{cloud} contained in the ion atmosphere is obtained by summing the charges dq contained in all the infinitesimally thick spherical shells. In other words, the total excess charge surrounding the reference ion is computed by integrating dq (which is a function of the distance r from the central ion) from a lower limit corresponding to the distance from the central ion at which the cloud is taken to commence to the point where the cloud ends. Now, the ion atmosphere begins at the surface of the ion, so the lower limit depends upon the model of the ion. The first model

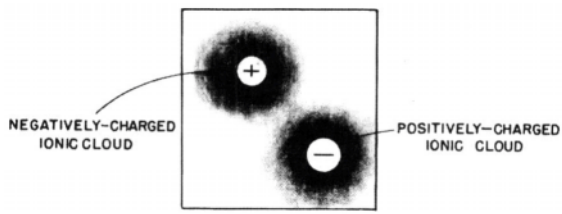

Fig. 3.12. A positively charged ion has a negatively charged ionic cloud, and vice versa.

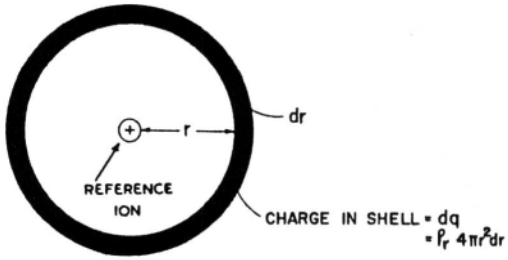

Fig. 3.13. A spherical shell of thickness *dr* at a distance *r* from the center of the reference ion.

chosen by Debye and Hückel was that of point-charge ions, in which case the lower limit is $r = 0$. The upper limit for the integration is $r \to \infty$ because the charge of the ionic cloud decays exponentially into the solution and becomes zero only in the limit $r \to \infty$.

Thus,

$$q_{\text{cloud}} = \int_{r=0}^{r\to\infty} dq = \int_{r=0}^{r\to\infty} \varrho_r 4\pi r^2 dr \tag{3.37}$$

and by substituting for ϱ_r from Eq. (3.35), the result is

$$q_{\text{cloud}} = -\int_{r=0}^{r\to\infty} \frac{z_i e_0}{4\pi} \kappa^2 \frac{e^{-\kappa r}}{r} 4\pi r^2 dr$$

$$= -z_i e_0 \int_{r=0}^{r\to\infty} e^{-\kappa r} (\kappa r)\, d(\kappa r) \tag{3.38}$$

The integration can be done by parts (Appendix 3.2), leading to the result

$$q_{\text{cloud}} = -z_i e_0 \tag{3.39}$$

which means that a central ion of charge $+z_i e_0$ is enveloped by a cloud containing a total charge of $-z_i e_0$ (Fig. 3.14). Thus, the total charge on the surrounding volume is just equal and opposite to that on the reference ion. This is of course precisely how things should be so that there can be electroneutrality for the ionic solution taken as a whole; a given ion, together with its cloud, has a zero net charge.

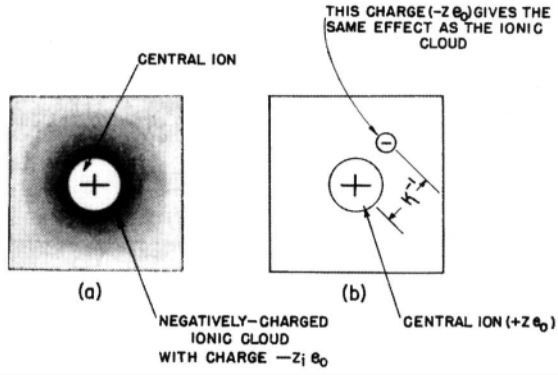

Fig. 3.14. The total charge $-z_i e_0$ on the ionic cloud is just equal and opposite to the charge $+z_i e_0$ on the central ion.

How is this equal and opposite charge of the ion atmosphere distributed in the space around the central ion? It is seen from Eqs. (3.35) and (3.36) that the net charge in a spherical shell of thickness dr and at a distance r from the origin is

$$dq = -z_i e_0 e^{-\kappa r} \kappa^2 r \, dr \tag{3.40}$$

Thus, the excess charge on a spherical shell varies with r and has a maximum value for a value of r given by

$$\begin{aligned} 0 &= \frac{dq}{dr} \\ &= \frac{d}{dr}[-z_i e_0 \kappa^2 (e^{-\kappa r} r)] \\ &= -z_i e_0 \kappa^2 \frac{d}{dr}(e^{-\kappa r} r) \\ &= -z_i e_0 \kappa^2 (e^{-\kappa r} - r\kappa e^{-\kappa r}) \end{aligned} \tag{3.41}$$

Since $(z_i e_0 \kappa^2)$ is finite, Eq. (3.41) can be true only when

$$0 = e^{-\kappa r} - r\kappa e^{-\kappa r}$$

or

$$r = \kappa^{-1} \tag{3.42}$$

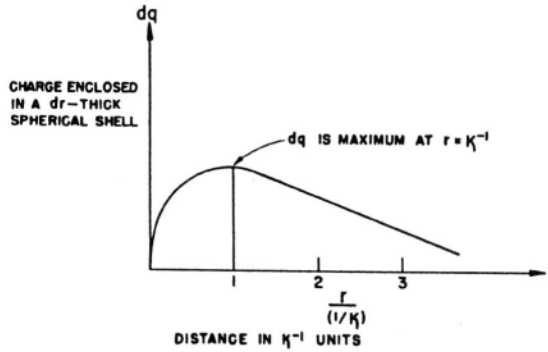

Fig. 3.15. The distance variation (in κ^{-1} units) of the charge dq enclosed in a dr-thick spherical shell, showing that dq is a maximum at $r = \kappa^{-1}$.

Hence, the maximum value of the charge contained in a spherical shell (of infinitesimal thickness dr) is attained when the spherical shell is at a distance $r = \kappa^{-1}$ from the reference ion (Fig. 3.15). For this reason (but see also Section 3.3.9), κ^{-1} is known as the *thickness*, or *radius*, of the ionic cloud that surrounds a reference ion. An elementary dimensional analysis [e.g., of Eq. (3.43)] will indeed reveal that κ^{-1} has the dimensions of length. Consequently, κ^{-1} is sometimes referred to as the *Debye–Hückel length.*

It may be recalled that κ^{-1} is given [from Eq. (3.20)] by

$$\kappa^{-1} = \left(\frac{\varepsilon kT}{4\pi} \frac{1}{\sum_i n_i^0 z_i^2 e_0^2} \right)^{1/2} \tag{3.43}$$

As the concentration tends toward zero, the cloud tends to spread out increasingly (Fig. 3.16). Values of the thickness of the ion atmosphere for various concentrations of the electrolyte are presented in Table 3.2.

3.3.9. Contribution of the Ionic Cloud to the Electrostatic Potential ψ_r at a Distance r from the Central Ion

An improved feel for the effects of ionic clouds emerges from considering the following interesting problem. Imagine, in a thought experiment, that the charge on the ionic cloud does not exist. There is only one charge now, that on the central ion. What is the potential at distance r from the central ion? It is simply given by the familiar formula for the potential at a distance r from a single charge, namely,

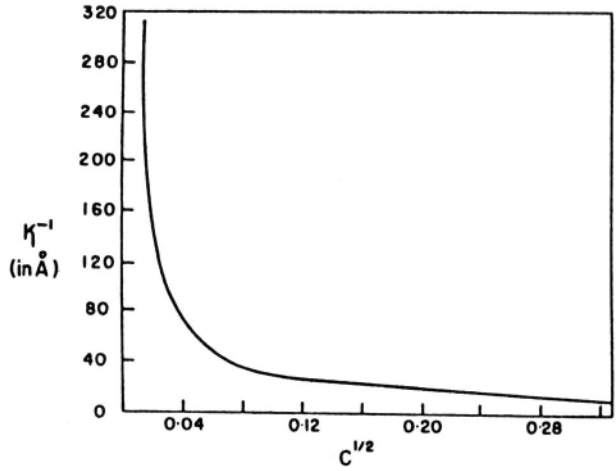

Fig. 3.16. The variation in the thickness κ^{-1} of the ionic cloud as a function of electrolyte concentration (1 Å = 0.1 nm).

$$\psi_r = \frac{z_i e_0}{\varepsilon r} \tag{3.44}$$

Then let the charge on the cloud be switched on. The potential ψ_r at the distance r from the central ion is no longer given by the central ion only. It is given by the law of superposition of potentials (Fig. 3.17); i.e., ψ_r is the sum of the potential due to the central ion and that due to the ionic cloud

$$\psi_r = \psi_{\text{ion}} + \psi_{\text{cloud}} \tag{3.45}$$

TABLE 3.2

Thickness of Ionic Atmosphere (nm) at Various Concentrations and for Various Types of Salts

Concentration (mol dm^{-3})	Type of Salt			
	1:1	1:2	2:2	1:3
10^{-4}	30.4	17.6	15.2	12.4
10^{-3}	9.6	5.55	4.81	3.93
10^{-2}	3.04	1.76	1.52	1.24
10^{-1}	0.96	0.55	0.48	0.39

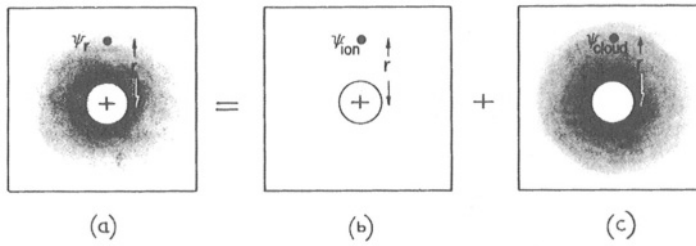

Fig. 3.17. The superposition of the potential ψ_{ion} due to the ion and the potential ψ_{cloud} due to the cloud yields the total potential at a distance r from the central ion.

The contribution ψ_{cloud} can thus be easily found. One rearranges Eq. (3.45) to read

$$\psi_{cloud} = \psi_r - \psi_{ion} \tag{3.46}$$

and substitutes for ψ_{ion} with Eq. (3.44) and for ψ_r with the Debye–Hückel expression [Eq. (3.33)]. Then,

$$\psi_{cloud} = \frac{z_i e_0}{\varepsilon} \frac{e^{-\kappa r}}{r} - \frac{z_i e_0}{\varepsilon r}$$

$$= \frac{z_i e_0}{\varepsilon r}(e^{-\kappa r} - 1) \tag{3.47}$$

The value of κ [*cf.* Eq. (3.20)] is proportional to $\Sigma n_i^0 z_i^2 e_0^2$. In sufficiently dilute solutions, $\Sigma n_i^0 z_i^2 e_0^2$ can be taken as sufficiently small to make $\kappa r << 1$,

$$e^{-\kappa r} - 1 \approx 1 - \kappa r - 1 \approx -\kappa r \tag{3.48}$$

and based on this approximation,

$$\psi_{cloud} = -\frac{z_i e_0}{\varepsilon \kappa^{-1}} \tag{3.49}$$

By introducing the expressions (3.44) and (3.49) into the expression (3.45) for the total potential ψ_r at a distance r from the central ion, it follows that

$$\psi_r = \frac{z_i e_0}{\varepsilon r} - \frac{z_i e_0}{\varepsilon \kappa^{-1}} \tag{3.50}$$

The second term, which arises from the cloud, reduces the value of the potential to a value less than that if there were no cloud. This is consistent with the model; the cloud has a charge opposite to that on the central ion and must therefore alter the potential in a sense opposite to that due to the central ion.

The expression

$$\psi_{\text{cloud}} = -\frac{z_i e_0}{\varepsilon \kappa^{-1}} \tag{3.49}$$

leads to another, and helpful, way of looking at the quantity κ^{-1}. It is seen that ψ_{cloud} is independent of r, and therefore the contribution of the cloud to the potential *at the site of the point-charge central ion* can be considered to be given by Eq. (3.49). But, if the entire charge of the ionic atmosphere [which is $-z_i e_0$ as required by electroneutrality—Eq. (3.39)] were placed at a distance κ^{-1} from the central ion, then the potential produced at the reference ion would be $-z_i e_0/(\varepsilon\kappa^{-1})$. It is seen therefore from Eq. (3.49) that the effect of the ion cloud, namely, ψ_{cloud}, is equivalent to that of a single charge, equal in magnitude but opposite in sign to that of the central ion, placed at a distance κ^{-1} from the reference ion (Fig. 3.18). This is an added and more important reason that the quantity κ^{-1} is termed the effective thickness or radius of the ion atmosphere surrounding a central ion (see Section 3.3.8).

3.3.10. The ionic Cloud and the Chemical-Potential Change Arising from Ion–Ion Interactions

It will be recalled (see Section 3.3.1) that it was the potential at the surface of the reference ion which needed to be known in order to calculate the chemical-potential change $\Delta\mu_{i-I}$ arising from the interactions between a particular ionic species i and the rest of the ions of the solution, i.e., one needed to know ψ_{cloud} in Eq. (3.3),

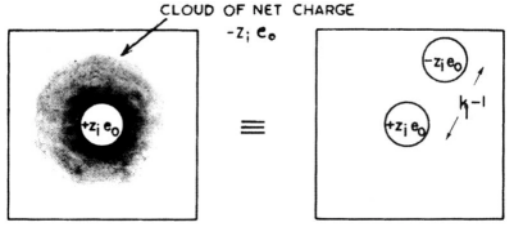

Fig. 3.18. The contribution ψ_{cloud} of the ionic cloud to the potential at the central ion is equivalent to the potential due to a single charge, equal in magnitude and opposite sign to that of the central ion, placed at a distance κ^{-1} from the central ion.

$$\Delta\mu_{i-I} = \frac{N_A z_i e_0}{2} \psi_{\text{cloud}} \tag{3.3}$$

It was to obtain this potential ψ that Debye and Hückel conceived their model of an ionic solution. The analysis presented the picture of an ion being enveloped in an ionic cloud. What is the origin of the ionic cloud? It is born of the interactions between the central ion and the ions of the environment. If there were no interactions (e.g., Coulombic forces between ions), thermal forces would prevail, distribute the ions randomly ($\varrho = 0$), and wash out the ionic atmosphere. It appears therefore that the simple ionic cloud picture has not only led to success in describing the distribution of ions but also given the electrostatic potential ψ_{cloud} at the surface of a reference ion due to the interactions between this reference ion and the rest of the ions in the solution (the quantity required for reasons explained in Section 3.3.1).

Thus, the expression (3.49) for ψ_{cloud} can be substituted for ψ in Eq. (3.3) with the result that

$$\Delta\mu_{i-I} = -\frac{N_A (z_i e_0)^2}{2\varepsilon\kappa^{-1}} \tag{3.51}$$

The Debye–Hückel ionic-cloud model for the distribution of ions in an electrolytic solution has permitted the theoretical calculation of the chemical-potential change arising from ion–ion interactions. How is this theoretical expression to be checked, i.e., connected with a measured quantity? It is to this testing of the Debye–Hückel theory that attention will now be turned.

3.4. ACTIVITY COEFFICIENTS AND ION–ION INTERACTIONS

3.4.1. Evolution of the Concept of an Activity Coefficient

The existence of ions in solution, of interactions between these ions, and of a chemical-potential change $\Delta\mu_{i-I}$ arising from ion–ion interactions have all been taken to be self-evident in the treatment hitherto presented here. This, however, is a modern point of view. The thinking about electrolytic solutions actually developed along a different path.

Ionic solutions were at first treated in the same way as nonelectrolytic solutions, though the latter do not contain (interacting) charged species. The starting point was the classical thermodynamic formula for the chemical potential μ_i of a nonelectrolyte solute

$$\mu_i = \mu_i^0 + RT \ln x_i \tag{3.52}$$

In this expression, x_i is the concentration[5] of the solute in mole fraction units, and μ_i^0 is its chemical potential in the standard state, i.e., when x_i assumes a standard or normalized value of unity

$$\mu_i = \mu_i^0 \quad \text{when} \quad x_i = 1 \tag{3.53}$$

Since the solute particles in a solution of a nonelectrolyte are uncharged, they do not engage in long-range Coulombic interactions. The short-range interactions arising from dipole–dipole or dispersion forces become significant only when the mean distance between the solute particles is small, i.e., when the concentration of the solute is high. Thus, one can to a good approximation say that there are no interactions between solute particles in dilute nonelectrolyte solutions. Hence, if Eq. (3.52) for the chemical potential of a solute in a nonelectrolyte solution (with noninteracting particles) is used for the chemical potential of an ionic species *i* in an electrolytic solution, then it is tantamount to ignoring the long-range Coulombic interactions between ions. In an actual electrolytic solution, however, ion–ion interactions operate whether one ignores them or not. It is obvious therefore that measurements of the chemical potential μ_i of an ionic species—or, rather, measurements of any property that depends on the chemical potential—would reveal the error in Eq. (3.52), which is blind to ion–ion interactions. In other words, experiments show that *even in dilute solutions,*

$$\mu_i - \mu_i^0 \neq RT \ln x_i$$

In this context, a frankly empirical approach was adopted by earlier workers not yet blessed by Debye and Hückel's light. Solutions that obeyed Eq. (3.52) were characterized as *ideal* solutions since this equation applies to systems of noninteracting solute particles, i.e., ideal particles. Electrolytic solutions that do not obey the equation were said to be *nonideal.* In order to use an equation of the form of Eq. (3.52) to treat nonideal electrolytic solutions, an empirical correction factor f_i was introduced by Lewis as a modifier of the concentration term[6]

$$\mu_i - \mu_i^0 = RT \ln x_i f_i \tag{3.54}$$

---

[5]The value of x_i in the case of an electrolyte derives from the number of moles of ions of species *i* actually present in solution. This number need not be equal to the number of moles of *i* expected of dissolved electrolyte; if, for instance, the electrolyte is a potential one, then only a fraction of the electrolyte may react with the solvent to form ions, i.e., the electrolyte may be incompletely dissociated.

[6]The standard chemical potential μ_i^0 has the same significance here as in Eq. (3.52) for ideal solutions. Thus, μ_i^0 can be defined either as the chemical potential of an ideal solution in its standard state of $x_i = 1$ or as the chemical potential of a solution in its state of $x_i = 1$ and $f_i = 1$, i.e., $a_i = 1$. No real solution can have $f_i = 1$ when $x_i = 1$; so the standard state pertains to the same hypothetical solution as the standard state of an ideal solution.

It was argued that, in nonideal solutions, it was not just the analytical concentration x_i of species i, but its effective concentration $x_i f_i$ which determined the chemical-potential change $\mu_i - \mu_i^0$. This effective concentration $x_i f_i$ was also known as the *activity* a_i of the species i, i.e.,

$$a_i = x_i f_i \tag{3.55}$$

and the correction factor f_i, as the *activity coefficient.* For ideal solutions, the activity coefficient is unity, and the activity a_i becomes identical to the concentration x_i, i.e.,

$$a_i = x_i \quad \text{when} \quad f_i = 1 \tag{3.56}$$

Thus, the chemical-potential change in going from the standard state to the final state can be written as

$$\mu_i - \mu_i^0 = RT \ln x_i + RT \ln f_i \tag{3.57}$$

Equation (3.57) summarizes the empirical or formal treatment of the behavior of electrolytic solutions. Such a treatment cannot furnish a theoretical expression for the activity coefficient f_i. It merely recognizes that expressions such as (3.52) must be modified if significant interaction forces exist between solute particles.

3.4.2. The Physical Significance of Activity Coefficients

For a hypothetical system of ideal (noninteracting) particles, the chemical potential has been stated to be given by

$$\mu_i \text{ (ideal)} = \mu_i^0 + RT \ln x_i \tag{3.52}$$

For a real system of interacting particles, the chemical potential has been expressed in the form

$$\mu_i \text{ (real)} = \mu_i^0 + RT \ln x_i + RT \ln f_i \tag{3.57}$$

Hence, to analyze the physical significance of the activity coefficient term in Eq. (3.57), it is necessary to compare this equation with Eq. (3.52). It is obvious that when Eq. (3 52) is subtracted from Eq. (3.57), the difference [i.e., μ_i (real) – μ_i (ideal)] is the chemical-potential change $\Delta\mu_{i-I}$ arising from interactions between the solute particles (ions in the case of electrolyte solutions). That is,

$$\mu_i \text{(real)} - \mu_i \text{ (ideal)} = \Delta\mu_{i-I} \tag{3.58}$$

and therefore,

$$\Delta\mu_{i-I} = RT \ln f_i \tag{3.59}$$

Thus, the activity coefficient is a measure of the chemical-potential change arising from ion–ion interactions. There are several well-established methods of experimentally determining activity coefficients, and these methods are treated in adequate detail in standard treatises (see Further Reading at the end of this section).

Now, according to the Debye–Hückel theory, the chemical-potential change $\Delta\mu_{i-I}$ arising from ion–ion interactions has been shown to be given by

$$\Delta\mu_{i-I} = -\frac{N_A(z_i e_0)^2}{2\varepsilon\kappa^{-1}} \tag{3.51}$$

Hence, by combining Eqs. (3.51) and (3.58), the result is

$$RT \ln f_i = -\frac{N_A(z_i e_0)^2}{2\varepsilon\kappa^{-1}} \tag{3.60}$$

Thus, the Debye–Hückel ionic-cloud model for ion–ion interactions has permitted a theoretical calculation of activity coefficients resulting in Eq. (3.60).

The activity coefficient in Eq. (3.59) arises from the formula (3.57) for the chemical potential, in which the concentration of the species i is expressed in mole fraction units x_i. One can also express the concentration in moles per liter (1 liter = 1 dm^3) of solution (molarity) or in moles per kilogram of solvent (molality). Thus, alternative formulas for the chemical potential of a species i in an ideal solution read

$$\mu_i = \mu_i^0(c) + RT \ln c_i \tag{3.61}$$

and

$$\mu_i = \mu_i^0(m) + RT \ln m_i \tag{3.62}$$

where c_i and m_i are the molarity and molality of the species i, respectively, and $\mu_i^0(c)$ and $\mu_i^0(m)$ are the corresponding standard chemical potentials.

When the concentration of the ionic species in a real solution is expressed as a molarity c_i or a molality m_i, there are corresponding activity coefficients γ_c and γ_m and corresponding expressions for μ_i,

$$\mu_i = \mu_i^0(c) + RT \ln c_i + RT \ln \gamma_c \tag{3.63}$$

and

$$\mu_i = \mu_i^0(m) + RT \ln m_i + RT \ln \gamma_m \tag{3.64}$$

3.4.3. The Activity Coefficient of a Single Ionic Species Cannot Be Measured

Before the activity coefficients calculated on the basis of the Debye–Hückel model can be compared with experiment, there arises a problem similar to one faced in the discussion of ion–solvent interactions (Chapter 2). There, it was realized the heat of hydration of an individual ionic species could not be measured because such a measurement would involve the transfer of ions of only one species into a solvent instead of ions of two species with equal and opposite charges. Even if such a transfer were physically possible, it would result in a charged solution[7] and therefore an extra, undesired interaction between the ions and the electrified solution. The only way out was to transfer a neutral electrolyte (an equal number of positive and negative ions) into the solvent, but this meant that one could only measure the heat of interactions of a *salt* with the solvent and this experimental quantity could not be separated into the individual ionic heats of hydration.

Here, in the case of ion–ion interactions, the desired quantity is the activity coefficient f_i,[8] which depends through Eq. (3.57) on $\mu_i - \mu_i^0$. This means that one seeks the free-energy change of an ionic solution per mole of ions of a single species *i*. To measure this quantity, one would have a problem similar to that experienced with ion–solvent interactions, namely, the measurement of the change in free energy of a solution resulting from a change in the concentration of one ionic species only.

This change in free energy associated with the addition of one ionic species only would include an undesired work term representing the electrical work of interaction between the ionic species being added and the charged solution. To avoid free-energy changes associated with interacting with a solution, it is necessary that after a change in the concentration of the ionic species, the electrolytic solution should end up uncharged and electroneutral. This aim is easily accomplished by adding an electroneutral electrolyte containing the ionic species *i*. Thus, the concentration of sodium ions can be altered by adding sodium chloride. The solvent, water, maintains its electroneutrality when the uncharged ionic lattice (containing two ionic species of opposite charge) is dissolved in it.

When ionic lattices, i.e., salts, are dissolved instead of individual ionic species, one eliminates the problem of ending up with charged solutions but another problem emerges. If one increases the concentration of sodium ions by adding the salt sodium chloride, one has perforce to produce a simultaneous increase in the concentration of chloride ions. This means, however, that there are two contributions to the change in

---

[7]The solution may not be initially charged but will become so once an ionic species is added to it.

[8]The use of the symbol γ for the activity coefficients when the concentration is expressed in molarities and molalities should be noted. When the concentration is expressed as a mole fraction, f_i has been used here. For dilute solutions, the numerical values of activity coefficients for these different systems of units are almost the same.

free energy associated with a change in salt concentration: (1) the contribution of the positive ions and (2) the contribution of the negative ions.

Since neither the positive nor the negative ions can be added separately, the individual contributions of the ionic species to the free energy of the system are difficult to determine. Normally, one can only measure the activity coefficient of the net electrolyte, i.e., of at least two ionic species together. It is necessary therefore to establish a conceptual link between the activity coefficient of an electrolyte in solution (that quantity directly accessible to experiment) and that of only one of its ionic species [not accessible to experiment, but calculable theoretically from Eq. (3.60)].

3.4.4. The Mean Ionic Activity Coefficient

Consider a uni-univalent electrolyte MA (e.g., NaCl). The chemical potential of the $\mathbf{M}^+$ ions is [Eq. (3.57)]

$$\mu_{M^+} = \mu^0_{M^+} + RT \ln x_{M^+} + RT \ln f_{M^+} \tag{3.65}$$

and the chemical potential of the $\mathbf{A}^-$ ions is

$$\mu_{A^-} = \mu^0_{A^-} + RT \ln x_{A^-} + RT \ln f_{A^-} \tag{3.66}$$

Adding the two expressions, one obtains

$$\mu_{M^+} + \mu_{A^-} = (\mu^0_{M^+} + \mu^0_{A^-}) + RT \ln (x_{M^+} x_{A^-}) + RT \ln (f_{M^+} f_{A^-}) \tag{3.67}$$

What has been obtained here is the change in the free energy of the system due to the addition of 2 moles of ions—1 mole of $\mathbf{M}^+$ ions and 1 mole of $\mathbf{A}^-$ ions—which are contained in 1 mole of electroneutral salt MA.

Now, suppose that one is only interested in the *average* contribution to the free energy of the system from 1 mole of both $\mathbf{M}^+$ and $\mathbf{A}^-$ ions. One has to divide Eq. (3.67) by 2

$$\frac{\mu_{M^+} + \mu_{A^-}}{2} = \frac{\mu^0_{M^+} + \mu^0_{A^-}}{2} + RT \ln (x_{M^+} x_{A^-})^{1/2} + RT \ln (f_{M^+} f_{A^-})^{1/2} \tag{3.68}$$

At this stage, one can define several new quantities

$$\mu_{\pm} = \frac{\mu_{M^+} + \mu_{A^-}}{2} \tag{3.69}$$

$$\mu^0_{\pm} = \frac{\mu^0_{M^+} + \mu^0_{A^-}}{2} \tag{3.70}$$

$$x_{\pm} = (x_{M^+} x_{A^-})^{1/2} \tag{3.71}$$

and

$$f_{\pm} = (f_{M^+} f_{A^-})^{1/2} \tag{3.72}$$

What is the significance of these quantities $\mu_{\pm}$, $\mu_{\pm}^0$, $x_{\pm}$, and $f_{\pm}$? It is obvious they are all average quantities—the mean chemical potential $\mu_{\pm}$, the mean standard chemical potential $\mu_{\pm}^0$, the mean ionic mole fraction $x_{\pm}$, and the mean ionic-activity coefficient $f_{\pm}$. In the case of $\mu_{\pm}$ and $\mu_{\pm}^0$, the arithmetic mean (half the sum) is taken because free energies are additive, but in the case of $x_{\pm}$ and $f_{\pm}$, the geometric mean (the square root of the product) is taken because the effects of mole fraction and activity coefficient on free energy are multiplicative.

In this notation, Eq. (3.68) for the average contribution of a mole of ions to the free energy of the system becomes

$$\mu_{\pm} = \mu_{\pm}^0 + RT \ln x_{\pm} + RT \ln f_{\pm} \tag{3.73}$$

since a mole of ions is produced by the dissolution of half a mole of salt. In other words, $\mu_{\pm}$ is half the chemical potential μ_{MA} of the salt.[9]

$$\tfrac{1}{2}\mu_{MA} = \mu_{\pm} = \mu_{\pm}^0 + RT \ln x_{\pm} + RT \ln f_{\pm} \tag{3.74}$$

Thus, a clear connection has been set up between observed free-energy changes μ_{MA} consequent upon the change from a state in which the two ionic species of a salt are infinitely far apart to a state corresponding to the given concentration and its mean ionic-activity coefficient $f_{\pm}$. Hence the value of $f_{\pm}$ is experimentally measurable. What can be obtained from $f_{\pm}$ is the product of the individual ionic-activity coefficients [Eq. (3.72)]. The theoretical approach must be to calculate the activity coefficients f_+ and f_- for the positive and negative ions [Eq. (3.60)] and combine them through Eq. (3.72) into a mean ionic-activity coefficient $f_{\pm}$ which can be compared with the easily experimentally derived mean ionic-activity coefficient.

3.4.5. Conversion of Theoretical Activity-Coefficient Expressions into a Testable Form

Individual ionic-activity coefficients are experimentally inaccessible (Section 3.4.3); hence, it is necessary to relate the theoretical individual activity coefficient f_i

[9]The symbol μ_{MA} should not be taken to mean that *molecules* of MA exist in the solution; μ_{MA} is the observed free-energy change of the system resulting from the dissolution of a mole of electrolyte.

[Eq. (3.60)] to the experimentally accessible *mean* ionic-activity coefficient $f_\pm$ so that the Debye–Hückel model can be tested.

The procedure is to make use of the relation (3.72)

$$f_\pm = (f_{M^+} f_{A^-})^{1/2} \tag{3.72}$$

of which the general form for an electrolyte that dissolves to give ν_+ z_+-valent positive ions and ν_- z_--valent negative ions can be shown to be (Appendix 3.3)

$$f_\pm = (f_+^{\nu} f_-^{\nu})^{1/\nu} \tag{3.75}$$

where f_+ and f_- are the activity coefficients of the positive and negative ions, and

$$\nu = \nu_+ + \nu_- \tag{3.76}$$

By taking logarithms of both sides of Eq. (3.75), the result is

$$\ln f_\pm = \frac{1}{\nu} (\nu_+ \ln f_+ + \nu_- \ln f_-) \tag{3.77}$$

At this stage, the Debye–Hückel expressions (3.60) for f_+ and f_- can be introduced into Eq. (3.77) to give

$$\ln f_\pm = -\frac{1}{\nu} \left[\frac{N_A e_0^2}{2\varepsilon RT} \kappa (\nu_+ z_+^2 + \nu_- z_-^2) \right] \tag{3.78}$$

Since the solution as a whole is electroneutral, $\nu_+ z_+$ must be equal to $\nu_- z_-$ and therefore

$$\begin{aligned} \nu_+ z_+^2 + \nu_- z_-^2 &= \nu_- z_- z_+ + \nu_+ z_+ z_- \\ &= z_+ z_- (\nu_+ + \nu_-) \\ &= z_+ z_- \nu \end{aligned} \tag{3.79}$$

Using this relation in Eq. (3.78), one obtains

$$\ln f_\pm = -\frac{N_A (z_+ z_-) e_0^2}{2\varepsilon RT} \kappa \tag{3.80}$$

Now, one can substitute for κ from Eq. (3.43)

$$\kappa = \left(\frac{4\pi}{\varepsilon kT} \sum n_i^0 z_i^2 e_0^2 \right)^{1/2} \tag{3.43}$$

but before this substitution is made, κ can be expressed in a different form. Since

$$n_i^0 = \frac{c_i N_A}{1000} \tag{3.81}$$

where *c is* the concentration in moles per liter, it follows that

$$\sum n_i^0 z_i^2 e_0^2 = \frac{N_A e_0^2}{1000} \sum c_i z_i^2 \tag{3.82}$$

Prior to the Debye–Hückel theory, $\frac{1}{2}\Sigma c_i z_i^2$ had been empirically introduced by Lewis as a quantity of importance in the treatment of ionic solutions. Since it quantifies the charge in an electrolytic solution, it was known as the *ionic strength* and given the symbol *I*

$$I = \tfrac{1}{2} \sum c_i z_i^2 \tag{3.83}$$

In terms of the ionic strength *I*, κ an be written as [Eqs. (3.43), (3.82), and (3.83)]

$$\kappa = \left(\frac{8\pi N_A e_0^2}{1000 \varepsilon kT} \right)^{1/2} I^{1/2} \tag{3.84}$$

or as

$$\kappa = BI^{1/2} \tag{3.85}$$

where

$$B = \left(\frac{8\pi N_A e_0^2}{1000 \varepsilon kT} \right)^{1/2} \tag{3.86}$$

Values of *B* for water at various temperatures are given in Table 3.3.

On the basis of the expression (3.85) for κ, Eq. (3.80) becomes

$$\ln f_{\pm} = -\frac{N_A (z_+ z_-) e_0^2}{2\varepsilon RT} BI^{1/2} \tag{3.87}$$

or

TABLE 3.3
Values of the Parameter *B* for Water at Various Temperatures

Temperature (°C)	$10^{-8}B$
0	0.3248
10	0.3264
20	0.3282
25	0.3291
30	0.3301
35	0.3312
40	0.3323
50	0.3346
60	0.3371
80	0.3426
100	0.3488

$$\log f_{\pm} = -\frac{1}{2.303}\frac{N_A e_0^2}{2\varepsilon RT} B(z_+z_-)I^{1/2} \tag{3.88}$$

For greater compactness, one can define a constant A given by

$$A = \frac{1}{2.303}\frac{N_A e_0^2}{2\varepsilon RT} B \tag{3.89}$$

and write Eq. (3.88) in the form

$$\log f_{\pm} = -A(z_+z_-)I^{1/2} \tag{3.90}$$

For 1:1-valent electrolytes, $z_+ = z_- = 1$ and $I = c$, and therefore

$$\log f_{\pm} = -Ac^{1/2} \tag{3.91}$$

Values of the constant A for water at various temperatures are given in Table 3.4.

In Eqs. (3.90) and (3.91), the theoretical mean ionic-activity coefficients are in a form directly comparable with experiment. How are such experiments carried out?

3.4.6. Experimental Determination of Activity Coefficients

A reasonably informative account has now been given as to how—albeit in very low concentrations—theoretical developments concerning interionic interaction give rise to theoretical values of the quantity (activity coefficient) by which the real

TABLE 3.4
Values of Constant *A* for Water at Various Temperatures

Temperature (°C)	*A*
0	0.4918
10	0.4989
20	0.5070
25	0.5115
30	0.5161
40	0.5262
50	0.5373
60	0.5494
80	0.5767
100	0.6086

(observed) behavior of electrolytes in solution can be linked to the behavior expected if there were zero electrostatic interactions between ions in solution.

During this presentation, the experimental mean activity coefficients showing up in the deductions have been taken for granted—nothing has been said about how they have been obtained. Obviously, one must be sure when dealing with theory that the experimental values with which the theory is compared are soundly based.

It is time then that some account be given about the means by which experimental values of activity coefficients are known. Only two methods will be presented because the material contains no new ideas and is only presented so the reader is assured that the ground is firm.

3.4.7. How to Obtain *Solute* Activities from Data on *Solvent* Activities

A characteristic of an ionic solution is that any vapor pressure due to the dissolved electrolyte itself is effectively zero. The vapor pressure of the solvent in the solution therefore falls with increasing concentration of the electrolyte in the solution. Thus, the solvent vapor pressure in the solution will be less than the vapor pressure of the pure solvent because the nonvolatile ions block out part of the surface from which, in the pure solvent, solvent molecules would evaporate.

Now, there is nothing mysterious about a solvent activity. It is determined by

$$a_1 = \frac{P_1}{P_1^*} \tag{3.92}$$

where P_1^* is the vapor pressure of *pure solvent* and P_1 is the vapor pressure of the solvent when it is a component of a solution. The relation of P_1 to P_1^* in the ideal condition will be governed by Raoult's law, that is,

$$P_1 = x_1 P_1^* \tag{3.93}$$

where x_1 is the mole fraction of the solvent. One allows for the nonideal behavior of the solvent in respect to its vapor pressure by writing

$$a_1 = f_1 x_1 \tag{3.94}$$

As $x_1 \to 1, f_1 \to 1$. Thus, the "standard state" is the pure solvent.

At this point, one calls into play the Gibbs–Duhem equation of thermodynamics, according to which[10]

$$\sum n_i \, d\mu_i = 0 \tag{3.95}$$

Or, for a two-component system (solvent and electrolyte)

$$n_1 \, d\mu_1 + n_2 \, d\mu_2 = 0 \tag{3.96}$$

where the subscript 1 represents the solvent and the subscript 2 represents the electrolyte solute.

It follows from $\mu_i = \mu_i^0 + RT \ln a_i$, that

$$d \ln a_2 = -\frac{n_1}{n_2} d \ln a_1 \tag{3.97}$$

or

$$\ln \frac{a_2}{c_2} = -\int_1^{a_1} \frac{n_1}{n_2} \, d \ln a_1 \tag{3.98}$$

Thus, if one measures a number of values of the vapor pressure of the solvent P_1 at a corresponding number of solute concentrations, x_2 (to which there are matching solvent concentrations x_1), one can plot the ln a_1 values against the n_1/n_2 ratios. Then the area of that plot will give ln a_2, the a_2 being the solute activity corresponding to the limit of the integral at a_1 (this a_1 being the measured solvent activity for a solution containing a solute, the activity of which is a_2).

The left-hand side of Eq. (3.98) came from

---

[10] Any initial impression that there is something unreasonable about the Gibbs–Duhem equation should be instantly quelled. It merely tells one that (for a two-component system) when an increase in $n_1 \, d\mu_1$ occurs, it causes a decrease in $n_2 \, d\mu_2$ of equal magnitude, a typically powerful and general result of thermodynamic reasoning.

$$\int_{a_2 \to 0}^{a_2} d \ln a_2$$

and $a_2 \to 0$ is simply c_2 because when the solute concentration (hence also activity) tends to zero, its activity becomes equal to its concentration.

This solvent vapor pressure method for measuring the activity of electrolytes has the advantage that the actual experiments one has to do are simple.[11] The method can be applied to any concentration (e.g., a 15 *M* solution!). The difficulty comes at low concentrations when the difference of the vapor pressure between the solution and that of the solvent becomes limitingly small. A huge amount of data (see Table 3.5) have been determined by this method, particularly in the 1950s by a long-term Australian–New Zealand collaboration between professors Stokes and Robinson.

3.4.8. A Second Method by Which One May Obtain Solute Activities: From Data on Concentration Cells and Transport Numbers

Thermodynamics treats electrochemical cells in equilibrium and indeed such hoary material, going back to the work of the great German physical chemist Nernst,[12] is a part of classical electrochemistry that is still being taught in universities to students as if it were representative of modern electrochemistry! Consider then the chemical potential of a metal as μ_M in the solid electrode.

The chemical potential of the ion is that of a solute in a solution and hence is given by

$$\mu_{M^+} = \mu^0_{M^+} + kT \ln a_{M^+} \tag{3.99}$$

---

[11]There is often no need for an absolute determination of vapor pressure. The solvent vapor pressure can be determined simply by setting up a closed system that contains a solution of large volume having an already known solvent activity. The unknown solution will change its concentrations (and hence its weight) until its solvent activity is the same as that of the reference system, which is known. Great accuracy in the weighing is essential and one should use platinum vessels to minimize possible dissolution.

[12]Walter Nernst was professor of chemistry in Berlin in the early years of the twentieth century. He epitomized the professor as a "Great Man." Among his many achievements was the work that led (via the Nernst heat theorem) to the third law of thermodynamics. He was active not only in chemistry but also made significant contributions to the theory of the expanding universe. Nernst was famous not only for his real (many and great) contributions to physical electrochemistry but also for the cold and rigid discipline he demanded from those who aspired to be his collaborators. Were one of these to arrive at his workplace after the scheduled hour of 7:00 a.m., he might find a note from the professor reminding him of the number of applicants who were waiting to occupy it.

One such collaborator (later himself a famous physical chemist) is known to have remarked that, in making the mixture for Nernst, the Herr Creator had put in an extra dose of the intellectual but left out the humanity.

TABLE 3.5

Experimental Activity Coefficients of NaCl at 298 K

$I(=c)$	$-\log f_{\pm}$ (Experimental Values)
0.000997	0.0155
0.001994	0.0214
0.004985	0.0327
0.009969	0.0446
0.01993	0.0599
0.049891	0.0859
0.09953	0.1072
0.1987	0.1308
0.4940	0.1593
0.9788	0.1671
1.921	0.1453
3.696	0.0477
5.305	−0.0789

Source: Reprinted from R. A. Robinson and R. H. Stokes, *Electrolyte Solutions*, 2nd ed. rev., Butterworth, London, 1968.

where a_{M^+} is the metal ion's activity in solution. Now the reaction that goes on at an electrode when an ion in solution exchanges electrons with the electrode can be written as

$$M^+ + e_0^- \rightleftharpoons M \tag{3.100}$$

Clearly, one has to make an allowance for the electron in the Nernst-type theories—which are thermodynamically valid (model free) and therefore can be used today. This was done by a term Ee_0 (potential × the electronic charge = energy in electrostatics). The E was thought of by Nernst as the potential between the metal and the solution.

Now, the thermodynamic equilibrium for Eq. (3.100)[13]

$$\mu_{M^+} - Ee_0 = \mu_M^0 - \mu_e^0 \tag{3.101}$$

Substituting μ_{M^+} from Eq. (3.99),

$$\mu_{M^+}^0 + kT \ln a_{M^+} - Ee_0 = \mu_M^0 - \mu_e^0 \tag{3.102}$$

or

[13]The negative sign arises because e_0^-, the magnitude of the charge on the electron, bears a negative sign.

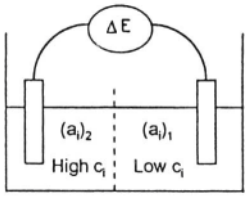

Fig. 3.19. Determination of individual ionic activity from the cell potential.

$$E = \frac{\Delta\mu^0}{e_0} + \frac{kT}{e_0} \ln a_{M^+} = E^0 + \frac{RT}{F} \ln a_{M^+} \tag{3.103}$$

where E^0 is the standard potential of the electrode reaction, at 25 °C and a unit activity of the ion i in solution; $N_A k = R$; $N_A e_0 = F$, the Faraday, or charge on 1 gram ion.

It follows that if one has two electrodes, each in contact with the same ions but at different activities, and the reactions are in thermodynamic equilibrium, then neglecting for a moment any potential that might exist at the contact between the two solutions, i.e., any *liquid-junction* potential, from Eq. (3.103),

$$E_{soln2} - E_{soln1} = E_{cell} = \frac{RT}{F} \ln \frac{a_{M^+,soln2}}{a_{M^+,soln1}} \tag{3.104}$$

and a schematic representation of this idea is shown in Fig. 3.19.

Thus, one could argue as follows: if one of the solutions in the cell has a sufficiently low concentration, e.g., $< 5 \times 10^{-3}$ mol dm^{-3} for 1:1 electrolyte, then the Debye–Hückel limiting law applies excellently. Hence, if one of the solutions has a concentration of $< 5 \times 10$ mol dm^{-3}, we know $a_{i,1}$, the activity of the ion i in that cell, so that Eq. (3.104) would give at once $a_{i,2}$ the activity of species i in the more concentrated cell.

Moreover—and still keeping the question of the liquid junction rigidly suppressed in one's mind—the answer would have one big advantage, it would give an *individual* ionic activity coefficient, f_i.

A method of such virtue must indeed have a compensating complication, and the truth is that the neglected liquid junction potential (LJP) may not be negligible at all.[14]

[14]It turns out that $E_{LJP}/E_{cell} = (t_+ - t_-)$ where t_+ and t_- are, respectively, the cationic and anionic transport numbers. There are cases (e.g., for junctions of solutions of KCl) where t_+ and t_- are almost the same and hence the $E_{LJP} = 0$ and the correction due to the liquid junction is negligible. In some cases the difference $t_+ - t_-$ may be quite considerable.

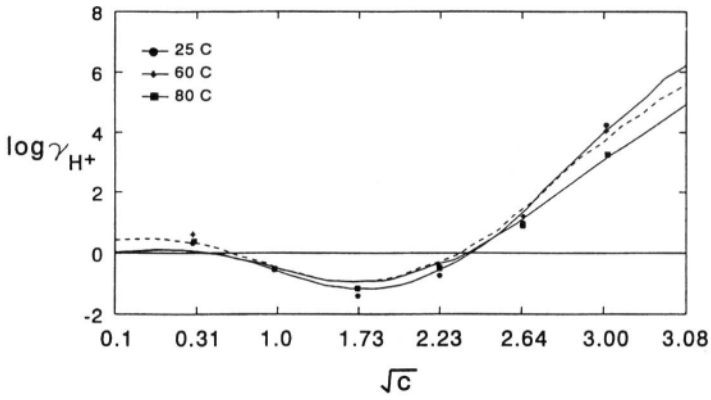

Fig. 3.20. Plot of log γ_{H^+} *vs.* $\sqrt{c}$ at different temperatures for CF_3SO_3H. (Reprinted from R. C. Bhardwaj, M. A. Enayetullah, and J. O'M. Bockris, *J. Electrochem. Soc.* **137**: 2070, 1990.)

Finding an equation for E_{LJP} is surprisingly difficult, but it is finally shown that [*cf.* the deduction of the Planck–Henderson equation, Eq. (4.291)]

$$E_{LJP} = (2t_+ - 1)\frac{RT}{F}\ln\frac{a_{i,soln2}}{a_{i,soln1}} \tag{4.291}$$

Using Eqs. (3.104) and (4.291), the cell potential *with* the liquid-junction potential is

$$E = \frac{RT}{F}\ln\frac{a_{M^+,soln2}}{a_{M^+,soln1}} + (2t_+ - 1)\frac{RT}{F}\ln\frac{a_{M^+,soln2}}{a_{M^+,soln1}} = 2t_+\frac{RT}{F}\ln\frac{a_{M^+,soln2}}{a_{M^+,soln1}} \tag{3.105}$$

If one knows t_+ at the concentration at which it is desired to know $a_{M^+,soln2}$, one can find the latter value by using the limiting law for $a_{M^+,soln1}$. Compared with the first method (Section 3.4.7), the advantage of being able to aim for an individual ion's activity coefficient is significant.

However, there are penalties to pay if one uses the electrochemical cell method. First, there is the question of the value of t_+—it should be known as a function of concentration, and such values are often not available and imply the need for a separate determination. Further, there is a nasty experimental point. One talks of "the liquid-junction potential" as though it were a clear and definite entity. The thermodynamic equation [Eq. (4.291)] *assumes that there is a sharp boundary with linear change of concentration across a small distance* (see Section 4.5.9). These conditions assumed in the deduction only last for a short time after the two solutions have been brought

TABLE 3.6

Experimental Values of Activity Coefficients of Various Electrolytes at Different Concentrations at 298 K

1:1 electrolyte, HCl					
Concentration, molal	0.0001	0.0002	0.0005	0.001	0.002
Mean activity coefficient	0.9891	0.9842	0.9752	0.9656	0.9521
2:1 electrolyte, $CaCl_2$					
Concentration (moles dm^{-3})	0.0018	0.0061	0.0095		
Mean activity coefficient	0.8588	0.7745	0.7361		
2:2 electrolyte, $CdSO_4$					
Concentration, molal	0.0005	0.001	0.005		
Mean activity coefficient	0.774	0.697	0.476		

into contact, even when the boundary is made very carefully.[15] Hence, the conditions under which Eq. (3.104) is valid are subtle and difficult to achieve. Nevertheless, the method has been used—with guarded admissions about the dangers of using it—when information on single ionic activities is desirable, e.g., in the study of O_2 reduction ($O_2 + 4\ H^+ + 4\ e \rightarrow 2\ H_2O$). Some results of the latter study— at very high concentrations—are given in Fig. 3.20. Note the extremely high values of the proton measured in the concentrated acid.

Further Reading

Seminal

1. P. Debye and E. Hückel, "The Interionic Attraction Theory of Deviations from Ideal Behavior in Solution," *Z. Phys.* **24**: 120 (1923).
2. H. S. Harned and B. B. Owen, *The Physical Chemistry of Electrolytic Solutions*, 3rd ed., Reinhold Publishing, New York (1958).
3. H. L. Friedman, "Electrolytic Solutions," in *Modern Aspects of Electrochemistry, No. 8*, J. O'M. Bockris and B. E. Conway, eds., Plenum, New York (1971).

Reviews

1. H. L. Friedman, "Theory of Ionic Solutions in Equilibrium," in *Physical Chemistry of Aqueous Ionic Solutions*, M.-C. Bellisent-Fund and G. W. Nielson, eds., *NATO ASI Series C* **205**: 61 (1986).

[15]There are several techniques for making an undisturbed boundary near in reality to that implicitly assumed in the theory (Section 5.6.7.2). In the one most usually used, two solutions of different concentrations are held apart by a glass slide that is slowly removed, allowing contact between the solutions with minimal coerciveness. In another, the two solutions are held apart in a tube, the one on top being restrained against gravity by means of reduced pressure. Very slow release of this pressure allows the gradual descent of the top solution to make a gentle junction with the lower one. The aim of each method is to avoid disturbance of the assumed ideal exact boundary.

2. J. C. Rasaiah, "Theories of Electrolyte Solutions," in *The Liquid State and Its Electrical Properties*, E. E. Kunhardt, L. G. Christophorou, and L. H. Luessen, eds., *NATO ASI Series B* **193**: 135 (1987).

Papers

1. C. F. Baes, Jr., E. J. Reardon, and B. A. Bloyer, *J. Phys. Chem.* **97**:12343 (1993).
2. H. P. Diogo, M. E. Minas da Piedade, and J. J. Moura Ramos, *J. Chem. Ed.* **70**: A227 (1993).
3. H. Schönert, *J. Phys. Chem.* **98**: 643 (1994).
4. H. Schönert, *J. Phys. Chem.* **98**: 654 (1994).
5. B. Honig and A. Micholls, *Science* **268**: 1144 (1995).
6. B. B. Laird and A. D. J. Haymet, *J. Chem. Phys.* **100**: 3775 (1996).

3.5. THE TRIUMPHS AND LIMITATIONS OF THE DEBYE–HÜCKEL THEORY OF ACTIVITY COEFFICIENTS

3.5.1. How Well Does the Debye–Hückel Theoretical Expression for Activity Coefficients Predict Experimental Values?

The approximate theoretical equation

$$\log f_{\pm} = -A(z_+z_-)I^{1/2} \tag{3.90}$$

indicates that the logarithm of the activity coefficient must decrease linearly with the square root of the ionic strength or, in the case of 1:1-valent electrolytes,[16] with $c^{1/2}$. Further, the slope of the log $f_{\pm}$ versus $I^{1/2}$ straight line can be unambiguously evaluated from fundamental physical constants and from (z_+z_-). Finally, the slope does not depend on the particular electrolyte (i.e., whether it is NaCl or KBr, etc.) but only on its valence type, i.e., on the charges borne by the ions of the electrolyte, whether it is a 1:1-valent or 2:2-valent electrolyte, etc. These are clear-cut predictions.

Even before any detailed comparison with experiment, one can use an elementary spot check: At infinite dilution, where the interionic forces are negligible, does the theory yield the activity coefficient that one would expect from experiment, i.e., unity? At infinite dilution, c or $I \to 0$, which means that $\log f_{\pm} \to 0$ or $f_{\pm} \to 1$. The properties of an extremely dilute solution of ions should be the same as those of a solution containing nonelectrolyte particles. Thus, the Debye–Hückel theory emerges successfully from the infinite dilution test.

Furthermore, if one takes the experimental values of the activity coefficient (Table 3.6) at extremely low electrolyte concentration and plots log $f_{\pm}$ versus $I^{1/2}$ curves, it

[16]That is, $I = \frac{1}{2}\Sigma c_i z_i^2$. For a 1:1 electrolyte, $I = \frac{1}{2}(c_i 1^2 + c_j 1^2)$. As $c_i = c_j = c$, $I = c$.

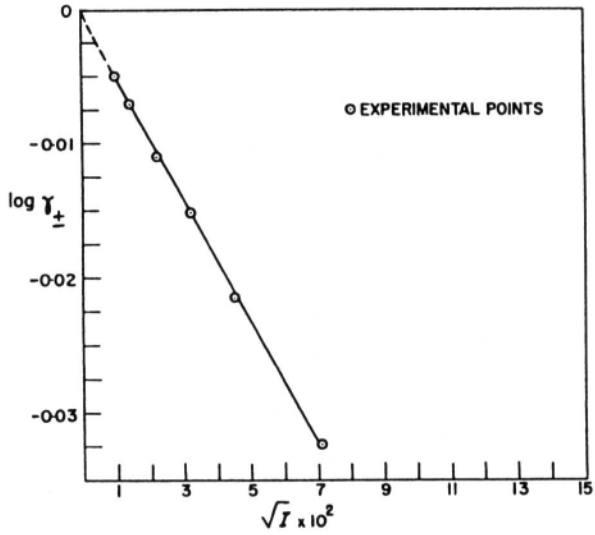

Fig. 3.21. The logarithm of the experimental mean activity coefficient of HCl varies linearly with the square root of the ionic strength.

is seen that: (1) They are linear (Fig. 3.21), and (2) they are grouped according to the valence type of the electrolyte (Fig. 3.22). Finally, when one compares the calculated and observed slopes, it becomes clear that there is excellent agreement to an error of ±0.5% (Table 3.7 and Fig. 3.23) between the results of experiment and the conclusions

TABLE 3.7

Experimental and Calculated Values of the Slope of log $f_{\pm} - \sqrt{I}$ for Alcohol–Water Mixtures at 298 K

Solvent Mole Fraction Water	Dielectric Constant	Slope	
		Observed	Calculated
	1:1 *type of salt, Croceo tetranitro diamino cobaltiate*		
1.00	78.8	0.50	0.50
0.80	54.0	0.89	0.89
	1:2 *type of salt, Croceo sulfate*		
1.00	78.8	1.10	1.08
0.80	54.0	1.74	1.76
	3:1 *type of salt, Luteo iodate*		
1.00	78.8	1.52	1.51

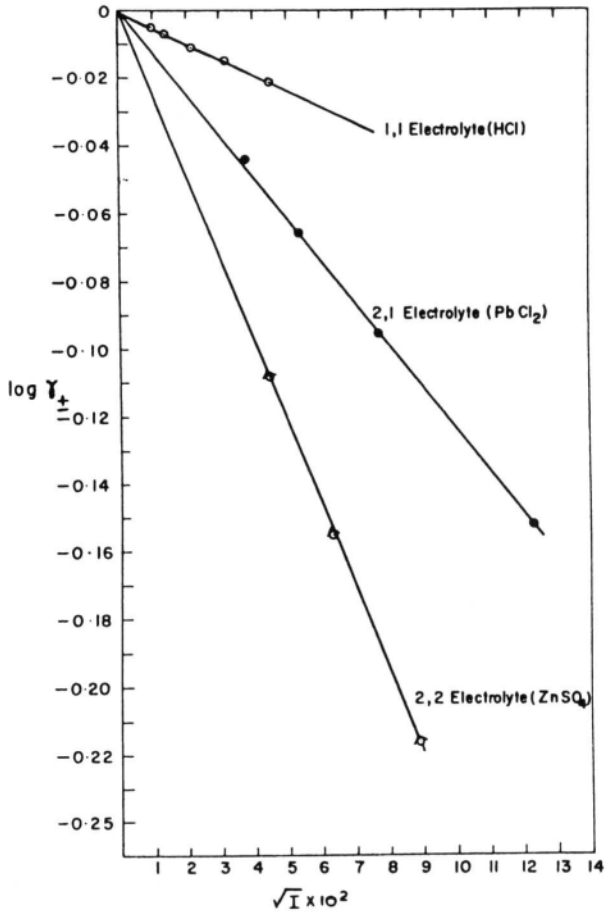

Fig. 3.22. The experimental log $f_{\pm}$ versus $I^{1/2}$ straight-line plots for different electrolytes can be grouped according to valence type.

emerging from an analysis of the ionic-cloud model of the distribution of ions in an electrolyte. Since Eq. (3.90) has been found to be valid at limiting low electrolyte concentrations, it is generally referred to as the *Debye–Hückel limiting law.*

The success of the Debye–Hückel limiting law is no mean achievement. One has only to think of the complex nature of the real system, of the presence of the solvent, which has been recognized only through a dielectric constant, of the simplicity of the Coulomb force law used, and, finally, of the fact that the ions are not point charges, to realize (Table 3.7) that the simple ionic cloud model has been brilliantly successful—almost unexpectedly so. It has grasped the essential truth about electrolytic

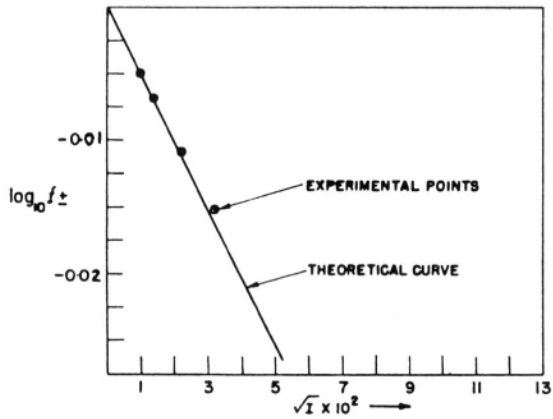

Fig. 3.23. The comparison of the experimentally observed mean activity coefficients of HCl and those that are calculated from the Debye–Hückel limiting law.

solutions, albeit about solutions of extreme dilution. The success of the model is so remarkable and the implications are so wide (see Section 3.5.6) that the Debye–Hückel approach is to be regarded as one of the most significant pieces of theory in the ionics part of electrochemistry. It even rates among the leading pieces of physical chemistry of the first half of the twentieth century.

The Debye–Hückel approach is an excellent example of electrochemical theory. Electrostatics is introduced into the problem in the form of Poisson's equation, and the chemistry is contained in the Boltzmann distribution law and the concept of true electrolytes (Section 3.2). The union of the electrostatic and chemical modes of

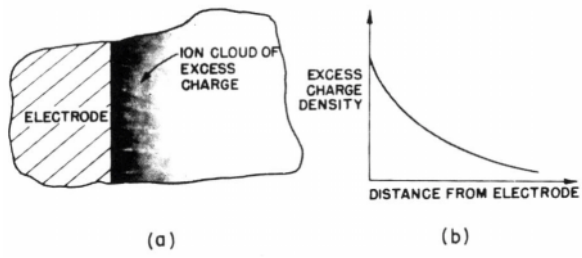

Fig. 3.24. An electrode immersed in an ionic solution is often enveloped by an ionic cloud [see Fig. 3.11] in which the excess charge density varies with distance as shown in (b).

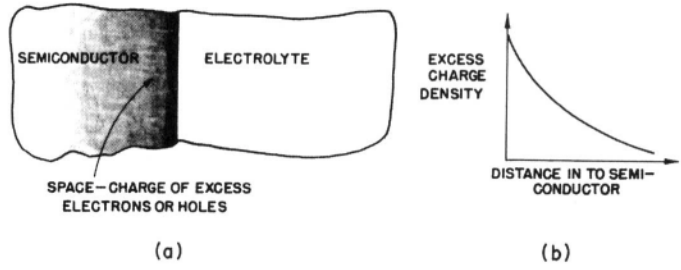

Fig. 3.25. (a) A space charge produced by excess electrons or holes often exists inside the semiconductor, (b) The space charge density varies with distance from the semiconductor–electrolyte interface.

description to give the linearized Poisson–Boltzmann equation illustrates therefore a characteristic development of electrochemical thinking.

It is not surprising that the Poisson–Boltzmann approach has been used frequently in computing interactions between charged entities. Mention may be made of the Gouy theory (Fig. 3.24) of the interaction between a charged electrode and the ions in a solution (see Chapter 6). Other examples are the distribution (Fig. 3.25) of electrons or holes inside a semiconductor in the vicinity of the semiconductor–electrolyte interface (see Chapter 6) and the distribution (Fig. 3.26) of charges near a polyelectrolyte molecule or a colloidal particle (see Chapter 6).

However, one must not overstress the triumphs of the Debye–Hückel limiting law [Eq. (3.90)]. Models are always simplifications of reality. They never treat all its complexities and thus there can never be a perfect fit between experiment and the predictions based on a model.

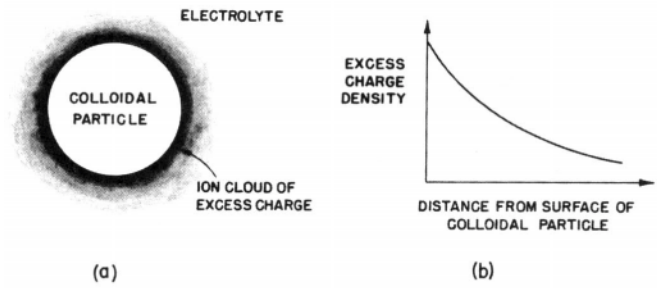

Fig. 3.26. (a) A colloidal particle is surrounded by an ionic cloud of excess charge density, which (b) varies with distance from the surface of the colloidal particle.

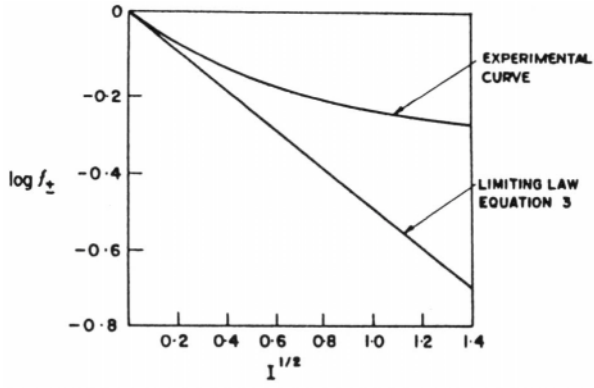

Fig. 3.27. The experimental log $f_\pm$ versus $I^{1/2}$ curve is a straight line only at extremely low concentrations.

What then are the inadequacies of the Debye–Hückel limiting law? One does not have to look far. If one examines the experimental log $f_\pm$ versus $I^{1/2}$ curve, not just in the extreme dilution regions, but at higher concentrations, it turns out that the simple Debye–Hückel limiting law falters. The plot of log $f_\pm$ versus $I^{1/2}$ is a curve (Fig. 3.27 and Table 3.8) and not a straight line as promised by Eq. (3.90). Further, the curves depend not only on valence type (e.g., 1:1 or 2:2) but also (Fig. 3.28) on the particular electrolyte (e.g., NaCl or KC1).

It appears that the Debye–Hückel law is the law for the tangent to the log $f_\pm$ versus $I^{1/2}$ curve at very low concentrations, say, up to 0.01 N for 1:1 electrolytes in aqueous solutions. At higher concentrations, the model must be improved. What refinements can be made?

3.5.2. Ions Are of Finite Size, They Are Not Point Charges

One of the general procedures for refining a model that has been successful in an extreme situation is to liberate the theory from its approximations. So one has to recall

TABLE 3.8

Comparison of Calculated [Eq. (3.90)] and Experimental Values of log $f_\pm$ for NaCl at 298 K

Concentration (molal)	$-\log f_\pm$ Experimental	$-\log f_\pm$ Calculated
0.001	0.0155	0.0162
0.002	0.0214	0.0229
0.005	0.0327	0.0361
0.01	0.0446	0.0510
0.02	0.0599	0.0722

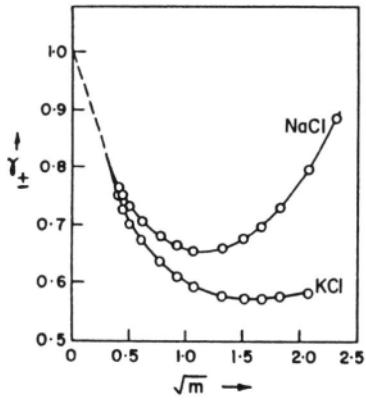

Fig. 3.28. Even though NaCl and KCl are 1:1 electrolytes, their activity coefficients vary indifferent ways with concentration as soon as one examines higher concentrations.

what approximations have been used to derive the Debye–Hückel limiting law. The first one that comes to mind is the point-charge approximation.[17] One now asks: Is it reasonable to consider ions as point charges?

It has been shown (Section 3.3.8) that the mean thickness κ^{-1} of the ionic cloud depends on the concentration. As the concentration of a 1:1 electrolyte increases from 0.001 *N* to 0.01 *N* to 0.1 *N*, κ^{-1} decreases from about 10 to 3 to about 1 nm. This means that the relative dimensions of the ion cloud and of the ion change with concentration. Whereas the radius of the cloud is 100 times the radius of an ion at 0.001 *N*, it is only about 10 times the dimensions of an ion at 0.1 *N*. Obviously, under these latter circumstances, an ion cannot be considered a geometrical point charge in comparison with a dimension only 10 times its size (Fig. 3.29). The more concentrated the solution (i.e., the smaller the size κ^{-1} of the ion cloud; Section 3.3.8), the less valid is the point-charge approximation. If therefore one wants the theory to be applicable to 0.1 *N* solutions or to solutions of even higher concentration, the finite size of the ions must be introduced into the mathematical formulation.

To remove the assumption that ions can be treated as point charges, it is necessary at first to recall at what stage in the derivation of the theory the assumption was

[17] Another approximation in the Debye–Hückel model involves the use of Poisson's equation, which is based on the smearing out of the charges into a continuously varying charge density. At high concentrations, the mean distance between charges is low and the ions see each other as discrete point charges, not as smoothed-out charges. Thus, the use of Poisson's equation becomes less and less justified as the solution becomes more and more concentrated.

Fig. 3.29. At 0.1 *N*, the thickness of the ion cloud is only 10 times the radius of the central ion.

invoked. The linearized P–B equation involved neither the point-charge approximation nor any considerations of the dimensions of the ions. Hence, the basic differential equation

$$\frac{1}{r^2}\frac{d}{dr}\left(r^2\frac{d\psi_r}{dr}\right)=\kappa^2\psi_r \tag{3.21}$$

and its general solution, i.e.,

$$\psi_r = A\frac{e^{-\kappa r}}{r} + B\frac{e^{+\kappa r}}{r} \tag{3.28}$$

can be taken as the basis for the generalization of the theory for finite-sized ions.

As before (Section 3.3.7), the integration constant B must be zero because otherwise one cannot satisfy the requirement of physical sense that, as $r \to \infty$, $\psi \to 0$. Hence, Eq. (3.28) reduces to

$$\psi_r = A\frac{e^{-\kappa r}}{r} \tag{3.29}$$

In evaluating the constant A, a procedure different from that used after (3.29) is adopted. The charge dq in any particular spherical shell (of thickness dr) situated at a distance r from the origin is, as argued earlier,

$$dq = \varrho_r 4\pi r^2 dr \tag{3.36}$$

The charge density ϱ_r is obtained thus

$$\varrho_r = -\frac{\varepsilon}{4\pi}\left[\frac{1}{r^2}\frac{d}{dr}\left(r^2\frac{d\psi_r}{dr}\right)\right] = -\frac{\varepsilon}{4\pi}\kappa^2\psi_r \tag{3.34}$$

and inserting the expression for ψ_r from Eq. (3.29), one obtains

$$\varrho_r = -\frac{\varepsilon}{4\pi}\kappa^2 A \frac{e^{-\kappa r}}{r} \tag{3.106}$$

Thus, by combining Eqs. (3.36) and (3.106)

$$dq = -A\kappa^2\varepsilon(e^{-\kappa r} r\, dr) \tag{3.107}$$

The total charge in the ion cloud q_{cloud} is, on the one hand, equal to $-z_i e_0$ [Eq. (3.39)] as required by the electroneutrality condition and, on the other hand, the result of integrating *dq*. Thus,

$$q_{\text{cloud}} = -z_i e_0 = \int_{?}^{\infty} dq\, dr = -A\kappa^2\varepsilon \int_{?}^{\infty} e^{-\kappa r} r\, dr \tag{3.108}$$

What lower limit should be used for the integration? In the point-charge model, one used a lower limit of zero, meaning that the ion cloud commences from zero (i.e., from the surface of a zero-radius ion) and extends to infinity. However, now the ions are taken to be of finite size, and a lower limit of zero is obviously wrong. The lower limit should be a distance corresponding to the distance from the ion center at which the ionic atmosphere starts (Fig. 3.30).

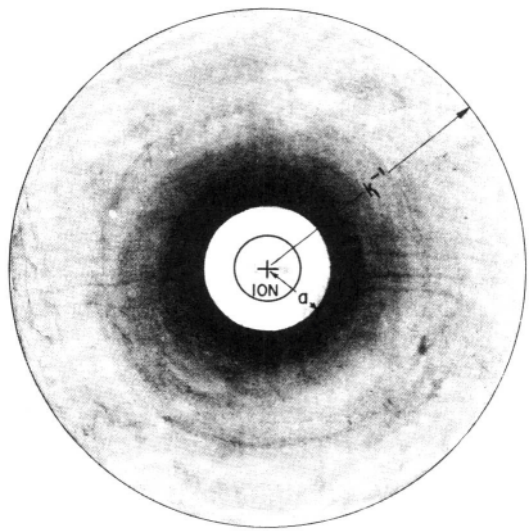

Fig. 3.30. For a finite-sized ion, the ion atmosphere starts at a distance *a* from the center of the reference ion.

As a first step, one can use for the lower limit of the integration a distance parameter that is greater than zero. Then one can go through the mathematics and later worry about the physical implications of the ion size parameter. Let this procedure be adopted and symbol a be used for the ion size parameter.

One has then

$$\int_a^\infty dq\, dr = -A\kappa^2\varepsilon \int_a^\infty e^{-\kappa r} r\, dr$$

$$= -A\varepsilon \int_a^\infty \kappa r e^{-\kappa r}\, d(\kappa r) \tag{3.109}$$

As before (Appendix 3.2), one can integrate by parts; thus,

$$\int_a^\infty \kappa r e^{-\kappa r}\, d\kappa r = -[\kappa r e^{-\kappa r}]_a^\infty + \int_a^\infty e^{-\kappa r}\, d(\kappa r)$$

$$= \kappa a e^{-\kappa a} - [e^{-\kappa r}]_a^\infty \tag{3.110}$$

Inserting Eq. (3.110) in Eq. (3.109), one obtains

$$\int_a^\infty dq\, dr = -A\varepsilon e^{-\kappa a}(1 + \kappa a) = -z_i e_0 \tag{3.111}$$

from which

$$A = \frac{z_i e_0}{\varepsilon} \frac{e^{\kappa a}}{1 + \kappa a} \tag{3.112}$$

Using this value of A in Eq. (3.29), one obtains a new and less approximate expression for the potential ψ_r at a distance r from a finite-sized central ion,

$$\psi_r = \frac{z_i e_0}{\varepsilon} \frac{e^{\kappa a}}{1 + \kappa a} \frac{e^{-\kappa r}}{r} \tag{3.113}$$

3.5.3. The Theoretical Mean Ionic-Activity Coefficient in the Case of Ionic Clouds with Finite-Sized Ions

Once again (see Section 3.3.9), one can use the law of superposition of potentials to obtain the ionic-atmosphere contribution ψ_{cloud} to the potential ψ_r at a distance r from the central ion. From Eq. (3.46), i.e.,

$$\psi_{\text{cloud}} = \psi_r - \psi_{\text{ion}} \tag{3.46}$$

it follows by substitution of the expression (3.113) for ψ_r and Eq. (3.44) for ψ_{ion} that

$$\psi_{\text{cloud}} = \frac{z_i e_0}{\varepsilon r}\frac{e^{\kappa(a-r)}}{1+\kappa a} - \frac{z_i e_0}{\varepsilon r}$$

$$= \frac{z_i e_0}{\varepsilon r}\left[\frac{e^{\kappa(a-r)}}{1+\kappa a} - 1\right] \tag{3.114}$$

It will be recalled, however, that, in order to calculate the activity coefficient from the expressions

$$RT \ln f_i = \Delta\mu_{i-I} \tag{3.59}$$

and

$$\Delta\mu_{i-I} = \frac{N_A z_i e_0}{2}\psi \tag{3.3}$$

i.e., from

$$\ln f_i = \frac{N_A z_i e_0}{2RT}\psi \tag{3.115}$$

it is necessary to know ψ, which is the potential at the surface of the ion due to the surrounding ions, i.e., due to the cloud. Since, in the finite-ion-size model, the ion is taken to have a size a, it means that ψ is the value of ψ_{cloud} at $r = a$,

$$\psi = \psi_{\text{cloud}} \quad r = a \tag{3.116}$$

The value of ψ_{cloud} at $r = a$ is obtained by setting $r = a$ in Eq. (3.114). Hence,

$$\psi = \psi_{\text{cloud}(r=a)} = -\frac{z_i e_0}{\varepsilon \kappa^{-1}}\frac{1}{1+\kappa a} \tag{3.117}$$

By substitution of the expression (3.117) for $\psi = \psi_{\text{cloud}(r=a)}$ in Eq. (3.115), one obtains

$$\ln f_i = -\frac{N_A (z_i e_0)^2}{2\varepsilon RT\kappa^{-1}}\frac{1}{1+\kappa a} \tag{3.118}$$

This individual ionic-activity coefficient can be transformed into a mean ionic-activity coefficient by the same procedure as for the Debye–Hückel limiting law (see Section 3.4.4). On going through the algebra, one finds that the expression for $\log f_{\pm}$ in the finite-ion-size model is

$$\log f_{\pm} = -\frac{A(z_+z_-)I^{1/2}}{1 + \kappa a} \tag{3.119}$$

It will be recalled, however, that the thickness κ^{-1} of the ionic cloud can be written as [Eq. (3.85)]

$$\kappa = BI^{1/2} \tag{3.85}$$

Using this notation, one ends up with the final expression

$$\log f_{\pm} = -\frac{A(z_+z_-)I^{1/2}}{1 + BaI^{1/2}} \tag{3.120}$$

If one compares Eq. (3.119) of the finite-ion-size model with Eq. (3.90) of the point-charge approximation, it is clear that the only difference between the two expressions is that the former contains a term $1/(1 + \kappa a)$ in the denominator. Now, one of the tests of a more general version of a theory is the *correspondence principle*; i.e., the general version of a theory must reduce to the approximate version under the conditions of applicability of the latter. Does Eq. (3.119) from the finite-ion-size model reduce to Eq. (3.90) from the point-charge model?

Rewrite Eq. (3.119) in the form

$$\log f_{\pm} = -A(z_+z_-)I^{1/2}\frac{1}{1 + a/\kappa^{-1}} \tag{3.121}$$

and consider the term a/κ^{-1}. As the solution becomes increasingly dilute, the radius κ^{-1} of the ionic cloud becomes increasingly large compared with the ion size, and simultaneously a/κ^{-1} becomes increasingly small compared with unity, or

$$\frac{1}{1 + a/\kappa^{-1}} \approx 1 \tag{3.122}$$

Thus, when the solution is sufficiently dilute to make $a << \kappa^{-1}$, i.e., to make the ion size insignificant in comparison with the radius of the ion atmosphere,the finite-ion-size model Eq (3.119) reduces to the corresponding Eq. (3.90) of the point-charge model because the extra term $1/(1 + a/\kappa^{-1})$ tends to unity

$$-\left[\frac{A(z_+z_-)I^{1/2}}{1+\kappa a}\right]_{a\ll\kappa^{-1}} = -A(z_+z_-)I^{1/2} \tag{3.123}$$

The physical significance of $a/\kappa^{-1} \ll 1$ is that at very low concentrations the ion atmosphere has such a large radius compared with that of the ion that one need not consider the ion as having a finite size *a*. Considering $a/\kappa^{-1} \ll 1$ is tantamount to reverting to the point-charge model.

One can now proceed rapidly to compare this theoretical expression for $\log f_\pm$ with experiment; but what value of the ion size parameter should be used? The time has come to worry about the precise physical meaning of the parameter *a* that was introduced to allow for the finite size of ions.

3.5.4. The Ion Size Parameter a

One can at first try to speculate on what value of the ion size parameter is appropriate. A lower limit is the sum of the *crystallographic* radii of the positive and negative ions present in solution; ions cannot come closer than this distance [Fig. 3.31 (a)]. But in a solution the ions are generally solvated (Chapter 2). So perhaps the sum of the solvated radii should be used [Fig. 3.3 l(b)]. However when two solvated ions collide, is it not likely [Fig. 3.31 (c)] that their hydration shells are crushed to some extent? This means that the ion size parameter *a* should be greater than the sum of the crystallographic radii and perhaps less than the sum of the solvated radii. It should best be called the *mean distance of closest approach*, but beneath the apparent wisdom of this term there lies a measure of ignorance. For example, an attempted calculation of just how crushed together two solvated ions are would involve many difficulties.

To circumvent the uncertainty in the quantitative definition of *a*, it is best to regard it as a parameter in Eq. (3.120), i.e., a quantity the numerical value of which is left to be calibrated or adjusted on the basis of experiment. The procedure (Fig. 3.32) is to assume that the expression for $\log f_\pm$ [Eq. (3.120)] is correct at one concentration, then to equate this theoretical expression to the experimental value of $\log f_\pm$ corresponding to that concentration and to solve the resulting equation for *a*. Once the ion size parameter, or mean distance of closest approach, is thus obtained at one concentration, the value can be used to calculate values of the activity coefficient over a range of other and higher concentrations. Then the situation is regarded as satisfactory if the value of *a* obtained from experiments at one concentration can be used in Eq. (3.120) to reproduce the results of experiments over a range of concentrations.

3.5.5. Comparison of the Finite-Ion-Size Model with Experiment

After taking into account the fact that ions have finite dimensions and cannot therefore be treated as point charges, the following expression has been derived for the logarithm of the activity coefficient:

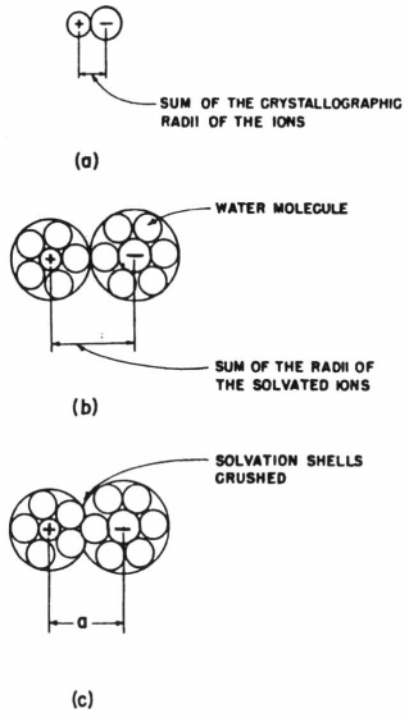

Fig. 3.31. The ion size parameter cannot be (a) less than the sum of the crystallographic radii of the ions or (b) more than the sum of the radii of the solvated ions and is most probably (c) less than the sum of the radii of the solvated ions because the solvation shells may be crushed.

$$\log f_{\pm} = -\frac{A(z_+z_-)I^{1/2}}{1 + BaI^{1/2}} \tag{3.120}$$

How does the general form of this expression compare with the Debye–Hückel limiting law as far as agreement with experiment is concerned? To see what the extra term $(1 + BaI^{1/2})^{-1}$ does to the shape of the $\log f_{\pm}$ versus $I^{1/2}$ curve, one can expand it in the form of a binomial series

$$\frac{1}{1+x} = (1+x)^{-1} = 1 - x + \frac{x^2}{2!} - \ldots \tag{3.124}$$

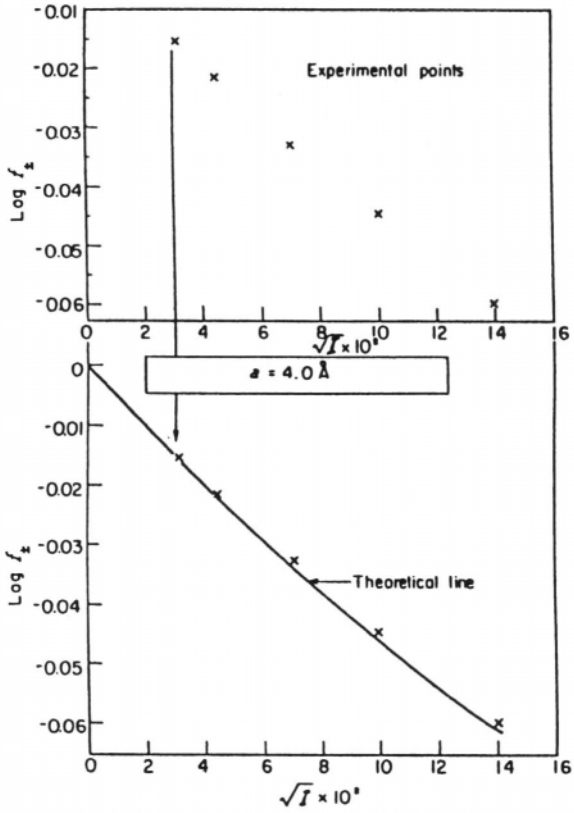

Fig. 3.32. Procedure for recovering the ion size parameter from experiment and then using it to produce a theoretical log $f_\pm$ versus $I^{1/2}$ curve that can be compared with an experimental curve.

and use only the first two terms. Thus,

$$\frac{1}{1 + BaI^{1/2}} = 1 - BaI^{1/2} \tag{3.125}$$

and therefore

$$\log f_\pm \approx -A(z_+z_-)I^{1/2}(1 - BaI^{1/2}) \tag{3.126}$$

$$\approx -A(z_+z_-)I^{1/2} + \text{constant}(I^{1/2})^2 \tag{3.127}$$

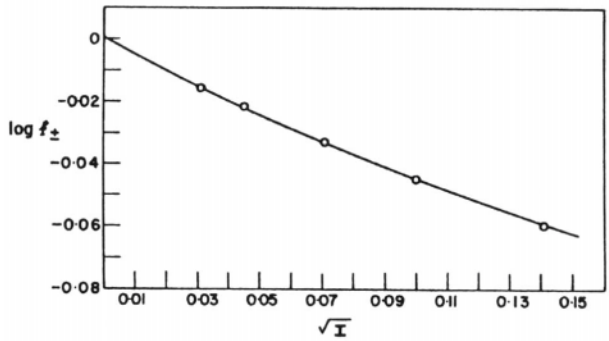

Fig. 3.33. Comparison of the experimental mean activity coefficients with theory for Eq. (3.126).

This result is encouraging. It shows that the log $f_\pm$ versus $I^{1/2}$ curve gives values of log $f_\pm$ higher than those given by the limiting law, the deviation increasing with concentration. In fact, the general shape of the predicted curve (Fig. 3.33) is very much on the right lines.

The values of the ion size parameter, or distance of closest approach, which are recovered from experiment are physically reasonable for many electrolytes. They lie around 0.3 to 0.5 nm, which is greater than the sum of the crystallographic radii of the positive and negative ions and pertains more to the solvated ion (Table 3.9).

By choosing a reasonable value of the ion size parameter a, independent of concentration, it is found that in many cases Eq. (3.126) gives a very good fit with experiment, often for ionic strengths up to 0.1. For example, on the basis of a = 0.4 nm, Eq. (3.126) gives an almost exact agreement up to 0.02 M in the case of sodium chloride (Fig. 3.34 and Table 3.10).

The ion size parameter a has done part of the job of extending the range of concentration in which the Debye–Hückel theory of ionic clouds agrees with experiment. Has it done the whole job? One must start looking for discrepancies between theory and fact and for the less satisfactory features of the model.

TABLE 3.9

Values of Ion Size Parameter for a Few Electrolytes

Salt	a (nm)
HCl	0.45
HBr	0.52
LiCl	0.43
NaCl	0.40
KCl	0.36

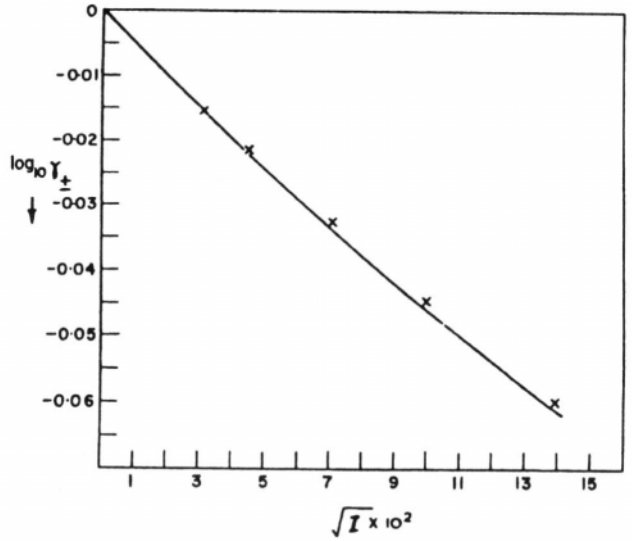

Fig. 3.34. Comparison of the experimental mean activity coefficients for sodium chloride with the theoretical log $f_{\pm}$ versus $I^{1/2}$ curve based on Eq. (3.126) with $a = 0.4$ nm.

The most obvious drawback of the finite-ion-size version of the Debye–Hückel theory lies in the fact that a is an *adjustable parameter.* When parameters that have to be taken from experiment enter a theory, they imply that the physical situation has been incompletely comprehended or is too complex to be mathematically analyzed. In contrast, the constants of the limiting law were calculated without recourse to experiment.

TABLE 3.10

Experimental Mean Activity Coefficients and Those Calculated from Eq. (3.126) with $a = 0.4$ nm at 25 °C at Various Concentrations of NaCl

Molality	Experimental Mean Activity Coefficient, $-\log f_{\pm}$	Calculated
0.001	0.0155	0.0155
0.002	0.0214	0.0216
0.005	0.0327	0.0330
0.01	0.0446	0.0451
0.02	0.0599	0.0609

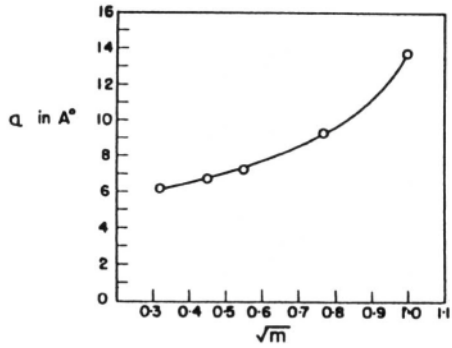

Fig. 3.35. The variation of the ion size parameter with concentration of NaCl.

The best illustration of the fact that a has to be adjusted is its concentration dependence. As the concentration changes, the ion size parameter has to be modified (Fig. 3.35). Further, for some electrolytes at higher concentrations, a has to assume quite impossible (i.e., large negative, irregular) values to fit the theory to experiment (Table 3.11).

Evidently there are factors at work in an electrolytic solution that have not yet been reckoned with, and the ion size parameter is being asked to include the effects of all these factors simultaneously, even though these other factors probably have little to do with the size of the ions and may vary with concentration. If this were so, the ion size parameter a, calculated back from experiment, would indeed have to vary with concentration. The problem therefore is: What factors, forces, and interactions were neglected in the Debye–Hückel theory of ionic clouds?

TABLE 3.11

Values of Parameter *a* at Higher Concentrations

Concentration (molality)	Value of a for HCl (nm)	Concentration (molality)	Value of a for LiCl (nm)
1	1.38	2	4.13
1.4	2.45		
1.8	8.50	2.5	−14.19
2	−41.12		
2.5	−2.79	3	−2.64
3	−1.48		

3.5.6. The Debye–Hückel Theory of Ionic Solutions: An Assessment

It is appropriate at this stage to recount the achievements in the theory of ionic solutions described thus far. Starting with the point of view that ion–ion interactions are bound to operate in an electrolytic solution, in going from a hypothetical state of noninteracting ions to a state in which the ions of species i interact with the ionic solution, the chemical-potential change $\Delta\mu_{i-I}$ was considered a quantitative measure of these interactions. As a first approximation, the ion–ion interactions were assumed to be purely Coulombic in origin. Hence, the chemical-potential change arising from the interactions of species i with the electrolytic solution is given by the Avogadro number times the electrostatic work W resulting from taking a discharged reference ion and charging it up in the solution to its final charge In other words, the charging work is given by the same formula as that used in the Born theory of solvation, i.e.,

$$W = \frac{z_i e_0}{2}\psi \tag{3.3}$$

where ψ is the electrostatic potential at the surface of the reference ion that is contributed by the other ions in the ionic solution. The problem therefore was to obtain a theoretical expression for the potential ψ. This involved an understanding of the distribution of ions around a given reference ion.

It was in tackling this apparently complicated task that appeal was made to the Debye–Hückel simplifying model for the distribution of ions in an ionic solution. This model treats only one ion—the central ion—as a discrete charge, the charge of the other ions being smoothed out to give a continuous charge density. Because of the tendency of negative charge to accumulate near a positive ion, and vice versa, the smoothed-out positive and negative charge densities do not cancel out; rather, their imbalance gives rise to an excess local charge density ϱ_r, which of course dies away toward zero as the distance from the central ion is increased. Thus, the calculation of the distribution of ions in an electrolytic solution reduces to the calculation of the variation of excess charge density ϱ_r with distance r from the central ion.

The excess charge density ϱ_r was taken to be given, on the one hand, by Poisson's equation of electrostatics

$$\varrho_r = -\frac{\varepsilon}{4\pi}\left[\frac{1}{r^2}\frac{d}{dr}\left(r^2\frac{d\psi_r}{dr}\right)\right] \tag{3.17}$$

and on the other, by the linearized Boltzmann distribution law

$$\varrho_r = -\sum\frac{n_i^0 z_i^2 e_0^2 \psi_r}{kT} \tag{3.18}$$

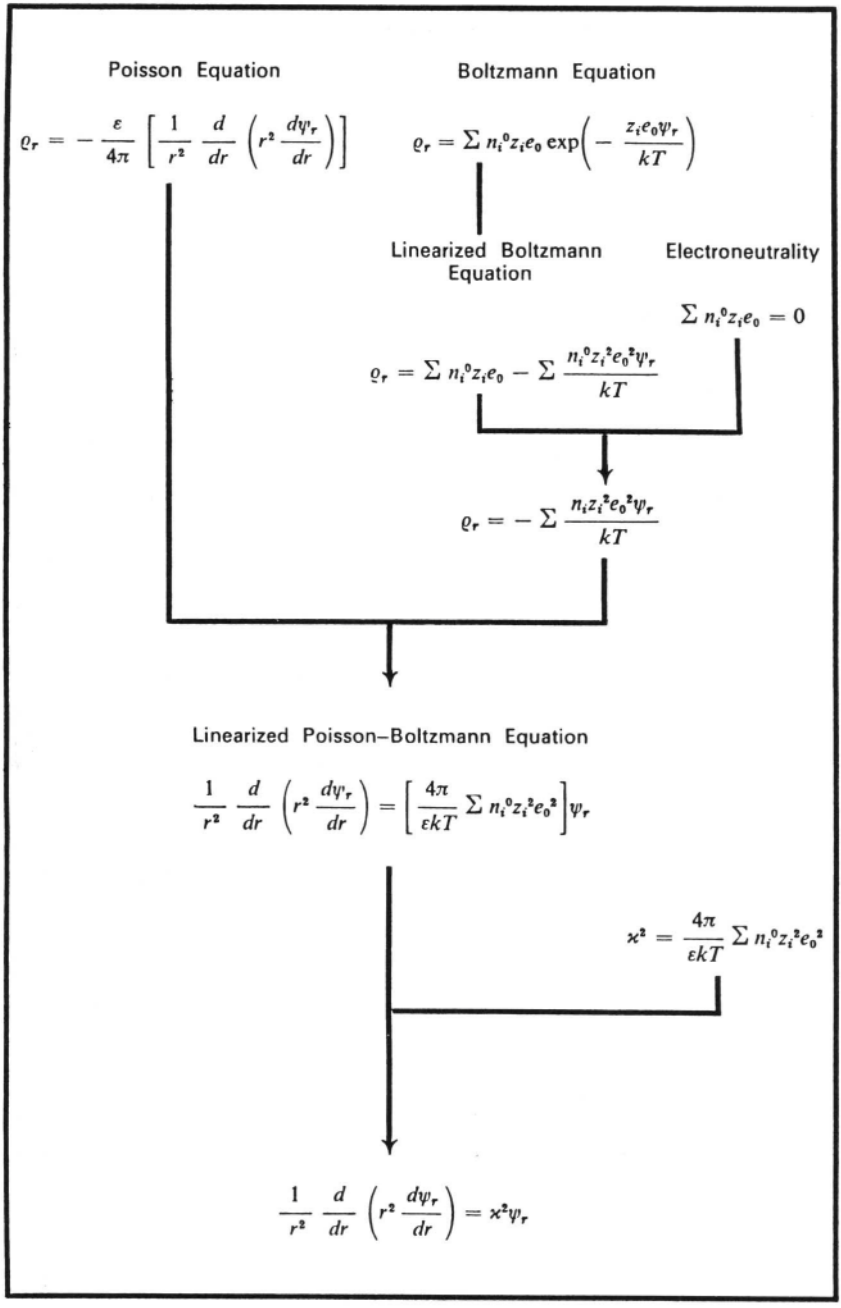

Fig. 3.36. Steps in the derivation of the linearized Poisson–Boltzmann equation.

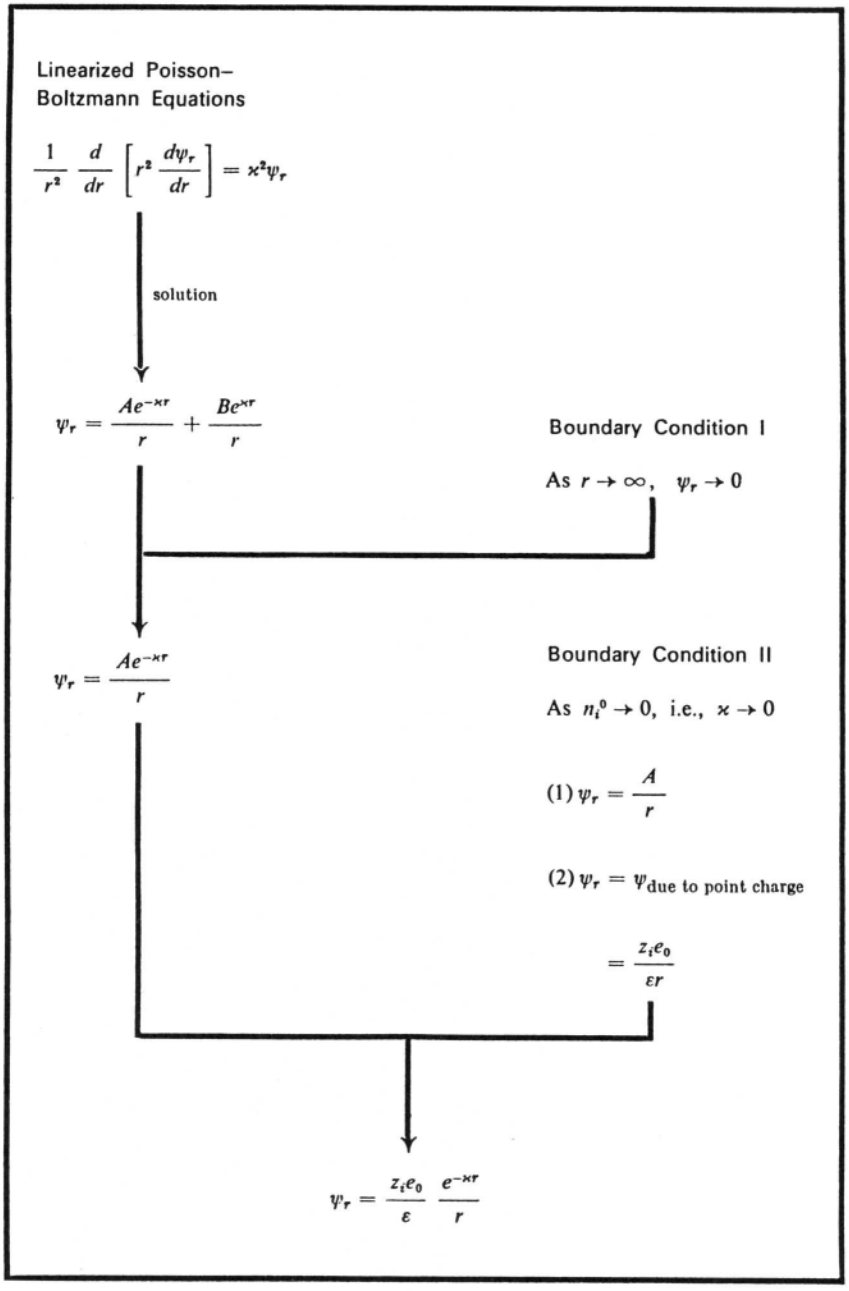

Fig. 3.37. Steps in the solution of the linearized Poisson–Boltzmann equation for point-charge ions.

The result of equating these two expressions for the excess charge density is the fundamental partial differential equation of the Debye–Hückel model, the linearized P–B equation (Fig. 3.36),

$$\frac{1}{r^2}\frac{d}{dr}\left(r^2\frac{d\psi_r}{dr}\right)=\kappa^2\psi_r \tag{3.21}$$

where

$$\kappa^2=\frac{4\pi}{\varepsilon kT}\sum n_i^0 z_i^2 e_0^2 \tag{3.20}$$

By assuming that ions can be regarded as point charges, the solution of the linearized P–B equation turns out to be (Fig. 3.37)

$$\psi_r=\frac{z_i e_0}{\varepsilon}\frac{e^{-\kappa r}}{r} \tag{3.33}$$

Such a variation of potential with distance from a typical (central or reference) ion corresponds to a charge distribution that can be expressed as a function of distance r from the central ion by

$$\varrho_r=-\frac{z_i e_0}{4\pi}\kappa^2\frac{e^{-\kappa r}}{r} \tag{3.35}$$

This variation of the excess charge density with distance around the central or typical ion yielded a simple physical picture. A reference positive ion can be thought of as being surrounded by a cloud of negative charge of radius κ^{-1}. The charge density in this ionic atmosphere, or ionic cloud, decays in the manner indicated by Eq. (3.35). Thus, the interactions between a reference ion and the surrounding ions of the solution are equivalent to the interactions between the reference ion and the ionic cloud, which in the point-charge model set up at the central ion a potential ψ_{cloud} given by

$$\psi_{\text{cloud}}=-\frac{z_i e_0}{\varepsilon\kappa^{-1}} \tag{3.49}$$

The magnitude of central ion–ionic-cloud interactions is given by introducing the expression for ψ_{cloud} into the expression (3.3) for the work of creating the ionic cloud, i.e., setting up the ionic interaction situation. Thus, one obtains for the energy of such interactions

$$\Delta\mu_{i-I}=-\frac{N_A(z_i e_0)^2}{2\varepsilon\kappa^{-1}} \tag{3.51}$$

In order to test these predictions, attention was drawn to an empirical treatment of ionic solutions. For solutions of noninteracting particles, the chemical-potential change in going from a solution of unit concentration to one of concentration x_i is described by the equation

$$\mu_i - \mu_i^0 = RT \ln x_i \tag{3.52}$$

However, in the case of an electrolytic solution in which there are ion–ion interactions, it is experimentally observed that

$$\mu_i - \mu_i^0 \neq RT \ln x_i$$

If one is unaware of the nature of these interactions, one can write an empirical equation to compensate for one's ignorance

$$RT \ln f_i = (\mu_i - \mu_i^0) - RT \ln x_i \tag{3.57}$$

and say that solutions behave ideally if the so-called activity coefficient f_i is unity, i.e., $RT \ln f_i = 0$, and, in real solutions, $f_i \neq 1$. It is clear that f_i corresponds to a coefficient to account for the behavior of ionic solutions, which differs from that of solutions in which there are no charges. Thus, f_i accounts for the interactions of the charges, so that

$$RT \ln f_i = \Delta\mu_{i-I} = -\frac{N_A(z_i e_0)^2}{2\varepsilon\kappa^{-1}} \tag{3.60}$$

Thus arose the Debye–Hückel expression for the experimentally inaccessible individual ionic-activity coefficient. This expression could be transformed into the Debye–Hückel limiting law for the experimentally measurable mean ionic-activity coefficient

$$\log f_{\pm} = -A(z_+ z_-) I^{1/2} \tag{3.90}$$

which would indicate that the logarithm of the mean activity coefficient falls linearly with the square root of the ionic strength $I (= \frac{1}{2}\Sigma c_i z_i^2)$, which is a measure of the total number of electric charges in the solution.

The agreement of the Debye–Hückel limiting law with experiment improved with decreasing electrolyte concentration and became excellent for the limiting tangent to the $\log f_{\pm}$ versus $I^{1/2}$ curve. With increasing concentration, however, experiment deviated more and more from theory and, at concentrations above 1 *N*, even showed an *increase* in $f_{\pm}$ with an increase in concentration, whereas theory indicated a continued decrease.

An obvious improvement of the theory consisted in removing the assumption of point-charge ions and taking into account their finite size. With the use of an ion size parameter a, the expression for the mean ionic-activity coefficient became

$$\log f_{\pm} = -\frac{A(z_+z_-)I^{1/2}}{1 + \kappa a} \tag{3.119}$$

However, the value of the ion size parameter a could not be theoretically evaluated. Hence, an experimentally calibrated value was used. With this calibrated value for a, the values of $f_{\pm}$ at other concentrations [calculated from Eq. (3.119)] were compared with experiment.

The finite-ion-size model yielded agreement with experiment at concentrations up to 0.1 *N*. It also introduced through the value of a, the ion size parameter, a specificity to the electrolyte (making NaCl different from KCl), whereas the point-charge model yielded activity coefficients that depended only upon the valence type of electrolyte. Thus, while the limiting law sees only the charges on the ions, it is blind to the specific characteristics that an ionic species may have, and this defect is overcome by the finite-ion-size model.

Unfortunately, the value of a obtained from experiment by Eq. (3.119) varies with concentration (as it would not if it represented simply the collisional diameters), and as the concentration increases beyond about 0.1 mol dm^{-3}, a sometimes has to assume physically impossible (e.g., negative) values. Evidently these changes demanded by experiment not only reflect real changes in the sizes of ions but represent other effects neglected in the simplifying Debye–Hückel model. Hence, the basic postulates of the Debye–Hückel model must be scrutinized.

The basic postulates can be put down as follows: (1) The central ion sees the surrounding ions in the form of a smoothed-out charge density and not as discrete charges. (2) All the ions in the electrolytic solution are free to contribute to the charge density and there is, for instance, no pairing up of positive and negative ions to form any electrically neutral couples. (3) Only long-range Coulombic forces are relevant to ion–ion interactions; short-range non-Coulombic forces, such as dispersion forces, play a negligible role. (4) The solution is sufficiently dilute to make ψ_r [which depends on concentration through κ—*cf.* Eq. (3.20)] small enough to warrant the linearization of the Boltzmann equation (3.10). (5) The only role of the solvent is to provide a dielectric medium for the operation of interionic forces; i.e., the removal of a number of ions from the solvent to cling more or less permanently to ions other than the central ion is neglected.

It is because it is implicitly attempting to represent all these various aspects of the real situation inside an ionic solution that the experimentally calibrated ion size parameter varies with concentration. Of course, a certain amount of concentration variation of the ion size parameter is understandable because the parameter depends upon the radius of solvated ions and this time-averaged radius might be expected to

decrease with an increase of concentration. One must try to isolate that part of the changes in the ion size parameter that does not reflect real changes in the sizes of ions but represents the impact of, for instance, ionic solvation upon activity coefficients. This question of the influence of ion–solvent interactions (Chapter 2) upon the ion–ion interactions will be considered in Section 3.6.

3.5.7. Parentage of the Theory of Ion–Ion Interactions

Stress has been laid on the contribution of Debye and Hückel (1923) to the development of the theory of ion–ion interactions. It was Debye and Hückel who ushered in the electrostatic theory of ionic solutions and worked out predictions that precisely fitted experiments for sufficiently low concentrations of ions. It is not often realized, however, that the credit due to Debye and Hückel as the parents of the theory of ionic solutions is the credit that is quite justifiably accorded to foster parents. The true parents were Milner and Gouy. These authors made important contributions very early in the growth of the theory of ion–ion interactions.

Milner's contribution (1912) was direct. He attempted to find out the virial[18] equation for a mixture of ions. However. Milner's statistical mechanical approach lacked the mathematical simplicity of the ionic-cloud model of Debye and Hückel and proved too unwieldy to yield a general solution testable by experiment. Nevertheless, his contribution was a seminal one in that for the first time the behavior of an ionic solution had been linked mathematically to the interionic forces.

The contribution of Gouy (1910) was indirect.[19] Milner's treatment was not sufficiently fruitful because he did not formulate a mathematically treatable model. Gouy developed such a model in his treatment of the distribution of the excess charge density in the solution near an electrode. Whereas Milner sought to describe the interactions between series of discrete ions, it was Gouy who suggested the smoothing out of the ionic charges into a continuous distribution of charge and took the vital step of using Poisson's equation to relate the electrostatic potential and the charge density in the continuum. Thus, Gouy was the first to evolve the ionic-atmosphere model.

It was with an awareness of the work of Milner and Gouy that Debye and Hückel attacked the problem. Their contributions, however, were vital ones. By choosing one ion out of the ionic solution and making an analogy between this charged reference ion and the charged electrode of Gouy, by using the Gouy type of approach to obtain the variation of charge density and potential with distance from the central ion and

---

[18] *Virial* is derived from the Latin word for *force*, and the virial equation of state is a relationship between pressure, volume, and temperature of the form

$$\frac{PV}{RT} = 1 + \frac{K_2}{V} + \frac{K_3}{V^2} + \ldots$$

where $K_2, K_3, \ldots$ the virial coefficients, represent interactions between constituent particles.

[19] Chapman made an independent contribution in 1913 on the same lines as that of Gouy.

thus to get the contribution to the potential arising from interionic forces, and, finally, by evolving a charging process to get the chemical-potential change due to ion–ion interactions, they were able to link the chemical-potential change caused by interionic forces to the experimentally measurable activity coefficient. Without these essential contributions of Debye and Hückel, a viable theory of ionic solutions would not have emerged.

Further Reading

Seminal

1. G. Gouy, "About the Electric Charge on the Surface of an Electrolyte," *J. Phys.* **9***:* 457 (1910).
2. S. R. Milner, "The Virial of a Mixture of Ions," *Phil. Mag.* **6**: 551 (1912).
3. P. Debye and E. Hückel, "The Interionic Attraction Theory of Deviations from Ideal Behavior in Solution," Z. *Phys.* **24**: 185 (1923).

Review

1. K. S. Pitzer, "Activity Coefficients in Electrolyte Solutions," in *Activity Coefficients in Electrolyte Systems*, K. S. Pitzer, ed., 2nd ed., CRC Press, Boca Raton, FL (1991).

Papers

1. C. F. Baes, Jr., E. J. Reardon, and B. A. Bloyer, *J. Phys. Chem.* **97**: 12343 (1993).
2. D. Dolar and M. Bester, *J. Phys. Chem.* **99**: 4763 (1995).
3. G. M. Kontogeorgis, A. Saraiva, A. Fredenslund, and D. P. Tassios, *Ind. Eng. Chem. Res.* **34**:1823 (1995).
4. A. H. Meniai and D. M. T. Newsham, *Chem. Eng. Res. Des.* **73**: 842 (1995).
5. M. K. Khoshkbarchi and J. H. Vera, *AlChE J.* **42**: 249 (1996).

3.6. ION–SOLVENT INTERACTIONS AND THE ACTIVITY COEFFICIENT

3.6.1. Effect of Water Bound to Ions on the Theory of Deviations from Ideality

The theory of behavior in ionic solutions arising from ion–ion interactions has been seen (Section 3.5) to give rise to expressions in which as the ionic concentration increases, the activity coefficient decreases. In spite of the excellent numerical agreement between the predictions of the interionic attraction theory and experimental values of activity coefficients at sufficiently low concentrations (e.g., $< 3 \times 10^{-3}$ *N*), there is a most sharp disagreement at concentrations above about 1 *N*, when the activity coefficient begins to increase back toward the values it had in limitingly dilute solutions. In fact, at sufficiently high concentrations (one might have argued, when the ionic interactions are greatest), the activity coefficient, instead of continuing to

decrease, begins to exceed the value of unity characteristic of the reference state of noninteraction, i.e., of infinite dilution.

A qualitative picture of the events leading to these apparently anomalous happenings has already been given in Chapter 2. There it has been argued that ions exist in solution in various states of interaction with solvent particles. There is a consequence that must therefore follow for the effectiveness of some of these water molecules in counting as part of the solvent. Those that are tightly bound to certain ions cannot be effective in dissolving further ions added (Fig. 3.38). As the concentration of electrolyte increases, therefore the amount of *effective* or free solvent decreases. In this way the apparently anomalous increase in the activity coefficient occurs. The activity coefficient is in effect that factor which multiplies the simple, apparent ionic concentration and makes it the *effective* concentration, i.e., the activity. If the hydration of the ions reduces the amount of free solvent from that present for a given stoichiometric concentration, then the effective concentration increases and the activity coefficient must increase so that its multiplying effect on the simple stoichiometric concentration is such as to increase it to take into account the reduction of the effective solvent. Experiment shows that sometimes these increases more than compensate for the decrease due to interionic forces, and it is thus not unreasonable that the activity coefficient should rise above unity.

Some glimmering of the quantitative side of this can be seen by taking the number of waters in the primary hydration sheath of the ions as those that are no longer effective solvent particles. For NaCl, for example, Table 2.18 indicates that this number is about 7. If the salt concentration is, e.g., 10^{-2} *N*, the moles of water per liter withdrawn from effect as free solvent would be 0.07. Since the number of moles of water per liter is 1000/18 = 55.5, the number of moles of free water is 55.43 and the effects arising from such a small change are not observable. Now consider a 1 *N* solution of NaCl. The water withdrawn is 7 mol dm^{-3}, and the change in the number of moles of free water is from 55.5 in the infinitely dilute situation to 48.5, a significant change. At 5 *N* NaCl,

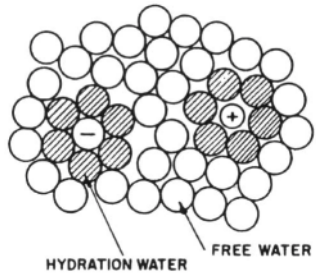

Fig. 3.38. The distinction between free water and hydration water that is locked up in the solvent sheaths of ions.

more than half of the water in the solution is associated with the ions, and a sharp increase of activity coefficient, somewhat of a doubling in fact, would be expected to express the increase in effective concentration of the ions. To what extent can this rough sketch be turned into a quantitative model?

3.6.2. Quantitative Theory of the Activity of an Electrolyte as a Function of the Hydration Number

The basic thought here has to be similar to that which lay beneath the theory of electrostatic interactions: to calculate the work done in going from a state in which the ions are too far apart to feel any interionic attraction to the state at a finite concentration c at which part of the ions' behavior is due to this. This work was then [Eq. (3.59)] placed equal to $RT \ln f$, where f is the activity coefficient, which was thereby calculated.

When one realizes that a reversal of the direction in which the activity coefficient varies with concentration has to be explained by taking into account the removal of some of the solvent from effectively partaking in the ionic solution's activity, the philosophy behind the calculation of this effect on the activity coefficient becomes clear. One must calculate the work done in the changes caused by solvent removal and add this to the work done in building up the ionic atmosphere. What, then, is the contribution due to these water-removing processes? [Note that ions are hydrated at all times in which they are in the solution. One is not going to calculate the heat of hydration; that was done in Chapter 2. Here, the task is to calculate the work done as a consequence of the fact that when water molecules enter the solvation sheath, they are, so to speak, no longer operating as far as the solvent is concerned. It is to be an $RT\ln(c_1/c_2)$ type of calculation.]

As a device for the calculation, let it be assumed that the interionic attraction is switched off. (Reasons for employing this artifice will be given.) Thus, there are two kinds of work that must be taken into account.

1. The $RT\ln(c_1/c_2)$ kind of work done when there is a change in concentration of the free solvent *water* caused by introducing ions of a certain concentration into the solution.
2. The $RT\ln(c_1/c_2)$ kind of work done when there is a corresponding change in concentration of the *ions* due to the removal of the water to their sheaths.

The work done for process 1 is easy to calculate. Before the ions have been added, the concentration of the water is unaffected by anything; it is the concentration of pure water and its activity, the activity of a pure substance, can be regarded as unity. After the ions are there, the activity of the water is, say, a_w. Then, the work when the activity of the water goes from 1 to a_w is $RT \ln (a_w/1)$.

However, one wishes to know the change of activity caused in the *electrolyte* by this change of activity of the water. Furthermore, the calculation must be reduced to that for 1 mole of electrolyte. Let the sum of the moles of water in the primary sheath per liter of solution for both ions of the imagined 1:1 electrolyte be n_h (for 1-molar

solutions, this is the hydration number). Then, if there are n moles of electrolyte in the water, the change in free energy due to the removal of the water to the ions' sheaths is $-(n_h/n)RT\ln a_w$ per mole of electrolyte.

One now comes to the second kind of work and realizes why the calculation is best done as a thought process in which the interionic attraction is shut off while the work is calculated. One wants to be able to use the ideal-solution (no interaction) equation for the work done, $RT\ln(c_1/c_2)$, and not $RT\ln(a_1/a_2)$. Thus, using the latter expression would be awkward; it needs a knowledge of the activities themselves and that is what one is trying to calculate.

Now, the change in free energy change due to the change in the concentration of the ions after the removal of the effective solvent molecule is

$$RT\ln\left[\frac{x_{\text{after water removal from free to solvated state}}}{x_{\text{before water removal from free to solvated state}}}\right]$$

where x is the mole fraction of the electrolyte in the solution.

Before the water is removed,

$$x_{\text{before}} = \frac{n}{n_w + n} \tag{3.128}$$

where n is the number of moles of electrolyte present in n_w moles of water. Then after the water is removed to the sheaths,

$$x_{\text{after}} = \frac{n}{n_w - n_h + n} \tag{3.129}$$

The change in free energy is

$$RT\ln\frac{n_w + n}{n_w + n - n_h}$$

Hence, the total free-energy change in the solution, calculated per mole of the electrolyte present, is

$$-\frac{n_h}{n}RT\ln a_w + RT\ln\frac{n_w + n}{n_w + n - n_h}$$

Now, one has to switch back to the Coulombic interactions. If the expression for the work done in building up an ionic atmosphere [e.g., Eq. (3.120)] were still valid in the region of relatively high concentrations in which the effect of change of concentration is occurring, then,[20]

[20]Here $\sqrt{c}$ has been written instead of the $I^{1/2}$ of Eq. (3.119). For 1:1 electrolytes, c and I are identical.

$$RT \log f_{\pm(\text{exp})} = -\frac{A\sqrt{c}}{1 + Ba\sqrt{c}} - 2.303\, RT \frac{n_h}{n} \log a_w$$

$$+ 2.303\, RT \log \frac{n_w + n}{n_w + n - n_h} \tag{3.130}$$

One sees at once that there is a possibility of a change in direction for the change in $\log f_{\pm}$ with an increase in concentration in the solution. If the last term predominates, $RT \log f_{\pm}$ may increase with concentration.

The situation here does have a fairly large shadow on it because of the use of the expression (3.120) in $\sqrt{c}$. It will be seen (Section 3.14) that, at concentrations as high as 1 *N*, there are some fundamental difficulties for the ionic-cloud model on which this $\sqrt{c}$ expression of Eq. (3.120) was based (the ionic atmosphere can no longer be considered a continuum of smoothed-out charge). It is clear that when the necessary mathematics can be done, there will be an improvement on the $\sqrt{c}$ expression, and one will hope to get it more correct than it now is. Because of this shadow, a comparison of Eq. (3.130) with experiment to test the validity of the model for removing solvent molecules to the ions' sheathes should be done a little with tongue in cheek.

3.6.3. The Water Removal Theory of Activity Coefficients and Its Apparent Consistency with Experiment at High Electrolytic Concentrations

If one examines the ion–solvent terms in Eq. (3.130), one sees that since $a_w \leq 1$ and in general $n_h > n$ (more than one hydration water per ion), both the terms are positive. Hence, one can conclude that the Debye–Hückel treatment, which ignores the withdrawal of solvent from solution, gives values of activity coefficients that are smaller than those which take these effects into account. Furthermore, the difference arises from the ion–solvent terms, i.e.,

$$-2.303\, RT \frac{n_h}{n} \log a_w + 2.303\, RT \log \frac{n_w + n}{n_w + n - n_h}$$

As the electrolyte concentration increases, a_w decreases and n_h increases; hence both ion–solvent terms increase the value of $\log f$. Furthermore, the numerical evaluation shows that the above ion-solvent term can equal and become larger than the Debye–Hückel $(\sqrt{c})$ Coulombic term. This means that the $\log f_{\pm}$ versus $I^{1/2}$ curve can pass through a minimum and then start rising, which is precisely what is observed (Fig. 3.39, where an activity coefficient is plotted against the corresponding molality).

On the other hand, with increasing dilution, $n_w + n >> n_h$, or $n_w + n - n_h \approx n_w + n$ and $a_w \to 1$, and hence the terms vanish, which indicates that ion–solvent interactions (which are of short range) are significant for the theory of activity

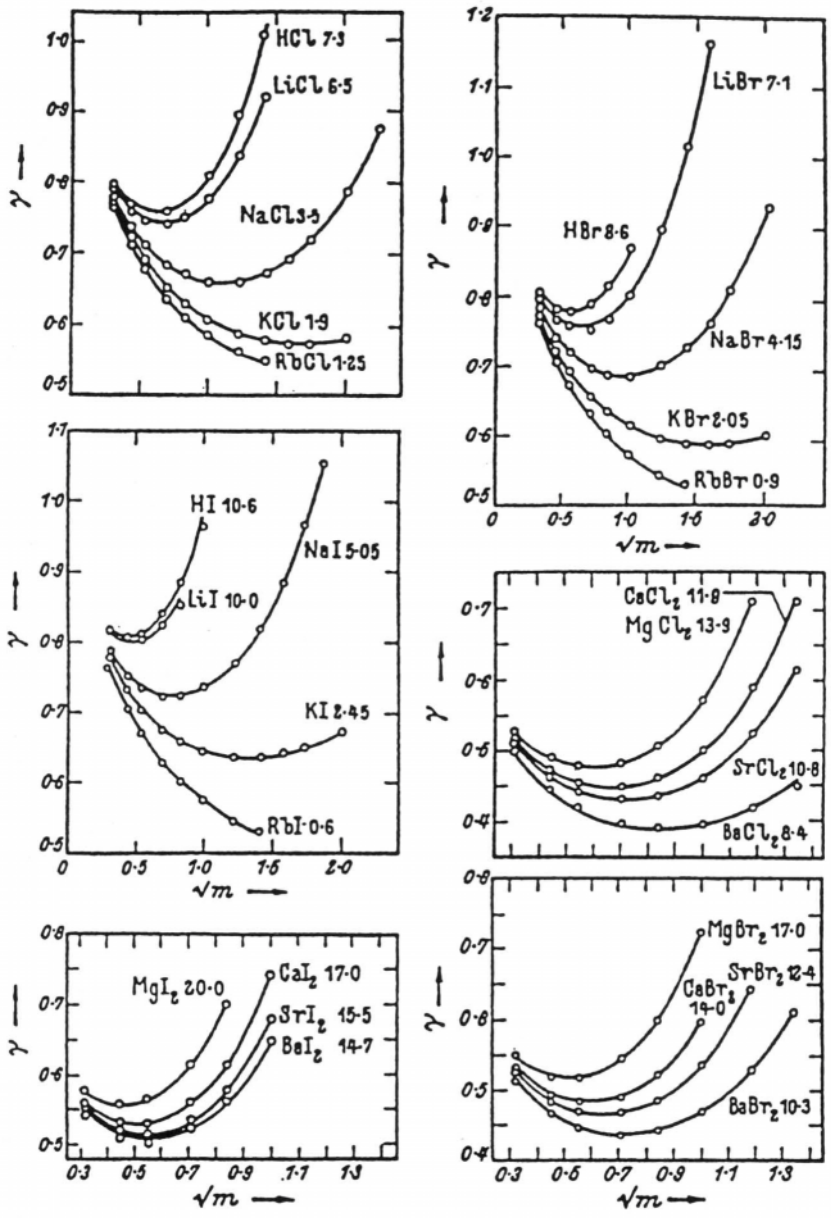

Fig. 3.39. Comparison of experimental activity coefficients with those predicted by the one-parameter equation as shown. (Reprinted from R. H. Stokes and R. A. Robinson, *J. Am. Chem. Soc.* **70**: 1870, 1948.)

TABLE 3.12
Water Activities in Sodium Chloride Solutions

M	a_w	M	a_w
0.1	0.99665	3	0.8932
0.5	0.98355	3.4	0.8769
1	0.96686	3.8	0.8600
1.4	0.9532	4.2	0.8428
1.8	0.9389	4.6	0.8250
2.2	0.9242	5	0.8068
2.6	0.9089	5.4	0.7883

coefficients only in concentrated solutions. At extreme dilutions, only the ion–ion long-range Coulombic interactions are important.

In order to test Eq. (3.130), which is a quantitative statement of the influence of ionic hydration on activity coefficients, it is necessary to know the quantity n_h and the activity a_w of water, it being assumed that an experimentally calibrated value of the ion size parameter is available. The activity of water can be obtained from independent experiments (Table 3.12). The quantity n_h can be used as a parameter. If Eq. (3.130) is tested as a two-parameter equation (n_h and a being the two parameters; Table 3.13), it is found that theory is in excellent accord with experiment. For instance, in the case of NaCl, the calculated activity coefficient agrees with the experimental value for solutions as concentrated as **5 mol dm^{-3}** (Fig. 3.39).

Since the quantity n_h is the number of moles of water used up in solvating $n = n_+ + n_-$ moles of ions, it can be split up into two terms: $(n_h)^+$ moles required to hydrate n_+ moles of cations, and $(n_h)^-$ moles required to hydrate n_- moles of anions. It follows that $[(n_h)^+/n_+]$ and $[(n_h)^-/n_-]$ are the hydration numbers (see Chapter 2) of

TABLE 3.13
Values of n_h of a 1 *M* Solution and *a*

Salt	n_h	a (pm)
HCl	8.0	447
HBr	8.6	518
NaCl	3.5	397
NaBr	4.2	424
KCl	1.9	363
$MgCl_2$	13.7	502
$MgBr_2$	17.0	546

TABLE 3.14

Nearest-Integer Hydration Numbers of Electrolytes from Eq. (3.130) and the Most Probable Value from Independent Experiments

Salt	Hydration Number from Eq. (3.130) (nearest integer)	Hydration Number from Other Experimental Methods
LiCl	7	7 ± 1
LiBr	8	7 ± 1
NaCl	4	6 ± 2
KCl	2	5 ± 2
KI	3	4 ± 2

the positive and negative ions and $[(n_h^+)/n_+] + [(n_h^-)/n_-]$ is the hydration number of the electrolyte.

It has been found that, in the case of several electrolytes, the values of the hydration numbers obtained by fitting the theory [Eq. (3.130)] to experiment are in reasonable agreement with hydration numbers determined by independent methods (Table 3.14). Alternatively, one can say that, when independently obtained hydration numbers are substituted in Eq. (3.130), the resulting values of $\log f_\pm$ show fair agreement with experiment.

In conclusion, therefore, it may be said that the treatment of the influence of ion–solvent interactions on ion–ion interactions has extended the range of concentration of an ionic solution which is accessible to theory. Whereas the finite-ion-size version of the Debye–Hückel theory did not permit theory to deal with solutions in a range of concentrations corresponding to those of real life, Eq. (3.130) advances theory into the range of practical concentrations. Apart from this numerical agreement with experiment, Eq. (3.130) unites two basic aspects of the situation inside an electrolytic solution, namely, ion–solvent interactions and ion–ion interactions.

3.7. THE SO-CALLED "RIGOROUS" SOLUTIONS OF THE POISSON–BOLTZMANN EQUATION

One approach to understanding the discrepancies between the experimental values of the activity coefficient and the predictions of the Debye–Hückel model has just been described (Section 3.6); it involved a consideration of the influence of solvation.

An alternative approach is based on the view that the failure of the Debye–Hückel theory at high concentrations stems from the fact that the development of the theory involved the linearization of the Boltzmann equation (see Section 3.3.5). If such a view is taken, there is an obvious solution to the problem: instead of linearizing the

Boltzmann equation, one can take the higher terms. Thus, one obtains the unlinearized P–B equation

$$\frac{1}{r^2}\frac{d}{dr}\left(r^2\frac{d\psi_r}{dr}\right)=-\frac{4\pi}{\varepsilon}\varrho_r=-\frac{4\pi}{\varepsilon}\sum z_i e_0 n_i^0 e^{-z_i e_0\psi_r/kT} \tag{3.131}$$

In the special case of a symmetrical electrolyte ($z_+ = -z_- = z$) with equal concentrations of positive and negative ions, i e., $n_+^0 = n_-^0 = n^0$, one gets

$$\sum z_i e_0 n_i^0 e^{-z_i e_0\psi_r/kT} = n^0 z_+ e_0 e^{-z_+ e_0\psi_r/kT} - n^0 z_- e_0 e^{+z_- e_0\psi_r/kT}$$

$$= n^0 z e_0 (e^{-ze_0\psi_r/kT} - e^{+ze_0\psi_r/kT}) \tag{3.132}$$

But

$$e^{+x} - e^{-x} = 2\sinh x$$

and therefore

$$\varrho_r = -2n^0 z e_0 \sinh\frac{ze_0\psi_r}{kT} \tag{3.133}$$

or

$$\frac{1}{r^2}\frac{d}{dr}\left(r^2\frac{d\psi}{dr}\right)=\frac{8\pi z e_0 n^0}{\varepsilon}\sinh\frac{ze_0\psi}{kT} \tag{3.134}$$

By utilizing a suitable software, one could obtain from Eq. (3.134) so-called rigorous solutions.

Before proceeding further, however, it is appropriate to stress a logical inconsistency in working with the unlinearized P–B equation (3.131). The unlinearized Boltzmann equation (3.10) implies a *nonlinear* relationship between charge density and potential. In contrast, the *linearized* Boltzmann equation (3.16) implies a *linear* relationship of ϱ_r to ψ_r.

Now, a linear charge density–potential relation is consistent with the law of superposition of potentials, which states that the electrostatic potential at a point due to an assembly of charges is the sum of the potentials due to the individual charges. Thus, when one uses an unlinearized P–B equation, one is assuming the validity of the law of superposition of potentials in the Poisson equation and its invalidity in the Boltzmann equation. This is a basic logical inconsistency which must reveal itself in the predictions that emerge from the so-called rigorous solutions. This is indeed the case, as will be shown below.

Recall that, after the contribution of the ionic atmosphere to the potential at the central ion was obtained, the Coulombic interaction between the central ions and the cloud was calculated by an imaginary charging process, generally known as the *Guntelberg charging process* in recognition of its originator.

In the Guntelberg charging process, the central ion i is assumed to be in a hypothetical condition of zero charge. The rest of the ions, fully charged, are in the positions that they would hypothetically have were the central ion charged to its normal value $z_i e_0$; i.e., the other ions constitute an ionic atmosphere enveloping the central ion (Fig. 3.40). The ionic cloud sets up a potential $\psi_{\text{cloud}} = -(z_i e_0 / \varepsilon \kappa^{-1})$ at the site of the central ion. Now, the charge of the central ion is built up (Fig. 3.40) from zero to its final value $z_i e_0$, and the work done in this process is calculated by the usual formula for the electrostatic work of charging a sphere (see Section 3.3.1), i.e.,

$$W = \frac{z_i e_0}{2} \psi \tag{3.3}$$

Since during the charging only ions of the ith type are considered, the Guntelberg charging process gives that part of the chemical potential due to electrostatic interactions.

Now, the Guntelberg charging process was suggested several years after Debye and Hückel made their theoretical calculation of the activity coefficient. These authors

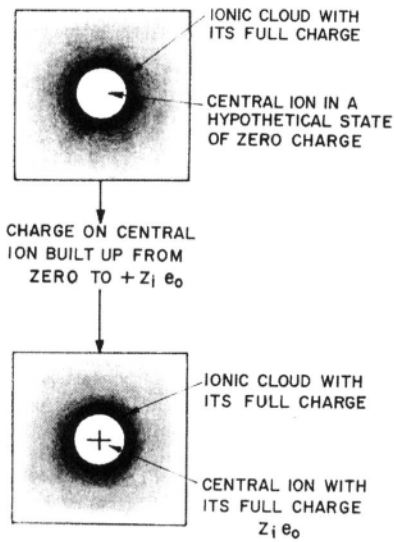

Fig. 3.40. The Guntelberg charging process.

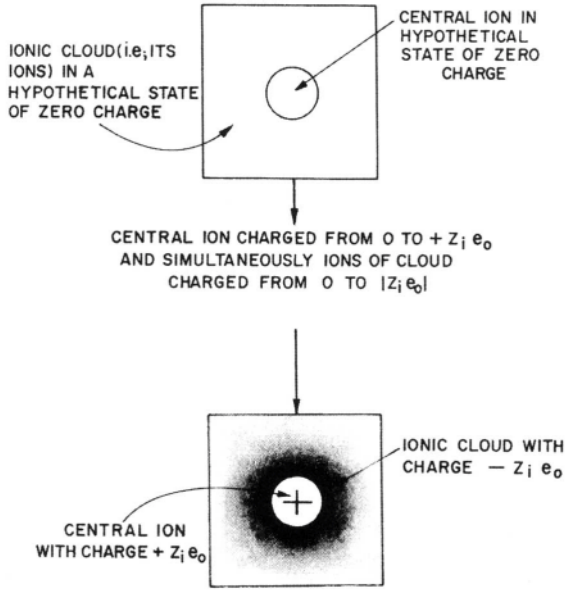

Fig. 3.41. The Debye charging process.

carried out another charging process, the *Debye*[†] *obtaining charging process.* All the ions are assumed to be in their equilibrium, or time-average positions in the ionic atmosphere (Fig. 3.41), but the central ion and the cloud ions are *all* considered in a hypothetical condition of zero charge. All the ions of the assembly are then simultaneously brought to their final values of charge by an imaginary charging process in which there are small additions of charges to each. Since ions of all types (not only of the *i*th type) are considered, the work done in this charging process yields the free-energy change arising from the electrostatic interactions in solution. Differentiation of the free energy with respect to the number of moles of the *i*th species gives the chemical potential

---

[†]Peter Debye is known not only for the seminal theory of the ionic atmosphere: he is the originator of the theory of dielectric constants in polar gases; and of ionic vibration potentials in electrolytes. During the '40's and '50's, his name was perhaps the most well known in the world of physical chemistry. He had a most fertile mind and it was humiliating to bring to him weighty problems which had puzzled you and your colleagues for months, for he generally had the solution in a few minutes and asked "Now what else shall we talk about?" He retained affection for his famous theory of the ionic atmosphere but when asked about it in later years would say: "You know, it applies much better than it should."

Debye was also a much appreciated lecturer at Cornell University in the '50's—particularly when he illustrated the random nature of diffusion movements by doing his "drunkard's walk" in front of the class. However, his eagerness to be an effective administrator was not so clearly manifest and after a year as Head of the Chemistry Department, he returned back to full-time research and teaching.

$$\frac{\partial \Delta G_{I-I}}{\partial n_i} = \Delta \mu_{i-I} \tag{3.135}$$

Using the rigorous solutions of the unlinearized P–B equation, one gets the cloud contribution to the electrostatic potential at the central ion and when this value of the electrostatic potential is used in the two charging processes to get the chemical-potential change $\Delta \mu_{i-I}$ arising from ion–ion interactions, it is found that the Guntelberg and Debye charging processes give discordant results. As shown by Onsager, this discrepancy is not due to the invalidity of either of the two charging processes; it is a symptom of the logical inconsistency intrinsic in the unlinearized P–B equation.

This discussion of rigorous solutions has thus brought out an important point: The disagreement between the chemical-potential change $\Delta \mu_{i-I}$ calculated by the Debye and Guntelberg charging processes cuts off one approach to an improved theory of higher concentrations for it prevents our using the unlinearized P–B equation, which is needed when the concentration is too high for the use of $z_i e_0 \psi / kT << 1$.

3.8. TEMPORARY ION ASSOCIATION IN AN ELECTROLYTIC SOLUTION: FORMATION OF PAIRS, TRIPLETS

3.8.1. Positive and Negative ions Can Stick Together: Ion-Pair Formation

The Debye–Hückel model assumed the ions to be in almost random thermal motion and therefore in almost random positions. The slight deviation from randomness was pictured as giving rise to an ionic cloud around a given ion, a positive ion (of charge $+ze_0$) being surrounded by a cloud of excess negative charge $(-ze_0)$. However, the possibility was not considered that some negative ions in the cloud would get sufficiently close to the central positive ion in the course of their quasi-random solution movements so that their thermal translational energy would not be sufficient for them to continue their independent movements in the solution. Bjerrum suggested that a pair of oppositely charged ions may get trapped in each other's Coulombic field. An *ion pair* may be formed.

The ions of the pair together form an ionic dipole on which the net charge is zero. Within the ionic cloud, the locations of such uncharged ion pairs are completely random, since, being uncharged, they are not acted upon by the Coulombic field of the central ion. Furthermore, on the average, a certain fraction of the ions in the electrolytic solution will be stuck together in the form of ion pairs. This fraction will now be evaluated.

3.8.2. Probability of Finding Oppositely Charged Ions near Each Other

Consider a spherical shell of thickness *dr* and of radius *r* from a reference positive ion (Fig. 3.42). The probability P_r that a negative ion is in the spherical shell is

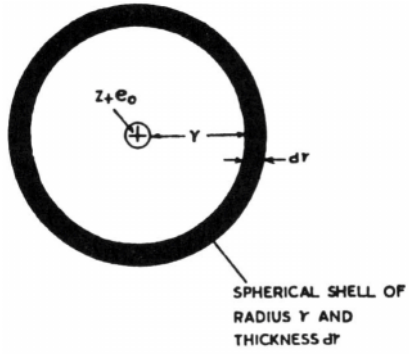

Fig. 3.42. The probability P_r of finding an ion of charge z_-e_0 in a dr-thick spherical shell of radius r around a reference ion of charge z_+e_0.

proportional, first, to the ratio of the volume $4\pi r^2 dr$ of the shell to the total volume V of the solution; second, to the total number N_- of negative ions present; and third, to the Boltzmann factor $\exp(-U/kT)$, where U is the potential energy of a negative ion at a distance r from a cation, i.e.,

$$P_r = 4\pi r^2 dr \frac{N_-}{V} e^{-U/kT} \tag{3.136}$$

Since N_-/V is the concentration n_-^0 of negative ions in the solution and

$$U = \frac{-z_-z_+e_0^2}{\varepsilon r} \tag{3.137}$$

it is clear that

$$P_r = (4\pi n_-^0) r^2 e^{z_-z_+e_0^2/\varepsilon rkT} dr \tag{3.138}$$

or, writing

$$\lambda = \frac{z_-z_+e_0^2}{\varepsilon kT} \tag{3.139}$$

one has

$$P_r = (4\pi n_-^0) e^{\lambda/r} r^2 dr \tag{3.140}$$

A similar equation is valid for the probability of finding a positive ion in a dr-thick shell at a radius r from a reference negative ion. Hence, in general, one may write for

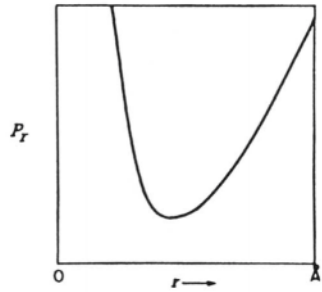

Fig. 3.43. The probability P_r of finding an ion of one type of charge as a function of distance.

the probability of finding an i type of ion in a dr-thick spherical shell at a radius r from a reference ion k of opposite charge

$$P_r = (4\pi n_i^0) e^{\lambda/r} r^2 dr \tag{3.141}$$

where

$$\lambda = \frac{z_i z_k e_0^2}{\varepsilon kT} \tag{3.142}$$

This probability of finding an ion of one type of charge near an ion of the opposite charge varies in an interesting way with distance (Fig. 3.43). For small values of r, the function P_r is dominated by $e^{\lambda/r}$ rather than by r^2, and under these conditions P_r *increases with decreasing* r; for large values of r, $e^{\lambda/r} \to 1$ and P_r *increases with*

TABLE 3.15
Number of Ions in Spherical Shells at Various Distances

	Number of Ions in Shell $\times 10^{22}$	
r (pm)	Of Opposite Charge	Of Like Charge
200	$1.77n_i$	$0.001n_j$
250	$1.37n_i$	$0.005n_j$
300	$1.22n_i$	$0.01n_j$
357	$1.18n_i$	$0.02n_j$
400	$1.20n_i$	$0.03n_j$
500	$1.31n_i$	$0.08n_j$

increasing r because the volume $4\pi r^2 dr$ of the spherical shell increases as r^2. It follows from these considerations that P_r goes through a minimum for a particular, critical value of *r*. This conclusion may also be reached by computing the number of ions in a series of shells, each of an arbitrarily selected thickness of 0.01 nm (Table 3.15).

3.8.3. The Fraction of Ion Pairs, According to Bjerrum

If one integrates P_r between a lower and an upper limit, one gets the probability P_r of finding a negative ion within a distance from the reference positive ion, defined by the limits. Now, for two oppositely charged ions to stick together to form an ion pair, it is necessary that they should be close enough for the Coulombic attractive energy to overcome the thermal energy that scatters them apart. Let this "close-enough" distance be *q*. Then one can say that an ion pair will form when the distance *r* between a positive and a negative ion becomes less than *q*. Thus, the probability of ion-pair formation is given by the integral of P_r between a lower limit of *a*, the distance of closest approach of ions, and an upper limit of *q*.

Now, the probability of any particular event is the number of times that the particular event is expected to be observed divided by the total number of observations. Hence, the probability of ion-pair formation is the number of ions of species *i* that are associated into ion pairs divided by the total number of *i* ions; i.e., the probability of ion-pair formation is the fraction θ of ions that are associated into ion pairs. Thus,

$$\theta = \int_a^q P_r\, dr = \int_a^q 4\pi n_i^0 e^{\lambda/r} r^2\, dr \tag{3.143}$$

It is seen from Fig. 3.44 that the integral in Eq. (3.143) is the area under the curve between the limits $r = a$ and $r = q$. It is obvious that as *r* increases past the minimum, the integral becomes greater than unity. Since, however, θ is a fraction, this means that the integral diverges.

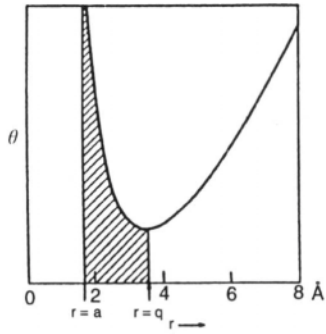

Fig. 3.44. Graphical representation of the integral in Eq. (3.143), between the limits *a* and *q*.

In this context, Bjerrum took an arbitrary step and cut off the integral at the value of $r = q$ corresponding to the minimum of the P_r vs. r curve. This minimum probability can easily be shown (Appendix 3.4) to occur at

$$q = \frac{z_+ z_- e_0^2}{2\varepsilon kT} = \frac{\lambda}{2} \tag{3.144}$$

Bjerrum argued that it is only short-range Coulombic interactions that lead to ion-pair formation and, further, when a pair of oppositely charged ions are situated at a distance apart of $r > q$, it is more appropriate to consider them free ions.

Bjerrum concluded therefore that ion-pair formation occurs when an ion of one type of charge (e.g., a negative ion) enters a sphere of radius q drawn around a reference ion of the opposite charge (e.g., a positive ion). However, it is the ion size parameter that defines the distance of closest approach of a pair of ions. The Bjerrum hypothesis can therefore be stated as follows: If $a < q$, then ion-pair formation can occur; if $a > q$, the ions remain free (Fig. 3.45).

Now that the upper limit of the integral in Eq. (3.143) has been taken to be $q = \lambda/2$, the fraction of ion pairs is given by carrying out the integration. It is

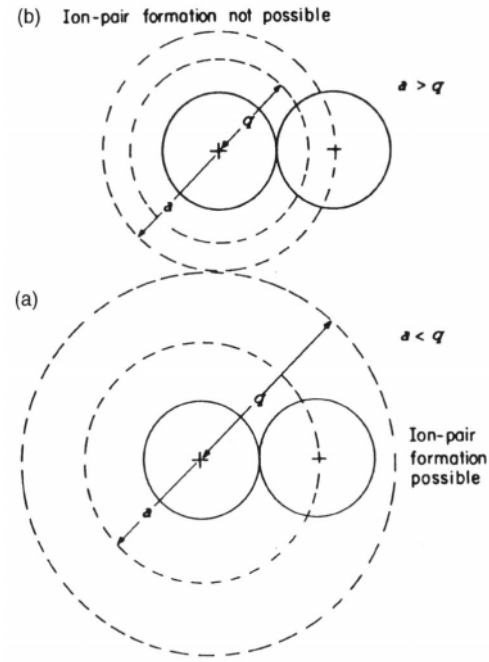

Fig. 3.45. (a) Ion-pair formation occurs if $a < q$. (b) Ion-pair formation does not occur if $a > q$.

TABLE 3.16
Values of the Integral $\int_2^b e^y y^{-4}\,dy$

b	$\int_2^b e^y y^{-4}\,dy$	b	$\int_2^b e^y y^{-4}\,dy$	b	$\int_2^b e^y y^{-4}\,dy$
2.0	0	3	0.326	10	4.63
2.1	0.0440	3.5	0.442	15	93.0
2.2	0.0843	4	0.550		
2.4	0.156	5	0.771		
2.6	0.218	6	1.041		
2.8	0.274				

$$\theta = 4\pi n_i^0 \int_a^{q=\lambda/2} e^{\lambda/r} r^2\,dr \tag{3.145}$$

For mathematical convenience, a new variable y is defined as

$$y = \frac{\lambda}{r} = \frac{2q}{r} \tag{3.146}$$

Hence, in terms of the new variable y, Eq. (3.145) becomes (Appendix 3.5)

$$\theta = 4\pi n_i^0 \left(\frac{z_+ z_- e_0^2}{\varepsilon kT}\right)^3 \int_2^b e^y y^{-4} dy \tag{3.147}$$

where

$$b = \frac{\lambda}{a} = \frac{z_+ z_- e_0^2}{\varepsilon akT} = \frac{2q}{a} \tag{3.148}$$

Bjerrum has tabulated the integral $\int_2^b e^y y^{-4} dy$ for various values of b (Table 3.16). This means that, by reading off the value of the corresponding integral and substituting for the various other terms in Eq. (3.147), the degree of association of an electrolyte may be computed if the ion sizes, the dielectric constant, and the concentrations are known (Table 3.17).

3.8.4. The Ion-Association Constant K_A of Bjerrum

The quantity θ yields a definite idea of the fraction of ions that are associated in ion pairs in a particular electrolytic solution at a given concentration. The ions that get associated are those that get sufficiently close to an ion of opposite sign so that the energy of Coulombic attraction is greater than the thermal energy of the pair.

TABLE 3.17
Fraction of Association, θ, of Univalent Ions in Water at 291 K

$a \times 10^8$ cm:	2.82	2.35	1.76	1.01	0.70	0.47
q/a:	2.5	3	4	7	10	15
c, moles dm^{-3} [a]						
0.0001	—	—	—	—	0.001	0.027
0.0002	—	—	—	—	0.002	0.049
0.0005	—	—	—	0.002	0.006	0.106
0.001	—	0.001	0.001	0.004	0.011	0.177
0.002	0.002	0.002	0.003	0.007	0.021	0.274
0.005	0.002	0.004	0.007	0.016	0.048	0.418
0.01	0.005	0.008	0.012	0.030	0.030	0.529
0.02	0.008	0.013	0.022	0.053	0.137	0.632
0.05	0.017	0.028	0.046	0.105	0.240	0.741
0.1	0.029	0.048	0.072	0.163	0.336	0.804
0.2	0.048	0.079	0.121	0.240	0.437	0.854

[a] c in moles dm$^{-3} = 1000 n_i^0 / N_A$.

It would, however, be advantageous if each electrolyte [e.g., **NaCl, $BaSO_4$,** and **$La(NO_3)_3$**] were assigned a particular number that would reveal, without going through the calculation of θ, the extent to which the ions of that electrolyte associate in ion pairs. The quantitative measure chosen to represent the tendency for ion-pair formation was guided by historical considerations.

Arrhenius in 1887 had suggested that many properties of electrolytes could be explained by a *dissociation* hypothesis: The neutral molecules AB of the electrolyte dissociate to form ions A^+ and B^-, and this dissociation is governed by an equilibrium

$$AB \rightleftharpoons A^+ + B^- \tag{3.149}$$

Applying the law of mass action to this equilibrium, one can define a dissociation constant

$$K = \frac{a_{A^+} a_{B^-}}{a_{AB}} \tag{3.150}$$

By analogy,[21] one can define an association constant K_A for ion-pair formation. Thus, one can consider an equilibrium between free ions (the positive M^+ ions and the negative A^- ions) and the associated ion pairs (symbolized IP)

[21] The analogy must not be carried too far because it is only a formal analogy. Arrhenius's hypothesis can now be seen to be valid for ionogens (i.e., potential electrolytes), in which case the neutral ionogenic molecules (e.g., acetic acid) consist of aggregates of atoms held together by covalent bonds. What is under discussion here is ion association, or ion-pair formation, of ionophores (i.e., true electrolytes). In these ion pairs, the positive and negative ions retain their identity as ions and are held together by electrostatic attraction.

$$M^+ + A^- \rightleftharpoons IP \tag{3.151}$$

The equilibrium sanctions the use of the law of mass action

$$K_A = \frac{a_{IP}}{a_{M^+} a_{A^-}} \tag{3.152}$$

where the a's are the activities of the relevant species. From (3.152) it is seen that K_A is the reciprocal of the ion pair's dissociation constant.

Since θ is the fraction of ions in the form of ion pairs, θc is the *concentration* of ion pairs, and $(1 - \theta)c$ is the concentration of free ions. If the activity coefficients of the positive and negative free ions are f_+ and f_-, respectively, and that of the ion pairs is f_{IP}, one can write

$$K_A = \frac{\theta c f_{IP}}{(1-\theta)cf_+(1-\theta cf_-}$$

$$= \frac{\theta}{(1-\theta)^2} \frac{1}{c} \frac{f_{IP}}{f_+ f_-} \tag{3.153}$$

or, using the definition of the mean ionic-activity coefficient [Eq. (3.72)],

$$K_A = \frac{\theta}{(1-\theta)^2} \frac{1}{c} \frac{f_{IP}}{f_\pm^2} \tag{3.154}$$

Some simplifications can now be introduced. The ion-pair activity coefficient f_{IP} is assumed to be unity because deviations of activity coefficients from unity are ascribed in the Debye–Hückel theory to electrostatic interactions. But ion pairs are not involved in such interactions owing to their zero charge and hence they behave ideally like uncharged particles, i.e., $f_{IP} = 1$.

Furthermore, in very dilute solutions: (1) The ions rarely come close enough together (i.e., to within a distance q) to form ion pairs, and one can consider $\theta \ll 1$ or $1 - \theta \approx 1$; (2) activity coefficients tend to unity, i.e., f_i or $f_\pm \to 1$.

Hence, under these conditions of very dilute solutions, Eq. (3.154) becomes

$$K_A \approx \frac{\theta}{c} \tag{3.155}$$

and substituting for θ from Eq. (3.147), one has

$$K_A = \frac{4\pi n_i^0}{c} \left(\frac{z_+ z_- e_0^2}{\varepsilon kT} \right)^3 \int_2^b e^y y^{-4} dy \tag{3.156}$$

TABLE 3.18
Ion-Association Constant K_A: Extent to Which Ion-Pair Formation Occurs

Salt	Solvent	Temperature (K)	ε	K_A
KBr	Acetic acid	303	6.20	9.09×10^6
KBr	Ammonia	239	22	5.29×10^2
CsCl	Ethanol	298	24.30	1.51×10^2
KI	Acetone	298	20.70	1.25×10^2
KI	Pyridine	298	12.0	4.76×10^3

But

$$n_i^0 = \frac{cN_A}{1000} \tag{3.157}$$

and therefore,

$$K_A = \frac{4\pi N_A}{1000}\left(\frac{z_+ z_- e_0^2}{\varepsilon kT}\right)^3 \int_2^b e^y y^{-1}\, dy \tag{3.158}$$

The value of the association constant provides an indication of whether ion-pair formation is significant. The higher the value of K_A, the more extensive is the ion-pair formation (Table 3.18).

What are the factors that increase K_A and therefore increase the degree of ion-pair formation? From Eq. (3.158), it can be seen that the factors that increase K_A are (1) low dielectric constant ε; (2) small ionic radii, which lead to a small value of a and hence [Eq. (3.148)] to a large value of the upper limit b of the integral in Eq. (3.158); and (3) large z_+ and z_-.

These ideas based on Bjerrum's picture of ion-pair formation have received considerable experimental support. Thus, in Fig. 3.46, the association constant is seen to increase markedly with decrease of dielectric constant.[22] The dependence of ion-pair formation on the distance of closest approach is seen in Fig. 3.47.

When numerical calculations are carried out with these equations, the essential conclusion that emerges is that in aqueous media, ion association in pairs scarcely occurs for 1:1-valent electrolytes but can be important for 2:2-valent electrolytes. (However, see the results of post-Bjerrum calculations in 3.13.) The reason is that K_A depends on z_+z_- through Eq. (3.156). In nonaqueous solutions, most of which have dielectric constants much less than that of water ($\varepsilon = 80$), ion association is extremely important.

[22]The critical dielectric constant above which there is no more ion-pair formation (as indicated by Fig. 3.46) is really a result of the arbitrary cutting off of ion-pair formation at the distance q.

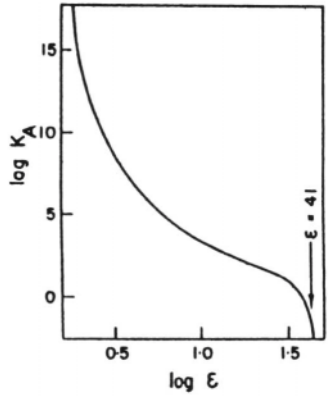

Fig. 3.46. Variation of the association constant K_A with the dielectric constant for 1:1 salts.

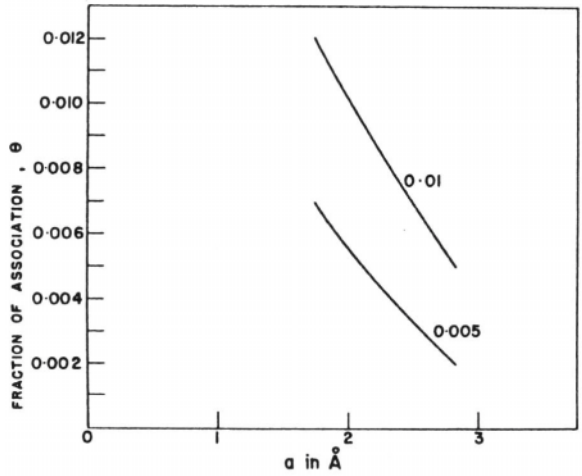

Fig. 3.47. Variation of θ, the fraction of associated ions, with a, the distance of closest approach (i.e., the ion size parameter).

3.8.5. Activity Coefficients, Bjerrum's Ion Pairs, and Debye's Free Ions

What direct role do the ion pairs have in the Debye–Hückel electrostatic theory of activity coefficients? The answer is simply: None. Since ion pairs carry no net charge,[23] they are ineligible for membership in the ion cloud, where the essential qualification is *charge*. Hence, ion pairs are dismissed from a direct consideration in the Debye–Hückel theory.

This does not mean that the Debye–Hückel theory gives the right answer when there is ion-pair formation. The extent of ion-pair formation decides the value of the concentration to be used in the ionic-cloud model. By removing a fraction θ of the total number of ions, only a fraction $1 - \theta$ of the ions remain for the Debye–Hückel treatment, which interests itself only in the free charges. Thus, the Debye–Hückel expression for the activity coefficient [Eq. (3.120)] is valid for the free ions, with two important modifications: (1) Instead of there being a concentration c of ions, there is only $(1 - \theta)c$; the remainder θc is not reckoned with owing to association. (2) The distance of closest approach of free ions is q and not a. These modifications yield

$$\log f_{\pm} = -\frac{A(z_+z_-)\sqrt{(1-\theta)c}}{1 + Bq\sqrt{(1-\theta)c}} \tag{3.159}$$

This calculated mean activity coefficient is related to the measured mean activity coefficient of the electrolyte $(f_{\pm})_{obs}$ by the relation (for the derivation, see Appendix 3.6)

$$(f_{\pm})_{obs} = (1 - \theta) f_{\pm} \tag{3.160}$$

or

$$\begin{aligned} \log (f_{\pm})_{obs} &= \log f_{\pm} + \log (1 - \theta) \\ &= -\frac{A(z_+z_-)\sqrt{(1-\theta)c}}{1 + Bq\sqrt{(1-\theta)c}} + \log (1 - \theta) \end{aligned} \tag{3.161}$$

This equation indicates how the activity coefficient depends on the extent of ion association. In fact, this equation constitutes the bridge between the treatment of solutions of true electrolytes and that of solutions of potential electrolytes.

3.8.6. From Ion Pairs to Triple Ions to Clusters of Ions

The Coulombic attractive forces given by $z_+z_-e_0^2/\varepsilon r^2$ are large when the dielectric constant is small. When nonaqueous solvents of low dielectric constant are used, the

[23] Remember that the equations for the Bjerrum theory as presented here are correct only for electrolytes yielding ions of the same valence z., i.e., only for symmetrical 1:1- or 2:2-valent electrolytes.

values of dielectric constant are small. In such solutions of electrolytes therefore it has already been stated that ion-pair formation is favored.

Suppose that the electrostatic forces are sufficiently strong then it may well happen that the ion-pair "dipoles" may attract ions and *triple ions* be formed; thus

$$M^+ + (A^-M^+)_{\text{ion pair}} = [M^+A^-M^+]_{\text{triple ion}} \tag{3.162}$$

or

$$A^- + (M^+A^-)_{\text{ion pair}} = [A^-M^+A^-]_{\text{triple ion}} \tag{3.163}$$

Charged triple ions have been formed from uncharged ion pairs. These charged triple ions play a role in determining activity coefficients. Triple-ion formation has been suggested in solvents for which $\varepsilon < 15$. The question of triple-ion formation can be treated on the same lines as those for ion-pair formation.

A further decrease of dielectric constant below a value of about 10 may make possible the formation of still larger clusters of four, five, or more ions. In fact, there is some evidence for the clustering of ions into groups containing four ions in solvents of low dielectric constant.

3.9. THE VIRIAL COEFFICIENT APPROACH TO DEALING WITH SOLUTIONS

The material so far presented has shown that a model taking into account the size of the ions, ion-pair formation, and the idea that some of the water in the solution was not to be counted in estimating the "effective" concentration—the activity—has allowed a fair accounting for the main arbiter of the interionic attraction energy, the activity coefficient, even at concentrations up to nearly 5 mol dm^{-3} (see, e.g., Fig. 3.39).

This position of ionic solution theory has, however, a challenger,[24] and, during the 1970s and 1980s, it was this radically different approach to ionic solution theory

[24]There might be some who would actually say that there was "something wrong" with the theory of Debye and Hückel, but this claim depends on which version of the theory one means. The limiting-law equation certainly is inconsistent with experiments above ~ 5×10^{-3} mol dm^{-3} for a 1:1 electrolyte and even smaller concentrations for electrolytes possessing ions with a valence above unity. The later developments of the theory, which take into account the space occupied by the ions, do much better and taking the effect of solvation into account gives agreement with experiment to concentrations up to 10 mol dm^{-3} (Fig. 3.39). One question relates to whether cations and anions should have the same activity coefficient (the simple, original Debye and Hückel theory predicts this), but if one extends the model to account for "dead water" around ions, it turns out that there is more of this with small cations (they cling to water tighter) than with big anions, where the ion–water electric field is less and hence adherent dead waters are less in number. This solvational difference would imply a higher activity coefficient at high concentrations for cations than for anions, for which there is some evidence.

that absorbed most of the creative energy of physical electrochemists interested in this field. Suppose, says this '70s and '80s view, that one manages to remove from one's mind the evidence that some ions stick together in pairs, that (at least with smaller ions) they stick to water, and that the word "solvent" applies only to the free water. Then one tries to replicate experimental data with bare ions (always present in the stoichiometric amount and always free; there are no associated pairs) and free water alone.

Suppose also one regarded the basic idea of an "atmosphere" of ions (see Fig. 3.11) as a bit too theoretical for comfort and wanted to try an approach that looked more directly at the ionic interaction of individual ions. Then one might easily think of an approach made earlier in the century to deal with intermolecular force interactions and size effects in real gases: van der Waals's theory of imperfect gases. McMillan and Mayer devised a theory for liquids of this kind (although it was based on the theory of imperfect gases) in 1945 but tried to do much more than van der Waals had done. They used some highly generalized statistical mechanical arguments to deduce equations for pressure in terms of a number of virial (= force) coefficients

$$\frac{PV}{RT} = 1 + \frac{A}{V} + \frac{B}{V^2} + \frac{C}{V^3} + \ldots \tag{3.164}$$

where P, V, and RT are as usually understood in physical chemistry; A, B, C, etc., are the so-called *virial coefficients* theorized to take into account the intermolecular forces.

Applied to ionic solutions by Mayer in 1950, this theory aimed to express the *activity coefficient* and the *osmotic pressure* of ionic solutions while neglecting the effects of solvation that had been introduced by Bjerrum and developed by Stokes and Robinson to give experimental consistency of such impressive power at high concentrations.

However, Mayer found it to be more difficult to obtain a total of the interionic forces than that of forces between uncharged molecules. The reason is that the latter decline very rapidly, their dependence on distance being proportional to r^{-7}. Hence, accounting for nearest-neighbor interactions only becomes an acceptable proposition.

Consider now the interaction between an ion and those in a surrounding spherical section of ions chosen here—in this simple example of the kind of difficulty Mayer encountered—to be all of opposite sign to that of the central ion.

The energy of attraction of the central positive ion and *one* negative ion is $-e_0^2/\varepsilon r$, where r is the distance apart of two ions of opposite sign and ε is the dielectric constant. If the ionic concentration is N_i ions cm^{-3}, the number of ions in the spherical shell of thickness dr_i is $4\pi r^2 N_i\, dr$; therefore the energy of interaction of the central ion with all the negative ones becomes

$$W = \frac{4\pi N_i e_0^2}{\varepsilon} \int_{r_i}^{\infty} r\, dr \to \infty \tag{3.165}$$

This is a difficulty that occurs with many problems involving Coulombic interaction.

Mayer then conceived a most helpful stratagem. Instead of taking the potential of an ion at a distance r as $\psi = e_0/\varepsilon r$, he took it as $\psi = e_0 e^{-\kappa r}/\varepsilon r$ [where κ is the same κ of Debye–Hückel; Eq. (3.20)]. With this approach he found that the integrals in his theory, which diverged earlier [Eq. (3.165)] now *converged*. Hence, the calculation of the interionic interaction energy—the interaction of a representative ion with both negative and positive ions surrounding it—could yield manageable results.

There are many writers who would continue here with an account of the degree to which experiments agree with Mayer's theory and pay scant attention to the justification of the move that underlies it.[25] However, it *is* possible to give some basis to Mayer's equation (Friedman, 1989) because in a mixture of ions, interaction at a distance occurs through many other ions. Such intervening ions might be perceived as screening the interaction of one ion from its distant sister, and one feels intuitively that this screening might well be modeled by multiplying the simple $e_0/\varepsilon r$ by $e^{-\kappa r}$, for the new term decreases the interaction at a given distance and avoids the catastrophe of Eq. (3.165).

Does Mayer's theory of calculating the virial coefficients in equations such as Eq. (3.165) (which gives rise directly to the expression for the osmotic pressure of an ionic solution and less directly to those for activity coefficients) really improve on the second and third generations of the Debye–Hückel theory—those involving, respectively, an accounting for ion size and for the water removed into long-lived hydration shells?

Figure 3.48 shows two ways of expressing the results of Mayer's virial coefficient approach using the osmotic pressure[26] of an ionic solution as the test quantity. Two versions of the Mayer theory are indicated. In the one marked **DHLL + B_2**, the authors have taken the Debye–Hückel limiting-law theory, redone for osmotic pressure instead of activity coefficient, and then added to it the results of Mayer's calculation of the second virial coefficient, B. In the upper curve of Fig. 3.48, the approximation within the Mayer theory used in summing integrals (the one called hypernetted chain or HNC) is indicated. The former replicates experiment better than the latter. The two approxi-

---

[25]One of the reasons for passing over the physical basis of the modified equation for the potential due to an ion in Mayer's view is that several mathematical techniques are still needed to obtain final answers in Mayer's evaluation of an activity coefficient. (To replace the ionic cloud, he calculates the distribution of ions around each other and from this the sum of their interactions.) Among these occur equations that are approximation procedures for solving sums of integrals. To a degree, the mathematical struggle seems to have taken attention away from the validity of the modified equation for the potential due to an ion at distance r. These useful approximations consist of complex mathematical series (which is too much detail for us here) but it may be worthwhile noting their names (which are frequently mentioned in the relevant literature) for the reader sufficiently motivated to delve deeply into calculations using them. They are, in the order in which they were first published, the Ornstein–Zernicke equation, the Percus–Yevich equation, and the "hypernetted chain" approach.

[26]Since Mayer's theory originated in a theory for imperfect *gases*, it naturally tends to calculate the nearest analogue of gas pressure that an ionic solution exhibits—osmotic pressure.

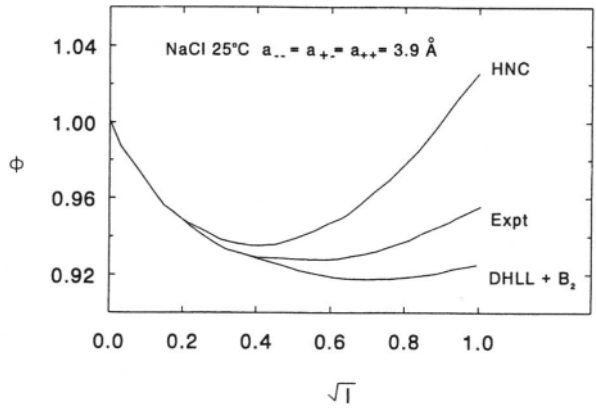

Fig. 3.48. Osmotic coefficients for the primitive model electrolyte compared with the experimental results for NaCl in aqueous solutions at 298 K. The $a_{\pm}$ parameters in the HNC and DHLL + B_2, approximations have been chosen to fit the data below 0.05 mol dm^{-3}. I is the ionic strength. (Reprinted from J. C. Rasaiah, *J. Chem. Phys.* **52:** 704, 1970.)

mations differ by ~12%. To get results which agree really well (±1%) with experiment up to, say, 1 mol dm^{-3}, the original theory tested here is not enough. One has to develop the interaction energy more realistically than by the use of Mayer's perceptive $e_0^2 e^{-\kappa r}/\varepsilon r$, using the addition of a number of "extra potentials," representing, for example, short-range repulsion energies on contact (Section 3.10.1). It is these closer approaches to physical reality rather than the solutions to difficult mathematical equations representing an overly simple model that now mark the way for electrolyte theory.

Further Reading

Seminal

1. N. Bjerrum, "Ionic Association," *Kgl. Danske Videnskab. Selskab.* **7**: 9 (1926).
2. W. G. McMillan and J. E. Mayer, "A Virial Coefficient Approach to the Theory of Fluids," *J. Chem. Phys.* **13**: 276 (1945).
3. J. E. Mayer, "A Virial Theory of Ionic Solutions," *J. Chem. Phys.* **18**: 1426 (1950).
4. R. M. Fuoss and L. Onsager, "Ionic Association in Electrolyte Theory," *Proc. Natl. Acad. Sci. U.S.A.* **41**: 274, 1010 (1955).
5. T. L. Hill, "A Simplified Version of the McMillan-Meyer Theory," *J. Chem. Phys.* **30**: 93 (1959).

Review

1. H. L. Friedman, E. O. Raineri, and O. M. D. Wodd, "Ion-Ion Interactions," *Chemica Scripta* **29A**: 49 (1989).
2. J. C. Rasaiah, "A Model for Weak Electrolytes," *Int. J. Thermodyn.* **11**: 1 (1990).
3. L. M. Schwartz, "Ion Pair Complexation in Moderately Strong Aqueous Acids," *J. Chem. Ed.* **72**: 823 (1995).

Papers

1. J.-L. Dandurand and J. Schott, *J. Phys. Chem.* **96**: 7770 (1992).
2. E. H. Oelkers and H. C. Helgeson, *Science* **261**: 888 (1993).
3. J. Gao, *J. Phys. Chem.* **98**: 6049 (1994).
4. J. Wang and A. J. Haymet, *J. Chem. Phys.* **100**: 3767 (1994).
5. M. Madhusoodana and B. L. Tembe, *J. Phys. Chem.* **99**: 44 (1995).
6. G. Sese, E. Guardia, and J. A. Padro, *J. Phys. Chem.* **99**: 12647 (1995).
7. M. Ue and S. Mori, *J. Electrochem. Soc.* **142**: 2577 (1995).

3.10. COMPUTER SIMULATION IN THE THEORY OF IONIC SOLUTIONS

All parts of the physical sciences are now served by calculation techniques that would not have been possible without the speed of electronic computers. Such approaches are creative in the sense that, given the law of the energy of interaction between the particles, the software allows one to predict experimental quantities. If agreement with experiment is obtained, it tells us that the energy of interaction law assumed is correct. Sometimes this approach can be used to calculate properties that are difficult to determine experimentally. Such calculations may allow increased insight into what is really happening in the system concerned or they may be used simply as rapid methods of obtaining the numerical value of a quantity.[27] There are two main computational approaches and these will be discussed next.

3.10.1. The Monte Carlo Approach

The Monte Carlo approach was invented by Metropolis (Metropolis, 1953). The system concerned is considered in terms of a small number of particles—a few hundred. The basic decision that has to be made is: What law are the particles i and j going to follow in expressing the interaction energy between them as a function of their distance apart? For example, a useful law might be the well-known Lennard-Jones equation:

[27]The major attraction of such computer simulation approaches is that they often result in lower costs. However, a prerequisite to their use is an experimental value on some related system, so that the As and Bs of equations such as Eq. (3.166) can be calibrated.

$$U_{ij} = -\frac{A}{r^6} + \frac{B}{r^{12}} \tag{3.166}$$

where r *is* the interparticle distance and A and B are constants, the values of which are not usually found from independent determinations but by assuming the law of interaction calculation procedure to be correct and finding the A's and B's that have then to be used to fit the experimental quantities.

What is the procedure? The N particles are started off in any configuration, e.g., in that of a regular lattice. Then each particle is moved randomly (hence the title of the procedure). A single but vital question is asked about each move: does it increase the energy of the particle (make its potential energy move positive) or decrease it (potential energy more negative)? If the former, the move is not counted as contributing to the final equilibrium stage of the system. If the latter, it is counted.

Such a calculation is then carried out successively on each particle many times. Since each can move to any point within the allotted space, a large enough number of moves allows one to reach the equilibrium state of the system while calculating a targeted quantity, e.g., the pressure of an imperfect gas. The result is compared with that known experimentally, thus confirming or denying the force law assumed (and other assumptions implicit in the calculation).

Card and Valleau (1970) were the first to apply the Metropolis Monte Carlo method to an electrolytic solution. Their basic assumption was that if

$$r < a_{ij} \quad U_{ij} = \infty$$

$$r > a_{ij} \quad U_{ij} = \frac{z_i z_j e_0^2}{\varepsilon} \tag{3.167}$$

In spite of the long-range nature of the interionic forces, they assumed that the yes/no answers obtained on the basis of the nearest-neighbor interactions could be relied upon. Using this nearest-neighbor-only approximation, and neglecting ion association and the effects of hydration in removing some of the water from circulation, their calculation replicated the experimentally observed minimum in the log $\gamma_\pm$ vs. $\sqrt{c}$ plot up to 1.4 mol $\mathbf{dm}^{-3}$, a point supporting the approach.

3.10.2. Molecular Dynamic Simulations

Another and now more widely used computational approach to predicting the properties of ions in solution follows from the Monte Carlo method. Thus, in the latter, the particle is made mentally to move randomly in each "experiment" but only one question is posed: Does the random move cause an increase or decrease of energy? In molecular dynamic (MD) simulations, much more is asked and calculated. In fact, a random micromovement is subjected to all the questions that classical dynamics can ask and answer. By repeating calculations of momentum and energy exchanges

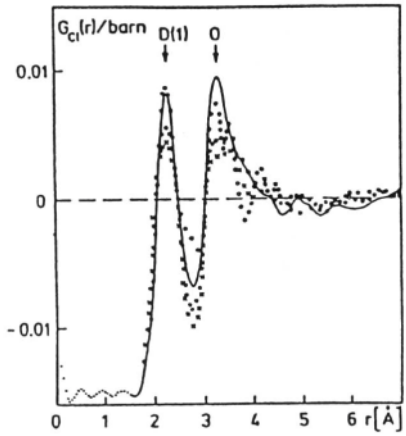

Fig. 3.49. Comparison of the weighted Cl^--water radial distribution function from an MD simulation of a 1.1 *M* $MgCl_2$ solution (solid line) with results from neutron diffraction studies of a 5.32 *M*NaCl(o), a 3 *M* $NiCl_2$ (x), and a 9.95 *M*LiCl (•) solution (1 Å = 0.1 nm). (Reprinted from P. Bopp, *NATO ASI Series* **206**: 237,1987.)

between particles as they approach each other at intervals of time of the order of a few femtoseconds, and then working out the dynamic consequences for each encounter for the few hundred particles considered, it is possible to calculate the distribution functions of the particles in respect to a central particle, $g(r)$. Knowing this calculated distribution function, many properties of an ionic system can be computed. Of course, as with the Monte Carlo approach, the MD calculations pertain to reality insofar as the two-body energy–distance law between the particles has been made to fit the system by using some experimental results to calculate the parameters in such equations as (3.166). The procedure is thus designed to give an experiment-consistent answer.

P. Bopp has carried out many MD simulations for aqueous ionic solutions, following the introduction of the method by Adler and Wainwright (1959). The type of agreement he can obtain between theory and experiment is illustrated in Fig. 3.49.

3.10.3. The Pair-Potential Interaction

Computer simulation studies are based on the need for an experimental value to start with! The A and B of Eq. (3.166) are not obtained from independent methods. Rather, they are adjusted so that even with a simple pair potential, the calculation is

correct. Thus in mechanics it is fundamentally not possible to calculate the final result of the interaction of more than two particles! Hence, the implicit assumption is made that the properties of a body depend on *pair*-potential (i.e., *two*-body) interactions only. Of course, this is not the case, and indeed the influence of particles apart from nearest neighbors is particularly strong for Coulombic interactions because of their long range. Thus A and B are not the real values for the interaction of a pair of particles in Eq. (3.166). They are values that make the simplified equations (two-body-interaction-only assumption) correct. The computation then becomes possible. The ability of the computation to get the right answer is bred into the calculation at an early stage.

This is a burden that MD (and Monte Carlo) procedures carry with them. Since the parameters are built in to give the right results on approximate model assumptions (no ion association, for example), the procedure is better suited for calculating quantities correctly than for finding out what is going on. Thus in electrolytic solution theory, the mean spherical approximation (MSA) and other procedures produce experimentally consistent values and properties, such as osmotic and activity coefficients up to a high concentration of 2 mol $\mathbf{dm}^{-3}$ (Section 3.16). However, in getting the right answer, they neglect the effects of hydration on the availability of water to act as part of the solution, although a substantial fraction of the ions are known to be associated and all the free ions are hydrated. The right answer is produced on the wrong model. Thus, computer-simulated solutions are good "answer-getters," but one had better look to spectroscopy to find out what is really going on.

3.10.4. Experiments and Monte Carlo and MD Techniques

In the brief description of computational approaches to the properties of solutions presented in this chapter, only the barest bones have been indicated (see also Chapters 2 and 5). The techniques actually used to move from the application of mechanics to the movement of particles to the computation of observable properties are beyond the scope of this book.

However, it is right to face an interesting question. The computational techniques described are widely used in research. They led to the rapid calculation of many properties of systems formerly laboriously determined by large numbers of white-coated experimentalists. They even allow calculation of some properties for which experimental determinations are nearly impossible.[28] Are the days of the white coats numbered?

There seems to be much going for this proposition. Before acceding to it completely, it is necessary to recall what has been written earlier about the use of pair potentials in place of multiparticle interactions. The quantities A and B in the Lennard-

[28]Excellent examples are the properties of the first one to two layers of water near an ion in a dilute solution or the properties of silicates at great pressures deep in the interior of the planet.

Jones equation are calculated from *experimentally obtained values.* Furthermore, it should be an experiment that duplicates as closely as possible the phenomena for which answers are being sought by means of calculation.

There is another reservation that should be mentioned for those who see Monte Carlo and MD techniques as all-conquering: they use classical mechanics. This is all very well for some movements, e.g., translation in imperfect gases. But what of the quantized vibration? Or what of quantal aspects in rate calculations or the tunneling of protons in the conduction of aqueous acid solutions (see Section 4.11.5), for example?

So, manufacturers of white coats may still have a market for a generation or more. But it will be a diminishing market! There is no doubt that computer-simulation techniques are making inroads into experimental data collection and that they will be increasingly used because they save time and cost.

Further Reading

Seminal

1. N. Metropolis, *J. Chem. Phys.* **21**: 1087 (1953).
2. B. J. Adler and T. E. Wainwright, *J. Chem. Phys.* **27**: 1208 (1959).
3. B. J. Adler and T. E. Wainwright, "Computer Simulation in Electrolytes," *J. Chem. Phys.* **33**: 1439 (1960).
4. H. L. Friedman, *Ionic Solution*, Interscience, New York (1962).
5. S. G. Brush, H. L. Saklin, and E. Teller, "A Monte Carlo Calculation of a One Component Plasma," *J. Chem. Phys.* **45**: 2102 (1965).
6. J. C. Rasaiah and H. L. Friedman, "Integral Equation Methods for Computations about Ionic Solutions," *J. Chem. Phys.* **48**: 2742 (1965).
7. G. Snell and J. L. Lebowitz, "Computational Techniques in Electrolytic Calculations," *J. Chem. Phys.* **48**: 3706 (1968).
8. P. S. Ramanathen and H. L. Friedman, "Study of a Refined Model for Electrolytes," *J. Chem. Phys.* **54**: 1080 (1971).
9. J. C. Rasaiah, "Ionic Solutions in Equilibrium," *J. Chem. Phys.* **56**: 3071 (1972).
10. L. Blum, "Mean Spherical Model for a Mixture of Hard Spheres and Hard Dipoles," *Chem. Phys. Lett.* **26**: 200 (1976).

Review

1. P. Turq, "Computer Simulation of Electrolytic Solutions," in *The Physics and Chemistry of Aqueous Solutions*, M. C. Bellisent-Funel and G. W. Neilson, eds., *NATO ASI Series*, **205**: 409 (1987).

Papers

1. D. N. Card and J. P. Valleau, *J. Chem. Phys.* **52**: 6232 (1970).
2. D. Smith, Y. Kalyuzhnyi, and A. D. J. Haymet, *J. Chem. Phys.* **95**: 9165 (1991).

3. T. Cartailler, P. Turq, and L. Blum, *J. Phys. Chem.* **96**: 6766 (1992).
4. J.-L. Dandurand and J. Schott, *J. Phys. Chem.* **96**: 7770 (1992).
5. B. Jamnik and V. Vlachy, *J. Am. Chem. Soc.* **115**: 660 (1993).
6. J. Gao, *J. Phys. Chem.* **98**: 6049 (1994).
7. D. E. Smith and L. X. Dang, *J. Chem. Phys.* **100**: 3757 (1994).
8. J. Wang and A. D. J. Haymet, *J. Chem. Phys.* **100**: 3767 (1994).
9. C. E. Dykstra, *J. Phys. Chem.* **99**: 11680 (1995).
10. C.-Y. Shew and P. Mills, *J. Phys. Chem.* **99**: 12988 (1995).

3.11. THE CORRELATION FUNCTION APPROACH

3.11.1. Introduction

Debye and Hückel's theory of ionic atmospheres was the first to present an account of the activity of ions in solution. Mayer showed that a virial coefficient approach relating back to the treatment of the properties of real gases could be used to extend the range of the successful treatment of the "excess" properties of solutions from 10^{-3} to 1 mol dm^{-3}. Monte Carlo and molecular dynamics are two computational techniques for calculating many properties of liquids or solutions. There is one more approach, which is likely to be the last. Thus, as shown later, if one knows the correlation functions for the species in a solution, one can calculate its properties. Now, correlation functions can be obtained in two ways that complement each other. On the one hand, neutron diffraction measurements allow their experimental determination. On the other, Monte Carlo and molecular dynamics approaches can be used to compute them. This gives a pathway purely to calculate the properties of ionic solutions.

3.11.2. Obtaining Solution Properties from Correlation Functions

To understand this section, it is best to review briefly the idea of a correlation function (see Section 2.11.3). Consider a hypothetical photograph of a number of ions in a solution. One looks for one ionic species i in a small volume dV at a series of distances r from a molecule of species j. The chance of finding the ion i in dV is

$$c_i g_{ij}(r)\, dV \tag{3.168}$$

where $c_i = N_i/V$ is the number of i ions per unit volume. In Eq. (3.168), g_{ij} is called the *correlation function.* This is a measure of the effect of species j in increasing or decreasing the number of i ions in dV. One way of writing g_{ij} is

$$g_{ij}(r) = c^{-w_{ij}/kT} \tag{3.169}$$

where w_{ij} is the reversible work to bring i and j from infinitely far apart to the distance r.

There are two kinds of ways to obtain g values, i.e., g_{ij}, g_{ii}, and g_{jj}. One is a computational approach using the Monte Carlo method or MD. In Fig. 3.49 one has seen the example of P. Bopp's results of such a determination using MD.

On the other hand, one can experimentally determine the various g's. Such determinations are made by a combination of X-ray and neutron diffraction measurements (see Section 2.11.3 and 5.2.3).

One now has to use the correlation functions to calculate a known quantity. One way of doing this (Friedman, 1962) is to use the following equation:

$$\left(\frac{\partial c}{\partial P}\right)_{N,T} = \frac{kT}{1 + 4Pr\int_0^{N/V} [g(r) - 1]r^2 dr} \tag{3.170}$$

The excess free energy can be shown to be

$$A^{ex} = N\int_0^c (P - ckT)c^{-2}dc \tag{3.171}$$

The process of relating A^{ex} back to $g(r)$, obtained theoretically or experimentally, is done by first calculating the pressure by computing $g(r)$ at various values of the distance r to get $\partial P/\partial c$ at a series of c's down to $P \sim ckT$, the ideal value, after which one integrates the equation to get

$$P(c) = ckT + \left\{\left(\frac{\partial P}{\partial c}\right) - kT\right\} dc \tag{3.172}$$

Having thus obtained P on the basis of a knowledge of the g's, one can use the expression given to obtain A^{ex} as a function of P. The procedure is neither brief nor simple but broad and general. It indicates that if one knows the distribution functions, one can compute the energy excess over that for zero interaction (and by implication any excess property).[29]

Why should one go to all this trouble and do all these integrations if there are other, less complex methods available to theorize about ionic solutions? The reason is that the correlation function method is open-ended. The equations by which one goes from the gs to properties are not under suspicion. There are no model assumptions in the experimental determination of the g's. This contrasts with the Debye–Hückel theory (limited by the absence of repulsive forces), with Mayer's theory (no misty closure procedures), and even with MD (with its pair potential used as approximations to reality). The correlation function approach can be also used to test any theory in the future because all theories can be made to give $g(r)$ and thereafter, as shown, the properties of ionic solutions.

[29] An excess property is one that indicates the difference between the real values of the property and the ideal value of the property that would exist in the absence of interionic attraction.

3.12. HOW FAR HAS THE MEAN SPHERICAL APPROXIMATION GONE IN THE DEVELOPMENT OF ESTIMATION OF PROPERTIES FOR ELECTROLYTE SOLUTIONS?

The latest models propose to represent electrolyte solutions as a collections of hard spheres of equal size, ions, immersed in a dielectric continuum, the solvent. For such a system, what is called the Mean Spherical Approximation, MSA, has been successful in estimating osmotic and mean activity coefficients for aqueous 1:1 electrolyte solutions, and has provided a reasonable fit to experimental data for dilute solutions of concentrations up to ~0.3 mol dm^{-3}. The advantage in this approach is that only one adjustable parameter, namely the single effective ionic radius, has to be considered.[30]

The abbreviation MSA refers here to the model implied by the simple correlation function stated and with the development which follows. More generally, the term refers to one or several integral equations used in the theory of liquids. It is appropriate to what is discussed here (charged hard spheres) because MSA equations have an analytical solution for that case.

What about the difficult problem of modeling electrolyte solutions at higher concentrations? In the MSA approach, attempts were made to extend the treatment by allowing the ion size parameter to be a function of ionic strength. Unfortunately, such an approach became unrealistic because of the sharp reduction of effective cation size with increasing electrolyte concentration.

In another attempt (Fawcett and Tikenen, 1996), the introduction of a changing dielectric constant of the solvent (although taken from experimental data) as a function of concentration has been used to estimate activity coefficients of simple 1:1 electrolyte solutions for concentrations up to 2.5 mol dm^{-3}.

In the mean spherical approximation, the interaction energy between any two particles is given by their pairwise interaction energy, independent of direction from one of the particles. This interaction is then used to define the direct correlation function. Under this approach,

$$g_{ij}(r) = 0 \quad \text{when} \quad r < \sigma$$

where σ is the diameter of the reference ion. In this hard sphere version, there is no steep tuning of the repulsive potential, but suddenly, at $r = \sigma$, $U_{ij} \rightarrow +\infty$.[31] However, when $r > \sigma$, the equation becomes complex to solve.

---

[30] Let's not forget that a model is only an attempt to represent the much more complex reality. Using one of different approaches—MSA, Monte Carlo, MD, etc.,—the scientist proposes a model starting with simple but reasonable assumptions that compares it with experimentally determined parameters. If the agreement is reasonable, then a complexity is added to the model, and the understanding of the system—of the reality—advances. Of course, all this is subjected to the limitations of the approach chosen, e.g., long computer times and complex integrals to solve.

[31] This is in contrast to the "soft-sphere approximation" where some distance-dependent function such as the second term in the Lennard-Jones equation (3.166) is used.

The simplest pairwise interaction equation for the electrostatic attraction of a positive and a negative ion to each other is

$$U_{ij} = \frac{z_i z_j e_0^2}{\varepsilon r} \tag{3.173}$$

Mayer achieved closure in integrals involved in his application of the McMillan–Mayer virial approach to ionic solutions by multiplying this equation by the factor $e^{-\kappa r}$ where κ^{-1} is the Debye length. Something similar is done in equations for the electrostatic attraction part of the MSA theory, but in this case the Ornstein–Zernicke integral equation is introduced.[32] Instead of κr, the term used is $2\Gamma r$ where

$$\Gamma = \frac{(1 + 2\sigma\kappa)^{1/2} - 1}{2\sigma} \tag{3.174}$$

If one takes the pairwise interaction equation (3.173) and modifies it by multiplying by $e^{-2\Gamma r}$, then one finds the correlation function becomes

$$g_{ij}(r) = \frac{z_i z_j e_0^2}{\varepsilon r k T} e^{-2\Gamma r} \tag{3.175}$$

In the primitive Debye–Hückel theory—one that did not allow for the size of ions—the value for the activity coefficient is given by Eq. (3.60). The corresponding equation in the MSA is

$$\ln (\gamma_i)_{es} = -\frac{z_i^2 e_0^2 \Gamma}{kT\varepsilon(1 + \Gamma\sigma)} \tag{3.176}$$

However, this is only the electrostatic attraction part of the theory. There is also the effect of the hard-sphere part of the theory, that upon contact ions immediately repel with infinite energy. This part of the activity coefficient is found to be given by

$$\ln (\gamma_i)_{hs} = \frac{6\eta}{1 - \eta} + \frac{3\eta^2}{(1 - \eta)^2} + \frac{2\eta}{(1 - \eta)^3} \tag{3.177}$$

Here the term η represents a *packing factor* and is given by

$$\eta = \frac{\pi\sigma^3}{6} \sum_i c_i \tag{3.178}$$

where c_i is the ionic concentration.

---

[32]This equation was first used to deal with problems in the theory of liquids. See, e.g., D.A. McQuarie, *Statistical Mechanics*, p. 269, Harper Collins, New York (1976).

Finally,

$$\ln \gamma_i = \ln(\gamma_i)_{es} + \ln(\gamma_i)_{hs} \tag{3.179}$$

It is easy then to develop equations for actual observables such as the mean activity coefficients (Section 3.4.4).

These equations all contain the value of ε, the dielectric constant of the solution. Many workers have approximated it by using $\varepsilon = 78$, the value for water. However, Blum (1977) was the first to point out that better agreement with experiment is achieved by using instead the actual dielectric constant of the solution. Fawcett and Tikanen (1996) took this into account, and by using a fit to results obtained much earlier by Hasted, found

$$\varepsilon = \varepsilon_0 - \delta_i c_i + b c_i^{3/2} \tag{3.180}$$

The σ values that were found by Fawcett and Tikanen to fit best are shown in Table 3.19 and the results for NaBr are shown in Fig. 3.50.

It is interesting to note that the $\gamma - c^{1/2}$ plot bends upward at higher concentrations. It is easy to see why. As the concentration increases, the solution, as it were, gets filled up with ions and there tends to be no more room. This is equivalent to too many ions per solvent and the *effective* ionic concentration becomes higher than would be

TABLE 3.19

Values of the Average Ionic Diameter σ Obtained from the Best Fit of the Model to Experiment[a]

	σ (pm)			
	F^-	Cl^-	Br^-	I^-
Li^+	—	435 (1.6 *M*)	448 (1.5 *M*)	489 (0.5 *M*)
Na^+	328 (1 *M*)[b]	388 (3 *M*)	407 (2.5 *M*)	427 (2.5 *M*)
K^+	365 (1.4 *M*)	362 (2.5 *M*)	376 (3 *M*)	394 (2.5 *M*)
Rb^+	389 (0.9 *M*)	349 (2.5 *M*)	349 (1.2 *M*)	351 (0.8 M)
Cs^+	408 (0.5 *M*)	317 (1 *M*)	318 (0.9 *M*)	311 (0.6 *M*)

Source: Reprinted from W. R. Fawcett and A. C. Tikanen, *J. Phys. Chem.* **100**: 4251, 1996.

[a] The concentration in parentheses gives the value over which a successful fit between theory and experiment was obtained.

[b] Experimental data available only up to 1 mol dm^{-3}

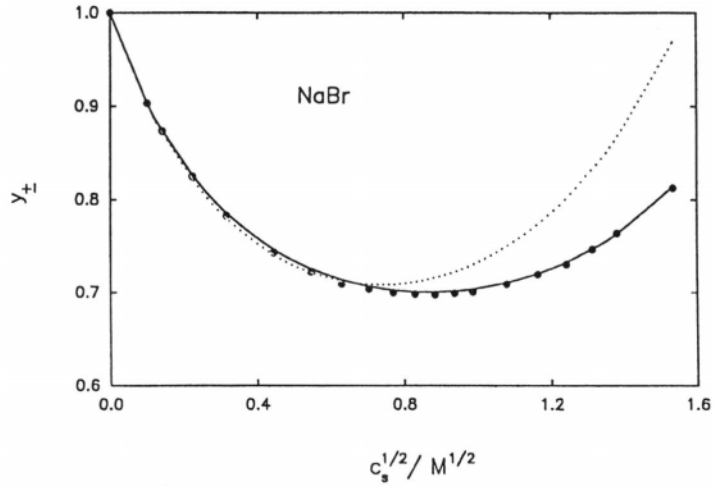

Fig. 3.50. Plot of the mean ionic activity coefficient for aqueous NaBr solutions against the square root of molarity. The solid line through the experimental points shows the MSA estimates with an optimized value of 407 pm for σ and a varying solvent ε. The dotted durve was calculated with an ε equal to that of the pure solvent and an optimized value of 366 pm for σ. (Reprinted from W. R. Fawcett and A. C. Tikanen, *J. Phys. Chem.* **100**: 4251, 1996.)

calculated on stoichiometric grounds, overcoming the tendency of γ to fall with increasing concentration due to increasing interionic attraction.[33]

The degree of fit in Fig. 3.50 looks excellent. Detailed considerations of results for all the alkali halides, however, show that there are discrepancies and these are most likely to be due to the neglected ion pairing.

3.13. COMPUTATIONS OF DIMER AND TRIMER FORMATION IN IONIC SOLUTION

In forming post-2000 theories of solutions, it is important to know what fraction of the ions in a solution are associated to form dimers and trimers and perhaps higher aggregates. Dimers are not charged and will interact with the surrounding ions as

[33]A similar result is obtained in the Stokes and Robinson application of the idea, i.e., that there is a removal of effective free solvent into hydration shells around ions (Section 2.4.1). Both ideas are similar to the effect of the $V - b$ term in van der Waals's equation of state for gases. If the a/V^2 attraction term is neglected, $P = kT/(V - b)$. As V is reduced to be comparable in value to b, P (which is analogous to the ionic activity) increases above that for the simple $PV = kT$ equation.

dipoles. Bjerrum was the first, in 1926, to give an estimate of dimer concentration (Section 3.8). In this theory, it was simply assumed that if the ions approach each other so that their mutual Coulombic attraction exceeds their total thermal energy ($2kT$), they will form a charge-free pair.

Experimental methods for determining dimer formation were published in an early book (Davies, 1962). The author interpreted conductance data in terms of degrees of association. His book had less impact than might have been thought reasonable because of ambiguities arising from allowance of the parallel effects of interionic attraction, as well as ion association to dipoles, in lowering equivalent conductance as the concentration increased.

One might suspect that Raman spectra would give an indication of ion pairs, but this is only true for pairs (such as those involving NO_3^-) where the ion pairing affects a molecular orbital (such as that in N–O). In a pair such as Na^+Cl^-, there are *no chemical bonds*—and it is these that produce spectra—so that ion pairs may exist without a spectral signature.

It follows that experimental determination of ion pairing has been difficult to carry out. Some theoretical works by Wertheim (1984) have contributed a correlation function approach to ion pairing that improves on the original work by Bjerrum (1926). The major difference is the form of the interaction energy between the ions, $U_{A^+B^-}$. In

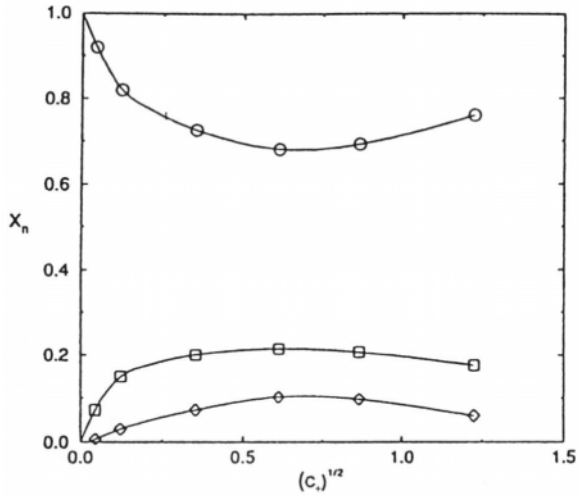

Fig. 3.51. Mole fraction of monomers, dimers, and + - + trimers as a function of the square root of the concentration $c_+^{1/2}$: monomer fraction (circles), dimer fraction (squares), and the fraction of + - + trimers (diamonds). (The lines are to guide the eye only.) (Reprinted from J. Wang and D. J. Haymet, *J. Chem. Phys.* **100**: 3767, 1994.)

Bjerrum's work it was simply Coulombic attraction, but in Wertheim the governing equation involves not only the attraction but also the repulsive forces, somewhat as in the Lennard-Jones equation. The actual equation used originated in work by Rossky and Friedman (1980).

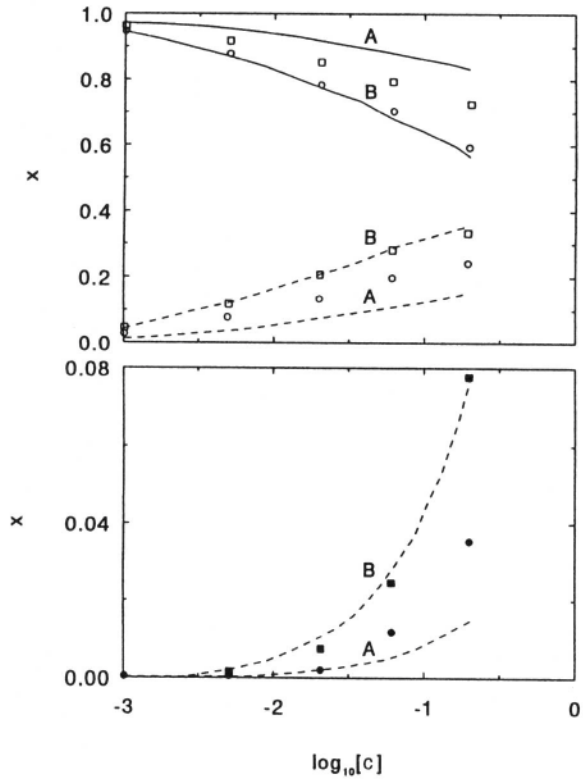

Fig. 3.52. Dependence of the fraction of *n*-mers (x_1,x_2,x_3) on the concentration at T= 298.16 K. The results of the "energy" A and "distance" B versions of the theory at $U_0/kT = -5.135$ and $r_0 = 5.5$ Å, respectively, are represented by the lines. The squares and circles are the MD results based on the distance (r_{in} = 3.191 Å, r_{out} = 5.5 Å) and energy [$U_0^{(MD)}/kT = -5.135$] criteria, respectively. The open symbols and solid lines represent the results for monomers, half-filled symbols and dashed lines represent the results for dimers, and filled symbols and dotted lines are the results for trimers and higher *n*-mers. (Reprinted from Y. V. Kalyuzhnyi et al. *J. Chem. Phys.* **95**: 9151, 1991.)

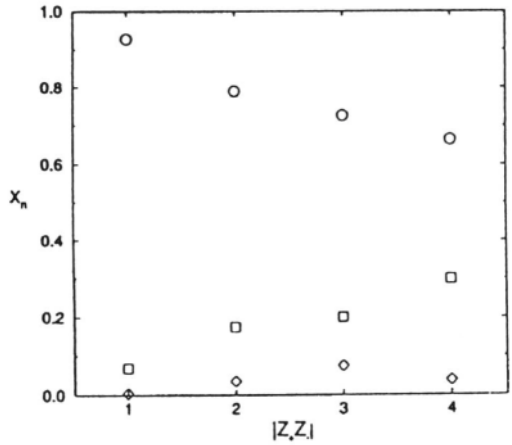

Fig. 3.53. The mole fraction of monomers, dimers, and total trimers for four model electrolytes at Debye length κ^{-1} = 0.61 nm, as a function of $|z_+z_-|$: monomer fraction (circles), dimer fraction (squares), and total trimer fraction (diamonds). (Reprinted from J. Wang and A. D. J. Haymet, *J. Chem. Phys.* **100**: 3767,1994.)

This formalism for calculating dimer formation begun by Wertheim has been applied extensively by Haymet (1991 and onward) to electrolytes. For example, 1:3 electrolytes (e.g., Na_3PO_4) have been examined following Wertheim's interaction equation. Some of the results are shown in Fig. 3.51. The calculations show not only that there is significant dimer formation at 0.1 *M* but that trimers of the type + – + are present at higher concentrations than those that are – + –.

Haymet also studied 2:2 electrolytes. Here, even at 0.1 mol dm^{-3}, the association with dimers is 10–20% (Fig. 3.52). The dependence of dimer and trimer formation on z_+z_- in Fig. 3.53 is for a constant value of the Debye–Hückel length, $1/\kappa$.

What is the significance of these results on dimer and trimer formation for ionic solution theory? In the post-Debye and Hückel world, particularly between about 1950 and 1980 (applications of the Mayer theory), some theorists made calculations in which it was assumed that all electrolytes were completely dissociated at least up to 3 mol dm^{-3}. The present work shows that the degree of association, even for 1:1 salts, is ~10% at only 0.1 mol dm^{-3}. One sees that these results are higher than those of the primitive Bjerrum theory.

There is much work to do to recover from the misestimate that entered into calculations made after Debye and Hückel by neglecting ion pairing and "dead water" (Section 3.8).

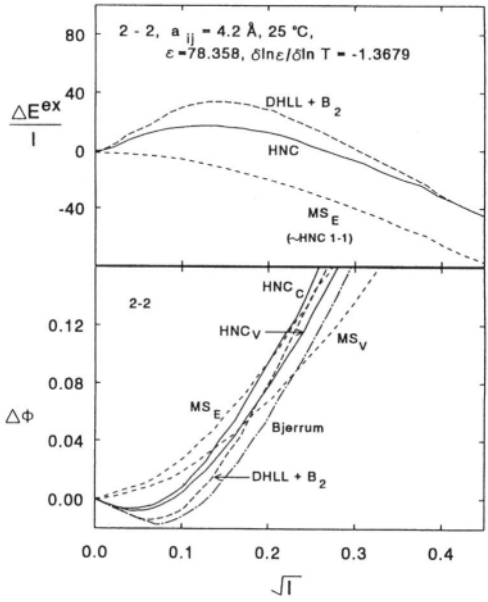

Fig. 3.54. Deviations from the Debye–Hückel limiting law (DHLL) for E^{ex} and ϕ of a 2:2 electrolyte for several theories. The ion-pairing cutoff distance d for the Bjerrum curve is 1.43 nm. I is the ionic strength. (Reprinted from J. C. Rasaiah, *J. Chem. Phys.* **56**: 3071, 1972.)

3.14. MORE DETAILED MODELS

By now this chapter has presented several modeling pathways that give rise to extensions of the Debye–Hückel limiting law of 1923. The results obtained from a few models developed in the half century that followed are illustrated in Fig. 3.54. The lines denoted "HNC" refer to versions of the Mayer theory utilizing the hypernetted chain approximation for evaluation of the integrals and the designation "MS" corresponds to theories using the mean spherical approximation.

No great superiority of one approximation over the other is apparent. However, there is something a little inconsistent, even dubious, about the comparisons. The approximation marked "Bjerrum" allows for ion association, and this is a fact known to be present at higher concentrations, as independently shown by Raman spectra of electrolytes containing, e.g., NO_3^- ions. The other models assume, however, that all the ions are free and unassociated, even in concentrations in which experiment shows strong ion-pair formation. Also, where is the allowance for Bjerrum's "dead water,"

i.e., water fixed in hydration shells that cannot be counted in calculating the ionic concentration?

In the post-Debye and Hückel developments surveyed above (virial coefficient theory, computer simulation, and distribution coefficients), it is frequently stated that the quantity that has the greatest influence on the result of an ionic solution is $U_{A^+B^-}$, the interaction potential. In discussing the validity of Monte Carlo and molecular dynamics calculations, the difficulty of expressing the potential of an ion in terms only of the nearest-neighbor interaction (when long-range Coulomb forces indicate that other interactions should be accounted for) was pointed out. Because computations that go further are too lengthy, the simple pair potential is the one generally used, but the previous generation's papers have progressively improved the potential.

Thus, theories using an U_{ij} that is simply

$$U_{ij} = \frac{e_i e_j}{\varepsilon r} \tag{3.181}$$

are said (Friedman, 1987) to be using the *primitive* model.

The simplest improvement is the mean spherical approximation model (Section 3.12), but a somewhat better version of this is what can be pictorially called the "mound model," because instead of having an abrupt change from simple Coulomb attraction to total repulsion between ions of opposite sign when they meet, this model (Rasaiah and Friedman, 1968) allows for a softer collision before the plus infinity of the hard wall is met (Fig. 3.55).

The fullest development along these lines (Ramanathan et al., 1987) is given by the following series:

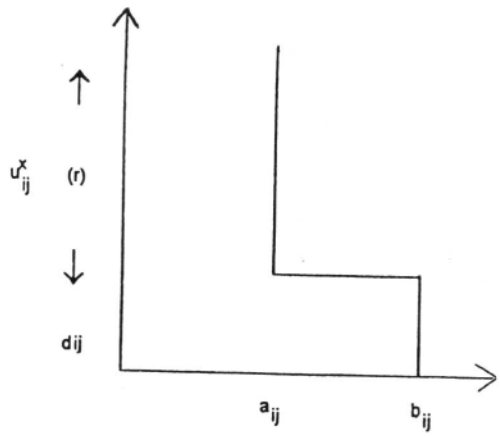

Fig. 3.55. The "mound model."

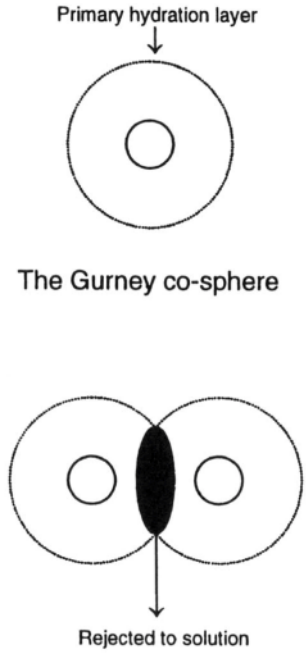

Fig. 3.56. Excluded solvent formed upon contact between two ions.

$$U_{ij}(r) = \frac{e_i e_j}{\varepsilon r} + COR_{ij} + CAV_{ij} + GUR_{ij} \tag{3.182}$$

Here COR_{ij} represents a short-range repulsion, the second term in the Lennard-Jones equation, or it is sometimes substituted for by a term becoming exponentially more positive as the interionic distance diminishes. CAV_{ij} is a term that accounts for the fact that the ions themselves are dielectric cavities in the solution that have a dielectric constant (<5) differing dramatically from that of the solution (~80). Thus, owing to this, one acts on the other in a way not allowed for in the first term in Eq. (3.182). (On the whole, this term is less important than the others.) Finally, the GUR_{ij} term gets its name from Gurney (Gurney, 1953), who stressed the existence of a primary solvation layer (Bockris, 1949). In effect, as far as interactions are concerned, this is like a hard rubber tire around the ion. Upon collision (*cf.* the mound model), two ions squelch into each other, knocking out a water molecule or two and making the distance of closest approach less than the sum of the hydrated radii. This hydrated layer around the ion, called by Bockris the "primary hydration layer," is called by Friedman the "Gurney co-sphere" (Fig. 3.56).

Figure 3.57 (originally drawn by Friedman) shows clearly how these various contributions to U_{ij} vary with distance as two ions approach each other. The diagram indicates

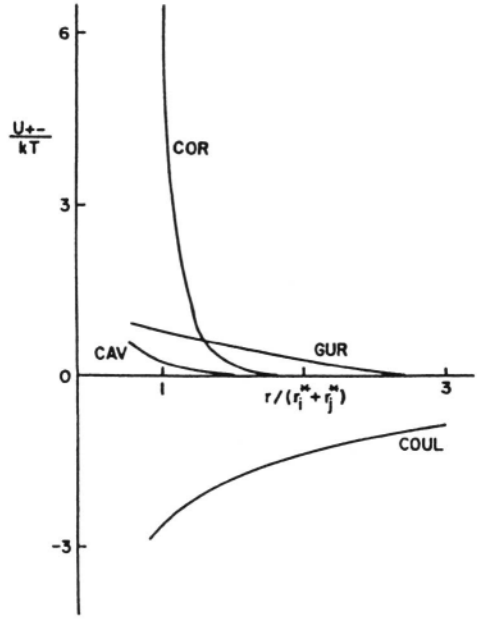

Fig. 3.57. Terms of the model potential for a (+–) pair in units of kT for an aqueous 1:1 electrolyte with $r_+^* + r_-^* = 0.28$ nm, $\varepsilon_{CAV} = 2$, and $(A_g)_{+-} = 100$ cal/mol. (Reprinted from H. L. Friedman, *Pure Appl. Chem.* **59**: 1003,1987.)

the complexity of ionic solution theory when the concentration is so high that most of the energies involved are effective the whole time and not only on closest approach.

Further Reading

Seminal

1. R. Gurney, *Ions in Solution,* Cambridge University Press, Cambridge (1940).
2. H. L. Friedman, *Ionic Solution,* Interscience, New York (1962).
3. C. W. Davies, *Ionic Association*, Butterworth, London (1962).
4. D. A. McQuarie, *Statistical Mechanics,* pp. 274–277, 355–356, Harper Collins, New York (1969).
5. H. L. Friedman, Computations of ionic properties, *Modern Aspects of Electrochemistry,* Vol. 6, J. O'M Bockris and B. E. Conway, eds., Plenum, New York (1971).
6. J. C. Rasaiah, "Comparison of Models for Ions in Solution," *J. Chem. Phys.* **56**: 5061 (1972).
7. L. Blum, *Mol. Phys.* **30**: 1529 (1975).

Reviews

1. K. S. Pitzer, "Activity Coefficients in Electrolyte Solutions," in *Activity Coefficients in Electrolyte Systems,* K. Pitzer, ed., 2nd ed., CRC Press, Boca Raton, FL (1991).
2. J. E. Enderby, *Chem. Soc. Review* **24**: 159 (1995).
3. G. W. Neilson and J. E. Enderby, "Aqueous Solutions," *J. Phys. Chem.* **100**: 1317 (1996).

Papers

1. J. O'M. Bockris, *Quant. Rev. Chem. Soc., London* **111**: 173 (1949).
2. R. Gurney, *J. Chem. Phys.* **19**: 1499 (1953).
3. J. C. Rasaiah and H. L. Friedman, *J. Chem. Phys.* **48**: 2742 (1968).
4. E. L. Blum, *Inorg. Chem.* **24**: 139 (1977).
5. P. J. Rossky and H. L. Friedman, *J. Chem. Phys.* **72**: 5694 (1980).
6. G. K. Wertheim, *Phys. Rev.* **30**: 4343 (1984).
7. H. L. Friedman, *NATO ASI Series C* **205**: 61 (1987).
8. K. V. Ramanathan and R. Pinto, *J. Electrochem. Soc:* **134**: 165 (1987).
9. J. Barthel and R. Buckner, *Pure Appl. Chem.* **63**: 1473 (1991).
10. Y. Wei, P. Chiang, and S. Sridhar, *J. Chem. Phys.* **96**: 4569 (1992).
11. J. F. Lu, Y. Yu, and Y. G. Li, *Fluid Phase Equilibria,* **85**: 81 (1993).
12. D. H. Powell, G. W. Nielson, and J. E. Enderby, *J. Phys. Condens. Matter* **5**: 5723 (1993).
13. R. H. Tromp, G. W. Nielson, and M. L. Bellisent-Fund, *J. Phys. Chem.* **98**: 13195 (1994).
14. S. Angell, R. H. Tromp and G. W. Nielson, *J. Phys. Condens. Matter* **7**: 1513 (1995).
15. J. Barthel, H. J. Gores, and L. Kraml, *J. Phys. Chem.* **100**: 1283 (1996).
16. W. R. Fawcett and A. C. Tikanen, *J. Phys. Chem.* **100**: 4251 (1996).

3.15. SPECTROSCOPIC APPROACHES TO THE CONSTITUTION OF ELECTROLYTIC SOLUTIONS

An understanding of the concentration dependence of activity coefficients required the postulation of the concepts of ion-pair formation and complex formation. Certain structural questions, however, could not be answered unequivocally by these considerations alone. For instance, it was not possible to decide whether pure Coulombic or chemical forces were involved in the process of ion association, i.e., whether the associated entities were ion pairs or complexes. The approach has been to postulate one of these types of association, then to work out the effect of such an association on the value of the activity coefficient, and finally to compare the observed and calculated values. Proceeding on this basis, it is inevitable that the postulate will always stand in need of confirmation because the path from postulate to fact is indirect.

It is fortunately possible to gain direct information on the constitution and concentrations of the various species in an electrolytic solution by "seeing" the species. These methods of seeing are based upon shining "light"[34] into the electrolytic solution

[34]The word *light* is used here to represent not only the visible range of the electromagnetic spectrum but all the other ranges for which analytical methods have been developed.

and studying the light that is transmitted, scattered, or refracted. The light emerging from the electrolytic solution in the ways just mentioned is altered or modulated as a result of the interaction between the free ionic or associated species and the incident light (*cf.* the corresponding use of light as a tool in Section 2.3.3).

There are many types of interactions between electromagnetic radiation and matter. A species as a whole can change its rotational state; the bonds (if any) within a species can bend, stretch, or twist and thus alter its vibrational state; the electrons in the species may undergo transitions between various energy states; and finally the atomic nuclei of the species can absorb energy from the incident radiation by making transitions between the different orientations to an externally imposed magnetic field.

All these responses of a species to the stimulus of the incident electromagnetic radiation involve energy exchange. According to the quantum laws, this energy exchange must occur only in finite jumps of energy. Hence, the light that has been modulated by these interactions contains information about the energy that has been exchanged between the incident light and the species present in the electrolytic solution. If the free, unassociated ions and the associated aggregates (ion pairs, triplets, complex ions, etc.) interact differently with the incident radiation, then information concerning the structures will be observed in the radiation emerging from the electrolytic solution.

There are various kinds of spectroscopy: visible and ultraviolet (UV) absorption spectroscopy, Raman and infrared spectroscopy, nuclear magnetic resonance spectroscopy, and electron-spin resonance (ESR) spectroscopy. A brief description of the principles of these techniques and their application to the study of ions in solution follows (see also Section 2.11).

3.15.1 Visible and Ultraviolet Absorption Spectroscopy

Atoms, neutral molecules, and ions (simple and associated) can exist in several possible electronic states; this is the basis of visible and UV absorption spectroscopy. Transitions between these energy states occur by the absorption of discrete energy quanta ΔE which are related to the frequency ν of the light absorbed by the well-known relation

$$\Delta E = h\nu$$

where h is Planck's constant. When light is passed through the electrolytic solution, there is absorption at the characteristic frequencies corresponding to the electronic transitions of the species present in the solution. Owing to the absorption, the intensity of transmitted light of the absorption frequency is less than that of the incident light. The falloff in intensity at a particular wavelength is given by an exponential relation known as the Beer–Lambert law

$$I = I^0 e^{-\varepsilon c l}$$

where I^0 and I are the incident and transmitted intensities, ε is a characteristic of the absorbing species and is known as *molar absorptivity,* l is the length of the material (e.g., electrolytic solution) through which the light passes, and c is the concentration of the absorbing molecules.

A historic use of the Beer–Lambert law was by Bjerrum, who studied the absorption spectra of dilute copper sulfate solutions and found that the molar absorptivity was independent of the concentration. Bjerrum concluded that the only species present in dilute copper sulfate solutions are free, unassociated copper and sulfate ions and not, as was thought at the time, undissociated copper sulfate molecules that dissociate into ions to an extent that depends on the concentration. For if any undissociated molecules were present, then the molar absorptivity of the copper sulfate solution would have been dependent on the concentration.

In recent years, it has been found that the molar absorptivity of *concentrated* copper sulfate solutions does show a slight concentration dependence. This concentration dependence has been attributed to ion-pair formation occurring through the operation of Coulombic forces between the copper and sulfate ions. This is perhaps ironic because Bjerrum's concept of ion pairs is being used to contradict his conclusion that there are only free ions in copper sulfate solutions. Nevertheless, there is a fundamental difference between the erroneous idea that a copper sulfate crystal dissolves to give copper sulfate molecules, which then dissociate into free ions, and the modern point of view that the ions of an ionic crystal pass into solution as free solvated ions which, under certain conditions, associate into ion pairs.

The method of visible and UV absorption spectroscopy is at its best when the absorption spectra of the free ions and the associated ions are quite different and known. When the associated ions cannot be chemically isolated and their spectra studied, the type of absorption by the associated ions has to be attributed to electronic transitions known from other well-studied systems. For example, there can be an electron transfer to the ion from its immediate environment (charge-transfer spectra), i.e., from the entities associated with the ion; or transitions between new electronic levels produced in the ion under the influence of the electrostatic field of the species associated with the ion (crystal-field splitting). Thus, there is an influence of the environment on the absorption characteristics of a species, and this influence reduces the clarity with which spectra are characteristic of species rather than of their environment. Herein lies what may be considered a disadvantage of visible and UV absorption spectroscopy.

3.15.2. Raman Spectroscopy

Visible and UV absorption spectroscopy are based on studying that part of the incident light transmitted (after absorption) through an electrolytic solution in the same direction as the original beam. However, a certain amount of light is scattered in other directions.

A simple view of the origin of the Raman effect (see also Section 2.11.5) is as follows: *Rayleigh scattering* is produced because the electric field of the incident light induces a dipole moment in the scattering species and since the incident field is oscillating, the induced dipole moment also varies periodically. Such an oscillating dipole acts as an antenna and radiates light of the same frequency as the incident light.

It is the deformation polarizability α_{deform} that determines the magnitude of a dipole moment induced by a particular field. If this polarizability changes from its time-averaged value, then the induced-dipole antenna will be radiating at a new frequency that is different from the incident frequency; in other words, there is a Raman shift. The changes in polarizability of the scattering species can be correlated with their rotations and vibrations and also their symmetry characteristics. Hence, the Raman shifts are characteristic of the rotational and vibrational energy levels of the scattering species and provide direct information about these levels. Though the presence of electrostatic bonding produces second-order perturbations in the Raman lines, it is the species with covalent bonds to which Raman spectroscopy is sensitive, and not purely electrostatic ion pairs. Another feature that makes Raman spectra useful is the fact that the integrated intensity of the Raman line is proportional to the concentration of the scattering species, i.e., allows the amount present to be determined.

The problem with Raman spectroscopy is the low intensity of the Raman lines, which permits easy detection of species only in concentrated solutions. Fortunately, the availability of lasers, which are intense sources of monochromatic light, is stimulating further applications of this powerful technique, which is noted for the lack of ambiguity with which it can report on the species in an electrolytic solution. Devices that distinguish a low-intensity signal from noise also help.

3.15.3. Infrared Spectroscopy

Infrared spectroscopy resembles Raman spectroscopy in that it provides information on the vibrational and rotational energy levels of a species, but it differs from the latter technique in that it is based on studying the light transmitted *through* a medium after absorption and not that *scattered* by it (see Section 2.11.2).

The techniques of Raman and IR spectroscopy are generally considered complementary in the gas and solid phases because some of the species under study may reveal themselves in only one of the techniques. Nevertheless, it must be stressed that Raman scattering is not affected by an aqueous medium, whereas the strong absorption in the infrared shown by water proves to be a troublesome interfering factor in the study of aqueous solutions by the IR method.

3.15.4. Nuclear Magnetic Resonance Spectroscopy

The nuclei of atoms can be likened in some respects to elementary magnets. In a strong magnetic field, the different orientations that the elementary magnets assume correspond to different energies. Thus, transitions of the nuclear magnets between

these different energy levels correspond to different frequencies of radiation in the short-wave, radio-frequency range. Hence, if an electrolytic solution is placed in a strong magnetic field and an oscillating electromagnetic field is applied, the nuclear magnets exchange energy (exhibit resonant absorption) when the incident frequency equals that for the transitions of nuclei between various levels (see Section 2.11.6).

Were this NMR to depend only on the nuclei of the species present in the solution, the technique could not be used to identify ion pairs. However, the nuclei sense the applied field as modified by the environment of the nuclei. The modification is almost exclusively due to the nuclei and electrons in the neighborhood of the sensing nucleus, i.e., the adjacent atoms and bonds. Thus, NMR studies can be used to provide information on the type of association between an ion and its environmental particles, e.g., in ion association.

Further Reading

Seminal Papers

1. M. Falk and P. A. Giguere, "I.R. Spectra in Solution," *Can. J. Chem.* **35**: 1195 (1957).
2. H. G. Hertz, "N.M.R. Spectra of Solutions," *Ber. Bunsen. Ges.* **67**: 311 (1963).
3. G. E. Walrafen, "Raman Spectra in Solution," *J. Chem. Phys.* **40**: 3249 (1964).

Review

1. P. L. Goggin and C. Carr, "Infrared Spectroscopy in Aqueous Solution," in *Water and Aqueous Solutions,* G. W. Nielson and J. E. Enderby, eds., Adam Hilger, Bristol, U.K. (1986).

Papers

1. H. J. Reich, J. P. Borst, R. R. Dykstra, and D. P. Green, *J. Am. Chem. Soc.* **115**: 8728 (1993).
2. E. Vauthey, A. W. Parker, B. Nohova, and D. Phillips, *J. Am. Chem. Soc.* **116**: 9182 (1994).
3. Y. Wang and Y. Tominaga, *J. Chem. Phys.* **101**: 3453 (1994).
4. F. Mafune, Y. Hashimoto, M. Hashimoto, and T. Kondow, *J. Phys. Chem.* **99**: 13814 (1995).
5. D. C. Duffy, P. B. Davies, and A. M. Creeth, *Langmuir* **11**: 2931 (1995).
6. P. W. Faguy, N. S. Marinkovic, and R. R. Adzic, *J. Electroanal. Chem.* **407**: 209 (1996).
7. V. Razumas, K. Larsson, Y. Miezis, and T. Nylander, *J. Phys. Chem.* **100**: 11766 (1996).
8. X. M. Ren and P. G. Pickup, *Electrochim. Acta* **41**: 1877 (1996).

3.16. IONIC SOLUTION THEORY IN THE TWENTY-FIRST CENTURY

Looking first back to the publication date of the famous theory of Debye and Hückel (1923), there is no doubt that their ionic-atmosphere calculation (Section 3.3) of the activity coefficient at very low concentrations is still the dominating peak of

this century in the field of ionic solutions. Not only is the theory effective in giving the theoretical means to calculate ionic activity coefficients at low concentrations, but its success also had ripple effects on other parts of the physical chemistry of solutions.

Bjerrum published his work on the calculations of the association of ions formed from salts (Section 3.8) in 1926 and then nothing much happened until the Mayer theory of 1950. The development of this exceedingly complex piece of statistical mechanics, largely by Friedman and Rasaiah, produced works of ever-increasing mathematical difficulty, but today these look much more like exercises in very difficult integrations rather than insights into what is really happening. The enormous improvement over the Debye and Hückel equations with which the virial approach was credited was based on a comparison with the most simple ("limiting law") equation of Debye and Hückel, rather than later versions of their theory. These later versions take into account the volume occupied by ions, ion pairing, and the removal of solvent in the solution from its natural role as a dissolver to spend significant time clamped tightly to ions, unable to move and act as a solvent to newly introduced ions. On the basis of this model, Stokes and Robinson were able to calculate good numerical values for activity coefficients in solutions of concentrations up to $10\ \text{mol dm}^{-3}$.

By the 1980s, it had to be admitted (Rasaiah, 1987) that several versions of the post-1950 theories (mostly developments based on Mayor's theory) could not be distinguished as to virtue when ranked by their ability to replicate experiments, nor were they markedly better than those obtainable from later developments of Debye and Hückel's ionic atmosphere theory.

However, there is no doubt that from the 1980s on, a very hopeful type of development has been taking place in ionic solution theories. It is the correlation function approach, not a theory or a model, but an open-ended way to obtain a realistic idea of how an ionic solution works (Fig. 3.58). In this approach, pair correlation functions that are experimentally determined from neutron diffraction measurements represent "the truth," without the obstructions sometimes introduced by a model. From a knowledge of the pair correlation function, it is possible to calculate properties (osmotic pressure, activities). The pair correlation function acts as an ever-ready test for new models, for the models no longer have to be asked to re-replicate specific properties of solutions, but can be asked to what degree they can replicate the known pair correlation functions.

It is rather easy to make a list of milestones in ionic solution theory:

- The peaklike beginning in 1923.
- The MM stage,[35] the theory of ionic solution based on concepts used to interpret the behavior of imperfect gases (1950–1980). During this long stage (a

[35]MM refers to the McMillan-Mayer theory of 1945. This was a general theory of interaction in gases which was applied to interpret the behaviors of solutions. Mayer's theory was produced in 1950 [J.E. Mayer, *J. Chem. Phys.* **18:** 1426 (1950)] and applied the MM theory particularly to ionic solutions where the dominance of long range interactions causes special mathematical difficulties.

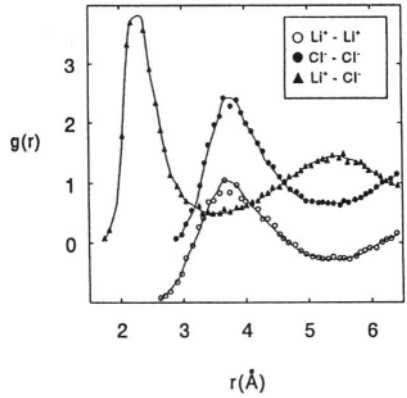

Fig. 3.58. Pair correlation functions from Monte Carlo simulation for charged soft sphere model for LiCl liquid at 883 K and 28.3 cm^3 mol^{-1}. (Reprinted from I. R. MacDonald and K. Singer, *Chemistry In Britain* **9**: 54, 1973.)

generation!), there developed an increasingly complex series of additions to the interaction energy U_{AB} which had first begun at the simplest level of $z_1 z_2 e_0^2/\varepsilon r$ but grew to encompass several extra terms, some of which had only a minimal effect on results.

- Pair correlation functions were discussed from the 1960s on, but not until the 1980s with the neutron diffraction contribution of Enderby and Neilson was it possible to make such determination with relative ease and certainty.
- Computer simulations began nearly half a century ago, but they did not really come into wide use for ionic solutions until the late 1980s (Heinziger, Bopp, Haymet). The convenience of being able to calculate the consequences of assuming a certain pair interaction law, to simulate an effect (the influence of high temperature and pressure, for example), and then find via the pair correlation functions the corresponding properties is a major advance because it brings a great increase in speed of obtaining new knowledge and a decrease in its expense.

There is yet a further stage for ionic solution theory that will not be presented here because it is still fragmentary in achievement and densely complex in the physical theory that underlies it. This "final" stage is the quantum mechanical one, in which an attempt is made to describe a solution at the Schrödinger equation level. Such work has been pioneered by Clementi and his colleagues since the mid-1980s.

APPENDIX 3.1. POISSON'S EQUATION FOR A SPHERICALLY SYMMETRICAL CHARGE DISTRIBUTION

A starting point for the derivation of Poisson's equation is Gauss's law, which can be stated as follows: Consider a sphere of radius r. The electric field X_r due to charge in the sphere will be normal to the surface of the sphere and equal everywhere on this surface. The total field over the surface of the sphere (i.e., the surface integral of the normal component of the field) will be equal to X_r times the area of the surface, i.e., $X_r 4\pi r^2$. According to Gauss's law, this surface integral of the normal component of the field is equal to $4\pi/\varepsilon$ times the total charge contained in the sphere. If ϱ_r is the charge density at a distance r from the center of the sphere, then $4\pi r^2 \varrho_r\, dr$ is the charge contained in a dr-thick shell at a distance r from the center and $\int_0 4\pi r^2 \varrho_r\, dr$ is the total charge contained in the sphere. Thus, Gauss's law states that

$$X_r 4\pi r^2 = \frac{4\pi}{\varepsilon} \int_0^r 4\pi r^2 \varrho_r\, dr$$

i.e.,

$$r^2 X_r = \frac{4\pi}{\varepsilon} \int_0^r r^2 \varrho_r\, dr \tag{A3.1.1}$$

Now, according to the definition of electrostatic potential ψ_r, at a point r,

$$\psi_r = -\int_\infty^r X_r\, dr \tag{A3.1.2}$$

or

$$X_r = -\frac{d\psi_r}{dr} \tag{A3.1.3}$$

Substituting Eq. (A3.1.2) in Eq. (A3.1.1), one gets

$$r^2 \frac{d\psi_r}{dr} = -\frac{4\pi}{\varepsilon} \int_0^r r^2 \varrho_r\, dr \tag{A3.1.4}$$

Differentiating both sides with respect to r,

$$\frac{d}{dr}\left(r^2 \frac{d\psi_r}{dr}\right) = -\frac{4\pi}{\varepsilon} r^2 \varrho_r$$

i.e.,

$$\frac{1}{r^2}\frac{d}{dr}\left(r^2\frac{d\psi_r}{dr}\right)=-\frac{4\pi}{\varepsilon}\varrho_r \tag{A3.1.5}$$

which is Poisson's equation for a spherically symmetrical charge distribution.

APPENDIX 3.2. EVALUATION OF THE INTEGRAL $\int_{r=0}^{r\to\infty} e^{-\kappa r}(\kappa r)\, d(\kappa r)$

According to the rule for integration by parts,

$$\int v\, du = uv - \int u\, dv$$

Thus,

$$\int_{r=0}^{r\to\infty} (\kappa r)e^{-\kappa r}\, d(\kappa r) = \left[-\kappa r e^{-\kappa r} - \int \frac{e^{-\kappa r}}{(-1)} d(\kappa r)\right]_{r=0}^{r\to\infty}$$

$$= \left[-\kappa r e^{-\kappa r} - e^{-\kappa r}\right]_{r=0}^{r\to\infty}$$

$$= \left[-e^{-\kappa r}(\kappa r + 1)\right]_{r=0}^{r\to\infty}$$

$$= +1 \tag{A3.2.1}$$

APPENDIX 3.3. DERIVATION OF THE RESULT $f_{\pm} = (f_+^{\nu_+} f_-^{\nu_-})^{1/\nu}$

Suppose that on dissolution 1 mole of salt gives rise to ν_+ moles of positive ions and ν_- moles of negative ions. Then, instead of Eqs. (3.65) and (3.66), one has

$$\nu_+\mu_+ = \nu_+\mu_+^0 + \nu_+RT\ln x_+ + \nu_+RT\ln f_+ \tag{A.3.3.1}$$

and

$$\nu_-\mu_- = \nu_-\mu_-^0 + \nu_-RT\ln x_- + \nu_-RT\ln f_- \tag{A.3.3.2}$$

Upon adding the two expressions (A3.3.1) and (A3.3.2) and dividing by $\nu = \nu_+ + \nu_-$ to get the average contribution to the free-energy change of the system per mole of both positive and negative ions, the result is

$$\mu_{\pm} = \frac{\nu_+\mu_+ + \nu_-\mu_-}{\nu} = \frac{\nu_+\mu_+^0 + \nu_-\mu_-^0}{\nu} + RT\ln(x_+^{\nu_+}x_-^{\nu_-})^{1/\nu} + RT\ln(f_+^{\nu_+}f_-^{\nu_-})^{1/\nu} \quad \text{(A3.3.3)}$$

which may be written as

$$\mu_{\pm} = \mu_{\pm}^0 + RT\ln x_{\pm} + RT\ln f_{\pm} \quad \text{(A3.3.4)}$$

where

$$\mu_{\pm}^0 = \frac{\nu_+\mu_+^0 + \nu_-\mu_-^0}{\nu} \quad \text{(A3.3.5)}$$

$$x_{\pm} = (x_+^{\nu_+}x_-^{\nu_-})^{1/\nu} \quad \text{(A3.3.6)}$$

and

$$f_{\pm} = (f_+^{\nu_+}f_-^{\nu_-})^{1/\nu} \quad \text{(A3.3.7)}$$

APPENDIX 3.4. TO SHOW THAT THE MINIMUM IN THE P_r VERSUS r CURVE OCCURS AT $r = \lambda/2$

From

$$P_r = 4\pi n_i^0 e^{\lambda/r} r^2 \quad \text{(A3.4.1)}$$

one finds the minimum in the P_r versus r curve by differentiating the expression for P_r with respect to r and setting the result equal to zero. That is,

$$\frac{dP_r}{dr} = 4\pi n_i^0 e^{\lambda/r} 2r - 4\pi n_i^0 r^2 e^{\lambda/r}\frac{\lambda}{r^2} = 0 \quad \text{(A3.4.2)}$$

i.e.,

$$2r_{\min} - \lambda = 0$$

or

$$r_{\min} = q = \frac{\lambda}{2} \quad \text{(A3.4.3)}$$

APPENDIX 3.5. TRANSFORMATION FROM THE VARIABLE r TO THE VARIABLE $y = \lambda/r$

From $y = \lambda/r$, it is obvious that

$$r^2 = \frac{\lambda^2}{y^2} \tag{A3.5.1}$$

$$dr = -\frac{\lambda}{y^2}\,dy \tag{A3.5.2}$$

$$e^{\lambda/r} = e^y \tag{A3.5.3}$$

Further, when $r = q = \lambda/2$, it is clear that

$$y = 2 \tag{A3.5.4}$$

and, when $r = a$, it follows that

$$y = \frac{\lambda}{a} = b \tag{A3.5.5}$$

By introducing the substitutions (A3.5.1), (A3.5.2), (A3.5.3), (A3.5.4), and (A3.5.5) into Eq. (3.145), the result is

$$\theta = 4\pi n_i^0 \lambda^3 \int_{y=2}^{y=b} e^y y^{-4}\,dy$$

or

$$\theta = 4\pi n_i^0 \left(\frac{z_+ z_- e_0^2}{\varepsilon \kappa T}\right)^3 \int_{y=2}^{y=b} e^y y^{-4}\,dy \tag{A3.5.6}$$

APPENDIX 3.6. RELATION BETWEEN CALCULATED AND OBSERVED ACTIVITY COEFFICIENTS

Consider a solution consisting of 1 kg of water in which is dissolved m moles of 1:1-valent salt. Ignoring the question of ion-pair formation, there are m moles of

positive ions and m moles of negative ions in the solution. Hence, the total free energy G of the solution is given by

$$G = \left(\frac{1000}{M_{H_2O}}\right)\mu_{H_2O} + m\mu_+ + m\mu_- \tag{A3.6.1}$$

where M_{H_2O} is the molecular weight of the water and μ_{H_2O}, μ_+, and μ_- are the chemical potentials of water, positive ions, and negative ions, respectively.

Now, if a fraction θ of the positive and negative ions form ion pairs designated (+ –), then the free energy of the solution assuming ion-pair formation is

$$G = \left(\frac{1000}{M_{H_2O}}\right)\mu_{H_2O} + (1-\theta)m\mu'_+ + (1-\theta)m\mu'_- + \theta m\mu'_{+-} \tag{A3.6.2}$$

where the primed chemical potentials are based on ion association.

Since, however, the free energy of the solution must be independent of whether ion association is considered, Eqs. (A3.6.1) and (A3.6.2) can be equated. Hence

$$\mu_+ + \mu_- = (1-\theta)(\mu'_+ + \mu'_-) + \theta\mu'_{+-} \tag{A3.6.3}$$

But ions are in equilibrium with ion pairs, and therefore

$$\mu_{+-} = \mu'_+ + \mu'_- \tag{A3.6 4}$$

Combining Eqs. (A3.6.4) and (A3.6.3), one has

$$\mu_+ + \mu_- = \mu'_+ + \mu'_- \tag{A3.6.5}$$

or

$$\mu^0_+ + RT\ln\gamma_+ m + \mu^0_- + RT\ln\gamma_- m = \mu^{0\prime}_+ + RT\ln\gamma'_+(1-\theta)m + \mu^{0\prime}_-$$

$$+ RT\ln\gamma'_-(1-\theta)m \tag{A3.6.6}$$

It is clear, however, that $\mu^0_+ = \mu^{0\prime}_+$ and $\mu^0_- = \mu^{0\prime}_-$ since, whether ion association is considered or not, the standard chemical potentials of the positive and negative ions are the chemical potentials corresponding to ideal solutions of unit molality of these ions. Hence

$$\gamma_+\gamma_- = (1-\theta)^2\gamma'_+\gamma'_- \tag{A3.6.7}$$

or

$$\gamma_{\pm} = (1 - \theta)\gamma'_{\pm} \tag{A3.6.8}$$

But $\gamma_{\pm}$ is the observed or stoichiometric activity coefficient and therefore

$$(\gamma_{\pm})_{obs} = (1 - \theta)\gamma'_{\pm} \tag{A3.6.9}$$

Similarly,

$$(f_{\pm})_{obs} = (1 - \theta)f_{\pm} \tag{3.160}$$

EXERCISES

1. Calculate the potentials due to the ionic cloud around cations in the following solutions: (a) 10^{-3} *M* NaCl, (b) 0.1 *M* NaCl, (c) 10^{-3} *M* $CaCl_2$, and (d) 10^{-3} *M* $CaSO_4$. (Kim)

2. For 0.001 *M* aqueous KCl solution, calculate the total potential in the ionic atmosphere and then that part of the total potential due to the ionic cloud.

3. Calculate the mean activity coefficient of a 0.002 *M* $LaCl_3$ solution, assuming that at this low concentration there is a negligible association between cations and anions.

4. What is the electrical work done in charging a body up to a charge q and a potential ψ? Prove the expression.

5. Compare the molarities and ionic strengths of 1:1, 2:1, 2:2, and 3:1 valent electrolytes in a solution of molarity c. (Constantinescu)

6. Calculate the ionic strength of the following solutions: (a) 0.04 *M* KBr, (b) 0.35 *M* $BaCl_2$, and (c) 0.02 *M* Na_2SO_4 + 0.004 *M* Na_3PO_4 + 0.01 *M* $AlCl_3$. (Constantinescu)

7. A 0.001 *M* $BaCl_2$ solution is mixed with an 0.001 *M* Na_2SO_4 solution. Calculate the ionic strength.

8. Assuming that a 10% error can be tolerated, calculate from the Debye–Hückel limiting law the highest concentration at 25°C at which activity can be replaced by concentration in the cases of (a) NaCl and (b) $CaSO_4$ solutions. (Constantinescu)

9. Calculate the activity coefficients in the following solution at 25°C by the Debye–Hückel limiting law: (a) 10^{-3} *M* NaCl, (b) 0.1 *M* NaCl, (c) 10^{-3} *M* $CaCl_2$, and (d) 10^{-3} *M* $CaSO_4$. (Kim)

TABLE P.1

KCl mol kg^{-1}	0.025	0.050	0.10	0.20
TlCl mol kg^{-1}	8.69×10^{-3}	5.90×10^{-3}	3.96×10^{-3}	2.68×10^{-3}

10. Calculate the activity coefficient of a 10^{-2} *M* NaCl solution by the extended Debye–Hückel limiting law with an ion-size parameter of 400 pm. (Kim)

11. Calculate the effect of water molecules on the activity coefficient in 1 *M* NaCl. The water activity in the solution is 0.96686 and the hydration number of the electrolyte is 3.5. The density of the solution is 1.02 g cm^{-3}. (Kim)

12. Calculate the mean activity coefficient of thallous chloride, the solubility of which has been measured in water and in the presence of various concentrations of potassium chloride solutions at 25 °C, as given in Table P.1. The solubility of this salt in pure water is 1.607×10^{-2} mol kg^{-1}. (Constantinescu)

13. Calculate the solubility product of $C_2O_4Ag_2$ if its solubility in pure water at 25 °C is 8×10^{-5} mol dm^{-3}. (Constantinescu)

14. Calculate the mean activity coefficient at 25 °C of 0.01 *N* solutions of (a) HCl, (b) $ZnCl_2$, and (c) $ZnSO_4$. (Constantinescu)

15. Utilize the known values of the Debye–Hückel constants *A* and *B* for water to calculate the mean activity coefficients for 1:1, 1:2, and 2:2-valent electrolytes in water at the ionic strengths 0.1 and 0.01 at 25 °C. The mean distance of closest approach of the ions *a* may be taken as 300 pm in each case. (Constantinescu)

16. Draw a diagram representing the Gurney co-sphere. When two ions collide, how does this sphere influence the parameters that go into the calculation of the activity coefficient?

17. In the text, an explanation is given which shows how the mean activity coefficient of an electrolyte can be given if the activity of water in the solution is known. Suppose you know the vapor pressure of water over the solution of an electrolyte. Could you still get the activity coefficient of the electrolyte in solution? How? Illustrate your answer by using the data in Table 3.5.

18. Calculate the chemical-potential change of the cations in the following solutions by the Debye–Hückel theory: (a) 10^{-3} *M* NaCl, (b) 0.1 *M* NaCl, (c) 10^{-3} *M* $CaCl_2$, and (d) 10^{-3} *M* $CaSO_4$. (Kim)

19. Use the values of the Debye–Hückel constants *A* and *B* at 25 °C to calculate $-\log f_{\pm}$ for a 1:1-valent electrolyte for ionic strengths 0.01, 0.1, 0.5, and 1.0,

assuming in turn that the mean distance of closest approach of the ions, a, is either zero or 100, 200, and 400 pm. (Constantinescu)

20. Electrolytes for which the concentration is less than 10^{-3} M can usually be dealt with by the Debye–Hückel limiting law. Utilize the Debye–Hückel theory extended by allowance for ion size and also for removal of some of the active solvent into the ion's primary solvation shell to calculate the activity coefficient of 5 M NaCl and 1 M $LaCl_3$ solutions (neglecting ion association or complexing). Take the total hydration number at the 5 M solution as 3 and at the 1 M solution as 5. Take r_i as 320 pm.

21. Use the Debye–Hückel limiting law to derive an expression for the solvent activity in dilute solutions. (Xu)

22. Use the above results to calculate the activity coefficients for water (Table 2.8). (Xu)

23. Calculate the Debye–Hückel reciprocal lengths for the following solutions: (a) 10^{-3} M NaCl, (b) 0.1 M NaCl, (c) 10^{-3} M $CaCl_2$, and (d) 10^{-3} M $CaSO_4$. (Kim)

24. Calculate the thickness of the ionic atmosphere in 0.1 N solutions of a uni-univalent electrolyte in the following solvents: (a) nitrobenzene ($\varepsilon = 34.8$), (b) ethyl alcohol ($\varepsilon = 24.3$), and (c) ethylene dichloride ($\varepsilon = 10.4$) at 25 °C. (Constantinescu)

25. Calculate the minimum distance at which the attractive electrostatic energy of the ions having charges z_+ and z_- in an electrolyte is greater than the thermal energy of an interacting cation and anion.

26. Determine the mean distance between ions in a solution of concentration c for a 1:1 electrolyte. Calculate $1/\kappa$ for a solution of 0.01 mol dm^{-3}.

27. Explain why κ^{-1} is called "the Debye length." Draw a figure that shows what this term means in terms of the concept of an ionic atmosphere.

28. Assume as a rough approximation that the distance of closest approach between two ions a is the sum of the ionic radii of cation and anion plus the diameter of water. Calculate κa for concentrations of CsCl of 10^{-4}, 5×10^{-4}, 10^{-3}, 5×10^{-3}, 10^{-2}, 5×10^{-2}, and 10^{-1} M at 25 °C and find the maximum concentration at which $\kappa a < 0.1$, i.e., the limiting law is applicable.

29. Prove that the ionic strength is actually a parameter reflecting the electrostatic field in the solution. (Hint: Show the effect of ionic valence charge on I.) (Xu)

30. Compute the ionic activity of 0.0001 M KCl. What change will be caused to the activity of KCl if 0.01 mole of $ZnCl_2$ is added to 1000 ml of the above solution? With the added salt, will the Debye–Hückel reciprocal length κ^{-1} increase or decrease? Why? (Xu)

31. Calculate the ion association constant K_A of CsCl in ethanol ($\varepsilon = 24.3$) according to Bjerrum's concept. $r(Cs^+) = 1.69$ Å and $r(Cl^-) = 1.81$ Å. (Kim)

32. Write down the full Taylor–MacClaurin expansion of e^x and e^{-x}. Find the difference between e^x and the expansion for $x = 0.1$, 0.5, and 0.9.

33. Derive the linearized Poisson–Boltzmann equation.

34. Write down a typical equation for the sum of the attractive and repulsive energies of an ion in an electrolyte. What is meant by the MSA approximation? Represent it diagrammatically and with equations.

35. Describe the basic principles of the Monte Carlo and molecular dynamic simulation methods applied to electrolytes. How are the adjustable parameters determined?

36. Explain in about 250 words the essential approach of the Mayer theory of ionic solutions and how it differs from the ionic-atmosphere view. The parent of Mayer's theory was the McMillan–Mayer theory of 1950. With what classical equation for imperfect gases might it be likened?

37. Among the outstanding contributors to the theory of ionic solutions after 1950 were Mayer, Friedman, Davies, Rasaiah, Blum, and Haymet. Write a few lines on the contributions due to each.

38. A number of acronyms are used in work on the theory of ion–ion interactions. Some are DHLL, HNC, MSA, COUL, and GUR. Give the full meaning of each and explain the significance of the concept it represents in the field of ion–ion interactions.

39. Spectroscopic methods are used to find out about the structure of an ionic solution. Write a few lines on what particular aspects of the solution structure are revealed by the use of the following kinds of spectra: (a) UV-visible, (b) Raman, (c) infrared, and (d) nuclear magnetic resonance.

PROBLEMS

1. Find the maximum potential of the ionic atmosphere at which the Poisson–Boltzmann equation can be linearized in a 1:1 electrolyte at 25 °C. After linearization, the charge density in the atmosphere is proportional to the potential. Can you see any fundamental objection to having ρ not proportional to ψ.

2. When the Debye–Hückel model was developed, an important hypothesis was made for mathematical convenience, i.e., $z_i e_0 \psi_r < kT$. Now, using an aqueous 1:1 electrolyte solution at 25 °C as an example, reassess the validity of the hypothesis. What is the physical nature of the hypothesis? (Xu)

TABLE P.2

Lowering of Vapor Pressure by Salts in Aqueous Solutions

g-mole salt / liter of water	KNO_3	KNO_2	LiBr	NaBr	NaI
0.5	10.3	11.1	12.2	12.6	12.1
1.0	21.1	22.8	26.2	24.9	25.6
2.0	40.1	44.8	60.0	57.0	60.2
3.0	57.6	67.0	97.0	89.2	99.5
4.0	74.5	90.0	140.0	124.2	136.7
5.0	88.2	110.0	186.3	159.5	177.3
6.0	102.1	130.7	241.5	197.5	221.0
8.0	126.3	167.0	341.5	268.0	301.5
10.0	148.0	198.8	438.0	—	370.0

Source: *CRC Handbook of Chemistry and Physics*, 58th ed., CRC, Boca Raton, FL

3. Explain from the Gibbs–Duhem equation how the determination of the activity of water can give rise to the activity of the electrolyte dissolved in it. Table P.2 shows data from the lowering of the vapor pressure of water by different salts at 100 °C at which $P^*_{H_2O} = 760$ torr. Plot $\log f_\pm$ against the ionic strength for each of the different salts. Discuss your results in the light of the data in Table P4.

4. Describe the difference between the Guntelberg and Debye charging processes. Which process should be more effective in deriving an equation for the activity coefficient?

5. Show that within the concentration range of the limiting law, the slope of the $\log f_\pm$ vs. $-\sqrt{I}$ line is 0.509 for aqueous solutions at 25 °C.

6. (a) The whitecoats built the cell below and managed to measure its potential at 25 °C as 0.35 V:

$$\text{Ag} \mid \text{AgCl(s)} \mid \text{AgCl(aq, saturated)} \mid$$
$$\mid \text{AgCl(aq, saturated in 0.05 } M \text{ CaCl}_2) \mid \text{AgCl(s)} \mid \text{Ag}$$

The solubility product of AgCl is known to be 1.77×10^{-10} at room temperature. Calculate the individual activity coefficient for Ag^+ in the $CaCl_2$ solution.
(b) Is there a way to obtain the individual activity coefficient for Cl^- in the same solution? (Xu)

7. The excess charge on an ionic atmosphere varies with distance out from the central ion. Show that the net change in the charge of a spherical shell of thickness dr is

$$dq = -z_i e_0 \, e^{-\kappa r} \kappa^2 r \, dr$$

Hence at a certain distance from the central ion, there will be a ring with a maximum charge. Find this distance.

8. Plot the values for the activity coefficient of the electrolyte as calculated in Problem 3 against the ionic strength. Then see what degree of match you can obtain from the Debye–Hückel law (one-parameter equation). Do a similar calculation with the equation in the text which brings in the distance of closest approach *(a)* and allows for the removal of water from the solution (two-parameter equation). Describe which values of a_i and n_h (the hydration number) fit best. Discuss the degree to which the values you had to use were physically sensible.

9. The radius of the ionic atmosphere is $1/\kappa$ where κ is defined in the text. Work out the average distance between ions (d) in terms of the concentration c_0, in mol dm^{-3}. If $d > 1/\kappa$, then one is confronting a situation in which the radius of the atmosphere is less than the average distance between ions. Describe what this means. Derive a general expression for c_0 at which this problem (coarse grainedness) occurs for a 2:2 electrolyte. Do you think an ionic atmosphere model applies when $d > 1/\kappa$?

10. Suppose the finite-sized center ion has a size parameter a; what will be the radial distribution of the total excessive charge $q(r)$ and $dq(r)$? Use the "correspondence principle" to confirm the validity of this expression. In the above case will the Debye–Hückel reciprocal length κ^{-1} depend on the ion size parameter a? (Xu)

11. Bjerrum's theory of ionic association gives rise to an expression for the fraction of ions in an ionic solution which are associated. Use the theory to calculate the degree of association of a 0.01 M $MgCl_2$ solution in ethanol ($\varepsilon = 32$).

12. Use the equations in the text that concern ion association. Find the concentration in an ethanol solution at which KCl manifests a 10% association. Compare the value you find with Haymet's calculations.

13. (a) As alternative to Bjerrum's model of ion association, you can use the results of the Debye–Hückel model to develop a qualitative but facile method for predicting ion-pair formation. (Hint: Compare the Debye–Hückel reciprocal length κ^{-1} and the effective distance for ion formation q.)
(b) In a lithium battery, usually a nonaqueous solution of lithium salts in organic solvents is used as an electrolyte. While the dielectric constants of such solvents range between 5 and 10, estimate the degree of ion-pair formation. (Xu)

14. The McMillan–Mayer theory is an alternative to the Debye–Hückel theory. It is called the virial coefficient approach and its equations bear some conceptual resemblance to the virial equation of state for gases. The key contribution in

applying the theory to electrolytes was made by Mayer, when he finally solved the equations by introducing a screening factor $e^{-\kappa r}$ when $1/\kappa$ is the Debye length. Plot $e_0/\varepsilon r$ and $e_0 e^{-\kappa r}/\varepsilon r$ against $1/r$ in the range $0.15 < r < 2.5$ nm for RbCl at 0.1 *M*. Determine the numerical effect of Mayer's screening factor.

15. Calculate $\log f_\pm$ from the Debye–Hückel equation with allowance for both the ion size and hydration terms for $AgNO_3$ solutions from 10^{-3} to 2 mol dm^{-3} and compare the result with those of the MSA equation:

$$\log f_\pm = \frac{e_0^2 z_i^2 \Gamma}{kT\varepsilon(1 + \Gamma\sigma)}$$

The term σ can be taken as the same as a_i in the Debye–Hückel expressions, Γ is defined in the text.

Compare each with the experimental values of Table P.3. Which is the more experimentally consistent approach?

16. Haymet and co-workers have calculated the mole fraction of dimers (associated ions) in electrolytic solutions, and some of their results are shown in Fig. 3.51. Use the equations of the Bjerrum theory applied to Na_3PO_4 and compare the results with those of the correlation function approach used by Haymet et al. The essential difference between the Haymet approach and that of Bjerrum is that

TABLE P.3

Molal Activity Coefficients of $AgNO_3$ Solutions at 25 °C

m	γ	m	γ
0.001	0.964	0.800	0.465
0.002	0.950	0.900	0.447
0.005	0.924	1.000	0.430
0.010	0.896	1.200	0.400
0.020	0.859	1.400	0.375
0.050	0.794	1.600	0.353
0.100	0.732	1.800	0.334
0.200	0.656	2.000	0.316
0.300	0.606	2.500	0.280
0.400	0.567	3.000	0.252
0.500	0.536	3.500	0.229
0.600	0.509	4.000	0.210
0.700	0.486	4.500	0.194

Source: Reprinted from W. Hamer and Y.-C. Wu, *J. Phys. Chem. Ref Data*, **1**: 1047 (1972).

the former more realistically involves repulsive as well as attractive forces. What is the percent difference in the two answers at 1 mol dm^{-3}?

17. What is the total charge on an ionic atmosphere around an anion of valence z? From the data in the text, examine $\log f_{\pm}$ vs. $\sqrt{m}$, where m is the molality of the solution, from 0 to 1 mol dm^{-3}. The plots always pass through a minimum. Use the fully extended Debye–Hückel theory, including the Bjerrum–Stokes and Robinson terms, to find the significance of the minimum at which the electrolyte concentration increases with the increase of the cation radius.

18. In most of the modern versions of the Debye–Hückel theory of 1923, it is still assumed that the dielectric constant to be used is that of water. The dielectric constant of solutions decreases linearly with an increase in the concentration of the electrolyte. Using data in the chapter, calculate the mean activity coefficient for NaCl from 0.1 *M* to 2 *M* solutions, using the full equation with correction for the space taken up by the ions and the water removed by hydration. Compare the new calculation with those of Stokes and Robinson. Discuss the change in "*a*" you had to assume.

19. Consider KCl and take "*a*" to be the sum of the ionic radii. Use data from tables to get these. Thus, one can calculate "*b*" of the Bjerrum theory over a reasonable concentration range and, using appropriate tables, obtain the value of the fraction of associated ions. Now recalculate the values of $\log f_{\pm}$ for KCl for 0.1 to 2 *M* solutions from the full Debye–Hückel theory involving allowance for ion size and hydration — but now also taking into account θ. In this approach, $c_0(1 - \theta)$ is the concentration of the ions that count in the expressions. (See Appendix 3.6.) Does this accounting for θ improve the fit?

20. Using the "point-charge version" of the Debye–Hückel model, derive the radial distribution of total excessive charge $q(r)$ from the central ion. Comment on the difference between $q(r)$ and the excessive charge in a dr-thickness shell $dq(r)$. (Xu)

21. (a) Using the above result, calculate the total excessive charge within the sphere of the radius of the Debye–Hückel reciprocal length κ^{-1}. How much of the overall excessive charge has been accounted for within the sphere of radius κ^{-1}? (b) Plot $q(r)$ vs. r for an aqueous solution of 10^{-3} *M* of a 1:1 electrolyte at 25 °C. (Xu)

22. Evaluate the Debye–Hückel constants *A* and *B* for ethyl alcohol and use the values to calculate the mean activity coefficients for 1:1, 1:2, and 2:2-valent electrolytes in ethyl alcohol at ionic strengths 0.1 and 0.01 at 25 °C. The mean distance of closest approach of the ions *a* may be taken as 300 pm in each case. Dielectric constant $\varepsilon = 24.3$. (Constantinescu)

23. Describe the correlation function as applied to ionic solutions. Sketch out a schematic of such a quantity for a hypothetical solution of $FeCl_2$. There are two entirely different types of methods of obtaining $g(r)$; state them. Finally, describe the "point" of knowing this quantity and comment on the meaning of the statement: "From a knowledge of the correlation function, it is possible to calculate solution properties (which may, in turn, be compared with the results of experiment). Hence the calculation of the correlation function is the aim of all new theoretical work on solutions."

24. The text gives the results of molecular dynamic calculations of the fraction of ion pairs as a function of concentration for univalent ions. Compare these values with those calculated by the Bjerrum theory.

25. Early work on solvation was dominated by the work of Born, Bernal and Fowler, Gurney and Frank. Which among these authors made the most lasting contributions? Why?

MICRO RESEARCH

1. One could use the Debye–Hückel ionic-atmosphere model to study how ions of opposite charges attract each other. (a) Derive the radial distribution of cation (n_+) and anion (n_-) concentration, respectively, around a central positive ion in a dilute aqueous solution of 1:1 electrolyte. (b) Plot these distributions and compare this model with Bjerrum's model of ion association. Comment on the applicability of this model in the study of ion association behavior. (c) Using the data in Table 3.2, compute the cation/anion concentrations at Debye–Hückel reciprocal lengths for NaCl concentrations of 10^{-4} and 10^{-3} **mol dm^{-3}**, respectively. Explain the applicability of the expressions derived. (Xu)

2. In the development of the theory of Debye and Hückel, it was assumed that two main changes had to be made: in the ion size (represented by the distance of closest approach a) and the diminution of the "available" waters due to hydration. Ion association was taken into account also.

   In a parallel series of developments, starting with the Mayer theory and continuing with the so-called mean spherical approximation, the effects of hydration and ion association were arbitrarily removed from consideration, in spite of their undeniable presence in nature.

   Utilizing equations of the text and values in Table P.4, follow through the calculations made to fit experiments in both approaches. Discover what adjustments are made in the MSA approach so that fair agreement (as in the work of Fawcett and Blum) with experiments can be obtained up to **2 mol dm^{-3}**, using model assumptions that neglect association and hydration.

TABLE P.4

Recommended Values for the Mean Activity Coefficient γ and Water Activity of $CaCl_2$ in H_2O at 25 °C

m/mol kg^{-1}	γ	a_w
0.001	0.8885	0.999948
0.002	0.8508	0.999897
0.003	0.8245	0.999848
0.004	0.8039	0.999798
0.005	0.7869	0.999749
0.006	0.7724	0.999701
0.007	0.7596	0.999653
0.008	0.7483	0.999605
0.009	0.7380	0.999557
0.010	0.7287	0.999510
0.020	0.6644	0.999042
0.030	0.6256	0.998583
0.040	0.5982	0.998127
0.050	0.5773	0.997674
0.060	0.5607	0.997221
0.070	0.5470	0.996769
0.080	0.5355	0.996316
0.090	0.5256	0.995863
0.100	0.5171	0.995408
0.200	0.4692	0.990782
0.300	0.4508	0.985960
0.400	0.4442	0.980912
0.500	0.4442	0.975621
0.600	0.4486	0.970072
0.700	0.4564	0.964256
0.800	0.4670	0.958163
0.900	0.4801	0.951785
1.000	0.4956	0.945117
1.250	0.5440	0.927142
1.500	0.6070	0.907271
1.750	0.6861	0.885497
2.000	0.7842	0.861853
2.250	0.9049	0.836413
2.500	1.0529	0.809293
2.750	1.2339	0.780655
3.000	1.4550	0.750702

Source: Reprinted from R. N. Goldberg and R. L. Nuttall, *J. Phys. Chem. Ref. Data* **7**: 263 (1978).

3. The MSA equation used by Fawcett, Blum, and their colleagues shows good results in the calculation of activity coefficients up to a 2 *M* solution. Such calculations are described in the text. In this approach to electrolyte behavior, there are two properties of solutions that are neglected: (1) The degree of association, θ. How to calculate it from Bjerrum's point of view and the results of calculating it from MD, are described in the text, together with how to take θ into account in activity coefficient calculations. (2) The effect on activity calculations of hydration, also described in the text. What effect would it have on the Blum–Fawcett MSA calculations if these two neglected phenomena were also accounted for?

4. This text contains descriptions of numerous methods for obtaining the solvation number of ions (corresponding tables of data are given). By and large, the methods can be divided into two classes: solution properties (mobility, entropy, compressibility, partial molar volume, dielectric constant, Debye potential) and spectroscopic methods (neutron diffraction, Raman, and NMR). The values that arise from the solution methods hang together fairly well, though it is clear that the methods are not very precise. The results of the spectroscopic methods are similar to each other. However, it has to be admitted that for a given ion, the spectroscopic values are much lower (about one-third to one-half lower) than the self-consistent values determined from the properties of solutions. By examining the literature quoted in the text (and other literature), validate the statements made above for the following ions: Na^+, Ca^+, and Cr^{3+}. Then examine the evidence in favor of and against the following two hypotheses concerning the discrepancy noted:

   (a) There is no basic discrepancy. The two approaches are measuring the same quantity. However, solvation numbers are dependent on concentration; they get larger as the dilution increases. In concentrations above about 1 *M* (as shown by the molar volume–Debye potential approach), the solvation number declines considerably. However, it is only at the higher concentrations that most of the spectroscopic measurements have been made. Conversely, the solution properties have tended to be measured in the 10^{-3} to 10^{-1} *M* range, where the solvation number is indeed larger.
   (b) There is a basic discrepancy. The spectroscopic methods are more precise and with some of them one can obtain the time of residence of the water molecule and be quite precise about waters that stay with the ion, for how long, etc. The solution properties methods are a heterogeneous group. It is remarkable that they lead to a fairly consistent sense of numbers. However, the molar volume–Debye potential method should be precise.

   Analyze all this and produce a clear and reasoned judgment, buttressed by reasonings in a multipage analysis. Include in your discussion a ranking of methods for primary solvation numbers.

This page intentionally left blank